DOE/METC-95/1017, Vol. 1
(DE95009703)
CONF-950494--Vol.1

# Proceedings of the Natural Gas RD&D Contractors Review Meeting Volume I

Rodney D. Malone

April 1995

Co-Hosted by

U.S. Department of Energy
Office of Fossil Energy
Morgantown Energy Technology Center

and

Southern University and
Agricultural and Mechanical College

# Disclaimer

DOE/METC-95/1017, Vol. 1
(CONF-950494)--Vol.1
(DE95009703)
Distribution Category UC-109
UC-110
UC-131
UC-132
UC-133

# Proceedings of the Natural Gas RD&D Contractors Review Meeting Volume I

Editor
Rodney D. Malone

Co-Hosted by

U.S. Department of Energy
Morgantown Energy Technology Center
P.O. Box 880
Morgantown, WV 26507-0880
(304) 285-4764
FAX (304) 285-4403/4469

and

Southern University and
Agricultural and Mechanical College
Southern Branch Post Office
Baton Rouge, LA 70813

April 4-6, 1995

# Foreword

The Natural Gas RD&D Contractors Review Meeting was held on April 4-6, 1995, at the campus of Southern University in Baton Rouge, Louisiana. This meeting was sponsored by the Morgantown Energy Technology Center, Office of Fossil Energy, U.S. Department of Energy (DOE) and co-hosted by Southern University.

**METC** periodically provides an opportunity to bring together all of the R&D participants in a DOE-sponsored Contractors Review Meeting to present key results of their research and to provide technology transfer to the active research community and the interested public. Current research activities in Natural Gas included discussions of results summarizing work being conducted in Resource and Reserves; Low Permeability Reservoirs; Drilling, Completion, and Stimulation; Natural Gas Upgrading; and Storage product lines. The meeting also included project and technology summaries related to the DOE Oil Program, Natural Gas Fuel Cells and Natural Gas Turbines as well as a summary of the activities of the Gas Research Institute and the Petroleum Technology Transfer Council. The format included both oral and poster session presentations.

This meeting contained ten formal sessions, two informal sessions, and one seminar, which included forty-three technical papers, fourteen poster presentations, and six exhibits.

- Keynote, Plenary and Opening Sessions (7 papers)
- Seminar
  - Northern Gulf of Mexico Oil and Gas Atlas
- Natural Gas Technology Product Lines
  - Resource and Reserves (4 papers)
  - Low Permeability Reservoirs (8 papers)
  - Drilling, Completion, and Stimulation (10 papers)
  - Natural Gas Upgrading (11 papers)
  - Natural Gas Storage (3 papers)

We gratefully acknowledge the participation of the Gas Research Institute, the Petroleum Technology Transfer Council, the University of Texas (Bureau of Economic Geology and the Minerals Management Service), and Southern University, as well as the research contractors and the various offices of DOE in the presentations provided in this document. The papers printed in these proceedings have been produced from camera-ready manuscripts provided by the authors. They have been neither refereed nor extensively edited.

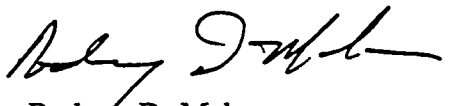

Rodney D. Malone
Conference Coordinator

# Contents

## Volume I

# Volume II

## Session 3B — Natural Gas Upgrading: Low-Quality Natural Gas



## Session 4B — Natural Gas Storage

## Poster Session

## Session 7 — Drilling, Completion, and Stimulation



## Appendices

# Session 1

*Plenary Session*

# 1.5 U.S. Department of Energy Power Generation Programs for Natural Gas

R. A. Bajura
Morgantown Energy Technology Center

## ABSTRACT

The U.S. Department of Energy (DOE) is sponsoring two major programs to develop high efficiency, natural gas fueled power generation technologies. These programs are the Advanced Turbine Systems (ATS) Program and the Fuel Cell Program. While natural gas is gaining acceptance in the electric power sector, the improved technology from these programs will make gas an even more attractive fuel, particularly in urban areas where environmental concerns are greatest.

Under the auspices of DOE's Office of Fossil Energy (DOE/FE) and Office of Energy Efficiency and Renewable Energy (DOE/EE), the 8-year ATS Program is developing and will demonstrate advanced gas turbine power systems for both large central power systems and smaller industrial-scale systems. The large-scale systems will have efficiencies significantly greater than 60 percent, while the industrial-scale systems will have efficiencies with at least an equivalent 15 percent increase over the best 1992-vintage technology. The goal is to have the system ready for commercial offering by the year 2000.

DOE/FE and DOE/EE also cooperate in the development of fuel cells. DOE/EE is responsible for transportation applications, while DOE/FE supports fuel cell development for stationary electric power. Fuel cell systems in the 100 kilowatt (kW) to several megawatt (MW) size range are an attractive technology for power generation because of their ultra-high energy conversion efficiency and extremely low environmental emissions. As modular units for distributed power generation, fuel cells are expected to be particularly beneficial where their by-product heat can be effectively used in cogeneration applications. The first generation of fuel cells for power generation is currently entering the commercial market. Advanced fuel cell power systems fueled with natural gas are expected to be commercially available by the turn of the century. The domestic and international market for this advanced technology is expected to be very large.

## INTRODUCTION

The U.S. will not be able to produce and use hydrocarbon fuels to their full potential—efficiently, affordably, and with environmental responsibility—unless new technology is developed and deployed. Failure to build on the substantial technological capabilities we already possess will put the U.S. at a competitive disadvantage to other countries who are pushing hard to dominate an increasingly "high-tech" global energy market.

The economic slowdown in the 1980s reduced the need for new electric power plants. Few large plants are being built today. With the economy growing again, the U.S. will require new electric power generating capacity early in the next century. The next generation of power plants, however, will have to meet new environmental standards, while still producing affordable electricity. Traditional technology cannot meet the more stringent standards and keep energy costs down and the economy growing.

The pace of technology development is critical. We can keep our domestic economy growing and stay ahead of our international competitors, only if new technology is ready in time to meet critical market "windows." We don't believe that will happen unless the Federal Government and the private and academic sectors join in concerted, forward-looking, risk-shared partnerships.

In today's highly competitive international marketplace, other countries have created their own public-private research and development (R&D) ventures in an effort to gain significant global advantages in developing and marketing energy technologies for the 21st century. In the U.S., our Government can provide the critical catalyst that stimulates the private sector to look beyond immediate financial benefits and invest in higher-risk technologies that can maintain our Nation's competitive edge. Industry participation also assures that the technology in which the Government invests has real market pull.

The DOE/FE Fiscal Year (FY) 1995 appropriation for natural gas R&D is $116 million. This appropriation includes $50 million for the Fuel Cell Program and $38 million for the ATS Program. The FY 1996 budget request for natural gas R&D is $145 million, which includes $55 million and $43 million, respectively, for the Fuel Cell and the utility scale portion of the ATS Programs. The DOE/FE's total funding for the Natural Gas R&D Program is illustrated in Table 1.

Natural gas is a rapidly resurging domestic energy option. The prevailing opinion of the 1970s that gas was a scarce resource, and has been replaced with a much better understanding of the tremendous domestic supply that actually exists. The National Petroleum Council, in the most extensive study to date, has concluded that nearly 1,300 trillion cubic feet of natural gas is technically recoverable in the lower 48 states. Far from being "scarce," this resource base represents a 60-year supply, with the likelihood that even more will be found as technology improves. The challenge is to turn this huge resource base into proven reserves.

While natural gas is gaining acceptance in markets such as the electric power sector, improved technology is needed to make gas an even more attractive fuel, particularly in urban areas where environmental concerns are greatest. Some potential customers, again largely

**Table 1. Budget Authority in Millions**

| Natural Gas Research and Development | FY 1995 Appropriations | FY 1996 Request |
|---|---|---|
| Fuel Cells | $49.60 | $55.50 |
| Advanced Turbine Systems | 37.70 | 44.00 |
| Natural Gas Production | 29.00 | 46.40 |
| **Total Natural Gas R&D** | **$116.30** | **$145.90** |

in markets such as power generation, still lack confidence in the supply and availability of natural gas. By developing improved ways to use natural gas for power generation, such as advanced gas turbines and fuel cells, we can offer new options for meeting future growth in electric power demand.

The focus of the ATS and Fuel Cell Programs has been on commercialization from the outset. Most work is performed by industrial teams which will ultimately commercialize the technologies, and they are generally directly responsible for any work which supports initial demonstration and commercialization. Some generic R&D is performed by universities, national laboratories, and others. This work is generally targeted for a somewhat longer timeframe than initial demonstration and will provide the foundation for later system improvements.

## ADVANCED TURBINE SYSTEMS PROGRAM

The ATS Program began in 1992 with the appropriation of funding for the planning of a comprehensive 10-year program. Support has been strong, and the Program has since been accelerated by 2 years so that demonstrations of full-scale systems will be completed by the year 2000. Budget projections show the total DOE cost of the program will be $470 million to be cost-shared with an additional $230 million of industrial funding.

Planning for the ATS Program has included the solicitation of views from interested groups. An important step was the conducting of two workshops in Greenville, South Carolina[1,2]. Sponsored by DOE and hosted by Clemson University, each workshop brought together more than 75 representatives from the gas turbine R&D and user communities. Gas turbine manufacturers, the electric utility industry, and the university community were represented, along with Government and private sector R&D sponsors. Input for program planning was provided at the workshops, including the identification of R&D needs and the assessment of program goals. A draft plan for the ATS program[3] was presented at the second workshop and the plan revised based on guidance received from workshop participants.

Further public input was obtained as the Program Plan evolved. The plan was presented in numerous other forums (e.g., Reference 4), and a Program Plan[4] required by Congress was jointly prepared by DOE/FE and DOE/EE. A public meeting was held in Pittsburgh, Pennsylvania, on June 4, 1993, for the purpose of soliciting public comment.

Forty-five (45) organizations offered their views on the Program, and their comments were forwarded to Congress along with the plan. The comments showed broad and enthusiastic support for the planned program, although many specific comments were offered for modification.

The objectives and structure of the Program Plan emerging from this process, and sent to Congress via a formal report[5], is described in the next two sections.

## PROGRAM OBJECTIVE

The objective of the ATS Program is to develop ATS for base load application in the utility, independent power producer, and industrial electric power markets. The systems should be ready to enter the commercial market by 2000 and have the following characteristics:

- Efficiency. More than 60 percent (lower heating value [LHV] basis) on natural gas for large-scale utility turbine systems. For

industrial power generation systems, greater than 15 percent improvement in heat rate compared to 1992-vintage gas turbine systems.

- Environment. Environmental superiority under full-load operating conditions without the use of post-combustion controls. Nitrogen oxide ($NO_x$) emissions should be less than 8 parts-per-million (ppm). Carbon monoxide and hydrocarbon emissions should each be less than 20 ppm. Because of changing environmental requirements, these targets will undergo periodic review.

- Fuel Flexibility. Natural gas-fired ATS designs are to be adaptable to coal or biomass firing.

- Cost of Power. Busbar energy costs 10 percent less than current state-of-the-art turbine systems meeting the same environmental requirements.

- Reliability and Maintainability. Equivalent to state-of-the-art turbine systems.

## PROGRAM STRUCTURE

The ATS Program is jointly funded and managed by DOE/FE and DOE/EE. A Steering Committee is composed of representatives of DOE/FE, DOE/EE, the Electric Power Research Institute (EPRI), the Gas Research Institute (GRI), and the U.S. Environmental Protection Agency. This committee assures that work under the ATS Program is complementary with other work supported by these funding organizations. It is also responsible for coordination of ATS Program work with that supported by other Federal, State, and private funding organizations and for liaison with industry groups.

Much of the major development activity in the ATS Program is conducted by teams led by U.S. turbine manufacturers. This work is performed under a series of competitively awarded agreements with DOE. At first, there are multiple projects for both industrial and utility applications, but these will eventually be reduced to one full-scale prototype demonstration in each area. For the major projects, cost-sharing began at about 10 percent at the outset of the Program and will rise to greater than 50 percent for demonstrations of prototype systems.

As illustrated in Figures 1 and 2, the ATS Program consists of four elements:

### Element I—Innovative Cycle Development

This element targets the initial development of concepts which will meet ATS Program goals. In the first phase of this element, six U.S. turbine manufacturers conducted studies to define systems which they would like to commercialize. In the second phase, teams led by turbine manufacturers have been competitively selected to advance ATS systems through concept development. Technical, economic, and environmental performance of the ATS are being evaluated for both coal and natural gas firing. The teams are completing conceptual designs, market studies, and designs of critical components. They are also initiating small-scale testing for natural gas-fired systems.

### Element II—Utility System Development and Demonstration

In this element, DOE/FE will support the development and demonstration of ATS for utility application. R&D will be completed for multiple systems, including development all the way through full-scale component and integrated subsystem testing. Only one full-scale prototype demonstration is planned.

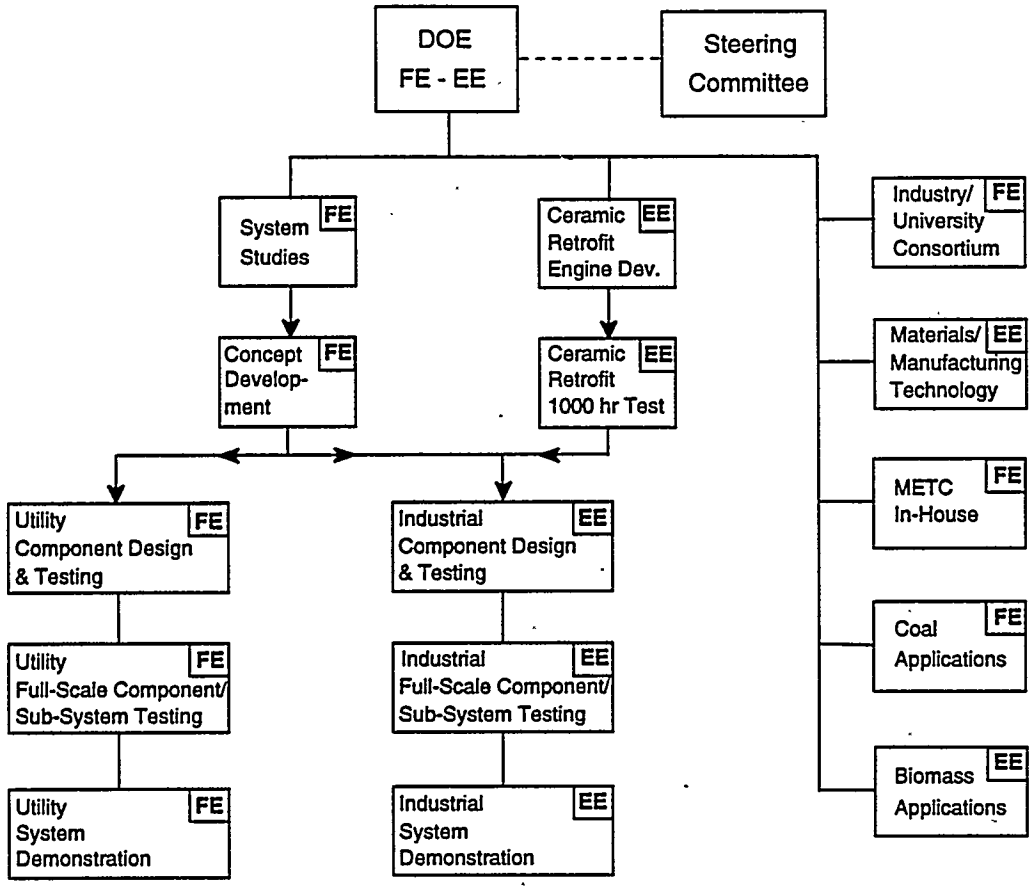


**Figure 1. Advanced Turbine Systems Program Structure**

## Element III—Industrial System Development and Demonstration

The first phase of this element was initiated by DOE/EE in parallel with Element I. Work is underway by Solar Turbines, Inc., to evaluate the benefits of upgrading existing industrial turbine designs by retrofitting with ceramic components. The study will culminate in the 4000-hour test of a 3.5-MW engine.

The second phase of this element will parallel Element II, and support the development of industrial ATS, leading to the demonstration of one full-scale prototype system.

## Element IV—Technology Base Development

R&D on generic technology issues supports the ATS development effort. Much of the Technology Base Development is performed by an industry/university consortium established by a cooperative agreement between DOE/FE and the South Carolina Energy Research and Development Center. Industrial co-sponsors identify critical technology needs and evaluate proposals prepared by the university participants.

A separate component of this element addresses critical materials and manufacturing technology issues for the whole Program. DOE/EE calls on the expertise of the Oak

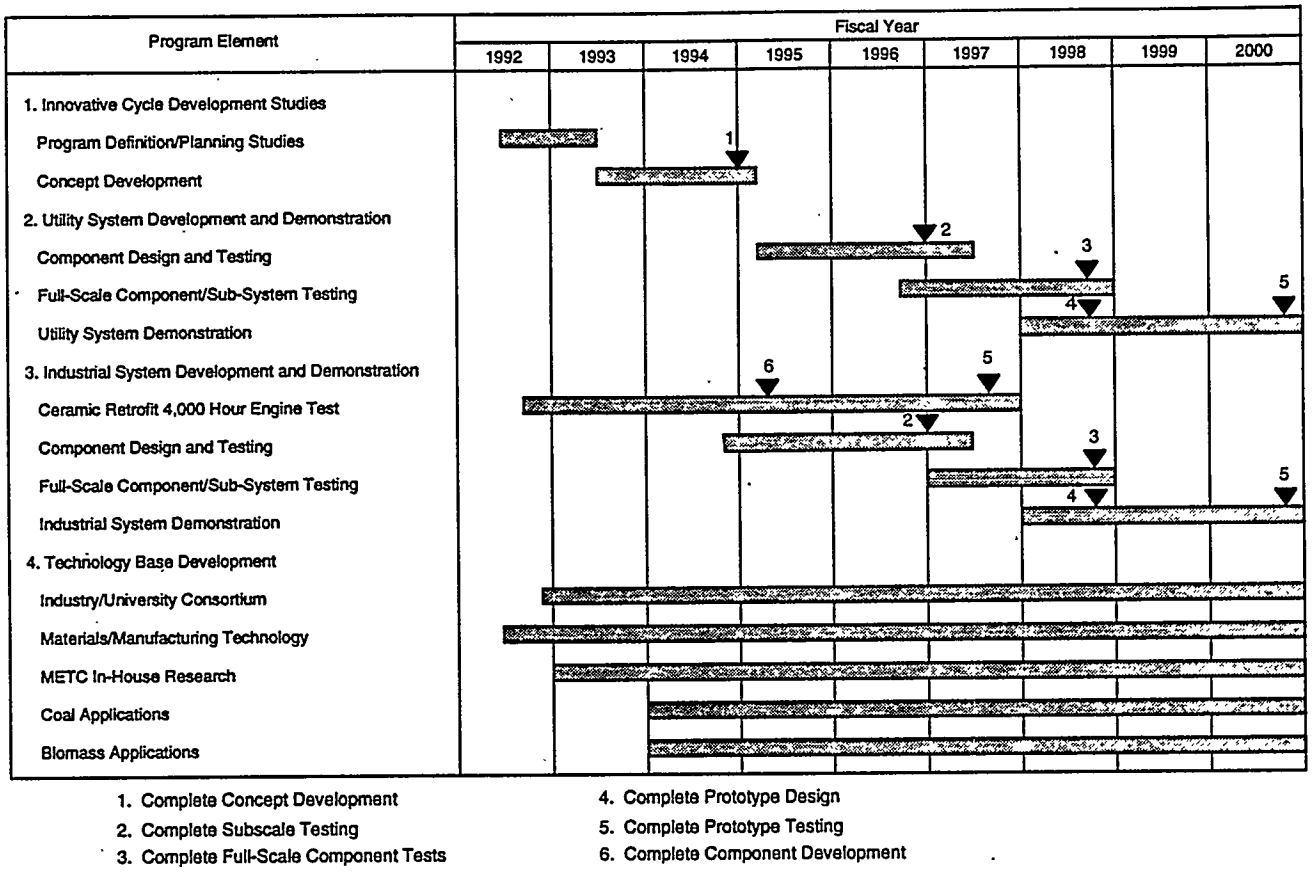


**Figure 2. Schedule for Advanced Turbine Systems Program**

Ridge Field Office for the management of this part of the Program. Projects are currently in place with PCC Airfoils, Inc., and Howmet Corporation to develop advanced turbine components.

The Morgantown Energy Technology Center (METC) in-house R&D organization also participates in this part of the Program. Much of METC's work is to be performed cooperatively with other organizations performing R&D in this program element and in program Elements I and II.

The Technology Base Development element also includes activities to address the application of ATS technology to the coal and biomass systems being developed in other DOE programs.

## PROGRAM STATUS

The initial systems studies of Element I have been completed, and Reference 6 includes papers describing the results obtained by Allison Engine Company, Asea Brown Boveri, General Electric, Solar Turbines, and Westinghouse. In general, each of the manufacturers explored a range of system possibilities and variations on the basic concepts. Advanced cycles were considered, along with significant improvements on basic combined cycle technology. All of the manufacturers

saw a need to increase turbine inlet temperature and planed to achieve this through improved cooling and materials technology. Combustor development will be needed to meet emission goals at the higher turbine inlet temperatures. The studies addressed both utility- and industrial-scale systems and included systems based on both heavy duty and aero-derivative technology.

Contracts have been awarded in the second phase of the Program, and the contractors are moving ahead with concept development. In parallel with the latter part of this work, DOE has issued solicitations for Phases 3 and 4. Awards under this round will cover the balance of the development through completion of demonstration. The target award date is late summer 1995. Although multiple awards are expected in both the industrial- and utility-scale categories, it is planned to down-select after component development and only have one demonstration project in each group.

The other elements of the Program are also well underway. Significant progress has been made in the ceramic retrofit project established with Solar Turbines, and results are being obtained. The Oak Ridge field office has established the Materials/Manufacturing Technology Program, and responses to initial solicitations are being processed. The industry/university consortium is off to a solid start, with more than 70 university members and 23 projects established in the first two annual solicitations. METC has completed shakedown of its Advanced Turbine Combustion Facility, and testing has begun.

## FUEL CELLS PROGRAM

Fuel cell systems offer the potential for ultra-high efficiency energy conversion and the enhancement of the quality of our environment. Because of this, DOE/FE is sponsoring the development of fuel cells for stationary power generation. The Department works closely with the private sector in the development and demonstration of this advanced energy conversion technology.

Concerns for the global environment are driving future power generation systems toward technologies that produce extremely low environmental emissions. Because of their high efficiencies, fuel cell power plants will help in reducing carbon dioxide emissions. Since combustion is not utilized in the process, fuel cells generate very low amounts of $NO_x$, and they emit very little sulfur oxides. Fuel cells have been exempt from air permitting requirements in southern California. Relying on electrochemistry instead of combustion, the fuel cell is attractive for both heavily polluted urban areas and remote applications. Not only will it emit none of the smog-causing pollutants associated with conventional power plants, it is ideal as a distributed power source; that is, it can be sited close to the electricity user—for example, at electrical substations, at shopping centers or apartment complexes, or in remote villages—minimizing long-distance transmission lines.

The Fuel Cell Program is a market-driven program which has more than 40 percent cost-sharing. The fuel cell developers enjoy the support of user groups with more than 75 utility and other end-user members. In addition, DOE cooperates with GRI and EPRI to fully and efficiently leverage funding for the U.S. Fuel Cell Program.

## FUEL CELL TECHNOLOGY

Fuel cells generate electricity and heat using an electrochemical process similar to a battery. A fuel cell will continuously produce power, as long as a fuel, such as natural gas; and an oxidant, air are supplied to the system. Because it is an electrochemical device, the electrical generation efficiency from the use of the fuel can be much more than that of conventional power plants. Present early

market systems are achieving over 45 percent (LHV) cycle efficiency. The next generation systems are expected to achieve 55 percent and eventually 70 percent (LHV) cycle efficiencies.

As shown in Table 2, several different types of fuel cells are being developed for stationary power applications. The electrolyte controls the operating temperature of the cells, which in turn determines the materials of construction. Phosphoric acid fuel cells (PAFC's) are now being commercialized, while molten carbonate fuel cells (MCFC's) and solid oxide fuel cells (SOFC's) promise even higher efficiencies for the future[7].

A basic fuel cell (Figure 3) consists of two electrodes, with the anode and cathode separated by an electrolyte. Fuel cell types are characterized by their electrolyte. For example, PAFC's utilize a phosphoric acid electrolyte in a matrix between anode and cathode electrodes. To produce a useable quantity of electric power, individual cells are assembled into a vertical "stack" of repeating components which are electrically interconnected. A fuel cell power plant (Figure 4) consists of the stack or power section integrated with a fuel processor and a power conditioner to convert the power from direct current to alternating current.

The fuel cell is inherently modular. Constructed as an assembly of individual cells, stacks ranging from 100 to 250 kW form a modular building block. Depending on the generating capacity required, 10 to 20 stacks can be grouped with a fuel processor and a power conditioner to create a 1- to 2-MW power plant. Larger plants will use a larger number of stacks. In high growth areas or remote sites, modular power plants located near the demand can offset the cost of right-of-way access and transmission lines.

Another attractive feature of fuel cell power plants is their use at sites where cogeneration is possible. High-grade heat or steam is available for industrial and commercial applications. Industrial drying, prisons, hotels, hospitals, and central heating and air conditioning are examples.

## PROGRAM STATUS

Because of cost-sharing by DOE and its predecessor agencies over the past 20 years, first-generation fuel cells are now in the initial states of commercialization. In the last 5 years, focus has shifted to advanced fuel cells, including molten carbonate and SOFC's. These systems offer higher efficiencies, the potential for lower capital cost, and because of higher operating temperatures, are more suitable for cogeneration.

**Table 2. Types of Fuel Cells**

| Characteristic | PAFC | MCFC | SOFC |
|---|---|---|---|
| Electrolyte | Phosphoric Acid | Lithium Carbonate/ Potassium Carbonate | Stabilized Zirconia |
| Operating Temperature | 400°F | 1200°F | 1800°F |
| Electrical Conversion Efficiency (LHV) | 45-50% | 50-65% | 50-60% |
| Materials | Carbon Platinum | Nickel Stainless Steel | Ceramic |

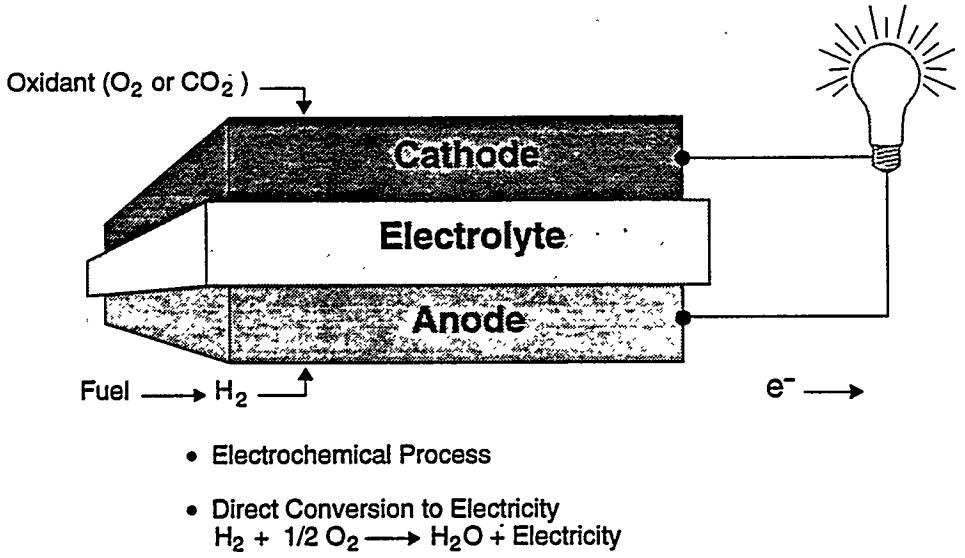


**Figure 3. Basic Fuel Cell**

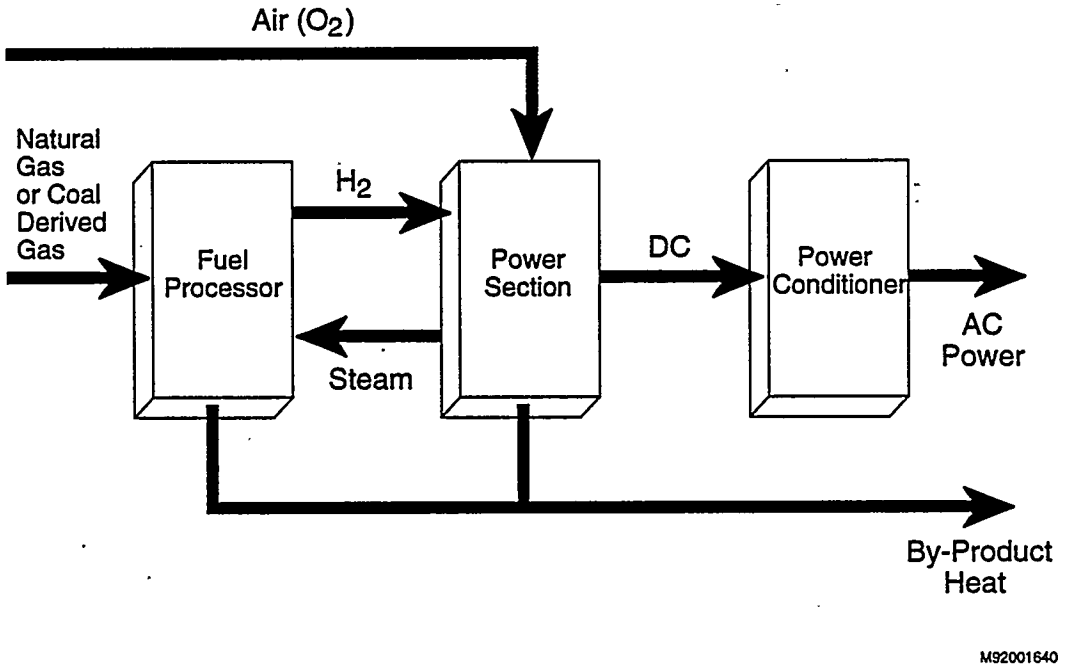


**Figure 4. Fundamentals of a Power Plant**

The Fuel Cell Program objectives are to develop and demonstrate cost effective fuel cell power generation, which can initially be commercialized using natural gas fuel by the year 2000. Figure 5[8] shows the major program activities. The DOE-sponsored PAFC development work was completed in 1992. ONSI Corporation located in South Windsor, Connecticut, has been actively involved in the development and marketing of on-site PAFC systems and has a 40-MW/year manufacturing facility. In their PAFC commercialization, the ONSI Corporation, a subsidiary of International Fuel Cells (IFC), is offering a complete packaged phosphoric acid power plant for $3000/kW. Named PC25, more than 50, 200-kW units are in operation in the U.S. and around the world. Operating experience has been excellent with availabilities of more than 90 percent. IFC is currently developing 1-MW class units based on a five-stack design and developing the PC25C which is lower in size and cost.

DOE is now cooperating with the Department of Defense in supporting the demonstration of the PAFC at customer sites. This activity is attempting to stimulate PC25 sales until the new PAFC fuel cell industry is self-sustaining.

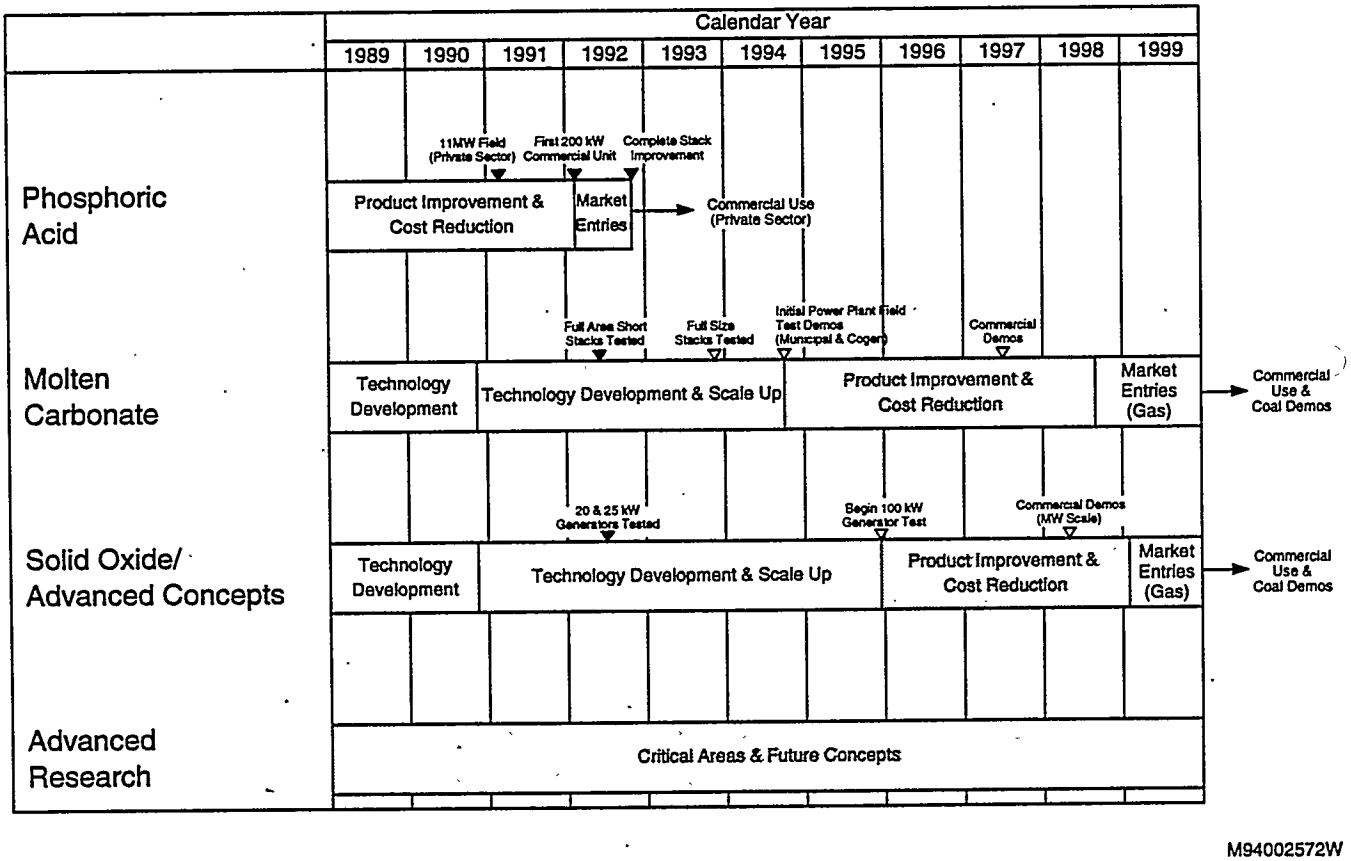


**Figure 5. Fuel Cell Program Activities**

There are two major U.S. developers of MCFC's. M-C Power (MCP), located in Burr Ridge, Illinois, is developing an internally manifolded design, while Energy Research Corporation (ERC) of Danbury, Connecticut, has developed a stack design based on internal reforming. Both of these developers have Product Design and Improvement cooperative agreements with DOE. The objective of the agreements is MCFC cost reduction, performance improvement, and packaging. MCFC's utilize a molten electrolyte composed of lithium and potassium carbonates. MCP is readying a 250-kW prototype of this next generation of fuel cell technology for testing at the Miramar Naval Air Station in San Diego, California. The heat produced by the fuel cell will be used for on-site heating. This cogeneration approach raises the overall efficiency to nearly 85 percent, meaning that this amount of the available energy in the fuel can effectively be utilized. In addition to this fully integrated test, a test of an 11-square foot, full-size stack is underway at UNOCAL's research center near Los Angeles. ERC will demonstrate an MCFC power plant system at the Santa Clara, California, municipal utility. Scheduled for operation in late 1995, the 2-MW demonstration will be a key milestone in the development of second-generation fuel cell technology. In the ERC fuel cell architecture, the Santa Clara Demonstration will be made up of 125-kW stacks linked together in four-stack modules.

In the 1997 timeframe, MCP and ERC are planning 1-MW and 2-MW demonstrations, respectively. These demonstrations are expected to trigger contingency orders and to finance the construction of larger manufacturing facilities. Commercialization is expected by 2000.

The Westinghouse Electric Corporation is the major and world's leading SOFC developer. Westinghouse is developing a tubular SOFC concept, with each tube made up of multiple ceramic layers bonded together. Multiple tubes are linked together to form power modules. The modules are then linked to form small generators or larger power plants. Two 25-kW generators have been tested in Japan. Two additional 25-kW tests are planned in 1995 at the southern California Edison National Fuel Cell Research Center near Riverside, California. These will be followed by 100-kW generators and later MW-size systems. Testing of a 100-kW generator is planned at a utility site in the Netherlands in mid-1996.

Longer range advanced research and technology development is being carried out by DOE's national laboratories and a number of private sector contractors.

Fuel cells operating with natural gas as a fuel, will enter the commercial market over the next few years. The technology is advancing rapidly as developers move from prototype to full commercial-size stacks and packaged integrated systems. Fuel cells are expected to offer long-term cost and environmental advantages. Early units will be limited to a few MWs in size until sufficient operating experience is gained. These first units will be used in dispersed generation and cogeneration applications. The manufacturing of fuel cells will create new industries and add growth to existing industries and services.

## BENEFITS TO THE GAS INDUSTRY

The ATS Program and the Fuel Cell Programs can make a significant contribution to the future strength of the natural gas industry. Each segment of the gas industry will share in the benefits of these programs.

**Potential to Increase Gas Use**

The efficiency, economic, and environmental benefits of fuel cell systems and ATS will lead to increased use of natural gas for electric power generation. For the near-term, PAFCs and technological spin-offs from the ATS Program will enter the marketplace. This will result in a modest acceleration of the ramp up in gas use. For the longer term, the efficiency and low-cost of these power generation systems will enlarge the economic "window" in which gas-fired systems are competitive with other types of fossil and renewable energy systems. This will ensure that gas consumption rates remain high, even in the face of rising gas prices in the post-2000 era.

**Reduce User Concerns of "Massive" Gas Price Increases**

Increased use of gas by the utility sector (or any other market segment) will tend to increase gas prices. The ATS and Fuel Cell Programs will protect against "massive" gas price increases in two ways. First, ATS designs are adaptable to coal or biomass firing. Thus, large ATS systems at central station utilities will be able to switch to an alternative fuel if gas prices rise beyond a certain level. Second, the higher efficiency of ATS and fuel cell systems will tend to moderate increases in gas use.

**Reduce Seasonal Variations in Natural Gas Consumption and Prices**

The ATS and the Fuel Cell Programs will help level seasonal peaks and valleys in natural gas consumption. Natural gas consumption has traditionally been highest in the December through March winter season. Most electric utilities in the U.S. are summer peaking. Gas fired power generation systems will help levelize consumption. This will make all segments of the natural gas industry more profitable.

Producers will have a much greater incentive for maintaining and expanding production capacity. New wells will have a much better payout, and capital investment decisions will be more easily justified. The transmission pipelines will similarly benefit, and it will be easier to justify adding new pipelines.

Local Distribution Companies (LDCs) will also benefit. Industrial-scale ATS and fuel cell systems could have wide-spread application in the dispersed power market and this would increase LDCs sales. While utilities may bypass LDCs in obtaining gas for large turbine systems, traditionally, LDCs have not played a dominant role in this market.

Greater stability in natural gas prices will be an important result of reducing seasonal variations in gas demand. This will increase user confidence in gas availability and reliability. This greater confidence will permeate all transactions with users, whether they are through LDCs, direct with producers, or through pipeline companies. It will also contribute to greater unity among the varied segments of the natural gas industry.

**More Efficient, Lower $NO_x$ Turbines for Pipeline Applications**

The goal of the ATS Program is to develop high-efficiency, environmentally benign, cost-effective gas turbine systems. The improved technology developed in this program is applicable to the turbines used in pipeline compressor stations. Additionally, a significant fraction of the gas and oil industry uses gas turbines systems for power generation. Thus, gas and oil industry sites are candidates for demonstration projects in the ATS Program.

## Economic Competitiveness

The ATS and Fuel Cell Programs will lead to additional U.S. jobs. The domestic market for power generation equipment is estimated to be 8 to 10 gigawatts (GW) per year; the total world market is estimated to be 100 GW per year. Gas turbine based power systems and fuel cell systems are well positioned to capture a significant fraction of this market. Turbines and fuel cells—as high-tech prime movers packaged in a small volume—are ideal candidates for export from the U.S. Thus, the ATS and Fuel Cell Programs will maximize the opportunity for U.S. suppliers to participate in this world market. The U.S. jobs created and maintained by the DOE investment in these programs will result in relatively affluent gas consumers—a benefit to all sectors of the U.S. gas industry.

## SUMMARY

The U.S. DOE is supporting the development of advanced, natural-gas fueled power generation technologies for the next century. These highly efficient and environmentally benign systems will contribute to the future strength of the natural gas industry.

## REFERENCES


1. *Proceedings of Workshop to Define Gas Turbine System Research Needs*, April 8-10, 1991, Greenville, South Carolina.

2. *Proceedings of Workshop to Define Gas Turbine System Research Needs—II*, January 7-8, 1992, Greenville, South Carolina.

3. Bajura, R. A., Webb, H. A., and Parsons, E. L., "A Proposed Plan for an Advanced Turbine Systems Program," *Proceedings of Workshop to Define Gas Turbine System Research Needs—II.*

4. Webb, H. A., and Bajura, R. A., "Development of Advanced Turbine Systems—Meeting Tomorrow's Needs," presented at the Energy Daily Conference: *Advanced Combustion Turbines: Looking Past the 90s*, June 25-26, 1992, Washington, DC.

5. *Report to Congress—Comprehensive Program Plan for Advanced Turbine Systems*, July 1993, Report Number DOE/FE-0279.

6. *Proceedings of Joint Contractors Meeting—Advanced Turbine Systems Conference/Fuel Cells and Coal-Fired Heat Engines Conference*, August 3-5, 1993, Morgantown, West Virginia, Report Number CONF-930893.

7. *Fuel Cells—A Handbook (Revision 3)*, Report Number DOE/METC-94/1006.

8. *Fuel Cell Systems Program Plan—Fiscal Year 1994*, Report Number DOE/FE-0311P.


RBAJUR\4:950798

# Session 2A

*Resource & Reserves — Resource Characterization*

## 2A.1 Reserves in Western Basins

### CONTRACT INFORMATION

| | |
|---|---|
| **Contract Number** | DE-AC21-91MC28130 |
| **Contractor** | The Scotia Group<br>4849 Greenville Avenue, Suite 1150<br>Dallas, Texas 75206<br>(214) 987-1042 |
| **Contractor Project Manager** | Robert H. Caldwell |
| **Principal Investigators** | Robert H. Caldwell<br>Bill W. Cotton |
| **METC Project Manager** | Karl-Heinz Frohne |
| **Period of Performance** | October 01, 1991 to September 30, 1995 |

### ABSTRACT

The objective of this project is to investigate the reserves potential of tight gas reservoirs in three Rocky Mountain basins: the Greater Green River (GGRB), Uinta and Piceance basins. The basins contain vast gas resources that have been estimated in the thousands of Tcf hosted in low permeability clastic reservoirs.

This study documents the productive characteristics of these tight reservoirs, re-quantifies gas in place resources, and characterizes the reserves potential of each basin. The purpose of this work is to promote understanding of the resource and to encourage its exploitation by private industry.

At this point in time, the GGRB work has been completed and a final report published. Work is well underway in the Uinta and Piceance basins which are being handled concurrently, with reports on these basins being scheduled for the middle of this year. Since the GGRB portion of the project has been completed, this presentation will focus upon that basin.

A key conclusion of this study was the subdivision of the resource, based upon economic and technological considerations, into groupings that have distinct properties with regard to potential for future producibility, economics and risk profile.

## 2A.2 Secondary Natural Gas Recovery—Infield Reserve Growth Joint Venture: Applications in Midcontinent Sandstones

### CONTRACT INFORMATION

| | |
|---|---|
| **Contract Number** | DE-FG21-88MC25031 |
| **Contractor** | Bureau of Economic Geology<br>The University of Texas at Austin<br>University Station, Box X<br>Austin, Texas 78713-8924<br>(512) 471-1534 |
| **Contractor Project Manager** | Robert J. Finley |
| **Principal Investigators** | Robert J. Finley<br>Bob A. Hardage |
| **METC Project Manager** | Charles W. Byrer |
| **Period of Performance** | September 1, 1988, to April 30, 1995 |

**Schedule and Milestones**

**FY95 Midcontinent Program Schedule**

| | O | N | D | J | F | M | A | M | J |
|---|---|---|---|---|---|---|---|---|---|
| Task 1.0 Selection of Resource Targets and Depositional Settings Within the Midcontinent | | | | | | | | | |
| • Evaluation of Suitable Plays and Resource Volumes | Completed | | | | | | | | |
| • Contact Operators to Determine Level of Activity and Interest | Completed | | | | | | | | |
| • Selection of Fields for Cooperative Studies | Completed | | | | | | | | |
| • Definition of Reservoir Targets | Completed | | | | | | | | |
| Task 2.0 Determination of Controls on Unrecovered Gas Resources | | | | | | | | | |
| • Framework for Target Reservoir Characterization | Completed | | | | | | | | |
| • Initial Reservoir Architecture Delineation | Completed | | | | | | | | |
| • Integrate Geophysical Analysis, Engineering Assessments, and Well Log Analysis | | | | | | | | | |

| | O | N | D | J | F | M | A | M | J |
|---|---|---|---|---|---|---|---|---|---|
| • Define Cooperative Data Collection and Testing | Completed | | | | | | | | |
| • Integrate Results of Field Data Collection to Refine Reservoir Characterization | ——— | ——— | ——— | ——— | | | | | |
| Task 3.0 Synthesis of Results and Development of Advanced Gas Recovery Strategies | | | | | | | | | |
| • Establish Extent of Flow Unit(s) | | | | ——— | ——— | | | | |
| • Define Flow Units Characteristics of Reservoirs | | | | ——— | ——— | | | | |
| • Determination of Extrapolation Potential | | | | | ——— | ——— | ——— | | |
| Task 4.0 Technology Transfer | | | | | | | | | |
| • Printed Reports and Presentations | | | | | | ——— | ——— | | |
| • Workshops to Transfer Results to Operators | | | | | | | * | ** | |
| • Development of Advanced Technology Transfer Products | | | | | | | | ——— | |
| • Economic Analysis of Reserve Growth Strategies | | | ——— | ——— | ——— | ——— | ——— | ——— | |

* Houston **Tyler, Texas, and Graham, Texas

## OBJECTIVES

The primary objective of the Infield Reserve Growth/Secondary Natural Gas Recovery (SGR) project is to develop, test, and verify technologies and methodologies with near- to midterm potential for maximizing the recovery of natural gas from conventional reservoirs in known fields. Additional technical and technology transfer objectives of the SGR project include:

- To establish how depositional and diagenetic heterogeneities in reservoirs of conventional permeability cause reservoir compartmentalization and, hence, incomplete recovery of natural gas.
- To document examples of reserve growth occurrence and potential from deltaic and valley-fill sandstones of the Midcontinent as a natural laboratory for developing concepts and testing applications to find secondary gas.
- To demonstrate how the integration of geology, reservoir engineering, geophysics, and well log analysis/petrophysics leads to strategic recompletion and well placement opportunities for reserve growth in mature fields.
- To transfer project results to a wide array of natural gas producers, not just as field case studies, but as conceptual models of how heterogeneities determine natural gas flow units and how to recognize the geologic and engineering clues that operators can use in a cost-effective manner to identify incremental, or secondary, gas.

The SGR project is a joint research effort of the Gas Research Institute (GRI), the U.S. Department of Energy (DOE), and the State of Texas conducted in cooperation with industry partners. Approaches to defining the distribution of unrecovered resources by depositional system and methods for maximizing their recovery are

being developed and tested. From 1988-93, the focus was on Texas Gulf Coast natural gas reservoirs as a major subset of the Nation's natural gas resource base. The current SGR Midcontinent project is designed to test and expand the application and benefits of reserve appreciation concepts and technology in a second major natural gas province characterized by different depositional systems and subsidence rates.

Results of the SGR project are enabling producers to economically recover this discovered but undeveloped natural gas resource through integrated geological, engineering, petrophysical, and geophysical assessments. Case studies conducted with the cooperation of independent producers have demonstrated the cost-benefit viability of an integrated SGR approach for small operators producing from gas reservoirs in similar and different depositional systems. However, project results indicate a lag time between technology transfer and producer response. Indications of higher yields per development well and higher development well success rates were first seen in 1993, some two years after technology transfer began.

## BACKGROUND STATEMENT

In the late 1970's and 1980's, the characterization of the internal geometry of reservoirs, mainly oil reservoirs, clearly demonstrated a greater degree of compartmentalization than had been previously recognized. Factors affecting this compartmentalization include the depositional system of the reservoir, structural configuration, and diagenetic history of the reservoir following deposition. These lessons were first learned for oil reservoirs, but starting in the late 1980's became increasingly evident for gas reservoirs. The conceptual view of the resource base in the lower 48 states changed drastically from the middle and late 1970's when estimates by M. K. Hubbert of more than 90 percent depletion were revised based on more recent analyses indicating that the natural gas resource base is only about 40 percent depleted (Fisher, 1993). Strategies developed during this research are being used by producers to target substantial reserve growth potential known to exist in known natural gas reservoirs.

Assessments of the reserve growth resource available for improved recovery of natural gas from mature fields have grown substantially over the last five years and also have gained wider acceptance. This acceptance has been in part the result of the SGR project. Three recent resource assessments are of particular significance. In 1990, the Energy Information Administration (1990) defined a reserve growth resource of 265 Tcf in the lower 48 states with deployment of advanced technology. This study used a newly-developed Oil and Gas Integrated Field File (OGIFF) to define field-level reserve appreciation trends. A later assessment by the National Petroleum Council (NPC) (1992) used an updated version of OGIFF to assess 236 Tcf of reserve growth resources, 203 of which were in conventional-permeability reservoirs. The NPC benefitted from input of early results of SGR project work in the Gulf Coast. Most recently, the U.S. Geological Survey (1995) assessed 290 Tcf of reserve growth resources in conventional reservoirs of the onshore lower 48 states as of December 31, 1991. This volume is up from 93 Tcf in the equivalent U.S. Geological Survey category in 1989. The use of an updated OGIFF underlies the new estimate, while the SGR project is helping define producer approaches to realize this substantial reserve growth potential.

The SGR Gulf Coast project focused on three major gas plays in the Frio and Vicksburg Formations and Wilcox Group during studies of the Gulf Coast Basin. Nongeopressured, conventional-permeability reservoirs like the middle Frio Formation (cumulative production >12 Tcf) were the primary emphasis in these SGR studies. These reservoirs were deposited as part of

a bedload-rich fluvial system that fed a major deltaic depocenter in South Texas. In contrast to the rapid subsidence and fluvial reservoirs in this setting, the Midcontinent SGR project is focusing on deltaic and valley-fill sandstones in a much less rapidly subsiding cratonic basin, the Fort Worth Basin.

## PROJECT DESCRIPTION

The reserve growth resource in a natural gas field will be contained in new infield reservoirs, untapped or incompletely drained reservoir compartments, bypassed reservoirs, and deeper pool reservoirs (figure 1). The latter have long been a recognized target for the producing industry, and for natural gas, deeper pool development benefits from the more gas-prone nature of deeper stratigraphic intervals. The SGR project's Technical Advisory Committee (TAC) determined that deeper pool reservoirs should not be a focus of the project because industry recognizes deeper pool reservoir potential and that the other, more difficult-to-develop, resources should be given priority.

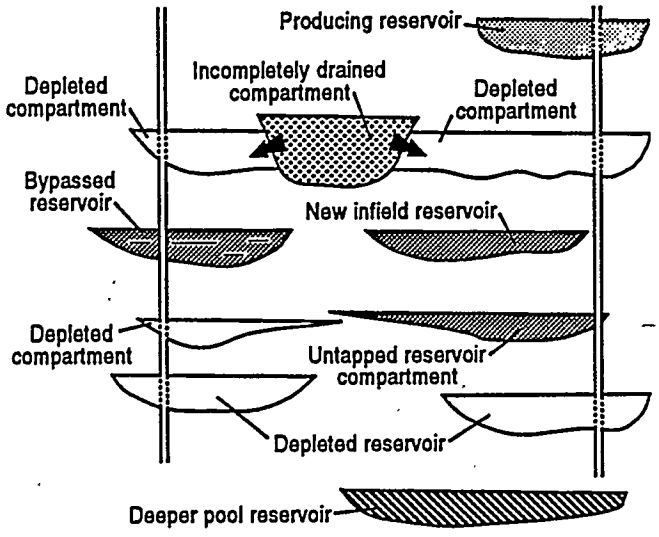


**Figure 1. Diagram of reservoir compartment terminology used in the SGR project**

New infield reservoirs are new reservoirs separated vertically and laterally from adjacent reservoirs that were not contacted during original development of the field. Often these reservoirs are found during deeper-pool development attempts. Untapped or incompletely drained reservoir compartments are parts of established producing reservoirs that may or may not have been contacted during original development of the field and are not in flow communication, or are in incomplete flow communication, with existing completions. Bypassed reservoirs are reservoirs contacted by existing wells that have not been produced. Bypassed reservoirs may have been thought nonproductive or noneconomic based on previous well log evaluations. All of these types of reservoirs are targets for incremental natural gas recovery based on understanding of depositional and diagenetic heterogeneity that leads to reservoir compartmentalization.

Although structural complexity also results in incomplete recovery, the focus of the SGR project has been to better understand depositional rather than structural reservoir variability. However, in the field selected for study in the Midcontinent, it was found that 3-D seismic revealed small-scale faulting not previously detectable using 2-D seismic lines. Trapping of natural gas in the study area is now interpreted to be a combination of stratigraphic and structural compartmentalization.

## RESULTS

### Geologic Summary

Although work is still in progress, several results have been obtained from the core- and log-based stratigraphic analysis, and a preliminary examination of the 3-D seismic data. Thirteen genetic sequences (similar to cycles or cyclothems in other terminology) have been observed in the Boonsville-Atokan strata. Genetic sequences average approximately 100 ft in thickness, and are defined and bounded by marine maximum

flooding surfaces (figure 2). A typical genetic sequence consists of an upward-coarsening facies succession that begins with dark gray, "maximum flooding" mudstones, and grades upward into "highstand" calcareous shoreface/delta front sandstones that are erosionally truncated and overlain by complex, "lowstand" valley-fill deposits composed of fluvial and deltaic conglomeratic sandstones. Valley-fill deposits are capped by muddy estuarine and carbonaceous floodplain deposits, which were commonly truncated by shoreface ravinement and overlain by transgressive deposits consisting of bioturbated, muddy sandstones or shallow-marine limestones. Cyclic stacking of Boonsville-Atokan genetic sequences probably resulted from glacioeustatically induced changes in accommodation space that were superimposed upon long-term subsidence of the Fort Worth Foreland Basin.

Natural gas reservoirs at Boonsville occur predominantly in "lowstand" valley-fill conglomeratic sandstones; they owe their existence to incisement and subsequent aggradation during low and early-phase base-level rise. "Highstand" deltaic and shoreface sandstones are also important reservoirs in some of the genetic sequences. The "highstand" reservoirs occur in the uppermost/updip parts of offlapping progradational lobes bounded by a series of inclined surfaces that can sometimes be detected in log and seismic sections as shingled clinoforms.

Syndepositional structural deformation played a major role in Boonsville-Atoka reservoir distribution. Many small-scale, near-vertical fault zones with oval or circular patterns are present on time-structure maps of Bend Conglomerate seismic horizons. Most of these high-angle normal and reverse faults have less than 100 ft of displacement, they rarely penetrate the overlying Strawn Group, and the fault zones are closely associated with karst-collapse features in the underlying Paleozoic platform carbonate units. "Low" areas on seismic time-structure maps roughly coincide with thick gross and net reservoir isopach fairways in many of the genetic sequences, suggesting that karst-collapse and associated faulting occurred during Bend Conglomerate deposition. Many of the thickest valley-fill sandstone reservoirs occur above or immediately adjacent to vertically faulted karst-collapse zones.

The stratigraphic knowledge gained from the core- and log-based evaluation has provided a springboard for the 3-D seismic interpretation. Besides providing physical stratigraphic benchmarks for time-depth conversion, the core- and log-based geologic framework is focusing the seismic interpretation on the identification of specific elements of reservoir architecture. In particular, seismic manifestations of key stratal surfaces, sequence stacking patterns, and isolated reservoir compartments will be critical aids to producers in strategic drilling and recompletion activities.

### 3-D Seismic Data Recording Program

The 3-D seismic grid at Boonsville field covered approximately 26-mi$^2$, starting at the west shore of Lake Bridgeport and extending westward across Wise County and into Jack County. The positions of the source and receiver lines within the 26-mi$^2$ survey area are shown in figure 3. Approximately half of the survey was positioned in Wise County and half in Jack County.

An extensive research effort was conducted to determine the optimum 3-D seismic field procedures that should be used to image the thin-bed reservoirs deposited in the low sediment-accommodation conditions that existed during Atoka time on this shelf margin of the Fort Worth

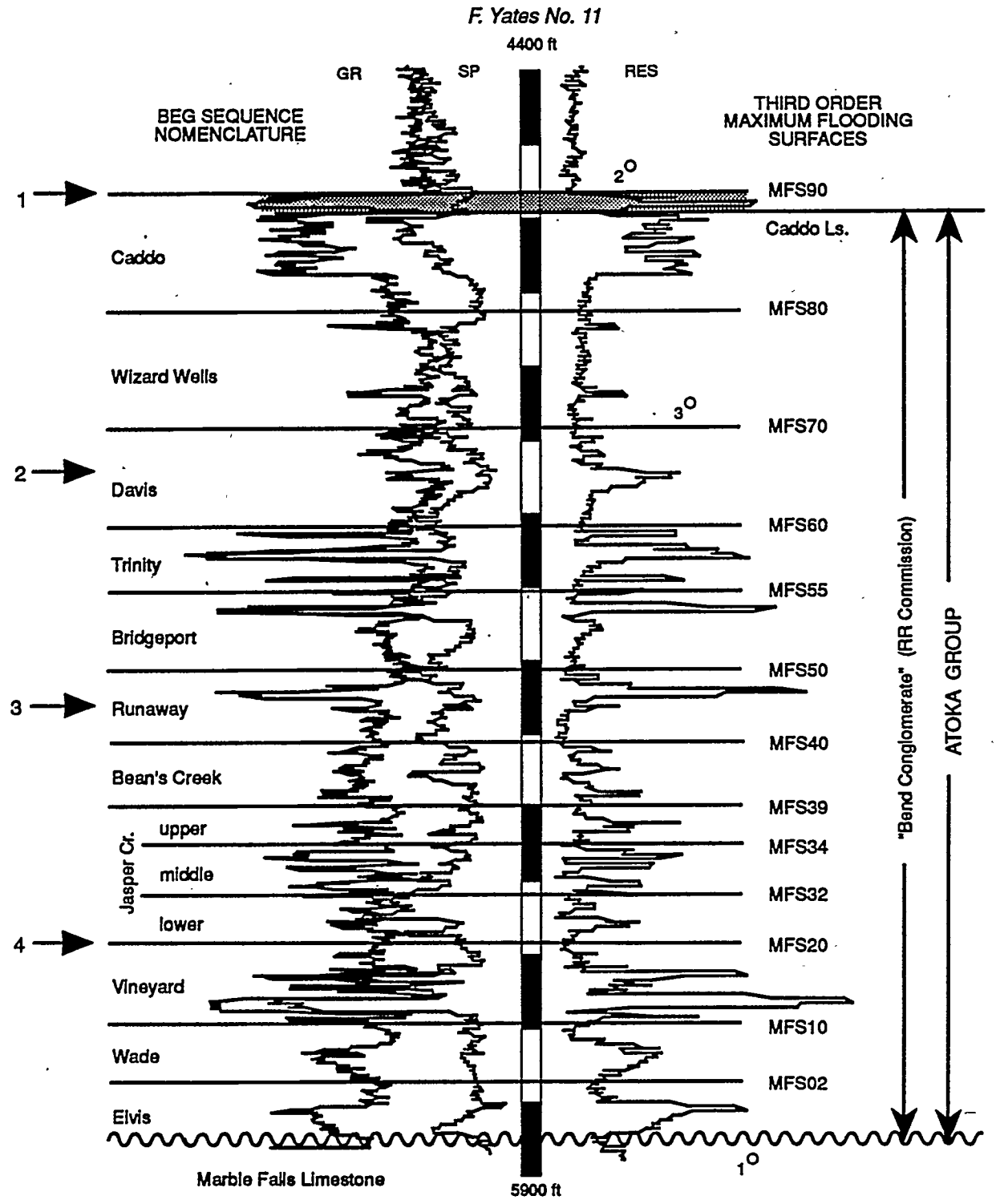


**Figure 2. Stratigraphic nomenclature used to define depositional units and sequence boundaries in Boonsville field. The numbers 1, 2, 3, and 4 on the left margin define the stratigraphic positions of the four seismic chronostratigraphic surfaces which were interpreted across the complete 26-mi$^2$ 3-D survey**

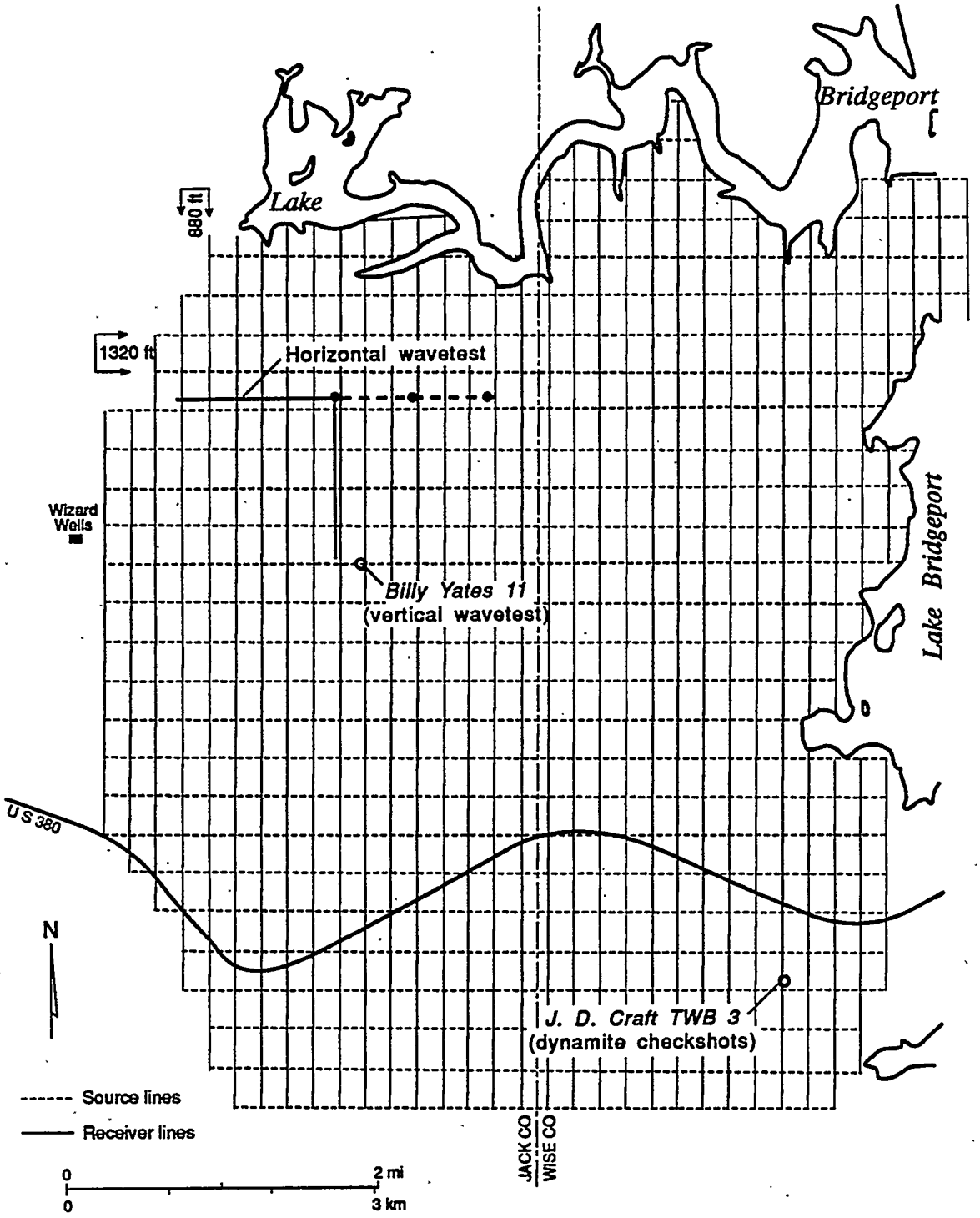


**Figure 3. Source-receiver grid used to record the Boonsville 3-D seismic data. Locations of key velocity control wells and wavetest sites are indicated. The north-south receiver lines are spaced at intervals of 880 ft, and the east-west source lines are separated a distance of 1320 ft. The horizontal wavetest site is further explained in figure 12**

basin. This seismic field program involved the following research efforts:

1. Establishing vertical wavetesting as a technique for comparing seismic sources and for selecting the optimum source parameters for imaging Midcontinent thin-bed reservoirs.

2. Demonstrating the value of horizontal wavetesting as a technique for determining the optimum receiver geometry to use in a 3-D seismic survey so that the recorded data have a maximum bandwidth.

3. Verifying the interpretational value of a novel, staggered-source-line, staggered-receiver-line recording geometry which allows 3-D data to be sorted into large bins with high stacking fold or into small bins with lower stacking fold.

4. Documenting the traveltime differences, if any, exhibited by an explosive source and a swept-frequency source in Midcontinent rocks.

5. Demonstrating the economic and technical advantages of using small explosive charges in shallow holes, rather than the usual convention of large charges in deep holes, as a 3-D seismic energy source in Midcontinent prospects.

Onsite inspection of the 3-D seismic area showed that almost half of the 26-$mi^2$ grid was heavily timbered, particularly in the northern and eastern portions abutted to Lake Bridgeport. Vibroseis sources could not be used in these forested areas due to permitting restrictions.

The explosive charge selected for testing was the C-10 design, composed of 10 oz of high velocity pentolite molded into a directional charge that focuses the energy in a downward direction. These charges were planted in holes 10 ft deep with the assumption that this hole depth was adequate for good energy coupling.

The C-10 charges were shot in a 5-hole pattern so that 50 oz of high velocity pentolite were detonated as a linearly distributed source spanning 40 ft and centered about the source flag. This design is a reasonable approximation to a point source. All five holes were wired in series so that if an electrical break occurred in any one of the five detonating caps, none of the charges would fire. This technique ensured that all shots recorded during wavetesting and during the subsequent 3-D recording would be consistent in that they each involved simultaneous detonation of five 10-oz charges.

The vertical wavetesting geometry used at Boonsville field to measure the bandwidth and signal-to-noise properties of the pentolite wavelet is illustrated in figure 4. Twelve 5-hole arrays were prepared at an offset distance of 420-ft (figure 4b), and the wavefields generated by these shots were recorded at vertical intervals of 500 ft as the receiver was lowered down the Billy Yates 11 well (figure 5). These vertical wavetest data were numerically analyzed to determine the energy level and the spectral bandwidth of the pentolite-generated wavelet as it propagated down to, and through, the targeted Atokan-age Bend reservoirs occurring between depths of 4500 ft and 6000 ft (approximately) in the Billy Yates 11 well.

The spectra of the downgoing pentolite wavelets were calculated within minutes of recording each wavelet so onsite decisions could be made about how to adjust the shot hole geometry and the number of shot holes if necessary. These onsite spectral calculations are plotted in figure 6 and show that these small, shallow, directional charges produce a remarkably broadband signal spectrum exceeding 200 Hz.

**Staggered-Line Geometry.** A unique 3-D source-receiver geometry, referred to as a

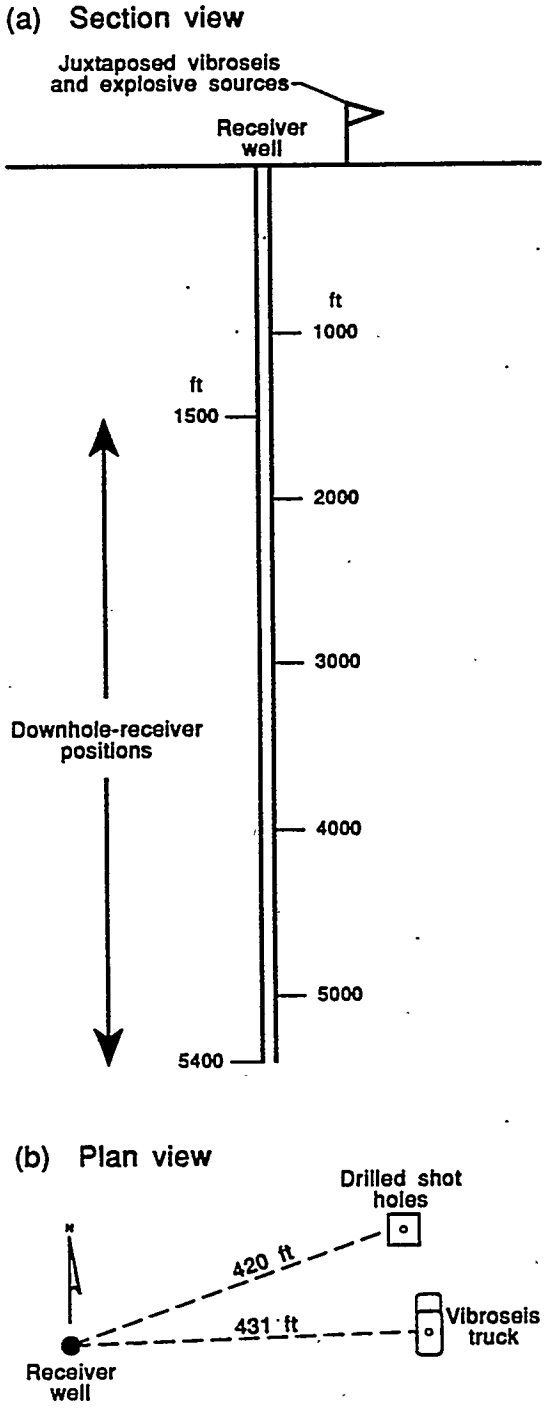


**Figure 4. Geometry used to record vertical wavetest data in the Billy Yates 11 well. Well location shown in figure 1. The objective of the test was to determine the relative bandwidths and vertical traveltimes of vibroseis and pentolite wavelets**

staggered-line grid, was implemented at Boonsville field. The geometrical pattern that was used is illustrated in figure 7. In this geometry, adjacent source lines were shifted by one-half of the source interval, and likewise, adjacent receiver lines were shifted by one-half of the receiver interval. This recording technique allowed the 3-D data traces to be sorted into large, higher-fold bins [measuring (0.5 × source interval) × (0.5 × receiver interval)] or into small, lower-fold bins [measuring (0.25 × source interval) × (0.25 × receiver interval)]. At Boonsville, the receiver and source intervals were both 220 ft, so the sizes of the two stacking bin options provided by this staggered-line geometry were 110 ft × 110 ft and 55 ft × 55 ft, as shown in figure 7. This recording geometry allowed higher-fold, large-bin data to be used as the primary data set for interpretation, and lower-fold, small-bin data to be used when greater lateral resolution was needed in the interpretation process.

**Creating Chronostratigraphic Surfaces.** Inspection of the Boonsville 3-D seismic data volume leads to the conclusion that most of the thin-bed reservoirs in the Atokan interval could be assumed to be conformable, in a local sense, to one of four seismic chronostratigraphic surfaces; these being the formation units and sequence boundaries defined in figure 2 as

1—Caddo (MFS90)
2—Davis (MFS70)
3—Runaway (MFS50)
4—Vineyard (MFS20)

**Pre-Atokan Karsting.** An interpreted Vineyard time surface was created that shows an eastward-dipping Vineyard topographic surface that is high along the western margin of the 3-D grid, toward the direction of the Bend Arch. The surface exhibits considerable topographic relief, with a dominant northwest-southeast-trending ridge extending across the central part of the 3-D survey area. Perhaps the most interesting topographic features are the several depressions

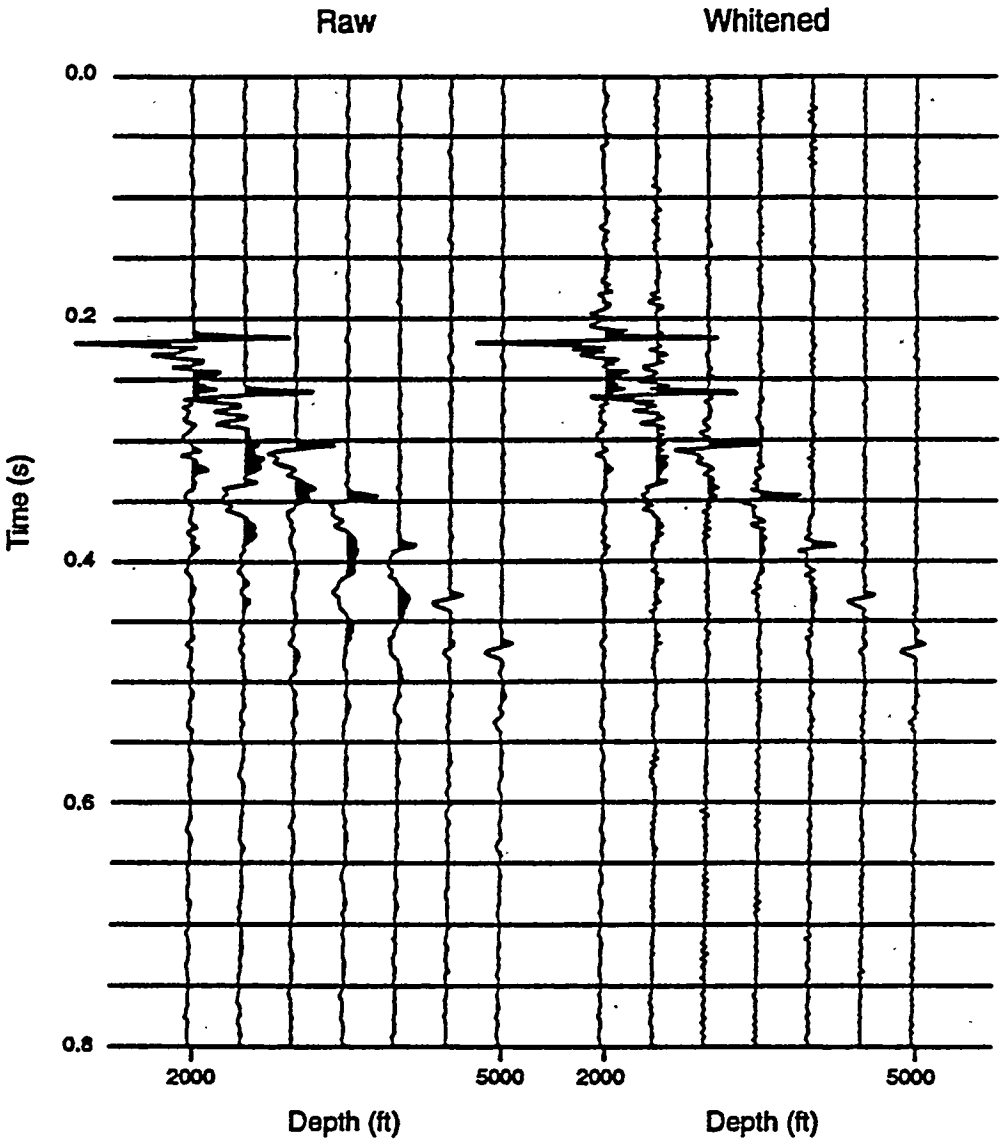


**Figure 5. Some of the vertical wavetest data generated by C-10 directional charges detonated in 5-hole patterns and recorded in the Billy Yates 11 well. The source-receiver geometry used to record these data is diagrammed in figure 4**

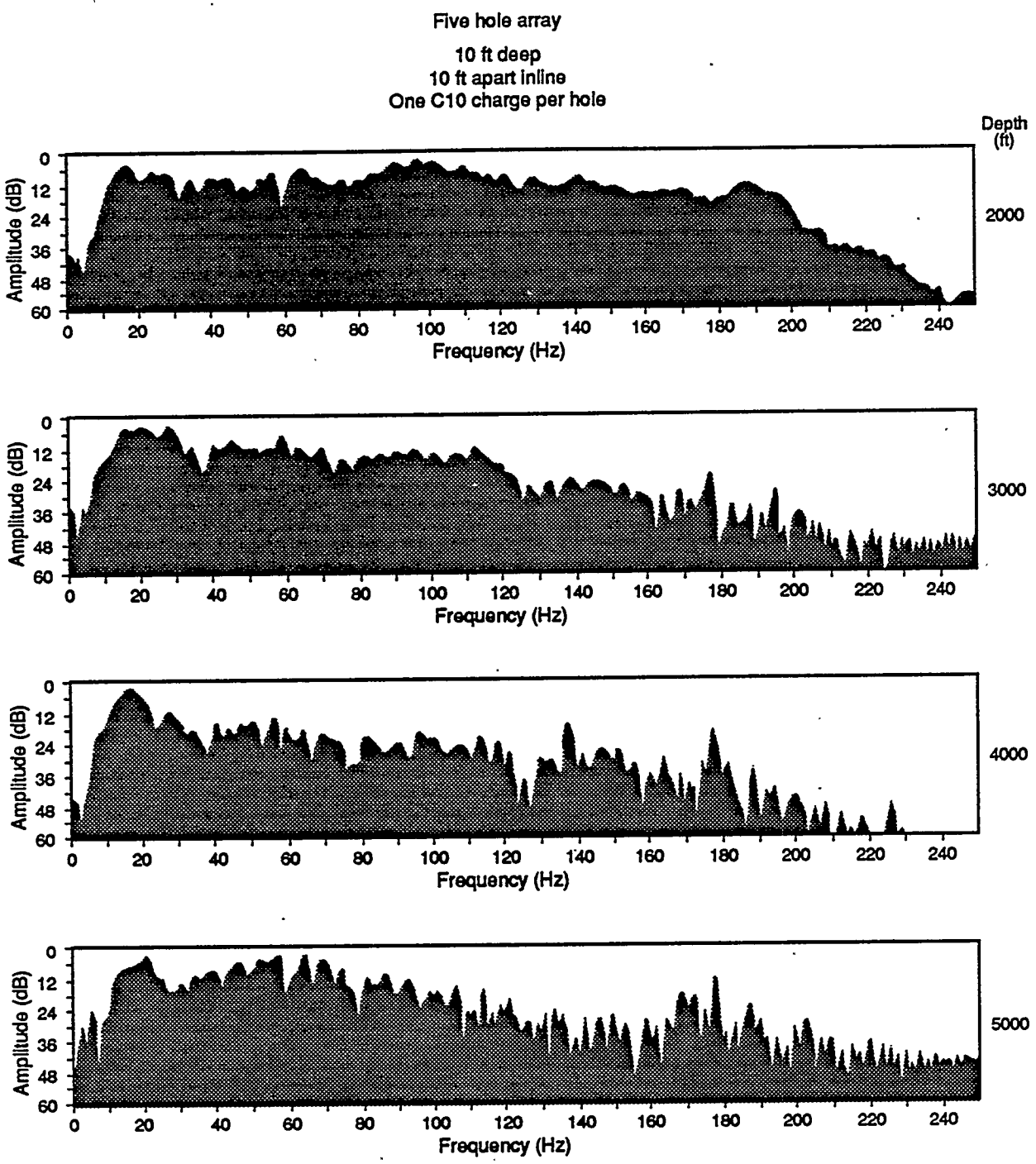


**Figure 6. Amplitude spectra of the pentolite-generated vertical wavetest data shown in figure 5. These spectra document that the pentolite wavelets are extremely broadband and contain frequency components exceeding 200 Hz. The recording system used in this test required that the wavelets be recorded at a sample rate of 2 ms, so the spectral roll-off above 180 Hz is produced by the 2 ms alias filter in the recording system and is not a true reduction of the wavelet energy. The numbers labeled on the right margin indicate the depths where the spectral analyses were done. The Atoka-age reservoirs begin at a depth of about 4500 ft**

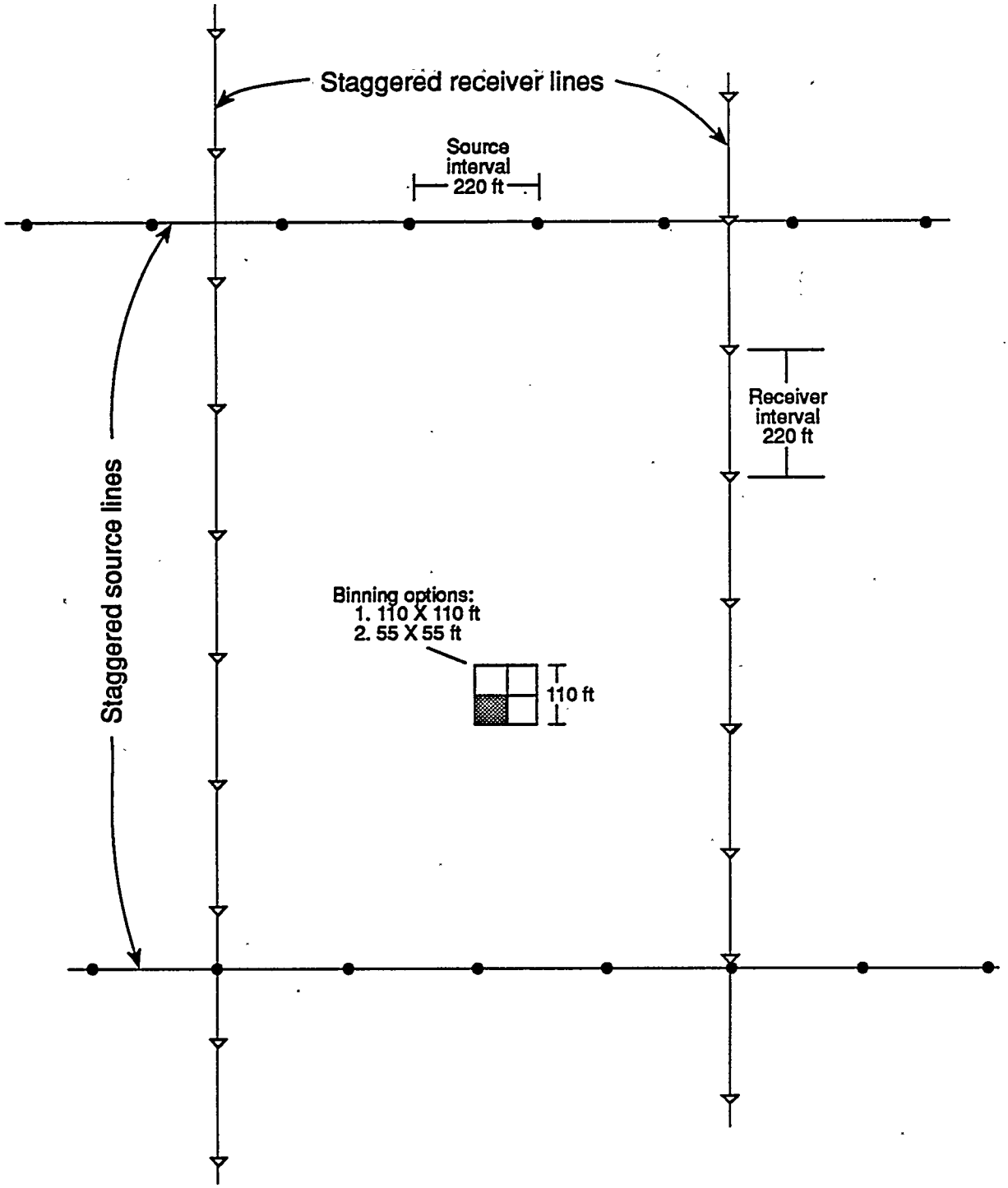


**Figure 7. Staggered-line geometry used at Boonsville field. Source flags and receiver flags were stationed 220 ft apart so that the size of the conventionally defined stacking bin was 110 ft x 110 ft. In the staggered-line technique, adjacent receiver lines were shifted north or south by one-half of the receiver interval (a shift of 110 ft), and adjacent source lines were shifted east-west by one-half of the source interval (a shift of 110 ft). This geometry allows the data to be sorted into stacking bins measuring 110 ft x 110 ft or into smaller bins measuring 55 ft x 55 ft**

dispersed across the surface, some almost perfectly circular, that pose intriguing questions as to their structural origin. The reflection amplitude behavior on this same surface is displayed as figure 8, and the circular character of many of these depressions is more obvious when viewed in the original color reflection amplitude format.

To help understand the origin of these topographic depressions, a section crossing three of the features was constructed along profile ABC. The depressions labeled 1, 2, 3 along this profile are shown in section view in figure 9. This vertical image showed that each Vineyard depression was a tall, vertical, collapse zone extending down to the interpreted top of Ellenberger at approximately 1.3 s. These collapsed zones persist throughout Atokan time, with some extending even as high as the Caddo interval.

The origin of these Atokan depressions was interpreted to be the effect of karsting occurring during or immediately after Ellenberger time. These karst areas were assumed to have collapsed when an appropriate sediment loading, perhaps 1000 ft or more, was created above the karsted void. Since karsts generally originate along faults where meteoric water can more easily gain access to the subsurface, such faults no doubt aided the collapse of the overburden. In figure 8, a series of offset northeast-southwest-trending linear features starting at the southwest corner of the map near the coordinates (inline, crossline) = (40,60) indicate that there is some fault control on the collapsed depressions in this local area of the 3-D grid. Other short fault trends occur juxtaposed to several other depressional lows, leading to the conclusion that fault-induced karsting generated the onset of all, or most, of the structural collapses. Once any basement collapse occurred, the resulting depression remained a persistent depositional low, invariant in size and position, throughout Atokan time.

During Atokan time, these karst-related topographic lows, when aerially exposed, had to affect the patterns of surface water flow and, when submerged, had to serve as significant sediment traps. These depressions were thus a dominant influence on Atokan erosion and sedimentation and show that important aspects of the Atoka stratigraphy, including reservoir compartmentalization, in Boonsville field are directly related to deep, seismic-basement features.

**Incised Valleys and Valley-Fills.** Well log facies interpretations imply that erosional processes created incised valleys and associated valley-fill facies throughout much of the Atokan period. A depositional surface which shows good examples of the size and complexity of some of these erosional features is the Runaway chronostratigraphic surface.

Valley-like depressions of various sizes exist on the Runaway surface, some of which can be traced for several miles. These incised valleys seem to always pass through at least one of the persistent depositional depressions that occur directly above each of the deep, karst-generated collapses of the pre-Atokan section.

**Seismic Images of Compartmentalized, Thin-Bed Reservoirs.** Two important objectives of the Boonsville research were to use modern geologic, petrophysical, and reservoir engineering concepts to determine where Atokan reservoir compartments existed inside the 26-$mi^2$ 3-D seismic grid and then to combine these conclusions with modern 3-D seismic technology to determine if these thin-bedded compartments can be seismically imaged. A third, and more important, objective was to use the knowledge gained to predict where uncontacted Atokan reservoirs exist inside the 3-D grid so future development wells can be properly sited. This section illustrates the results of extracting seismic

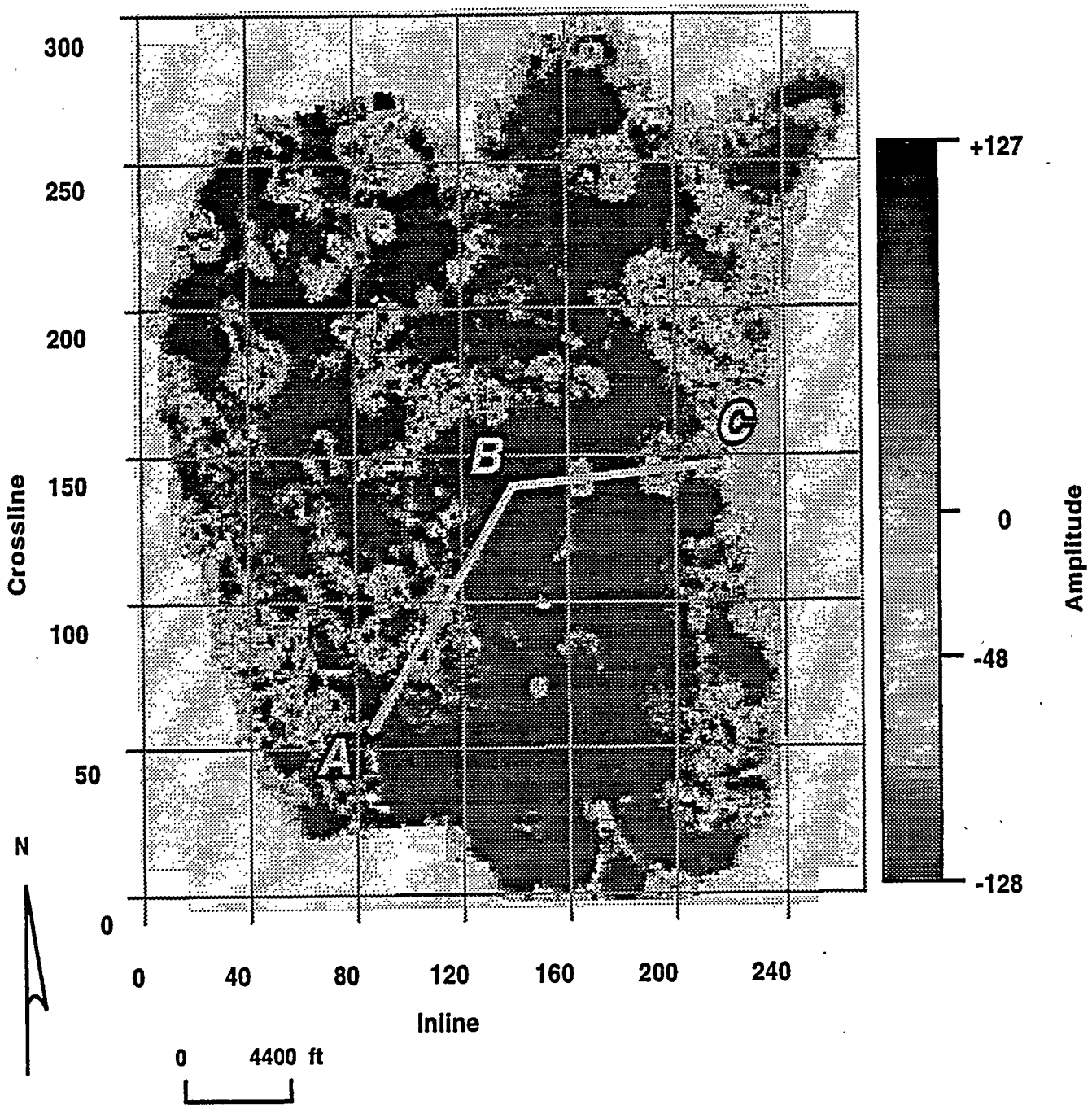


**Figure 8. Seismic reflection behavior on the Vineyard chronostratigraphic surface. Most of the surface is a consistent color (black) because the chronostratigraphic surface follows a consistent reflection trough. White discontinuities in this surface correspond to topographic lows in the Vineyard chronostratigraphic surface. This reflection amplitude map emphasizes the circular character of many of these depressions**

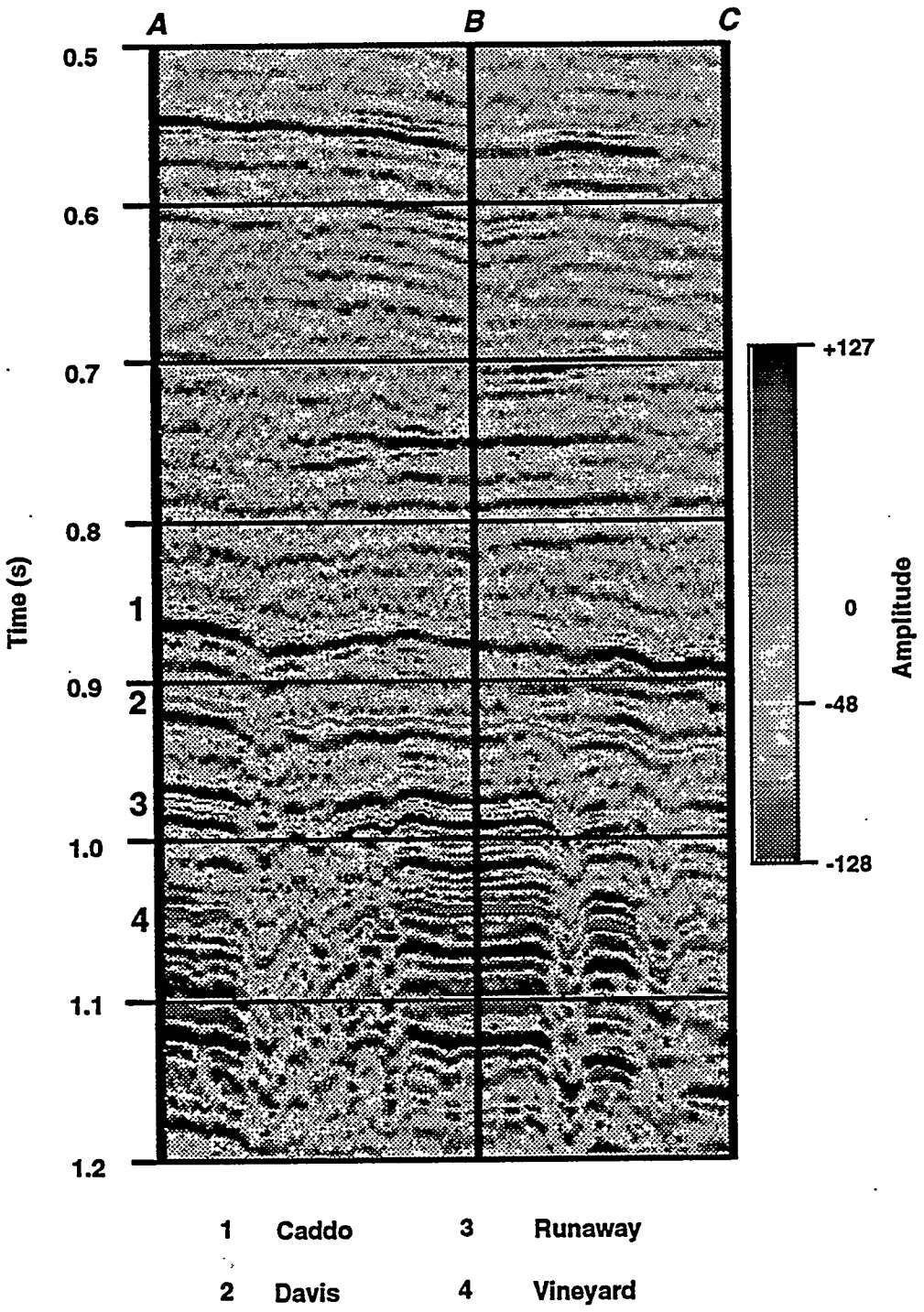


**Figure 9. Section view along the profile ABC labeled in figure 8. This section traverses three of the circular depressions in the Vineyard chronostratigraphic surface. In each instance, the depression is positioned directly above a collapsed zone that extends down to seismic basement**

images of known thin-bed reservoir compartments from the 3-D data volume.

**Small-Scale Jasper Creek Compartments.** Production data from four closely spaced wells (I. G. Yates 9 and 33 and Dewbre 2 and 3) in the southeast quadrant of the 3-D grid substantiated that these wells contacted rather small reservoir compartments at the Jasper Creek level. A summary of these data is given in figure 10. Checkshot information from the J. D. Craft TWB #3 well, approximately 1 m southeast of the 4-well site, was used to define the correct time position of the horizon slice that would properly image the Jasper Creek reservoirs perforated in these four wellbores. When the logged depths of the perforated zones in the wells were converted to seismic depths, the desired horizon slice was calculated to be a surface 33 ms below, and conformable to, the Runaway chronostratigraphic surface. The seismic reflection amplitude behavior on this surface is shown as figure 11.

In this image, the Jasper Creek reservoirs appear as small, disjointed bodies (compartments?) whose areal sizes are approximately the same sizes as those given in the reservoir engineering calculations in figure 10. For example, the seismic anomaly centered about the I. G. Yates 33 well covers 9 acres, compared to the 12-acre size calculated for a constant thickness reservoir (figure 10). The east-west section view in figure 12 passes through the I. G. Yates 33 and the Dewbre 3 wells and illustrates the heterogeneous nature of the Jasper Creek reservoirs at these well locations.

We concluded that, in this instance, reservoirs as small as 8 to 10 acres and as thin as 10 ft (figure 10) could indeed be seismically imaged with the Boonsville 3-D data.

**Large-Scale Caddo Compartments.** The recently drilled (1993) J. M. Robinson A5 well apparently penetrated a large-scale Caddo reservoir and has produced 1.5 MMscf per day since completion. The well is immediately south of the 4-well complex previously used as an imaging objective for small-scale Jasper Creek compartments (the Dewbre 2, Dewbre 3, I. G. Yates 9, and I. G. Yates 33 wells in figure 11). These four wells did not penetrate Caddo reservoirs as productive as that found in the J. M. Robinson A5 well, so the Caddo reservoir facies must be compartmentalized in the local area of these five wells.

An east-west crossline cutting through each of the five study wells is displayed in figure 13. Note in this crossline view that the J. M. Robinson A5 well is positioned in one of the basement-related collapsed zones that persisted as a depositional low through Atokan time. Immediately below the Caddo chronostratigraphic surface, this section view shows a valley fill sequence labeled "Caddo anomaly" infilling this depression. This same sequence appears on crosslines 94 and 98 at the labeled positions.

A map view of the seismic reflection behavior on a horizon slice conformable to, and 12 ms below, the Caddo chronostratigraphic surface is displayed as figure 14. This image shows the J. M. Robinson A5 well to be positioned in a large northeast-southwest-trending anomaly, while the less productive (at Caddo level) Dewbre 2, Dewbre 3, I. G. Yates 9, and I. G. Yates 33 wells are outside the anomaly.

Because of the correlation between productive wells being inside the reflection anomaly and less productive wells being outside, we conclude that the Boonsville 3-D seismic data are capable of imaging this particular Caddo reservoir compartment.

**Technology Deployment and Demonstration.** The SGR research in the Gulf Coast has been "leading by example" by demonstrating to operators how the strategic application of technology, existing and advanced, can recover incremental natural gas. This has been

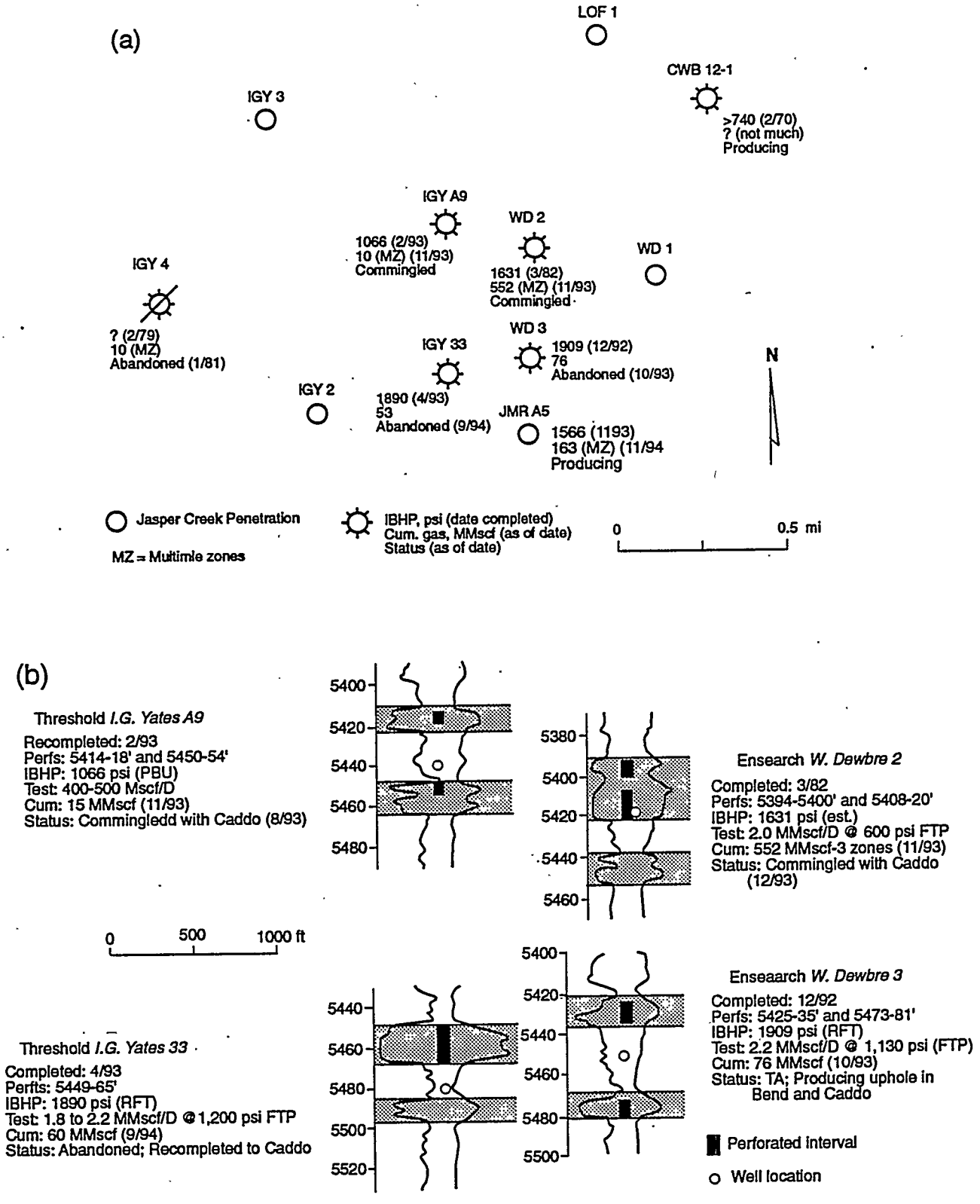


**Figure 10. Perforation intervals and reservoir compartment analyses for four wells that penetrated small-scale Jasper Creek compartments**

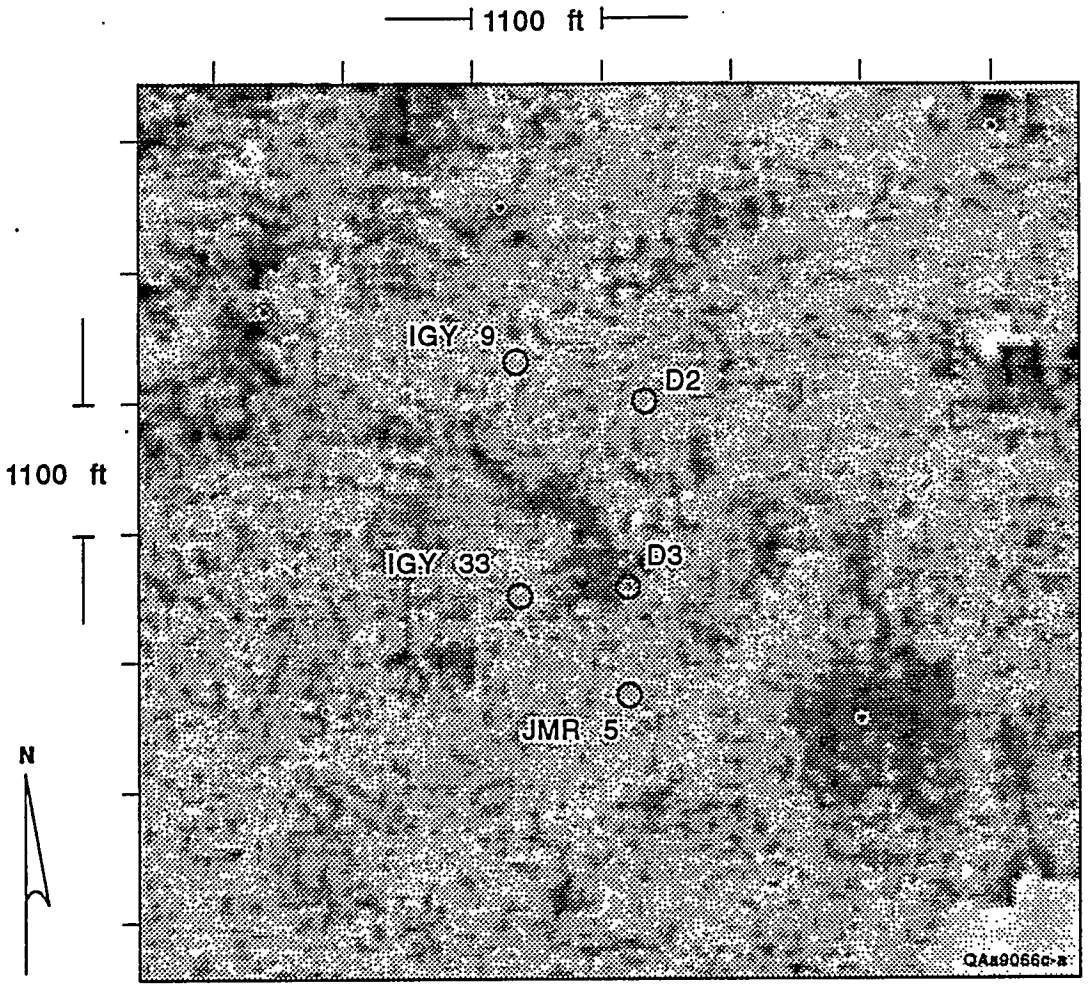


**Figure 11. Seismic reflection behavior on the horizon surface passing through the Jasper Creek perforations in the Dewbre 2, Dewbre 3, I. G. Yates 9, and I. G. Yates 33 wells**

done by showing operators how to identify and develop new infield reservoirs, incompletely drained compartments, and bypassed reservoirs and by doing so in a way that minimizes development risk and costs. Producing industry partners in the Gulf Coast project included large and small operators: Shell Western Exploration & Production Inc., Mobil Exploration & Production U.S. Inc., Oryx Energy, Union Pacific Resources Company, Pintas Creek Oil Company, and Anaqua Oil & Gas Company. Between 1989 and 1992 a total of $5.7 million was committed to the SGR project as industry co-funding. This represented one-third of the SGR Gulf Coast project total expenditures. Service company partners—Mobil Research & Development, Halliburton Geophysical, Halliburton Geochemical, Sierra Geophysics, Western Geophysical, Landmark Graphics, Advance Geophysical, Green Mountain Geophysics, and IBM—provided $678,700 in cofunding to the Gulf Coast project. The total industry cofunding represented almost 35 percent of the Gulf Coast project expenditures.

Six field studies were completed in the SGR Gulf Coast project. Important new technology products and insights on innovative, more powerful applications of existing tools resulted

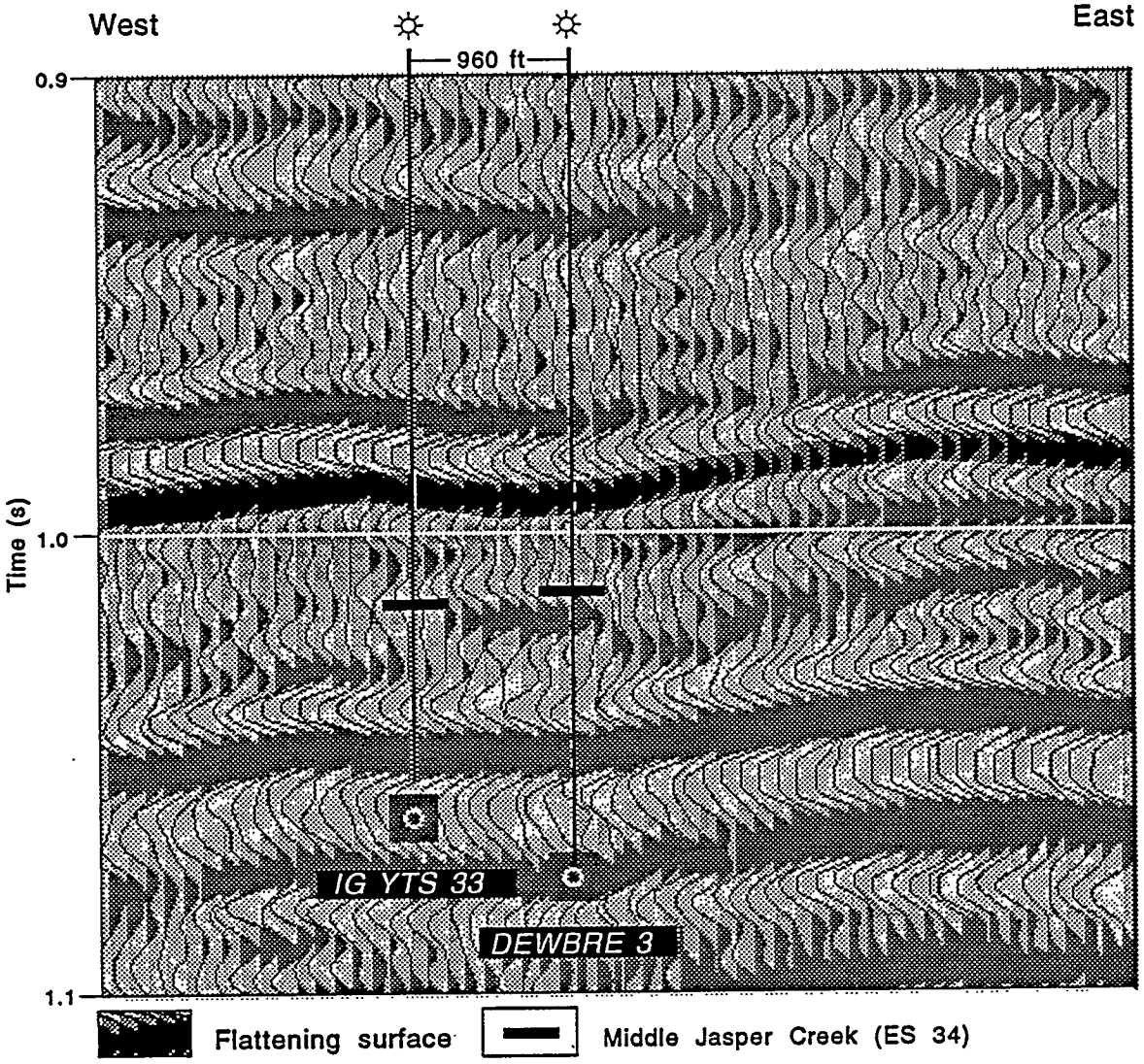


**Figure 12. East-west section view showing the heterogeneous nature of the Jasper Creek reservoir system in the vicinity of the I. G. Yates 33 and Dewbre 3 wells**

from each field study. These technology products pertain to the four major disciplines—reservoir engineering, petrophysics, geology, and geophysics—that provided the foundation for the SGR research investigation. The new technologies included screening and evaluation tools, stochastic techniques for formulation of infield development strategies, reserve vertical seismic profiling (VSP), use of specially configured geophysical surveys to study specific compartment boundary problems, and geophysical calibration of thin-bed stratigraphy.

A problem operators face when trying to develop incremental gas reserves is to screen pressure and production data for clues to the presence of incompletely drained compartments and to estimate the potential volume of reserves remaining in such compartments. The Gas-Wizard (G-WIZ) is a PC-based compartmented reservoir

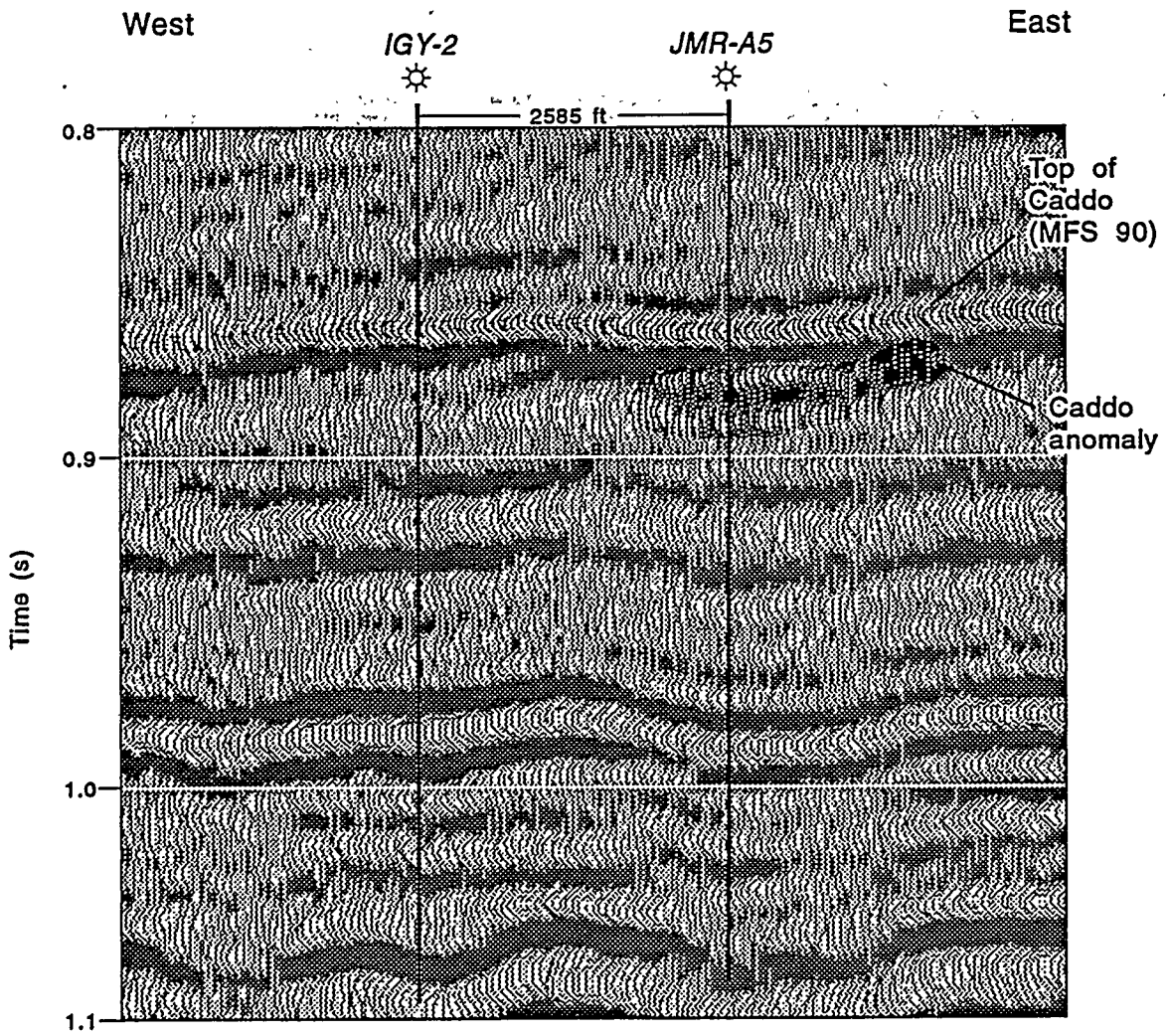


**Figure 13. East-west profile passing through the J. M. Robinson A5 and I. G. Yates 2 wells showing a Caddo-age valley-fill sequence**

simulator that was developed by the SGR project as a reservoir management tool. The simulator accepts pressure and production data from external files and performs material balance and rate-time history-matching simulations for easy identification of compartment behavior and estimation of reserve growth potential (Lord and Collins, 1991; Collins and Lord, 1992). This technology product can analyze hundreds of completions to yield compartment size distributions and it can perform stochastic modeling to evaluate the ideal well spacing to maximize natural gas recovery. Well spacings of 340, 200, and 60 acres (or less) were determined to provide the maximum gas-contact efficiency in large, medium and small compartment class reservoirs, respectively, within the Frio Formation in South Texas. Although the stochastic modeling results were developed to evaluate reserve growth potential within the FR-4 play in the Texas Gulf Coast, the technique should be broadly applicable in other plays. To facilitate rapid dissemination of this technology and promote increased use by operators, a videotape was produced to explain

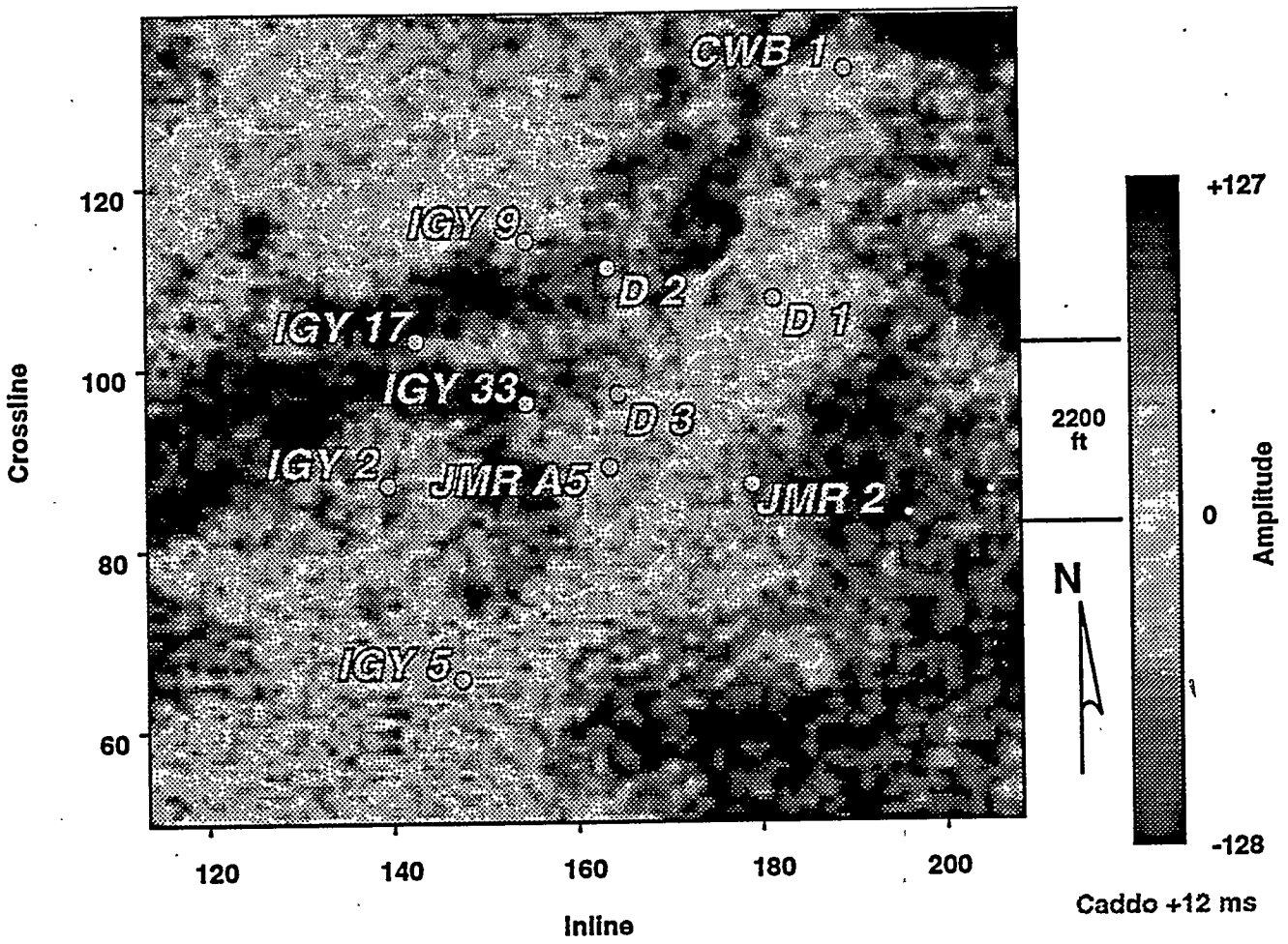


**Figure 14. Seismic reflection amplitude behavior on the horizon slice passing through the Caddo-age valley-fill sequence**

the use of the model. Furthermore, a software program to use the model was made available on a disk for user-friendly use on a PC. This product is commercially available and has been purchased by operators in the U.S. and Canada.

The SGR field investigation at Seeligson field produced the first 3-D reserve VSP or RVSP ever recorded in the world (Ambrose and others, 1992). RVSP refers to the placement of the energy source in the well and the receivers on the surface. A major technical challenge was to identify a source that would not harm the cement bond in the well. A downhole source was specifically designed for this field investigation and tested. As the world's first RVSP, this was a major technical breakthrough; it will provide significant economic benefits for operators in the future if this technology is adopted because receivers are inexpensive and sources are expensive. There are substantial cost savings to operators if they can maximize the use of receivers and minimize the use of sources.

Although there is published technical literature on interpretation of isolated thin beds, the interpretation of closely stacked thin-bed reservoirs is a different and much more challenging problem. Recently, published research results from Stratton field provided the first public

documentation of a technique for properly interpreting closely stacked thin-bed reservoirs (Hardage and others, 1994). This public documentation is critical because it allows industry to access and understand the techniques and the potential benefit of applying them as part of their own infield resource development strategies.

There were four 3-D seismic case history evaluations of fluvially deposited thin-bed reservoirs in the Stratton field investigation (Hardage and others, 1994). The thin-bed interpretation procedure developed by SGR is based on thin-bed depth-versus-time calibration and the definition of chronostratigraphic depositional surfaces. The Stratton field study illustrated to operators that although fluvial deposition creates numerous compartment boundaries, determining which stratigraphic changes in seismic images are flow boundaries requires the integration of geologic and reservoir engineering data, especially reservoir pressure data, into the seismic interpretation. VSP-calibrated 3-D seismic data interpretation for Stratton field verified that subtle fluvial features 200 to 300 ft wide and 10 to 15 ft thick can be imaged at depths of 6,000 to 6,500 ft. Techniques were developed to accurately define and display 3-D seismic surfaces that image thin beds only 2 to 4 ms thick. Facies geometry and resultant flow boundaries between wells identified from pressure buildup tests indicated channel widths averaging 220 ft that confirmed seismic interpretations. It was also determined that well locations and bottom hole coordinates must be known precisely to fully interpret 3-D seismic images of reservoir compartments in fluvial systems where the depositional stratigraphy varies rapidly in the lateral direction. The result of the Stratton investigation was over 65 Bcf of reserve growth potential identified in a large lease block in the 40-year-old Stratton field that had produced over 400 Bcf of gas from 1937 to 1979. A 2-mi$^2$ section of the 3-D data set collected in this field investigation is now available in SEG-format with a well log data set from 21 wells, including a vertical seismic profile for use by operators to test hardware and software products, train individuals in the use of 3-D seismic data and well log information, and illustrate the complex stratigraphy and structure of Gulf Coast fluvial natural gas reservoirs.

In the North McFaddin field, the state-of-the-art array induction tool was used to identify thin-bed high productivity reservoirs. Detailed stratigraphic analysis of multiple thin-bed intervals in combination with resistivity cutoffs and spontaneous potential ratios were used to choose the well and recompletion locations. In the Agua Dulce field, integrated formation evaluation using the new open-hole, high-resolution array induction log, spectral gamma ray measurements, wireline pressure tests, and core analysis were used to identify gas fluvial depositional reservoir facies segmented by structural compartments and affected by stratigraphic variability and diagenesis. The result was that in 21 reservoirs in these 2 mature fields with original gas in place of 37.0 Bcf and cumulative production of 9.0 Bcf, an incremental 9.6 Bcf was identified as economically recoverable risk-weighted reserves. The total cost of developing the McFaddin thin-bed reservoirs using risk-weighted reserves was determined to be $0.58 per Mcf, excluding royalties. The total cost to develop and produce the Agua Dulce reservoirs using risk-weighted reserves was determined to be $0.83 per Mcf, excluding royalties. In both cases, because the production and development costs have been calculated using risk-weighted reserves, these cost estimates are conservative.

**Technology Transfer**

Technology transfer to the gas industry from 1989 to 1994 has included 81 research presentations at international, national, and

regional meetings and technical publications from 1989 to 1994. Twelve short courses and workshops have been taught in three states (Texas, Oklahoma, and Louisiana) in the cities of Houston, Corpus Christi, Midland, San Antonio, Oklahoma City, and New Orleans and attended by over 550 participants. Approximately 150 additional individuals have participated in half-day presentations included in gas reserve growth technology workshops sponsored by the Texas Independent Producers and Royalty Owners Association in Austin, Dallas, Amarillo, and Houston.

Seventy-five percent of the short course participants indicated that they will make direct application of the short course material to their gas reservoir development. Seventy-seven percent of the participants said that they are working with gas fields that can benefit from the short course material and ninety-eight percent stated that they believe that research of this nature is worthwhile.

A seven-stage comprehensive technology development strategy was implemented. Over 3,000 brochures summarizing the technology results of the Gulf Coast project have been distributed to operators in 3 states as well as overseas. A videotape that highlights Secondary Gas Recovery strategies for infield reserve growth opportunities has been requested by and distributed to 275 individuals or companies. A CD-ROM with complete documentation of all the technical reports from the research project, and a compilation of all published articles and technical presentation of the research results, has been purchased by 124 individuals or companies. The 3-D seismic data set from the Stratton field has been purchased by 146 individuals or companies. As of mid-March, 1995, 176 requests had been received for the "How-To Manual," which will be distributed by summer, 1995.

While it has been important to document technology transfer activities, it is more important to recognize that a production response is now becoming evident in the Texas Gulf Coast region. This response is adding substantial reserve growth reserves.

### Texas Gulf Coast Producer Response

The technology transfer effort under the SGR project that was launched in October, 1991, began to affect natural gas production in the Texas Gulf Coast in 1993. Two different responses were seen: 1) development well success rates rose 4 to 5 percent in the Upper Coast and Lower Coast, respectively, and 2) reserves added per development well were up 48 percent in the Texas Gulf Coast region compared to the 1991-92 average. These responses were evident in data developed by the American Petroleum Institute (1994) and the Energy Information Administration (1994). While it is difficult to judge what part of these changes are directly attributable to the SGR project, it is noteworthy that in a survey of producers in January, 1995, 25 percent of 499 respondents indicated that their companies had realized additional reserves or production by using SGR concepts or technologies. In addition, 75 percent of respondents (393) indicated that they were familiar with the studies being conducted by the SGR project. Taken together with requests for technology transfer products, these responses suggest that the SGR project has had an important impact on Texas Gulf Coast gas production as producers pursue opportunities to develop reserve growth resources.

In defining the development well success rate in the onshore Texas Gulf Coast basin, it is necessary to evaluate the Upper Coast (Railroad Commission of Texas District 3) and the Lower Coast (Railroad Commission of Texas District 4) separately from the Middle Coast. This distinction must be made because of the difference in depositional style of the Frio Formation across these areas. The Upper and Lower Coasts were major Frio deltaic depocenters, whereas the Middle Coast contains Frio barrier-strandplain

deposits. The latter have a higher degree of continuity than fluvial channel deposits and are therefore expected to have fewer opportunities for reserve growth than the vertically stacked fluvial channels and crevasse splays of the deltaic depocenters.

The success rates for natural gas development wells in Districts 3 and 4 were analyzed for 1987-93. District 3 (Upper Coast) showed the highest success rate (83 percent) for the period in 1993, 4 percent better than the 1991-92 average and 7 percent better than the 1990-92 average. District 4 (Lower Coast) showed the highest success rate (78 percent) for the period in 1993, 5 percent better than the 1990-92 average. Both districts were the sites of cooperative data collection with producers and of technology transfer efforts reaching more than 550 individuals in SGR workshops. These percentage improvements led to an estimated $8.8 million in gas industry dry hole cost savings in 1993 alone.

Additional benefits were also realized in terms of greater volumes of reserves added per development well in 1993 than in previous years. District 4 saw yields of 3.07 Bcf/development well, compared to an average of 2.28 Bcf/development well in 1991-92. For all three districts in the onshore Texas Gulf Coast, reserve growth was 2.98 Bcf/development well in 1993, compared to 2.02 Bcf/development well for the 1991-92 average, or an increase of 48 percent. This increase compares to a decline for the rest of onshore Texas from 1.35 Bcf/development well in 1991-92 to 1.16 Bcf/development well in 1993. If valued at an in-ground purchase price of $0.50/Mcf, the incremental gas per well (0.91 Bcf, after allowing for a 5 percent negative revision) is worth $455,000, which is comparable to a drilled and completed Middle Frio well at a cost of about $350,000 (1994 $). Thus, the improvement in yield per well will dramatically affect producer economics and, if sustained, will make a major contribution to reserve growth realization on a regional and national basis.

## FUTURE WORK

Technical project work on Midcontinent reservoirs will be completed with scheduled project conclusion on June 30, 1995. Any follow-up efforts will be aimed at additional technology transfer to producers.

## REFERENCES


Ambrose, W. A., J. D. Grigsby, B. A. Hardage, R. P. Langford, L. A. Jirik, and R. A. Levey, 1992, Secondary natural gas recovery: targeted technology applications for infield reserve growth in fluvial reservoirs in the Frio Formation, Seeligson field, South Texas: The University of Texas at Austin, Bureau of Economic Geology, topical report prepared for the Gas Research Institute under contract no. DE-FG21-88MC25031, Report No. GRI-92/0244, 200 p.

American Petroleum Institute, 1995, Quarterly completion report, fourth quarter 1994: vol. X, no. 4, 86 p.

Collins, R. E., and M. E. Lord, 1992, Simulation system for compartmented gas reservoirs: targeted technology applications for infield reserve growth: Research & Engineering Consultants, Inc., topical report prepared for The University of Texas at Austin, Bureau of Economic Geology; the Gas Research Institute under contract no. 5088-212-1718; and the U.S. Department of Energy under contract no. DE-FG21-88MC25031; Report No. GRI-92/0104, 75 p.

Fisher, W. L., 1993, Natural gas in the U.S.: will supplies be there when needed?: CERI North American Natural Gas Conference, Calgary, Alberta, Canada, March 1993.

Hardage, B. A., R. A. Levey, V. Pendleton, J. Simmons, and R. Edson, 1994, A 3-D seismic case history evaluating fluvially deposited thin-bed reservoirs in a gas-producing property: Geophysics, November, p. 1650–1665.

Levey, R. A., B. A. Hardage, R. P. Langford, A. R. Scott, R. J. Finley, M. A. Sipple, R. E. Collins, J. M. Vidal, W. E. Howard, J. R. Ballard, J. D. Grigsby, and D. Kerr, 1993, Targeted technology applications for infield reserve growth in fluvial reservoirs in the Stratton field, South Texas: The University of Texas at Austin, Bureau of Economic Geology, topical report prepared for the Gas Research Institute under contract no. 5088-212-1718, Report No. GRI 93/0178, 244 p.

Lord, M. E., and R. E. Collins, 1991, Detecting compartmented gas reservoirs through production performance: Society of Petroleum Engineers, paper no. SPE 22941, p. 575–581.

U.S. Department of Energy, Energy Information Administration, 1994, U.S. crude oil, natural gas, and natural gas liquids reserves 1993 annual report, 155 p.

U.S. Department of Energy, Energy Information Administration, 1990, The domestic oil and gas recoverable resource base: supporting analysis for the National Energy Strategy, Report No. SR/NES/90-05, 56 p.

U.S. Department of Energy, National Petroleum Council, 1992, The potential for natural gas in the United States: Executive Summary, 58 p.

U.S. Geological Survey National Oil and Gas Resource Assessment Team, 1995, 1995 national assessment of United States oil and gas resources: U.S. Geological Survey Circular 1118, 20 p.

# Session 3A

## *Resource & Reserves — Modeling and Data Bases*

## 3A.1 Development of a Gas Systems Analysis Model (GSAM)

CONTRACT INFORMATION

| | |
|---|---|
| **Contract Number** | DE-AC21-92MC28138 |
| **Contractor** | ICF Resources Incorporated<br>9300 Lee Highway<br>Fairfax, Virginia 22033<br>(703) 934-3000<br>(703) 691-3349 |
| **Contractor Manager** | Michael L. Godec |
| **Principal Investigators** | Alan B. Becker<br>William J. Pepper |
| **METC Project Manager** | Anthony Zammerilli |
| **Period of Performance** | June 22, 1992 - July 21, 1995 |

---

| **Schedule and Milestones** | Prior FY | FY95 Program Schedule<br>O N D J F M A M J J |
|---|---|---|
| Review Models | 1994 | |
| Review Technologies | 1994 | |
| Model Design | 1994 | |
| Model Development | 1994 | ----------C |
| Data Development | | S---------C |
| Peer Review | | X |
| Document, Test, and Validate | | S----------P |
| Final Report | | S----------P |

S = Start
P = Planned Completion
C = Complete

## OBJECTIVES

The objectives of developing a Gas Systems Analysis Model (GSAM) are to create a comprehensive, non-proprietary, PC based model of domestic gas industry activity. The system is capable of assessing the impacts of various changes in the natural gas system within North America. The individual and collective impacts due to changes in technology and economic conditions are explicitly modeled in GSAM. Major gas resources are all modeled, including conventional, tight, Devonian Shale, coalbed methane, and low-quality gas sources.

The modeling system assesses all key components of the gas industry, including available resources, exploration, drilling, completion, production, and processing practices, both for now and in the future. The model similarly assesses the distribution, storage, and utilization of natural gas in a dynamic market-based analytical structure. GSAM is designed to provide METC managers with a tool to project the impacts of future research, development, and demonstration (RD&D) benefits in order to determine priorities in a rapidly changing, market-driven gas industry.

## BACKGROUND INFORMATION

The effective planning of RD&D to meet changing future needs requires a comprehensive resource assessment and technology evaluation tool. METC in an effort to enhance its planning functions has developed GSAM. This modeling system and preliminary data provide a comprehensive planning capability to assess the impact of RD&D on future gas production, reserves, and gas prices, both regionally and nationally.

The diverse circumstances that affect recovery and use of natural gas to meet national energy needs requires thorough analysis of complex, inter-related systems. Simple evaluation of extraction technology R&D will not provide insights into the full needs of producers. The location of the gas resource and the existing infrastructure may not allow profitable development, production, and transportation to market of the gas at prevailing prices. Similarly within exploration and production (E&P) activities, multiple, coordinated advances in extraction practices and reductions in overall costs may be needed to allow economic development of remote resources.

The rapidly changing requirements for environmental compliance also impacts METC's RD&D program. Full economic and risk analysis on a reservoir specific basis is critical to understanding the multiple impacts of new environmental conditions faced by operators. GSAM is being expanded to also provide an integrated system for assessing related impacts of environmental compliance requirements on future E&P activities.

## PROJECT DESCRIPTION

GSAM was designed to quickly and thoroughly assess the relative impacts of various individual or collective improvements in technology. The diverse set of issues that must be addressed by DOE planners using GSAM demand an integrated, quick turn-around analytical structure.

The modeling system has been designed on a modular basis, with individual segments of the system analyzing and converting data,

References and illustrations at end of paper

modeling reservoir performance, conducting economic evaluations, and reporting detailed and summary results. This design was selected to speed future analysis by allowing each segment of the model to be run independently. Intermediate results can be used for many analytical requirements reducing the time and manpower needed to complete evaluations. Each module can also be individually tested and validated against other systems and modules, as well.

To complete this work, a comprehensive plan was developed including five major tasks:

- Review current technologies
- Review existing data and models
- Develop methodology
- Develop model and databases
- Test and validate system

Initial development has been completed and a trial version of GSAM delivered to METC for testing and initial use. Final testing, calibration, and validation of all modules and initial databases is underway. System training will be scheduled at METC later this spring.

The GSAM project was significantly expanded over the last year to provide an Environmental Module, designed to more comprehensively assess regulatory requirements. The module is designed to convert data from various sources into details on operating conditions, costs, and environmental impacts needed to assess current and future environmental compliance efforts. This work has been carefully incorporated into ongoing tasks.

Additional tasks were also added to develop complete databases for the known and undiscovered resources, to allow full testing and validation of the system. These initial databases contain information on the rock and fluid properties for over 8,500 gas reservoirs nationwide. Additionally, the undiscovered database contains resource descriptions for over 600 TCF (original gas-in-place) of remaining undiscovered gas reservoirs nationwide.

The system was reviewed by a panel of industry experts last fall. Based on their favorable comments and recommendations, key aspects of GSAM have been enhanced. Additional modifications and enhancements, beyond the initial scope of the development phase, have been identified. Final model development work, including expanded data analysis capability, is being reviewed by METC.

## RESULTS

### General GSAM Design

GSAM design has been fully developed and is undergoing rigorous testing, validation, and calibration. Figure 1 shows the overall design of GSAM and the key modules that make up the full analytical system. GSAM assess both supply and demand for natural gas under alternative future economic, technology, and policy conditions in order to quantify impacts of ongoing and future R&D to improve performance or reduce costs. Using the full integrated approach to program planning, METC hopes to direct future R&D to the highest payoff efforts.

The analysis of data and development of reservoir level resource descriptions are critical to the functioning of GSAM. As shown in Figure 2, the modeling system has a resource module that analyzes available data from several sources and produces consistent databases for the known and undiscovered reservoirs in key gas plays. GSAM, therefore, can quantify the known

and undiscovered resource that will be available to meet future natural gas demand. Additional work has also been completed to provide a comprehensive database of unconventional resources for initial GSAM analyses.

A key feature of GSAM is the source databases. These files contain information on the origin and evaluation of each element in the resource databases. This information is used to update and validate the data, assumptions, and analytical procedures resident in the resource module.

Figure 3 shows the logic flow of the upstream, E&P segment of GSAM. The model consists of consistent, parallel, but independent modules to assess the annual production levels, recovery potential, project costs, and summary economic results for individual reservoirs nationwide. Figure 4 displays the characteristics of the six reservoir performance (type-curve) models use in GSAM. These models use reservoir level rock and fluid properties to determine the technically feasible production response for various reservoir types. These preliminary results are further evaluated with detailed costing and cashflow models to generate summary project economics.

The summary information is then used to determine the probable timing of development for each reservoir based on regional and national prices and cost factors. The system consists of intermediate databases that allow analyses to be completed without running the entire analytical system. The results of the upstream model flow to the integrating model to determine market conditions and timing of development.

Figure 5 shows the market logic of the GSAM system and how it balances competing resources, R&D outcomes, policy considerations, and market realities to arrive at a single, comprehensive description of future gas potential. This evaluation can be run for a single gas price forecast, or in integrated mode to solve for regional and sectoral prices which balance end-use and production.

Figure 6 shows how GSAM tracks various aspects of natural gas resource discovery, development, production, and abandonment. The remaining resource database contains information on the location, character, and economics of key resources left to be developed or produced. This detailed assessment provides METC with targets and key program elements to use in directing future research. If required, the remaining resource database can be expanded to provide additional details on key attributes of the remaining gas resource as well.

## Resource Description Summary

The initial GSAM database was developed using information from the U.S. Geologic Survey (USGS)[1], the National Petroleum Council (NPC)[2]. The domestic resource described includes known reservoirs developed using data from NRG Associates database[3]. This data contains reservoir specific rock and fluid properties, production histories, and location information on over 10,000 non-associated gas reservoirs nationwide. Based on the information available, a detailed description of the gas resource in known, producing reservoirs was fully developed.

The NRG data provided an important element to the database; the assignment of all reservoirs to unique geologic-based plays[4]. This data element was used to develop default elements based on average properties for reservoirs in each play. This

provided a method for determining reasonable values for key missing data elements for some reservoirs. Play descriptions and resource characterization analysis methods were fully incorporated into GSAM.

Additionally, using the data available from the NRG file and cross-walking to information from the USGS, an undiscovered resource database was initially constructed for use in GSAM. This data uses average properties for known reservoirs to describe reservoirs that remain to be discovered in each play. Additional reservoir descriptions for zones in hypothetical plays, those identified as having resource but no current production, were developed based on plays with similar geologic characteristics.

For selected offshore and unconventional resources, and where data was not available (i.e. Canada and Appalachia) reservoir data sets were created to calibrate the model. This step involved using information developed for the recent NPC study *The Potential for Natural Gas in the United States*[5], as well as data available from the National Energy Board[6] of Canada. This data is intended to serve as a surrogate until additional information on these key resources can be collected and analyzed.

The resource description in GSAM provides a starting point for initial analyses and final model development. As additional data is collected, GSAM provides the framework to incorporate, validate, and utilize it for R&D planning. Additional work is warranted to document the data and fully develop the GSAM resource files.

Supply Model Results

The initial analyses using GSAM indicate significant remaining resource recovery potential in domestic reservoirs. Consistent with the findings of recent national analyses, the availability of natural gas in most regions seems to be assured in the foreseeable future. The initial GSAM findings indicate an increase in production from the Rockies region and a somewhat smaller contribution from the Gulf Coast and offshore reservoirs.

Technology can substantially increase recovery potential and lower the overall cost of delivering natural gas. GSAM's detailed performance and cost assessment of individual reservoirs allows technology to be evaluated in detail. Figure 7 shows how new technology, e.g. longer fracture lengths in tight reservoirs, could lower the required wellhead price by increasing recovery from the zone. However, lower costs for fracturing operations combined with better completion and stimulation technology may be required to allow operators to cost-effectively develop many tight and unconventional gas reservoirs.

Integrated Market Results

GSAM results indicate that, consistent with current conditions, regional gas price differentials will continue into the future. However, imports from Canada could be limited over the next twenty years unless new, lower cost technologies are applied to the diverse resources in Alberta and elsewhere.

Coalbed methane, shale gas, tight sands, and naturally fractured zones will play an increasingly important role in meeting future gas needs. As associated gas production declines and non-associated, conventional resources mature, more production must come from complex unconventional sources to meet demand. Additional research in drilling, completion, and processing to

improve current practices and limit costs and risks will be needed to develop and produce these resources at reasonable gas prices.

Green River Basin Examples

Production from tight sands, especially in the Rockies, will need to increase in the future as gas demand expands and transportation infrastructure matures. The Green River Basin in southern Wyoming is a key area for application of new technologies for tight gas sands. With 56 to 83 TCF of estimated technically recoverable resource[6], this basin is a key future supply source for tight gas production.

Preliminary GSAM analysis indicates that current drilling, completion, stimulation, and production practices will limit economic recovery of the resource to only 7 to 8 TCF including reserves developed through the year 2010. Most critical seems to be the need for cost-effective hydraulic fracturing technology.

Technology improvements could substantially increase productivity, reserve potential, and economic attractiveness of Green River reservoirs. New techniques must provide economic incentives to develop the resource at prevailing regional gas prices. If stimulation processes can be improved and costs reduced by 30% of current costs, reserve potential in the basin could increase to around 10 TCF based on current GSAM resource description.

Figure 8 shows the potential impact on future production from reservoirs in the Eastern Green River Basin. As shown, the application of new technology to improve recovery or lower costs could have a profound impact on future production levels. However, the application of new technologies will have a downward impact on gas prices in the Rockies, Canada, and elsewhere.

METC research must overcome economic limitations to production from Green River reservoirs under level to slightly rising gas prices likely to be seen by operators. This figure also shows the effect of the combined impact of improved fracture technology and lower stimulation costs relative to current practices.

This initial basin analysis shows that cost-effective stimulation techniques must be developed and demonstrated in key reservoir settings in Green River. Development of more efficient fracture stimulation methods, providing longer, more conductive fractures at comparable costs are required.

GSAM analyses provide the capability to comprehensively analyze the impact of individual or combined technology improvements for E&P operations, evaluating the impact of improvements in reservoir performance, reductions in costs, and management of operator risk. The capability to analyze potential improvements in detail allow METC to plan and focus research on the most critical needs. By linking to the downstream demand estimates, GSAM provides a realistic projection of the economic conditions that will define future production activities.

## FUTURE WORK

Initial GSAM development is complete and documentation is being reviewed and finalized. Additional deliverables will include a complete documentation of the modeling system, databases, and analytical procedures used. A comprehensive users' guide is also being prepared.

Additional testing and validation is being completed consistent with recommendations and initial plans. The full validation and model installation will be complete prior to July.

Additional work to improve GSAM is being considered by METC. In addition, enhancements to the environmental module to increase data coverage and streamline analyses of cost/benefits are being planned. Initial use of GSAM for policy and program planning will be initiated upon final development activity.

The GSAM design provides a solid framework for additional model development, data collection and analysis, and system refinements. The additional enhancements can be quickly integrated within the modeling system.

## REFERENCES


1. United State Geologic Survey, *Estimates of Remaining Hydrocarbon Deposits*, Washington, DC, 1989.

2. National Petroleum Council, *The Potential for Natural Gas in the United States*, Volumes I-VI, Washington, DC, 1992

3. NRG Associates, *Significant Oil and Gas Fields of the United States Database*, 1994.

4. NRG Associates, *U.S. Oil and Gas Plays*, Colorado Springs, CO, 1993.

5. NPC, Volume II, Chapter 4.

6. NPC, Volume II, p. 104.

## Figure 1. GSAM Structure

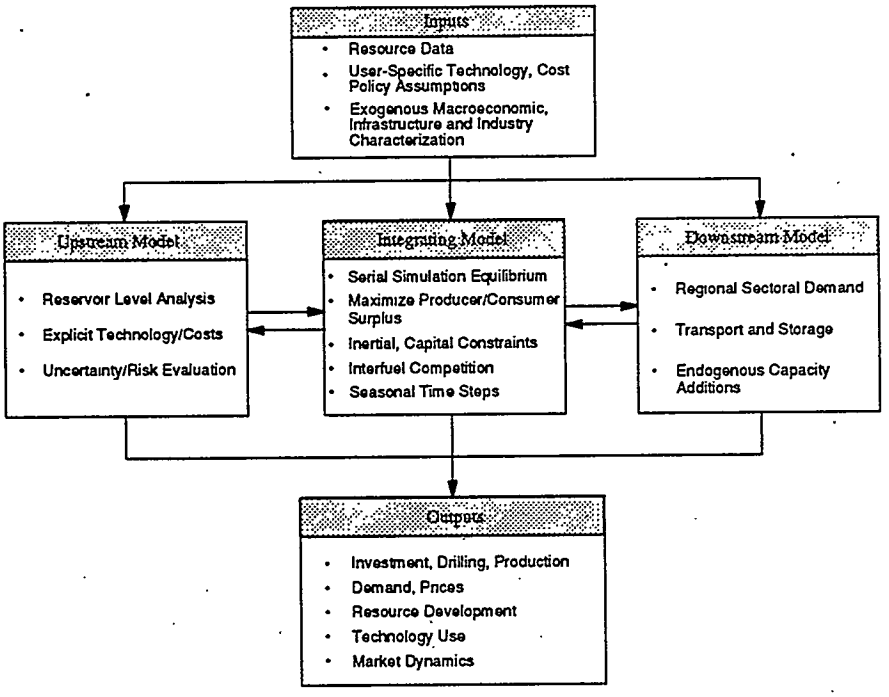


## Figure 2. GSAM Resource Data Development Method

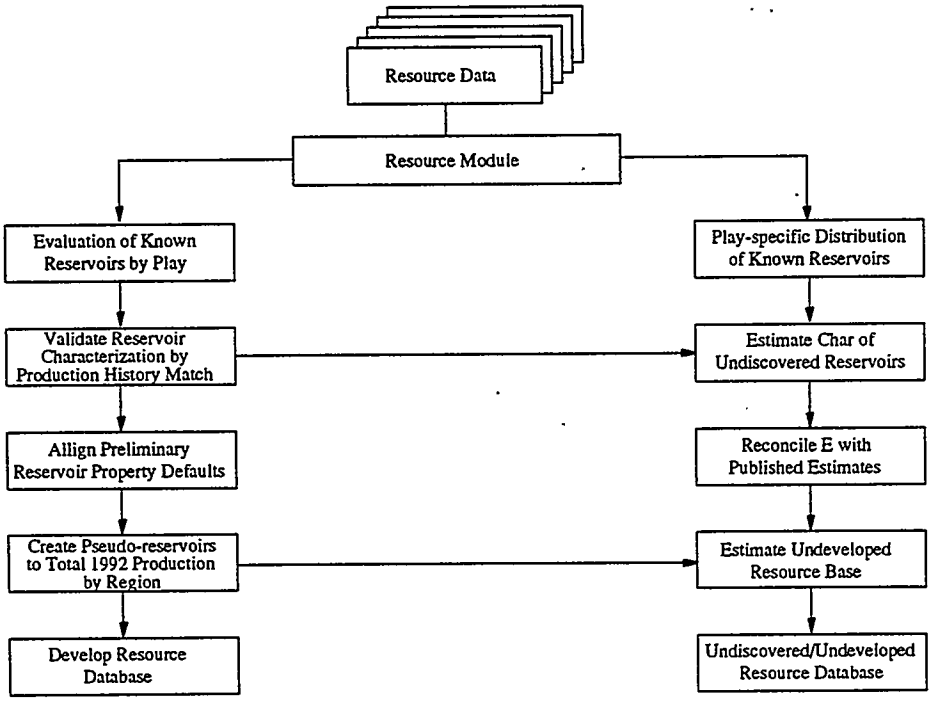

## Figure 3. GSAM Upstream Model Flowchart

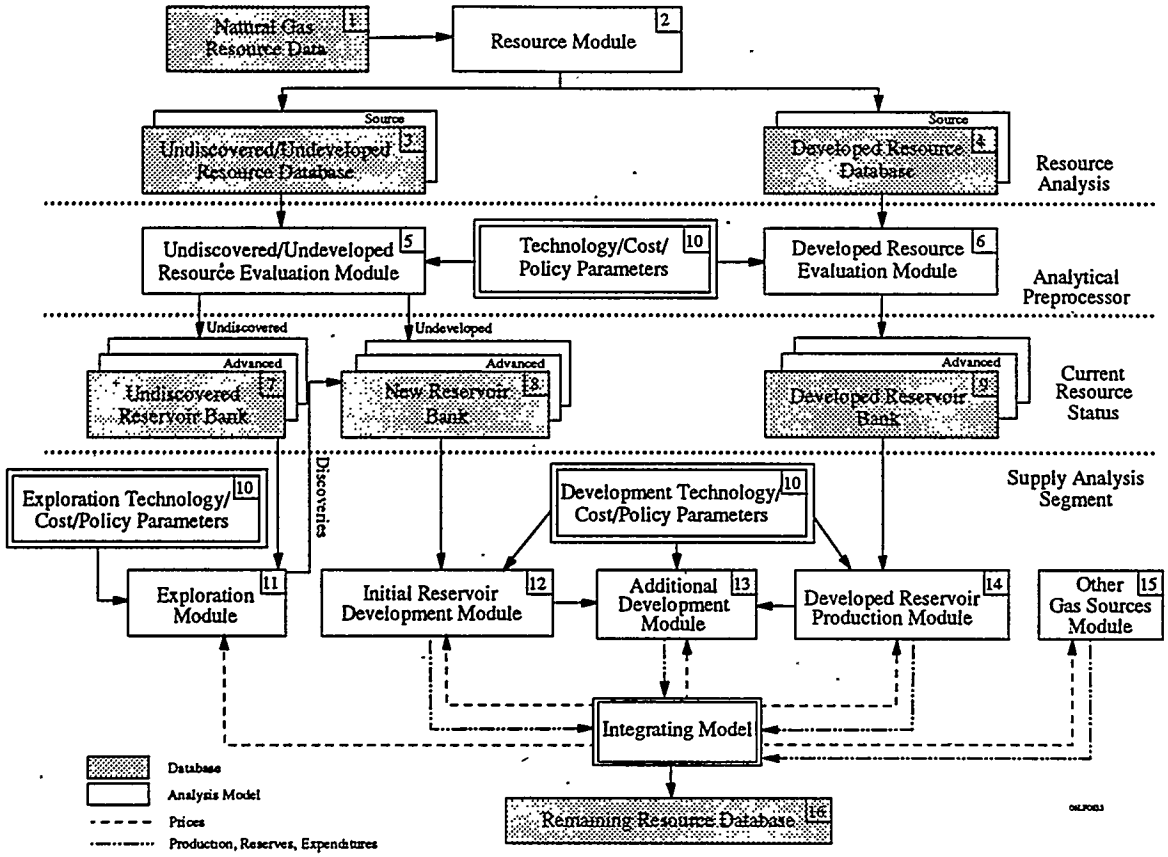


## Figure 4. GSAM Reservoir Performance Models

| Module | Reservoir Type | Drive Mechanism | Flow Geometry | Porosity Type | Number of Fluids |
|---|---|---|---|---|---|
| I | Conventional/ Tight | Fluid Expansion | Radial | Single | Single Fluid* (Gas) |
| II | Horizontal well/ Induced fracture | Fluid Expansion | Linear | Single | Single Fluid (Gas) |
| III | Conventional | Fluid Expansion | Radial | Dual | Single Fluid (Gas) |
| IV | Horizontal well/ Induced fracture | Fluid Expansion | Linear | Dual | Single Fluid (Gas) |
| V | Natural Fracture | Water-Drive | Radial | Single | Two Fluids (Gas & Water) |
| VI | Coal/Shale | Diffusion/ Desorption | Radial | Dual | 1 or 2 Fluids (Gas or Water/Gas) |

*Geopressured aquifers can be analyzed using Module I; mobile phase is water

## Figure 5. GSAM Logic Flow

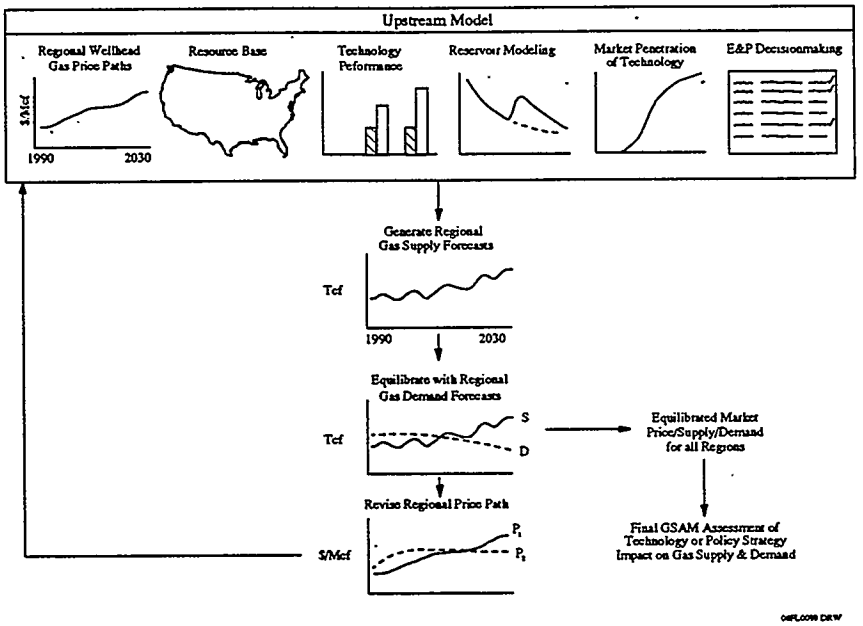


## Figure 6. Analysis of Natural Gas Resources by GSAM Modules and Databases

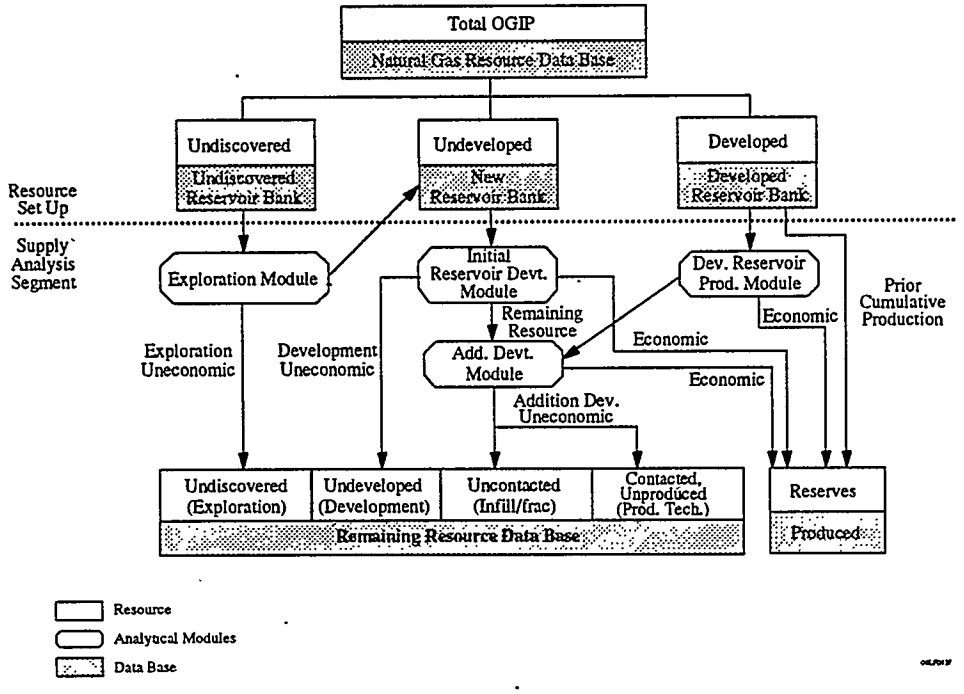

**Figure 7. Economic Recovery May Require Improved Technology and Lower Cost**

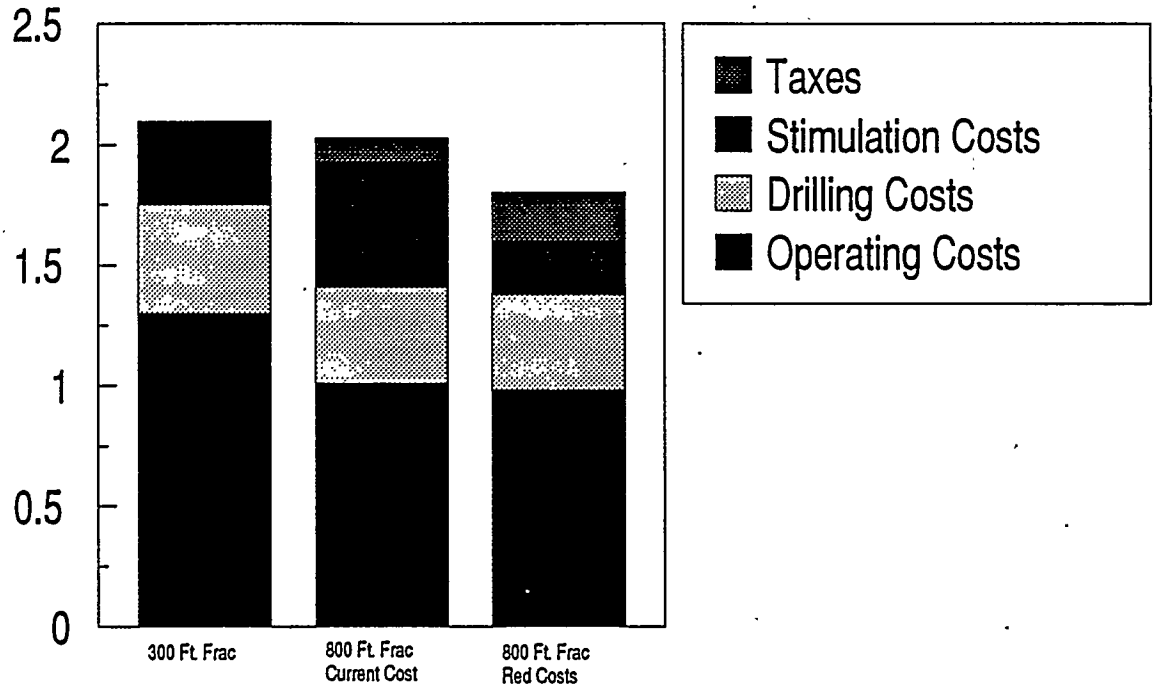


**Figure 8. Gas Production Potential From Eastern Green River Basin**

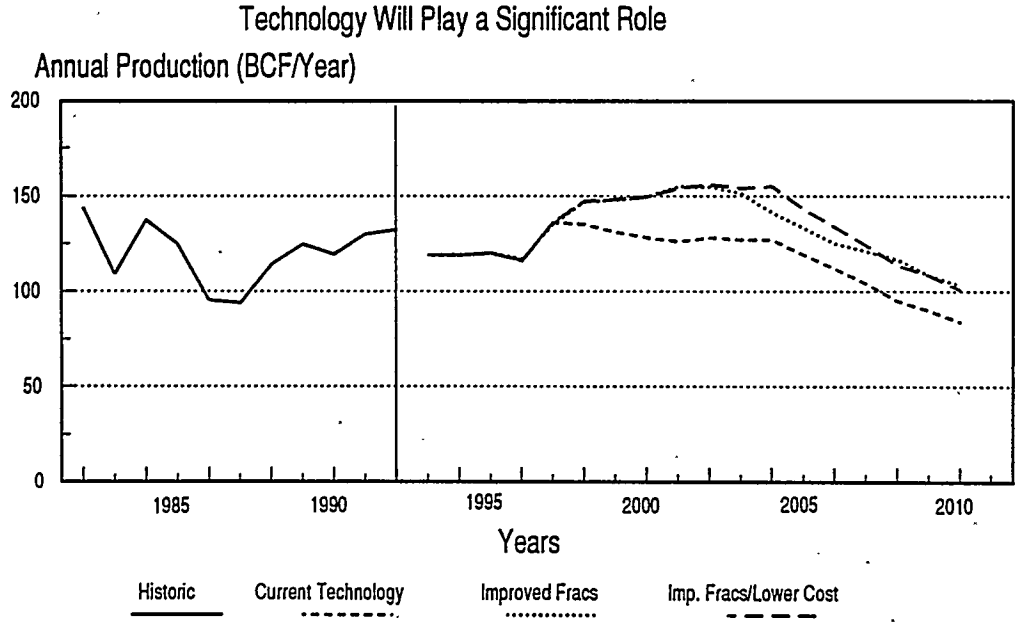

## 3A.2 Development of the DOE Gas Information System (GASIS)

**CONTRACT INFORMATION**

| | |
|---|---|
| **Contract Number** | DE-AC21-93MC28139 |
| **Contractor** | Energy and Environmental Analysis, Inc.<br>1655 North Fort Myer Drive, Suite 600<br>Arlington, VA 22209<br>(703) 528-1900 (telephone)<br>(703) 528-5106 (fax) |
| **Other Funding Sources** | |
| **Contractor Project Manager** | E. Harry Vidas |
| **Principal Investigators** | E. Harry Vidas<br>Robert H. Hugman<br>Peter S. Springer |
| **METC Project Manager** | Harold D. Shoemaker |
| **Period of Performance** | May 17, 1993 to May 16, 1996 |
| **Schedule and Milestones** | |

**FY95 Program Schedule**

| | S O N D J F M A M J J A |
|---|---|
| 1. User Survey | Completed |
| 2. Source Directory Development | ——— |
| 3. Reservoir Database Development | ——— |
| • Prototype/software development | ——— |
| • Processing of data sources | ——— |
| • Reservoir studies | ——— |

## OBJECTIVES

The primary goal of the GASIS project is the development of a national database of geological, engineering, and production and ultimate recovery data for U.S. oil and gas reservoirs. The database will include the information interpreted and assembled by the regional GRI/DOE Gas Atlas projects. GASIS data will be used to develop or expand reservoir data input files for DOE reservoir-based technology assessment models such as GSAM, and as a stand-alone database for gas resource characterization and assessment.

Another goal is to promote the development of domestic natural gas resources by providing the oil and gas industry with the first national public domain reservoir property database. The GASIS "Source Directory" will also assist industry by documenting supply-related databases and information centers. GASIS will be made available on CD-ROM with retrieval software, and will have applications in the areas of exploration, development, planning, resource characterization, and technology and market assessment.

The reservoir database will combine the electronic Gas Atlas data, data from Dwight's, new GASIS interpreted reservoir data, GRI data, and new "processed" data elements into a single database with approximately 20,000 records. The data matrix will contain about 180 data fields for each reservoir.

A large-scale geological data collection and analysis effort is a major component of the project. This field and reservoir study effort will greatly improve the quality and coverage of reservoir and fluid property data and will provide the first true "reservoir definition" for many fields in the Mid-Continent and elsewhere. The geological studies will also provide DOE with an improved database for analysis of low permeability reservoirs in several basins.

## BACKGROUND INFORMATION

The GASIS project may be viewed as an extension of the Gas Research Institute/ Department of Energy Gas Atlas project, which has resulted in the development and publication of four regional reservoir databases, with two more regions in progress. Completed Gas Atlas projects include Texas, the Mid-Continent, the Central and Eastern Gulf Coast, and the Rockies. The Appalachian atlas has not yet been published and the Gulf of Mexico atlas is still in progress.

A major contribution of the Gas Atlas project has been the definition and geological description of exploration plays in each region and the assignment of reservoirs to these plays. This work has resulted in the first public domain play classification system for the U.S. Play description and classification is valuable because reservoirs within a specific play often display many similar geological and engineering characteristics. This allows a modeler or explorationist to make generalizations about play attributes. In addition, the discovery history of exploratory plays provides insight into future potential.

Energy and Environmental Analysis (EEA) is the lead contractor for GASIS. EEA is managing database design and development, software development, special data analysis projects, and Source Directory development.

The primary subcontractor to EEA is Dwight's Energydata. Dwight's field and reservoir group in Oklahoma City is conducting field and reservoir geological studies and related data collection activities.

## PROJECT DESCRIPTION

### Scope of GASIS

Figure 1 shows the two major components of the Gas Information System. The primary component is the Reservoir Data System, which will consist of approximately 20,000 reservoir records containing reservoir and fluid properties, play classification, and summary production data. Each record will contain approximately 180 data fields. The other component of GASIS is the Source Directory, which will document over 200 oil and gas supply-related databases and information centers currently available to industry. Both components of GASIS will be assembled on a single CD-ROM, along with Windows-based search and retrieval software.

### User Needs Assessment

The initial phase of the GASIS project, completed in 1994, was a survey of potential database users to guide the development of GASIS. This survey included representatives of majors, independents, consultants, GRI, state and federal agencies, financial institutions, and other groups. Topics included current data sources, potential GASIS applications, priorities by type of data and data format and software issues. The results of the survey and recommendations for GASIS were published in a topical report to DOE. (Hugman and others, 1994)

### Reservoir Data System

Figure 2 shows the types of data planned for the Reservoir Data System. Included will be field and reservoir identification, location, producing status, play classification, reservoir and fluid properties, geologic information, production data, and estimated remaining reserves. Also planned are reservoir area and average well spacing, completion level ultimate recovery data, a geological type well (for reservoir studies), drilling and completion data, and gas composition.

### Source Directory

The Source Directory will document public domain and commercial databases that contain geological, engineering, production, well completion, and related data of interest to oil and gas producers and the research community. The Source Directory will also document major oil and gas information centers, sample repositories, and technology transfer centers.

### Software

The CD-ROM will come with Windows-based software for data retrieval and manipulation. For the Reservoir Data System, the software will allow query and retrieval, screen display, report generation, and exporting of data in standard formats. The software will also allow query and retrieval of the Source Directory information.

### Reservoir Studies

In addition to database development, the GASIS project includes a large-scale field and reservoir study effort designed to obtain new, high quality reservoir data in selected regions and plays. This work includes regional and field level log correlation, log analysis, data collection, and geological interpretation. In the Mid-Continent, GASIS reservoir studies will result in the first accurate assignment of gas completions to specific reservoirs ("reservoir definition").

### Project Schedule

Figure 3 is a summary of the GASIS schedule. The project was initiated in May, 1993 and was scheduled for completion in May of 1996. A contract extension is being implemented to include all of the Gas Atlas

data, because the complete Gulf of Mexico atlas database will not be available until the Fall of 1996. Extension through mid-1998 will be necessary to compile the full range of information that will be needed to meet DOE's data requirements for GSAM and other models.

Figure 3 also shows the schedule for GASIS reservoir studies, and the planned dates for release of the initial and final GASIS database.

## RESULTS

### Information Included in Reservoir Data System

Figure 4 is a summary table of the data elements that are planned for the Reservoir Data System. This summary represents the information that will be covered by approximately 150 individual data elements. An additional 30 data elements will report information sources for key reservoir parameters.

Field and reservoir identification, codes, reservoir type and status information will be reported. Reservoir type will include the official state designation (oil or gas) as well as the gas reservoir classifications used in the atlas project (non-associated, gas cap, or dissolved gas). Tight gas, coalbed methane, and shale reservoirs will be identified.

Geological and engineering parameters will include standard data items such as net pay, porosity, and water saturation collected by the Gas Atlas project, as well as additional data types collected in the GASIS reservoir studies. For the standard data items, both Gas Atlas and Dwight's data are available. Since both sources will be used in developing GASIS, the data coverage will generally be better than for each source individually. Additional data types being collected in the reservoir studies include a heterogeneity evaluation, and ranges for net pay and porosity.

Both published and calculated reservoir area and well spacing data will be included. Gas productive area and calculated average gas well spacing will be determined through analysis of Dwight's gas completion database.

Drilling, completion, and stimulation data are also included. Currently, this information is being collected as a component of the reservoir studies. In the future, we expect to use electronic well history data to identify artificially stimulated reservoirs and to characterize basic drilling and completion practices. Identification of horizontally drilled reservoirs is part of the current project and will be based upon information in Dwight's databases.

GASIS will include documentation of a "geological type well" for each of the reservoir studies. It is the well which is considered to have a representative reservoir section. Type wells and producing intervals will be identified in the database.

GASIS will also include statistical information on completion level ultimate recovery. Using Dwight's DOGR completion level database, an ultimate recovery estimate will be made for each gas completion in non-Appalachian areas. (DOGR does not cover the Appalachian Basin). The minimum, maximum, mean, and median completion level ultimate recoveries will be reported for each reservoir. These recovery statistics can be used for reservoir screening, characterization, and economic analysis. The most representative or "median recovery" well will also be identified.

Also included will be cumulative oil and gas production and the most recent year of annual production. The full historical annual production data series is considered proprietary Dwight's data and will not be included on the CD-ROM.

Reserve-to-production (R/P) ratios will be used to estimate remaining reserves of oil and gas for each reservoir. The R/P ratios will be determined from state and district level EIA production and reserve data, and will be applied to reservoir level production. More sophisticated reserve estimation methods may be used in the future to obtain better estimates.

Original gas-in-place (OGIP) information is sparsely covered in both public and commercial reservoir databases, and where present, has generally been taken from published sources. Published estimates of OGIP or ultimate recovery have limited value because they are generally dated and the methodology is unknown or undocumented. Despite this, GASIS will include OGIP where it has been published by the atlas project or is present in Dwight's database. Development of new estimates of OGIP using historical pressure and production data is not a part of the current GASIS project.

Wellhead gas composition will be reported by component, including C1 through C6-plus, nitrogen, carbon dioxide, and $H_2S$, and will be derived from the GRI database developed by EEA using Bureau of Mines and other data (Hugman and others, 1993a).

**Primary Data Sources - Reservoir Data System**

Figure 5 summarizes the principal data sources for the reservoir database. Major sources include the regional Gas Atlas datasets, new GASIS reservoir studies, Dwight's reservoir and completion-level databases, and the GRI Tight Gas and Gas Composition databases.

The regional GRI/DOE Gas Atlases cover the major gas producing areas of the U.S. Each project has produced a bound atlas containing play descriptions and reservoir groupings and an electronic dataset of reservoir data. Figure 6 summarizes the play and reservoir coverage of each regional project. The Gas Atlas series was initiated in 1989 with the publication of the "Atlas of Major Texas Gas Reservoirs" by the Bureau of Economic Geology (BEG) for GRI (Kosters and Bebout, 1989). GRI also supported the Central and Eastern Gulf Coast and Mid-Continent atlases, which are also available through the BEG (Bebout, 1993a and 1993b). The Rocky Mountain atlas has been completed and is available through the New Mexico Bureau of Mines and Mineral Resources (Robertson and Broadhead, 1993). DOE is funding the Appalachian atlas, which is nearing completion. DOE, GRI, and the Minerals Management Service are funding the Northern Gulf of Mexico Atlas, which is scheduled to be published in two parts (in 1995 and 1996).

The onshore Gas Atlas databases include reservoirs with cumulative total gas production of either 5 billion cubic feet (Rockies) or 10 billion cubic feet (most other areas). GASIS reservoirs will be selected using the same cumulative production criteria that were used in the Gas Atlas projects, although GASIS will use more recent production data than most of the atlases. All Lower-48 producing regions that are covered by the Gas Atlas project will be included on the CD-ROM. Excluded areas are the Michigan/Illinois Basins, onshore and offshore California, and the Williston Basin.

Prior to the Gas Atlas project, public domain reservoir data were widely scattered in regional oil and gas field compilations and state files. Major contributions of the project include play definition and description, assignment of reservoirs to plays, and the collection and reporting of reservoir data in a standard format. The atlas play assignments are the only large-scale source of such information available currently in the public domain.

Dwight's has made available a large amount of geological and engineering information for GASIS. Dwight's PDS (Petroleum Data System) "TOTL" field and reservoir file is the primary source of data. This information has been assembled from numerous sources including industry compilations, state oil and gas agencies, and reservoir studies.

The Dwight's "DOGR" (Dwight's Oil and Gas Reports) database contains gas production and pressure data at the individual well completion level. (Oil production is included in DOGR as well, but is often reported only at the lease level). This database will be used to calculate productive gas area (number of sections) and average current gas well spacing. Periodic pressure data in this database can also be used to estimate current reservoir pressure.

The GRI Gas Composition and Tight Gas databases will also be incorporated into GASIS. The Gas Composition database was developed by EEA from the U.S. Bureau of Mines gas sample database, which contains composition data for gas samples from over 15,000 wells (Hugman and others, 1993a). The GRI Tight Gas Database identifies all of the reservoirs in non-Appalachian areas that fall within the Federal Energy Regulatory Commission tight gas formation areas (Hugman and others, 1993b).

**Source Directory Development**

Figure 7 lists the major subject areas that are currently planned for the database portion of the GASIS Source Directory. As discussed earlier, the Source Directory will document public domain and commercial databases that contain reservoir property, geological, engineering, production, and related data. Of primary interest are electronic databases at the well, reservoir, or field level. Also included are major electronic bibliographical compilations, such as the GEOREF database developed by AGI.

Each Source Directory record documenting a database will include the information shown in Figure 8. This will include: title, database type or major subject area, developer name and address, specific subjects, an abstract, time period covered, geographic area covered, number of records, availability, and format. Where available, specific data elements or categories will be listed.

In developing the Source Directory, several large existing database directories were researched, including the Earth Science Data Directory (ESDD) developed by the U.S.G.S.

**Software and Prototype Development**

The GASIS CD-ROM will include Windows-based software that will allow manipulation of both the reservoir database and the Source Directory information. The software is being developed using the Foxpro commercial software development package.

Most of the GASIS software development has been completed and is being tested and demonstrated as part of the GASIS "prototype." The prototype consists of test versions of the reservoir database and Source Directory datasets and the software for query

and retrieval. The prototype reservoir database covers the Rocky Mountain region and contains the full GASIS data matrix (all GASIS data elements and formats). It is populated for development purposes primarily by the information included in the Rocky Mountain Gas Atlas.

The software contains query and retrieval, display, report, and data export functions. Basic queries by state, basin, or field name will be assisted by scrolling selection lists. A detailed query screen will allow record selection on the basis of any data field (such as depth, cumulative production, or geological age.) Logical operators can be applied to any numeric data element or combinations of elements. (An example would be "all reservoirs in the Green River Basin with depths greater than 10,000 feet and porosities greater than 10 percent.) Data can be displayed on the screen in either a single record format or "browse" mode with one row for each record. Data sets can be exported in standard formats for manipulation with other software packages. Export format options will include ASCII, Lotus, and dBASE.

**Reservoir Studies**

A major reservoir study effort is underway to improve the coverage and quality of geological and engineering data in selected areas. A total of about 400 reservoir studies are currently planned and cover portions of the Mid-Continent, Texas, the Central and Eastern Gulf Coast, and the Rockies. No studies are planned for the Gulf of Mexico or Appalachian regions. The Gulf of Mexico Atlas project is expected to produce an excellent dataset, and field or reservoir studies in the Appalachian states are not planned for GASIS because of the need to first incorporate the information collected in the atlas project.

As summarized in Figure 9, a large dataset of geological and engineering information is being collected for each studied reservoir. These parameters include net pay, porosity, permeability, initial pressure, and gas and fluid properties. In addition to reservoir averages, an observed range of values is also reported for major parameters. A geological "type well" for each reservoir is also being selected and documented in the database.

A primary consideration in prioritizing the reservoir study effort is to address the "reservoir definition" issue in certain regions. Reservoir definition is the identification of the completions that produce from a reservoir, and is a serious problem in the Mid-Continent, South Louisiana and some other areas. In some states, reservoir level production data are not reported by the regulatory agency. To create a reservoir level production database in these areas, it is necessary to sum well level production within each reservoir using the reservoir name information. In many cases the reservoir name on the well record is either missing or inadequate to correctly define a reservoir. For example, the "reservoir name" may be a geological age such as "Pennsylvanian" that may contain multiple reservoirs in a field. Reservoir definition problems can be dealt with only through detailed log correlation and production database modification.

Figure 10 shows the current or potential GASIS reservoir study areas in the Mid-Continent, Texas, and the Central and Eastern Gulf Coast. The Mid-Continent effort is concentrating on the Anadarko Basin, the major gas producing basin in the region. Other basins where studies are planned are East Texas, the Arkla Basin, and the Mid-Gulf Coast Basin. Future GASIS studies within the area shown in Figure 10 may target the Arkoma Basin and portions of the Permian Basin and South Texas.

The GASIS Mid-Continent reservoir study effort (including the Texas Panhandle) is nearing completion and will include evaluation of approximately 200 10-plus Bcf gas reservoirs. The project has included a comprehensive reservoir definition effort targeted on the "problem" stratigraphic intervals of Pennsylvanian age. Figure 11 shows the distribution of reservoir studies by Gas Atlas play in the Anadarko Basin. Figure 12 shows the map distribution of reservoir studies in the Oklahoma portion of the Anadarko. The reservoir definition and stratigraphic work in this area alone will be one of the major contributions of the GASIS project.

A significant portion of the reservoir study effort will be directed toward analysis of low permeability plays and reservoirs, especially in areas other than the Mid-Continent. Improvement of the scope, coverage, and reliability of tight gas data will allow DOE to more effectively evaluate their research in this area. Our work in the Green River Basin and elsewhere in the Rockies will be designed to complement and incorporate the tight gas log analysis work done by the Scotia Group of Dallas for METC over the past few years. (Scotia Group, 1993).

### Identification of Data Sources

An effort is being made to identify and evaluate sources of low permeability reservoir data that could be used for database development and resource characterization. A large amount of data have been compiled by DOE, GRI, the USGS, and other groups. Much of this data has been collected and reported at the well or sample level, rather than the reservoir level. An example of this type of data is the rock mechanics and reservoir property data collected by GRI on cooperative tight gas research wells.

## FUTURE WORK

### Reservoir Studies

Studies of 10-plus Bcf gas reservoirs are either underway or planned for 1995 for East Texas, North Louisiana, the Mid-Gulf Coast Basin, and the Green River Basin. The North Louisiana and Gulf Coast studies will target conventional reservoirs in major gas-prone plays, while the East Texas studies will include evaluation of tight reservoirs in the Cotton Valley and Travis Peak.

The Green River Basin studies will include both conventional and tight reservoirs, but will emphasize tight sandstone reservoirs in the Mesaverde Group and several other intervals.

### Database Development

Much of the development of the GASIS reservoir database will be accomplished in 1995. Major components of this work include final processing of the Dwight's completion and reservoir databases with data through 1994, evaluation and incorporation of the Appalachian and (initial) Gulf of Mexico Gas Atlas data, updating the South Louisiana reservoir production database developed for the atlas project, development of "processed data elements" such as productive area, and processing of the GRI tight gas and gas composition data.

Other projects include evaluation of rock mechanics data collected by GRI on their cooperative research wells, determination of available data in the FERC tight gas files, development of a method to create data source codes for key data elements, implementation of quality control algorithms, and finalization of GASIS software.

## REFERENCES


Bebout, D.G., 1993, "Atlas of Major Central and Eastern Gulf Coast Gas Reservoirs," 94 page atlas and computer database, Texas Bureau of Economic Geology, Austin, TX.

Bebout, D.G., 1993, "Atlas of Major Mid-Continent Gas Reservoirs," 91 page atlas and computer database, Texas Bureau of Economic Geology, Austin, TX.

Hugman, R.H., P.S. Springer, and E.H. Vidas, 1993, "Chemical Composition of Discovered and Undiscovered Natural Gas in the United States - 1993 Update," prepared for Gas Research Institute, Report Numbers 93-0456.1 through 0456.3 (three volumes and database on diskette).

Hugman, R.H., E.H. Vidas, and P.S. Springer, 1994, "DOE GASIS Reservoir Data System: User Needs Assessment and Recommendations," report prepared by Energy and Environmental Analysis for DOE/METC, September 14, 1994.

Hugman, R.H., P.S. Springer, and E.H. Vidas, 1993, "Tight Gas Field, Reservoir, and Completion Analysis of the United States - 1993 Update," prepared for Gas Research Institute, Report Numbers 93-0364.1 and 0364.2 (two volumes).

Kosters, E.C., and D.G. Bebout, 1989, "Atlas of Major Texas Gas Reservoirs," 161 page atlas and computer database, Texas Bureau of Economic Geology, Austin, TX.

Robertson, J.M., and R.F. Broadhead, 1993, "Atlas of Major Rocky Mountain Gas Reservoirs," 201 page atlas and computer database, New Mexico Bureau of Mines and Mineral Resources, Socorro, NM.

Scotia Group, 1993, "Reserves in Western Basins. Part 1: Greater Green River Basin," topical report prepare by the Scotia Group, Dallas, for DOE/METC, October, 1993.

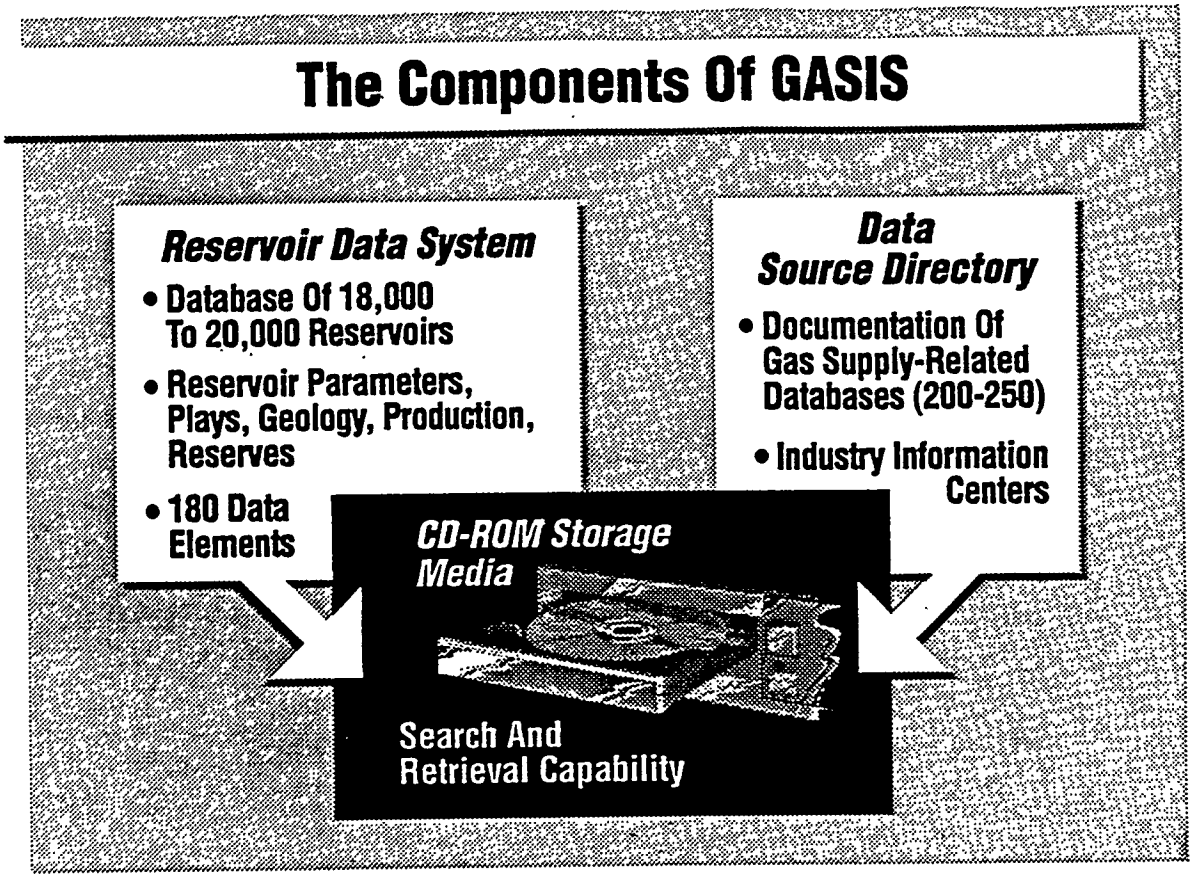


**Figure 1.** The Components of GASIS

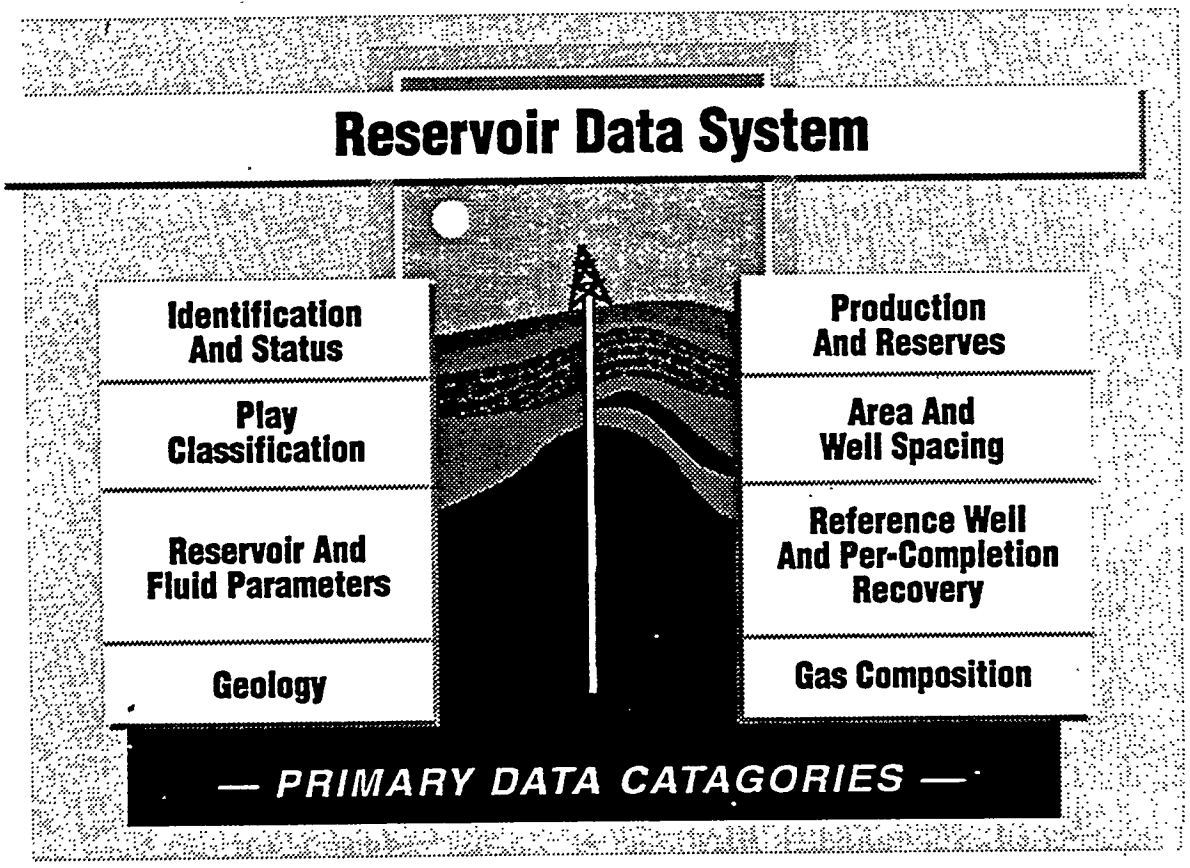


**Figure 2.** Reservoir Data System

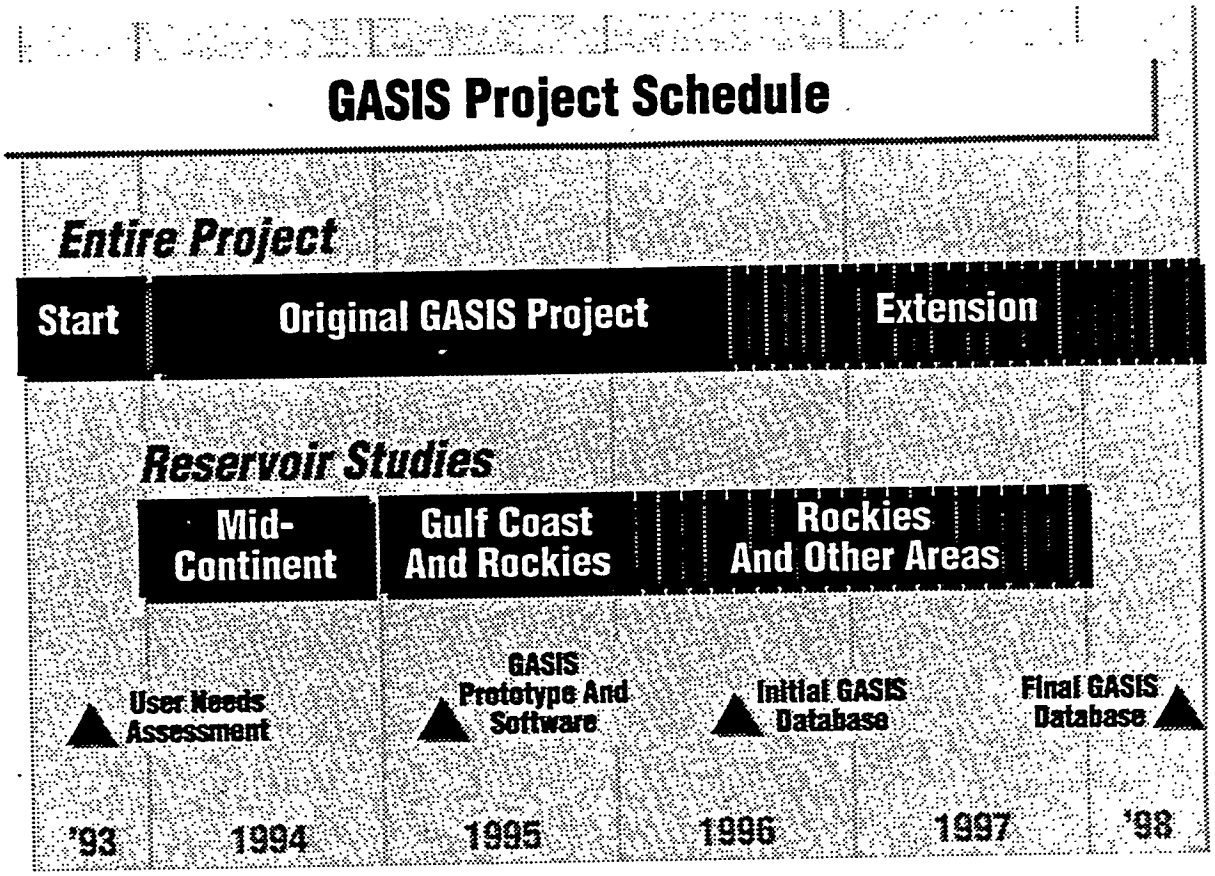


**Figure 3.** GASIS Project Schedule

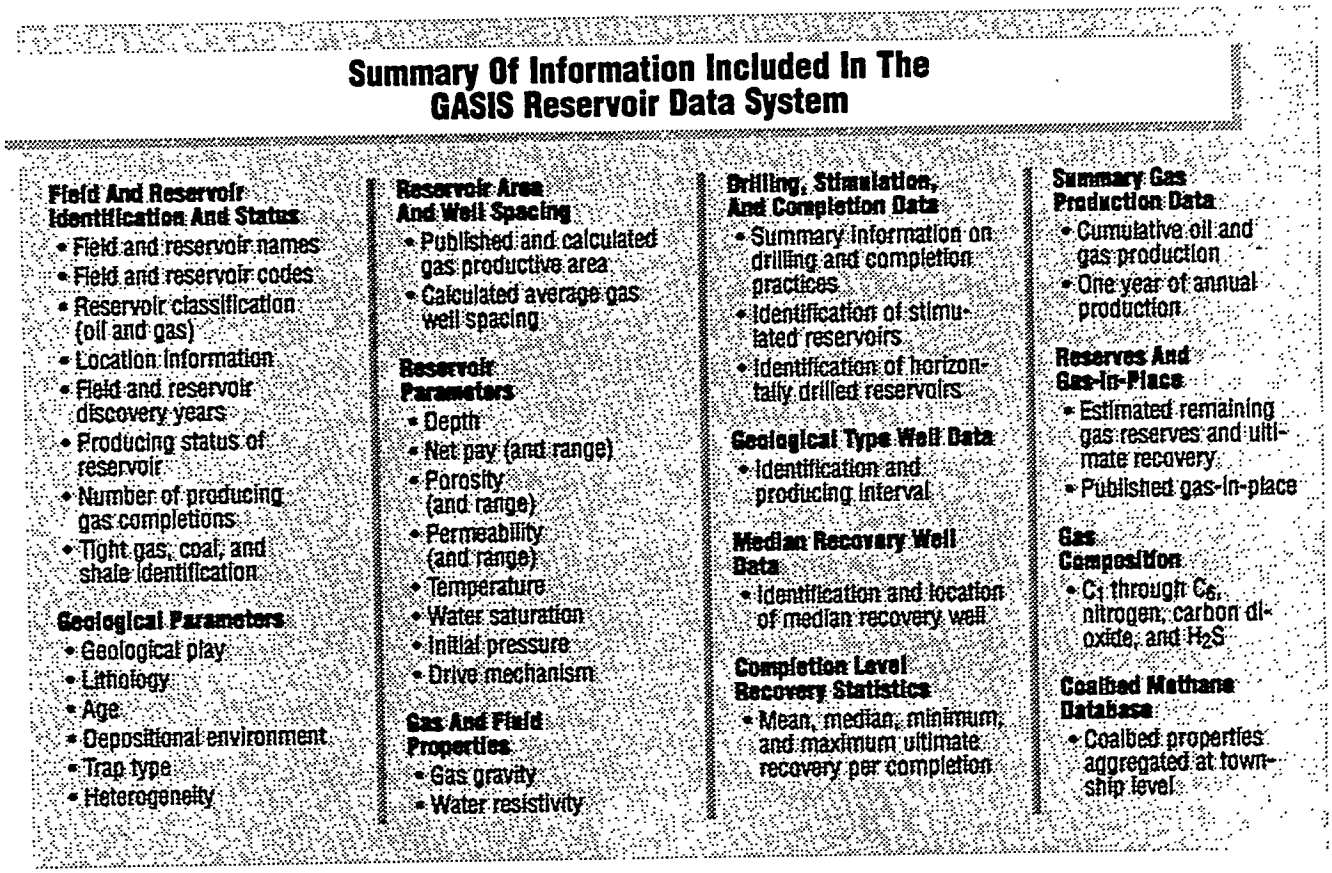


**Figure 4.** Summary of Information Included in the Reservoir Data System

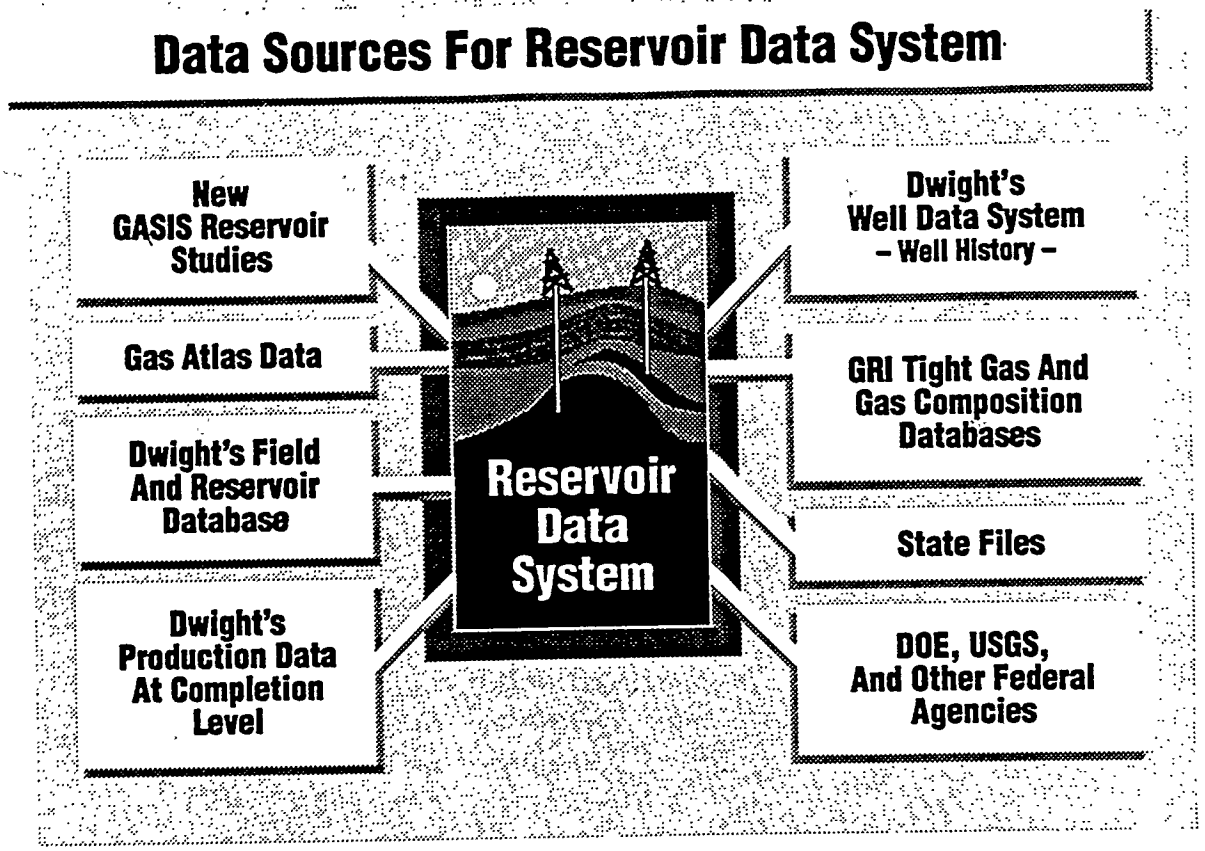


**Figure 5.** Data Sources for Reservoir Data System

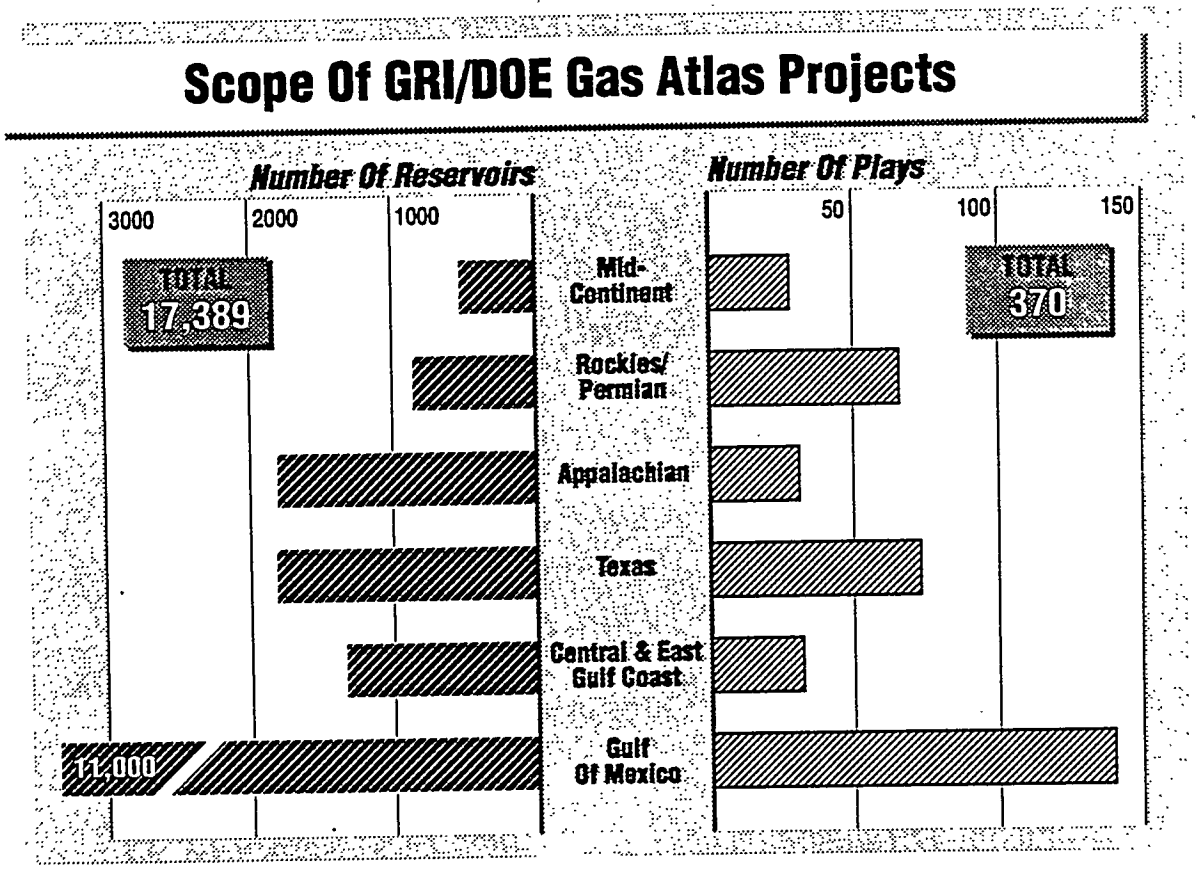


**Figure 6.** Scope of GRI/DOE Gas Atlas Projects

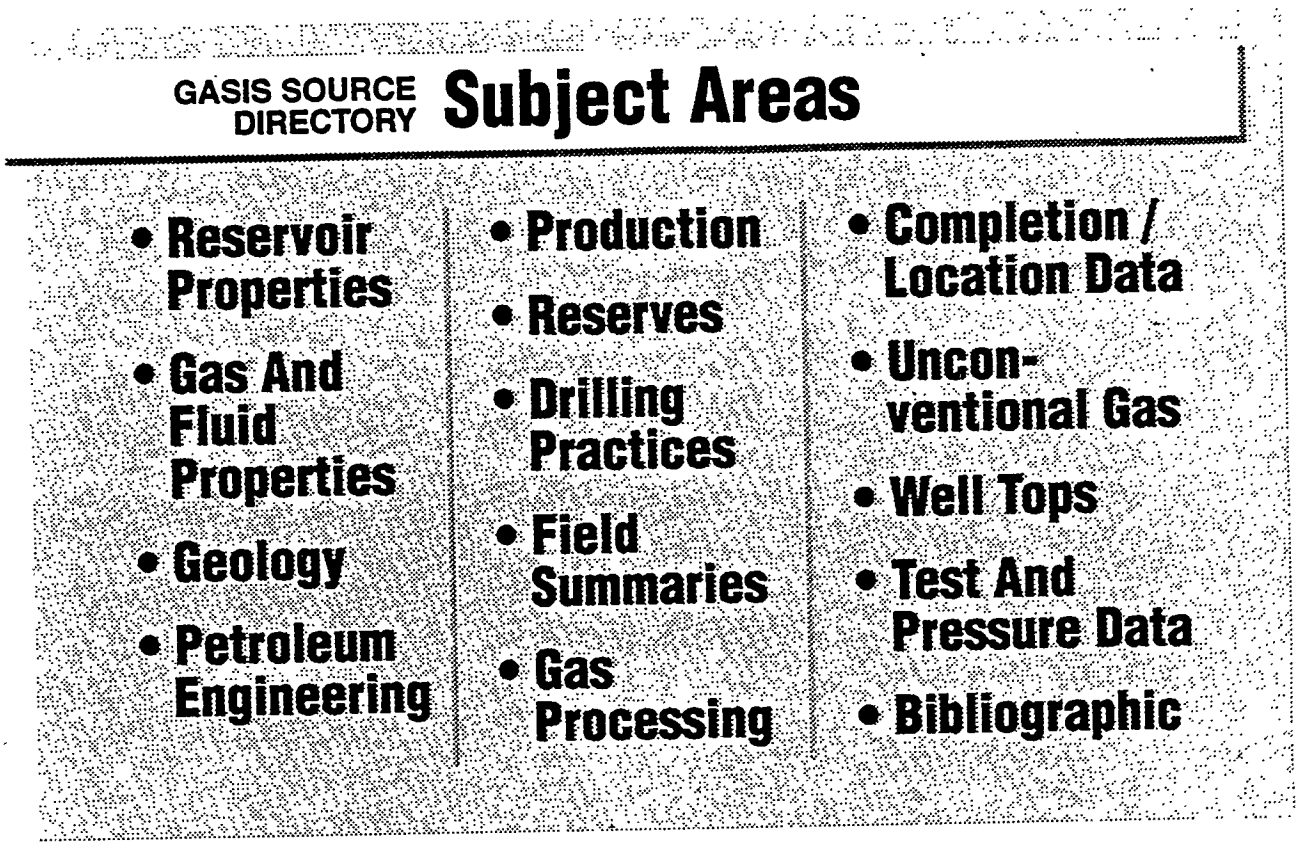


**Figure 7.** Major Source Directory Database Subjects

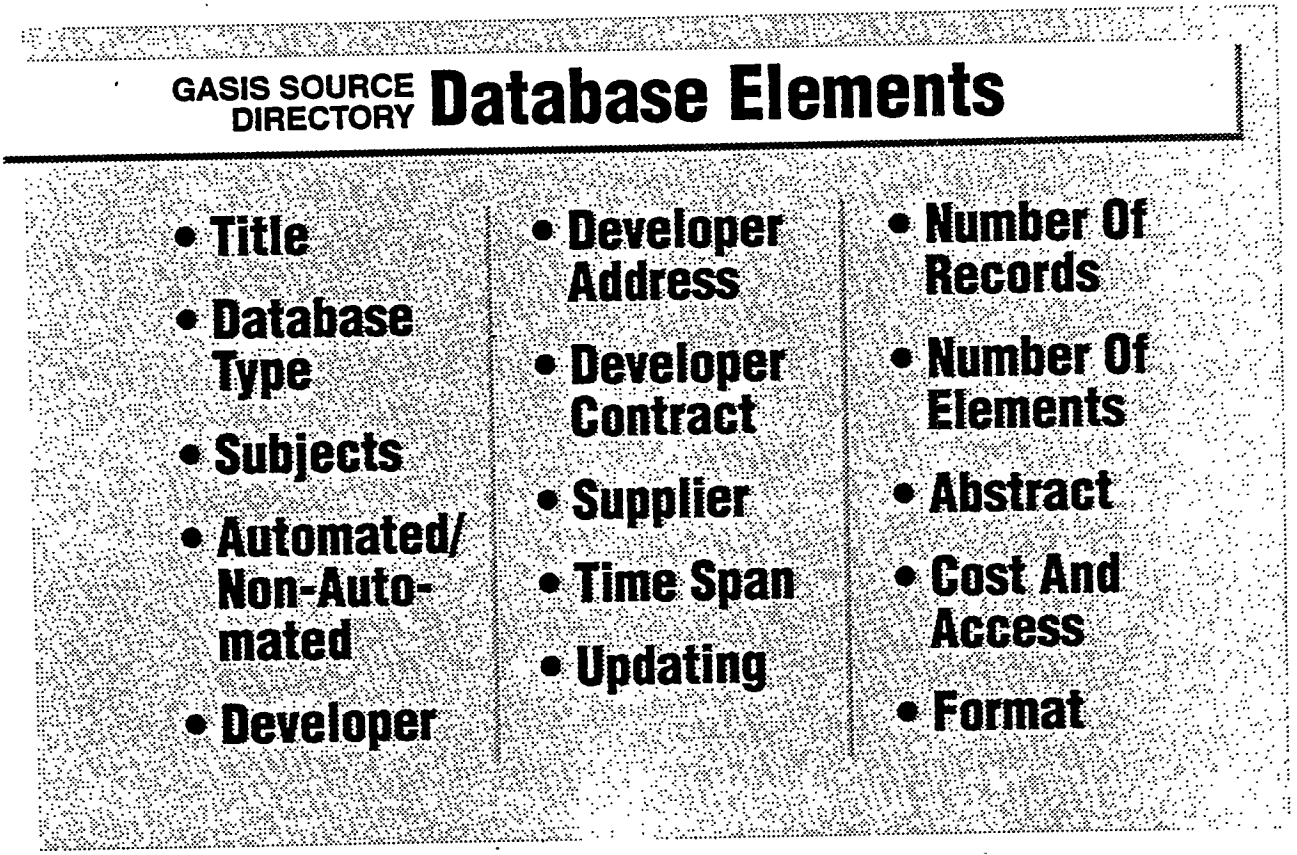


**Figure 8.** GASIS Source Directory Elements

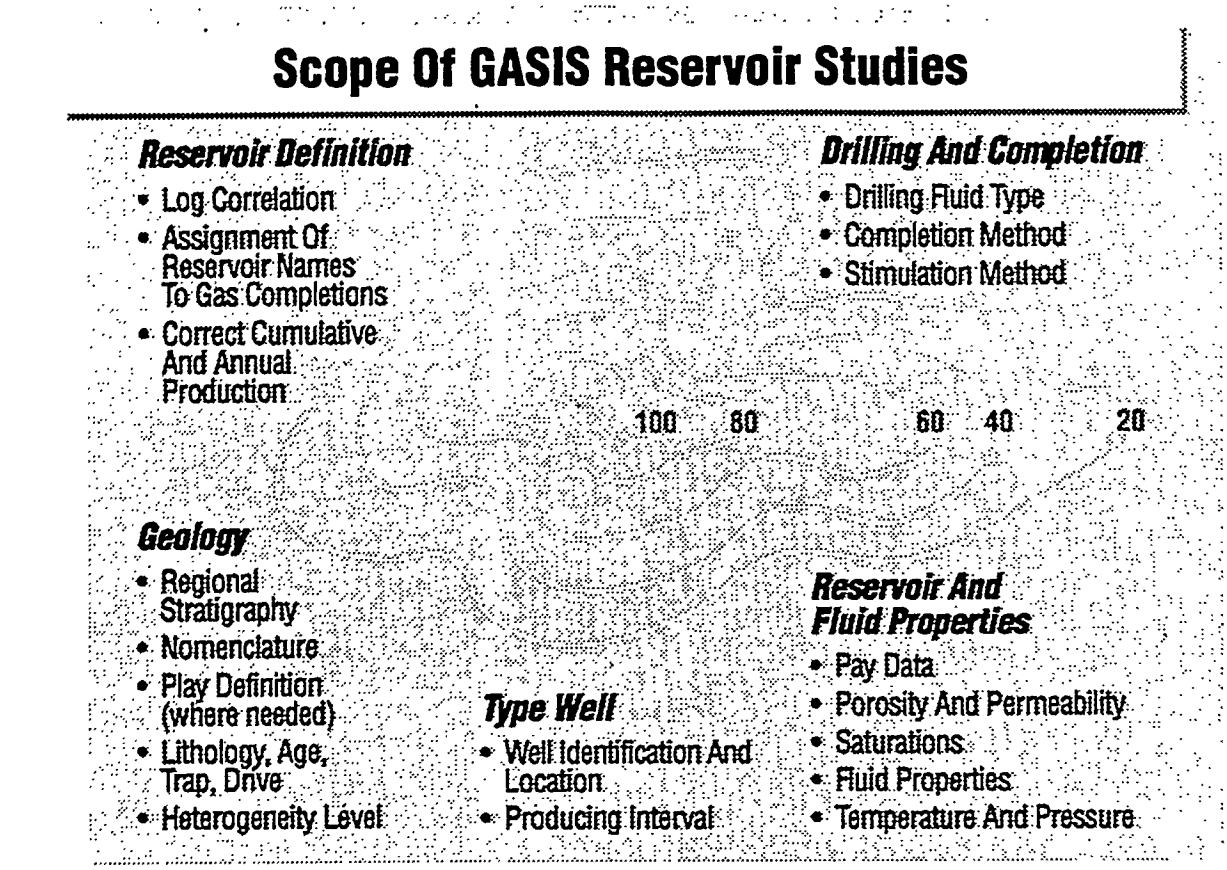


**Figure 9.** Scope of GASIS Reservoir Studies

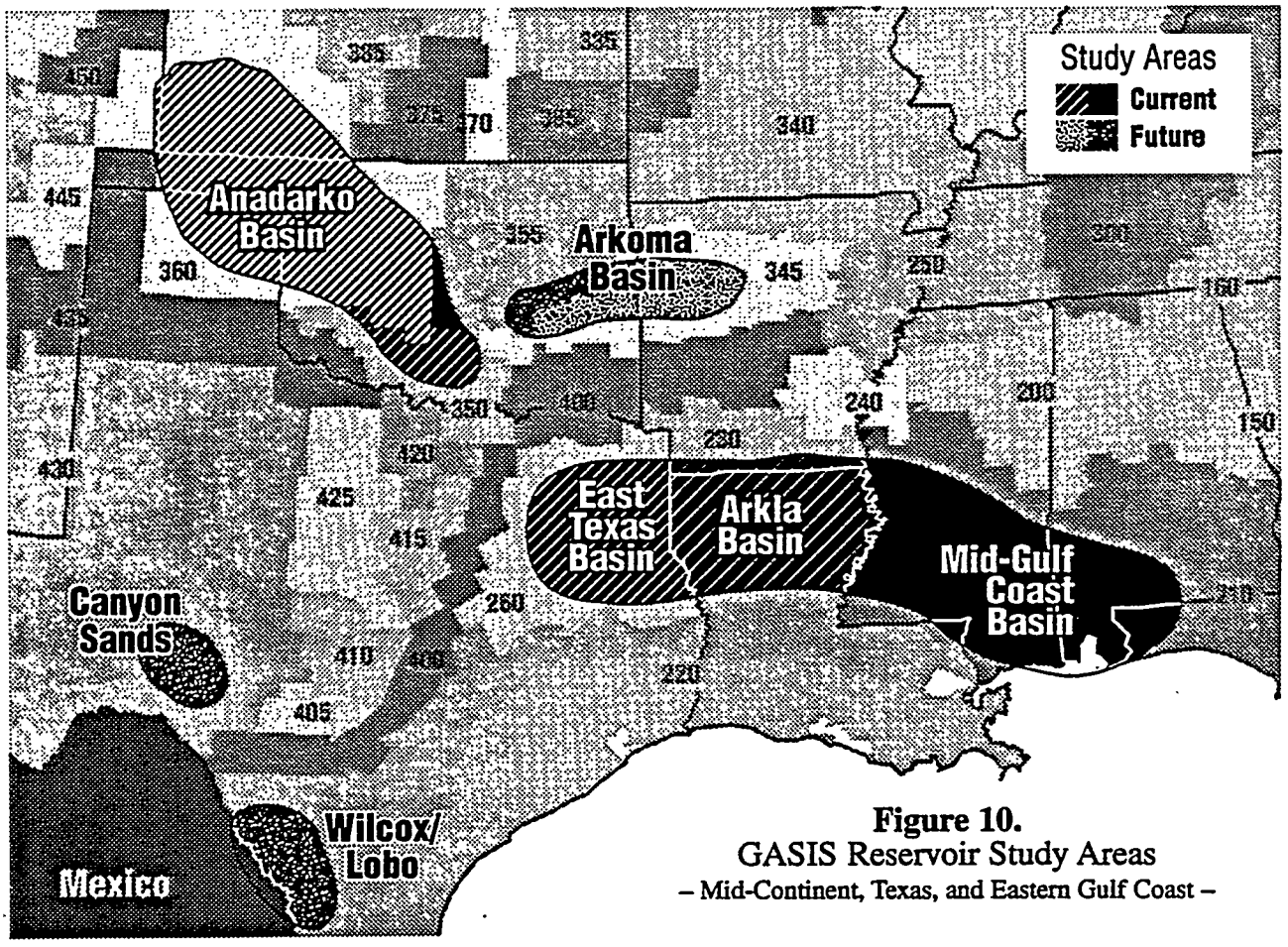


**Figure 10.**
GASIS Reservoir Study Areas
– Mid-Continent, Texas, and Eastern Gulf Coast –

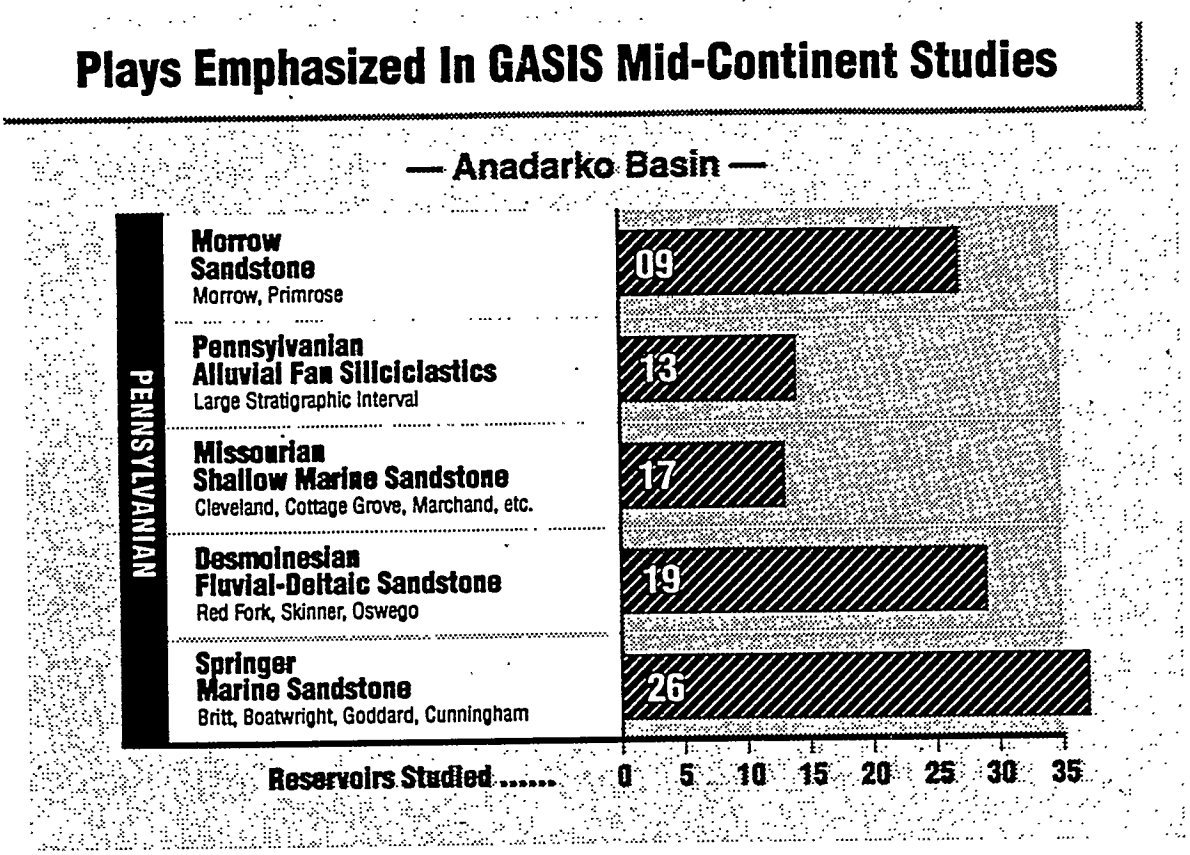


**Figure 11.** Plays Emphasized in GASIS Mid-Continent Studies

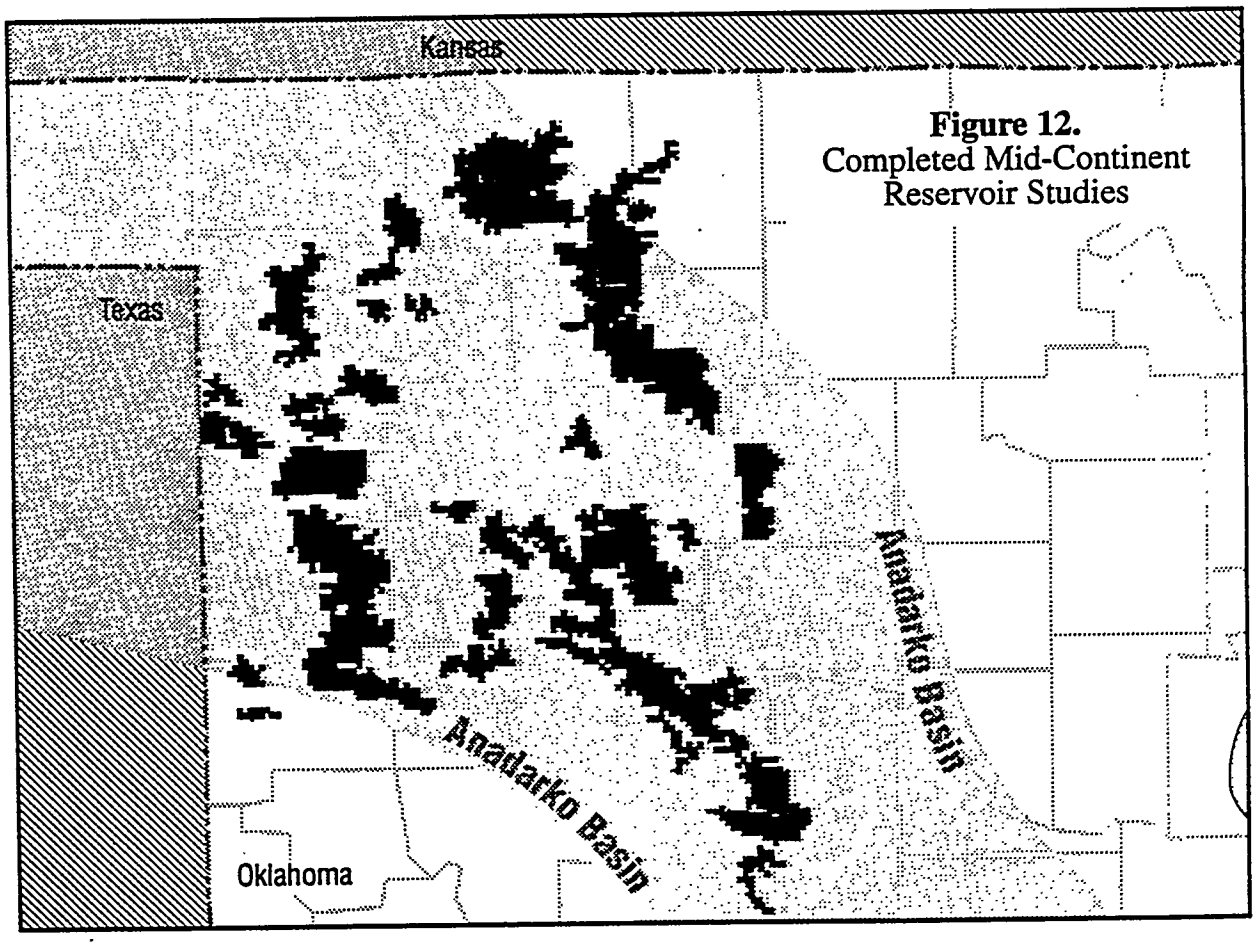


**Figure 12.**
Completed Mid-Continent Reservoir Studies

# Session 4A

## *Low Permeability Reservoirs — Low Permeability Reservoir Characterization*

# 4A.1 Multistrata Exploration and Production Study

## CONTRACT INFORMATION

| | |
|---|---|
| **Contract Number** | DE-AC21-89MC26026 |
| **Contractor** | The College of West Virginia<br>P.O. Box AG<br>Beckley, WV USA 25802-2830 |
| **Contract Project Manager** | Linda K. Hawkins |
| **Principal Investigators** | Ronald G. Brunk<br>John R. Maestas<br>Pat Parsons |
| **METC Project Manager** | Charles W. Byrer |
| **Period of Performance** | October 1, 1989, to March 31, 1995 |


## ABSTRACT

The objective of this project was to develop and verify a geotechnical/geostatistical approach to find natural gas resources and to verify the process by drilling, completing, testing, and producing wells located by the process.


## BACKGROUND INFORMATION

Research conducted on the Eccles 7.5' quadrangle in Raleigh County, WV, in 1990, pinpointed several target areas. Immediate landowners, gas companies, and mineral rights owners were contacted to determine their willingness to assist the College in conducting the research. Extensive talks were held and as a result, agreements were drawn up between the College and the owners. Test Well 1 (TW1) was completed in May 1991 and Test Wells 2 and 3 (TW2, TW3) in November, 1991. The wells were shut in for one year thereafter, while the parties involved negotiated agreements. The wells were placed on line at the close of fiscal year 1992. The following section summarizes the activities conducted in fiscal years 1993 and 1994.

## PROJECT DESCRIPTION

Activities for the Multistrata Project began in Fiscal Year 1993 with the placement of the three Test Wells into production full force. By turning all three wells in line October 1, 1992, gas began flowing as designed by the agreements negotiated in Fiscal Year 1992. All the parties involved began to see tangible results as the gas moved from the College's gathering lines into the systems of Ramco, Columbia, and Mountaineer Gas Companies.

The College of West Virginia began work as specified in the Field Test Plan for Phase II, Task 12. The TW1 and TW3 sites were successfully automated. The College coordinated the automation activities, which included selecting and installing electric motors and controls for each site. It also required electricians and Appalachian Power Company to set several poles, hang 5000 feet of line, and install two transformers.

Prior to running electricity to these sites, the pumps used to dewater the coal seams were operated on a manual basis. By running them 12 hours a day, three days per week, coal gas production increased an average 6 mcfd. Following automation, production from the coals increased another 4 mcfd on average. A number of pump rates and schedules were attempted in order to achieve maximum dewatering.

Water disposal has been addressed on a continuing basis, and permission has been granted from the State of West Virginia to apply water from the coal seams directly to the surface since the coal seam water has been analyzed and found to be potable. There are certain guidelines, of course, such as requirements to monitor the disposal, to avoid erosion, etc. Several meetings have been held with the State Oil & Gas Division and the Division of Environmental Protection, and the subject will continue to be discussed.

It should also be noted that water production from the coals is minimal. Water from the coals on TW1 averages about 2.2 bbls per pumping hour, and TW3 coal water is only 1.2 bbls per actual pumping hour. Based on swabbing and echometer tests done during workover, the water influx rate appears to be near 2 bbls per day from the coals on each well.

The most recent field activities in the WV Task involved the installation of a small 16hp compressor into the main CWV sales line. The purpose of this action was to observe the response of the coal zones to producing against 1-2 pounds suction pressure.

The results of compression near atmospheric pressure have been impressive with TW3 production quadrupling and TW1 coal gas increasing by a factor of 18. Pressure was held back to 25-30 psi on the deeper producing zones (sandstones and limestones) in order to prevent drowning these formations. Overall a 55% increase in gas production has been seen.

The College experimented with many approaches to dewatering the coal zones on these wells. The following general conclusions can be drawn from the research:

- As expected, dewatering greatly enhances gas production, tripling it within two weeks. Without continual dewatering efforts, production from these coals (Poca #3, Beckley) drops quickly in about 10 days to 0 mcfd.

- Long periods of pumping, in the range of 8-12 hours on followed by 8-10 hours off, are more beneficial to gas production than more elaborate timing schedules and methods (e.g. one hour on, one hour off throughout each 24 hour period).

- For coal zones in southern WV, experience indicates that standard pump jack units perform more effectively and efficiently than progressive cavity or rotary

pumps. The dangers of pumping dry, the accumulation of coal fines or other debris, and the rate of system shut-down/stoppage prove more damaging to the rotary pumps.

- Water production from CWV coal zones averages 12 bbls per day during peak dewatering efforts, and the water is potable.

**COMPARISON OF AVERAGE DAILY PRODUCTION LEVELS**
**Expressed in Thousands of Cubic Feet Per Day**

| | | Prior to Compression Jan 1994 | After Compression Jan 1995 |
|---|---|---|---|
| TW1 | Coal Zones | 1 | 18 |
| | Sandstone/Limestones | 40 | 40 |
| TW2 | Sandstone/Limestones | 9 | 10 |
| TW3 | Coal Zone | 5 | 17 |
| | TOTALS | 55 | 85 |

## NEW PROJECTS

As the College of West Virginia refined and perfected its processes, the Department of Energy determined that the College's work in West Virginia could produce major benefits in other areas. Two projects were developed including the establishment of methane gas wells in Alaska, and a Brine Separation project in Poland.

Alaska has nearly 200 isolated Native villages who must rely primarily on diesel fuel to provide heat for the winter. They import nearly 250,000 gallons of fuel per year, and must spend from 33% to 50% of their annual salaries for fuel. The State of Alaska has three trillion tons of coal reserves. The installation of gas wells in this coal rich area will bring the price of electricity to nearly $.06 from the current rate of $.76 per kilowatt.hour. The methane gas well is expected to provide for the power needs of a tribe for nearly thirty years.

The disposal of brine is a major environmental problem. The College has entered into a working relationship with Aquatech Services, Inc. of California. This company has developed a cost effective strategy for reducing or disposing of brine through a reserve osmosis process. The Company has completed phase one, a demonstration project, in Katowice, Poland. The highlights include the reduction of brine water into the environment by creating both potable water and commercially usable salt.

## REFERENCES

1. Overbey, W.K., T.K. Reeves, S.P. Salamy, C.D. Locke, H.R. Johnson, R. Brunk, and L.K. Hawkins. A Novel Geotechnical/ Geostatistical Approach for Exploration and Production of Natural Gas from Multiple Geologic Strata. Topical report submitted to U.S. Department of Energy, under Contract DE-AC21-89MC26026, May 1991.

## 4A.2 Brine Disposal Process for Morcinek Coal Mine

### CONTRACT INFORMATION

| | |
|---|---|
| **Contract Number** | DE - AC21 - 89 MC 26026-20-13 |
| **Contractor** | Aquatech Services, Inc.<br>7745 Greenback Lane<br>Citrus Heights, California 95610<br>P.O. Box 946<br>Fair Oaks, California 95628<br>Phone (916) 723 - 5107<br>Facsimile (916) 723 - 6709 |
| **Other Funding Sources** | Environmental Protection Agency |
| **Contract Project Managers** | John H. Tait, Aquatech Services, Inc.<br>Linda K. Hawkins, College of West Virginia |
| **Principal Investigator** | John H. Tait |
| **METC Project Manager** | Charles W. Byrer |
| **Period of Performance** | July 1994 to March 1995 |

**FY94 Program Schedule**

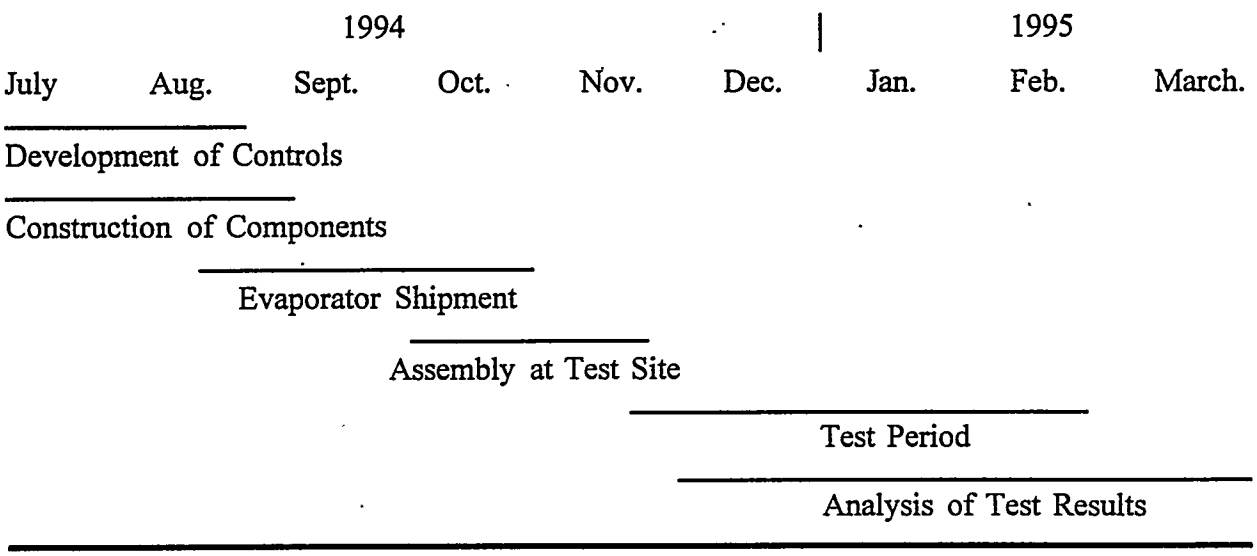

## ABSTRACT

This paper describes the work to develop a commercial brine disposal process for the Morcinek mine, located 45 km south of the city of Katowice in Poland. Currently, brine is discharged into the Odra river and methane from the mine is released into the atmosphere. The process would use the released methane and convert a large percentage of the brine into potable water for commercial use. Thus, the proposed process has two environmental benefits.

The brine salinity is about 31,100 ppm. Major brine components are Na (10,300 ppm), Ca (1,170 ppm), Mg (460 ppm), $Cl^-$ (18,500 ppm) and $SO_4^{2-}$ (252 ppm). Present in smaller amounts are K, S, Sr, B, Ba and $NO_3^-$.

The process integrates a reverse osmosis (RO) unit and a submerged combustion evaporator. Extensive studies made at the Lawrence Livermore National Laboratory established the pretreatment method of the brine before it enters the RO unit. Without adequate pretreatment, mineral phases in the brine would become supersaturated and would precipitate in the RO unit. The pretreatment consists of first adding sodium carbonate to increase both the pH and the carbonate concentration of the brine. This addition causes precipitation of carbonate solids containing Ca, Mg, Sr, and Ba. After filtration of these precipitates, the fluid is acidified with HCl to prevent precipitation in the RO unit as the brine increases in salinity.

A chemical modeling computer code was used to calculate the mineral saturation states during the pretreatment and RO processes. After an optimum pretreatment strategy was found, the results were verified by means of laboratory experiments using a simulated brine.

In the commercial configuration, the brine from the RO unit would be pumped into a submerged combustion evaporator. In submerged combustion evaporation, a mixture of mine gas and air is combusted in a burner that is placed above a liquid bath. Combustion takes place above the brine level while the combustion gases are vented through the brine. An evaporator was successfully tested during extended Phase I operations since October 1994.

The evaporator had a capacity to evaporate 50 $m^3$/day (315 bpd) of brine. However, during the Phase I experiments, the evaporator operated at a capacity of 33 $m^3$/day (208 bpd) with limited combustion air blower capacity and reduced methane content in the mine gas stream. The mine gas available for the test had an average methane concentration of 50.4 per cent and a flow rate of 3.4 $m^3$/min (120 $ft^3$/min).

Specifications were developed during Phase I of the project for both a Phase II pilot RO demonstration unit and a full-scale combined RO and evaporator commercial unit .

In commercial operations, part of the heat in the exhaust stack of the evaporator will be used to preheat the brine feed stream to the RO unit, and to heat the concentrated brine flowing from the RO unit into a submerged combustion evaporator.

[1] Geochemist, Lawrence Livermore National Laboratory, Livermore, California.

[2] Technical Director, Aquatech Services, Inc., Fair Oaks, California.

[3] Principal, Aquatech Services, Inc., Fair Oaks, California.

In a typical operation, a brine feed stream of 1,000 $m^3$/day (6,291 bpd) with a total dissolved salt concentration (TDS) of 31,100 ppm would be separated into a product stream of 585 $m^3$/day (3,680 bpd) with a TDS of 500 ppm and a concentrated brine stream of 415 $m^3$/day (2,610 bpd) with a TDS of 74,300 ppm. The submerged combustion evaporator concentrates this latter stream to a concentration of 250,000 ppm and reduces the volume to 124 $m^3$/day (780 bpd).

Energy costs to operate the reverse osmosis unit are primarily pumping costs of approximately 0.03 MJ/kg (13 Btu/lb). The submerged combustion evaporator uses approximately 2.75 MJ/kg (1,182 Btu/lb) to evaporate water from the brine. The cost to process this type of brine is approximately \$4.72/$m^3$ (\$0.75/barrel) at a methane price of \$0.044/$m^3$ (\$1.25/mcf) and an electrical cost of \$0.04/kwh.

The Phase II pilot demonstration of the RO and evaporator system is expected to start at the Morcinek mine this summer. The demonstration will verify process variables and operating costs for a commercial-scale process.

## Introduction

The treatment process for coal mine waste water (brine) uses a reverse osmosis (RO) unit and a submerged combustion evaporator. Water from the mine (Figure 1) is first pumped through a pretreatment stage, where it is chemically conditioned to avoid scaling and fouling of the RO membranes. The RO unit produces potable water and a concentrated waste stream which is fed into a submerged combustion evaporator, in which evaporation of water produces a mixture of saturated brine and suspended salt crystals. The present plan is to pump the mixture into an abandoned mine shaft. The mixture also could be processed further by a dryer that could dry the mixture to a low moisture salt.

During the Phase I activities of this project, the brine from the Morcinek mine in Upper Silesia, Poland was delivered to a submerged combustion evaporator. The evaporator operated at the mine from October 1994 to December 1994. During the planned Phase II pilot demonstration, both a reverse osmosis unit and the evaporator will be integrated into a single brine treatment process. The Phase II pilot demonstration will establish operating costs and technical data under local field conditions. The Phase II demonstration is expected to begin during the summer of 1995. Upon successful completion of the Phase II demonstration, a commercial system will be designed that would treat the entire mine effluent of 2,500 $m^3$/day (15,730 bpd).

This paper discusses the pretreatment method developed at the Lawrence Livermore National Laboratory and the results of the submerged combustion evaporator test at the Morcinek mine.

## Reverse Osmosis Pretreatment

A computer chemical model is used to simulate the pretreatment and reverse osmosis processes. The simulation provides a cost-effective method for evaluating potential pretreatment techniques such as water softening, the addition of threshold or chelating anti-scaling compounds, and other types of scale inhibitors. The model can also be used to simulate fluid passage through the reverse osmosis membrane to predict whether inorganic scale will form. When combined with pilot-scale laboratory simulations, the simulation provides a method for optimizing the treatment process by selecting the best treatment method and by minimizing the amounts of pretreatment chemicals that are used.

The chemical modeling codes [1,2] contain provisions for calculating aqueous phase speciation, mineral saturation states, kinetically controlled mineral dissolution and precipitation reactions, redox disequilibria, surface charge and

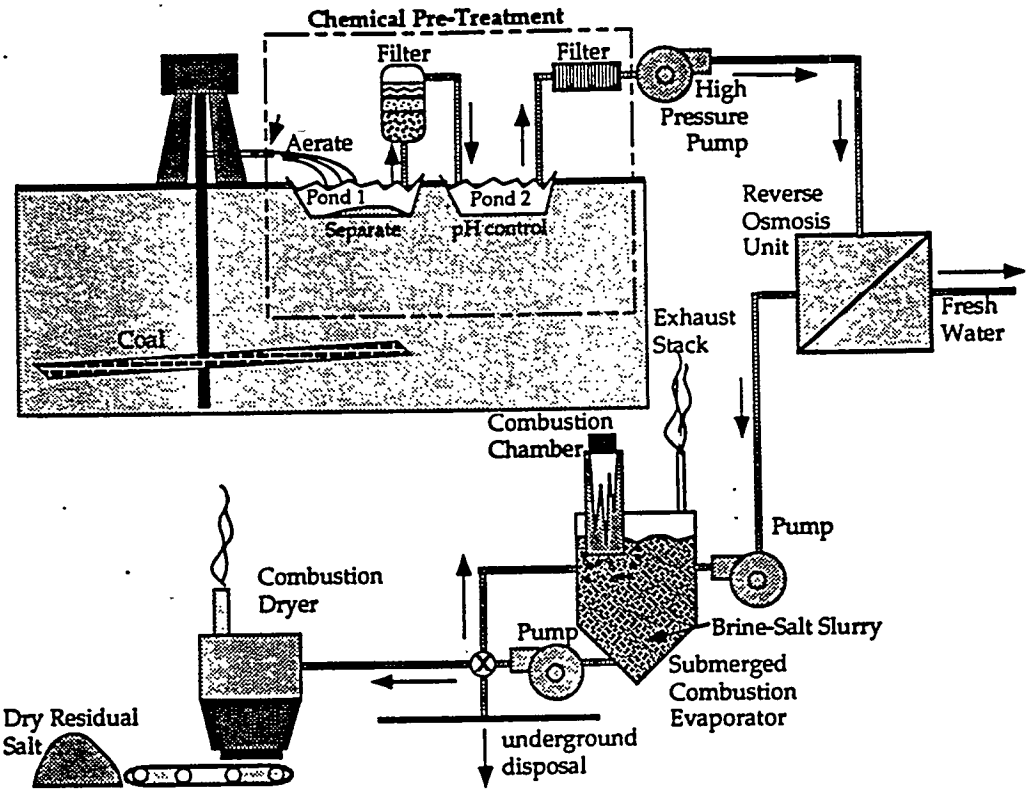


**Figure 1. Schematic of Coal Mine Brine Treatment Process**

**Table 1. Concentrations of Elements during Pretreatment Process**

| Element | Waste Water | After $Na_2CO_3$ (Predicted) | After RO (Predicited) |
|---|---|---|---|
| Na | 10,300 | 10,250 | 24,470 |
| Cl | 18,500 | 18,500 | 44,230 |
| $SiO_2$ | 6.5 | 1.5 | 4.6 |
| Mg | 460 | 445 | 1,062 |
| Ca | 1,170 | 923 | 2,205 |
| Sr | 42 | 2.3 | 5.6 |
| Ba | 2 | 0.05 | 0.11 |
| pH | 6.6 | 7.5 | 5.9 |
| TDS | 31,100 | 31,120 | 74,300 |

complexation, and gaseous equilibria (the major chemical processes taking place during pretreatment). The thermodynamic database which supports the codes has data for 850 aqueous species, 920 solids, and 80 gases, and includes Pitzer data for brines [3].

The computer models are currently limited in some applications by the lack of: (1) thermodynamic data at high temperatures and high concentrations for some species; (2) good kinetic data for some mineral precipitation processes; and (3) data for surface complexation reactions.

The use of chemical modeling codes provides important advantages over less rigorous methods of estimating scaling potential of brines. For example, methods which use the Langlier index [4] or Stiff-Davis index [5] are valid only for a narrow compositional range of "standard" brines. These types of methods do not work well with fluids that contain significant amount of species which form strong ion pairs with $Ca^{2+}$, and also do not account for other species, such as carboxylic acids, which are often present and erroneously included in the measured alkalinity [6]. Both of these effects can give rise to substantial error in the estimated carbonate saturation index.

In contrast, the chemical modeling codes explicitly account for ion-ion interactions and the effect of other species on alkalinity measurements. They also can be used to calculate the effects of adding anti-scaling agents, such as chelating agents, to these fluids.

## Example of Pretreatment Simulation

A brine having the composition shown in Table 1 is saturated with calcium carbonate. Without proper pretreatment, the brine will supersaturate and begin precipitating calcite if the solution is concentrated in the reverse osmosis unit. Therefore the brine is treated by adding sodium carbonate, which causes the pH to rise and the carbonate concentration to increase. Both effects cause precipitation of carbonate minerals which contain Ca, Mg, Sr, and Ba. These precipitates are filtered out. The solution is then acidified and passed into the RO unit. The chemical model is used to determine the amount of sodium carbonate to be added to the brine in order that the fluid does not re-saturate with carbonate minerals during the reverse osmosis concentration. Figure 2a shows the elemental concentration and Figure 2b indicates the predicted pH during this process.

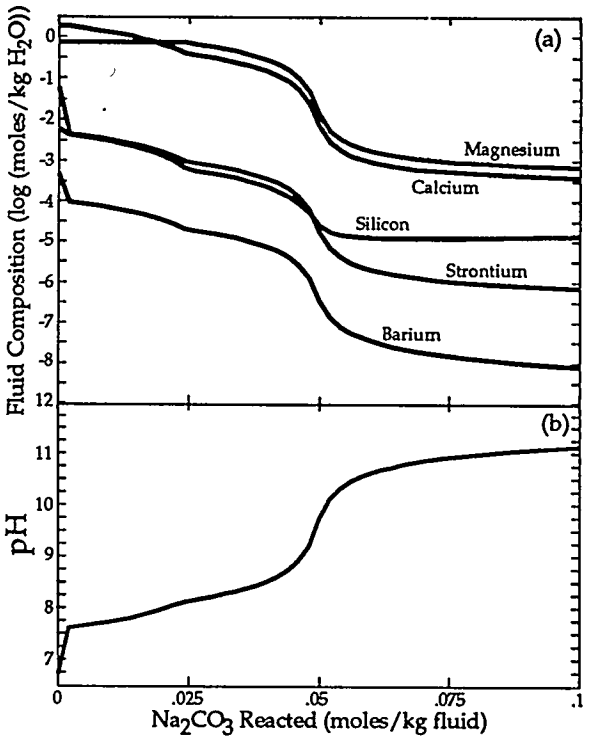


**Figure 2. Simulation Process of Adding $Na_2CO_3$ to Brine**

Alternatively, the chemical models could be used to predict the amounts of anti-scalant chemicals which need to be added to prevent scaling. The cost of each method can be calculated based on the amounts of additives needed and their associated processing costs. The most cost-effective method can then be selected for any given application.

The simulations should always be supported with pilot scale laboratory tests to ensure that real fluids behave as the simulator predicts. The tests were made at the Lawrence Livermore National Laboratory with a simulated brine of the same composition as the Morcinek brine.

**Submerged Combustion Evaporation**

After the reverse osmosis process, the concentrated brine is delivered to a submerged combustion evaporator. In submerged combustion evaporation, a mixture of coalbed gas and air is combusted in a burner that is placed above a brine bath. Combustion takes place above the brine level [7], while the combustion gases are vented through the brine thereby evaporating part of the brine in the evaporator. Figure 3 is a photograph of the evaporator at the Morcinek mine. In the foreground is the blower for the combustion air. The small building to the right houses the process controls.

The submerged combustion evaporator uses the combustion energy in an efficient manner to evaporate the brine. The fuel and air enter the submerged combustion evaporator at ambient temperature and the exhaust gases leave the stack at approximately 85°C (185°F). The brine consists of a mixture of a saturated solution and a suspension of solid salt particles. The particles remain in suspension as a result of the stirring action of the combustion gases and the action of a recirculation pump.

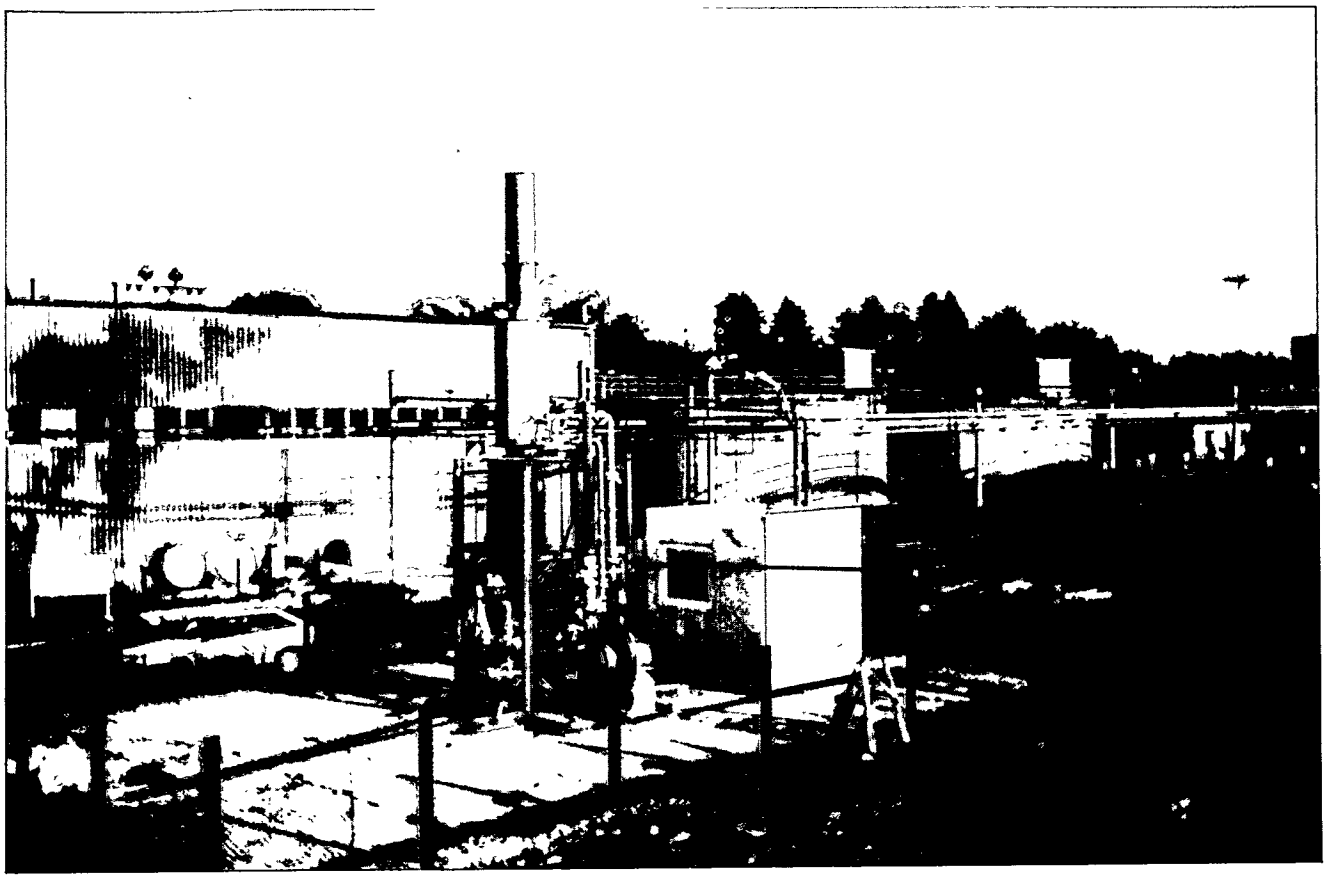

**Figure 3. Photograph of Submerged Combustion Evaporator at Morcinek Mine**

Because the particles in the evaporator fluid would settle out and form a deposit upon shutdown of the evaporator, the unit is equipped with controls that drain the unit during shutdown.

Typically, the submerged combustion evaporator operates with excess air ranging from 50 to 75 per cent [7]. In this case the oxides of nitrogen concentration ranges from 21 to 13 ppm while the carbon monoxide concentration ranges from 30 to 15 ppm. In the test at the Morcinek mine, the blower operated at 3,000 RPM which is less than the rated speed of 3,600 RPM. The reduction of speed was caused by the lower electrical frequency of 50 cycles per second compared to the U.S. 60 cycles per second. As a result of this speed reduction, the average brine flow to the evaporator was reduced from 50 $m^3$/day (315 bpd) to 33 $m^3$/day (208 bpd). Furthermore, the methane gas from the mine was substantially diluted. Measurements of the gas composition indicated that the methane concentration ranged from 49 to 52 per cent. The average methane concentration during the test was 50.4 per cent. The dilution of the methane required modification of the gas-air piping and the control strategy.

The oxides of nitrogen and the carbon monoxide from the exhaust stack were measured at both 72 and 128 per cent of excess air. At 128 per cent of excess air, the concentration of the oxides of nitrogen was 13 ppm while the carbon monoxide concentration was 14 ppm.

Heat losses by convection and conduction from the submerged combustion evaporator are less than 1.5 per cent of the energy input. Another loss is the heat carried away by the brine that is discharged from the evaporator. Depending on the ratio of the salt concentrations of the brine in the evaporator and in the feedstream, the heat carried by the discharged brine ranges from 0.4 to 2 per cent of the heat supplied.

The heat added to evaporate water from the brine mixtures typically ranges from 2.65 to 2.75 MJ/kg (1,137 to 1,182 Btu/lb) depending on the gas to air ratio. The maximum value of this range translates to 90 $m^3$ methane per $m^3$ brine (0.51 mcf/barrel) [7,8]. At the Morcinek test, the gas consumption was 174.2 $m^3$ per $m^3$ brine with a gas consisting of 50.4 per cent methane.

The evaporator has a mist eliminator in the exhaust stack (See Figure 3). Test of the evaporator exhaust stack gases indicated that the mist eliminator effectively scrubbed the exhaust gases from brine droplets and salt crystals. In a typical application, the submerged combustion evaporator would concentrate the brine to a concentration of 30 per cent [7-11]. During the Morcinek test, this figure was 25 per cent.

**Final Brine Processing**

Several methods are available to deal with the concentrated brine mixture from the evaporator. One method under consideration is to dispose of the brine mixture in an abandoned mine shaft. Another method is to dry the brine mixture to a low moisture salt. Spray drying is a practical means to do this.

The surface area of the feed stream presented to the hot surroundings governs the evaporation rate and temperature time history of the material being processed. Energy consumption of spray drying methods range from 4.5 to 9.0 MJ/kg (1,935 to 3,870 Btu/lb) of water removed [12].

Aquatech evaluated a pulse combustion drying process for a coalbed brine. A 30 per - cent brine mixture of sodium chloride and sodium bicarbonate was delivered to a pulse combustion dryer. The energy to evaporate water from the brine mixture was approximately 4.15 MJ/kg (1,783 Btu/lb). The pulse combustion dryer produced a fine-grained dry salt in powder form [9].

## Conclusions

A combination of chemical pretreatment, reverse osmosis separation and submerged combustion evaporation can be used to perform cost-effective disposal of waste waters associated with coal mining and methane production. The pretreatment process needed to prevent fouling of the reverse osmosis membranes can be optimized by using a chemical modeling program developed at the Lawrence Livermore National Laboratory to simulate the process.

The cost to process this type of brine in Poland is approximately $\$4.72/m^3$ ($0.75/barrel) at a methane price of $\$0.044/m^3$ ($1.25/mcf) and an electrical cost of $0.04/kwh.

## Acknowledgments

This research was funded in part by DOE's Research Grants Nos. DE-FG03-91ER 81105 A002 and A003 as well as DE-AC21-89MC 26026 managed by the College of West Virginia, and in part under the auspices of the USDOE by the Lawrence Livermore National Laboratory under contract W-7405-Eng-48.

## References

1. Bethke, C.M., "The Geochemist's Workbench: A Users Guide to Rxn, Act 2, Tact, React and Gtplot", U. of Illinois Press, 1992.
2. Wolery, T.J., "EQ3/6, A Software Package for Geochemical Modeling of Aqueous Systems: Package Overview and Installation Guide", Lawrence Livermore National Laboratory, UCRL-MA-110662, 1992.
3. Pitzer, K.S., "Thermodynamics of Electrolytes - I. Theoretical Basis and General Equations.", Journal of Physical Chemistry, 77: 2-68-277, 1973.
4. Langlier, W.F., "Chemical Equilibrium in Water", J. of the American Water Works Association, 1946.
5. Stiff, H.A. and Davis, L.E., "A Method for Predicting the Tendency of Oil Field Waters to Deposit Calcium Carbonate", Petroleum Transactions AIME, v. 195, 1952.
6. Butler, J.N., "Carbon Dioxide Equilibria and Their Applications", Addison-Wesley Publishing Company, 1982.
7. Brandt, H. and Tait, J.H., "Process Eases Coalbed Brine Disposal.", Am. Oil & Gas Rep., 1992.
8. Brandt, H. and Jackson, K.J., "Process for Coalbed Brine Disposal", in DOE Fuels Technology Review Meeting, Nov. 16-18, Morgantown, West Virginia, 1993.
9. Brandt, H., Bourcier, W.L., and Jackson, K.J., "Integrated Process for Coalbed Brine Disposal", International Petroleum Environmental Conference, Houston, Texas, 1994.
10. Brandt, H. and Bourcier, W.L., "Treatment Process for Coal Mine Waste Water", Second International Symposium on Environmental Contamination in Central and Eastern Europe. Budapest, Hungary, 1994.
11. Brandt, H. and Bourcier, W.L., "Treatment Process for Waste Water Disposal of the Morcinek Mine Using Coalbed Methane", Silesian International Conference on Coalbed Methane Utilization, Katowice, Poland, 1994.
12. Mujumdar, A.S., "Handbook of Industrial Drying", Marcel Dekker, Inc. New York, 1987.

# 4A.3 Preliminary Geologic Characterization of Upper Cretaceous and Lower Tertiary Low-Permeability (Tight) Gas Bearing Rocks in the Wind River Basin, Wyoming

## CONTRACT INFORMATION

| | |
|---|---|
| **Contract Number** | DE-AT21-93-MC30139 |
| **Contractor** | United States Geological Survey<br>Branch of Petroleum Geology<br>MS 934, Denver Federal Center<br>Denver, Colorado 80225-0046 |
| **Contractor Project Manager** | Vito F. Nuccio |
| **Principle Investigators** | Ronald C. Johnson, Thomas M. Finn, William R. Keefer, Romeo M. Flores, C. William Keighin, Richard J. Szmajter, and Vito F. Nuccio |
| **METC Project Manager** | Karl-Heinz Frohne |
| **Period of Performance** | October 1, 1993 to September 30, 1994 |

## OBJECTIVES

The Wind River Basin is one of several Rocky Mountain basins that contain significant resources of gas in low-permeability or tight reservoirs. Low-permeability gas reservoirs have an in situ permeability to gas of 0.1 millidarcies or less. These reservoirs cover vast areas of the structurally deeper parts of Rocky Mountain basins. They have also been referred to as "continuous-type (unconventional) hydrocarbon accumulations" (Schmoker, 1995) or simply basin-centered accumulations. They differ from conventional oil and gas deposits in that they (1) cut across stratigraphic units, (2) commonly are structurally down dip from more permeable water-filled reservoirs, (3) have no obvious structural or stratigraphic trapping mechanism, and (4) commonly are either abnormally overpressured or underpressured. The abnormal pressures of these reservoirs indicate that water, in hydrodynamic equilibrium with outcrop, is not the pressuring agent. Instead, hydrocarbons within the tight reservoirs are thought to pressure these rocks. The objectives of the Wind River Basin tight gas sandstone project are to define the limits of the tight gas accumulation, characterize the geology of the sandstone reservoirs, estimate the in-place tight gas resources, and to estimate recoverable gas resources.

## BACKGROUND INFORMATION

The Wind River Basin is a complex structural and sedimentary basin formed during the Laramide orogeny in latest Cretaceous, Paleocene, and early Eocene time (Figure 1). It is bounded on the north by the Absaroka Range, Owl Creek Mountains, and Bighorn Mountains; on the east by the Casper Arch; on the south by the the Granite Mountains; and on the west by the Wind River Range. The Wind River Basin is asymmetrical, with the deep trough adjacent to the east-west trending Owl Creek Mountains, which were

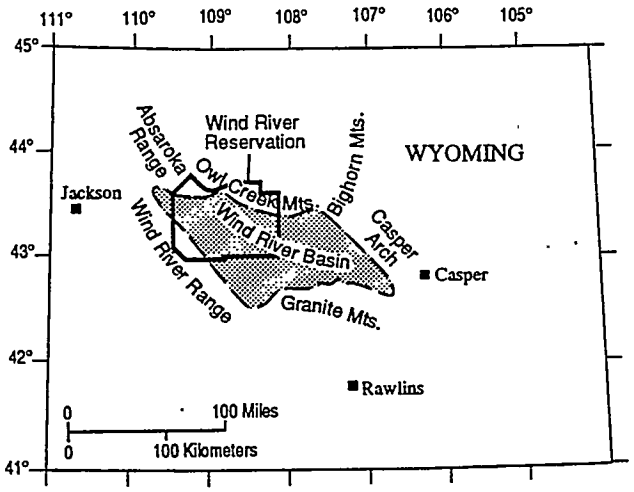


**Figure 1. Index map showing location of Wind River Basin and surrounding uplifts. Location of Wind River Reservation is shown by heavy black line.**

uplifted and faulted southward over the sedimentary basin. The west and southwest margins dip fairly gently away from the Wind River Range and the south margin dips away from the Granite Mountains. Numerous northwest-trending anticlines, many of which are bounded by reverse faults, occur along the basin margins.

Defining the limits of the basin-centered tight gas accumulation in the Wind River Basin is difficult because of the general sparseness of drilling data. Only a few permeability measurements from core in in the basin have been published, and most of these measurements were not taken under in-situ pressure conditions. The Wind River Basin differs significantly from other Rocky Mountain basins that contain basin-centered hydrocarbon accumulations. It is more faulted and generally more complex structurally than the Piceance Basin, the Greater Green River Basin, and the Uinta Basin. The Wind River Basin has far less topographic relief than the Piceance and Uinta Basins, and it is the only Rocky Mountain basin that contains a thick Paleocene-age lacustrine shale, the Waltman Shale Member of the Fort Union Formation. Understanding these differences is important in defining the limits of the basin-centered gas accumulation as well as in predicting the economics of producing tight gas in the Wind River Basin. Several techniques used to define basin centered accumulations in other Rocky Mountain basins were tested in the Wind River Basin.

The Upper Cretaceous and lower Tertiary interval (Figure 2) in the Wind River Basin is capable of producing gas throughout a large area in the central part of the basin. Many of these formations, including the Upper Cretaceous Mesaverde, Meeteetse, and Lance Formations, and the Paleocene Fort Union Formation have been given tight sandstone designation. These gas-charged reservoirs vary from normally pressured, having conventional permeabilities in the shallower areas of the basin, to highly

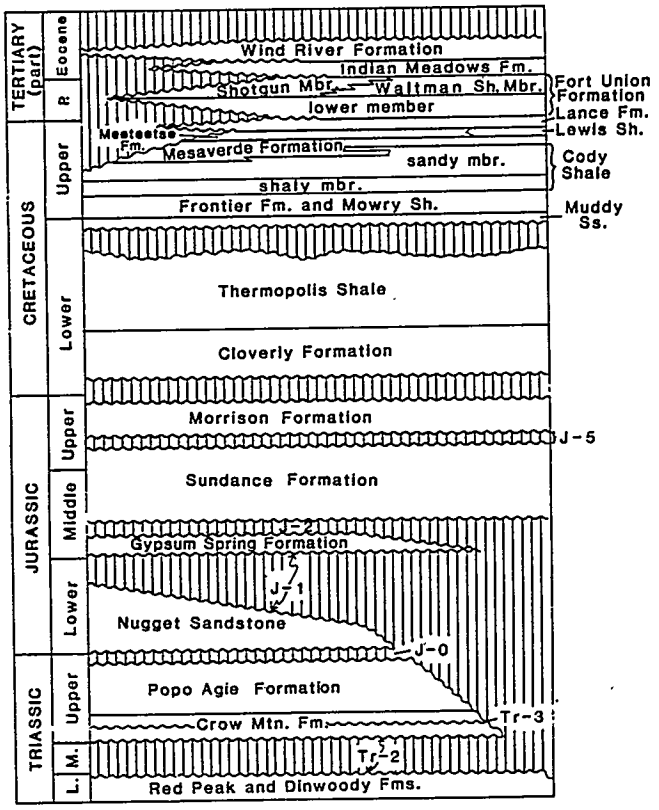


**Figure 2. Generalized stratigraphic chart of Mesozoic and lower Cenozoic rocks, Wind River Basin, Wyoming. Patterns of vertical lines indicate hiatuses. Locations of Triassic unconformities (Tr-2, Tr-3) and Jurassic unconformities (J-0, J-1, J-2, J-5) from Pipiringos and O'Sullivan (1978).**

overpressured and having generally low permeabilities in the deeper areas of the basin. Although this interval appears to be able to produce gas throughout a large area of the basin, significant production is now established in only a handful of fields. Most of these fields occur on structural closures and structural noses. Many are single well gas fields that are shut in because there are no pipelines nearby. The fact that no further development occurred in these fields after gas rather than oil was discovered underlines the importance of pipeline availability in the development of the gas resources of the Wind River Basin. Frenchie Draw field, in contrast (Figure 3), occurs along a major pipeline and was developed largely because of the existence of this pipeline.

## RESULTS

### Source Rocks

Rich source rocks for oil and gas in the Upper Cretaceous and Lower Tertiary interval in the basin include the Upper Cretaceous Mowry Shale, the shaley member of the Upper Cretaceous Cody Shale, the lower part of the Upper Cretaceous Mesaverde Formation, the Upper Cretaceous Meeteetse Formation, and the lower unnamed member and Waltman Shale Member of the Paleocene Fort Union Formation (Figure 2). The Mesaverde and Meeteetse Formations, and the lower unnamed member of the Fort Union Formation contain mainly gas-prone Type III organic matter, while the Mowry Shale, the lower shaley member of the Cody Shale, and the Waltman Shale Member contain mixes of Type II (oil and gas prone) and Type III organic matter. Thermal maturity studies, using vitrinite reflectance, indicate that the Mowry Shale, the shaley member of the Cody Shale, the lower part of the Mesaverde Formation, and the Meeteetse Formation have reached a thermal maturity level of Rm 0.73 percent, sufficient for significant gas generation throughout the area of the tight-gas accumulation in the basin. In contrast, the lower unnamed member and the Waltman Shale Member of the Fort Union Formation are thermally mature in only the deep trough area of the basin (Nuccio and Finn, 1993).

### Evidence for Gas Migration in the Basin

Recent work on the chemical and isotopic composition of gases in the Wind River, Piceance, and Uinta Basins, (Johnson and Rice, 1993; Johnson and others, 1994a; 1994b) suggests that there has been considerable vertical migration of gases from mature Cretaceous-age source rocks into overlying marginally mature to immature lower Tertiary reservoirs in all three basins. In the Wind River Basin, the Waltman Shale Member acts as a seal, keeping gas from migrating vertically into younger formations above the Waltman or venting to the surface. Shale seals are seldom considered in conjunction with low-permeability gas accumulations, however, Masters (1984, p. 10) stressed the importance of the Lower Cretaceous Joli Fou Shale as a regional seal inhibiting the vertical migration of hydrocarbons out of the low-permeability hydrocarbon accumulation in the Alberta Deep Basin. Gases from below the Waltman are isotopically much heavier than gases produced from sandstones within or above the Waltman and are probably sourced by mature Upper Cretaceous source rocks. At Pavillion and Muddy Ridge fields, in the western part of the basin, where the Waltman is not present, gas has migrated vertically from Upper Cretaceous source rocks into units as young as the Eocene Wind River Formation (Figure 3) (Johnson and Rice, 1993).

Figure 3 is a structure contour map of the base of the Waltman Shale Member and its lateral equivalent. The contour map was extended beyond the limit of the Waltman by contouring the base of the sandy marginal lacustrine equivalent of the Waltman in the Shotgun Member of the

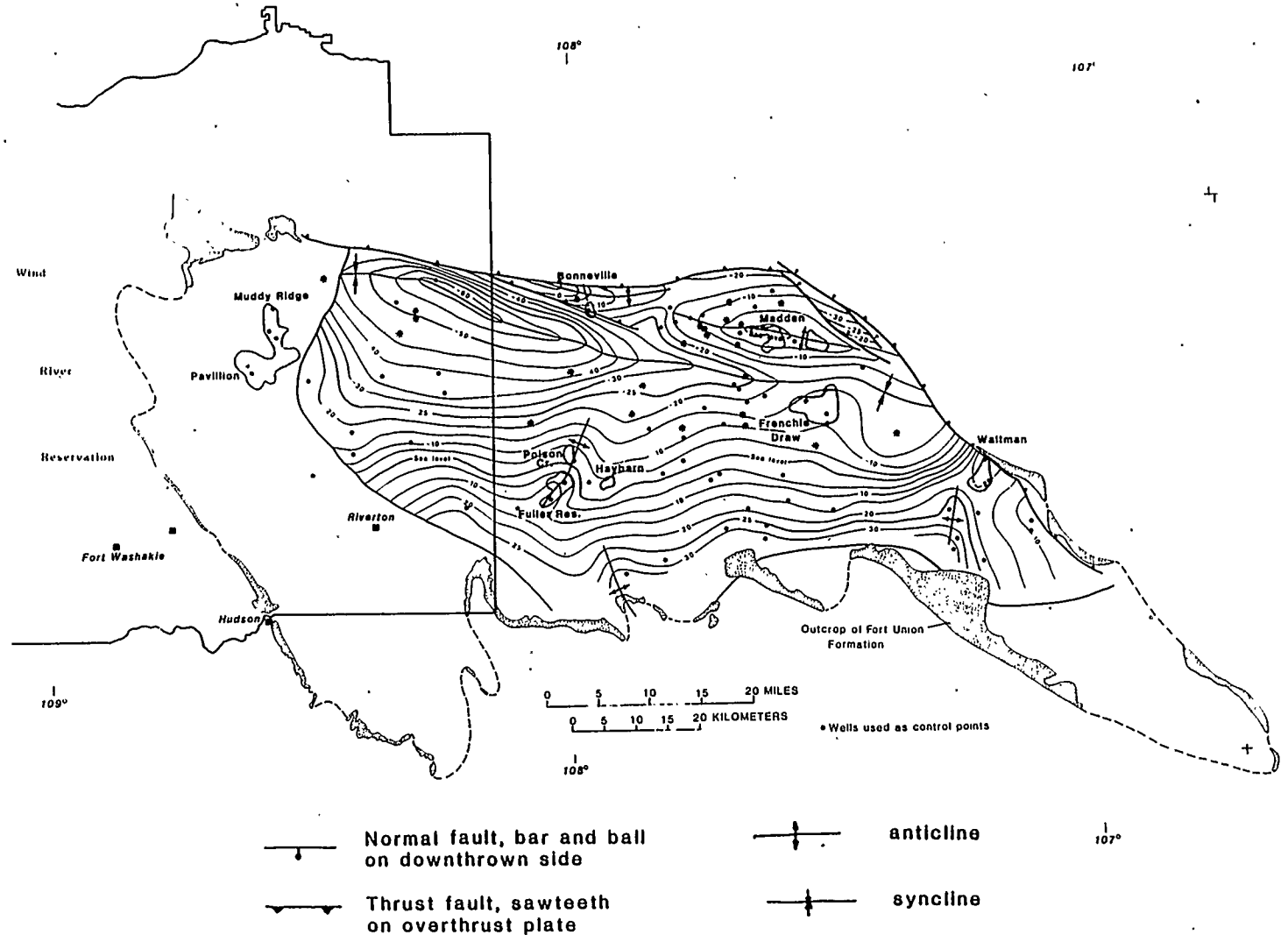


**Figure 3. Structure contour map drawn on the base of the Waltman Shale Member of the Paleocene Fort Union Formation and its marginal-lacustrine equivalent in the Shotgun Member of the Fort Union. Contour interval: 500 ft. Heavy line shows limit of Waltman Shale Member and its equivalent. Gas shows and fields that produce from the lower unnamed member of the Fort Union Formation beneath the Waltman are shown.**

Fort Union. Gas fields which produce from the underlying lower unnamed member of the Fort Union Formation are shown. Wells which had nearly continuous gas shows on mudlogs of the lower member are shown with an astrisk. Gas appears to be more-or-less ubiquitous in the lower unnamed member wherever the Waltman Shale is present. In many shallow fields such as Waltman (Ptasynski, 1989), Fuller Reservoir (Specht, 1989), Haybarn (Evans, 1989), and Poison Creek (Morton, 1989), the lower unnamed member appears to have conventional permeabilities. Deeper production from the lower unnamed member appears to be from either low-permeability sandstones or sandstones with unknown permeabilities.

**Defining the overpressured pocket using mud weights**

Mud weights used during drilling and pressures from drillstem tests were examined to help define the overpressured pocket in the basin. It should be remembered that tight accumulations can also be underpressured, and hence studying heavy mudweights will only define that part of the tight accumulation that is overpressured. The overpressured pocket in the Wind River Basin is unusual in that 1) normally pressured reservoirs or reservoirs occur interbedded with highly overpressured reservoirs, and 2) significant water is produced from many fields completed in overpressured rocks. On Madden Anticline, the Sussex Sandstone Member equivalent of the Cody Shale is normally pressured, with a pressure gradient of about 0.41 to 0.44 psi/ft, while pressure gradients in underlying and overlying sandstones are as much as 0.76 psi/ft (Dunleavy and Gilbertson, 1986). The normally pressured Sussex equivalent appears to be in communication with the regional hydrodynamic system while the overlying and underlying intervals are not. This problem is discussed further below. Water production on Madden Anticline from the overpressured interval as of 1989, include 1,522,245 barrels from the Mesaverde Formation and 562,683 barrels from the Cody Shale (Brown and Shannon, 1989). At the Bonneville field west of Madden, significant water was produced with gas in the overpressured Upper Cretaceous Lance Formation (Gilbert, 1989).

The depths at which 10 lb mud and 12 lb mud were used during drilling were converted into elevations above and below sea level and plotted on Figure 4. Ten pound mud indicates a pressure gradient of 0.494 psi/ft or moderate overpressuring, while 12 lb mud indicates a pressure gradient of 0.625 psi/ft or significant overpressuring. The elevations of the 10 lb mud level shown on Figure 4 are probably somewhat below the true onset of overpressuring in the basin since normal hydrostatic pressure is significantly less than the 0.494 lbs/ft represented by the 10 lb mud weight. In addition, overpressuring is commonly not detected immediately while drilling through tight intervals.

Elevations where 10 lb mud was used generally fall between -5,500 and -8,500 ft throughout most of the basin, except on the Madden Anticline where 10 lb mud was used at elevations of +290 to -1,935 ft, and in some wells along the north margin of the basin where 10 lb mud was not used until elevations of from -11,000 to -12, 395 ft were reached (Figure 4). Overpressuring on Madden Anticline begins at the base of the Waltman Shale Member, further evidence of the importance of the Waltman as a seal against vertical migration of gas in the basin. This overpressuring at relatively shallow depths has traditionally been attributed to a long gas column beneath the Waltman. A single long gas column supported by an underlying column of water seems unlikely. The lower unnamed member is productive through over a 3,500 ft stratigraphic interval, yet water has been recovered from as little as 200 ft below the crest of the anticline (Schmitt, 1975) indicating multiple gas-water contacts. There is no reliable permeability data available for the lower unnamed member of the

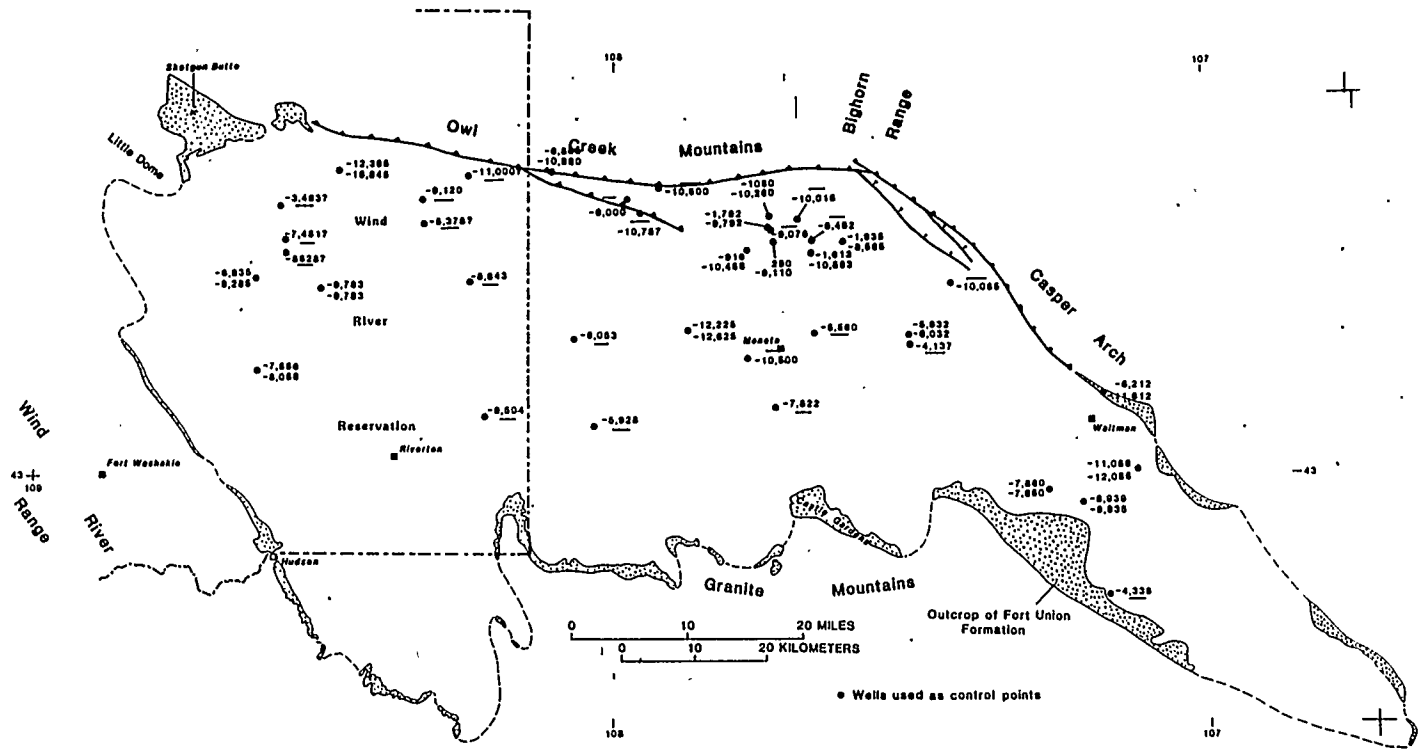


**Figure 4. Map of Wind River Basin showing elevations in feet at which 10 lb mud or greater (upper number) and 12 lb mud or greater (lower number) was used during drilling.**

Fort Union Formation at Madden (Brown and Shannon, 1989) but the interval has some characteristics in common with low-permeability reservoirs. As in many tight intervals, defining potentially productive zones in the lower unnamed member at Madden using geophysical log interpretations has proven unreliable (Dunleavy and Gilbertson, 1986, p. 111-112).

Twelve pound mud was used generally between elevations of -10,000 to -12,700 ft except on the Madden Anticline where 12 lb mud was used at somewhat higher elevations and along the northern margin of the basin where 12 lb mud use occurs at somewhat lower elevations (Figure 4). The limited drillstem test information available generally supports the outline of the overpressured pocket defined from mudweights. Figures 5 and 6 are schematic north-south and east-west cross sections through the basin showing the approximate positions where 10 lb and 12 lb mud weights were used. The shallow depth for the onset of overpressuring on Madden Anticline is clearly anomalous when compared to onset of overpressuring in the rest of the basin.

## Using Variations in Thermal Maturity to Help Define the Low-Permeability Gas Accumulation

Variations in thermal maturity were examined to help define the limits of the basin-centered gas accumulation, particularly in areas where little pressure data is available. Thermal maturity defines areas where potential source rocks have generated gas at some time in the past. In the Piceance Basin (Johnson and others, 1987) used a vitrinite reflectance (Rm) of 1.1% to define the limits of the basin-centered accumulation while an Rm of 0.73 to 1.1% was used to define a transition zone containing both tight and more conventional reservoirs. Masters (1984, p. 27, Fig. 25), in a study of the basin-centered gas accumulation in the Deep Basin of Alberta, shows that an Rm of 1.0 corresponds approximately to the limit of the accumulation. In the Greater Green River Basin (Law and others, 1989), found that an Rm of 0.80 generally corresponds to the top of overpressuring.

The approximate elevations of the Rm 0.73% and Rm 1.1% are shown on Figures 7 and 8. Vitrinite reflectance data is from Pawlewicz (1993) and from Nuccio and Finn (unpublished data). The elevations of the Rm 0.73 and 1.1% level are highest in the central part of the basin and lowest in the western and eastern parts. The Rm 0.73% and Rm 1.1% levels are also plotted on schematic north-south and east-west cross sections (Figures 5 and 6). The position of the Rm 1.1% thermal maturity level is approximately 1,000 to 2,000 ft above the 10 lb mud level throughout much of the basin except on Madden Anticline, where it dips below the 10 lb mud level and in the western part of the basin where the 10 lb mud level and the position of the Rm 1.1% thermal maturity level are nearly the same. The elevation of the Rm 0.73 thermal maturity level varies from about 3,000 ft above the 10 lb mud level in the eastern and western parts of the basin to about the same level as the 10 lb mud level at Madden Anticline in the central part of the basin.

## Using Present-Day Formation Temperatures to Help Define the Low-Permeability Gas Accumulation

Present-day formation temperatures have also been used to help determine the boundaries of overpressured basin-centered accumulations in Rocky Mountain basins. Rates of gas generation are directly related to temperature. Spencer (1989) suggested that rates of gas generation need to exceed rates of gas loss in order to maintain abnormally high pressures in Rocky Mountain basin-centered gas accumulations and that this generally occurs at present-day temperatures of about 200° F or greater. A corrected geothermal gradient map for the basin, recently constructed by Pawlewicz (1993), showed that gradients vary

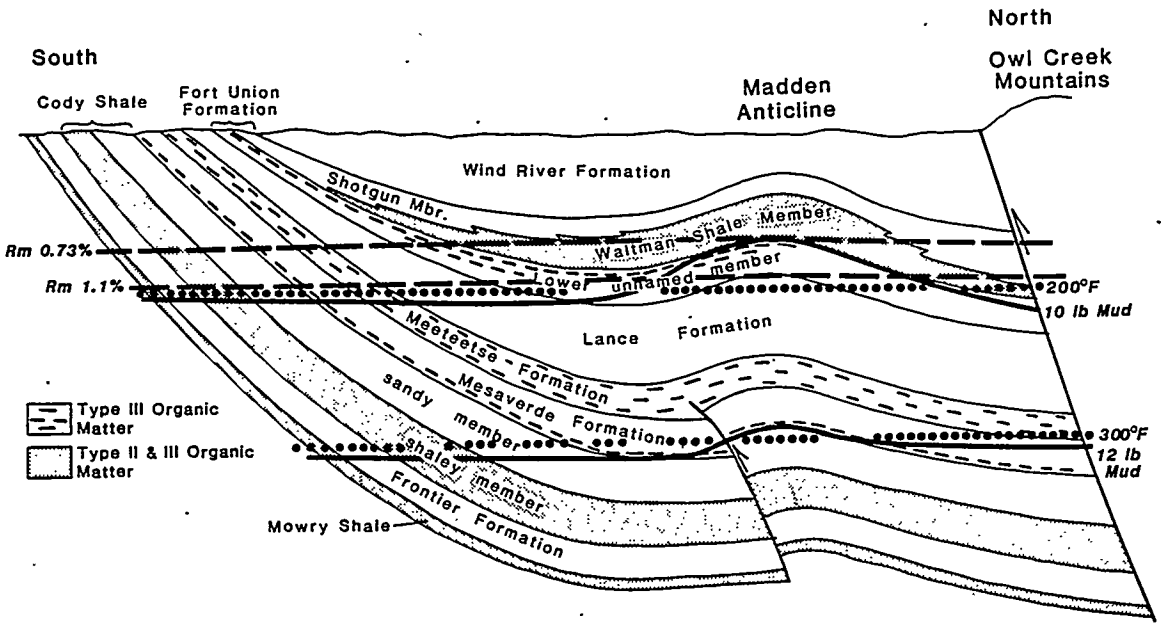


**Figure 5. Schematic north-south cross section through the Wind River Basin, Wyoming showing Upper Cretaceous and lower Tertiary stratigraphic units, potential source rocks, approximate positions where 10 lb and 12 lb mud was used during drilling, approximate positions of Rm 0.73% and Rm 1.1% vitrinite reflectance levels, and approximate positions of 200° and 300° present-day isotherms.**

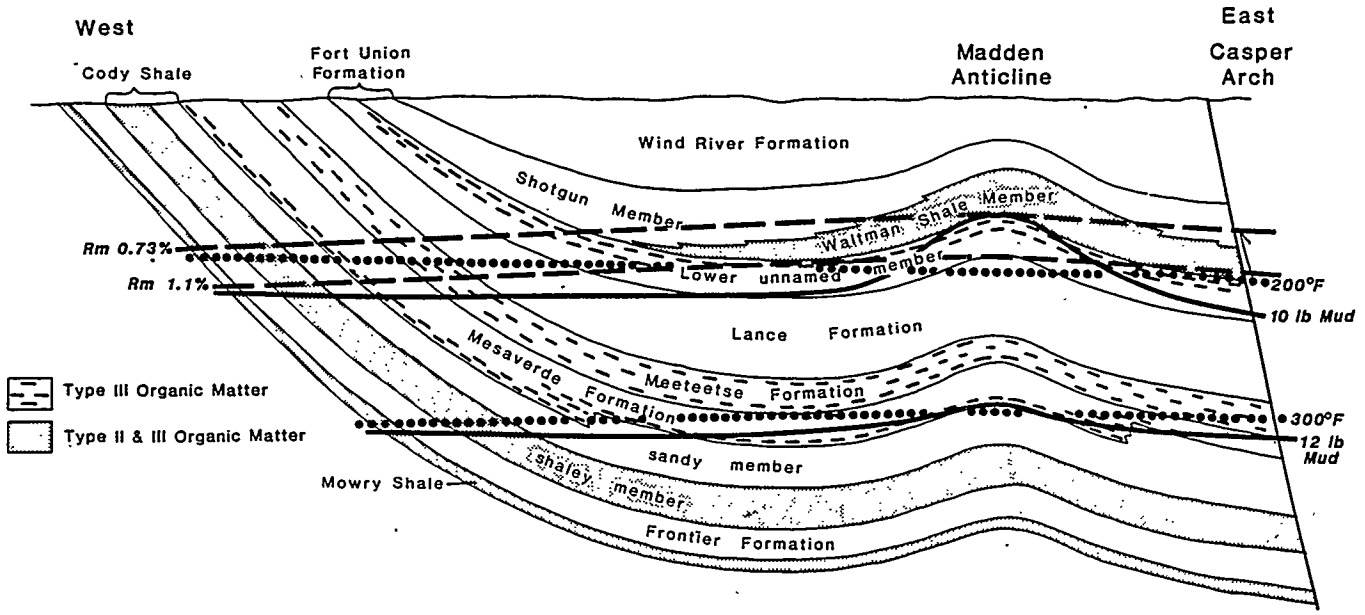


**Figure 6. Schematic east-west cross section through the Wind River Basin, Wyoming showing Upper Cretaceous and lower Tertiary stratigraphic units, potential source rocks, approximate positions where 10 lb and 12 lb mud was used during drilling, approximate positions of Rm 0.73% and Rm 1.1% vitrinite reflectance levels, and approximate positions of 200° and 300° present-day isotherms.**

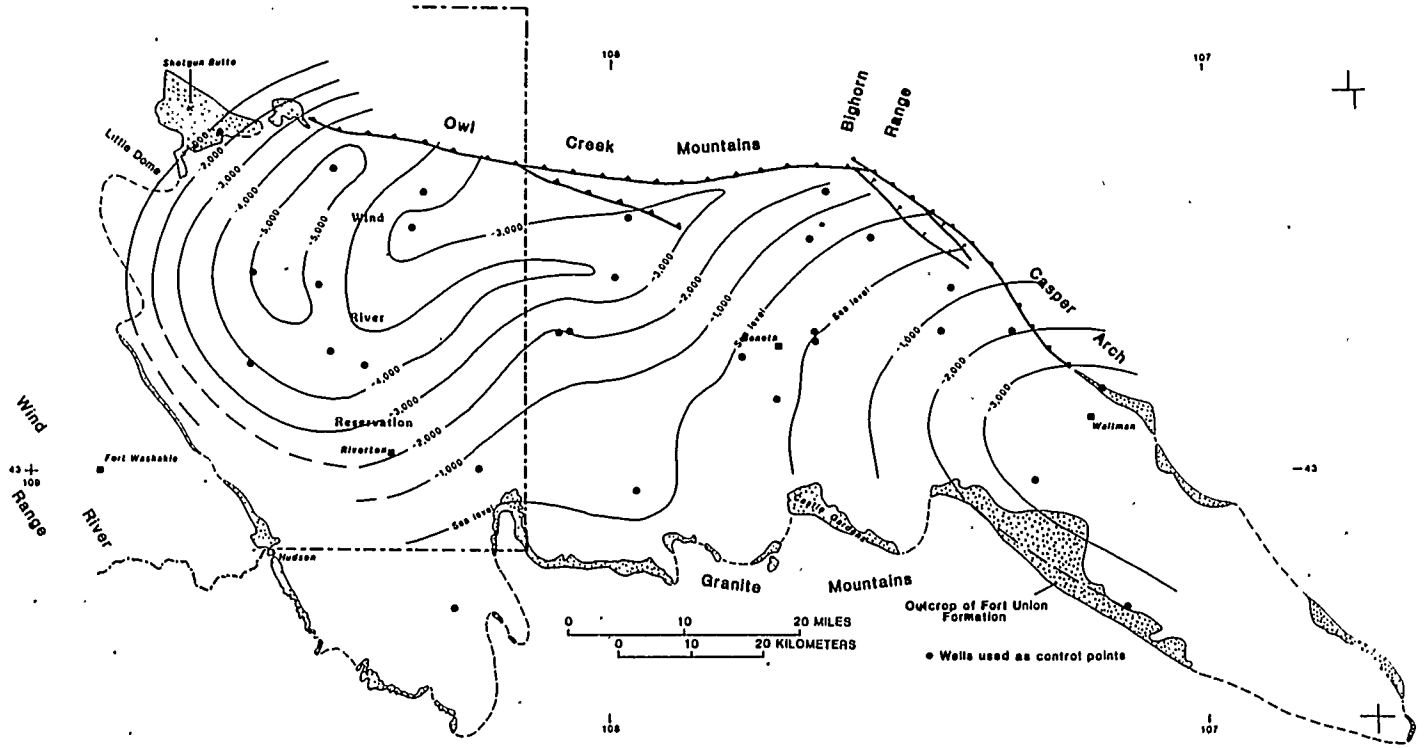


**Figure 7. Map showing approximate elevation of the Rm 0.73 vitrinite reflectance level in the Wind River Basin. Contour interval: 1,000 ft. Data from Pawlewicz (1993), and Nuccio and Finn (unpublished data).**

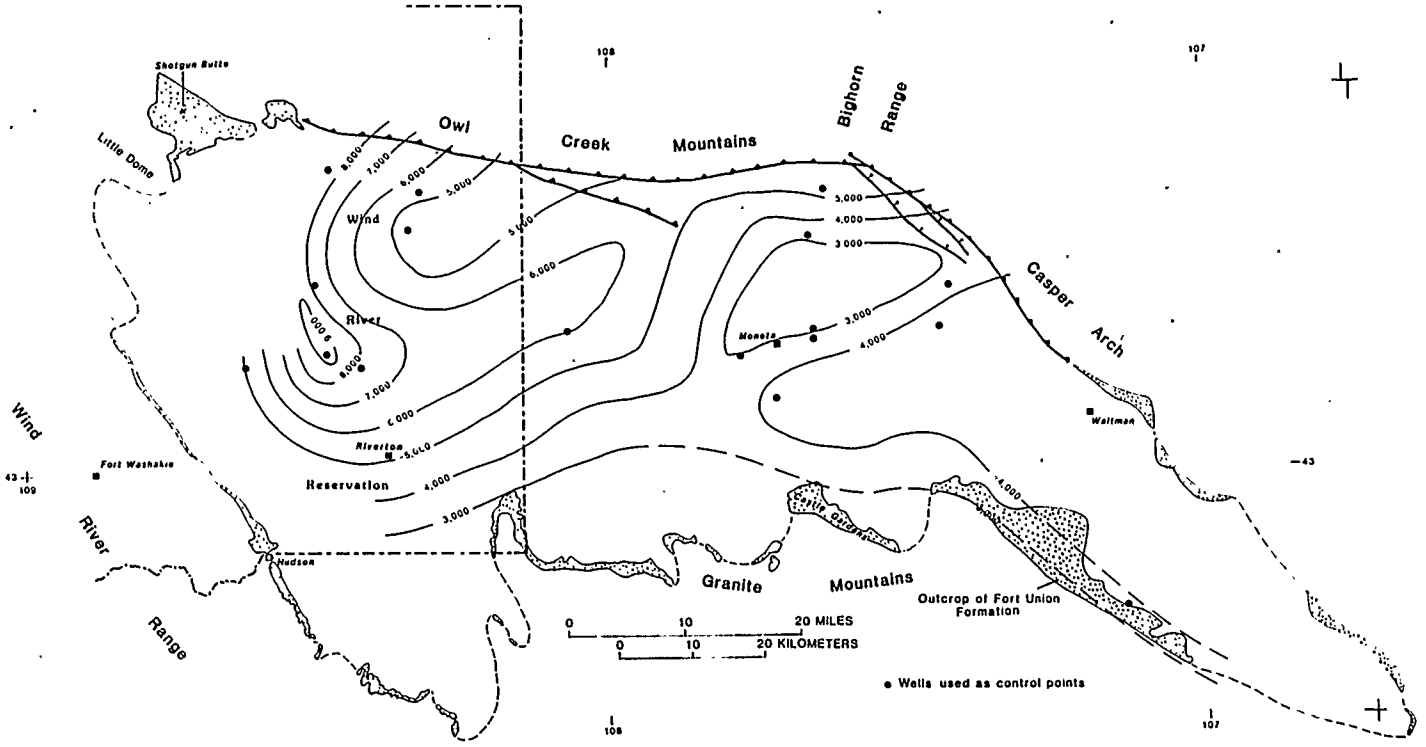


**Figure 8. Map showing approximate elevation of the Rm 1.1 vitrinite reflectance level in the Wind River Basin. Contour interval: 1,000 ft. Data from Pawlewicz (1993), and Nuccio and Finn (unpublished data).**

irregularly across the basin from less than 1.2°F/100 ft to over 2.0°F/100 ft. Geothermal gradients are on average somewhat higher in the central part of the basin where high thermal maturities were found but there is considerable scatter.

The geothermal gradient map of Pawlewicz (1993) was used to determine the approximate positions of two isotherms, the 200° F and the 300° F on the cross sections (Figures 5 and 6). On both cross sections, the 300°F isotherm fairly closely follows the 12 lb mud weight line. On the north-south cross section in the central part of the basin (Figure 5), the 200° isotherm closely follows the Rm 1.1% line; however, on the east-west cross section (Figure 6) the distance between the 200° isotherm and the Rm 1.1 line increases toward the east and west ends of the basin. This indicates that variations in present-day thermal gradients do not closely follow variations in thermal maturity throughout the basin, suggesting that thermal gradients in the basin have changed significantly since the presently observed thermal maturities were established.

A comparrison between variations in thermal maturity, present-day temperatures, and overpressuring indicated by mud weights, (Figures 5 and 6) indicates that both the 200° isotherm and the Rm 1.1% level fairly closely follow the top of the overpressured pocket in the central part of the basin. However, toward the western margin of the basin, only the Rm 1.1% line fairly closely tracks the 10 lb mud line. This suggests that the position of the Rm of 1.1% thermal maturity level in the basin may fairly closely correspond to the onset of overpressuring.

## Geologic Characterization of Stratigraphic Units Within the Low-Permeability Accumulation

A comprehensive geologic characterization of each formation within a low-permeability gas accumulation can lead to a better understanding of some of the variations in production characteristic found within the accumulation. Although water production is not typically a problem in low-permeability accumulations until gas production is well into decline, certain intervals produce significant water from the start. The Mesaverde Formation in the Wind River Basin is use here as an example of the importance of geologic characterization. The Mesaverde Formation was deposited along the western margin of the Upper Cretaceous interior seaway as the seaway gradually retreated eastward across Wyoming. The thickness of the Mesaverde varies from over 2,400 ft in the western part of the basin to less than 500 ft in the eastern part (Figure 9). The Mesaverde thins largely by grading laterally into the underlying marine Cody Shale in an easterly direction. This lateral facies change is not gradual across the basin, however, but occurs in two distinct jumps (indicated as datum changes), where significant thicknesses of Mesaverde Formation grade into Cody over relatively short distances. This indicates that the eastward retreat of the shoreline stalled near these two positions for considerable periods of time.

The Mesaverde Formation can be subdivided into a lower sequence containing mainly regressive shoreface sandstones and an upper sequence of mainly fluvial sandstones. The two positions where the eastward retreat of the shoreline stalled for considerable periods of time are readily apparent on an isopach map of the thickness of the lower shoreface sequence (Figure 10). An interval of stacked shoreface sandstones over 1,200 ft thick occur just westward of the western facies change. These shoreface sandstones trend generally north-south or parallel to the paleoshoreline. Sandstones were also deposited on the continental shelf east of the Cretaceous shoreline, and these sandstone also appear to trend generally north-south. More lenticular sandstones in the overlying fluvial part of the Mesaverde trend generally east-west or perpendicular to the paleoshoreline.

The shoreface sandstones and their shelf equivalents commonly extend to outcrop along the south margin of the basin. They appear to be

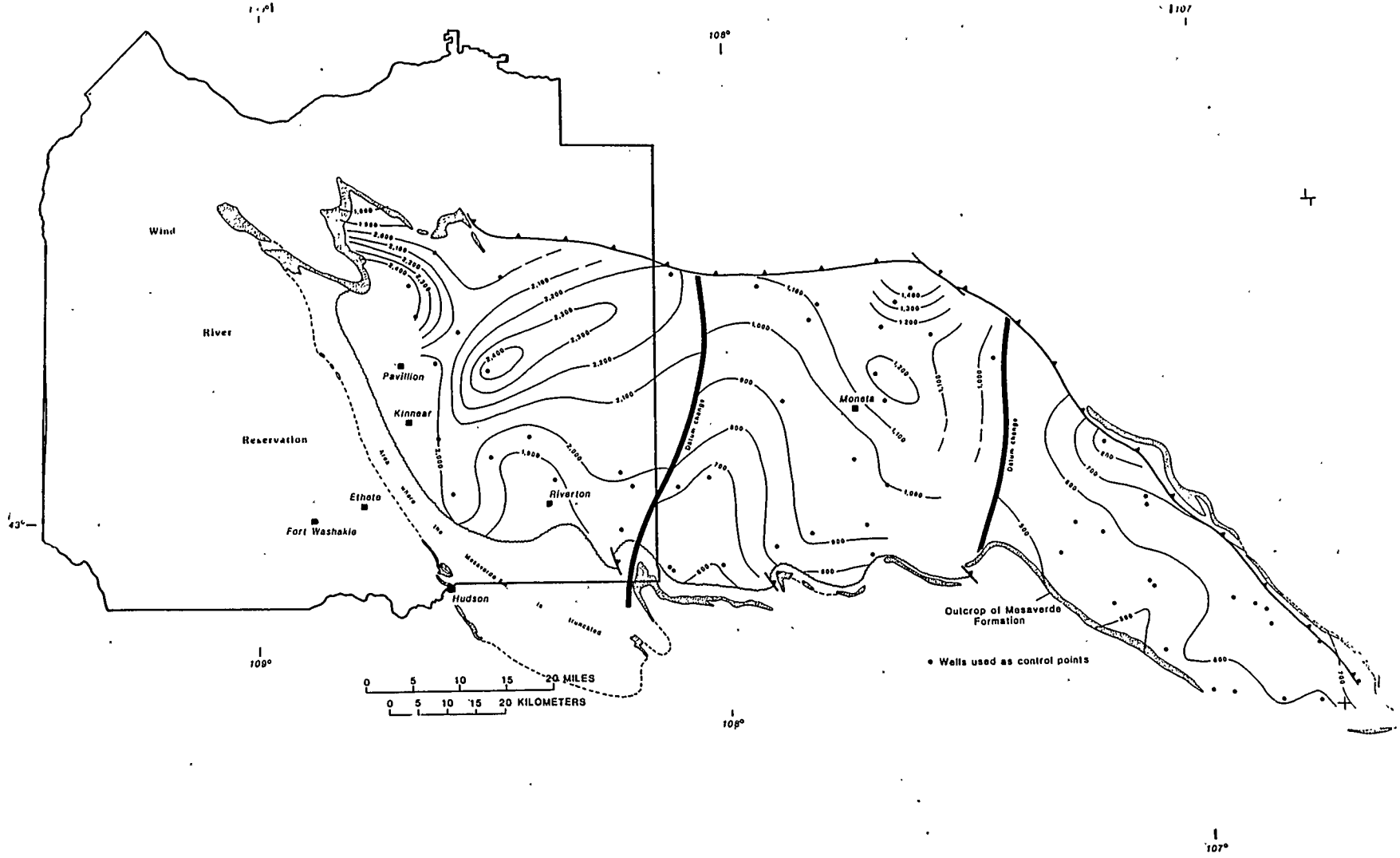


**Figure 9. Isopach map of the Upper Cretaceous Mesaverde Formation, Wind River Basin, Wyoming. Contour interval: 100 ft.**

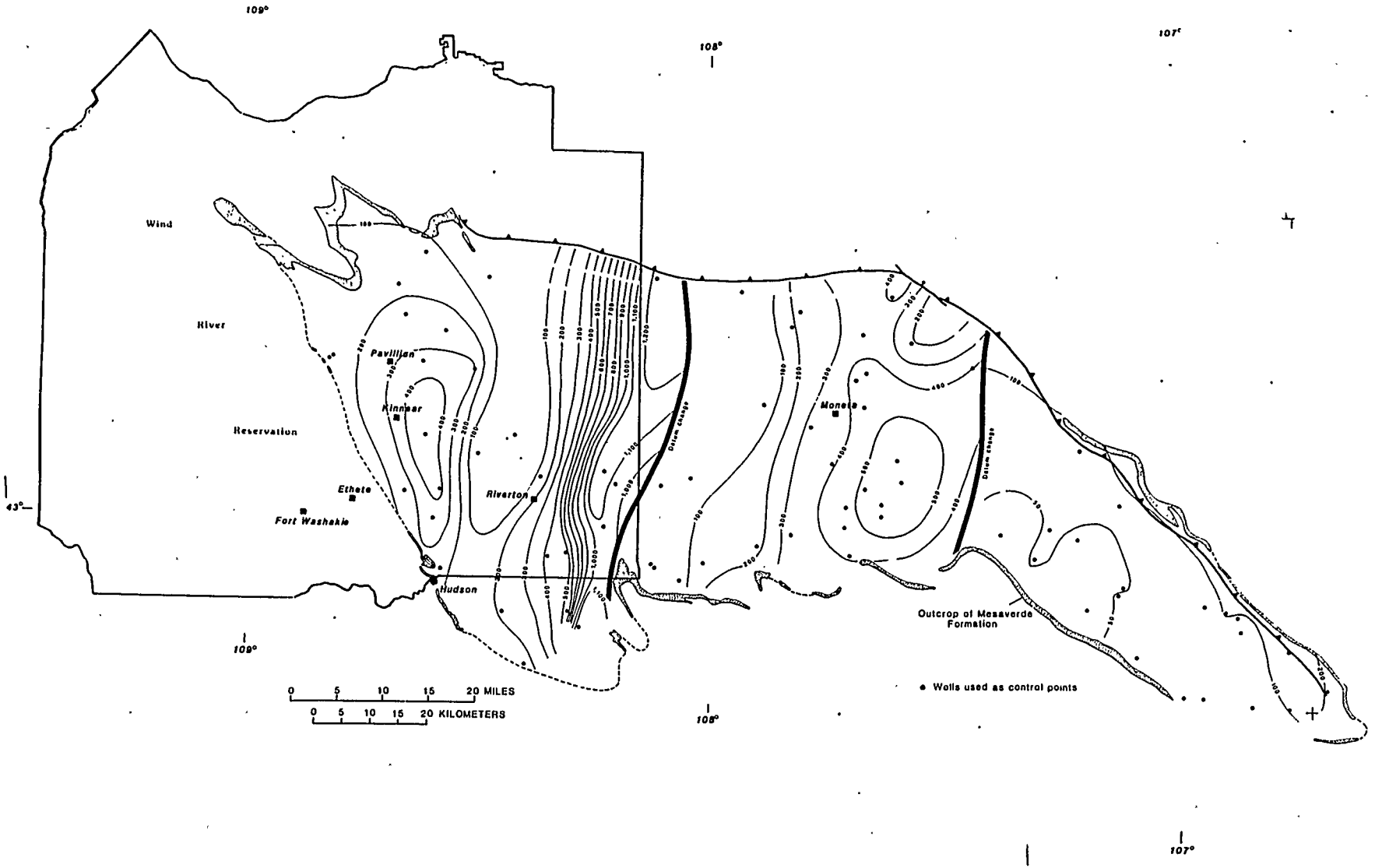


**Figure 10. Isopach map of the lower shoreface sequence in the Mesaverde Formation, Wind River Basin, Wyoming. Contour interval: 100 ft.**

recharged by fresh-water from these outcrops and are water-wet far down dip into the basin. Water production problems are far less common in the overlying fluvial sandstones which lense out before reaching recharge areas along the southern margin of the basin. This recharge can reach to the deepest parts of the basin. As previously mentioned, the Sussex Sandstone Member equivalent of the Cody Shale is in the highly overpressured interval on Madden Anticline near the deep trough of the basin but is normally pressured and in apparent hydrodynamic equilibrium with the outcrop.

## FUTURE WORK

Our studies of the low-permeability gas accumulation in the Wind River Basin are nearing completion. A combination of mudweights, levels of thermal maturities, and present-day formation temperatures will be used to generally define the limits of the accumulation. Sandstone isopach maps will be used in conjunction with porosity and water saturation estimates, and pressure estimates to estimate in-place gas resources. Estimates of economically recoverable gas will be made using the in-place gas estimates, production chraracteristics from existing fields, and geologic characterization studies.

## REFERENCES


Brown, R. G., and Shannon, L. T., 1989, Madden (Greater)-Long Butte: Wyoming Oil and Gas Symposium Bighorn and Wind River Basins; Wyoming Geological Association, p. 292-295.

Dunleavy, J. M., and Gilbertson, R. L., 1986, Madden Anticline: growing giant: in Noll, J. H., and Doyle, K. M., eds., Rocky Mountain Oil and Gas Fields: Wyoming Geological Association 1986 Symposium, p. 107-157.

Evans, J. G., 1989, Haybarn: Wyoming Oil and Gas Symposium Bighorn and Wind River Basins; Wyoming Geological Association, p. 228-229.

Gilbert, N. M., 1989, Bonneville: Wyoming Oil and Gas Symposium Bighorn and Wind River Basins; Wyoming Geological Association, p. 68-69.

Johnson, R. C., Crovelli, R. A., Spencer, C. W., and Mast, R. F., An assessment of gas resources in low-permeability sandstones of the Upper Cretaceous Mesaverde Group, Piceance Basin, Colorado: U.S. Geological Survey Open-File Report 87-357, 165 p.

Johnson, R. C., and Rice, D. D., 1993, Variations in composition and origins of gases from coal bed and conventional reservoirs, Wind River Basin, Wyoming: in Keefer, W. R., and Metzger, W. J., and Godwin, L. H., eds, Oil and Gas and Other Resources of the Wind River Basin, Wyoming: Wyoming Geological Association Special Symposium Volume, p. 319-335.

Johnson, R. C., Rice, D. D., and Fouch, T. D., 1994a, Evidence for gas migration from Cretaceous basin-centered accumulations into lower Tertiary reservoirs in Rocky Mountain basins: Rocky Mountain Association of Geologists and Colorado Oil and Gas Association First Biennial Conference, Natural Gas in the Western United States Proceedings, Oct. 17-18, 1994, 8 p.

Johnson, R. C., Rice, D. D., and Fouch, T. D., 1994b, Gas migrating from basin-center low-permeability hydrocarbon accumulations in the Rocky Mountain basins-where does it go?: American Association of Petroleum Geologists Annual Meeting, Denver Co., June 12-15, 1994, Abstracts With Program, p. 181-182.

Law, B. E., Spencer, C. W., Charpentier, R. R., Crovelli, R. A., Mast, R. F., Dolton, G. L., and Wandrey, C. J., 1989, Estimates of gas resources in overpressured low-permeability Cretaceous and Tertiary sandstone reservoirs, Greater Green River Basin, Wyoming, Colorado, and Utah: in Eisert, J. A., ed, Gas Resources of Wyoming: Wyoming Geological Association Fortieth Field Conference, p. 39-61.

Masters, J. A., 1984, Lower Cretaceous oil and gas in western Canada: in Masters, J. A. ed., Elmworth-Case Study of a Deep Basin Gas Field: American Association of Petroleum Geologists Memoir 38, p. 1-33.

Morton, D., 1989, Poison Creek: Wyoming Oil and Gas Symposium Bighorn and Wind River Basins; Wyoming Geological Association, p. 374-376.

Nuccio, V. F., and Finn, T. M., 1993, Structural and thermal history of the Paleocene Fort Union Formation, central and eastern Wind River Basin, with emphasis on petroleum potential of the Waltman Shale: in Flores, R. M., Mehring, K. T., Jones, R. W., and Beck, T. L., eds., Organics and the Rockies Field Guide: Wyoming State Geological Survey Public Information Circular No. 23, p. 53-68.

Pawlewicz, M., 1993, Vitrinite reflectance and geothermal gradients in the Wind River Basin, central Wyoming: in Keefer, W. R., and Metzger, W. J., and Godwin, L. H., eds, Oil and Gas and Other Resources of the Wind River Basin, Wyoming: Wyoming Geological Association Special Symposium Volume, p. 295-305.

Pipiringos, G. N., and O'Sullivan, R. B., 1978, Principal unconformities in Triassic and Jurassic rocks, Western Interior United States—A Preliminary survey: U.S. Geological Survey Professional Paper 1035-A, 29 p.

Ptasynski, H., 1989, Waltman, Bullfrog Unit: Wyoming Oil and Gas Symposium Bighorn and Wind River Basins; Wyoming Geological Association, p. 522-526.

Schmitt, G. T., 1975, Madden-Baswater field, Fremont and Natrona Counties, Wyoming: in Bolyard, D. D. ed, Deep Drilling Frontiers of the Central Rocky Mountains: Rocky Mountain Association of Geologists, p. 245-254.

Schmoker, J. W., 1995, Method for assessing continuous-type (unconventional) hydrocarbon accumulations: in Gautier, D. L., Dolton, G. L., Takahashi, K. I., and Varns, K. L., eds., 1995 National assessment of United States oil and gas resources on CD-ROM: U.S. Geological Survey Digital Data Series 30.

Specht, R. W. 1989, Fuller Reservoir: Wyoming Oil and Gas Symposium Bighorn and Wind River Basins; Wyoming Geological Association, p. 178-180.

Spencer, C. W., 1989, Review of characteristics of low-permeabillity gas reservoirs in western United States: American Association of Petroleum Geologists Bulletin, v. 73, no. 5, p. 613-629.

## 4A.4 Geotechnology for Low Permeability Gas Reservoirs, 1995*

### CONTRACT INFORMATION

| | |
|---|---|
| **Contract Number** | DE-AC04-94AL85000 (FEW 2086) |
| **Contractor** | Sandia National Laboratories<br>Geomechanics Department 6117, MS0751<br>P. O. Box 5800<br>Albuquerque, NM 87185-0751<br>(505) 844-4342 (telephone)<br>(505) 844-7354 (telefax) |
| **Other Funding Sources** | |
| **Contractor Project Manager** | Wolfgang R. Wawersik<br>David A. Northrop |
| **Principal Investigators** | Stephen R. Brown<br>Trent Boneau<br>Hugo Harstad<br>David J. Holcomb<br>John C. Lorenz<br>Lawrence W. Teufel<br>Norman R. Warpinski<br>Christopher J. Young |
| **METC Project Manager** | Royal J. Watts |
| **Period of Performance** | October 1, 1993 to February 28, 1995 |

* This work was performed at Sandia National Laboratories, which is operated for the U. S. Dept. of Energy under contract number DE-AC04-94AL85000.

**Schedule and Milestones** **FY94 - FY95 Program Schedule**

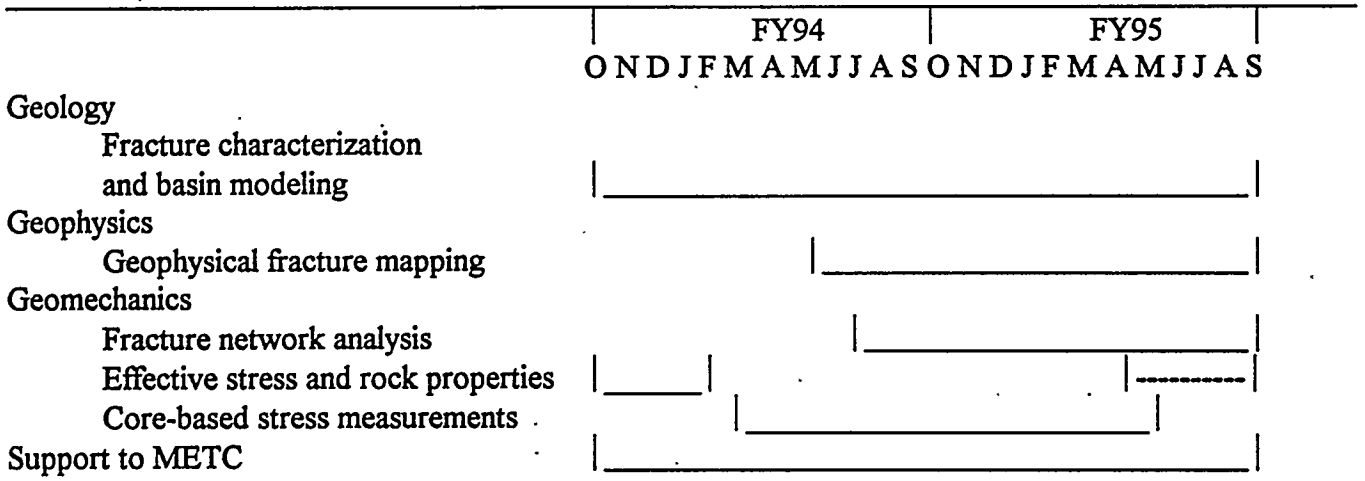


## OBJECTIVES

The objectives of this program are to (1) apply and refine a basinal and local analysis methodology for natural fracture exploration and exploitation, and (2) determine the important characteristics of natural fracture systems for their use in completion, stimulation, and production operations.

## BACKGROUND OF OVERALL PROJECT

The permeability, and thus the economics, of tight reservoirs are largely dependent on natural fractures, and on the in situ stresses that both originated fractures and control subsequent fracture permeability. Natural fracture permeability ultimately determines the gas (or oil) producibility from the rock matrix. Therefore, it is desirable to be able to predict, both prior to drilling and during reservoir production, (1) the natural fracture characteristics, (2) the mechanical and transport properties of fractures and the surrounding rock matrix, and (3) the present in situ stress magnitudes and orientations.

The project is a follow-on of a systematic study at the Multiwell Experiment (MWX) Site (now M-Site) in the southern Piceance basin which demonstrated the importance of natural fractures for gas production from tight reservoirs. The study was aided by extensive measurements of the in situ stress state, its variation with lithology, and its influence on the permeability anisotropy in reservoirs. The study was supported by a geomechanics laboratory program to examine the applicability of the conventional effective stress parameter, $\alpha$, to develop methods for determining $\alpha$, and to determine the effect of stress path on reservoir petrophysical properties and reservoir response.

The combination of activities described in this report extends the earlier work to other Rocky Mountain gas reservoirs. Additionally, it extends the fracture characterizations to attempts of crosswell geophysical fracture detection using shear wave birefringence and to obtaining detailed quantitative models of natural fracture systems for use in improved numerical reservoir simulations. Finally, the project continues collaborative efforts

to evaluate and advance cost-effective methods for in situ stress measurements on core.

## CURRENT ACTIVITIES

### Fracture Characterization and Basin Modeling in the Green River Basin

**Background.** Sandstones of the Frontier formation contain significant volumes of natural gas, and relatively shallow Frontier reservoirs have been successfully tapped with vertical wells in several areas of the basin (i.e., over the Moxa Arch). The Frontier formation also contains important volumes of gas where it is more deeply buried, but the economics of accessing that gas are currently unfavorable due to uncertainties in the characteristics of the permeability-enhancing natural fractures at depth. Work in 1994 has focused on the characterization of natural fractures in outcrop, and on methods for predicting fracture characteristics and in situ stresses in the deeper parts of the basin. Such predictions are useful in efficient application of advanced technologies (such as horizontal drilling) to the problem of extraction of natural gas from deep, fractured reservoirs.

**Project Description and Results.** During the summer of 1994, field work was designed to map and otherwise characterize natural fractures in outcrops of Frontier sandstones at the margins of the basin. The natural fractures in specific outcrops of Frontier sandstone, located along the margins of the Greater Green River basin, have been mapped in detail (Figures 1, 2). Mapping has shown that although fracture characteristics, primarily orientations, vary significantly in different parts of the basin, there is usually a through-going, older fracture set that is connected by younger, shorter, cross fractures. The younger fractures terminate at intersections with the older set and are commonly related to surface exposure; they are thus inferred to be rare in the subsurface where stress release or later tectonism have not occurred.

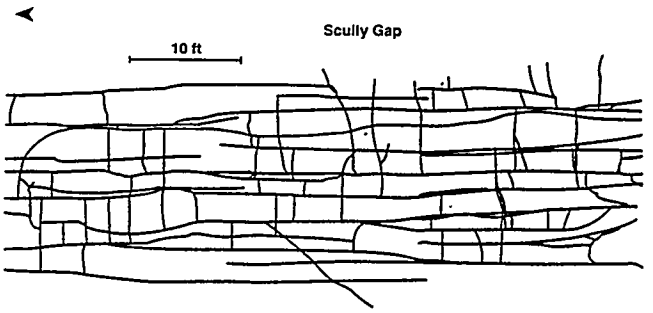


**Figure 1. Map of planview fractures on sandstone bedding plane of Frontier formation at southwestern edge of the Green River basin. Through-going fractures trend north-south.**

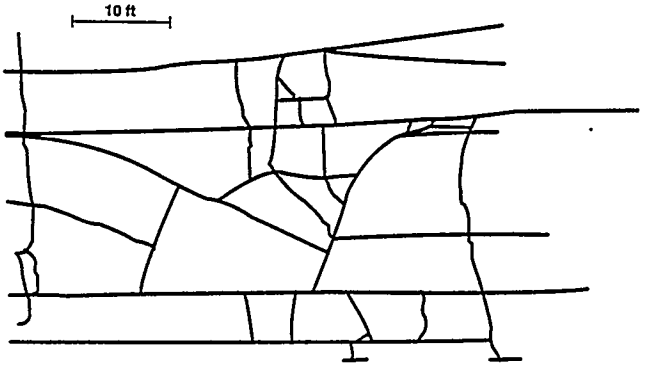


**Figure 2. Map of planview fractures on sandstone bedding plane of Frontier formation at southwestern edge of the Green River basin. Through-going fractures trend north-south.**

Populations of fracture parameters in Frontier outcrops display Weibull patterns that are similar to other fracture populations: i.e., frequency diminishes with length. This holds for fracture lengths and fracture spacings, and probably for fracture apertures. (Apertures are

not definitive in outcrops where significant weathering has occurred). Most outcrops are extensively fractured, and thus fracture "swarms" are rare. Bed thickness has some control on fracture spacing: thicker beds are less intensely fractured as a general rule, although a consistent, mathematical relationship is not yet evident.

The geometry of outcrop fracture patterns can be analyzed and is being used to calculate the most likely characteristics of the permeability enhancement due to a given fracture pattern. Progress along these lines is detailed in a later section of this paper. However, it is immediately relevant that permeability enhancement appears to be most sensitive to fracture apertures, whereas fracture orientations and lengths dictate the orientation and degree of permeability anisotropy, respectively.

Characterization of outcrop fracture patterns is a worthwhile exercise only if one or more aspects of the fractures in outcrop are analogous to fractures in subsurface reservoirs. The tectonic/stress histories of a given suite of strata may locally be similar for both outcrop and subsurface occurrences. In these circumstances the fracture patterns seen in outcrop would be expected to be similar to the reservoir fractures. However, it is also likely that the outcropping strata have been uplifted and exposed by secondary geologic events that did not effect the equivalent subsurface strata. In this case, only one or none of the fracture sets from the outcrops may have a subsurface analog. Thus, through-going fractures are inferred to have direct application to the subsurface whereas the shorter cross fractures are considered to be surface related.

The reconstructed stresses derived from tectonic events have been cross-referenced to a reconstruction of the fracture susceptibility of the strata through time, in order to indicate when, and in what orientation, fractures are likely to have formed. Fracture susceptibility is largely a function of the effective stress on the strata, which in turn is a combination of stresses derived from depth of burial, tectonic compression/extension, and pore pressure (Lorenz et al., 1993).

Several large-scale thrusts indent into the basin margins, creating local compression that increased the differential horizontal stress within the adjacent strata. Strata immediately adjacent to thrusts underwent the most severe compression, which also served to increase local pore pressure. Strata further from the thrust fronts experienced significantly less differential stress. The Laramide Wind River and Uinta Mountains thrust systems are inferred to have imparted significantly more stress in the mid-basin strata than the thin-skinned Sevier thrust belt to the west. Organic material within the more deeply buried strata underwent higher levels of maturation, resulting in larger volumes of natural gas and higher pore pressures, thus increased fracture susceptibilities in the deepest parts of the basin. Stress orientations and dominant fracturing within the deep, mid-basin strata are suggested by preliminary modeling to trend north-south between the Wind River and the Uinta Mountains thrusts. Further knowledge of the detailed local structure of the basin center may alter these conclusions.

Present-day conditions provide a tie-point for this modeling effort: if the model can replicate the present stress orientations across the basin, a degree of confidence can be inferred for the model and its sometimes subjective input parameters. Figure 3 portrays the few data points available on present in situ stress orientations, as measured from wellbore breakouts (oriented caliper logs) across the western part of the Green River basin. This map suggests that maximum horizontal stress is commonly oriented normal to an adjacent thrust front, or along a line between two nearby thrusts, as suggested by the model.

Ten of the better exposures of the Frontier Formation sandstone outcrops around the basin have been mapped, and four of these will be characterized in detail. A separate report describing the tectonic history of the basin and the fracture susceptibility through time of the strata will make preliminary predictions of the fracture orientations and stresses in the central, deep parts of the Green River basin.

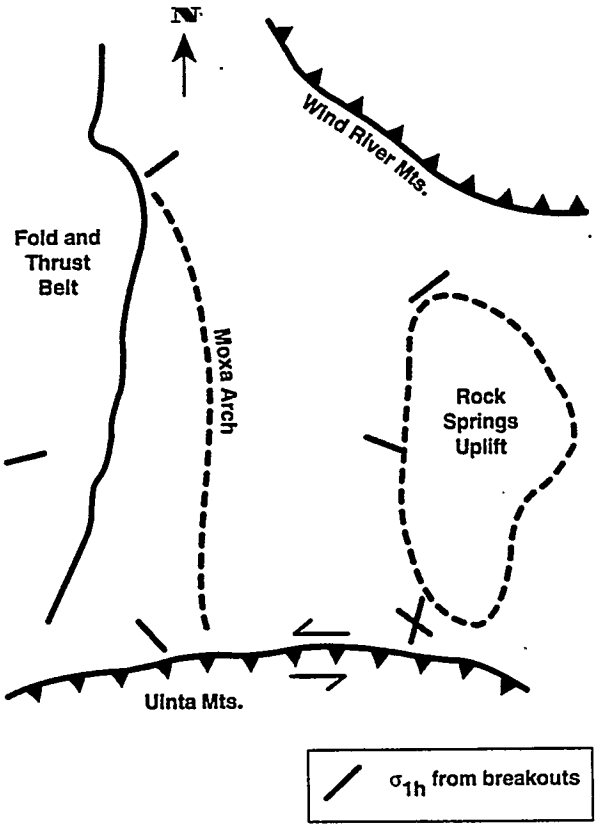


**Figure 3. Present-day in situ maximum horizontal compressive stresses in the Green River basin derived from wellbore breakouts.**

## Geophysical Fracture Mapping

**Background.** The presence of a natural fracture has been shown to cause seismic anisotropy in an in situ rock mass (Beydoun et al, 1985). In seismic data, this anisotropy manifests itself as shear wave birefringence, or simply, shear wave splitting. Observations of this wave splitting represent a potential tool for determining the density and azimuthal distribution of a natural fracture system.

When an S-wave passes through an anisotropic medium, the particle motion is polarized into two orthogonal components of differing velocities normally referred to as the S1 (fast), and S2 (slow), wave (Crampin 1989). The faster polarization corresponds to particle motion in the direction in which the rock is the least compliant, while the slower wave is polarized in the most compliant direction. As the S-waves propagate, the separation between the S1 and S2 waves becomes larger until shear wave splitting can potentially be observed. Birefringence is normally characterized by this time "lag" which represents the density of the fractures, and the wave polarization angles which describe the orientation of the anisotropy.

Traditionally, shear wave splitting has been identified in reflection surveys utilizing surface sources and receivers. In that case, the fast shear wave is polarized parallel to the fracture direction and the slow wave has particle motion perpendicular to the fracture system. However, S-wave particle motions are not necessarily confined to those orientations for non-vertical ray paths such as those found in a crosswell data set (Liu et al, 1989).

An extensive crosswell velocity survey was conducted in 1993 at the M-Site as part of the GRI project on hydraulic fracture detection. Seismic surveys were performed using triaxial receivers with over ten thousand source-receiver combinations between two wells separated by approximately two hundred feet. S-wave data in the survey were quite prominent and offer a

unique opportunity to investigate the effects of natural fractures on crosswell shear waves (Figure 4).

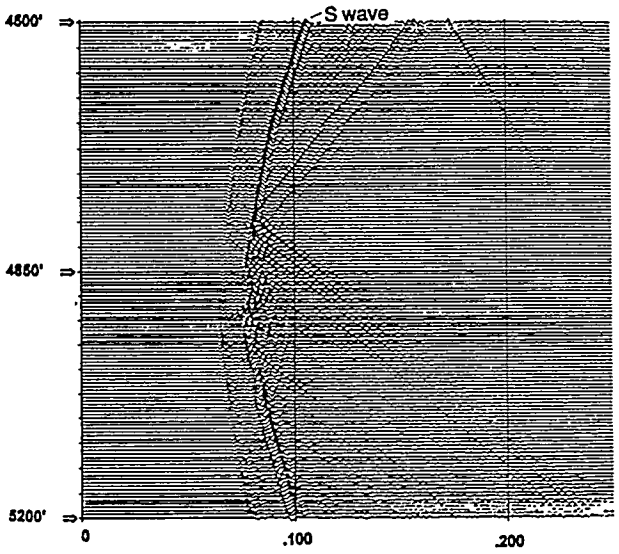


**Figure 4. Airgun depth-time records showing evidence of shear wave propagation in M-Site crosswell survey.**

**Project Description and Results.** The S-wave particle-motion data at the M-Site will be used to identify and characterize the fast and slow waves in a crosswell data set. If the shear wave is not split in the rock mass, the particle motion at the receiver during the S-wave arrival will show a single linear direction of polarization corresponding to the direction of the source. On the other hand, if splitting occurs between the source and receiver, the arrival of the fast S-wave will cause a linear particle motion related to the fracture direction which will degrade when the slower S2 wave arrives. At that point, a coordinate transformation will occur that will separate the shear wave into its two orthogonal components (Alford 1986); one axis will contain S2 wave energy while the other will only contain S1 energy.

The periods of linear motion corresponding to the S1 arrival can be identified using either particle motion diagrams (hodograms) or rectilinearity plots shown in Figures 5 and 6. Hodograms represent a projection of the 3-D receiver data onto a 2-D plane yielding a (nearly) straight line during periods of linear particle motion. The more complex rectilinearity method constructs a 3-D covariance matrix over a given time window and uses the eigenvalue solution of the matrix to test for linear motion (Jurkevics 1988). This is equivalent to finding the principle axes (i.e., eigenvectors) of a body consisting of point masses representing the 3-D displacement values for a small time increment of the data. If the particle motion is linear for that time window, the constructed body is "slender" and the matrix has a single, large eigenvalue. Rectilinearity itself is a measure of the relative magnitudes of the eigenvalues and approaches unity when the motion is linear and a single eigenvalue dominates. Both the hodogram and rectilinearity methods have been previously used to observe the transition from linear to non-linear particle motion which occurs during S1 and S2 arrivals as well as determining the polarization angle of that motion (Zhang & Schwartz 1994). However, because rectilinearity offers a 3-D view of the linear motion and lends itself to automated processing schemes, it has more promise in identifying the axes which contains purely S1 or S2 motion for our large data set.

Ongoing work entails the use of rectilinearity analysis to identify the existence and arrivals of S1 and S2 waves from the crosswell data set that were collected as part of the hydraulic fracturing work at the M-Site. Attention is directed at determining which ray paths exhibit splitting and how the time lag and polarization angles of the split waves relate to the fracture/ray path geometry. To this end, a routine was constructed to locate the periods of high rectilinearity and characterize them by their

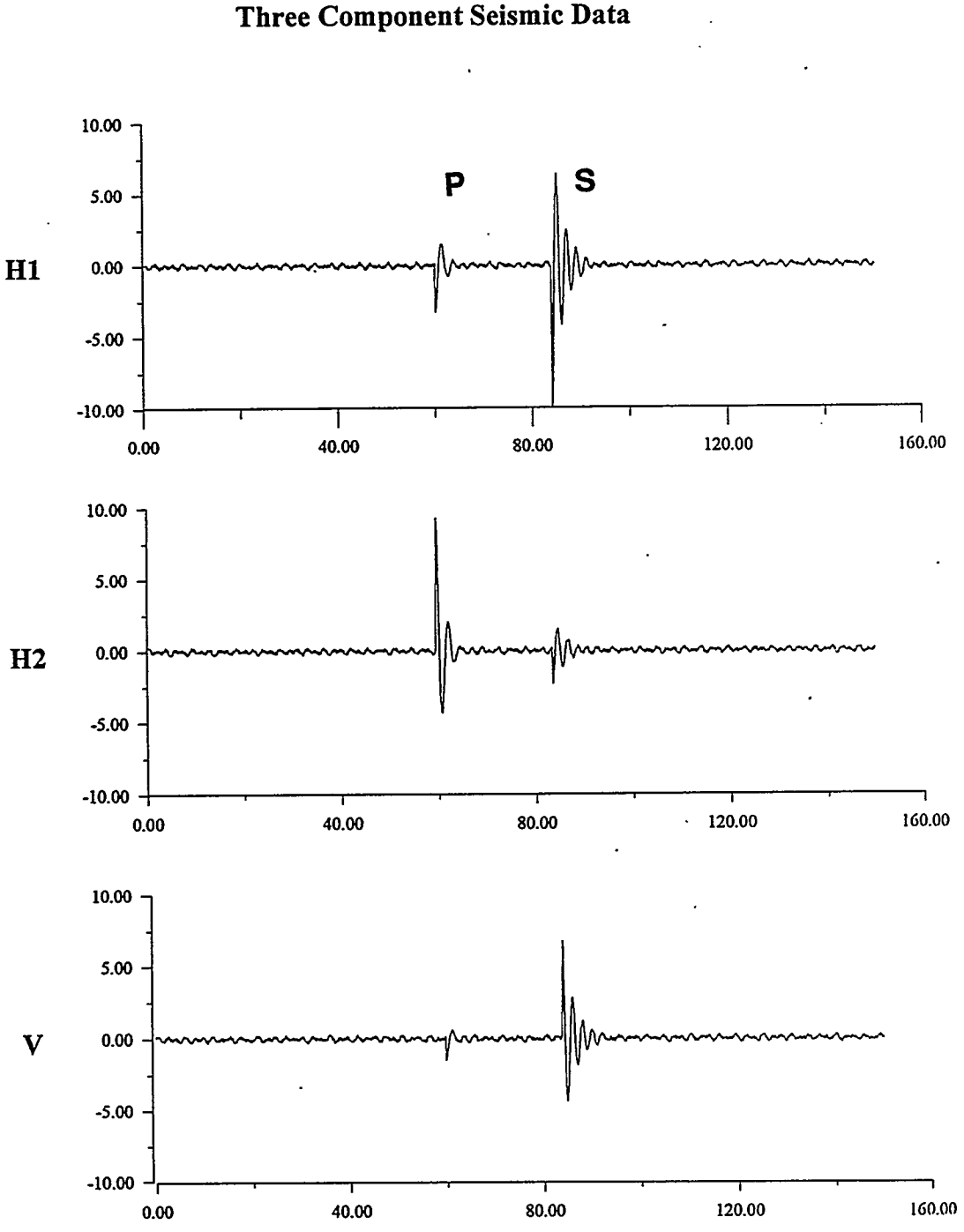


**Figure 5. Sample of seismic data containing P and S waves.**

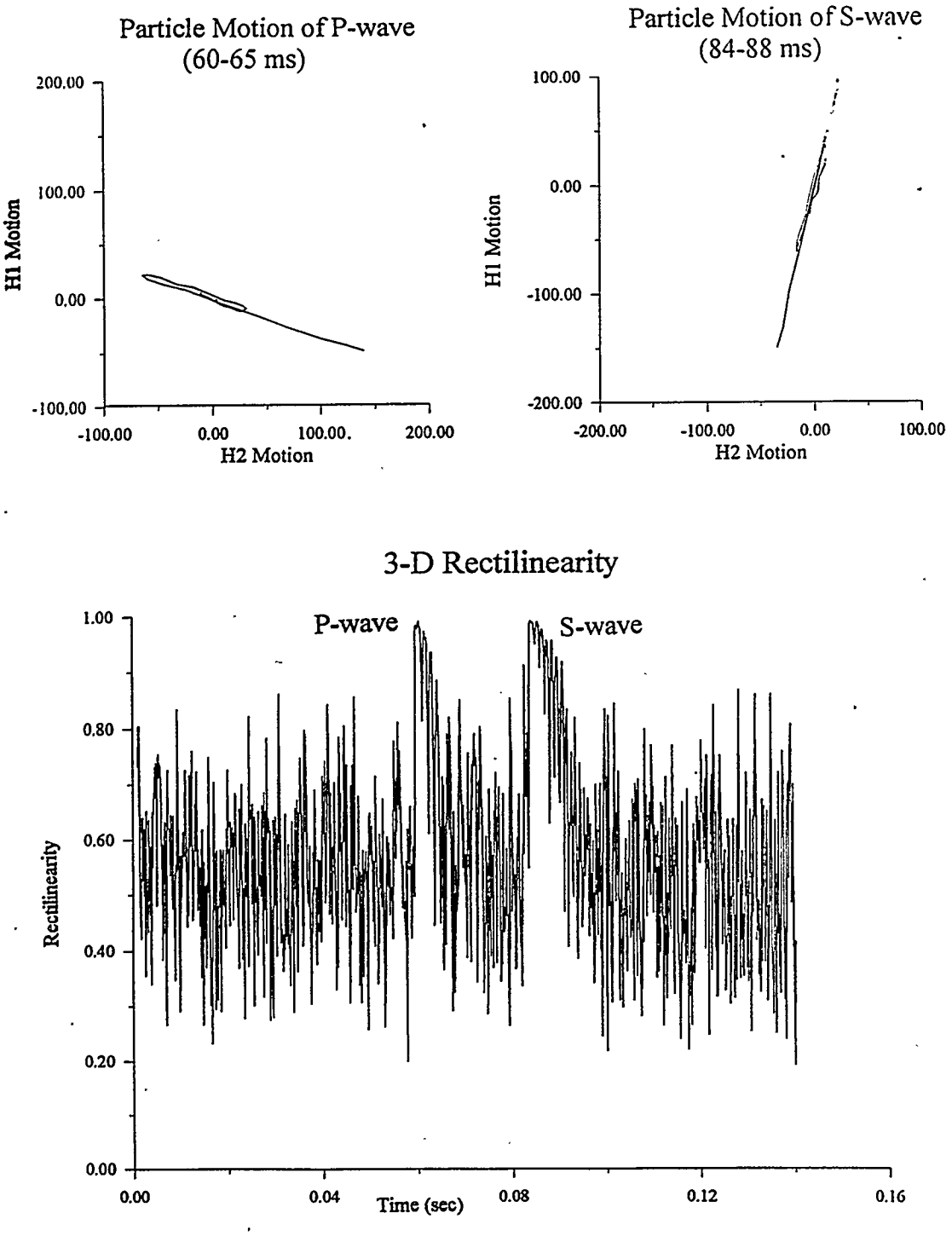


**Figure 6. Linear particle motion of sample data using hodograms and rectilinearity.**

respective linear particle motions. Preliminary results indicate that this data set does not show consistent shear wave polarizations parallel and perpendicular to the (known) fracture system. There is also evidence to suggest that the identification of the S2 wave will be difficult for crosswell data for which the distance between the source and receiver is small (Liu et al, 1991). If a relationship between the splitting parameters and the fracture system can be established, a means of back-projecting the data may be selected and implemented.

Parallel to the shear wave analysis, some background work is being performed. The rectilinearity method is being used to determine the unknown alignment of the horizontal receivers (H1 & H2) for each geophone location. This is accomplished by determining the P-wave azimuthal polarization for each geophone and relating the known source/receiver geometry to the polarization angle. A 2-D horizontal coordinate transformation can transform all of the data to a single, consistent N-E (and vertical) coordinate system. Additionally, some filtering issues are being investigated using the raw data and MicroMax® software. The correct filtering and the geophone orientations are both crucial to any extended shear wave interpretation.

Lastly, and separate from the birefringence issue, an automated routine for picking S-wave arrivals is being tested in the interests of constructed an S-wave tomogram of the data. This method uses a combination of the rectilinearity analysis, the P-wave arrival information, and a wave front selection algorithm. First-break shear wave data will aid in the overall M-Site effort to locate micro seismic events. They may also prove to be useful in the construction of a P-to-S velocity model.

**Fracture Network Analysis and Reservoir Modeling**

**Background.** The state of the art in simulation of fluid flow in fractured reservoirs relies on the application of dual porosity numerical models. These models contain two separate (possibly anisotropic) overlapping porous media, one for a permeable matrix and one for fractures in an impermeable medium. The flow of fluid in both media is coupled so that fluid can move from one to the other. The properties of each of the two components can vary from grid block to grid block as is typical in a finite element analysis. The fractured medium is equivalent to an anisotropic medium. Its permeability is defined as if it contained three mutually orthogonal regular sets of infinitely long parallel-plate fractures with a constant spacing and aperture.

There are several problems with this approach. First, natural fracture systems do not consist of three mutually orthogonal sets of smooth parallel planes. Therefore, some method is needed to describe the geometries of real fracture networks in such a way that the associated data provide useful input into the framework of conventional or improved reservoir models. Two particularly complicated issues in this process involve the consideration of scaling and spatial heterogeneity. Hence, an understanding is needed of the scale at which fracture geometries must be observed and how the relevant input data for modeling are extrapolated for a specific grid block.

Another major issue arises because the mechanical and transport properties of fractures are stress sensitive, much more so than the rock matrix, which renders the fluid transport behavior of the entire reservoir stress sensitive as well. At this time, much is known about the deformation of single fractures and how this affects the permeability (Brown, 1987). However, no proven

method has yet been developed by which the effective elastic compliance and stress-dependent permeability for a grid-block-sized piece of a fracture system can be calculated.

**Project Description and Results.** To solve the analysis of fracture networks, at least the following are needed: (1) development of methods for the quantitative analysis of fracture pattern, maps, and images, (2) use of data derived from this analysis to study scaling relations and the spatial heterogenity within fracture systems, and (3) establishment of methods to derive permeability tensors and the associated elasticity tensors for gridblocks from fracture patterns and other pertinent data.

Ongoing work under this project focuses on the problem of defining approximate fracture permeability and elasticity tensors for each grid block in a fractured reservoir from maps (including photographs) of natural fractures that were created during surveys of outcrops in the Green River basin. As a practical first step, a statistical model of randomly or systematically distributed cracks due by Oda (1982, 1984, 1985, 1986) is being implemented. The model relates elastic compliance and permeability tensors to the crack geometry through "fabric" tensors that are volume averages of the contribution from each crack in the population. The volume average contains functions of the crack orientation, length, and aperture, so that long cracks or wide cracks contribute relatively more than their smaller cousins. Elasticity is in this model is implicitly coupled to fluid flow through an assumed relationship between crack aperture and normal stress across the crack.

Oda's model and its current implementation are practical at the expense of rigor because there are many simplifying assumptions which reduce the generality of the results. However, the model is easy to apply and probably retains the essential features of real natural fracture populations to be a significant improvement over assuming that cracks reside in three infinitely long orthogonal sets. The latter concept constitutes the core of the existing dual porosity reservoir simulators. It is also significant that the permeability tensors derived from Oda's model can easily be translated into the proper inputs for the available dual porosity models.

At this point, considerable work has been done in an attempt to develop a method to digitize fracture location, length, and orientation automatically from scanned digital images. This problem has proved to be difficult due to a combination of the poor contrast between fractures and the background, and the presence of many other objects such as trees with similar gray-scale intensity as the fractures themselves. However, success was achieved in enhancing linear features in digital photographic images with spatial filters, ultimately making the work of digitizing by hand somewhat easier. Several digitized outcrop fracture maps have been used to calculate permeability tensors. Figures 7 to 9 illustrate one such sequence from scanned photograph, to digitized fracture pattern, to the 2-D permeability tensor. Additionally, work is in progress to include a realistic model of crack closure under normal stress in the model, allowing the evaluation of changes in the permeability tensor under changes in stress state.

## Core-Based In Situ Stress Measurements at the M-Site

**Background.** Total and effective stress measurements provide the boundary conditions for reservoir simulations during the exploration and production phases. Although hydraulic fracturing is accepted as the standard for determining orientation and magnitude of the minimum horizontal stress, it is expensive, leading to relatively infrequent use and widely spaced data

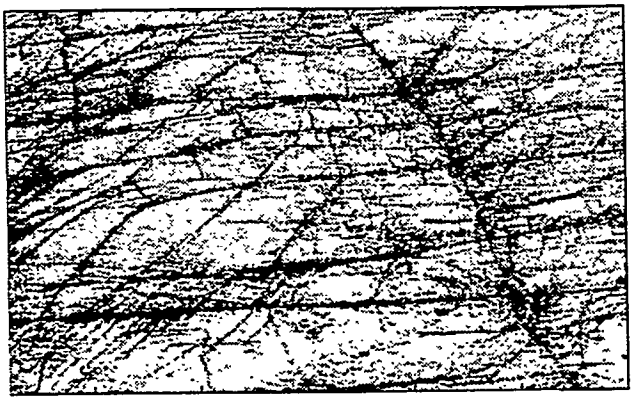

**Figure 7. Photograph of fractures within a marine sandstone unit of Frontier formation east of Kemmerer, Wyoming (Lorenz and Laubach, 1994). The area shown is approximately 1000x2000 ft.**

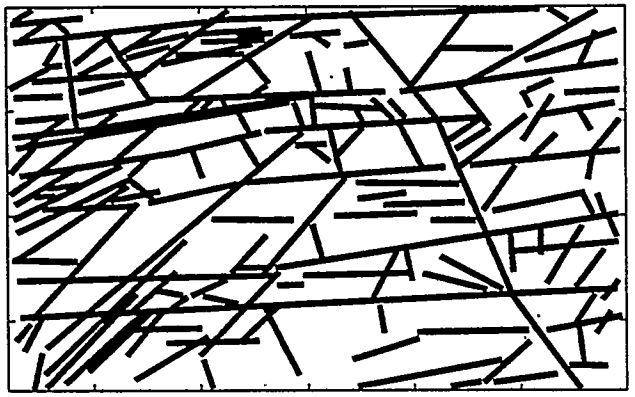

**Figure 8. Digitized map of fractures in Figure 7. Fractures are approximated as straight lines. The aperture is assumed to be proportional to the fracture length.**

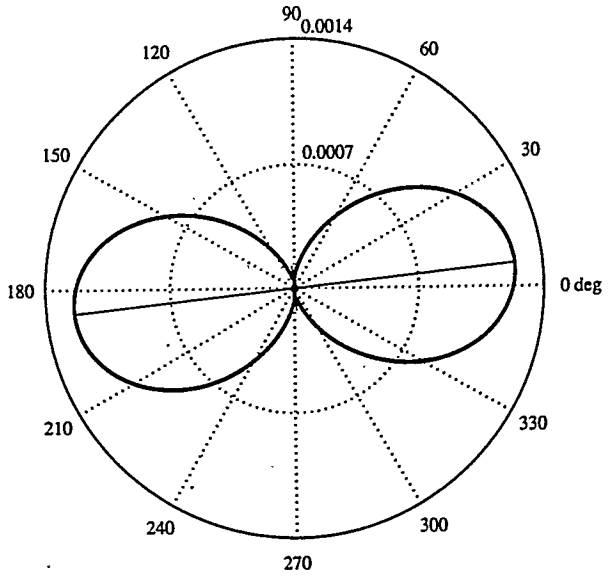


**Figure 9. Permeability tensor (permeability as function of orientation) for fractures shown in Figure 8. The ratio of maximum to minimum permeabilities is 23; the principal permeability is aligned with the orientation of the longest fractures.**

points. An alternative approach is based on measurements on oriented core. These "core-based" methods include Anelastic Strain Recovery (ASR), Differential Strain Curve Analysis (DSCA), Kaiser Effect, compressional and shear wave velocity measurements, and shear wave birefringence. The most established of these methods is the determination of the orientation of the velocity anisotropy. DSCA is also employed to evaluate the ratio of the principal in situ stresses. ASR provides answers quickly but must be applied on fresh core in the field. In some cases, ASR has also been used to estimate stress magnitudes as well as determine stress orientation. The Kaiser effect technique offers possibilities for determining stress orientations and magnitudes without knowledge of any physical rock properties.

Except for the Kaiser effect, core-based methods depend on the assumption that relaxation cracks form when the core is cut free and locked-in residual stresses are released. Driven by the largest locked-in stresses, more relaxation cracks open in the direction of the maximum in situ compressive stress. Rock properties that depend on crack density and degree of opening can detect the anisotropic orientation of the relaxation cracks, and this indicates the orientation of the in situ stress.

The Kaiser effect is based on the observation that many materials emit high frequency bursts of sound when loaded. The bursts of sound, called acoustic emissions or AE, are due to grain-scale failures, such as pore collapse or grain cracking. Typically, AE increase in number as the load on a sample is increased, drop sharply during unloading, and remain low until the previous peak stress is surpassed. An abrupt increase in AE rate at that stress is a marker of the previous peak stress.

**Project Description and Results.** Extensive knowledge concerning the in situ stress state at the M-Site motivated a comparison of all six methods above. Oriented sandstone core from 4314 and 4567 ft in Monitor Well #1 was used. First, attempts were made to measure ASR and monitor AE from fresh core. Subsequently, ultrasonic velocity, DSCA strain, and AE data were gathered at atmospheric conditions, in hydrostatic compression, and in uniaxial, triaxial, and extensile deviatoric loading experiments. Triaxial tests demonstrated significant nonlinearity and a nearly 300% increase in tangent (elastic) modulus at stresses up to 100 MPa, consistent with compaction and crack closure.

Compression and shear wave velocities were measured as a function of azimuth on core from both depths. The results are shown in Figures 10 and 11, which are polar plots with the minimum velocity subtracted off to emphasize the angular velocity variations. The observed velocity anisotropies are 3-10 % and indicate minimum in situ principal stress directions of N28E for core from 4314 ft and N5W for core from 4567 ft. Shear wave data for horizontally and vertically polarized waves in the sample from 4567 ft indicate somewhat smaller anisotropies but the same minimum principal stress direction. (Figure 11.)

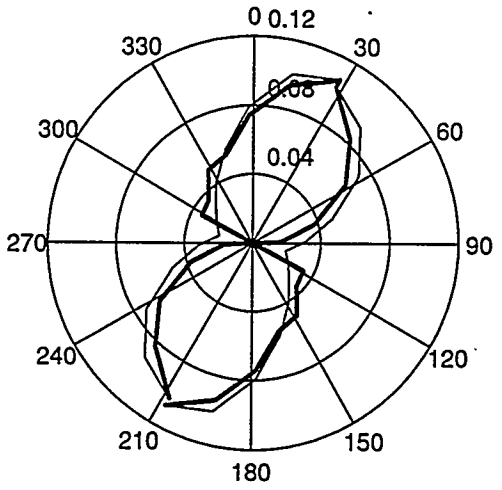


**Figure 10. Two independent measurements of compressional wave velocities on core from 4314 ft as a function of azimuth. Velocities were normalized to $V_{min}$=4.08 km/s.**

Shear wave birefringence was invoked earlier as a tool for detecting natural fractures in situ. Shear wave birefringence can also be related to the preferred orientation of relaxation microcracks in rock, and therefore, to in situ stress orientations (Yale and Sprunt, 1989). Figure 12 shows the amplitude of shear waves propagating along the axis of core from 4567 ft between transducers with crossed polarization. Normalized amplitudes are plotted as a function of the angle between the transmitter polarization and North as the core was rotated. The amplitude follows a

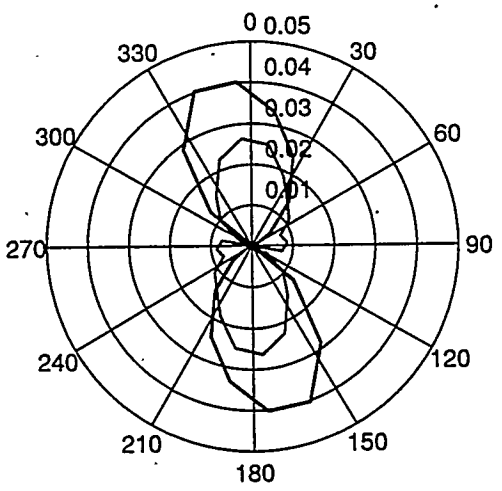


**Figure 11. Shear wave velocities (SH and SV) as a function of azimuth on core from 4567 ft. Velocities were normalized to $V_{min}$=2.51 and 2.23 km/s.**

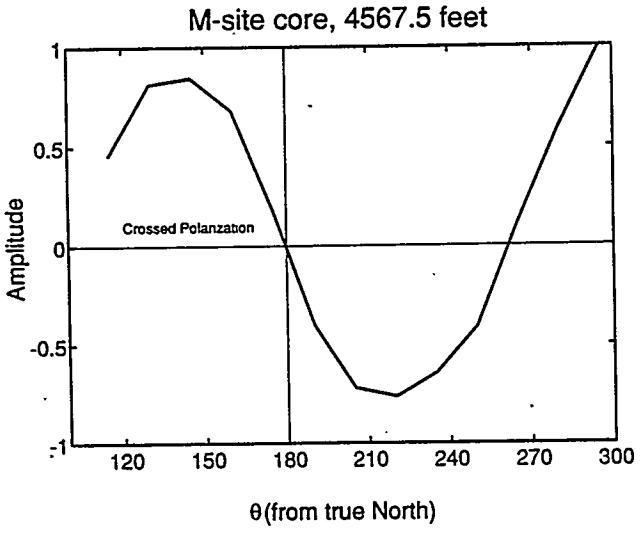


**Figure 12. Signal amplitude for cross-polarization shear transducers, propagating a shear wave parallel to core axis (vertical). Note polarity change at 180 and 270 degrees.**

cos2θ distribution with a change in sign (phase reversal) when the fast and slow directions, corresponding to the directions of maximum and minimum stresses, are rotated into and back out of alignment with the transducer polarizations.

Strain measurements (DSCA) showed that the principal strain axes were closely aligned with the in situ stress directions inferred from velocity and previous measurements (Warpinski and Teufel, 1989). No evidence was found for an increase in stiffness correlated to the magnitude of the in situ stress.

Kaiser effect measurements relied on uniaxial, conventional triaxial, and extensile compression tests on plugs cored at various orientations to the full core as it was received. AE interpretations were made based on both uniaxial loading measurements and on extensional loading (Holcomb, 1993). The underlying idea of the latter is that uniaxial testing for determining in situ stress is flawed because of the rotational invariance of the stress, resulting in the possible growth of cracks of many different orientations. Therefore, the onset of AE, produced by crack growth, is not uniquely linked to the orientation of the uniaxial stress. Figure 13 is a plot of threshold stress at the onset of AE in triaxial extension tests with a maximum at about 30°. According to Holcomb (1993), this direction should coincide with the direction of the minimum principal horizontal stress.

Surprisingly, no ASR or AE signals were obtained on fresh core. This means that time-dependent strains were small to zero, and only a few AE events were detected. Apparently, the relaxation either did not occur or was completed before instrumentation was installed. Based on past experience at the M-Site, it is unlikely that the strain relaxation was completed before the instrumentation was installed, approximately 6 hours after the core was cut. In light of the

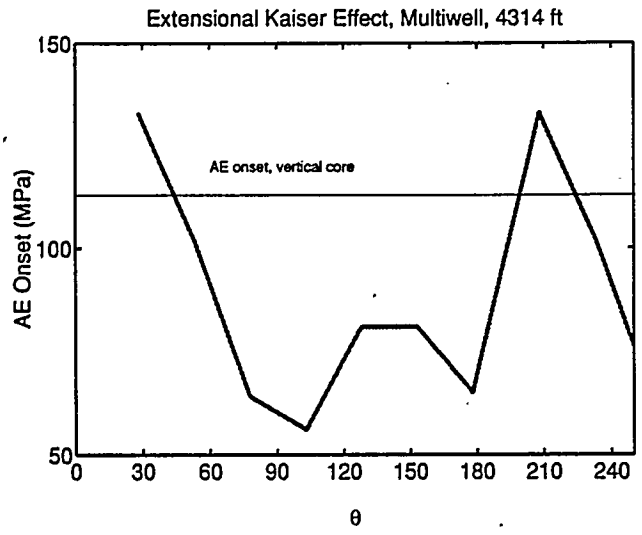


**Figure 13. AE onset for extensional tests.**

velocity and strain results mentioned earlier, however, it is conceivable that relaxation cracks were already formed in situ. They might have developed when pore pressure increased during the maturation phase or during the tectonic evolution of the reservoir.

## FUTURE WORK

Future Work in FY'95-96 will focus on basin fracture characterizations, the advancement of fracture network modeling, and the documentation of the results obtained from core-based stress measurements at the M-Site. Laboratory geomechanics measurements will be resumed as project involvement in subsurface reservoir analyses demands.

## ACKNOWLEDGEMENTS

The network analysis of fracture systems in this report was jointly funded by the Morgantown Energy Technology Center and the Bartlesville Project Office of the U. S. Department of Energy. The Gas Research Institute also funded a substantial portion of the evaluation of the core-based methods for in situ stress measurements.

## REFERENCES

Alford, R. M., 1986. Shear data in the presence of azimuthal anisotropy: Expanded Abstracts, 56th Annual International SEG Meeting, 1986, Houston, pp. 476-479.

Brown, S. R., Fluid flow through rock joints: the effect of surface roughness, J. Geophys. Res.,92, 1337-1347, 1987.

Beydoun, W. B., C. H. Cheng, and M. N. Toksoz, Detection of open fractures with vertical seismic profiling, J. Geophys. Res., 90, 4557-4566, 1985.

Crampin, S., Suggestions for a consistent terminology for seismic anisotropy, Geophys. Prosp., 37, 753-770, 1989.

Holcomb, D. J., Observations of the Kaiser effect under multiaxial stress states: implications for its use in determining in situ stress, Geophys. Res. Lett., 20, pp. 2119-2122, 1993.

Holcomb, D. J., General theory of the Kaiser effect, Int. J. Rock Mech. Min. Sci. & Geomech. Abs., 30, pp. 929-935, 1993.

Jurkevics, A., Polarization analysis of three-component array data, Bull. Seismol. Soc. Am, 78, 1725-1743, 1988.

Liu, E., S. Crampin, and D. B. Booth, Shear-wave splitting in cross-hole surveys: modeling, Geophysics, 54, 57-65, 1989.

Liu, E., S. Crampin, and J. Queen, Fracture detection using crosshole surveys and reverse seismic profiles at the Conoco Borehole Test Facility, Oklahoma, Geophys. Journal Int., 107, 449-463, 1991.

Lorenz, J. C., and S. E. Laubach, Description and interpretation of natural fracture patterns in sandstones of the Frontier Formation along the Hogsback, southwestern Wyoming: Gas Research Institute Topical Report, GRI 94/0020 89 p., 1994.

Lorenz, J. C., N. R. Warpinski, and L. W. Teufel, Rationale for finding and exploiting fractured reservoirs, based on the MWX/SHCT-Piceance basin experience: Sandia Report SAND93-1342, 147 p., 1993.

Oda, M., Fabric tensor for discontinuous geological materials, SoilsFdns., 22, 96-108, 1982.

Oda, M., K. Suzuki, and T. Maeshibu. Elastic compliance for rock-like materials with random cracks, Soils Fdns., 24, 27-40, 1984.

Oda, M., Permeability tensor for discontinuous rock masses, Geotechnique, 35, 483-495, 1985.

Oda, M., An equivalent continuum model for coupled stress and fluid flow analysis in jointed rock masses, Water Resour. Res., 22,1845-1856, 1986.

Warpinski, N. R., and L. W. Teufel, In-Situ Stresses in Low-Permeability, Nonmarine Rocks, J. Petr. Tech., April, pp. 405-414, 1989.

Yale, D. P. and E. S. Sprunt, Prediction of Fracture Direction Using Shear Acoustic Anisotropy, The Log Analyst, March-April, pp. 65-70, 1989.

Zhang, Z. & S. Schwartz, Seismic anisotropy in the shallow crust of the Loma Prieta segment of the San Andreas fault system, Journal of Geophysical Research, 99, 9651-9661.

# Session 5A

## *Low Permeability Reservoirs — Natural Fracture Detection*

# 5A.1 LBL/Industry Fractured Reservoir Performance Definition Project

**Progress Report:** April 1, 1995

**Contract Number** DE-AC03-76SF00093

**Contractor** Lawrence Berkeley Laboratory
1 Cyclotron Road
Berkeley, CA 94720

**Contractor Project Manager** Sally M. Benson

**Principal Investigators** Ernest L. Majer
Jane C.S. Long

**METC Project Manager** Royal J. Watts

**Period of Performance** Sept. 10, 1991 to Sept. 10, 1996

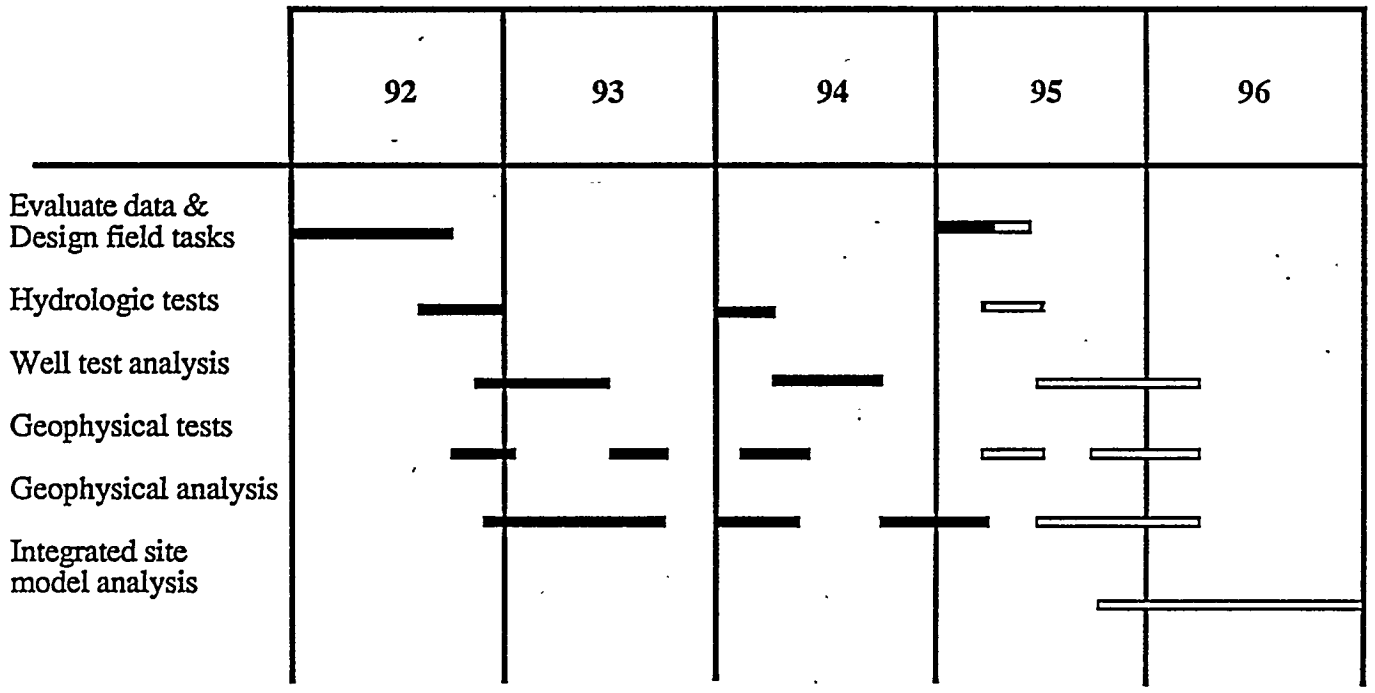

## OBJECTIVES

One of the problems facing the petroleum industry is the recovery of oil from heterogeneous, fractured reservoirs and from reservoirs that have been partially depleted. In response to this need, several companies, notably British Petroleum USA, (BP) and Continental Oil Company (CONOCO), have established integrated reservoir description programs. Concurrently, LBL is actively involved in developing characterization technology for heterogeneous, fractured rock, mainly for DOE's Civilian Nuclear Waste Program as well as Geothermal Energy programs. The technology developed for these programs was noticed by the petroleum industry and resulted in cooperative research centered on the petroleum companies test facilities. The emphasis of this work is a tightly integrated interdisciplinary approach to the problem of characterizing complex, heterogeneous earth materials. In this approach we explicitly combine the geologic, geomechanical, geophysical and hydrologic information in a unified model for predicting fluid flow. The overall objective is to derive improved integrated approaches to characterizing naturally fractured gas reservoirs.

## BACKGROUND INFORMATION

In the previous three years a series of joint LBL/Conoco-Amoco field experiments have been conducted at Conoco's Newkirk, Oklahoma Borehole Test Facility (Figure 1). The facility (Queen et al. 1992), contains a number of deep and shallow wells used for geophysical and hydrological tests. The site occupied for the subject experiments consists of five wells in a "5-spot" pattern (GW wells) with the outside wells approximately 50 meters away from the center well (Figure 1). Past work to characterize the shallow structure at the test site has included a series of crosswell seismic surveys and hydrologic well tests. The shallow wells penetrate a fractured shale and limestone sequence of the Lower Permian Chase Group (Queen and Rizer 1990). The regional dip of the formations is less than 1 degree west-southwest. As noted in Queen and Rizer (1990) two orthogonal sets of vertical fractures have been mapped: a systematic set striking N70°E and a non-systematic set at N25°W. The velocity variations between the shale and the limestone are sizable: contrasts of 2 to 1 exist (Lines et al. 1992, Harlan 1990). The LBL work described in this paper is focused on the Fort Riley limestone, a 10 to 15 meter thick fractured formation approximately 16 meters below the surface. This formation is bounded by layers of much lower seismic velocities. Shown in Figure 2 in a velocity log derived from the single well data in GW-3.

The processing of previous crosswell seismic and hydrologic data from the Conoco site indicated that there is strong evidence for open and conductive fractures trending N70°E, (Datta-Gupta et. al., 1994). This is approximately parallel to a line extending from GW-2 to GW-5 (Figure 1). That is, the dominant fracture direction inferred from the seismic and hydrologic data is consistent with the stress and geologic data as described in Queen and Rizer (1990). From the hydrologic inversions there was also an indication that there are either a greater number, or larger hydrologically conductive fractures between GW-3 and GW-1, parallel to a line connecting GW-5 and GW-2, (Datta-Gupta, et. al., 1994). Our initial crosshole work also indicated that there may be a reflector (vertical fracture striking NE?) in the subsurface a few meters north of GW-3. However, it was clear from the initial work that we had not unambiguously identified a single "target" fracture that could be responsible for the hydrologic results that showed a "fast path" between GW-5 and GW-2.

## PROJECT DESCRIPTION

Under DOE funding, LBL participates in the geologic and geophysical investigations at the test facility. LBL scientists work cooperatively CONOCO personnel in both the exploration and and production departments. Amoco and Phillips Petroleum are also involved with the Conoco test facility and are contributing to this effort. The basic concept of the work is to develop and integrate the various geophysical and hydrologic methods through a focused research effort a a few well-calibrated and characterized sites. The first phase of the work was modeling and planning field experiments by applying the techniques described above adapted from the technology

developed in DOE nuclear waste and geothermal programs to existing seismic and hydrologic data. The second stage, described here is to actually carry out DOE/CONOCO field experiments at the industry sites. To date the work has focused on using high resolution crosshole, and single well, seismic imaging and VSP for fracture detection in both the shallow and deep test holes. This is being combined with the development and application of the hydrologic inversion methods for fractured reservoirs.

## RESULTS

In order to enhance the seismic visibility of the suspected fracture we decided to inject air into the formation, the assumption being that the air would travel in the permeable fractures and increase the reflectivity, or attenuation properties of the fractures. The plan was to inject air into GW-5 and drawdown GW-2 below the Fort Riley formation, an attempt to force air into the assumed fracture. If there is a fast fracture path from GW-5 to GW-2, as indicated by the hydrologic data, then air would possibly follow that path and provide an improved seismic target.

In June of 1994 an air injection experiment was performed. The concept was to do a before and after seismic imaging experiment to determine the effect of air injection, and also to perform a "differencing" type of experiment to locate the elusive conductive fracture. The GW wells had been completed with slotted PVC casing and a sand backing over the Fort Riley limestone sequence. Above and below the limestone the wells were completed with unslotted PVC casing with bentonite behind the casing. Well GW-5 was packed off over the slotted section and air injected uniformly over the packed off region using an air compressor at 50 psi (we were careful to keep the pressure below the parting pressure of the formation). This was a rather crude means of air injection but this was not meant to be a precise injection of air for inferring transport behavior, but a means to increase the seismic visibility of the conductive fractures. During the air injection the water level in GW-2 was kept below the bottom of the limestone in order to create a negative pressure gradient in GW-2 to further encourage flow of the air towards GW-2.

Before the air was injected a series of cross well measurements were taken between the well pairs GW-3 and GW-1, GW-3 and GW-2, GW-3 and GW-4, and GW-3 and GW-5. The procedure for the crosshole measurements was to move the transmitter (piezoelectric) and 8-channel receiver string (hydrophones) in 0.25 meter increments up the holes concurrently, from a few meters below the Fort Riley to a few meters about the formation. The transmitter was positioned such that it was directly across from the center of the receiver string. The differences in well head height (relative to sea level) were accounted for when the data were taken. All surveys utilized a high-frequency imaging system (Majer et al. 1991). A piezoelectric source was used with swept frequencies from 1,000 to 10,000 Hz over a 50 millisecond time window with a recording time of 80 milliseconds at 0.020 milliseconds/sample.

Single well reflection surveys were also performed in wells GW-1 and GW-3. The procedure for acquiring the single well data was to use the 8-channel receiver hydrophone string with 1/4 meter intervals between receivers. As the string of receivers were held in place, the source was moved from one meter below the bottom receiver to the approximate bottom of the Fort Riley formation at 0.25 meter intervals. The receiver string was then moved up 1/4 meter and the procedure repeated until the entire Fort Riley was covered. This procedure was then repeated with the source above the receiver string. The result was a multifold imaging data set using a split spread.

After these "before" surveys were performed we then began injecting air into the formation. The effect of the air injection on the Fort Riley formation was continuously seismically monitored between GW-1 and GW-4 by placing the piezoelectric transmitter at the center of the formation in GW-1 and centering the receiver string in the formation in GW-4. The transmitter and receiver were not moved during this monitoring. The data were taken at various time intervals over the day. After the completion of the air injection, cross well measurements were again taken between wells GW-3 and GW-1, GW-3 and

GW-2, GW-3 and GW-4, and GW-3 and GW-5 with both the source and receiver at the same elevation. The single well reflection surveys in GW-3 and GW-1 were also repeated with the exact geometry as before injection.

## Results of Seismic Monitoring During Air Injection

Our previous seismic and hydrologic work had determined that the target fracture was between wells GW-3 and GW-1. It was unknown whether the injected air would follow a path along a fracture or whether it could be seismically detected. Therefore, the injection process was monitored from GW-4 to GW-1, a distance of 100 meters, to ensure that as many fractures as possible between the two wells were monitored so that the air produced the maximum effect on the seismic signal.

The monitoring began 30 minutes before the start of the air injection and repeated at two minute intervals. After one hour there was absolutely no change in the signal and monitoring was increased to every ten minutes. After two hours of injecting air there was a detectable decrease in travel time. This effect lasted about an hour, when the travel time returned to the original value. The travel times then immediately began to increase and the amplitudes began to decrease. This suggests that as the air front displaced the water there was an initial increase in velocity detected by the crosswell measurements due to an increase in pressure of the water in the fracture. After this pressure front passed and the air displaced the water, the velocities and amplitudes decreased in response to the air in the fracture.

The air injection was terminated overnight, but the seismic source and receivers were not removed but left in the exact same place to reduce any ambiguity upon continuation of the monitoring the next day. Figure 3 is a summary of the seismic monitoring between wells GW-4 and GW-1 during the air injection. In Figure 3. the time from the start of the air injection increases from the top of the figure to the bottom, the top trace being just before the air injection and the bottom trace being at the end of the air injection. The entire air injection was spread over two days. The middle set of traces in Figure 3 are the result of monitoring every two minutes the next morning after the air injection pump was turned back on. The first arrival amplitudes are slightly higher than the amplitudes seen just before the pump was turned off. This indicated that only a small amount of air had been replaced by water overnight. It is obvious from the crosswell data in Figure 3 that the air injection had a large effect on the seismic properties. The air significantly reduced the amplitudes of the seismic signal by an order of magnitude and decreased the travel time of the initial arrival by several samples. Our hope, was that due to increased acoustic impedance contrasts, a reflection from the air filled zone would be observed.

## Analysis of the Crosswell Imaging Data After Injection

The results of the monitoring during the air injection indicate that one would expect a significant effect on the crosswell data if air had migrated between any of the crosswell pairs. The crosswell results can be quantified by calculating a summed spectral amplitude over a specified frequency band (4000 to 6000 Hz) in 0.08 millisecond time steps along each trace at each depth. The result is a time-amplitude plot for each trace. Figure 4 shows the crosswell data between well pairs GW-3/GW-1 and GW-3/GW-4 before and after air injection. Almost for all traces a sharp decrease in the amplitude of the initial signal is observed. However, the GW-3 to GW-4 crosswell first arrival signals look virtually identical before and after the air injection. This also is an indication of the repeatability of the data. The only significant difference between the before and after data from GW-3 to GW-4, is the increase in amplitude of a secondary arrival at 17 milliseconds. The large decrease in seismic energy produced when introducing air into the fracture is easily seen in these plots. The crosswell pairs GW-3 to GW-5 and GW-3 to GW-2 are similar to GW-3 to GW-1.

Although very little effect was seen in the before and after results for the GW-3 to GW-4 P-wave arrivals, there is an increase in energy at about 7 milliseconds after the P-wave for traces in the 23 meter range of depths. This may be a

reflection from a vertical fracture set. The other crosswell data indicates that the there may be a fracture or set of fractures which intersects the planes between well GW-3 and the wells GW-5, and GW-1. The data from GW-5 may be misleading because air was pumped into the entire length of the well and it is probable that some air remained in the rock matrix or sand pack around the well when the measurements were taken. However, because of the speed in which the air traveled, it is likely that there is a fast, fracture-like path extending from near GW-5 to near GW-2. Since the air filled fracture produces an order of magnitude drop in amplitude, it is likely that there would be reflected energy from this feature. The increase in energy at 7 milliseconds after the P-wave in the GW-3 to GW-4 data could be caused by such reflected energy. At 4000 m/s velocity, this would put a vertical feature about 14 meters from GW-3. The strike of such a feature cannot be determined; the location between GW-3 and GW-1 is based on the drop in amplitude between those boreholes.

**Analysis of Single Well CDP Data**

The single well experiment was designed with the intention of processing the data as a common CDP reflection survey. Data were acquired from wells GW-3 and GW-1 before and after the air injection. The before and after injection traces were each initially sorted into CDP gathers for GW-3. These gathers show a low amplitude P-wave arrival at a velocity of 4000 m/s, and very large secondary arrivals with a velocity of 2200 m/s. The radiation pattern of the piezoelectric source used is such that the P-wave energy is largest at 90° to the borehole and is quite small parallel to the borehole. The radiation pattern for the S-wave has maximum energy 45° to the borehole (Gibson, 1994). These radiation patterns are consistent with our data and taken with the velocities, indicate that the secondary arrivals are S-waves. The data are surprisingly free of tube waves which are commonly seen in borehole data. Shown in Figure 5 are several shot gathers from the single well profiling. The strong secondary arrival is an S-wave, not a tube wave. The absence of tube waves may be due to the sand packing that was used to pack the slotted PVC casing, which is necessary for hydrologic testing, but the high frequencies used are also a great advantage in tube wave minimization.

The strong S-wave energy had to be removed from the data before stacking. Muting these arrivals is not advisable since reflectors are expected close to the well and as much energy as possible should be preserved in this time window. F-K filtering was performed instead of the mute on receiver gathers before sorting into CDP gathers. Velocities from 1000 m/s to 4200 m/s at all frequencies were removed using a fan filter. A simple stack was then performed with a constant stacking velocity of 4000 m/s, which is consistent with the present cross well data and with borehole logs. In this case the velocity logs represented a "horizontal" velocity variation with respect to the "downhole reflection line." The CDP's ranged from 17 meters to 28 meters at 0.25 meter increments, which extended the survey to the higher velocities at the top of the Fort Riley limestone formation, and into the lower velocities at the bottom of the formation. This "horizontal" velocity variation is difficult to remove and was ignored for this application, we were interested in the central part of the formation and not the edges.

The resulting CDP stacks before and after the air injection in GW-3 are shown in Figure 6. The two sections representing before and after injection are almost identical except for a strong reflector at 7 milliseconds after injection. This reflector was observed at the same time as the proposed reflector seen in the GW-3 to GW-4 crosswell data. The reflection is strong from a depth of 19 meters to 26 meters, which is a region of relatively constant velocity. The reflector appears to extend to a depth of 29 meters, but is less continuous due to large velocity contrasts in this region. There is evidence of reflected energy above 19 meters, but the large velocity contrasts at these depths produce poor stacks. The reflector is observed on the before-injection section, but it is not as strong and not as extensive.

The exact same processing was performed on single well data acquired from GW-1, Figure 7. The travel time between GW-1 and GW-3 is about 12.5 milliseconds. Therefore, if the targeted reflector is between GW-3 and GW-1 the two-way travel time from GW-1 should be 18 milliseconds. Depending on the depth in the well,

there does appear to be an increase in energy at 15 to 18 milliseconds from before injection to after injection (Figure 7). However, the reflector appears very weak, probably due its distance from GW-1. Also the disadvantage of using a constant velocity stack is more pronounced at larger distances from the reflector.

### Water Level Monitoring and Hydrologic Inversion

During the 1994 air injection test, while air was injected at a constant pressure in well GW-5 and water was pumped out of well GW-2, water levels were monitored in wells GW-1, GW-3, and GW-4. The transient response of these monitoring wells on June 11 is shown in Figure 8. The larger response at GW-3 is expected as it is slightly closer to the injection well than are GW-1 and GW-4. Overall, the three wells show a smooth, consistent response that should be amenable to analysis, thus providing an estimate of average flow properties at the borehole test facility.

Figure 8 also shows analytical solutions for idealized models representing water injection at a constant pressure into a homogeneous medium with either linear or spherical flow geometry around the injection well. The corresponding solution for radial flow geometry does not exist in a simple closed form, but would fall between the linear and spherical cases, much as the observed data does. Based on the geology and well spacings, and previous well-test analyses [Datta-Gupta et al., 1994], radial flow geometry is expected for a pump or injection test from GW-5 to GW-1, GW-3, and GW-4. This is in contrast to the strong connection between wells GW-5 and GW-2, hypothesized to be a large fracture or fracture zone, which would yield a more nearly linear flow geometry. Thus the present water-level analysis, while still very preliminary, is consistent with previous well-test analysis.

Future work will take either a semi-analytical or numerical approach to predicting the water level response for radial flow geometry. Then, by matching the observed data, an average hydraulic diffusivity (hydraulic conductivity divided by specific storage) may be inferred. The solution will also determine the air injection rate, which must be large relative to the pumping rate from well GW-2, in order for radial flow geometry to be valid. If this is not the case, further numerical modeling may be conducted to more accurately represent the dipole nature of the air injection test. If such modeling is done, it will also be of interest to compare the effects specific to injecting air rather than water, to see if the simpler solutions which treat air as though it were water are reasonable approximations.

### Resolution and Uncertainty of Hydrogeologic Data at the Conoco Borehole Test Facility

#### Introduction

The concepts of resolution and uncertainty have been used in geophysical characterization as ways to quantify the reliability of geophysical interpretations obtained through the inversion of geophysical data (Backus and Gilbert, 1967, 1968). Resolution measures how well subsurface properties can be determined as a function of space. The uncertainty is a measure of the variability of estimates of the Earth's properties. We are beginning to apply the concepts of resolution and uncertainty to hydrologic characterization (Vasco et al., 1995). In particular, we are examining the resolution and uncertainty associated with hydrologic tests conducted at the Conoco Borehole Test Facility.

#### Averaging Kernels

Hydrologic data, such as drawdown or tracer concentration measurements, are functionals of the transmissivity and storativity distribution between observation points. What this means is that the observations may be thought of as a mapping from a parameter distribution defined over some region of space $\chi$, say $X(r)$ to the real line $R$,

$$d_i = g_i[X]$$

where $d_i$ denotes the i-th datum and $g_i[X]$ represents the functional. For any nearby model $X(r)$ we may expand $g_i[X]$ in a Taylor series about $\delta X(r) = X(r) - X^*(r)$,

$$g_i[X] = g_i[X^*] + \int_x \delta X(r) G_i(r) dr + O(\delta X)^2$$

The term $O(\delta X)^2$ denotes all elements of the expansion greater than first order in $\delta X$. To first order,

$$d_i = \int_x X(r) G_i(r) dr$$

which may be written in matrix notation,

$$d = Gx \qquad (1)$$

The row of the matrix $G$ relates slight changes in the subsurface permeability to changes in the observed data. In Figure 9 the row of $G$ is shown for the PUMP58 test at the Conoco Borehole Test Facility. In this test water was produced from well GW-5 and the pressure monitored at wells GW-1, GW-2, GW-3, and GW-4. More details of the PUMP58 test may be found in Datta-Gupta et al. (1995). In Figure 10 the row of $G$ corresponding to the observed pressure at well GW-4, 0.31 days into the test is shown. The most significant sensitivity is associated with permeabilities between the pumping and observing (GW-4) wells. Also, note the sensitivity of the observed pressure to permeabilities behind each well.

Because the matrix $G$ is approximately singular, it cannot be inverted exactly. However, there are numerous methods (Menke 1984) to arrive at an approximate inverse, the generalized inverse $G^\dagger$, with which we may estimate variations in permeability, $\hat{x}$,

$$\hat{x} = G^\dagger d \qquad (2)$$

## The Resolution Matrix

As noted in the section on averaging kernels, it is only possible to estimate averages of the actual Earth structure. These averages are given by our calculated solution $\hat{x}$. Given the generalized inverse, $G^\dagger$, we need a quantitative estimate of the spatial averaging inherent in our estimate. That is, we would like to have an approximation of the averaging kernels for our discretized problem. Such an estimate may be derived by substituting equation (1) into equation (2),

$$\hat{x} = G^\dagger G x_t \qquad (3)$$

where $x_t$ is the 'true' permeability structure. The quantity $R = G^\dagger G$, known as the resolution matrix, may be thought of as the filter through which we view the Earth structure. The elements of the matrix $R$ are the averaging coefficients, e.g. $R_{ij}$ denotes the contribution of the j-th parameter to the estimate of the i-th parameter. For example, consider a row of the resolution matrix associated with block 821, a cell located just above and to the east of well GW-3. Note the significant averaging over the region between wells GW-1, GW-2, and GW-3. The diagonal elements of the resolution matrix provide an indication of how well one may resolve the permeability at a particular location (Figure 11). The size of the diagonal elements varies from 0 (complete unresolved) to 1 (perfectly resolved). Figure 11 displays the diagonal elements associated with the resolution matrix for the PUMP58 test. The diagonal elements of the resolution matrix are plotted at the corresponding locations. The most well resolved region surrounds the pumping well GW-5. Here, the resolution was as high as 0.85 (the scale saturates at 0.2). Also, the resolution is greatest on the sides of the observing wells nearest and furthest from the pumping well (GW-5).

## The Covariance Matrix

Another consideration in estimating subsurface structure is the uncertainty of calculated values. The conventional measure of model parameter uncertainty is the covariance matrix $C_{\hat{x}\hat{x}}$. For linear or linearized problems the model parameter covariance matrix is directly related to the data covariance matrix, $C_{dd}$,

$$C_{\hat{x}\hat{x}} = G^\dagger C_{dd} G^{\dagger^T} \qquad (4)$$

(Menke 1984). Note that the model parameter covariance matrix depends on the uncertainties in

the data as well as on the elements of the generalized inverse. The diagonal elements of the covariance matrix associated with the PUMP58 test are shown in Figure 12. We set the errors in our observations to 10 percent of the peak drawdown. The diagonal elements represent the standard errors associated with estimates of permeability. The standard errors are uniformly low for the PUMP58 test.

We are extending the analysis to include tracer data as well as production data. In the future we shall apply the methodology to a set of tracer data gathered at the test facility. In addition, we hope to conduct an analysis of production data from an actual producing field.

### Discussion and Conclusions

There are several accomplishments from these experiments: 1) They have shown that replacement of water with a gas (in this case air) produces large changes in the seismic signal, and 2) Single well reflection surveys are possible, enabling the imaging of vertical features. 3) The inversions for flow paths gave consistent results with the geophysics and geology.

The single well reflection data were characterized by a lack of tube waves, but large shear wave energy. The tube waves may have been attenuated by the sand packing around the boreholes and must be anticipated that strong tube waves would exist in other single well surveys. It is difficult to determine the effect strong tube waves would have on the processing, but the shear wave energy was easy to remove with F-K filtering so it can be assumed that tube wave could just as easily be removed. Using standard processing techniques, fracture zones were located which could be detected, but not located, by other means.

### Acknowledgments

This work was supported by the Assistant Secretary for Fossil Energy, Office of Oil Gas and Shale Technologies, U. S. Department of Energy under Contract No. DE-AC03-76SF00098. We are grateful to John Queen, Dale Cox, Peter D'Onfro, William Rizer, and John Sinton of Conoco Inc. for his support of this project and to Henery Tan for Amoco's continued support and interest in this work. Computations were carried out at the Center for Computational Seismology, LBL.

## FUTURE WORK

Future work will now shift to the application of the technology to actual gas reservoirs, through cooperative projects with industry partners. Out-year work will involve final technique development and validation.

## REFERENCES

Backus, G. and Gilbert, J.F., 1967. Numerical applications of a formalism for geophysical inverse prolems, *Geophys J. R. Astron. Soc.*, 13, 247-276.

Backus, G. and Gilbert, J.F., 1968. The resolving power of gross earth data, *Geophys. J. R. Astron. Soc..*, 16, 169-205.

Datta-Gupta, A., Vasco, D. W., Long, J. C. S., 1994, Detailed Characterization of a Fractured Limestone Formation Using Stochastic Inverse Approaches: SPE/DOE Paper 27744, 71-86.

Gibson, R. L., Jr., 1994, Radiation from seismic sources in cased and cemented boreholes: Geophysics, vol. 59, 518-533.

Harlan, W. S., 1990, Tomographic estimation of shear velocities from shallow crosswell seismic data: SEG Expanded Abstracts, 16th Annual Meeting, 86-89.

Lines, L. R., Kelly, K. R. and Queen, J. H., 1992, Channel waves in cross-borehole data: Geophysics, vol. 57, 334-342.

Majer, E. L., Peterson, J. E., Benson, S. M., and Long, J. C. S., 1991. High-frequency seismic tomographic imaging for hydrologic properties of near-surface materials: in Earth Sciences Division Annual Report 1990, Lawrence Berkeley Laboratory, Berkeley, CA.

Menke, W., 1984. Geophysical Data Analysis: Discrete Inverse Theory, Academic Press, Orlando, Florida.

Queen, J. H., and Rizer, W. D., 1990, An integrated study of seismic anisotropy and the natural fracture system at the Conoco Borehole Test Facility, Kay County, Oklahoma: J. Geophys. Res., vol. 95, 11255-11273.

Queen, J. H., Rizer, W. D., Liu, E., Crampin, S., and Lines, L. R., 1992, A review of downhole Source Effects at the Conoco Borehole Test Facility: in Symp of the Geophysical society of Tulsa, eds, L. Lines and J. Queen, Geophys. Soc. of Tulsa, Tulsa, OK. 62-63.

Vasco, D.W., Datta-Gupta, A., and Long, J.D.S., 1995. Resolution and uncertainty in hydrologic characterization, *Water resources Res.*, (submitted).

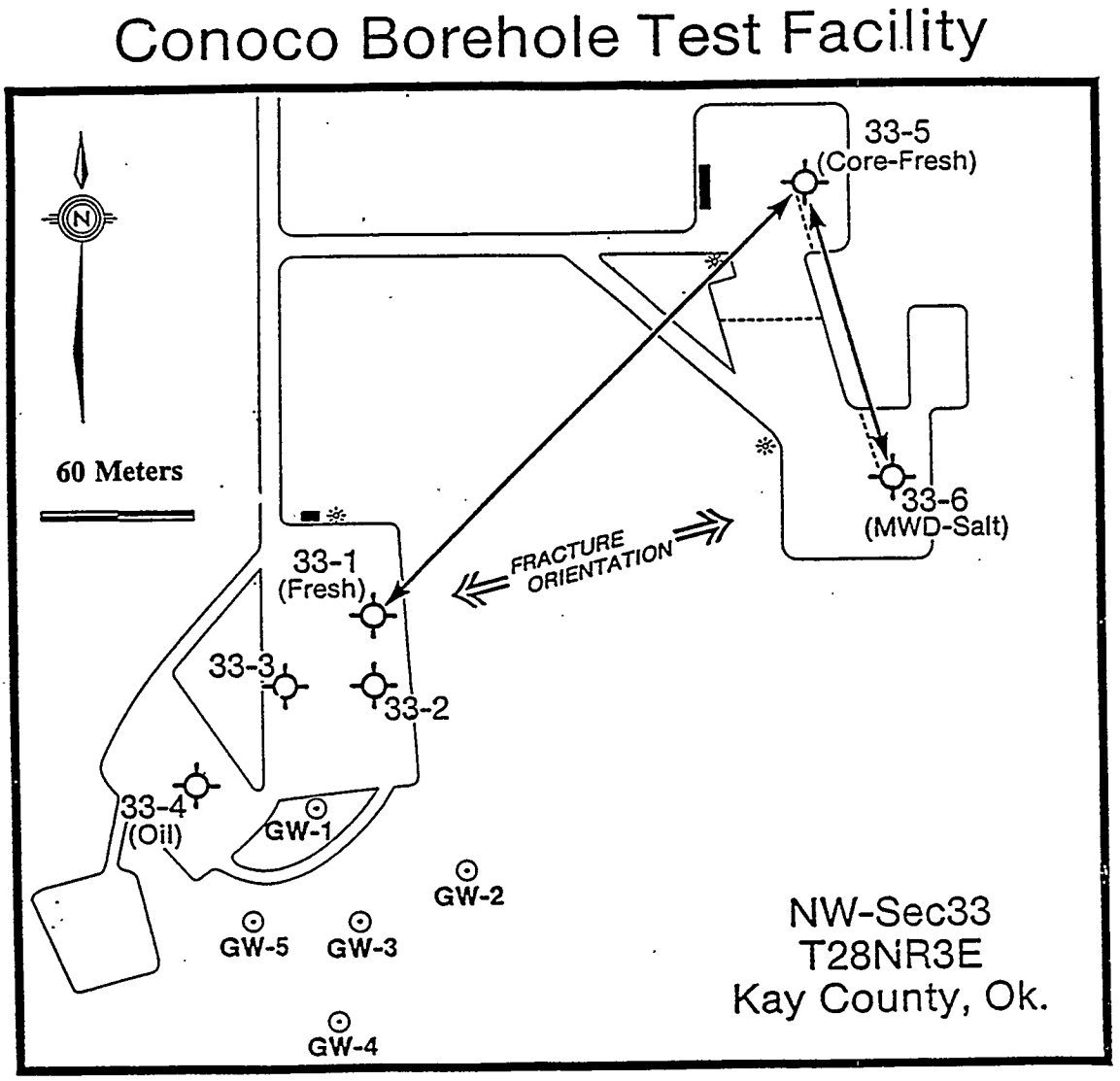


**Figure 1. Plan View of the Conoco Test Facility Showing the Geometry of the Wells Used (the Gw Wells) and the Predominant Fracture Direction As Inferred From Mapping Near-By Outcrops of the Limestone Formation In Which the Seismic Imaging Was Performed.**

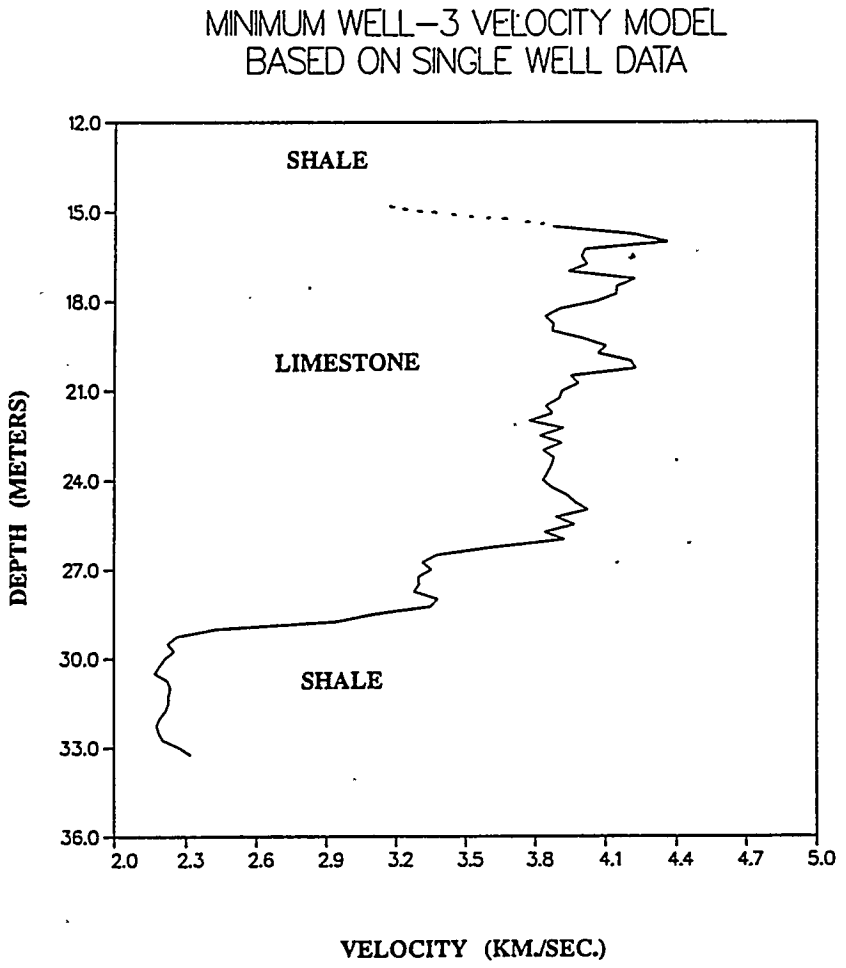


**Figure 2. The Velocity of the Subject Limestone Formation As A Function of Depth In Well Gw-3 As Derived From The Near offset Data In The Single Well Survey. The Single Well and Crosswell Measurements Were Carried Out Over the 15 To 30 Meter Depth Range.**

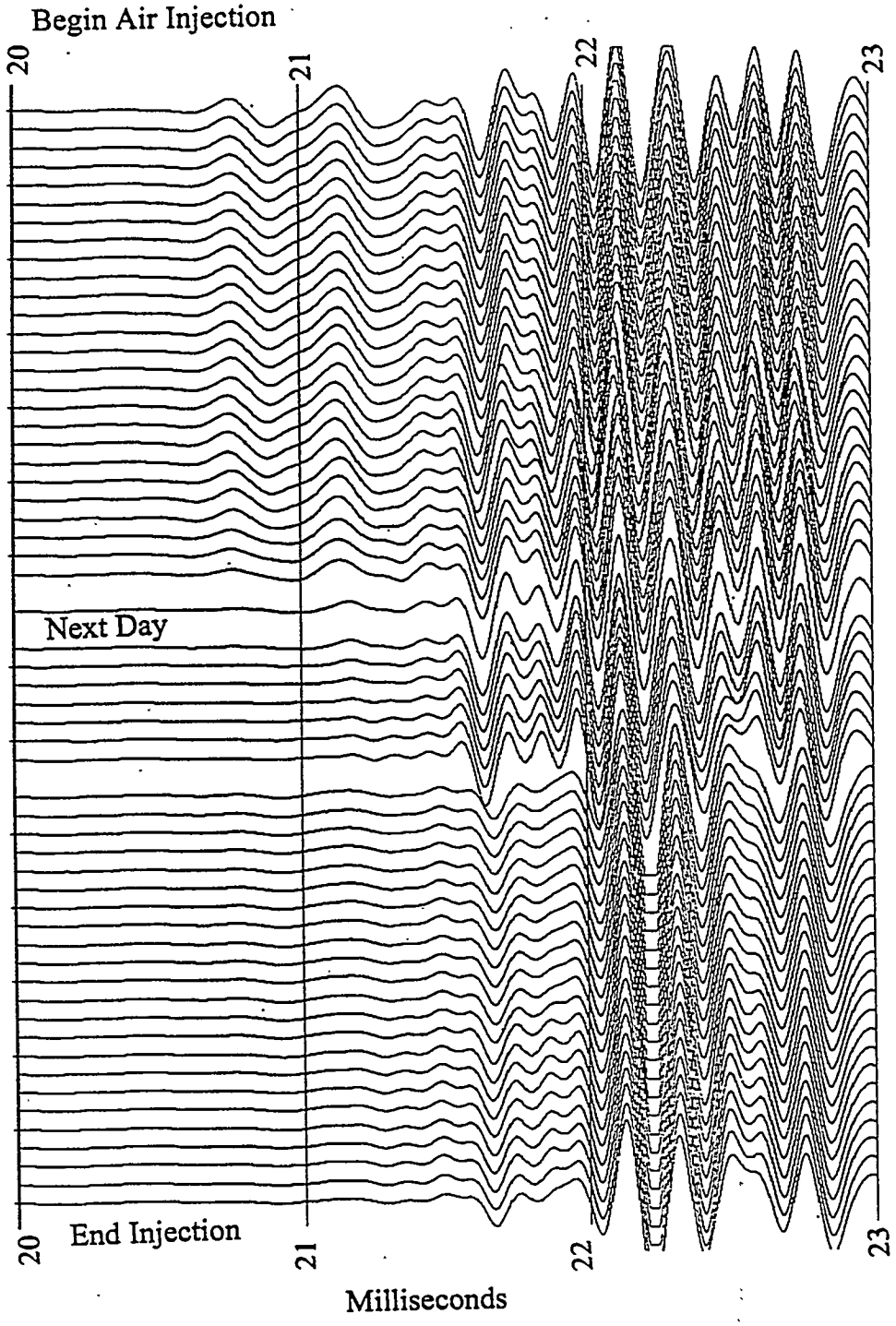


**Figure 3. Crosswell Data As A Function of Time Between Wells Gw-4 and Gw-1. The Top Trace Is Background Data Before the Air Injection Started, Time Increases From the Top of the Figure To the Bottom. The Total Time Span Is the Two Days Over Which Monitoring Occurred.**

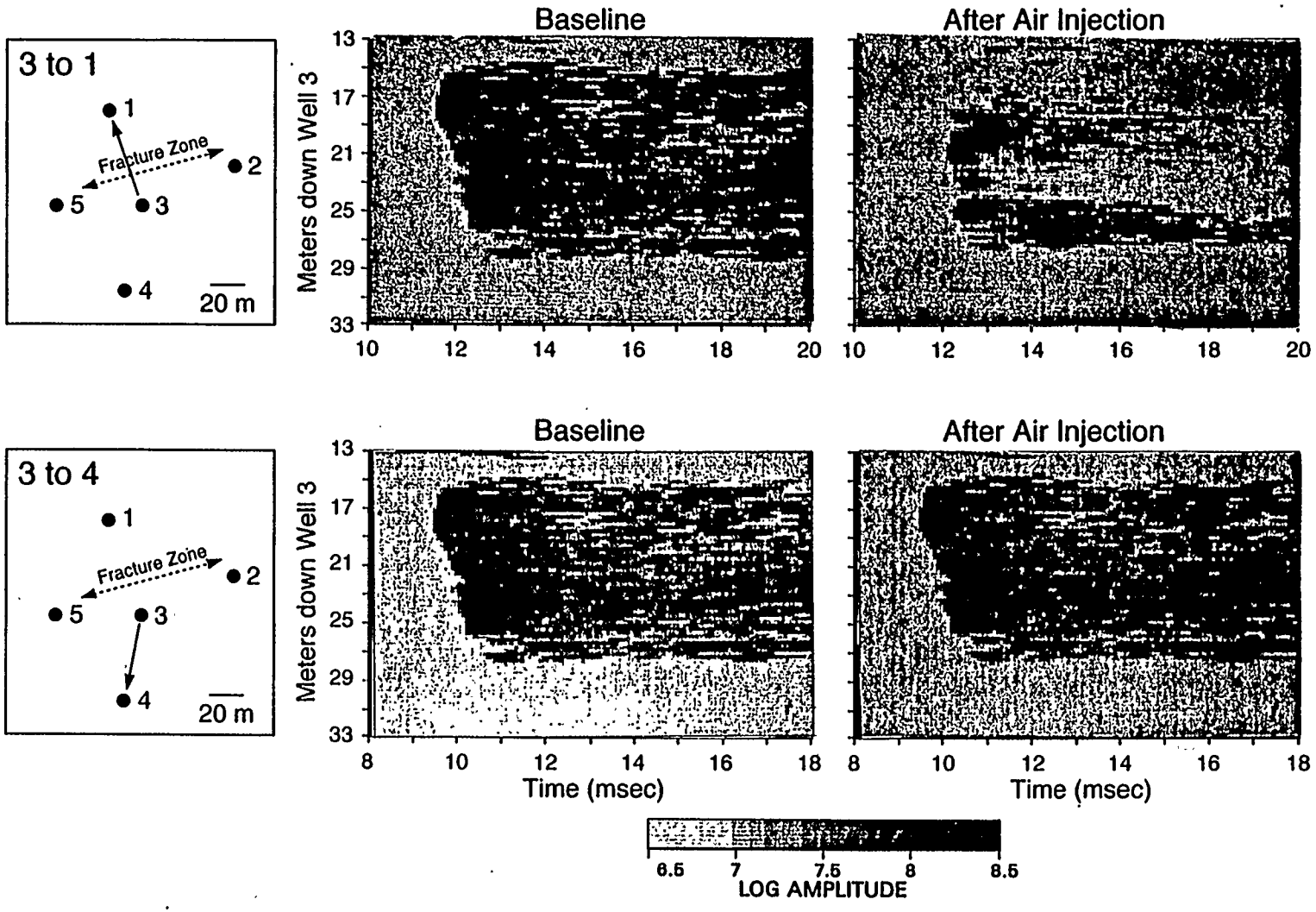


**Figure 4. Crosswell Amplitude Data As A Function of Depth and Time Between Well Pairs Gw-3/Gw-1 (Figure A) and Gw-3/Gw-4 (Figure B) Before Air Injection and After Air Injection.**

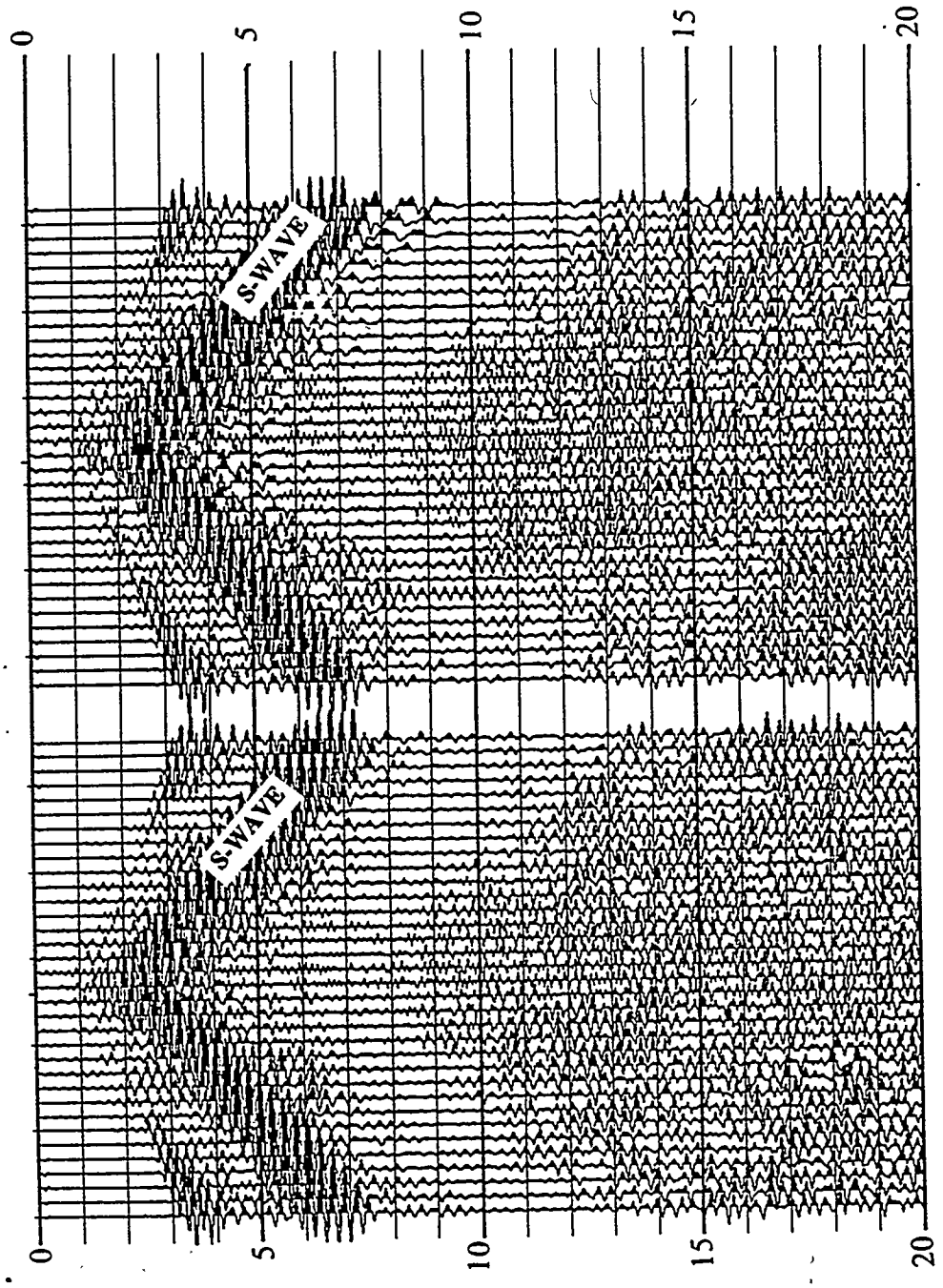


**Figure 5. Several Typical Shot Gathers From the Single Well Reflection Profile In Gw-3. Receiver Spacing Was 0.25 Meters.**

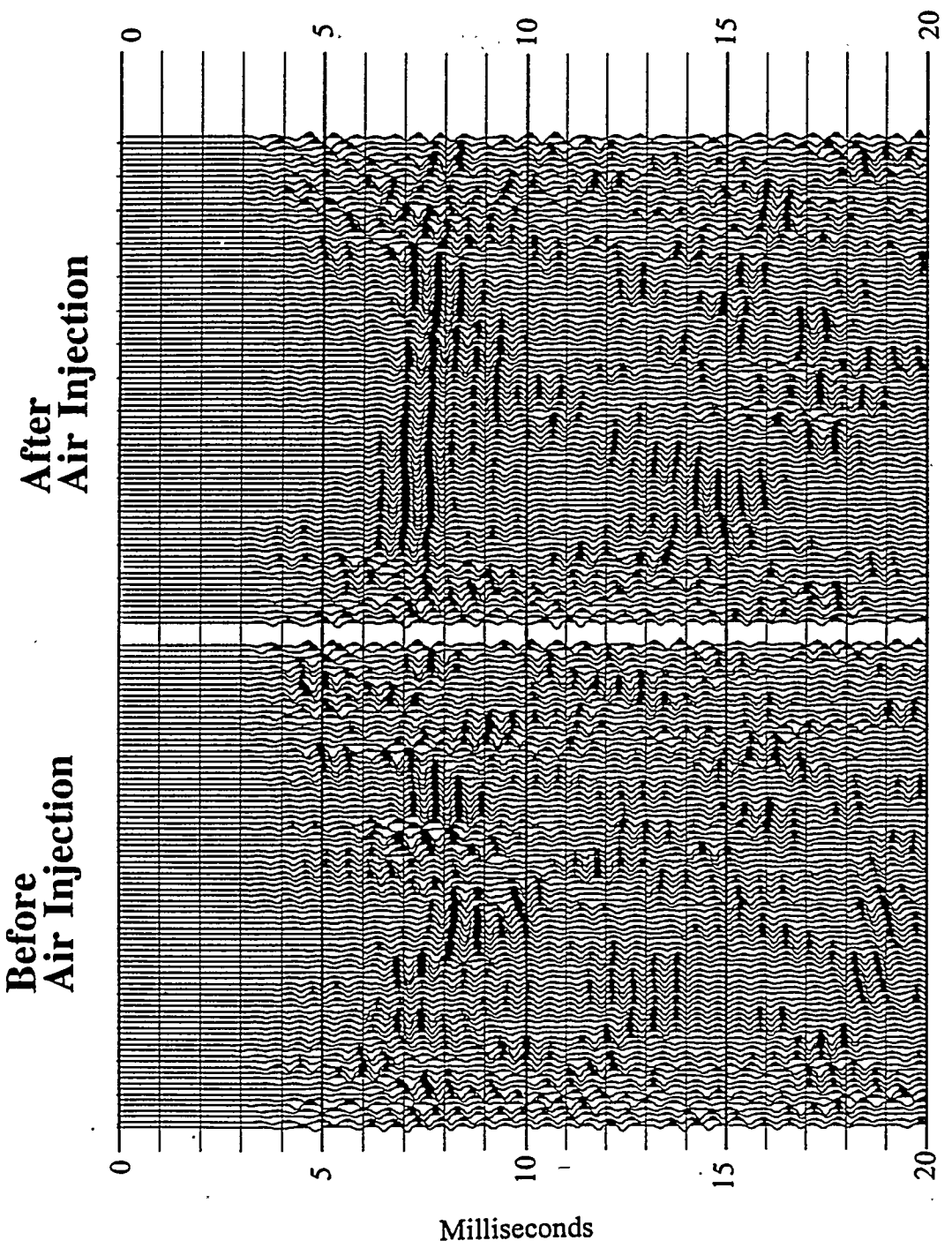


**Figure 6. A Cdp Stack of the Single Well Reflection Data From Gw-3 Before the Air Injection (Bottom) and After the Air Injection (Top). Note the Increase In the Reflected Energy At 7 Milliseconds When Air Fills the Fracture Zone.**

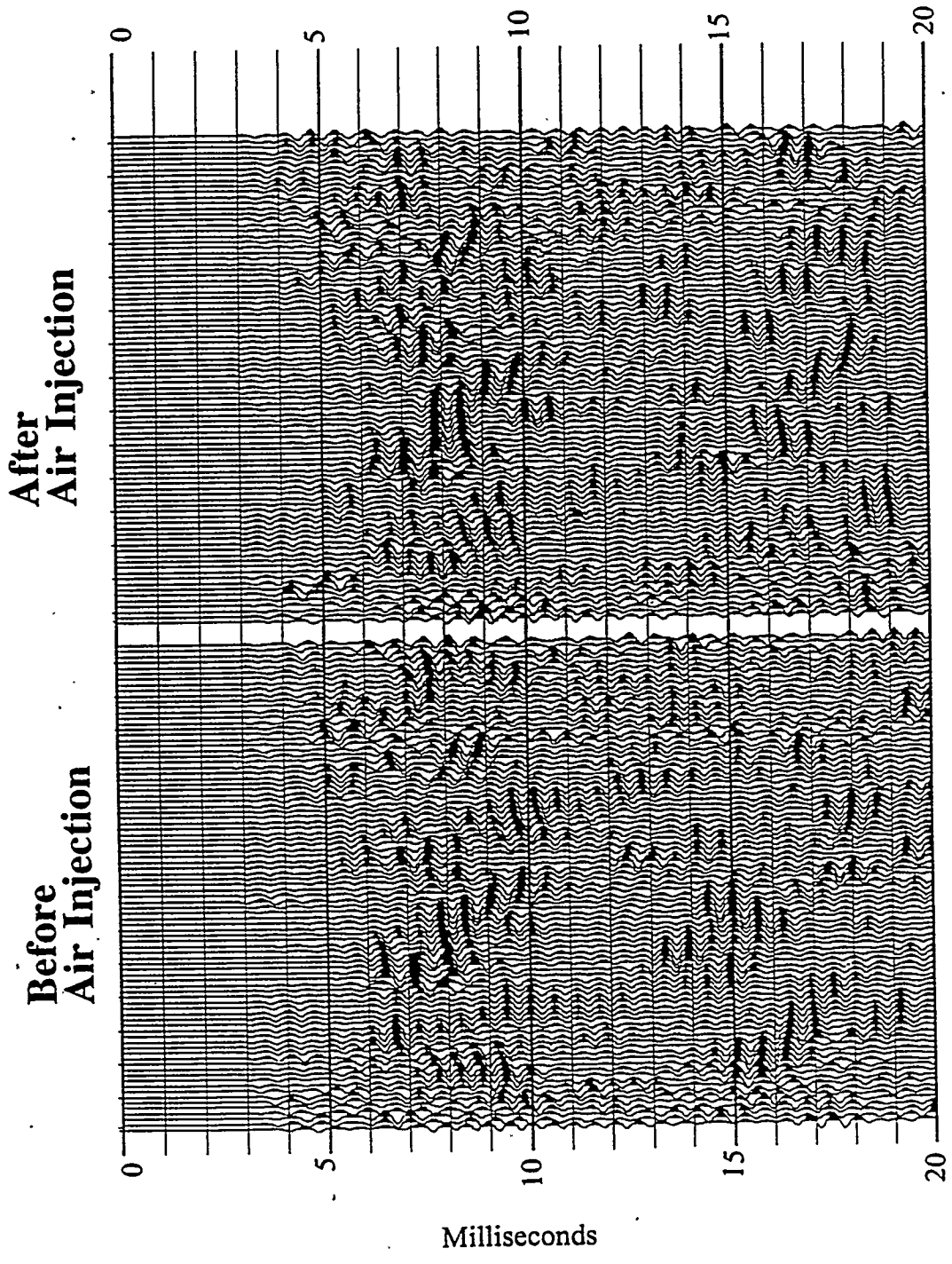


**Figure 7. A Cdp Stack of the Single Well Reflection Data From Gw-1 Before the Air Injection (Bottom) and After the Air Injection (Top). Although there Is an Increase In the Reflected Energy Between 15 and 18 Milliseconds When Air Fills the Fracture Zone, the Energy Is Weaker Due To the Larger Distance the Fracture Is Away From Gw-1 Than Gw-3.**

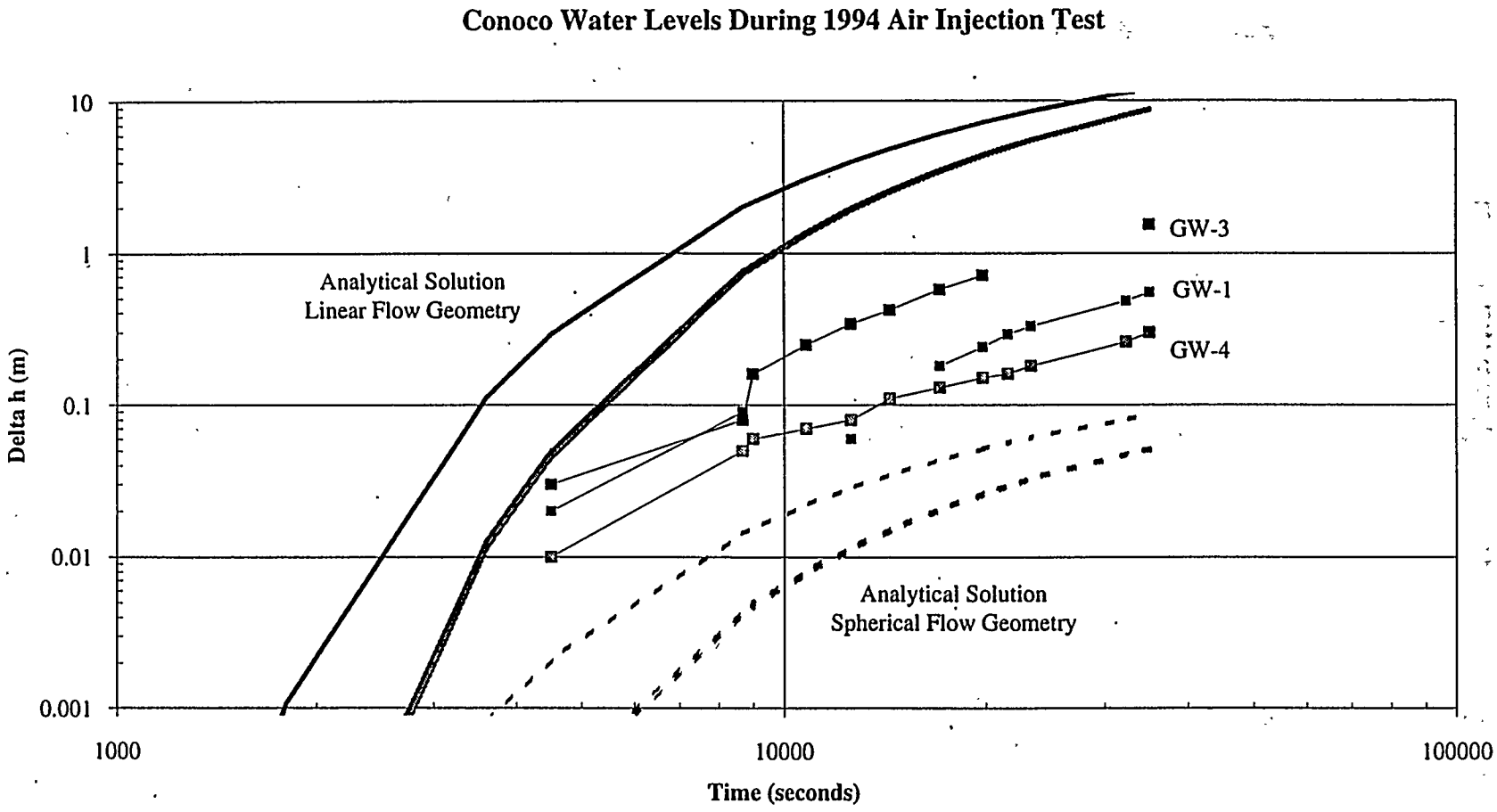


**Figure 8. Conoco Water Levels During 1994 Air Injection Test**

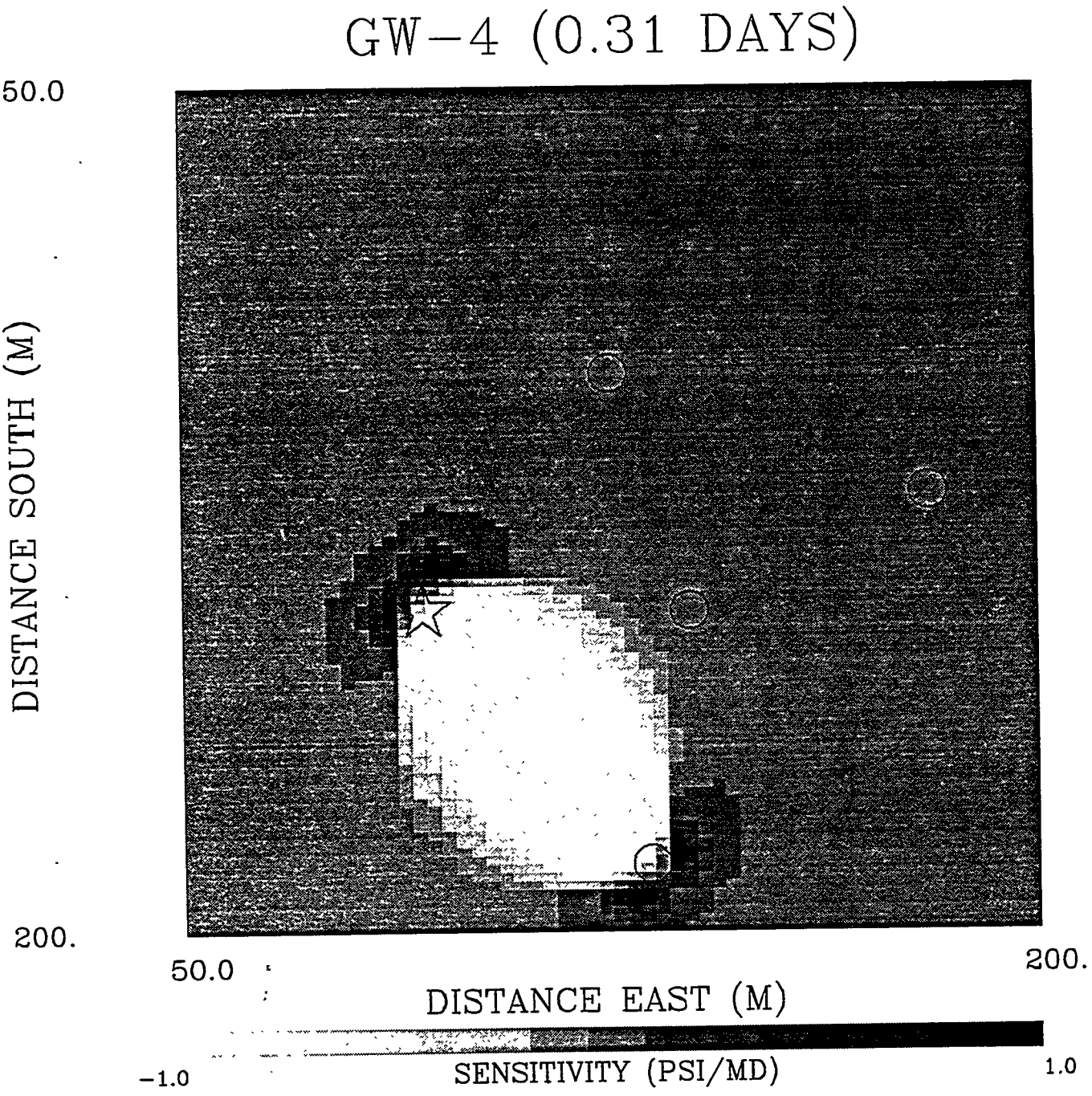


**Figure 9. Sensitivity Kernel Associated With The Pump58 Test. The Sensitivity Measures the Change In the Observed Pressure At Well Gw-4, 0.31 Days Into the Test, With Respect To Variations In Permeability At the Conoco Borehole Test Facility.**

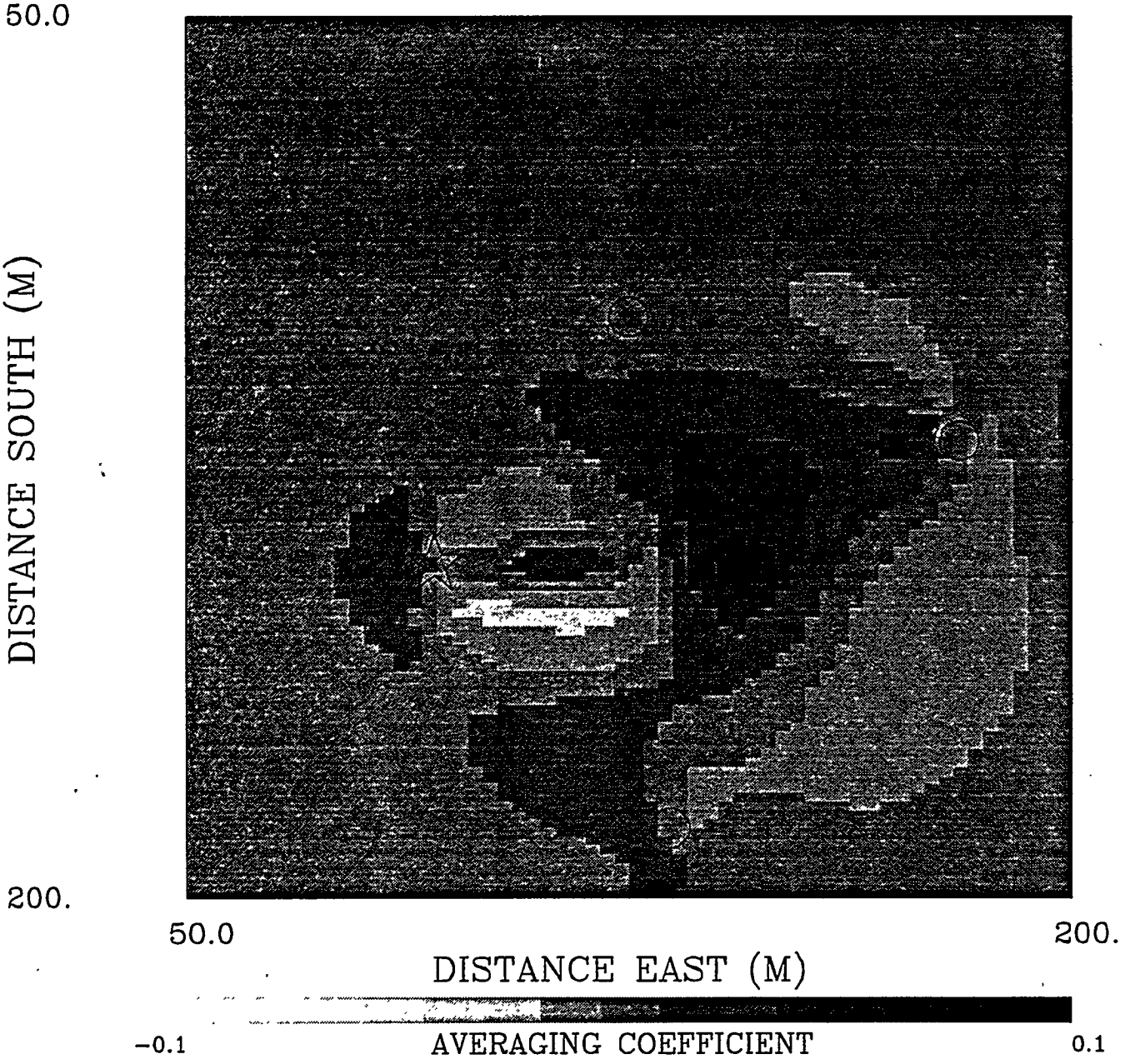


**Figure 10. Averaging Kernal Associated With Cell 821. This Row of the Resolution Matrix Signifies the Contribution of Permeability Variations Within the Subsurface to an Estimate of Permeability in Cell 821, Just to the North-East of Well GW-3.**

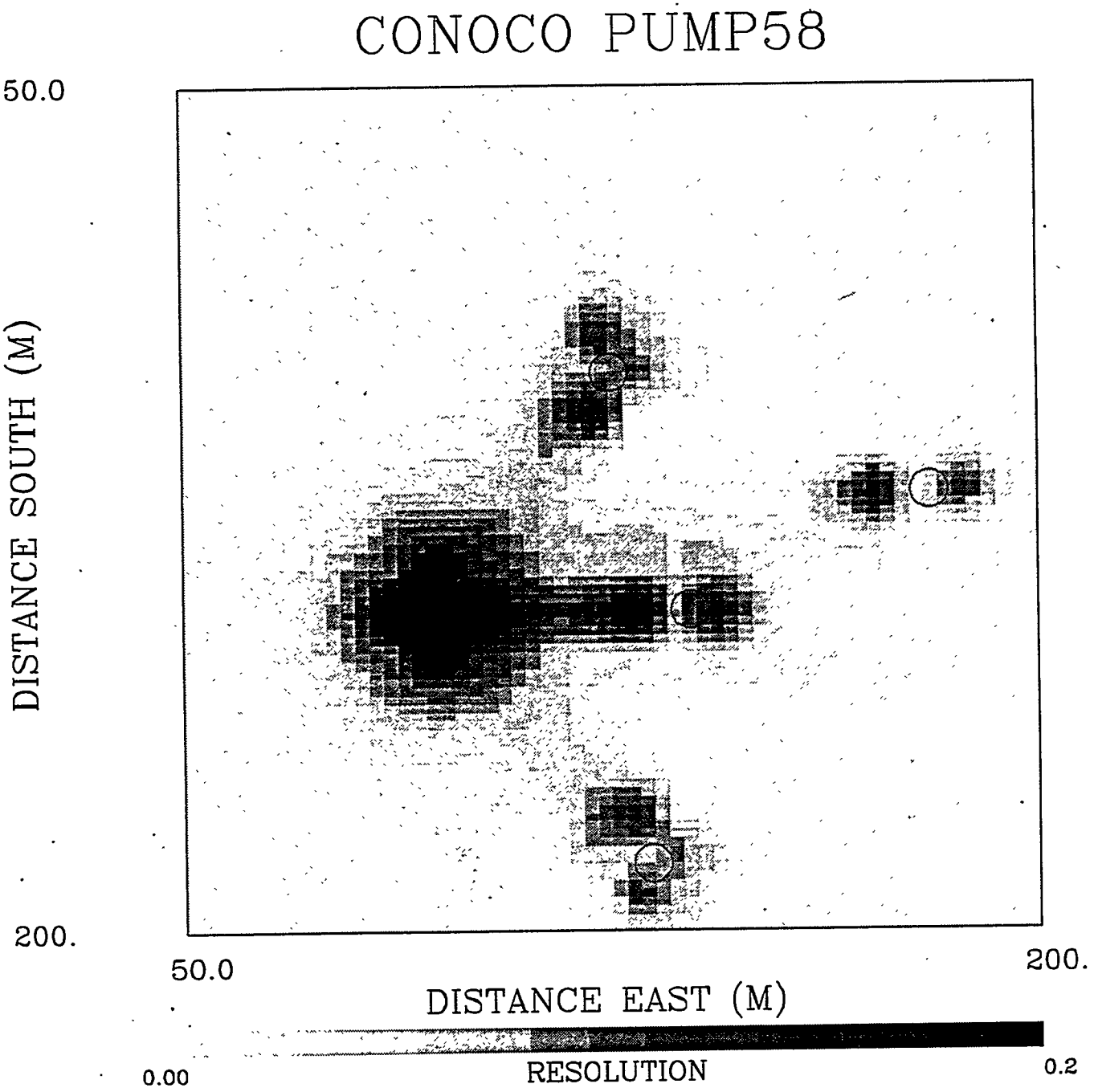


**Figure 11. Diagonal Elements of the Resolution Matrix.**

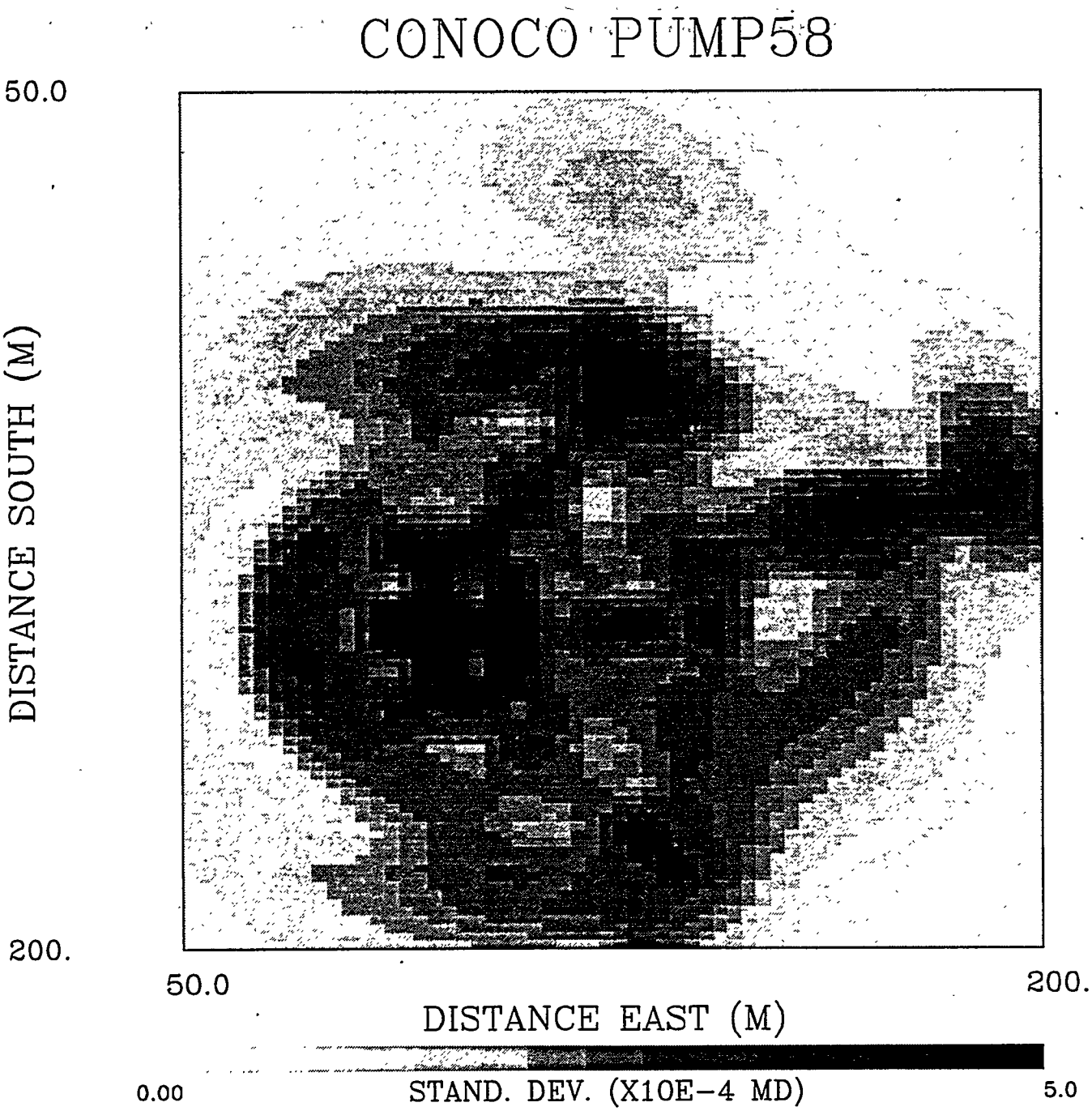


**Figure 12. Square-Root of the Diagonal Elements of the Covariance Matrix.**

# 5A.2. The Detection and Characterization of Natural Fractures Using P-Wave Reflection Data, Multicomponent VSP, Borehole Image Logs and the In-Situ Stress Field Determination

## CONTRACT INFORMATION

| | |
|---|---|
| **Contract Number** | DE-AC21-92MC28135 |
| **Contractor** | Coleman Research Corporation<br>201 S. Orange Avenue, Suite 1300<br>Orlando, FL 32801 |
| **Contractor Project Manager** | Dr. Pieter Hoekstra, Coleman Research |
| **Principal Investigators** | Dr. Heloise I. Lynn, Lynn Incorporated<br>Dr. C. Richard Bates, Coleman Research |
| **METC Project Manager** | Royal J. Watts |
| **Period of Performance** | September 23, 1992, to October 1, 1995 |

## OBJECTIVES

The objectives of this project are to detect and characterize fractures in a naturally fractured tight gas reservoir, using surface seismic methods, borehole imaging logs, and in-situ stress field data. Further, the project aims to evaluate the various seismic methods as to their effectiveness in characterizing the fractures, and to formulate the optimum employment of the seismic methods as regards fracture characterization.

## BACKGROUND INFORMATION

### General

The project site is in Duchesne County, Utah, which contains the Bluebell-Altamont field in the Uinta Basin. The Uinta Basin of northeast Utah is an asymmetric east-west trending basin with a steep north flank bounded by a thrust and a gently sloping (1 to 2 degrees) south flank. Bluebell-Altamont field is located along the basin axis and north-central portion of the basin in Duchesne and Uintah counties (Figure 1). Production is mainly from numerous sandstones and carbonates in the Tertiary Wasatch, lower Green River, and upper Green River formations. The fractured gas reservoirs of the upper Green River are the focus of this report.

Pennzoil Exploration & Production is the industry partner in the project. Pennzoil is a major operator in the Bluebell-Altamont field and operates almost all of an upper Green River formation gas field located in Duchesne County, Utah. Oil in the Bluebell-Altamont area was originally discovered in the lower Green River formation at the old Roosevelt Unit (1949) which was later discovered to have deeper Wasatch pay (1970). Pennzoil

recognized upper Green River commercial gas potential in 1987 when a shut-in well, the Boren #211A2, ruptured its casing and blew out with a very high volume of gas from the upper Green River. Since then, Pennzoil has completed five gas wells in the field.

**Geology of the Uinta Basin and the Upper Green River**

The Uinta Basin covers approximately 23,000 square miles and is the second largest basin in Utah. Erosion from the Duchesne River and its tributaries has significantly affected the topography of the Uinta Basin. This erosion has created a highly developed badlands type terrain, typical of erosional surfaces formed in soft, young geologic formations. Principal features include smooth, gently sloping benches or mesas; broad to narrow valley flood plains; low stream terraces; alluvial fans and steep foot slopes between the bench or mesa escarpments and the valley flood plains; and the steep, rough, broken and eroded badlands area. Many of the hydrocarbon bearing rocks of interest throughout the basin underlie the Uintah-Ouray Reservation. The Basin lies within an elevation range of 5,000 to 8,000 feet with the nearby Uinta Mountains to the north.

From latest Cretaceous to late Eocene, the Uinta Basin was the site of an inland lake known as Lake Uinta where up to 15,000 feet of sandstone, shale, and carbonate sediments were deposited in alluvial, marginal-lacustrine and lacustrine environments. Figure 2 shows the generalized stratigraphic column of the Late Cretaceous and Tertiary for Bluebell-Altamont. The upper Green River (40 m.y.B.P.) represents the last major lacustrine deposition within the Uinta Basin. Gas reservoirs within the upper Green River are trapped by updip pinchouts of the prograding lake margin. Producing intervals consist of fractured lake-margin sandstones encased within tight shales and carbonates of the lacustrine deposits. Within the marginal wedge are sandstone reservoirs that have been mapped using SP logs. Individual sandstones are about 5 to 20 feet thick, but occasionally they stack to give the appearance of thicker sands up to 80 feet thick.

Natural gas is being produced from the upper Green River formation in the Bluebell-Altamont field at depths from 6,500 to 8,500 feet (Figure 2). Producing rates from these zones range from 100 MCFPD to over 5,000 MCFPD. The sandstones which produce gas have matrix porosity of < 8 percent and permeability of < 1 md. Production has been enhanced in several wells with hydraulic sand fracturing. Several wells have producing rates that are much higher than would be possible if only the matrix were effective. Cores, FMS logs, sonic logs, and mud log samples have shown natural fractures which are the likely cause of the high producing rates in several wells. Sandstones in non-fractured wellbores are capable of producing rates of 100 to 300 MCFPD, whereas sandstones with naturally or artificially fractured wellbores produce at rates from 1,000 to 5,000 MCFPD.

Evidence for the regional stress regime is shown in Figure 3. Of particular note are the orientations of gilsonite dykes or veins in the study area. Gilsonite or uintahite is a black to green shiny asphalite found almost uniquely in veins in Utah. The veins are found from inches to 10 to 20 feet wide and can propagate for many miles as continuous events. Fouch, et al. (1992), have postulated that the veins form subsequent to hydrofracture of the rock

perpendicular to the minimum horizontal stress. Since the veins cut the upper Green River, Uinta, and Duchesne formations, they are interpreted to indicate recent stress field orientation. In the project area, the veins have rotated from the dominant NW-SE orientation to NNW-SSE.

At depth within the Bluebell-Altamont field, the regional stress orientation has been mapped from four arm caliper data with the maximum horizontal stress direction N30-45W. The formation micro-scanner (FMS) results from a number of boreholes close to the seismic lines indicate two major fracture orientations in the upper Green River, namely NW and NE.

The location of seismic acquisition is over the naturally fractured gas reservoirs of the Eocene Upper Green River formation on the Bluebell-Altamont field in the Uinta Basin, Northeastern Utah. The Bluebell-Altamont field produces commercial hydrocarbons from naturally fractured reservoirs in predominantly marginal-lacustrine facies of the Paleocene/ Eocene Wasatch formation (oil and associated gas), and lacustrine to marginal-lacustrine facies of the Eocene upper Green River formation (gas). It is Pennzoil's belief that most reservoirs in this field have load-parallel extension fractures that preferentially affect brittle sandstones and carbonates.

## PROJECT DESCRIPTION

The project includes the acquisition, processing, and interpretation of 9-component (9-C) surface seismic and 9-C borehole seismic datasets, and the integration of these seismic data with information obtained from geological outcrop measurements, borehole image logs, and core analyses.

### Surface Mapping

During the summer of 1993 and spring of 1994, outcrop mapping was conducted by Lynn Inc., CRC, and Pennzoil. The fractures mapped were typically 10 cm to 2 m long with clean sides and little evidence of movement from slickensides. The fracture orientation information, together with that for fractures from the borehole, was used to locate and orient the seismic lines to be approximately parallel and perpendicular to the fractures in the upper Green River formation. This orientation was determined to evaluate the potential to observe an azimuth amplitude variation with offset (AVO) anomaly due to fracture density at the seismic line tie.

### Seismic Program

The field seismic program included a 9-C vertical seismic profile (VSP) and approximately 10 miles of 9-C surface seismics. The surface seismic was laid out in 2 intersecting lines parallel and perpendicular fractures and the supposed regional maximum horizontal stress directions (Figure 4). The VSP was conducted by Schlumberger, Canada, in the Duncan 3-7A1 well. The VSP was acquired using a total of 7 source locations at various offsets. This number was needed to mitigate tube wave noise; however, the overall quality of the data was good throughout. The Schlumberger ASI sonde was used to collect the data. The ASI sonde is a magnetically clamped 5-stage tool with each stage consisting of a 3-component receiver. Four shear vibrators at 6 to 64 Hz and 4 P-vibrators sweeping at 10 to 100 Hz were used for the sources.

The surface seismic was acquired by Bay Geophysical and Lockheed Geophysical using four Amoco Mertz build

shear vibrator trucks and four Mertz compressional vibrators. The surface seismic lines were acquired using conventional multicomponent techniques with vibration motion in-line, cross-line and vertically, with three-component receiver oriented in-line and cross-line.

Processing of the VSP was done by Schiumberger, Canada; surface seismic processing was done by Pulsonic Geophysical, Canada.

## RESULTS

### Outcrop Mapping

The results of the outcrop mapping, with two dominant orientations seen at N30°W and N68°E, are displayed in Figure 5. These orientations are compared with fracture evidence from other sources, including seismics, FMS logs and cores, to deduce the fracture orientation at upper Green River depths.

### P-Wave Seismic

Results of the seismic effort are shown in Figures 6 through 18. Figure 6 shows the P-Wave sonic log from the Duncan 3-7A1 well together with the density and gamma ray. From these logs, the P-Wave synthetic seismogram was calculated and is shown to the right of the figure. Also depicted is the P-P corridor stack generated from the VSP. An excellent match is shown between the corridor stack and the synthetic seismogram from which strong reflection events associated with the target zone can be identified. Gas pay is usually concentrated near the top of upper Green River above the Mahogany Bench and "Z" marker horizons.

The 9-C VSP P-Wave corridor stack and synthetic seismogram from the Duncan 3-7A1 have also been spliced into Line 2 surface seismic (Figure 7). Once again, the match in data is excellent through the target zone.

### Amplitude Variation with Offset (AVO) Effects

Perhaps the most significant result to date is the observation of azimuthal dependence of amplitude variation with offset (AVO). AVO is an interpretative technique that utilizes the behavior of reflector amplitudes as a function of offset or more strictly as a function of incidence angle. Changes in AVO have been attributed to lithologic changes, pore constituent changes, the presence of gas being the most often used phenomenon, and more recently, changes in fracture density. For isotropic, brine-saturated rocks, a slight decrease in magnitude of reflector amplitude is seen with increasing offset. Changes other than this decrease are, therefore, attributed to one or more of the phenomena listed previously. At the Bluebell-Altamont field, the surface seismic lines were deployed in a cross pattern parallel and perpendicular to the regional stress field, and therefore, also the potential fracture directions. The hypothesis to be tested was that the AVO response would be different when the source-receivers were parallel or perpendicular to the dominant fracture direction. The gas in the fractures should increase the effect of the crack-induced anisotropy. This would hold true if lithology remained constant. By comparing both the shear and compressional wave data, the potential change in lithology could be evaluated.

Figure 8 shows the near-offset stack (0 to 5,980 feet) of Lines 1 and 2 at the tie point. Reflector match is excellent throughout the section with a 10 msec

static shift. Figure 9 shows the far-offset stack (5,980 feet to maximum offset 9,000 feet) for the tie point at Lines 1 and 2. Here the match is not as clearly made with individual reflectors showing distinct amplitude differences. These differences are summarized in Table 1.

Table 1

| Reflector | AVO | |
|---|---|---|
| Top of Green River | Dim | Strong |
| Z | Dim | Strong |
| Mahogany Bench | Dim | Strong |

The rationale for using a near offset gather to 5,980 feet offset is clearly demonstrated in Figure 10. This figure shows supergathers of 9 CDPs at the tie point for Lines 1 and 2 with the offset of 5,980 feet highlighted. The increase in amplitudes of the Z reflector and the Mahogany Bench reflector can be seen to the right (further offset) on Line 2 which is perpendicular to the fractures. This figure of super gathers also shows that some reflection events have an azimuthally isotropic AVO response, for example, the P-Wave reflectors at 1.08 and 1.12 seconds have the same AVO response on both lines. The reflector at 1.08 seconds is only on the near offsets, while the reflector at 1.12 seconds is only on the far offsets.

To further demonstrate this phenomenon, a synthetic AVO gather was modeled by Applied Geophysical Analysts (AGA), Denver, for the Duncan 3-7A1 logs. The AGA model uses the wireline logs (including sonic, density, neutron porosity, deep resistivity, spontaneous potential [SP] and gamma ray [GR]), the lithology, porosity, and pore content from both empirical data and theoretical relations to calculate the shear wave velocity. With the shear wave velocity, P-Wave velocity and density, the P-P AVO synthetic seismogram can be calculated. This is shown in Figure 11. Note on this figure that the reflection amplitudes diminish with offset for the top Green River, Z, TN1, and Mahogany Bench. The calculations for synthetic AVO response were made to assume no cracks in the rock.

To this point, the data for Lines 1 and 2 are interpreted as follows. Along Line 1, the reflection amplitudes diminish with offset as predicted by theory and empirical relations, and therefore it is interpreted that few cracks intersect the far offsets on this line between the top of Green River and Mahogany Bench. Along Line 2, the reflection amplitudes increase with offset, contrary to the empirical relations for non-cracked rock models. This observation is interpreted as resulting from a cracked rock. A schematic representation of this is shown in Figure 12. Wild and Crampin (1991) have modeled the change in shear wave (VS) and P-Wave (VP) velocity propagation directions, and their model is also given in Figure 13. In cracked media, VP and VS, and hence Poisson's ratio, change as a function of azimuth and angle of incidence. A greatly decreased VP and slightly decreased VS are interpreted to exist along Line 2 (perpendicular to cracks) at the tie point on far offsets, thus causing a low Poisson's ratio to be sensed. The P-Wave seismics are, therefore, influenced by the NW-SE cracks more than other crack orientations. This may be due to these cracks showing larger apertures, longer continuity, or that they are open and most likely gas filled.

## Shear Wave Seismics

Subsequent to the P-P VSP analysis, the S1-S1 corridor stacks were calculated. These are shown in Figure 16 together with the P-P corridor stack. Note that the S1-S1 stack has a compressed time scale compared to the P-P stack to compensate for the slow velocity of the shear waves; however, the character correlation between the stacks is pronounced. In Figure 15, the S1-S1 and S2-S2 corridor stacks are shown for two of the offsets from the well (approximately 550 feet to the west and 1,121 feet to the east). The character tie between S1 and S2 stacks is once again good; however, when the stacks are aligned on the Z marker, misties in time are observed for the top of Green River and Mahogany Bench. This mistie, or the amount of time delay, is equal for both offsets. Analysis of the time delay is given in Figure 16. From surface to 2,800 feet, 3 percent anisotropy was recorded. From 2,800 feet to top of Green River, 1 percent anisotropy was recorded. From top of Green River through the Z marker to Mahogany Bench, anomalous anisotropy of 8 percent was recorded. Of note also in Figure 15 is the reflection amplitude decrease in S2 stacks at the top of the anomalous anisotropy zone. A similar decrease in reflection coefficient compared to S1 was observed by Mueller (1991) in the Austin Chalk over a local highly fractured area.

The consistency in the polarization direction of the S1 and S2 shear waves with depth is demonstrated in Figure 17. This figure shows hodogram analysis for selected depth levels from 2,800 to 8,650 feet. The S1 (fast shear) shows a consistent azimuth at N33°W suggesting that the dominant fractures which influence the shear wave seismics also are consistent with azimuth over this depth range.

## Conclusions

From the analysis of results to date, the following conclusions are suggested:

1. The P-Wave AVO response seen at far offset on surface seismic Lines 1 and 2 indicates an azimuth dependence of the P-Wave AVO related to fracture azimuth and relative fracture density at this field.

2. Three-dimensional P-Wave surveys with source-receiver azimuths acquired and processed in the two important natural azimuths can be diagnostic to locate high fracture density zones in similar geologic settings (i.e., gentle dips or mild structure).

3. Anomalous high S-Wave bire-fringence was observed in the interval corresponding to the fractured gas reservoir interval that produces in the field. In addition, S1 and S2 reflection coefficients showed distinct differences associated with zones of anomalous anisotropy.

4. Fracture azimuths mapped in outcrop adjacent to the seismic lines are parallel to the S1 direction as determined from the VSP survey.

## FUTURE WORK

### Seismic

Remaining work on the project includes finalizing the data processing of the S-Wave surface seismic, and interpretation of the final S-Wave seismic data. The interpretation will compare the S-Wave lines with the P-Wave lines to evaluate the relation between P- and S-Wave responses along the lines, which

can be indicative of lithology, pore fluid, and relative fracture density.

To aid in the interpretation phase of the project, several modeling efforts have been initiated. The first of these is 2-D stratigraphic modeling along the seismic lines based on seismic response calculated from sonic logs (P-Wave synthetic seismogram modeling). This modeling results in synthetic seismic sections which represent a "baseline case" simulating only stratigraphic changes along the lines, without effects of fracturing.

Modeling of the seismic response to cracked rocks will be done using calculation of the full elastic response of the P- and S-Waves to fractures, in this way the fracture effect by azimuth can be obtained.

The amplitude variation with offset response of the P-Wave seismic will be compared to the well results and calibrated.

**Core Analyses**

All available cores from the upper Green River will be analyzed for evidence of fractures, for porosity-permeability determination, and for environment of deposition. The core studies will include thin section, scanning electron-microscope, and X-ray diffraction analyses.

**Engineering/Production Data**

Single-well pressure tests and any available multi-well tests will be analyzed for evidence of preferred flow direction which would indicate fracture azimuth.

**Stress Field**

The stress field as calculated from earthquake focal mechanisms will be investigated for any recent earthquakes in and near the study area. This approach is based on the conclusion of several earthquake researchers that focal mechanisms of earthquakes can be reliable indicators of regional stresses. This will widen our data base for in-situ stress field data, and should add confidence to the resulting stress field determination.

**REFERENCES**

Fouch, T., V. Nuccio, J. Osmond, L. MacMillan, W. Cashion, and C. Wandrey, 1992. Oil and Gas in Uppermost Cretaceous and Tertiary Rock, Uinta Basin, Utah; in Hydrocarbon and Mineral Resources of the Uinta Basin, Utah and Colorado. Utah Geological Association. *Guidebook 20*, Fouch, Nuccio, and Chidsey, Ed., published by the Utah Geological Association, Salt Lake City, Utah.

Mueller, M., 1991. Prediction of Lateral Variability in Fracture Intensity Using Multicomponent Shear-Wave Surface Seismic as a Precursor to Horizontal Drilling in the Austin Chalk, *Geophysical Jour. Inter.*, 107, pp. 409-415.

Wild, P., and S. Crampin, 1991. The Range of Effects of Azimuthal Isotropy and EDA Anisotropy in Sedimentary Basins, *Geophysical Jour. Inter.*, 107, pp. 513-529.

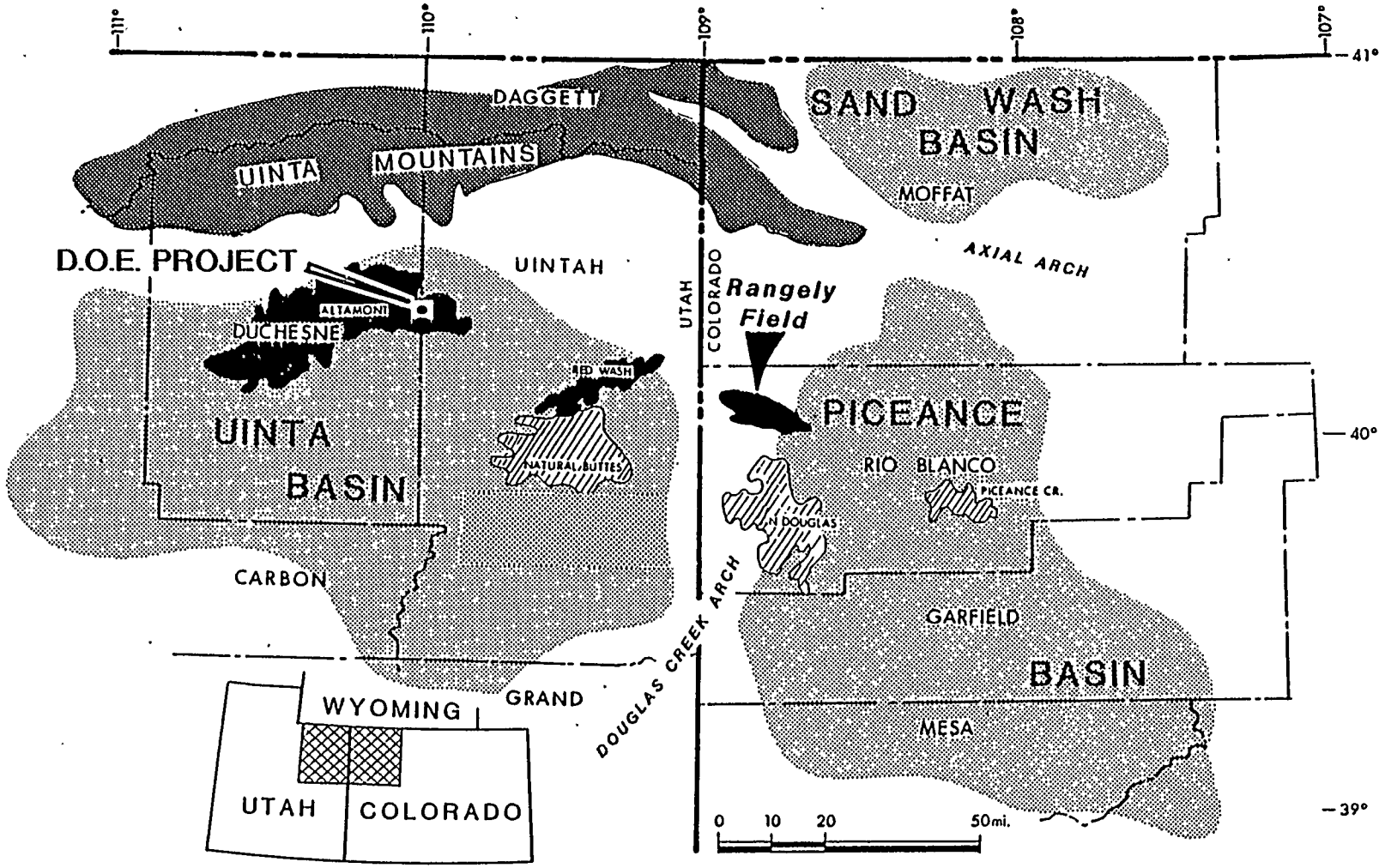


**Figure 1. Location Map—D.O.E Study Area**

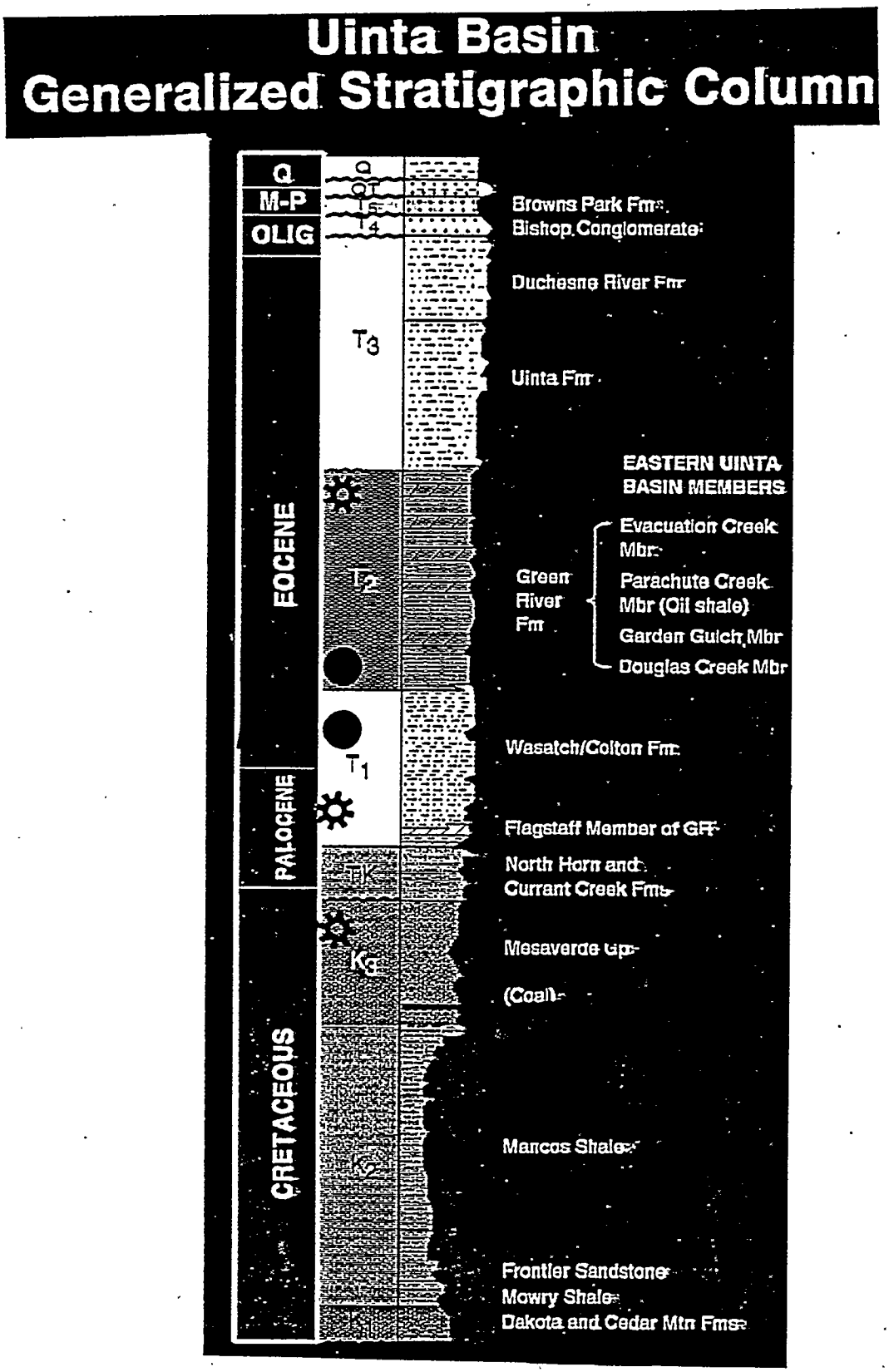
Uinta Basin
Generalized Stratigraphic Column
Q
M-P
OLIG
EOCENE
PALOCENE
CRETACEOUS
Q
QT
T5
T4
T3
T2
T1
K
Kg
K2
K1
Browns Park Fm
Bishop Conglomerate
Duchesne River Fm
Uinta Fm
EASTERN UINTA BASIN MEMBERS
Green River Fm
Evacuation Creek Mbr
Parachute Creek Mbr (Oil shale)
Garden Gulch Mbr
Douglas Creek Mbr
Wasatch/Colton Fm
Flagstaff Member of GFF
North Horn and Currant Creek Fms
Mesaverde Gp
(Coal)
Mancos Shale
Frontier Sandstone
Mowry Shale
Dakota and Cedar Mtn Fms

**Figure 2**

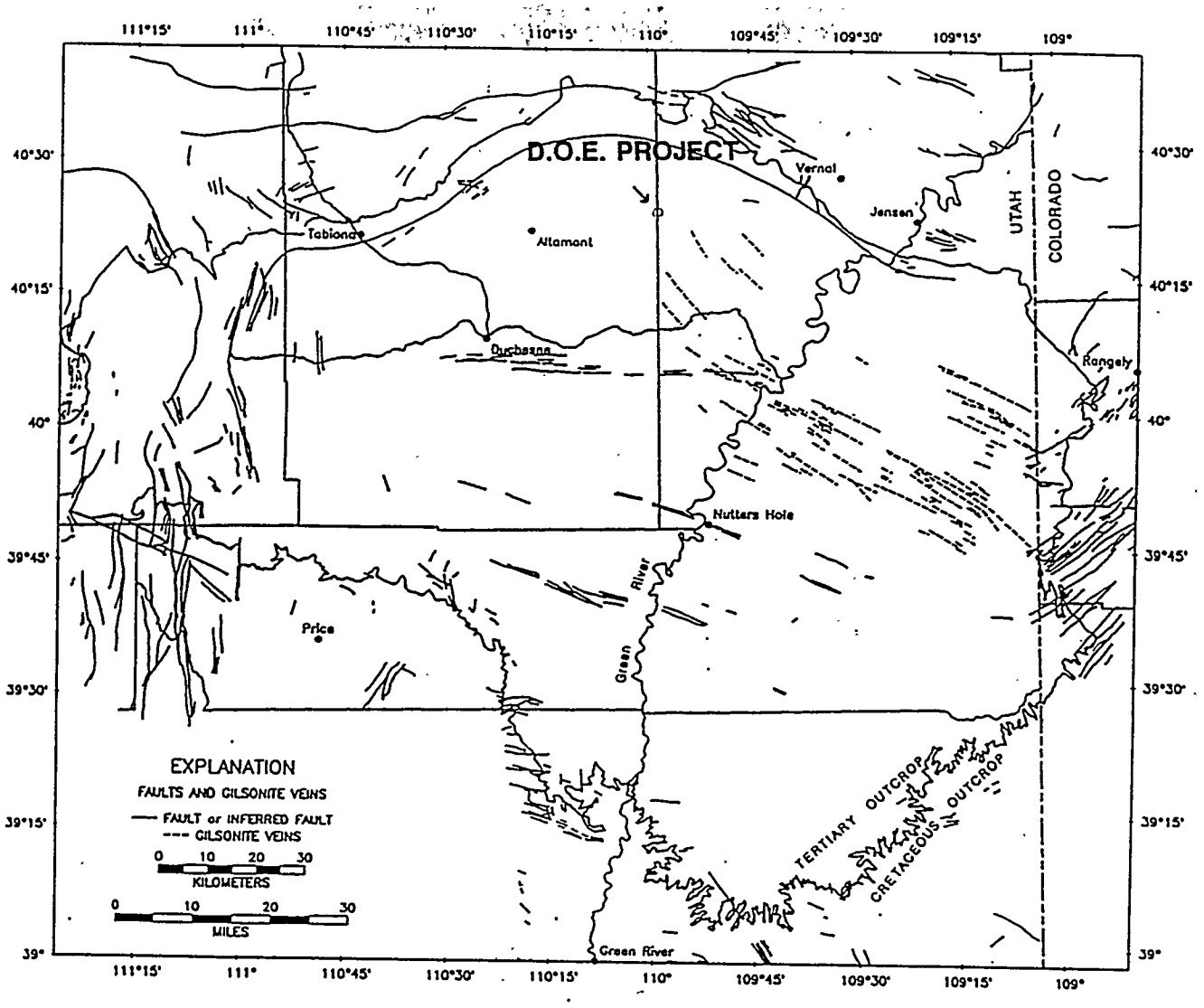


Gilsonite veins (dased lines) and major faults (solid heavy lines) in Upper Cretaceous and Tertiary rock of the Uinta Basin (from Fouch and others, 1991).

**Figure 3. Regional Setting**

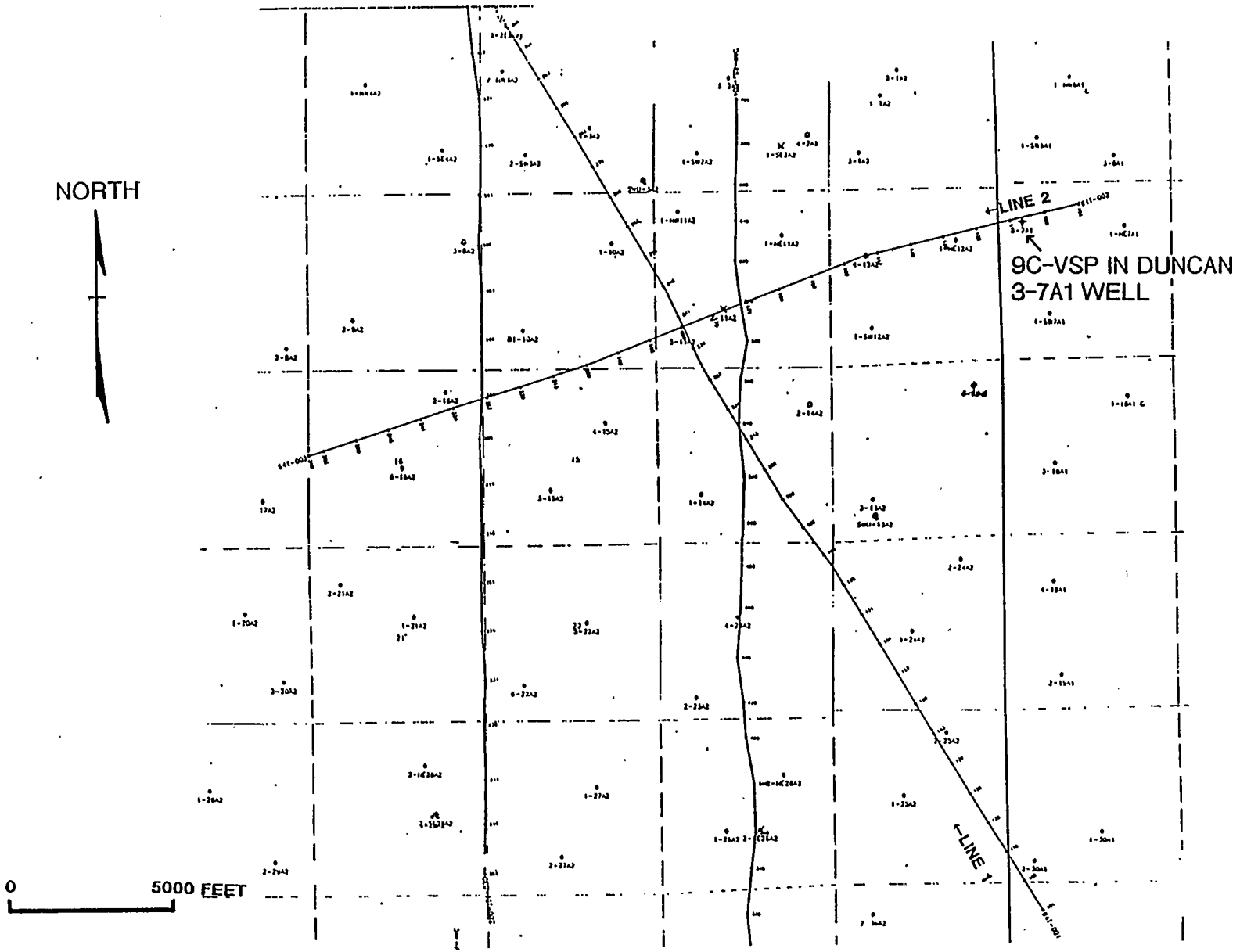


**Figure 4. Base Map: D.O.E. Project Bluebell-Altamont, UT**

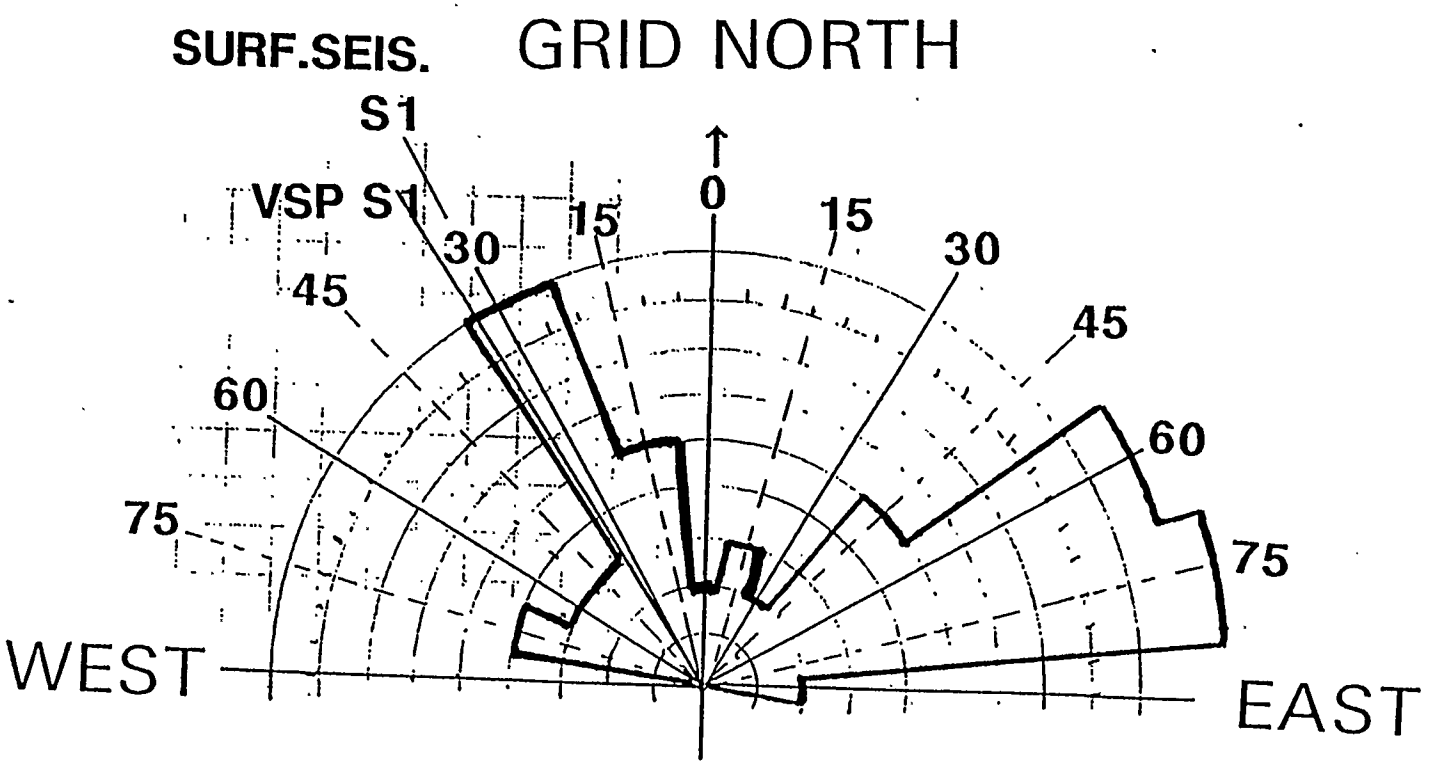


**Figure 5. Fracture Azimuths Mapped in Outcrops Adjacent to Seismic Lines**

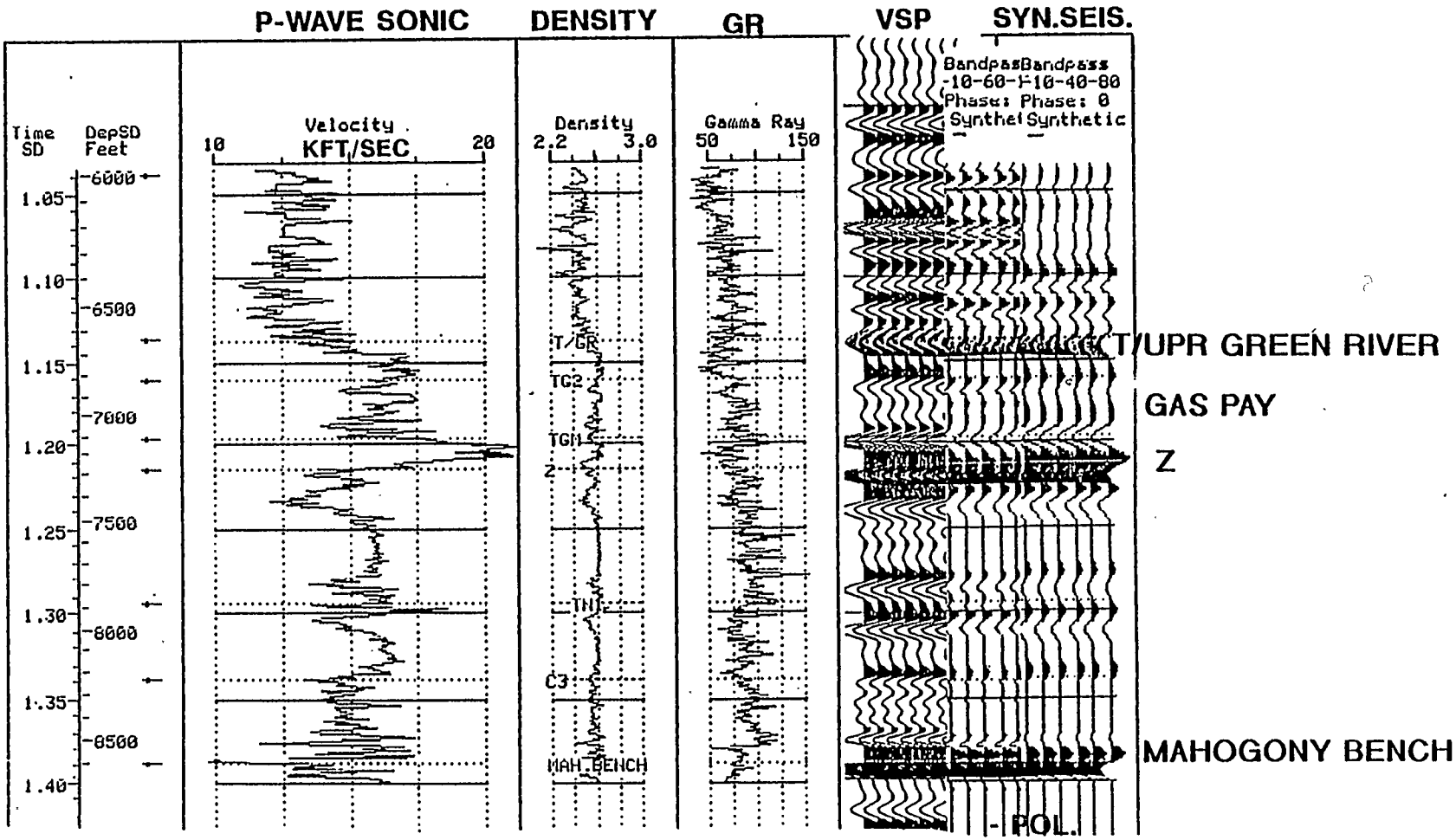


**Figure 6. Sonic, Density, GR, Synthetic Seismogram and VSP Corridor Stack in 9C VSP Well**

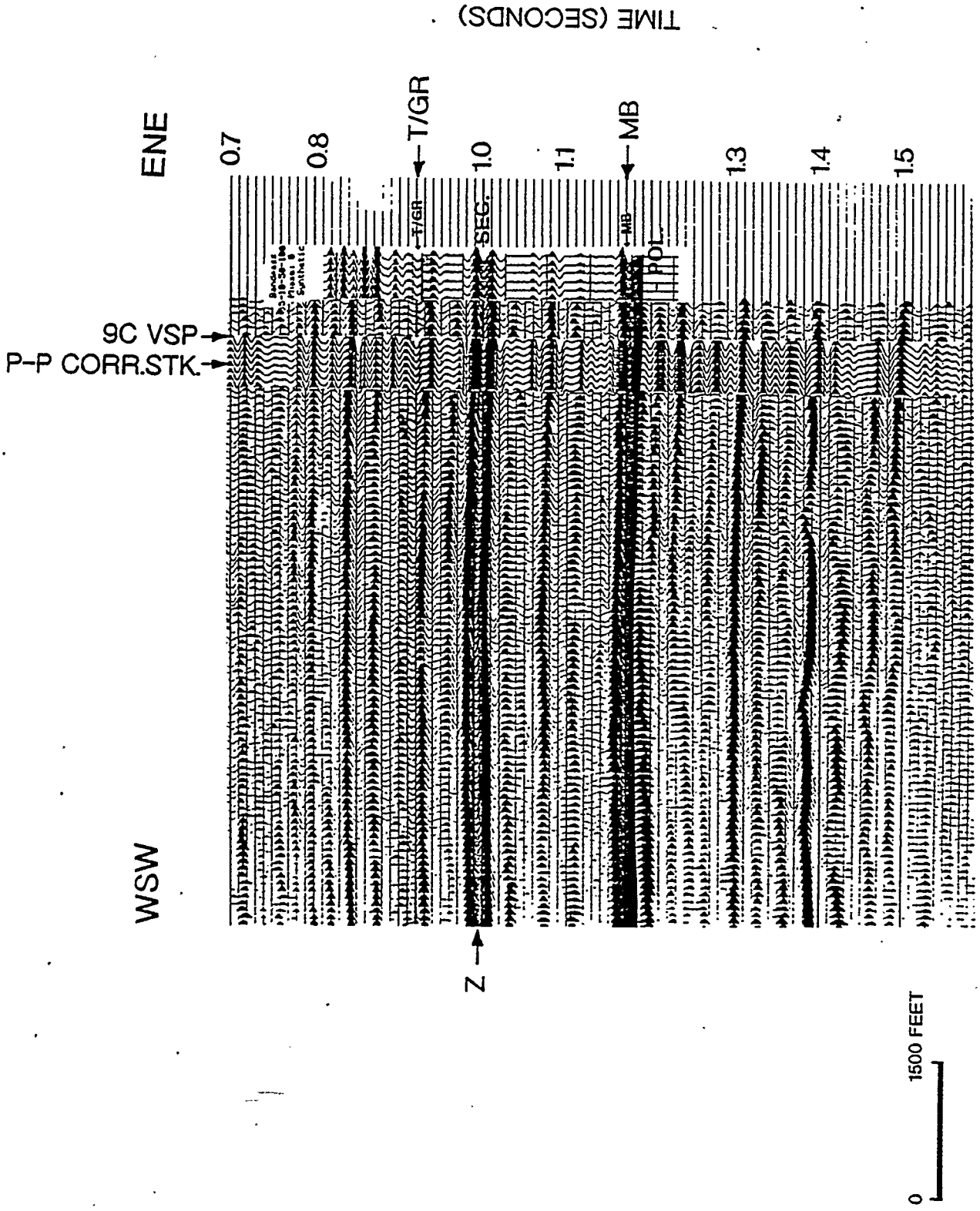


**Figure 7. Migrated P-P Line 2**

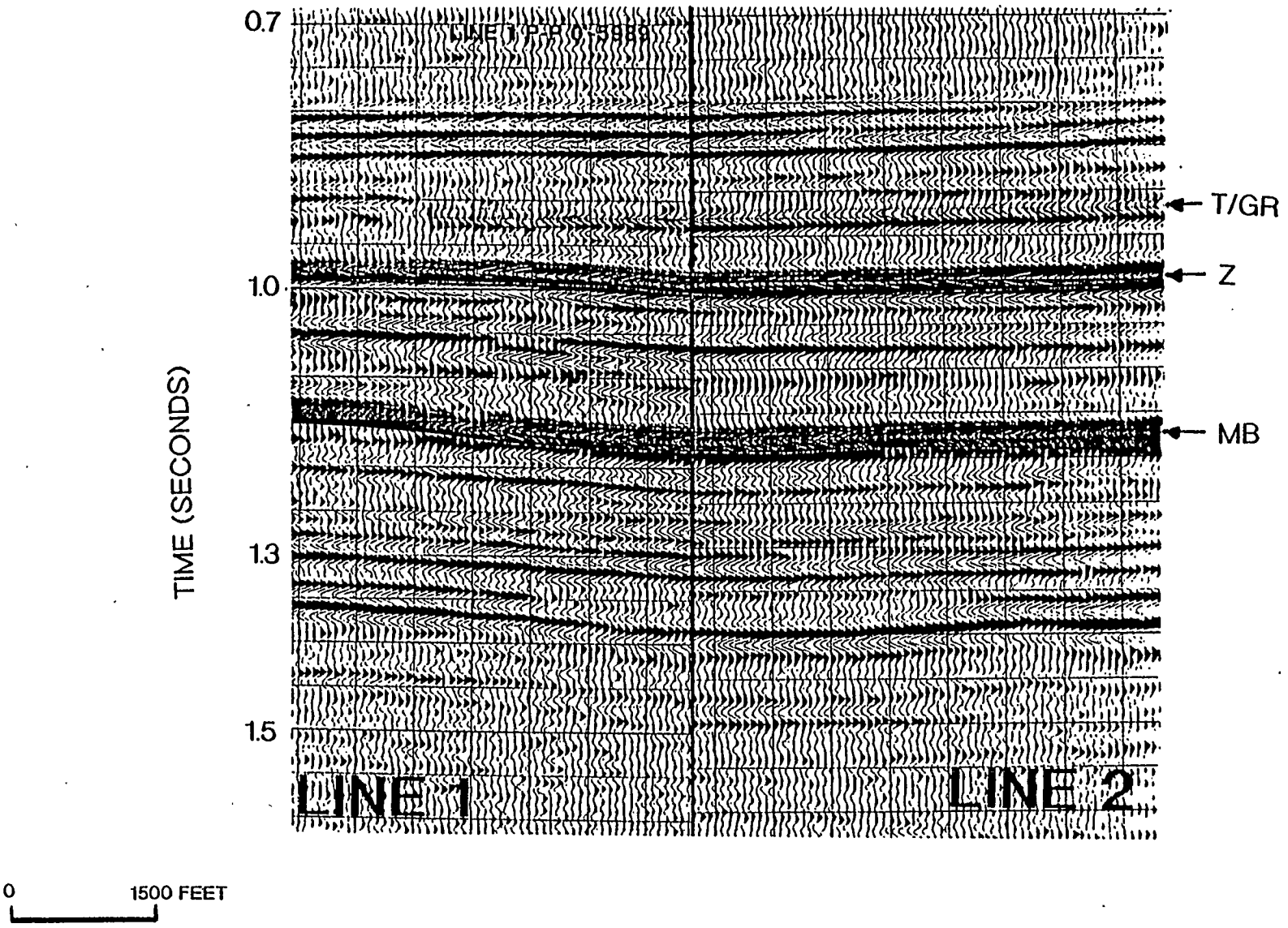


**Figure 8. P-P Near Offset Stack Line 1 and Line 2 at Tie Point**

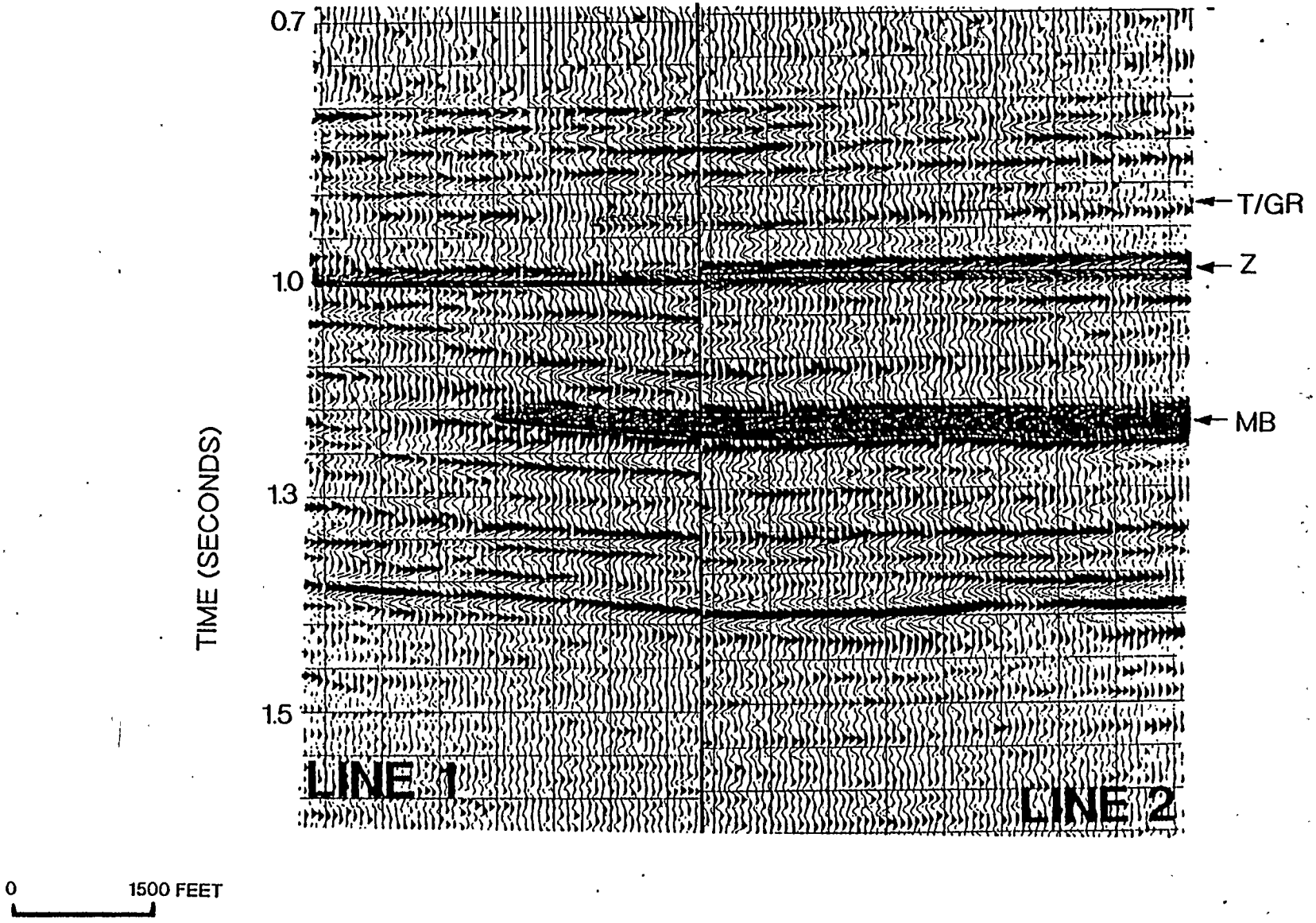


**Figure 9. P-P Far Offset Stack Line 1 and Line 2 at Tie Point**

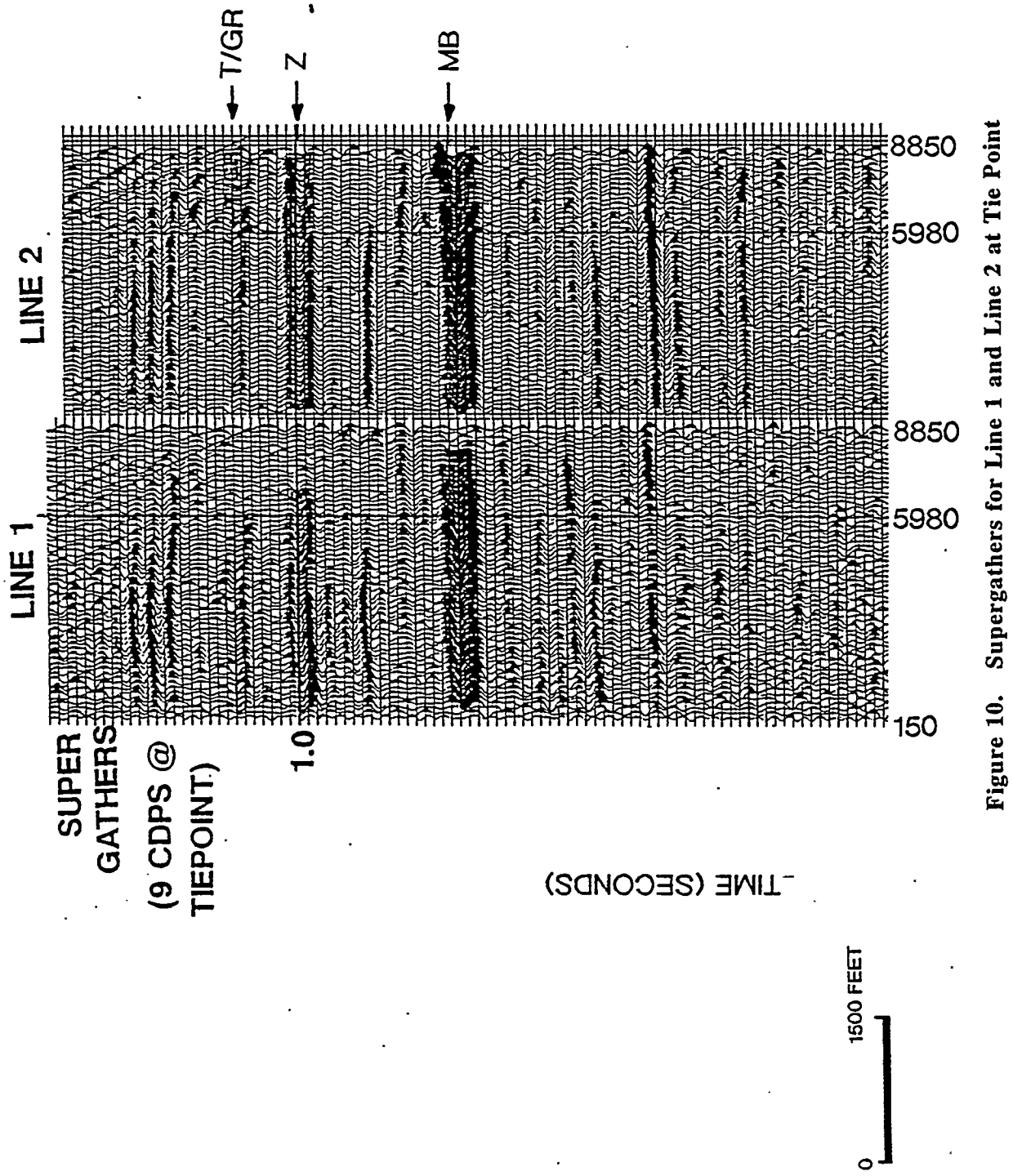


**Figure 10. Supergathers for Line 1 and Line 2 at Tie Point**

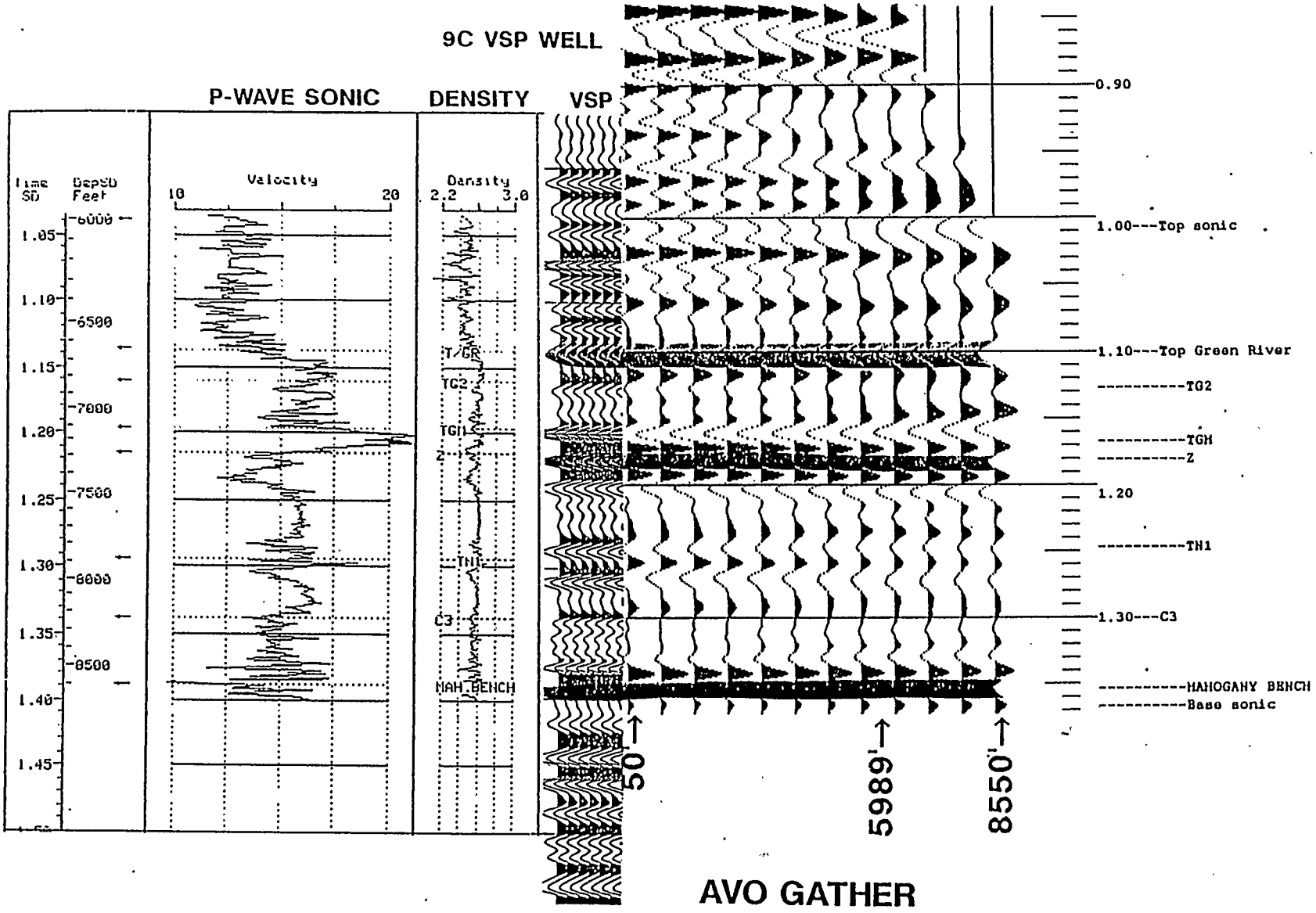


**Figure 11. P-P AVO Seismogram**

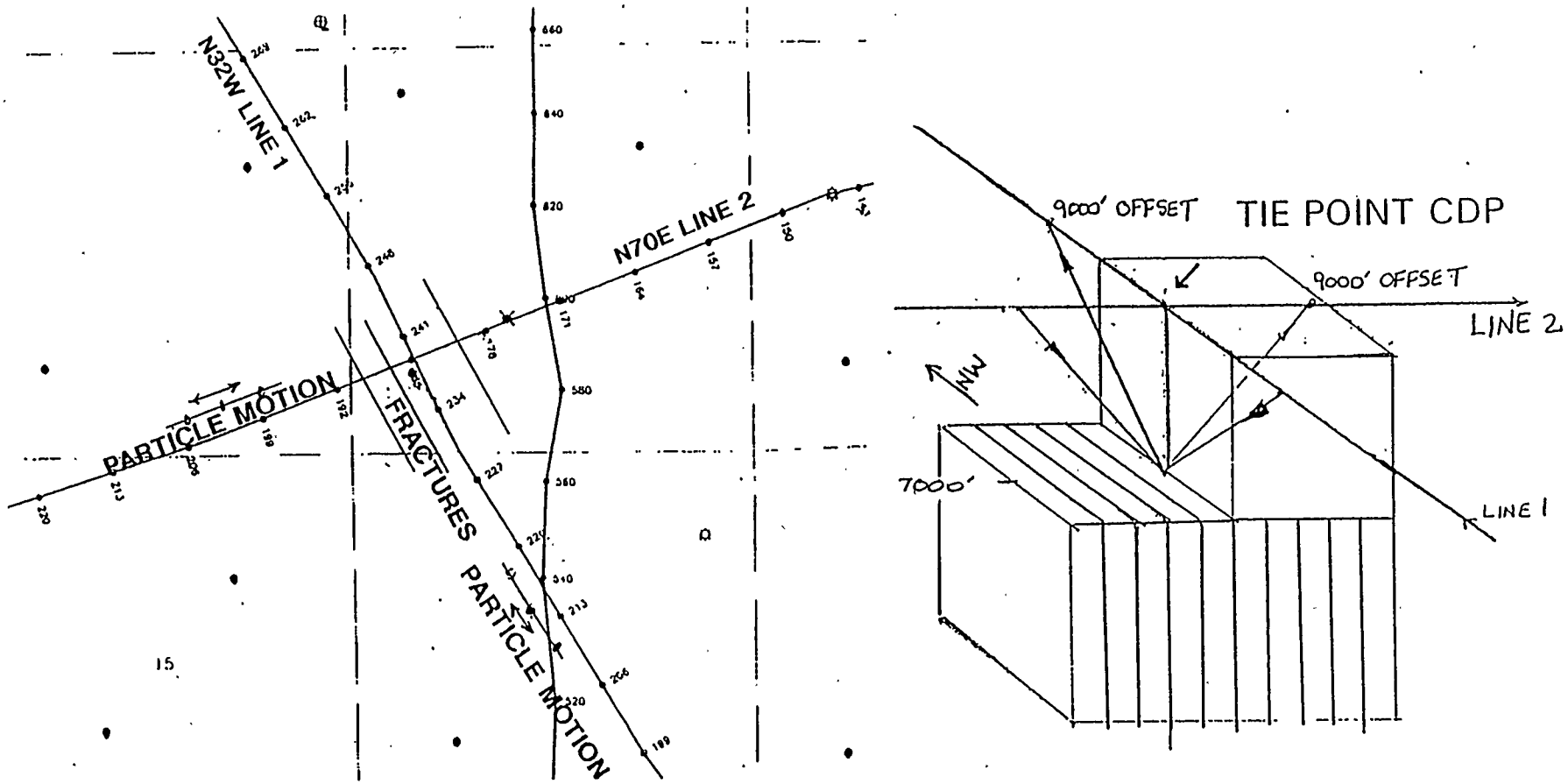


**Figure 12. Schematic — Azimuthal AVO Anomaly**

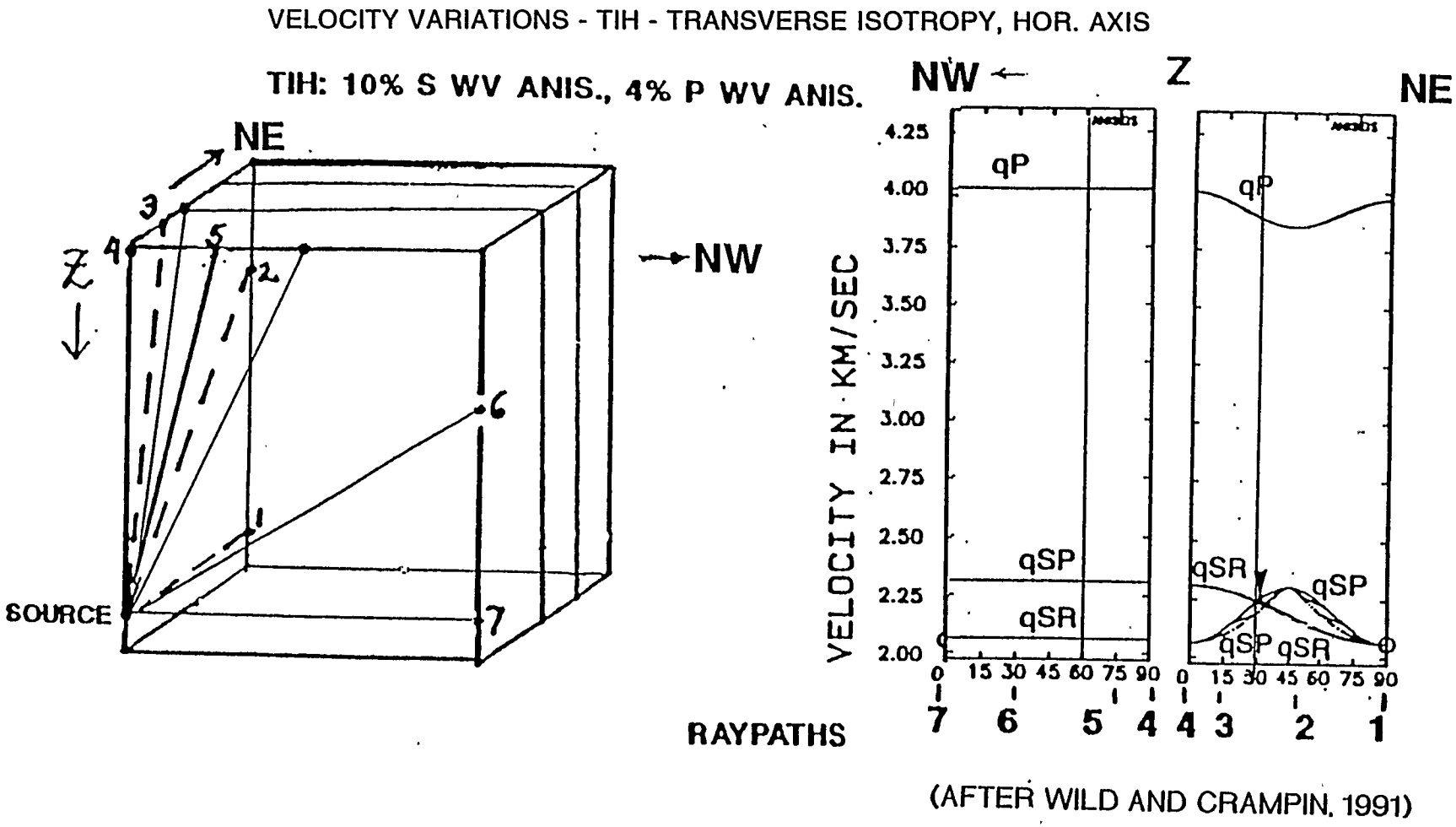


**Figure 13. Velocity Variations in Medium with Vertical Aligned Cracks and/or Unequal Hor. Stresses**

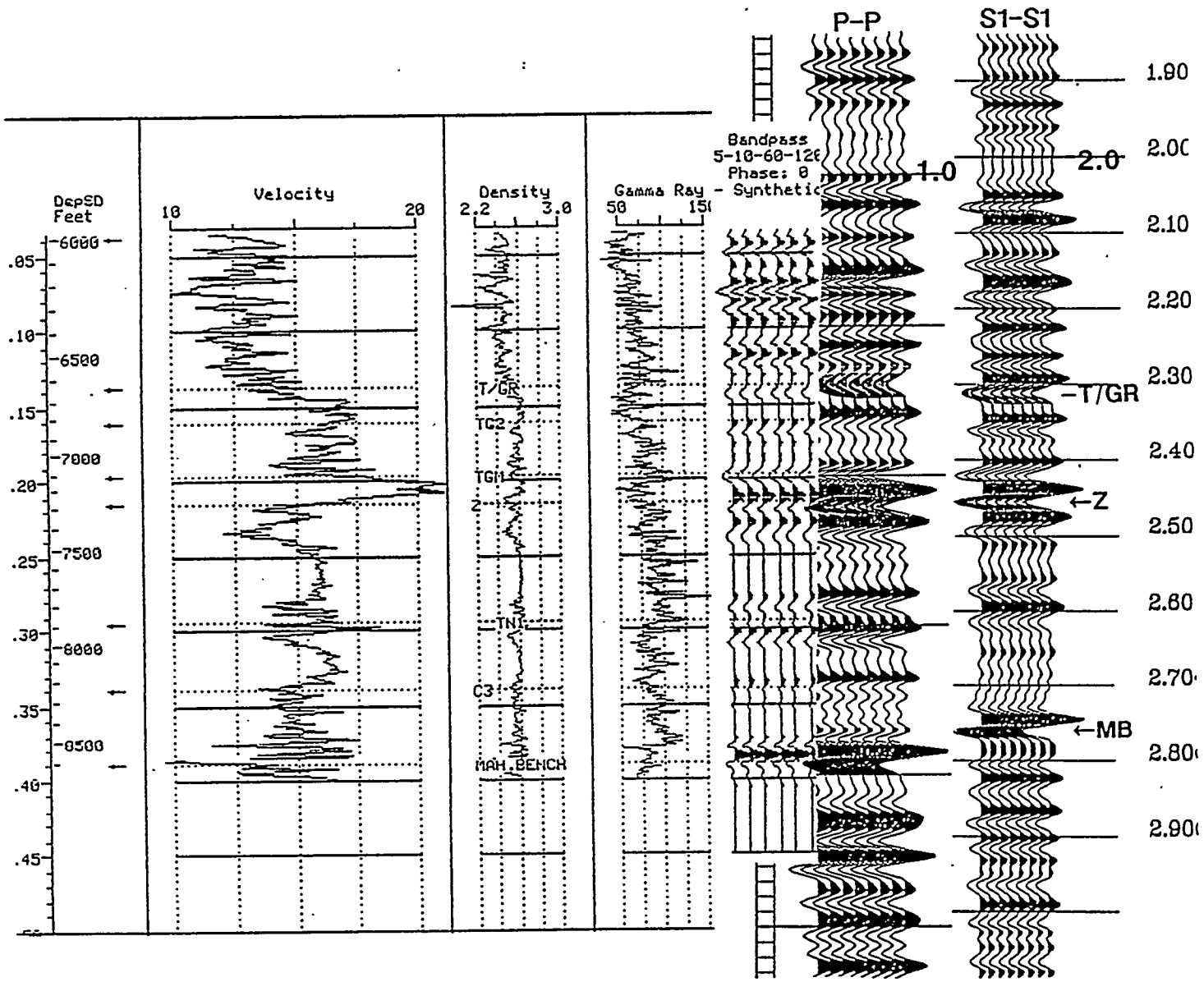


**Figure 14. P-P and S1-S1 Corridor Stacks**

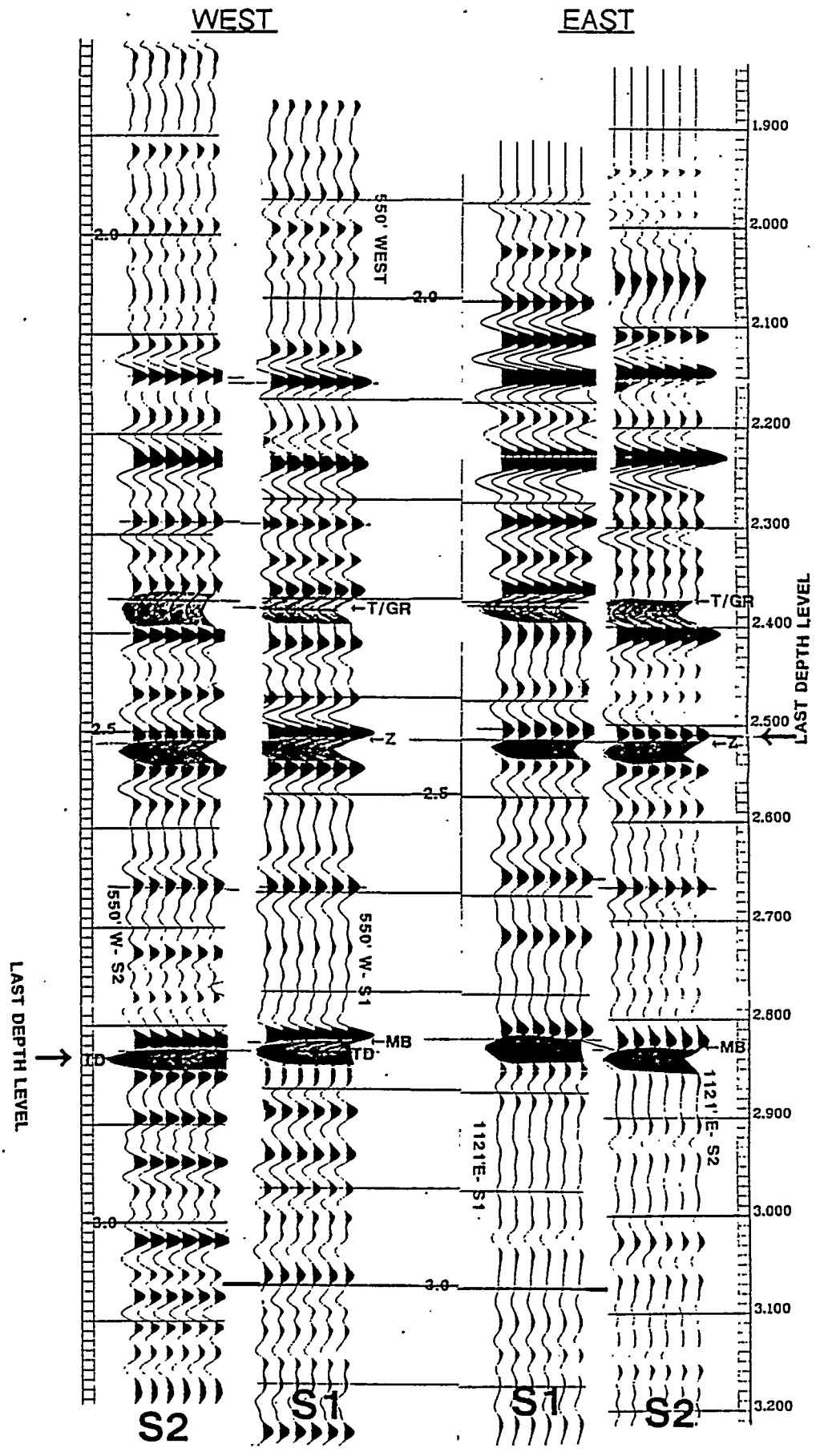


**Figure 15. S1-S1 and S2-S2 Corridor Stacks**

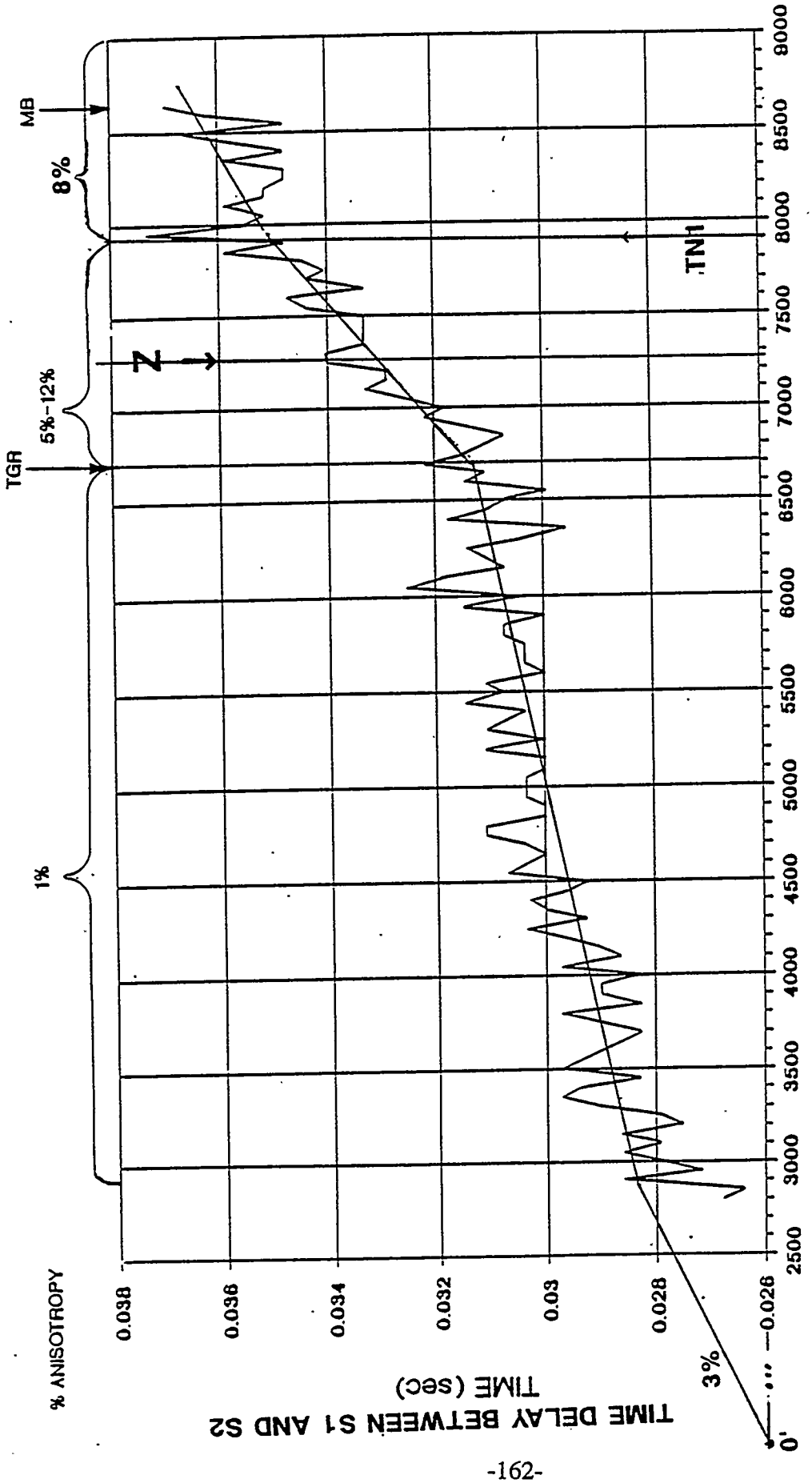


Figure 16. Time Delay Between S1 and S2 Arrivals

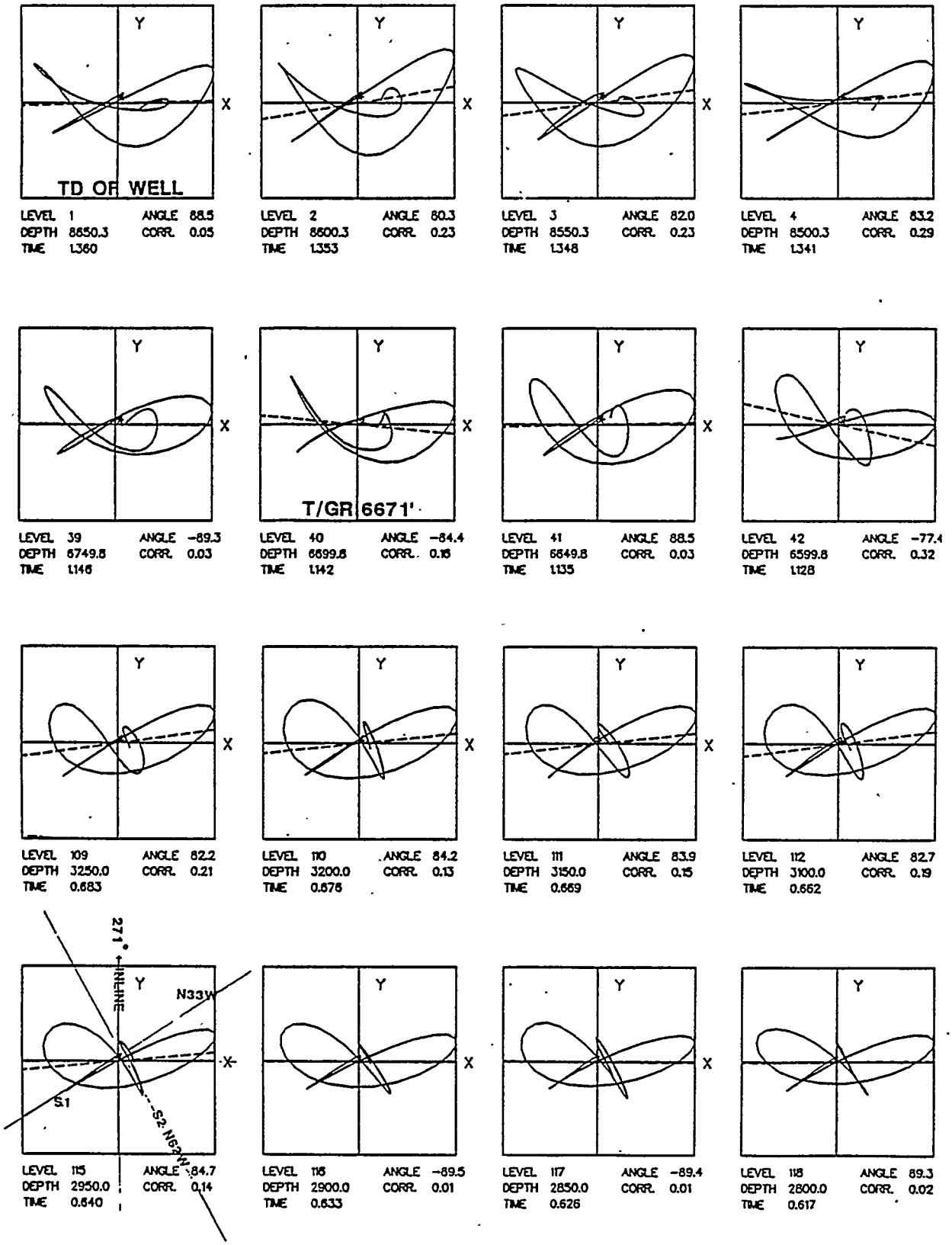


**Figure 17. Hodograms From SV Source, 2,800 ft. - 8,650 ft.**

## 5A.3 Naturally Fractured Tight Gas Reservoir Detection Optimization

### CONTRACT INFORMATION

**Contract Number:** DE-AC21-93MC30086

**Contractor:**
Advanced Resources International, Inc.
1110 North Glebe Road, Suite 600
Arlington, VA 22201
(703) 528-8420 (Telephone)
(703) 528-4039 (Fax)

**Contractor Project Manager:** Vello Kuuskraa

**Principal Investigator:** David Decker

**METC Project Manager:** Royal J. Watts

**Period of Performance:** September 30, 1993 - March 31, 1997

**Schedule and Milestones**

| **Program Schedule** | **FY 1994** | | | | **FY 1995** | | | | **FY 1996** | | | | **FY 1997** | |
|---|---|---|---|---|---|---|---|---|---|---|---|---|---|---|
| Field | $Q_1$ | $Q_2$ | $Q_3$ | $Q_4$ | $Q_1$ | $Q_2$ | $Q_3$ | $Q_4$ | $Q_1$ | $Q_2$ | $Q_3$ | $Q_4$ | $Q_1$ | $Q_2$ |
| **Task 1 - Site Selection** | ——— | | | | | | | | | | | | | |
| Remote Sensing Imagery | | | | | | | | | | | | | | |
| High Resolution Aeromagnetics | | | | | | | | | | | | | | |
| Field Studies | | | | | | | | | | | | | | |
| Structural Studies | | | | | | | | | | | | | | |
| **Task 2 - Field Test Plan** | | | | | | | ——— | | | | | | | |
| **Task 3 - 3-D Multicomponent Shear wave** | | | | | | | | | ——— | | | | | |
| Acquisition | | | | | | | | | | | | | | |
| Processing | | | | | | | | | | | | | | |
| Interpretation | | | | | | | | | | | | | | |
| **Task 4 - Project Summary** | | | | | | | | | | | | | ——— | |

## OBJECTIVES

The objectives of the fracture detection optimization program are to 1) Develop and optimize an integrated exploration approach utilizing advanced remote sensing imagery, high-resolution aeromagnetics, stratigraphic mapping and dynamic tectonic modeling that will reliably predict fracture prone areas and 2) Demonstrate application of 3-D multicomponent seismic array for siting wells within the selected fracture prone area to target naturally fracture tight gas reservoirs.

## BACKGROUND INFORMATION

Natural fracture intensity and diversity of orientation is a requirement for commercial production from the vast store house of natural gas held in tight gas reservoirs. Identifying and defining the location of fractured reservoirs with advanced seismic technologies such as shear wave birefringence has shown promise (Martin and others, 1987). Unfortunately, its high cost constrains the use of these technologies for exploration and reconnaissance mapping. Surface seismic fracture detection technologies however, maybe cost effectively applied in regions where fractures are already known to exist. Current geologic models for locating open fracture systems are qualitative (Lorenz and others, 1991) and as such too speculative to justify the expense commitment of using advanced seismic methods to verify their location and characteristics. Quantification of fracture characterization is possible by improving and correct application of existing geological and geophysical techniques.

Prediction of subsurface fractures will be accomplished by integrating and optimizing existing fracture detection tools. The research concept being pursued in this project is that fractures are generated by multiply reactivated basement faults. Structural warps associated by basement faults both fracture the overlying rocks and establishes regions of low stress settings allowing dilation of the natural fracture system. Therefore the development of an exploration strategy designed to identify these important but frequently subtle basement features is critical to locating fractured regions in advance of drilling. Infield development of the predicted fractured area can be most cost effectively accomplished by targeting fracture systems utilizing advanced seismic fracture detection technologies such as 3-D multicomponent shear wave surveys.

## PROJECT DESCRIPTION

A field demonstration site will be located in the Piceance Basin, northwestern Colorado. The Piceance Basin is an ideal area for the project due to 1) the wealth of subsurface fracture data collected at the MWX site, critical for calibration of the project fracture detection methodology 2) high drilling activity targeting tight gas reservoirs and support by the industry for optimizing fracture detection technology 3) widespread distribution of tight gas reservoirs within the basin that could be accessed by successful deployment of the technologies developed under this project.

An aggressive technical program involving a multi-disciplinary approach to meet the challenge of optimizing fracture detection technologies is the project foundation. Data acquisition, compilation, interpretation and synthesis as displayed on figure 1 is the first project phase. The key element in the first phase is determining the relationship of permeability anisotropy orientation to basement structures. Permeability anisotropy can be established through iso-production contouring of wells producing from fractured tight gas reservoirs. The presence and orientation of basement features has been determined by utilizing advanced basement imaging tools. Establishment of the relationship to known favorable permeability

fairways to mappable basement features will provide an exploration analog for the identification of undrilled basement structures and associated fractured tight gas reservoirs. A 3-D muticomponent shear wave program will be acquired, processed and interpreted over the area predicted to be fractured. Barrett Resources will drill and complete wells targeted by the seismic shoot. Well testing and reservoir simulation of historical production trends will determine reservoir permeability and thereby verify if wells drilled under this project have encountered better permeability than wells drilled without the benefit of integrated fracture detection technologies. An economic analysis will be performed to determine if the economic benefits of the fracture detection technologies are offset by increased gas reserves.

## RESULTS

A rigorous approach to structural analysis has been undertaken to successfully determine basement features controlling shallow structural development. To provide a foundation for structural interpretation, a high resolution aeromagnetic survey was acquired and processed over the southern basin (figure 2). To minimize interpretation subjectivity and establish credibility of interpreted features, basement features were also interpreted utilizing 400 line miles of seismic surveys, and utilizing Landsat Thematic Mapper (TM) and Side Looking Airborne Radar (SLAR) imagery for the basin and surrounding areas.

Spatially detailed aeromagnetic maps were used to interpret zones of basement structure. Basement structures, some verified by seismic profiles, corresponded to steep magnetic gradients and linear trending contours. Utilizing this technique, first order and second order basement features have been located on the reduced-to-pole total field magnetic intensity contour map (figure 3). The most prominent features include an interpreted paleobasement high in the east central portion of the basin flanked on the east and west by northwest trending faults NW3 and NW4 and on the north and south by EW3 and EW2 respectively interpreted as east - west trending faults. Seismic coverage (figure 4) has confirmed the basement high which has caused truncation of the Paleozoic section. At basement level, structural lineament NW4 is formed by low angle thrust faults that typically terminate within the Mancos shale. Mild warping and draping of the sediments occurs along the fault termination boundaries.

Coincident features to the identified first and second order northwest lineaments have been mapped through linear feature analysis of TM imagery. These lineaments are a composite of individual linear features as interpreted from Landsat Thematic Mapper imagery. Northwest-trending linear features were contoured with respect to frequency of occurrence. Imagery lineaments are defined as zones of aligned and concentrated linear features, which are linear elements interpreted directly from imagery. Figure 5 presents lineaments interpreted from NW-trending linear features in the southern portion of the basin. Note on figure 5 the close correlation of lineaments as interpreted from imagery to basement faults as interpreted from aeromagnetics. This close correlation and further calibration from seismic lines establishes interpreted NW lineament features as significant structural lineaments. Analysis of the E-W trending features is in progress. Preliminary interpretation of E-W structural elements suggests lateral movement along fault zones. Stratigraphic interpretation indicates the NW4 structural element acted as a basin hingeline during Cretaceous deposition.

## Structurally Aligned Reservoir Compartmentalization

The best production from Cameo coals and overlying tight gas sands of the Piceance Basin has been established in the Rulison, Parachute and Grand Valley Fields. Iso-production contouring of these three fields has been performed separately on the coal and tight gas sand as part of an effort to determine geologic controls on gas production. The strong NW trend of the production contouring from both intervals implies a common event causing permeability anisotropy. The close proximity and alignment of northwest trending basement faults (figure 6) to the production anisotropy is interpreted as being fracture controlled. Fractures have been generated by basement faults causing the northwest aligned production trend. A region of high stress occurring within close proximity to the structural lineament causes closure of the fracture system and results in a no-flow boundary. Gas migrating southward out of the gas-centered basin became trapped along the no flow boundary causing an overpressuring along the northwest flanks of the basin hingeline NW4. Southwest of the hingeline, the Cretaceous reservoirs are gas saturated and underpressured because the hingeline has isolated water recharge from the Northeastern basin elevated outcrop from the southwestern basin. High fracture permeability and overpressuring conditions are responsible for better reservoir performance observed at Rulison field when compared to other fields producing from Cameo coals and overlying tight gas sands. Since the favorable reservoir properties at the Rulison Field are associated with the basin hingeline, similar reservoir compartments are likely to exist northwest and southeast of the Rulison field along the basin hingeline.

## CONCLUSIONS

Fractured production anisotropy in Piceance Basin Mesaverde Group gas reservoirs are controlled by basement fault trends. These basement faults and associated fracture permeability trends can be accurately located using an integration and optimization of remote sensing imagery, high resolution aeromagnetics, stratigraphic mapping and dynamic tectonic modeling. Although some of the basement-related fracture trends have been drilled, the majority of the fracture prone area's identified in the southern Piceance Basin by this project, not yet drilled, represent significant exploration targets.

## FUTURE WORK

An area interpreted to be underlain by natural fractures will be selected by June 1995 as the site for field demonstration of the 3-D multicomponent shear wave program. The 3-D shear wave survey will be calibrated with a multicomponent VSP survey in the central portion of the test site. The VSP survey will provide critical information on shear wave attenuation and fracture orientation, thereby serving as an aide in designing the 3-D shear wave survey. Preliminary 3-D shear wave survey design calls for a 4.45 $mi^2$ array which at average targeted depths of 4,000 - 6,000 feet would yield a 3-D portrait of 2 $mi^2$ when wave migration is considered. Survey acquisition is planned for early 1996. Data processing and interpretation will locate zones of maximum fracture intensity within fluvial sections of the Mesaverde Group. Barrett Resources will drill wells to encounter the fractured zones as interpreted from the seismic survey. The zones will be stimulated and production tested. Permeability of the completed interval and gas reserve forecasts will be determined through reservoir simulation and production history matching. A comparison of reserves will be made between wells drilled with

and without utilization of the fracture detection technology. An economic analyses will determine relative benefits of the fracture detection technology and associated higher costs.

## REFERENCES

Lorenz, J., Teufel, L., and Teufel, N., 1991, Regional Fractures I: A mechanism for the formation of regional fractures at depth in flat-lying reservoirs, American Association of Petroleum Geologists Bulletin, 75, 1714-1737.

Martin, M.A. and Davis, T.L., 1987, Shear-Wave Birefringence: A New Tool for Evaluating Fractured Reservoirs, *Geophysics: The Leading Edge of Exploration*, Oct. 22-28.

FIGURE 1

# KEY ELEMENTS OF INTEGRATED DOE-METC FRACTURE DETECTION TECHNICAL APPROACH

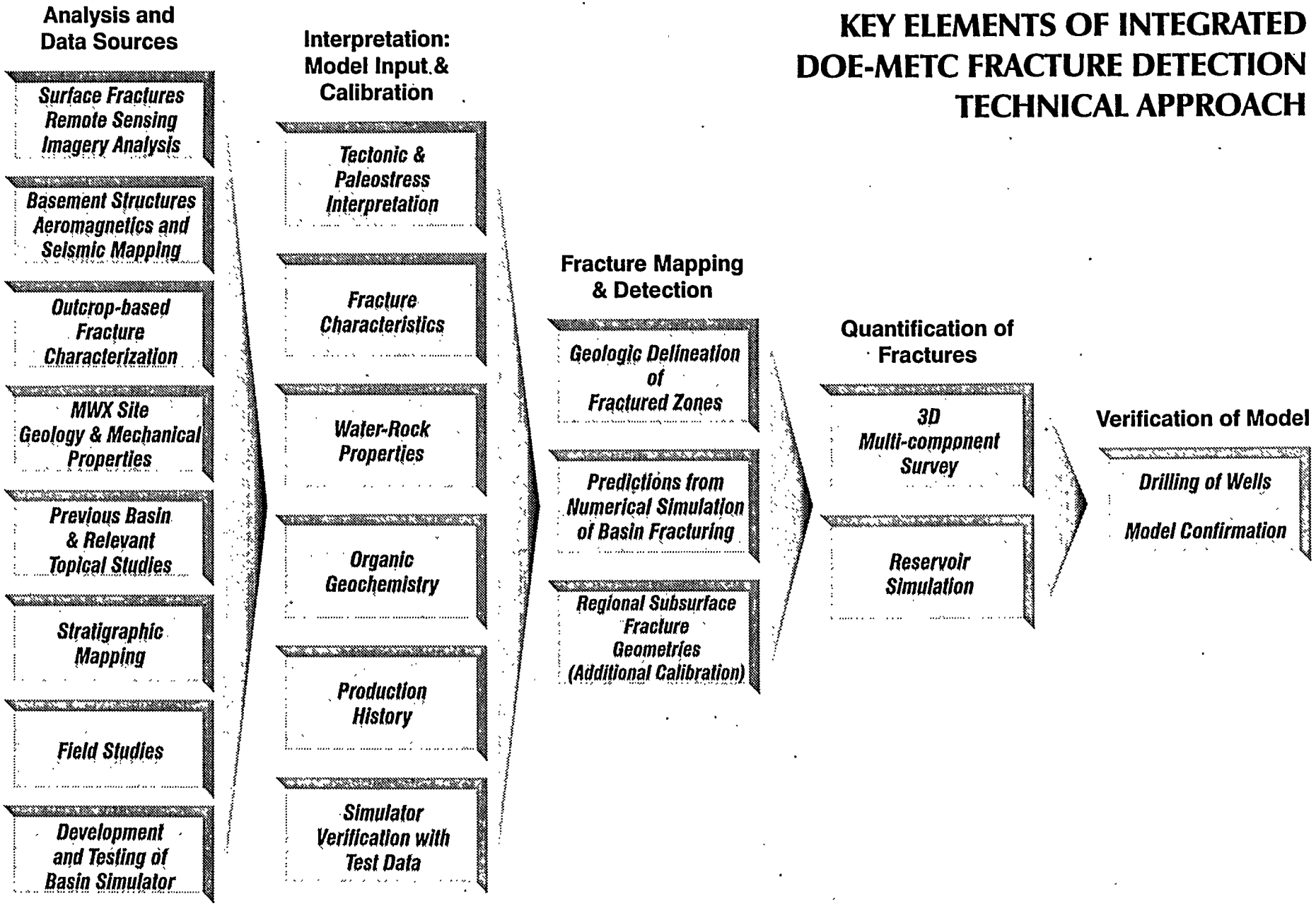

FIGURE 2

# AEROMAGNETIC SURVEY AREA AND SEISMIC GRID, PICEANCE BASIN

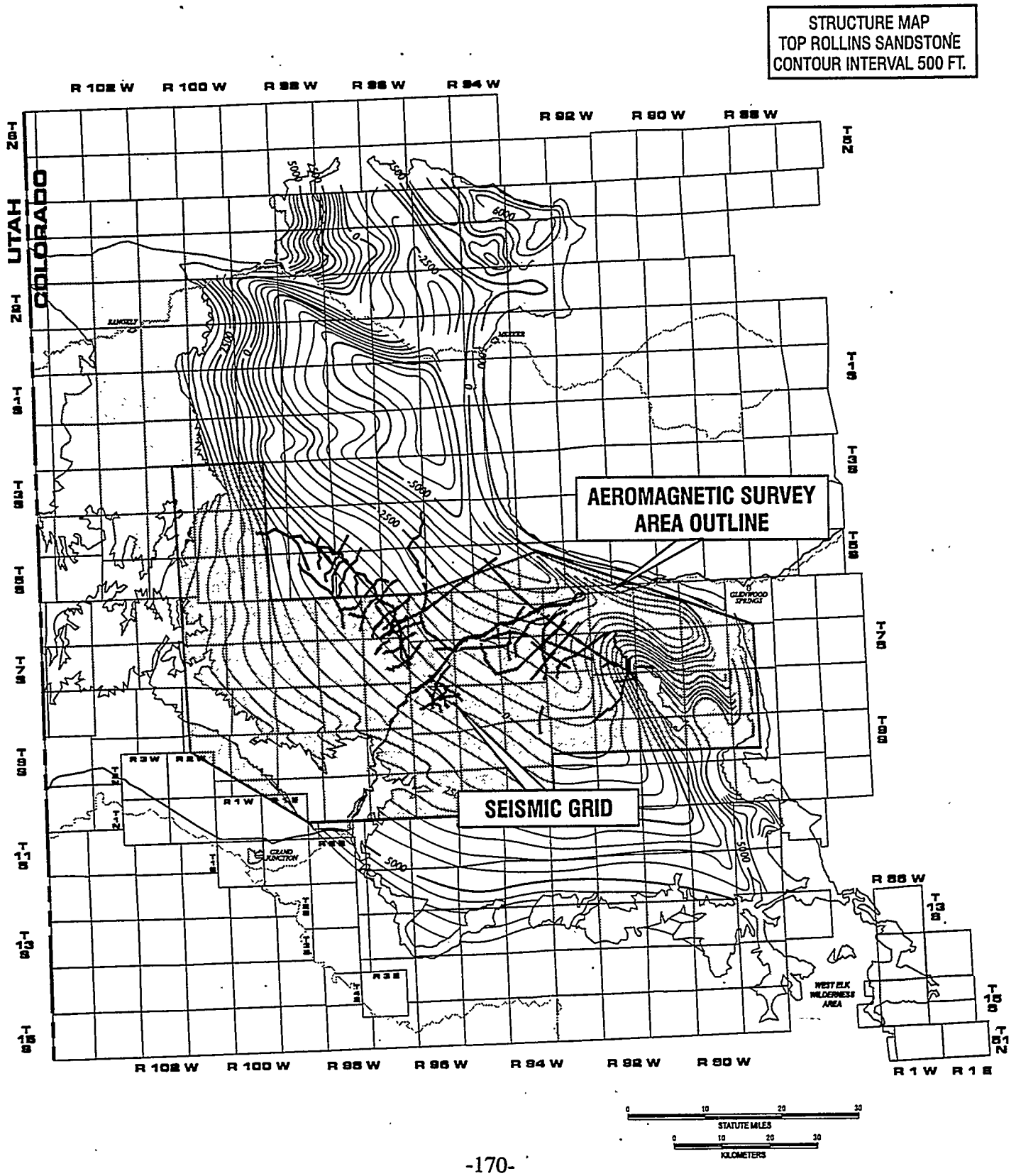

# REGIONAL HIGH-RESOLUTION REDUCED-TO-POLE TOTAL FIELD MAGNETIC INTENSITY

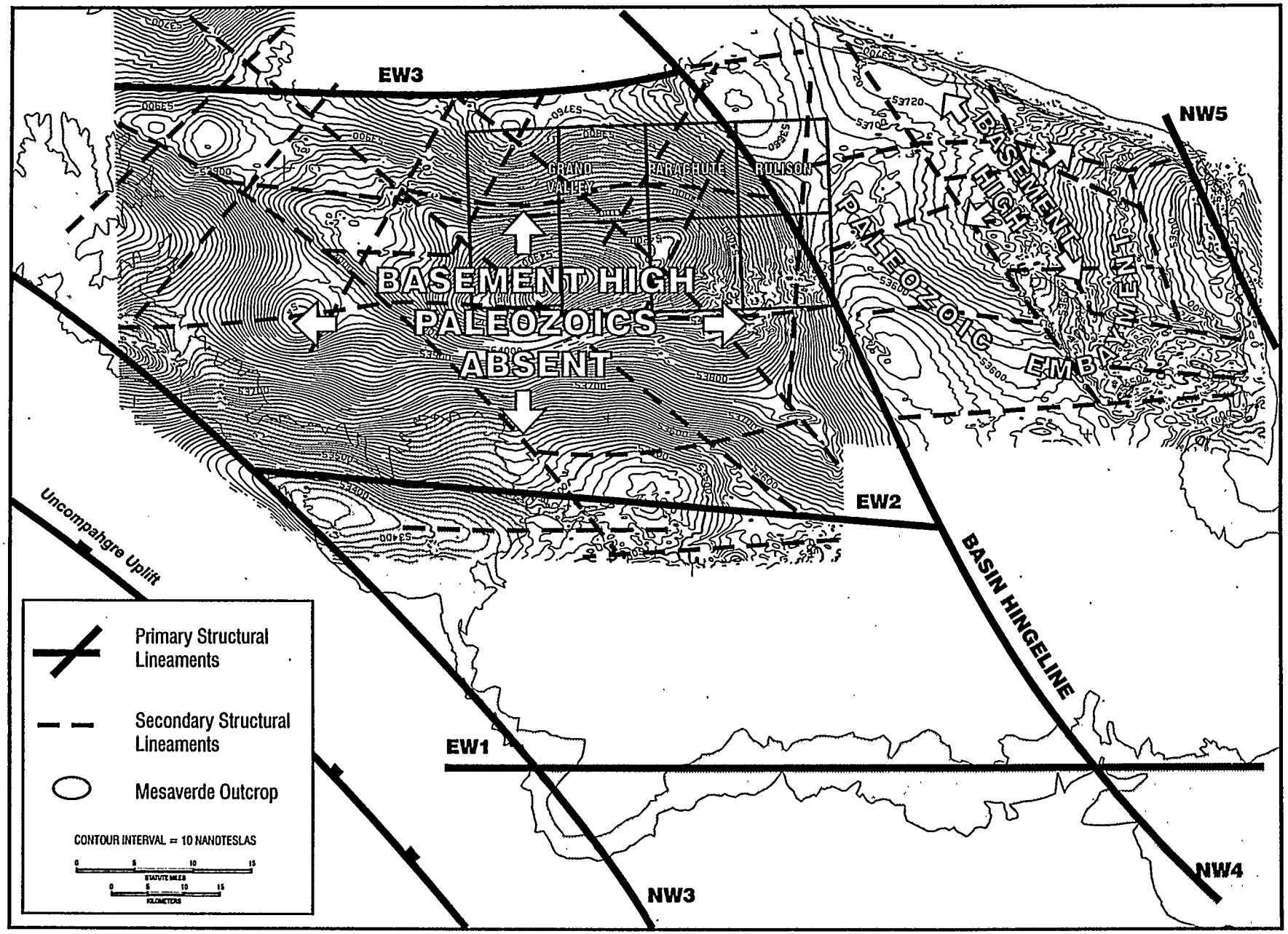

FIGURE 4

# BASEMENT FAULTS INTERPRETED FROM SEISMIC

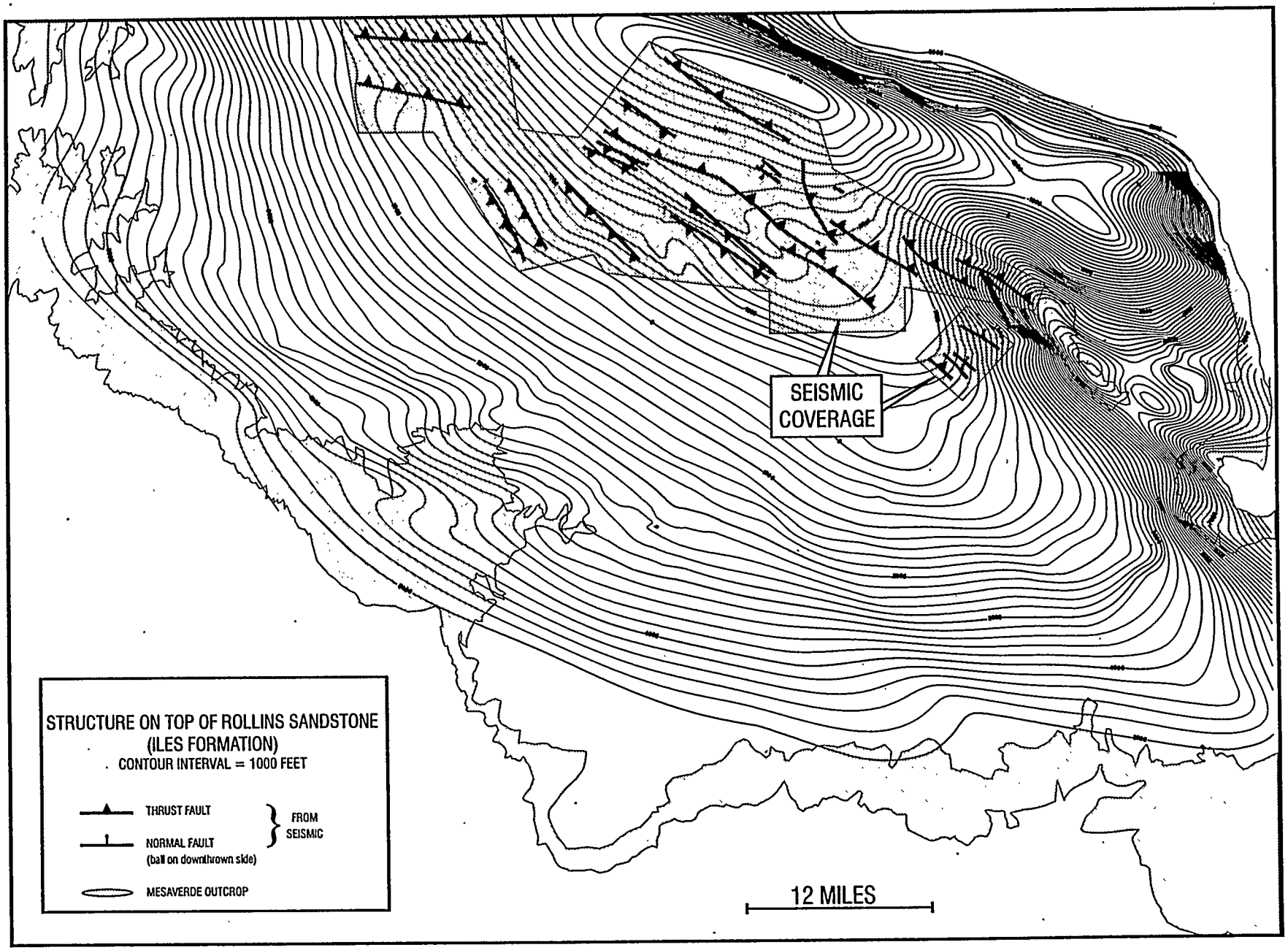

FIGURE 5

# LINEAR FEATURE ANALYSIS - NW TRENDING INTERVAL
# CONTOURED LINEAR FEATURE FREQUENCY

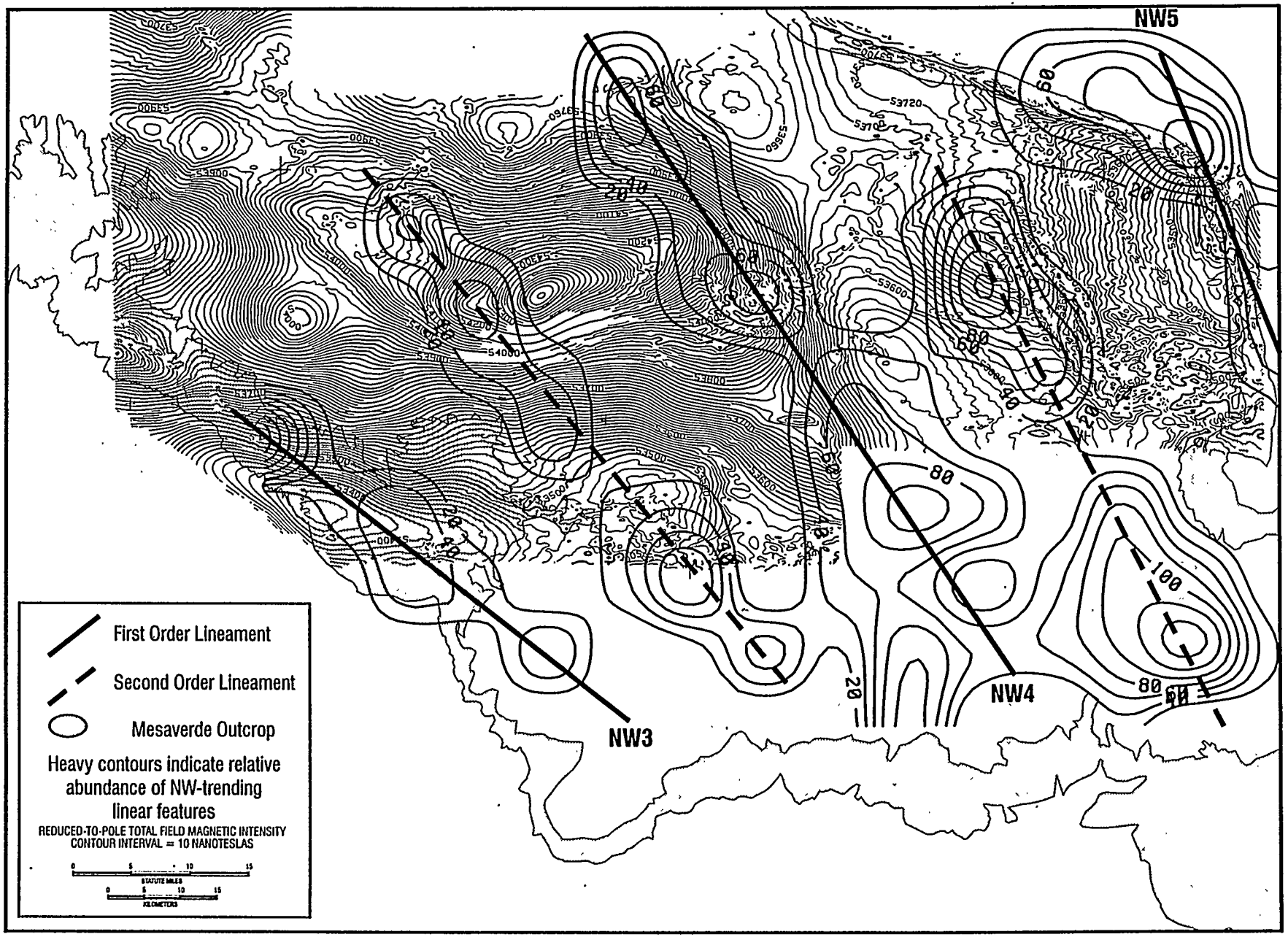

FIGURE 6

# RELATIONSHIP BETWEEN STRUCTURE AND PRODUCTION

## Grand Valley, Parachute and Rulison Fields, Piceance Basin

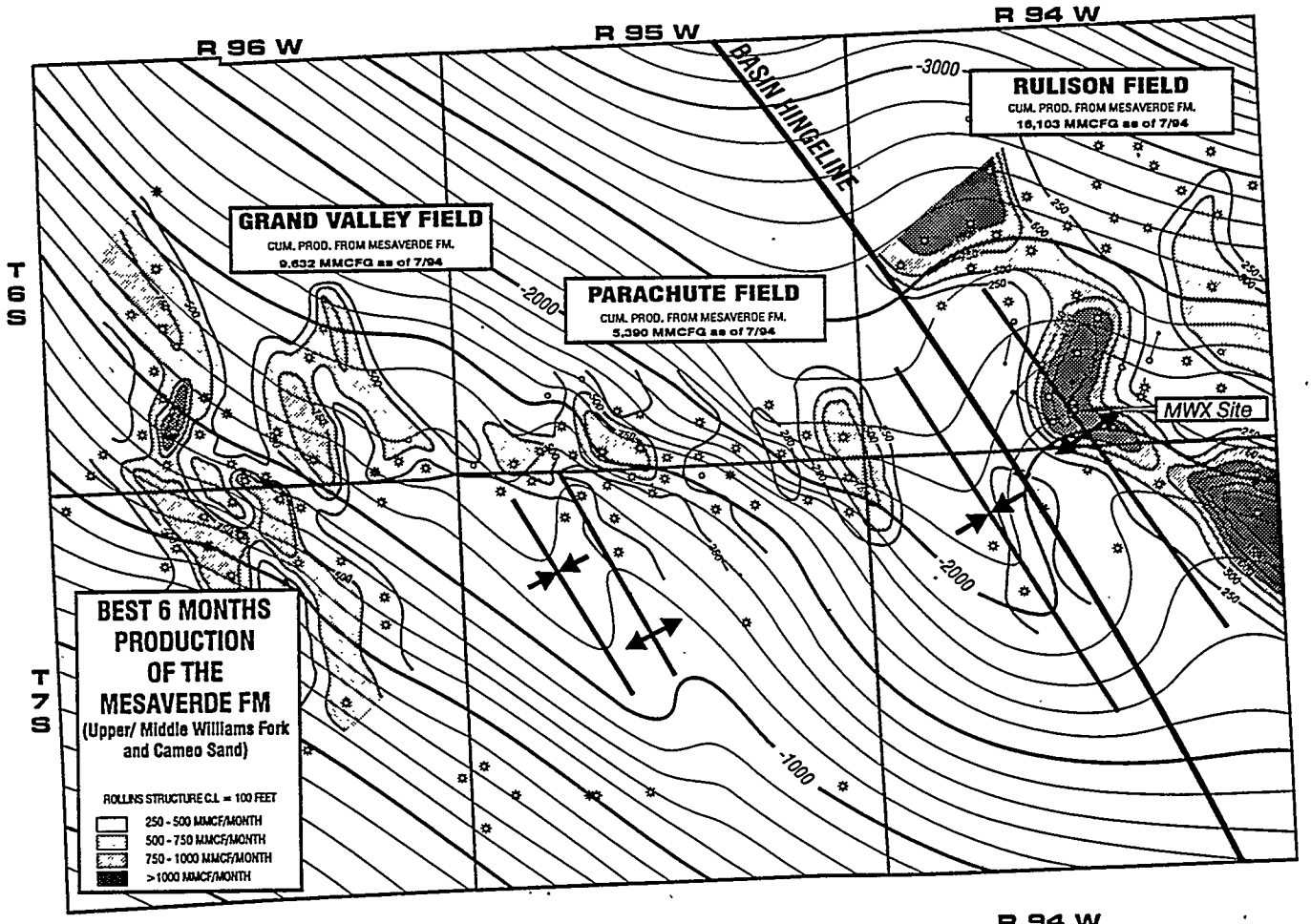


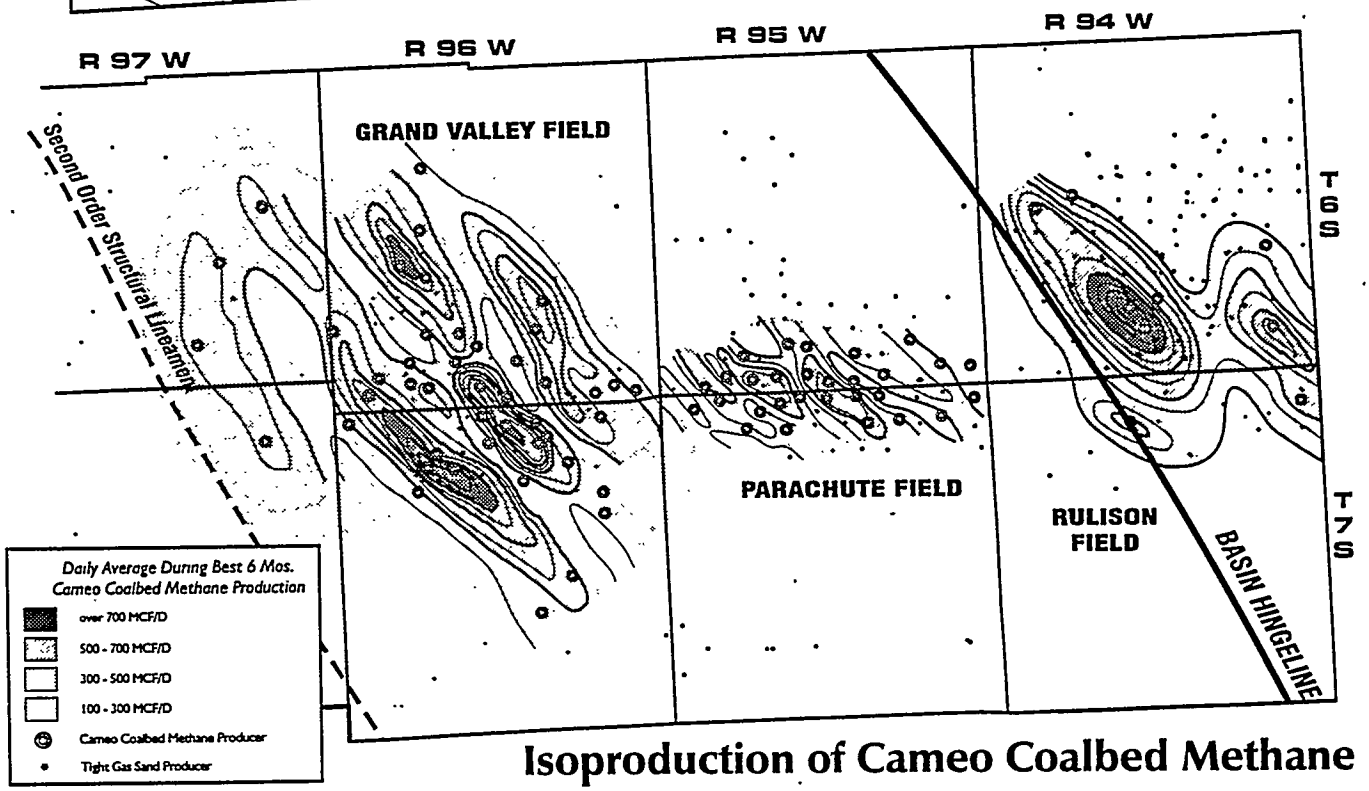


**Isoproduction of Cameo Coalbed Methane**

## 5A.4 Naturally Fractured Tight Gas Reservoirs Detection Optimization

### CONTRACT INFORMATION

| | |
|---|---|
| **Contract Number** | DE-RP21-93MC30086 |
| **Contractor** | Coleman Research Corporation<br>201 S. Orange Avenue, Suite 1300<br>Orlando, FL 32801 |
| **Other Funding Sources** | Louisiana Land and Exploration<br>Suite 1200, One Civic Center Plaza<br>1560 Broadway<br>Denver, CO 80202 |
| **Contractor Project Manager** | Dr. Pieter Hoekstra, Coleman Research |
| **Principal Investigators** | Dr. Heloise I. Lynn, Lynn Incorporated<br>Dr. C. Richard Bates, Coleman Research |
| **METC Project Manager** | Royal J. Watts |
| **Period of Performance** | June 1, 1994, to September 1, 1997 |

**Schedule and Milestones**

**FY94-95 Program Schedule**

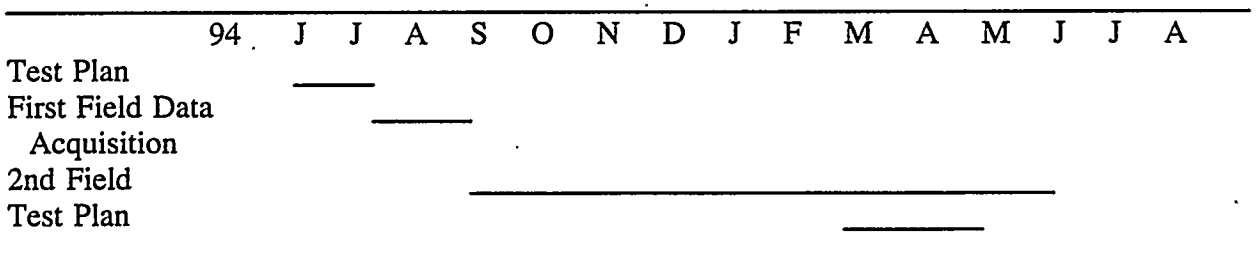


This contract is a joint project between METC and Louisiana Land and Exploration, planned to extend for 3 years. Substantial help and key information has been provided at the field by the owner/operator. All their well logs, cores, production data, geologic data, and geophysical data are available for study in this project. Their commitment in this technology development is demonstrated by their proposed contribution in the form of cost sharing: (1) obtaining the P-Wave (compressional wave) 3-D survey, (2) furnishing a borehole in which to acquire the

9-C vertical seismic profile (VSP), and (3) drilling and completing a test well for verification of the seismic anomaly. Also of significance is the direct involvement and participation of their professional staff. This staff has been responsible for generating and maintaining the database at the field and will form part of the team which evaluates the seismic data's findings.

## OBJECTIVES

The objective of the project is to determine optimum technologies for detecting fractures from which natural gas is produced in tight gas reservoirs. For the testing and evaluation of the technologies, a gas field in the Wind River Basin in central Wyoming was selected. In the field, gas is produced from naturally fractured reservoirs from 5,000 to 20,000 foot depths, although the target of this project is the Lower Fort Union, from 5,000 to 10,000 foot depths. The original seismic dataset is the owner/operators 3-D P-Wave survey. P-Wave anomalies associated with high fracture density and potential commercial gas pay will be surveyed using 3-D to 3-C in order to record the mode-converted shear wave arrivals. Shear waves carry more diagnostic and clear-cut information than P-Waves concerning the fracture density and the fracture orientation; however, multicomponent seismic data can cost 50 to 500 percent more to acquire and process than P-Wave (conventional) seismic data. Further testing of one of the seismic anomalies will be by the owner/operator drilling a well. Therefore, if fracturing associated with commercial pay can be detected using properly acquired and properly processed P-Wave data, the industry will be better able to apply seismic technology for drilling producers.

The seismic technologies to be evaluated and ranked for cost benefit are P-P (compressional-compressional) 3-D seismic, P-S (compressional-shear) 3-D seismic, and some S-S 2-D reflection seismic. P-Wave seismic is the widespread easily used technology commonly available in the oil and gas industry today; shear wave seismic reflection, or multicomponent reflection, is more expensive, more difficult to acquire and process, and not commonly used; however, because of its inherent characteristics, it provides more diagnostic information on fracture density and orientation. If most of the fracture information usually obtained through shear wave seismic can be demonstrated as obtainable from P-Wave seismic, through special acquisition and processing, then the lower cost, more robust tool would be the tool of choice.

## BACKGROUND INFORMATION

The structural setting is an east-west trending anticline, with the crest (7 miles by 3 miles) being slivered with many faults. Production in the Lower Fort Union is currently concentrated along the crest. Evidence that the natural fractures allow and control the gas production in the field is found in production history data, wireline data, and cores.

## PROJECT DESCRIPTION

Four avenues of investigation will be pursued and interlinked: (1) the seismic response to changes in relative fracture density, and/or changes in fracture orientation; (2) the evidence of the natural fractures, as found in wireline data, oriented core, production data, surface outcrops, and stratigraphic setting; (3) the in-situ stress field; and (4) the evidence of zones of enhanced permeability and fluid flow directionality within the Lower Fort Union,

on the scale of hundreds of meters in production data, DSTs, etc.

## RESULTS

To document the shear wave and P-Wave time-depth-velocity function, in order to guide the P-S interpretation of the data, a 9-C VSP was acquired in the Lower Fort Union in September 1994. Feasibility tests to show type of signal and noise contained in multicomponent surface seismic were acquired in July through August 1994, during the field operator's acquisition of a P-Wave 3-D surface seismic reflection survey. This 3-D P-Wave survey deployed circular geophone arrays, which provide the required azimuthally isotropic array response. The feasibility tests which recorded multicomponent receivers sourced by dynamite shots revealed P-S signal in the zone of interest (2 to 3.5 seconds), and deeper (to 4.5 seconds or 15,000 feet). Twelve 3-C phones per ground station recorded are needed in this field to acquire good shear wave data. A crossed dipole shear wave sonic log was also acquired in the VSP borehole, behind casing, in order to evaluate the shear wave birefringence (or anisotropy) at the wireline log scale and compare it to the gas kicks, lost circulation zones, and intervals of anisotropy observed in the VSP. The log documented an elevated amount of shear wave anisotropy, 15 percent, at the zone where at least 3,000 barrels of drilling fluid had been lost (at 9,200 to 9,215 feet). The orientation of the fast shear wave is not known, since the log was acquired behind casing.

To use P-Wave 3-D seismic for fracture detection involves analyzing two different source-receiver azimuths: parallel to the fractures and perpendicular to the fractures. At the field, the fractures are believed to trend east/west in the lower zones of interest. "Azimuth supergathers" from the 3-D data volume show P-P common-azimuth reflection data in 18 different azimuths from N to S, each with a range of offsets from 50 to 10,000 feet. An azimuth supergather is produced from a 1,980-foot by 1,980-foot bin in the subsurface. These plots indicate that the N/S stacking velocities are slower than the E/W stacking velocities which is consistent with the presence of E/W trending fractures. Moreover, the fast shear wave is polarized E/W in the 9-C VSP well, which would be consistent with a dominant E/W fracture set. The 5 azimuth supergathers also show that reflection coefficients, the amplitude variation with offset (AVO), and the attenuation are azimuth-dependent quantities. CDP lines excerpted from the P-Wave 3-D survey, in which E/W azimuths were segregated from N/S azimuths, also display what is seen in the azimuth gathers, and furthermore, indicate that in the locations of 4 azimuth supergathers, minimal dip is present. These observations lead us to conclude that specific azimuth-dependent 3-D data processing for the entire dataset and subsequent interpretation will yield a better understanding of the structure and the relative fracture density than conventional (azimuth-blind) processing.

## FUTURE WORK

To confirm that the P-Wave seismic is sensitive to fracture anisotropy, and to confirm that the cause of the identified P-Wave anomalies is due to high fracture density, shear wave seismic will also be acquired. The acquisition of 3-D dynamite-sourced three-component receiver data is scheduled for fall 1995 or spring 1996; shear wave vibrator sources will be tested on two 2-D lines in the 3-D survey.

Based upon the preliminary observations from the P-Wave 3-D data described above, we believe that azimuth-dependent processing of the 3-D data volume is necessary to properly process and understand this data volume. Moreover, azimuth-dependent processing is necessary in order to locate and identify, in space, all of the anomalies contained in the dataset. This processing will be done in March through July 1995.

# Session 6A

*Drilling, Completion, and Stimulation*

## 6A.1 Development of a Near-Bit MWD System

### CONTRACT INFORMATION

**Contract Number** DE-AC21-93MC29252

**Contractor**

Maurer Engineering Inc.
2916 West T.C. Jester
Houston, Texas 77018-7098
(713) 683-8227 (telephone)
(713) 683-6418 (telefax)

**Other Funding Sources** None

**Contractor Project Manager** William J. McDonald, Ph.D.

**Principal Investigators** William J. McDonald, Ph.D.
Gerard T. Pittard

**METC Project Manager** Al Yost

**Period of Performance** September 30, 1993 to August 30, 1995

**Schedule and Milestones:**

| TASKS | 0 | | | | | | | | | | | | FY95 | | | | | | | | | | | |
|---|---|---|---|---|---|---|---|---|---|---|---|---|---|---|---|---|---|---|---|---|---|---|---|---|
| | O | N | D | J | F | M | A | M | J | J | A | S | O | N | D | J | F | M | A | M | J | J | A | S |
| 1. Define System Requirements | x | x | m | | | | | | | | | | | | | | | | | | | | | |
| 2. System Electronic & Mechanical Designs | | | x | x | x | m | | | | | | | | | | | | | | | | | | |
| 3. Fabrication of Near-Bit MWD Prototype | | | | | | x | x | m | | | | | | | | | | | | | | | | |
| 4. Conduct Laboratory Performance Tests | | | | | | | | x | x | x | x | x | m | | | | | | | | | | | |
| 5. Phase 1 Final Report | | | | | | | | | | | | | x | x | m | | | | | | | | | |
| 6. Develop Commercial Sensor Suite | | | | | | | | | | | | | | | x | x | x | x | m | | | | | |
| 7. Shock & Vibration Testing | | | | | | | | | | | | | | | | | | x | x | x | m | | | |
| 8. Fabrication & Testing of Field Prototypes | | | | | | | | | | | | | | | | | | | | x | x | x | m | |
| 9. Implement Design Changes | | | | | | | | | | | | | | | | | | | | | | x | x | |
| 10. Phase 2 Final Report | | | | | | | | | | | | | | | | | | | | | | x | x | m |

## OBJECTIVES:

The project objective is to develop a measurements-while-drilling (MWD) module that provides real-time reports of drilling conditions at the bit. The module is to support multiple types of sensors and to sample and encode their outputs in digital form under microprocessor control. The assembled message is to be electromagnetically transmitted along the drill string back to its associated receiver located in a collar typically 50 - 100 feet above the bit. The receiver demodulates the transmitted message and passes it data to the third party wireline or MWD telemetry system for relay to the surface. The collar also houses the conventional MWD or wireline probe assembly.

The completed Phase 1 program began with the preparation of detailed performance specifications and ended with the design, fabrication and testing of a functioning prototype. The prototype was sized for operation with 6-3/4-inch multi-lobe mud motors due to the widespread use of this size motor in horizontal and directional drilling applications. The Phase 1 prototype provided inclination, temperature and pressure information.

The Phase 2 program objective is to expand the current sensor suite to include at least one type of formation evaluation measurement, such as formation resistivity or natural gamma ray. The Near-Bit system will be subjected to a vigorous series of shock and vibration tests followed by field testing to ensure it possesses the reliability and performance required for commercial success.

## BACKGROUND INFORMATION:

The Near-Bit MWD project was initiated following an unsolicit ed proposal submitted to the Department of Energy's Morgantown Energy Technology Center by Maurer Engineering Inc. and Guided Boring Systems, Inc. The proposed development effort addresses a significant opportunity to improve oil and gas extraction from underground formations as a result of more accurate and timely information of bottom-hole conditions being provided to personnel on the rig floor by the Near-Bit MWD technology.

The need for a Near-Bit MWD system is the direct result of the success of directional drilling in general, and horizontal drilling in particular, in increasing both production rates and ultimate recoveries in challenging formations and in mitigating production problems such as water coning and excessive sand production.

Correspondingly, as horizontal drilling technology has improved through evolution, the lengths of deviated sections have grown longer and the range of applications broadened. This has made the need for more accurate well placement more critical. The reliance on obtaining directional data and formation properties some 50 to 100 feet behind the bit becomes progressively less acceptable as turning radii decrease and target formations become thinner. This is because the impact of standoff distance, namely examining what has occurred instead of what is now transpiring at the bit, can result in missing thin targets, falling outside of productive seams or dipping into the water or gas cap. Necessary corrections may entail significant costs such as plugging back and redrilling the bottom portion of the hole. Combined inclination and formation data obtained directly at the bit eliminates these problems - allowing placement of the well to be optimized. Optimized well placement will in turn result in lower drilling and production costs. The R&D program therefore fits well with DOE's mission to improve the nation's oil and gas recoveries.


**Figure 1. Guidance Problems from MWD-to-Drill Bit Standoff**

## PROJECT DESCRIPTION:

The Phase 1 project first focused on establishing the performance and operating specifications of the Near-Bit MWD module. The environmental specifications were selected to satisfy the more strenuous loading conditions found at the drill bit while the sensor performance ratings were compared to those for existing commercial MWD and steering tool systems to assure they represented the current state-of-the-art. The industry's preference concerning the informational content and features the Near-Bit MWD system should possess were also tabulated and used to prioritize sensor development to assure inclusion of the most beneficial sensors first.

Interface protocols employed by various MWD and wireline steering tool manufacturers were identified and used to prepare the specifications of the receiver-to-host communications. As with the other specifications, they were thoroughly reviewed since they formed the basis for the follow on design activities.

The detailed design effort had the goal of producing a prototype unit which had the required form and functionality suitable for downhole operation. Design efforts were separated into mechanical and electronic elements.

The Near-Bit mechanical housings were designed to afford maximum protection to the electronics and downhole batteries. Several shock mounting and vibration damping techniques were evaluated along with alternative methods of PCB board fabrication and component options to provide reliable operation under the higher levels of loading that will be experienced from the system's placement in direct proximity to the drill bit. Substantial use of multi-chip modules, surface mount technologies and special stress bars were employed to extend the system's mean-time before failure.

Apart from the survivability of the Near-Bit module, the overall sub length was to be kept as small as possible to minimize the increase in bending moment on the Moineau motor bearing packs and its effect on steering response.

The mechanical housing was also designed to exceed the torque and overpull ratings of the drill motors with which they would be used. Flow areas were maximized to minimize pressure drops and support the passage of lost circulation materials.

The electric impedance properties of the drill string-earth-drilling fluid environment were bounded and applied to our understanding of EM signal propagation to define the most effect means of transmitting data from the bit sub to the drill collar containing the Near-Bit receiver.

The completed designs were then used to fabricate and assemble a complete Near-Bit MWD module plus one set of spare parts. The unit was then subjected to laboratory testing of its range under various simulated borehole environments and for its reliability under vibrational loads.

## RESULTS:

### Phase 1 Project (Complete)

Technical specifications of commercial MWD and wireline steering tools were examined in terms of sensor measurement accuracies, pressure and temperature ratings and operating life. The collected information was then used to establish the performance specifications of the prototype Near-Bit MWD sensor and support electronics. These specifications are listed in Table 1. Maximum overpull and torsional load carrying capacities of standard drill collar/mud motor combinations were then applied along with maximum borehole pressure

and temperature ratings to specify properties of the mechanical housings whose primary function is to provide protection to the electronics and to transmit/react drilling loads.

The above process resulted in the detailed design and fabrication of a 6-3/4-inch Near-Bit MWD prototype shown in Figures 2 - 5. Referring to Figures 2 and 3, the device operates as follows:

1. The control program residing in EEPROM of the downhole processor periodically collects the tri-axes accelerometer, temperature and pressure sensor data via its multiplexed A/D convertor. The operating software was prepared so that all aspects of the data collection process can be adjusted under operator control.

2. The collected sensor data along with the system status information is assembled by the microprocessor into a digitally formatted message string.

3. The message string is then digitally impressed onto the drill string using the high power transmitter circuit. The transmitter employs frequency shift key encoding and features a wide dynamic range from low, near-DC frequencies to frequencies in excess of 50 kHz. As with the message string length and content, the transmission trigger, message repetition and duration are fully programmable.

4. The transmitted message is received by the receiver-demodulator located in a standard drill collar placed up to 100 feet above the Near-Bit MWD sensor/transmitter sub. The receiver decodes the message and is designed to pass the data elements to a third party MWD or wireline host for integration and subsequent transmission to the surface. To maximize communication flexibility, the project team designed the Near-Bit MWD receiver to support data transfer to the host as either a fully buffered digital or analog message.

5. Operating power for the both the Near-Bit sensor/transmitter sub and the receiver are supplied by on-board battery packs. Rechargeable nickel-cadmium and lithium batteries are both supported depending upon the borehole temperatures to be encountered.

The Near-Bit MWD mechanical sub, shown in Figures 4 and 5, employs a coaxial design in which the sensors, electronics and batteries are mounted to a specially machined mandrel. The batteries are mounted on the inside of the mandrel while the sensor and support electronics are mounted on the mandrel's periphery. Proprietary shock mounts and full potting are employed to protect against possible damage during operation. The mandrel is keyed to the lower bit box assembly using two, high precision keys. This assures fixed orientation of the sensors on assembly. A steel pressure housing screws onto the bit box housing and provides a lower seal, This is followed by placement of a threaded cap on the top of the pressure which completes the pressure-tight seal of the electronics from the pressurized drilling fluid. Start up, reprogramming and battery charging can be accomplished by removing an access cap which covers a high pressure, multi-pin connector.

An outer housing is also threaded onto the lower bit box. Its function is as a mechanically robust member for transmitting loads between the drill motor and the drill bit. Inspection of the overall design shows that no drilling loads are directly carried by the instrumentation housing.

**Table 1. Preliminary Near-Bit MWD Specifications**

| | |
|---|---|
| **MECHANICAL** | |
| Sub Diameter | 6.750 Inches |
| Sub Length | 34 Inches Assembled |
| Flow Area | 7.85 Square Inches |
| Over Pull Capacity | >200,000 Lb |
| Pressure Rating | 15,000 psi |
| Material of Construction | 4140 CHT |
| Tool Joints | 41/2 API Reg. Pin x 41/2 API Reg. Box (down) |
| **SENSORY** | |
| Type of Sensor Data: | |
| Triaxial Acceleration | +/- 1g Range |
| Inclination | 0.1 Degrees Accuracy |
| Temperature | 125 Degrees C |
| Pressure | 15,000 psi |
| **COMMUNICATIONS** | |
| Telemetry | EM Frequency Shift Keying |
| Transmit Frequencies | Selectable |
| Baud Rate | Selectable |
| Transmission Trigger | Stop pumps (Stop Rotation) |
| Near-Bit to Conventional MWD Data Transfer | RS-232, Parallel and Analog Transfer |
| **OTHER** | |
| Power Source | Lithium or Ni-Cad Batteries |
| Operating Life | 200 Hours |
| Lost Circulation Materials | Pass |
| Retrieval | Overshot |

The drilling fluid exiting the motor travels through the annulus formed between the outside diameter of the inner pressure barrel and the inside diameter of the outer load bearing housing. The area of the annulus is almost 8 square inches - minimizing pressure drop across the sub.

## Prototype Testing

Following assembly and calibration, the Near-Bit prototype was subjected to a series of performance and reliability tests. The performance tests examined the ability of the EM telemetry link to transmit error free data across a 100 ft. Transmitter-to-Receiver separation distance. Tests were performed which simulated both mud- and air-drilled boreholes. In addition, several different methods of signal coupling were investigated; including direct and capacitive coupling.

Of the signal coupling methods investigated, direct signal coupling provided superior signal-to-noise ratios and worked in both borehole extremes. The tests further validated the performance of the automatic gain control circuit to prevent saturation in drilling environments which are only weak attenuators and to provide the required signal amplification in the other extreme of either highly attenuating mud-borehole combinations (low AC drive impedance.)

The Near-Bit sensors and electronics were also assessed on the ability of the prototype design to successfully withstand vibrations. The prototype was placed on a shake table and tested for 50 hours at a frequency of 5 hertz followed by 100 hours at 10 Hertz. The probe was fully powered throughout all these tests and the transmit trigger was deactivated in place of a sending a complete message once every 3 seconds. Data was received by the receiver which in turn periodically recorded the data to diskette. The message data was examined and the unit's pre- and post-test calibration constants examined for change.

The unit was also disassembled and visually inspected for damage upon completion of the 150 hour test cycle. No change in the calibration constants, fall off in performance or component damage were observed. While more strenuous testing will obviously be required in Phase 2, the results were quite promising.

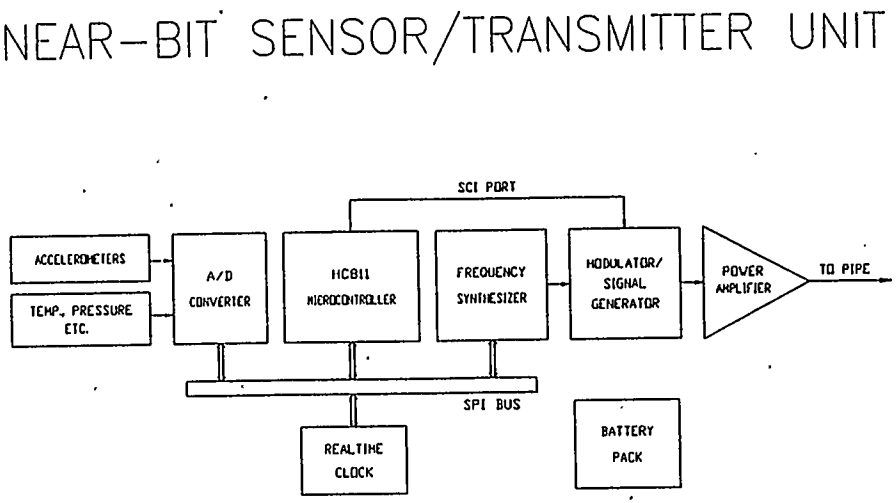


**Figure 2. Transmitter Block**

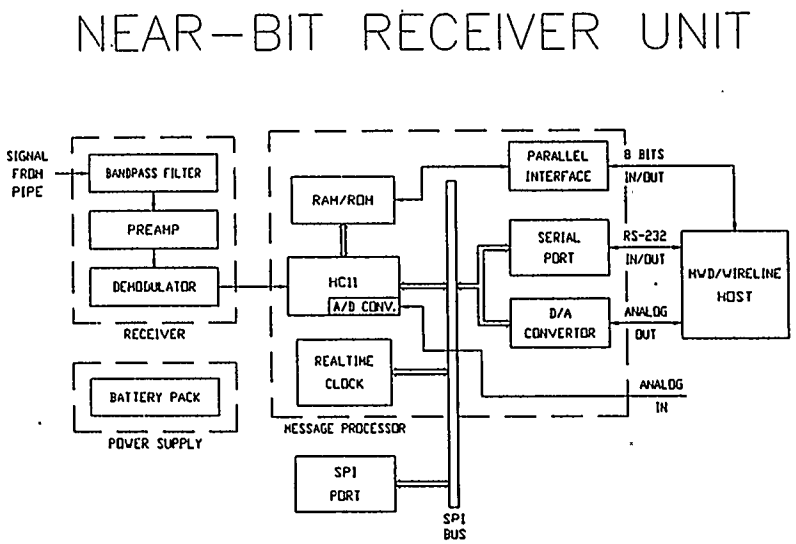


**Figure 3. Receiver Block Diagram**

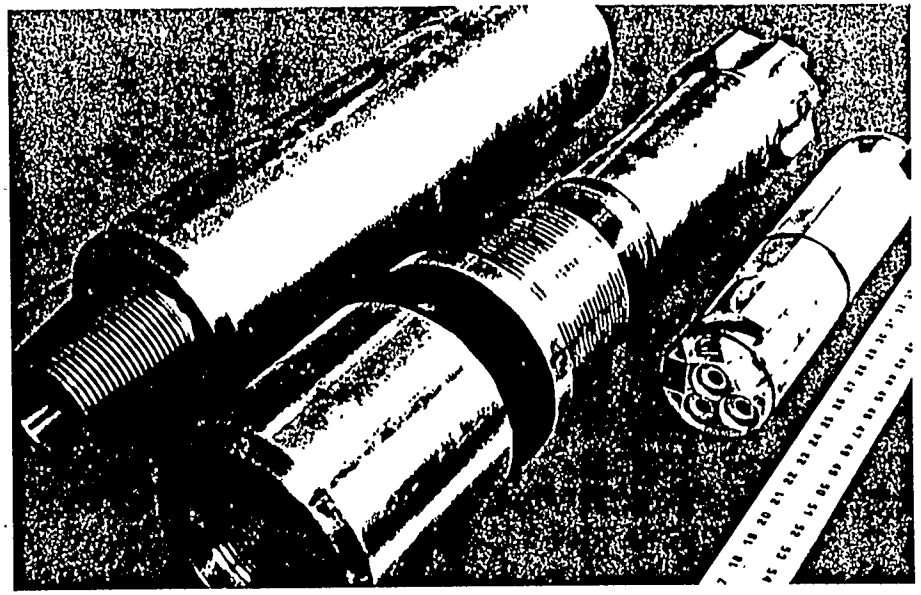

**Figure 4. Mechanical Components**

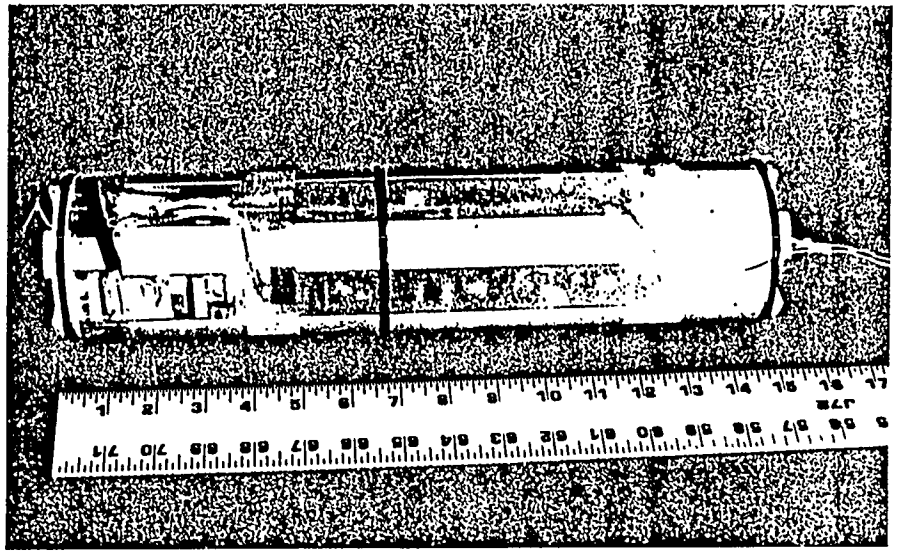

**Figure 5. Near-Bit Electronics Mandrel**

## FUTURE WORK:

The Phase 2 Near-Bit MWD project is currently in the first quarter of work. As such, a significant number of tasks remain to be completed.

The Near-Bit MWD receiver has been configured as a data recorder to enable rapid evaluation of the unit under actual well drilling conditions without the time and costs that would otherwise be required to integrate the Near-Bit MWD communications with a third party MWD or wireline probe. The fabrication of this board is now in progress. Once completed, the recording function will be validated in a test well with the transmitter in a non-drilling environment.

The current sensor suite will be expanded to include at least one type of formation property measurement. The research team is currently evaluating inclusion of either formation resistivity or natural gamma ray. A choice of sensor type must be made and incorporated into the existing design.

More strenuous vibration and shock tests must be conducted prior to field evaluation in order to identify design areas in need of improvement. These tests will pay particular consideration to the transverse loading since loading in this direction is a primary culprit in electronic component failures in downhole tools.

Upon completion of the above activities, the expanded Near-Bit MWD system will be evaluated for performance and reliability in at least two wells. The minimum reliability goal is a 100 hour MTBF.

Final design modifications necessary for commercialization will then be instituted based on the test results and the system offered to the market.

## REFERENCES:

McDonald, W.J., et al, "Borehole Telemetry Systems Key to Continuous Downhole Drilling Measurements," Oil and Gas Journal, September 15, 1995.

McDonald, W.J., et al, "AccuNav® - Remote Guidance Instrumentation for Directional Drilling, No-Dig Int'l Conference, Washington, D.C., April 20-24, 1992.

McDonald, W.J., et al, "Wireless Downhole Electromagnetic Data Transmission System and Method," U.S. Patent (Pending).

Pittard, G.T. and McDonald, W.J., "Development of Near-Bit MWD System," Proposal to DOE Morgantown Energy Technology Center, March 1992.

## 6A.2 Slim-Hole Measurement-While-Drilling (MWD) System for Underbalanced Drilling

(CONTRACT NO. 1 An MWD System for Air Drilling)
(CONTRACT NO. 2 A Slim-Hole MWD System for Underbalanced Drilling)

| CONTRACT INFORMATION | CONTRACT NO. 1 | CONTRACT NO 2 |
|---|---|---|
| **Contract Number:** | DE-AC21-88MC25105 | DE-AC21-94MC3 1196 |
| **Contractor:** | Geoscience Electronics Corporation<br>725-A Lakefield Road<br>Westlake Village, CA 91361 | |
| **Contractor Project Manager:** | William H. Harrison | |
| **Principal Investigators:** | William H. Harrison<br>James D. Harrison<br>Llewellyn A. Rubin | |
| **METC Project Manager:** | Albert B. Yost II | John R. Duda |
| **Period of Performance:** | Sept. 30, 1988<br>to May. 31, 1995 | Sept. 21, 1994<br>May 30, 1996 |

**Schedule and Milestones (Contract No. 2)**

**FY 1995 Program Schedule**

| | S | O | N | D | J | F | M | A | M | J | J | A |
|---|---|---|---|---|---|---|---|---|---|---|---|---|
| Task 1 Preliminary System Design | ---------- | | | | | | | | | | | |
| Task 2 Detailed Subsystem Design | | | | | | ---------- | | | | | | |
| Task 3 Fabrication | | | | | | | | | --------- | | | |
| Task 4 Laboratory Tests | | | | | | | | | | --------- | | |

## OBJECTIVES

The objective of both of these programs, the first of which is entitled "MEASUREMENT-WHILE-DRILLING (MWD) DEVELOPMENT FOR AIR DRILLING, " and the second of which is entitled, SLIM-HOLE MEASUREMENT-WHILE-DRILLING SYSTEM FOR UNDERBALANCED DRILLING, is to make commercially available, wireless MWD tools to reliably operate in air, air-mist, air-foam, and other underbalanced drilling environments during oil and gas directional drilling operations in conjunction with downhole motors and/or (other) bottom-hole assemblies. The application of this technology is required for drilling high angle (holes) and horizontal well drilling in low-pressure, water sensitive, tight gas formations that require use of underbalanced drilling fluids.

Contract No. 2 essentially picks up where the work, that was started in Contract No. 1 and furthered by GEC (under contract with Sperry-Sun Drilling Services) with the development of the Model 28, left off, to extend the capability of the technology to include slim-hole and use of a repeater to enhance performance. The end product will be Model 29 MWD System which will have specific features to satisfy the contract beyond those of the Model 28.

The specific objectives of Contract No. 2 include:

- A small diameter downhole instrumentation unit suitable for use in 6-1/4" well bores.
- A drill string repeater to facilitate higher data rates to greater depths.
- Retrievability of the Repeater Unit.
- Reliable operation in all formation types, drilling fluid media and well bore orientations.
- Compatibility with other steering, data acquisition equipment necessary to orient and steer, and to measure formation properties and drilling parameters.

The resultant Model 29 Slim-Hole MWD for underbalanced drilling will be designed to operate in air, air-mist, air-foam, nitrogenized water, and other fluids used in underbalanced drilling, and in standard muds. The Model 29 will be compatible with all oil and gas drilling scenarios, including: use of downhole motors, steerable assemblies, and other setups.

## BACKGROUND INFORMATION

Geoscience Electronics has been a supplier of EM-MWD Systems since 1980. Model 29 EM-MWD is the fifth generation of GEC's oilfield EM-MWD Systems. A synopsis of their evolutionary history starting with the initial involvement of the DOE is shown in Table 1.

1985 - The Model 20B was GEC's first oilfield EM-MWD System. It followed the Model 20A which was a converted "near surface" Model 10 EM-MWD used for drilling of boreholes under rivers and other natural and man made bodies. It under went a number of field tests in conventional mud drilling before being tried in an air drilled well under the control of DOE. The more severe air drilling environment caused mechanical failures.

**TABLE 1 History of GEC EM MWD Evolutionary Development**

| DATE | MODEL | PARTNER | PURPOSE | RESULT |
|---|---|---|---|---|
| 1985 | M20B | BDM | Prototype EM-MWD, Air Drilling Demo | Mechanical Failure |
| 1986-1988 | M20C | ARCO | Demo of Repeater Real Time Fraccing | Communication through Repeater to 9500 Feet in Casing |
| 1988-1992 | M27 | DOE | Customize for High Reliability Air Drilling and Field Test | Demonstrate Reliability Growth to > 100 Hrs. MTBF in 7 Field Tests |
| 1993 -1994 | M27 | SSDS | Evaluate in Horizontal / Under Balanced Scenarios | Viability Confirmed in 16 Field Tests |
| 1994→ | M28 | SSDS | Demo in Horizontal / Under Balanced with Repeater | Basic Functionality with Repeater Demo-ed to XXXX Meters in the 1st Field Test. |
| 1994-1995 | M29 | DOE / SSDS | Develop Slim-hole EM-MWD with Retrievable Repeater for Under-balanced drilling | Preliminary Design Completed |

**1986 - 1988 -** The Model 20C evolved from the Model 20B. Certain improvements were made to enhance performance and improve reliability. These improvements were not aimed specifically at air drilling performance. Even though the Model 20C was designed specifically as an EM-MWD System, its most important accomplishments were in an ARCO program associated with collecting real-time data in open casing fraccing. It was here that the viability of operating with an "In-Drill String Repeater" was demonstrated.

**1988 - 1992 -** In cooperation with the DOE, the Model 20C was evolved to become the Model 27, the first EM-MWD specifically for air-drilling. Over this period, the Model 27 was field tested in 7 different air drilled wells. It under went a continual improvement in demonstrated reliability as failures exposed weak aspects of the system. At the completion of the test series, the Model 27's Mean-Time-Between-Failure (MTBF) was in excess of the target goal of 100 hours.

**1993 - 1994 -** In cooperation with Sperry-Sun Drilling Systems (SSDS), the Model 27 was further tested in directionally drilled wells in Canada. A total of 16 field tests were performed in wells including horizontal / under-balanced scenarios using nitrogenizes water drilling fluid. Data was successfully communicated from depths of up to 2000 meters.

**1994 - 1995** - In cooperation with SSDS, the Model 28 was developed. The primary advances over the Model 27 were improved Downhole Antennae designs and the addition of a Downhole Repeater Unit (DRU). The functionality of the Model 28 operating with it Downhole Repeater Unit was recently demonstrated to 2147 meters in its initial field test.

**1994 - 1995** - In cooperation with DOE, the "Slim-Hole MWD System for Underbalanced Drilling" program was undertaken. The objective of the program is to upgrade the Model 28 EM-MWD design by adding specific features and to test it. The modified tool design is known as the Model 29 EM-MWD System. As with the Model 28, it is intended to operate in an air, air-mist, air-foam, nitrogenized mud or other under-balanced environment during oil and gas directional drilling operations in conjunction with downhole motors and/or (other) bottom-hole assemblies.

ORIGINAL CONTRACT

Under Contract No. 1, (DE-AC21-88MC25105, a new tool, the Model 27 was developed and four field tests were conducted in the Appalachian areas in the time frame October through December 1989.

Field Test No. 5 (Phase III) was conducted from 12/6/90 to 12/14/90, near Fairmont, WV. While on the whole, the results were very good and all test goals were successfully met, an unfortunate twistoff of the 6-1/4-inch transducer occurred.

Field Test No. 6 was conducted in Barbour County, West Virginia in air in October, 1992. This was the most successful complete-hole test to date, and improved the MTBF to just under 100 hours.

In June of 1993, Field Test No. 7 was conducted, using the 4-3/4-inch transducer for the first time, in air-mist at a site near Pratt, Kansas. The Model 27 tool was able to operate at the start of the build section, but because of the lack of spare units, was unable to commit to the balance of the hole when sticky conditions persisted.

Phase V of Contract No. 1 was authorized to provide a special version of Model 27 for use behind a steerable air hammer. This phase is scheduled to end in May, 1995.

The Model 27 was tested in 16 additional wells, including underbalanced wells, utilizing nitrogenized water, in Canada, from April 1993 through October, 1994. These tests were not an official part of the DOE Contract. The purpose of these test were to gain experience in the capabilities and limits of the EM-MWD in conjunction with the development of the Model 28 MWD. The Model 28 overcomes certain known problems plus adds a Downhole Repeater System.

## MODEL 29 PROJECT DESCRIPTION

### DESIGN CONSTRAINTS

The preliminary system design task for the Model 29, was initiated with the following ground rules and constraints in effect:

- The current Model 28 Downhole Subsystem is believed to partially satisfy the Model 29 requirements. It does not provide a widened-gap or flexible power amplifier capability, essential to the requirement for better wide-range impedance-matching.

- The Antenna Subsystem for the Downhole Repeater Unit (DRU) must accommodate the requirement of retrievability of the DRU as well as widened-gap capability. A modified version of the Model 28 antenna will be used as the basis of the design for the Model 29 antennas.

- The current SSDS DEP-1, Integrated Sensor Stack appears to satisfy the basic functions needed in the Model 29 DTU and may be used with minimum software modifications.

- The above DEP-1, does not satisfy the need for the Central Processor Unit (CPU). GEC will design a unit that satisfies the basic functions needed in the Model 29.

- The Downhole Power Amplifier will need to be modified to accommodate the wide-range impedance-matching requirement.

- The functional requirements of the surface system to reliably receive the DTU/DRU transmission over a wide range of formations, depths and operating conditions will likely require the use of site-generated noise reduction techniques. Optimum implementation of such a surface subsystem is viewed as an Up hole Terminal Unit (UTU) that consist of a 486-based IBM compatible Personal Computer that contains certain commercially available "add-in" circuit cards.

- The functional requirements of the surface system also require an external Signal Preprocessor Unit (SPU). The SPU provides the interface to the Surface Antenna(e) and to the sensors associated with noise reduction. This is envisioned as a unit having 8 to 16 low level, limited bandwidth input channels. The sensitivity of the unit would be dynamically controlled by the PC. This unit may also contain the Down Link Power Amplifier which would be under control of the PC.

### KEY FEATURES OF THE MODEL 29

The Model 29 consists of three primary units: 1) Downhole Terminal Unit (DTU), which contains the directional sensor suite, 2) Retrievable Downhole Repeater Unit, and 3) the Surface System, which consists of the Barrier Box, Uphole Terminal Unit, and PC LapTop Computer. The key features contained within the Model 29 are delineated below.

**TABLE 2 Key Features of the Model 29 EM-MWD**

- SSDS SENSOR PACKAGE (DEP1)
  - DIGITAL INTERFACE
  - ON-BOARD CALIBRATION
- REPEATER
  - INCREASED DATA RATE
  - INCREASED DEPTH
  - RETRIEVABLE
- DOWNHOLE ANTENNA
  - IMPROVED COMMUNICATION
  - MECHANICAL STRENGTH
  - CORROSION RESISTANT
- PRESSURE CASES
  - REPLACEABLE MODULES
  - REPLACEABLE CENTRALIZERS
  - IMPROVED MECHANICAL INTERFACES
  - IMPROVED ELECTRICAL INTERFACES
  - IMPROVED MAINTAINABILITY AND TRANSPORTABILITY
- NARROW PRINTED CIRCUITS BOARDS
  - DIGITAL PROCESSOR
  - DOWNLINK RECEIVER
  - POWER AMP
  - 130° C OPERATION
- MODERN DIGITAL PROCESSOR
  - DOWN LOADABLE PROGRAMS
  - SOLID GROWTH PATH
- POWER AMPLIFIER
  - WIDE FORMATION IMPEDANCE MATCHING
  - INCREASED EFFICIENCY
- SURFACE SUBSYSTEM
  - MULTI CHANNEL SIGNAL PROCESSOR UNIT (SPU)
  - 486 PC BASED UPHOLE TERMINAL UNIT (UTU)
  - IMPROVED NOISE REDUCTION

The Model 29 System uses a rugged and compact LapTop PC as the Uphole Terminal Unit computer.
Additionally, the PC furnishes both input and output devices. The internal software generates "screens" for each phase of the system operation.

One of the important screens is the one shown in Figure 1.This screen results from the command for a single survey, while using the repeater. All of the important system status readings and the actual survey data are presented. Following this "screen," the operator inputs the length of the joint(s) added since the last survey.

```
TIME: 22:31  BIT     0.00  SURVEY  10:2

         Survey # 10 Received                    X         Y         Z         TOTAL
                                               G  -.1997     .9783     .0052     .9985
   Gtotal    Btotal     HSG.       MagDip      B-41.4871   33.2945  -11.7021   54.4669
     .9985   54.4669  348.4607    48.6039
                                               AZI 109.3  INC 89.7  DIP 48.60   C 27.7
Survey # 10                        Time 22:31
ANGLE DATA        WAS     CHANGE     NOW       POWER AMP    UTU       DRU       DTU
                                               LEVEL R-X    36-24     3-3       2-2
 INCLINATION      89.70      0.00     89.70    VOLTAGE       2.199     0.78       .151v
 TOOLFACE        348.46      0.00    348.46    CURRENT        .165     3.7       2.564a
 AZIMUTH         109.32      0.00    109.32    POWER .        .363     2.8        .386w
                                               IMPEDENCE    13.327    0.21       .059o
                                               BATTERY      16.8      20.0      14.6
 DTU Checksum Status:   . 0                    AD590          -       43.0      24.6C
 DRU Checksum Status      0
                                               D/L Logdac   OUT        1.6       1.791V
 Press [C] to continue or [ESC] to dump
                                               CHANNEL 12        ATTN 36.0     SEN# 2011
```

**Figure 1. Initial Survey Angles Display**

In addition to the "single survey" mode of operation, the M29 System is capable of operation in the "Continuous Tool-Face" (CTF) mode. In this mode, upon reception of an appropriate downlink command, the Downhole Terminal Unit (DTU) transmits continuous tool-face updates until commanded to cease. The "screen" in this case is, as shown in Figure 2.

```
HIGHSIDE CTF        TIME        DATE

 #  14      10.0      1:03:06   03-03-95
 #  15      56.6      1:09:16   03-03-95
 #  16      66.1      1:15:25   03-03-95
 #  17      76.3      1:21:35   03-03-95
 #  18      88.8      1:27:45   03-03-95
 #  19      90.3      1:33:55   03-03-95
 #  20      92.7      1:40:05   03-03-95
 #  21      93.2      1:46:15   03-03-95
 #  22      95.3      1:51:25   03-03-95
 #  23      95.4      1:57:35   03-03-95
```

**Figure 2. CTF Display Format**

## RESULTS

Phase I, Task 1 Preliminary System Design - Overview

GEC has completed the preliminary system design of the Slimhole ElectroMagnetic (EM)-based MWD system. The system includes, but is not limited to the following components: downhole instrumentation unit, including power pack, sensors, etc.; in line retrievable two-way repeater unit; site-generated-noise-reduction unit; and surface processing units.

GEC performed detailed calculations and analyses to provide a sound basis for successful design of the system, including appropriate safety factors. The effort has ensured that the slimhole EM MWD system is compatible with other drilling products, and that the tool housing and connections (end details) conform with API/IADC recommendations for strength and fishability.

The design effort considered the downhole environment in which the commercial system is to operate. Aspects of that environment include, but are not limited to, downhole mechanical forces, pressures to 10,000 psi, and a sustained operating temperature of 130°C.

Other design aspects that were considered include:

- Small diameter downhole instrumentation (for use with widely available slimhole (maximum well bore diameter of 6-1/4 inches) tubulars, and other slimhole drilling equipment; multiple housings (subs) may be required to accommodate various drill string designs for slimhole drilling,

- A drill string repeater(s) addition to facilitate higher data transmission rates to greater depths. compared to conventional EM-based MWD equipment,

- Reliability in all formation types, drilling fluid media,

- Retrievability of the downhole repeater unit,

- Compatibility with other steering, data acquisition equipment necessary to orient and steer, and to measure formation properties and drilling parameters.

Engineering/fabrication drawings resulting from Task 1 (Preliminary System Design) have been prepared and cross-checked. At the end of February, 1995, GEC submitted the documented, preliminary design package for the slimhole EM-MWD system to the DOE COR for review and comment.

Detailed Summary of TASK 1 SubTask Progress

SubTask 1. Preliminary design the Model 29 DTU and DRU-Retrievable Antennas and Pressure Barrel interface. This sub task has been completed, and Task 2 work is underway.

SubTask 2. Analyze the existing SSDS Micro Processor PCB (μP) design to assure that it has the potential to perform the Model 29 CPU mission. SSDS has submitted the background documentation, and everything has been accomplished.

SubTask 3. Modify the existing (μP) design to add the functionality required to perform the EM signal processing and transmitter/receiver control. Make any other modifications required to allow the μP to operate independently of the existing SSDS sensor stack. Define the digital interface between the CPU and DEP. This effort is now complete, and documented.

SubTask 4. Convert the existing Model 28 DTU/DRU software to execute on the new μP. Integrate/merge the existing DEP-1 sensor sampling, sensor error compensation, and survey calculations with the EM software to create The Model 29 DTU/DRU software. The new software specification is now complete.

SubTask 5. Package and/or integrate the DEP-1 and CPU, with the remainder of the DTU and DRU subassemblies. This subtask is complete and documented.

SubTask 6. Modify the Model 28 Downhole Power Amplifier design to meet the wide-range impedance-matching requirements of all underbalanced drilling. The trade off study has been done, but the sub task is not complete due to lack of field data from early M28 testing.

SubTask 7. Instrument several operational drilling sites using a wide dynamic range digital recording system combined with appropriate ElectroMagnetic sensors. Record the signal/noise measured by the sensors. Analyze the data to determine the characteristics of the signal/noise and develop noise reduction strategies. This sub task likewise is delayed due to the late M28 deliveries.

SubTask 8. Design the Uphole Terminal Unit (UTU). Work has proceeded up to the point where the PC and add-in card requirements have been specified.

SubTask 9. Design the Signal Processing Unit (SPU). A preliminary specification has been prepared.

SubTask 10. Convert the existing Model 28 and other surface software to perform the Model 29 UTU functions. Develop new software, and integrate it with the basic UTU software. The architecture is complete. Detailed software codes are now being developed, as scheduled, in Task 2.

Results to Date

Although it has taken an additional month beyond that scheduled, GEC/SSDS completed essentially all of the required preliminary system design sub tasks required in Task 1, Phase I.

Some of the work was further deferred due to the late delivery of the Model 28 Systems, to the field for initial test and evaluation. This has impacted the noise reduction, and power amplifier preliminary design effort. However, GEC/SSDS intend to expend additional effort to catch up with these delayed sub tasks during the next few months.

## FUTURE WORK

GEC and SSDS are continuing the program by commencing Task 2 effort. The primary activities of Task 2 will be detailed design of:

- the new CPU,
- the revised UTU,
- the SPU, and
- the retrievable repeater and its antenna sub.

In addition, GEC/SSDS will, as part of the M28 field test and evaluation program:

- evaluate options for enhancing power-amplifier impedance-matching performance, and complete the detailed design of the candidate approach,
- continue software development, and
- gather noise data (not part of the M29 program),

Finally, GEC/SSDS will prepare the M29 Laboratory Test Plan, and submit it to the DOE COR.

# Session 2B

## *Natural Gas Upgrading — Gas-to-Liquids Conversion*

## 2B.1 Catalytic Conversion of Light Alkanes—Proof of Concept Stage

### CONTRACT INFORMATION

| | |
|---|---|
| Contract Number | DE-FC21-90MC26029 |
| Contractor | Sun Company, Inc.<br>Research and Development Department<br>P.O. Box 1135<br>Marcus Hook, PA 19061<br>(610) 859-1731 |
| Contractor Business Manager | Allen W. Hancock |
| Principal Investigator | James E. Lyons |
| METC Project Manager | Rodney D. Malone |
| Period of Performance | November 1, 1993 to October 31, 1994 |
| Schedule and Milestones | |

N D J F M A M J J A S O

Phase 1V $C_1$-$C_4$ Research
- Synthesize 2nd Generation Cat. ---(complete)
- Design and Synth. 3rd Gen. Cat. ----------(complete)
- Test 2nd and 3rd Gen. Cat. for $C_1$-$C_4$ activity ----------(complete)

Phase V Process Dev. i-$C_4$ -->TBA
- Determine Commercial Targets ----------(complete)
- Achieve for One-Step Route ----------
- Achieve for Two-Step Route ----------(complete)

Phase VI $C_1$-$C_3$ Research
- Modify 3rd Gen. Cat for $C_3$ _____
- Test 3rd Gen. Cat for $C_3$ ox ____
- Design More Active Catalyst _____
- Synthesize Family of MAC's _____

## OBJECTIVES

The objective of the work presented in this paper is to develop new, efficient catalysts for the selective transformation of the light alkanes in natural gas to alcohols for use as liquid transportation fuels, fuel precursors and chemical products. There currently exists no direct catalytic air-oxidation process to convert these substrates to alcohols. Such a one-step route would represent superior useful technology for the utilization of natural gas and similar refinery-derived light hydrocarbon streams. Processes for converting natural gas or its components (methane, ethane, propane and the butanes) to alcohols for use as motor fuels, fuel additives or fuel precursors would not only add a valuable alternative to crude oil but would produce a clean-burning, high octane oxygenate which would be a major component of reformulated gasoline (RFG).

## BACKGROUND INFORMATION

Natural gas is an abundant resource that can provide an inexpensive feedstock for production of $C_1$-$C_4$ alcohols. The low molecular weight alcohols, methanol, ethanol, isopropyl alcohol and tert-butyl alcohol have seen application both as alternative fuels and in reformulated gasoline. The ethers that are made from these alcohols: methyl-tert-butyl ether, MTBE, ethyl-tert-butyl ether, ETBE, diisopropyl ether,DIPE, and tert-amyl methyl ether, TAME, are major oxygenate components of RFG. These oxygenates have high blending value octane numbers, BVON, and good gasoline properties. Of these, MTBE has seen the most widespread use and the most rapid growth in RFG.

Working with ideas generated from recent understanding of biological systems responsible for enzymatic oxidations, Sun has developed a number of new catalyst systems for the direct oxidation of light alkanes to alcohol-rich oxygenate mixtures (1-40). The relative ease of oxidation of natural gas components with our catalyst systems has been found to be: isobutane>propane> ethane>methane. For this reason, the first oxidation reaction to reach the proof-of-concept stage was the oxidation of isobutane to TBA. TBA has been used as a high-octane fuel component and is the major precursor to MTBE. MTBE has excellent fuel properties. Among these are the apparent reduction of CO emissions from automotive exhaust. MTBE is currently the oxygenate of choice for RFG.

Field butanes have historically found a large number of liquid fuel precursor applications. Traditionally, this $C_4$ component was blended into gasoline for octane and vapor pressure. Light hydrocarbons, however, whether from natural gas or petroleum refining are rejected in large part from the gasoline pool in response to environmental regulations of vapor pressure emissions. After isomerization, the isobutane can be dehydrogenated to isobutylene which is a precursor to alkylate and MTBE - both high octane, clean-burning RFG components. Dehydrogenation is costly, however. Direct oxidation of isobutane to TBA is a way to avoid this expensive process step. The TBA produced is a viable high octane fuel oxygenate and a precursor to MTBE as well. Sun catalytic technology, therefore is able to convert a $C_4$ stream into a fuel oxygenate without requiring a costly dehydrogenation step.

Thus, in summary, the direct reaction of a light alkane with air or oxygen to give an alcohol-rich oxidate would: a) utilize an inexpensive feedstock unacceptable for liquid transportation fuel use, b) produce a material that would have superior gasoline performance properties such as driveability and high octane, and c) produce a clean-burning

alternative to conventional gasoline for use in areas that fail to meet air quality standards.

## PROJECT DESCRIPTION

During the stage at which this work ended, our program consisted of two phases which were running concurrently, a research phase and a proof-of-concept phase. The function of the research phase is to design synthesize and perform laboratory tests on new materials in order to enhance the catalytic properties of the suprabiotic systems generated in our laboratories. Increases in catalytic activity and process selectivity as well as extensions of structure-activity relationships are examined. The research phase is intended to provide the process development phases with catalysts having superior properties for light alkane oxidation. The second concurrent phase, is the proof-of-concept phase. In this phase process development of oxidations which have succeeded in the research phase are carried out in a pre-pilot PDU. At the conclusion of the cooperative agreement we were developing a process for the conversion of isobutane to TBA. We have identified two routes for this transformation: a one-step route directly from isobutane to TBA, and a two-step route in which the isobutane is oxidized first to tert-butyl hydroperoxide and then transformed into TBA catalytically. This paper will present the results of these activities.

## RESULTS

One Step Oxidation of Isobutane to TBA. There are currently no efficient catalysts for the direct oxidation of isobutane to TBA, eq. 1. Cobalt salts and complexes have been used

$$i\text{-}C_4H_{10} + 1/2\ O_2 \rightarrow t\text{-}C_4H_9OH \quad (1)$$

(41) but in order to achieve good rates, high catalyst concentrations are needed as well as high temperature. Under these conditions poor selectivity is achieved. In the research phase of our work we have designed, synthesized, and tested a family of metal complexes that are very effective catalysts for the selective low temperature oxidation of isobutane to TBA. These catalysts, the perhaloporphyrinatometal complexes, were designed based on biomimetic considerations. The halogen ligands on the periphery of the porphyrin ring withdraw electrons from the metal center, increase the M(III)/M(II) reduction potential and enhance the alkane oxidation activity. We have further shown that iron perhaloporphyrins have the greatest activity of any of the metalloporphyrins studied. Figure 1 shows that as the degree of electron withdrawal (number of halogens on the porphyrin macrocycle) increases, the reduction potential of a series of iron porphyrin complexes increases and the activity of the catalysts steadily increases. Table 1 shows that these perhaloporphyrin catalysts are effective soluble catalysts in neat isobutane and give unprecedented rates and selectivities for converting isobutane to TBA.

The same iron perhaloporphyrin complexes that were found to be effective for the direct oxidation of isobutane to TBA were also shown to be excellent catalysts for the decomposition of t-butylhydroperoxide, TBHP, to TBA, Figure 2, Table 2. Again, perhaloporphyrin complexes were over an order of magnitude more active than previously known catalysts. The same relationship was found between Fe(III)/Fe(II) reduction potential as in the direct oxidation reaction, Table 3. Since TBHP is made commercially by non-catalytic oxidation of isobutane (42), our work suggested the possibility of a competitive two-step route from isobutane to TBA, eq. 2, 3.

**Figure 1. Catalyst Activity vs. Redox Potential**

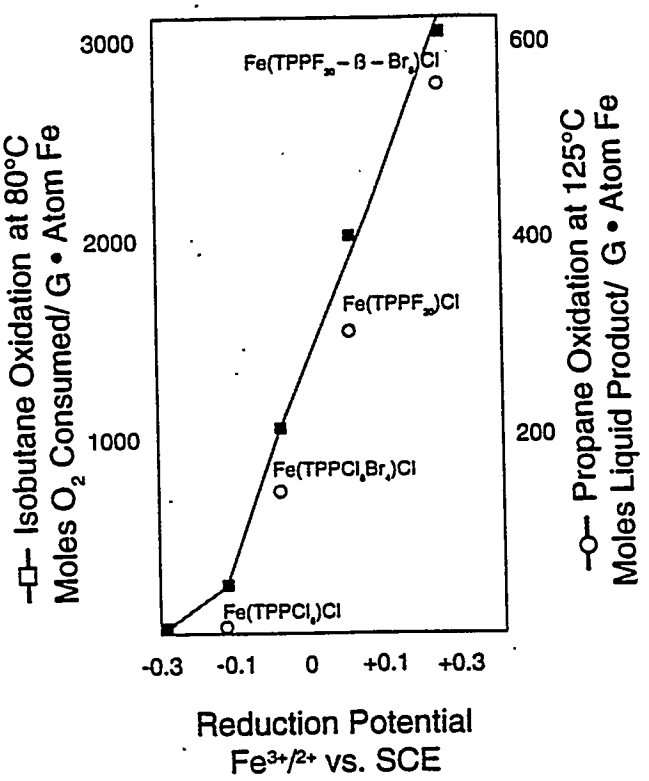


**Figure 2. TBA from TBHP**

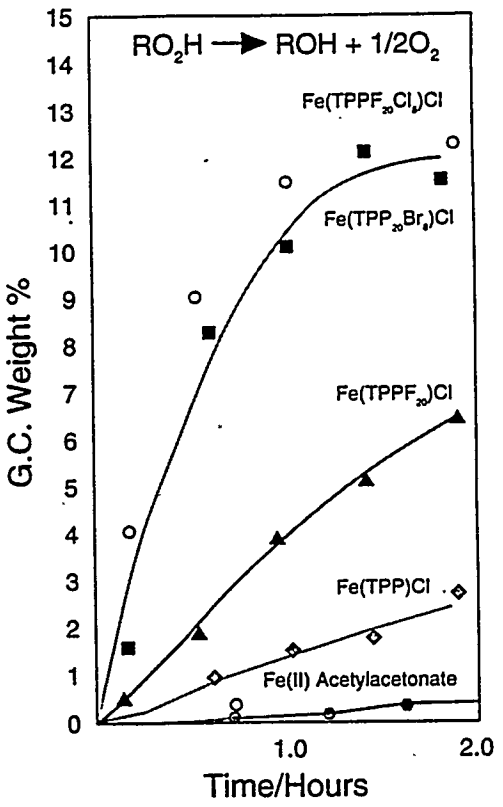


**Table 1. Iron Haloporphyrin - Catalyzed Isobutane Oxidation**

| | | | Charge to Reactor | | Conversion | Select | |
|---|---|---|---|---|---|---|---|
| Catalyst | T. °C | T. Hrs | *i*-$C_4H_{10}$ | $O_2$ | *i*-$C_4H_{10}$ % | TBA %[b] | TON[c] |
| Fe(TPPF$_{20}$β-Br$_8$)Cl | 80 | 3 | 1870 | 53 | 17 | 87 | 10,660 |
| | 80 | 3 | 1862 | 100 | 28 | 83 | 17,150 |
| | 80 | 3 | 1865 | 47 | 14 | 91 | 8,420 |
| | 25 | 71.5 | 1862 | 53 | 22 | 92 | 13,560 |
| Fe(TPPF$_{20}$)OH | 24 | 143 | 1871 | 53 | 18 | 95 | 12,150 |

[a] Isobutane oxidized by an oxygen - containing gas (75 ATM, diluent = $N_2$), liq. phase (180 ml), 3 hours. $O_2$ added as used
[b] (Moles TBA/molls liquid product) x 100
[c] Models (TBA + acetone) produced/mole catalyst used

## Table 2. Conversion of TBHP to TBA

| Catalyst | Time Hours | t-$BuO_2H$ Conv., % | Product, Molar Sel., % t-BuOH | $(t\text{-}BuO)_2$ | $(CH_3)_2CO$ |
|---|---|---|---|---|---|
| $Fe(ACAC)_3$ | 2.3 | <5 | 67 | tr | 32 |
| Fe(TPP)Cl | 1.9 | 27 | 82 | 7 | 11 |
| $Fe(TPPF_{20})Cl$ | 3.3 | 72 | 87 | 10 | 3 |
| $Fe(TPPF_{20}\beta\text{-}Br_8)Cl$ | 1.9 | 95 | 90 | 8 | 2 |
| $Fe(TPPF_{20}\beta\text{-}Cl_8)Cl$ | 3.3 | 100 | 90 | 8 | 2 |

[a] The catalyst, 2 x $10^{-4}$ mmoles, in 2.4 ml p-xylene was rapidly added to a stirred solution of 10 ml t-$BuO_2H$ (90%) in 48 mls benzene. $O_2$ evolved was measured manometrically and liquid samples taken periodically and analyzed by standardized gc

## Table 3. Electron Affinity Reduction Potential and Catalytic Activity

| Species | EA (eV) | $E_{1/2}$ (V) vs. SCE | TO $iC_4$-ox[a] | TBA Yield[b] TBHP-dec |
|---|---|---|---|---|
| Fe(TPP)Cl | 2.15 | -.29 | 0 | 4.8 |
| $Fe(TPPF_{20})Cl$ | 3.14 | +.08 | 1160 | 16.0 |
| $Fe(TPPF_{20}\beta Cl_8)Cl$ | 3.35 | +.29 | 1800 | 67.2 |

[a] Moles $O_2$ taken up in 60°C oxidations of isobutane after 6 hours
[b] Yield of TBA from TBHP decomposition in 0.5 hours

$$i\text{-}C_4H_{10} + O_2 \text{ ---> } t\text{-}C_4H_9OOH \qquad (2)$$

$$t\text{-}C_4H_9OOH \text{ ---> } t\text{-}C_4H_9OH \qquad (3)$$

Since both of these reactions work so well, we determined to proceed with evaluating the concept of potentially commercial routes from isobutane to TBA using both the one-step and the two-step processes. Together with a joint R&D partner we set proprietary hypothetical commercial targets for each process. The concept was proven, therefore, if our catalytic processes met these criteria. We first examined the direct one-step oxidation route. Our process concept is shown schematically in Figure 3. Using our best perhaloporphyrin complex as a catalyst we met all targets except that of catalyst cost. Efforts using new catalysts with lower costs failed to meet rate and selectivity targets. Efforts to lower the cost of manufacture of the

## Figure 3. Isobutane Oxidation - One Step Process

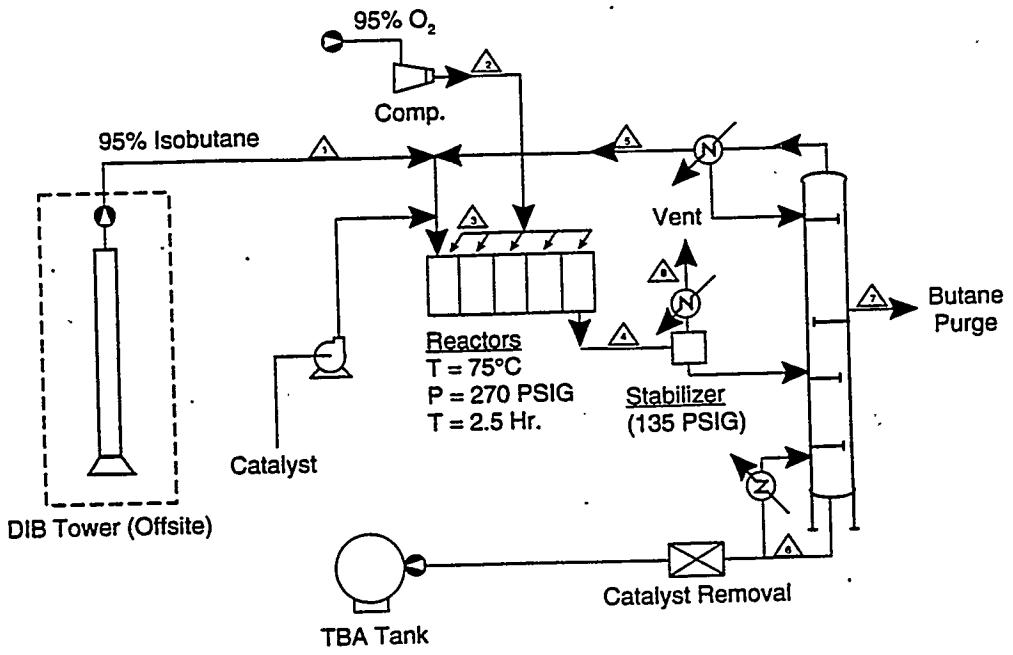


perhaloporphyrin complexes failed to achieve costs that were even close to what was needed. When the project ended we had found a way to make the inexpensive, first row metals including iron, far more active for oxidation of an alkane, than had ever been observed. How to do this with a low-cost ligand system is the one remaining technical problem with the one-step route.

Figure 4 shows a schematic flow diagram of the proposed two step process for manufacture of TBA. Catalyst cost again was a problem for the iron perhaloporphyrins. In this case, however we were able to find proprietary new catalyst systems that met the catalyst cost criterion. At the conclusion of the cooperative agreement we had met or exceeded all of the performance criteria for a two-step process. Table 4 summarizes our progress vs goals up until the end of the project in October, 1994.

## CONCLUSIONS

During the period of the cooperative agreement we have uncovered a family of catalysts which have shown unprecedented activity for the oxidation of alkanes to alcohol-rich oxidates. These catalysts have a ligand system which confers unusually high oxidation activity to inexpensive first row transition metals, especially iron. If less expensive analogs can be produced, they should ultimately have great practical value in converting natural gas components to fuel oxygenates. Isobutane can be converted to TBA in excellent selectivity at acceptable rates for a practical process if catalyst cost can be lowered. In the case of the conversion of isobutane to TBA we have found a two step route through the hydroperoxide that could have value in a retrofit of an existing plant.

## Figure 4. Isobutane Oxidation - Two Step Process

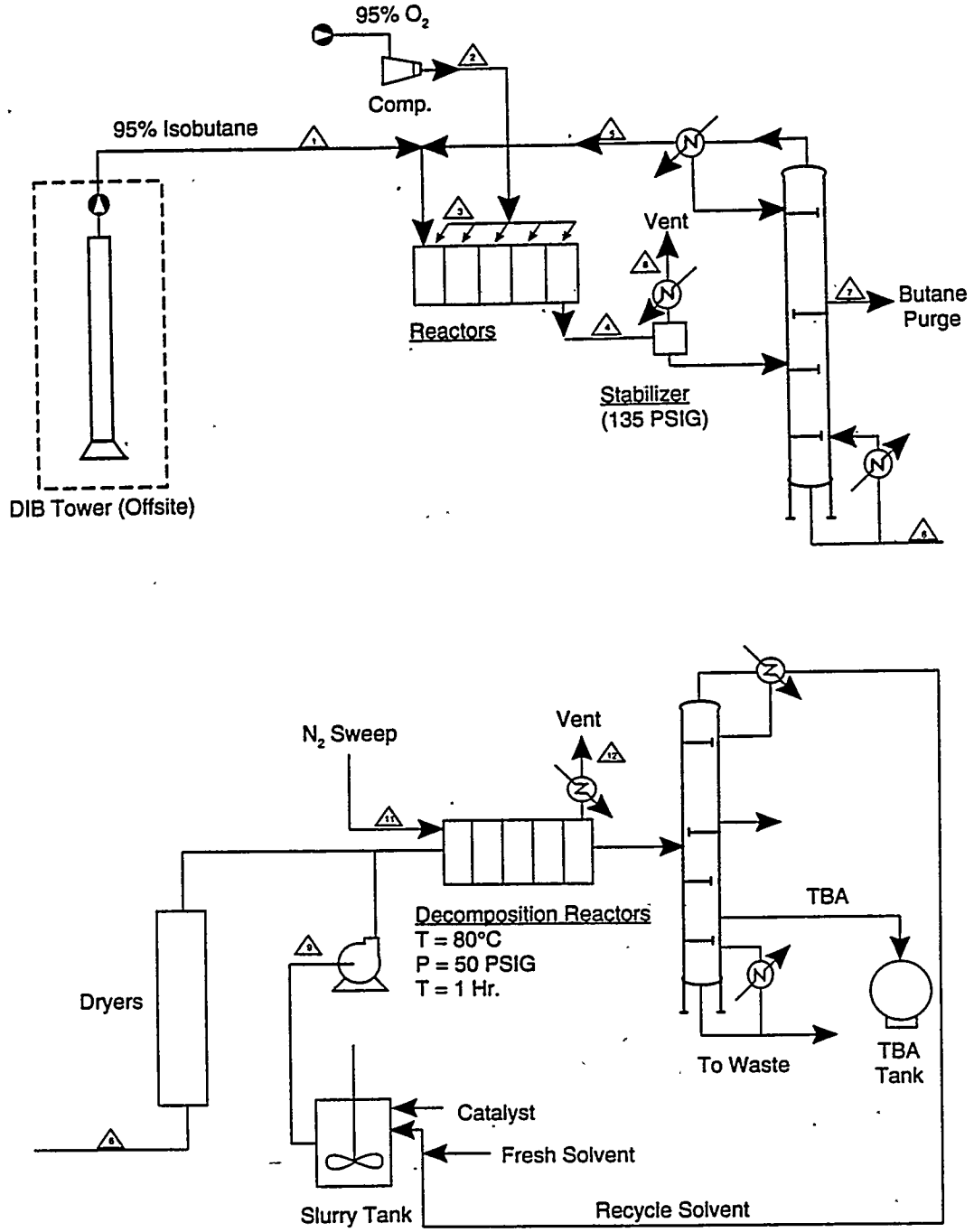

## Table 4. Isobutane to TBA - Proof -of-Concept Criteria For New Retrofit Process

**Process Mode 2**

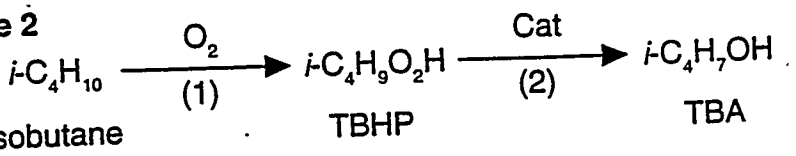


| | | |
|---|---|---|
| Rate: | Proprietary | (Achieved) |
| Catalyst cost: | <$100/lb | (Achieved) |
| TBA selectivity: | ≥85% | (Achieved) |
| (2) Conversion: | 99% | (Achieved) |

**Process Mode 1**

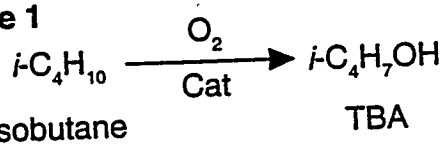


| | | |
|---|---|---|
| Rate: | Proprietary | (Achieved) |
| Catalyst cost: | 5¢/gal. TBA | (Not achieved) |
| TBA selectivity: | ≥85% | (Achieved) |
| Conversion: | 50% | (Achieved) |

## REFERENCES


(1) P. E. Ellis, Jr. and J. E. Lyons, J. Chem. Soc. Chem. Commun., (1987) 1187.

(2) P. E. Ellis, Jr. and J. E. Lyons, J. Chem. Soc. Chem Commun., (1989) 1189.

(3) P. E. Ellis, Jr. and J. E. Lyons, J. Chem. Soc. Chem. Commun., (1989) 1315.

(4) P. E. Ellis, Jr. and J. E. Lyons, Catalysis Letters 3, (1989) 389.

(5) P. E. Ellis, Jr. and J. E. Lyons, Preprints of the Division of Petroleum Chemistry, ACS, Vol. 35, No. 2, April (1990).

(6) P. E. Ellis, Jr. and J. E. Lyons, Coordination Chem. Rev., 105 (1990) 181.

(7) J. E. Lyons and P. E. Ellis, Jr., Catalysis Letters, 8 (1991) 45.

(8) J. E. Lyons and P. E. Ellis, Jr., Applied Catalysis A General, 84 (1992) L1-L6.

(9) J. E. Lyons, P. E. Ellis, Jr., R. W. Wagner, P. B. Thompson, H. B. Gray, M. E. Hughes and J. A. Hodge, Preprints Pet. Div., 37 (1992) 307.

(10) J. E. Lyons, "Catalytic Conversion of Light Alkanes," GRI Contractor Review Meeting, Methane Reaction Science Program, Paris, France, Aug. 25-27 (1991).

(11) Unpublished Work by H. B. Gray, W. P. Schaefer, et al.

(12) Related structures have been determined: a) R. E. Marsh, W. P. Schaefer, J. A. Hodge, M. E. Hughes, H. B. Gray, J. E. Lyons and P. E. Ellis, Jr., Acta Cryst. Sec. C, V 49 (1993) 1339. b) W. P. Schaefer, J. A. Hodge, M. E. Hughes, H. B. Gray, J. E. Lyons, P. E. Ellis, Jr. and R. W. Wagner, Acta Cryst. Sec. C, V 49 (1993) 1342.

(13) J. E. Lyons, P. E. Ellis, Jr. and V. A. Durante, Proceedings of the Natural Gas R&D Contractors Review Meeting, DOE/METC - 89/6103 (1989) 164.

(14) J. E. Lyons, Proc. Nat. Gas R&D Contractors Review Meeting, DOE/METC - 91/6117 (1990) 276.

(15) J. E. Lyons, P. E. Ellis, Jr., H. K. Myers, Jr., G. Suld and W. A. Langdale, U. S. Patent 4,803,187, Feb. 7 (1989).

(16) P. E. Ellis, Jr. and J. E. Lyons, U. S. Patent 5,091,354, Feb. 25 (1992).

(17) J. E. Lyons, P. E. Ellis, Jr., W. A. Langdale and H. K. Myers, Jr., U. S. Patent 4,916,101, Apr. 23 (1990).

(18) P. E. Ellis, Jr. and J. E. Lyons, U. S. Patent 4,898,989, Feb. 6 (1990).

(19) J. E. Lyons, P. E. Ellis, Jr., H. K. Myers, Jr., G. Suld and W. A. Langdale, U. S. Patent 4,859,798, Aug. 22 (1989).

(20) J. E. Lyons, Proc. Nat. Gas R&D Review Meeting, DOE/METC - 92/6125 (1992) 266.

(21) J. E. Lyons, P. E. Ellis, Jr. and V. A. Durante, Studies in Surface Science and Catalysis, 67, Elsevier, N.Y. (1991) 99.

(22) P. E. Ellis, Jr. and J. E. Lyons, U. S. Patent 5,254,740, Oct. 19 (1993).

(23) P. E. Ellis, Jr. and J. E. Lyons, U. S. Patent 5,212,300, May 18 (1993).

(24) P. E. Ellis, Jr. and J. E. Lyons, U. S. Patent 5,120,882, June 9 (1992).

(25) P. E. Ellis, Jr. and J. E. Lyons, U. S. Patent 5,118,886, June 2 (1992.

(26) P. E. Ellis, Jr., J. E. Lyons and H. K. Myers, Jr., U. S. Patent 5,093,491, Mar. 3 (1992).

(27) P. E. Ellis, Jr. and J. E. Lyons, U. S. Patent 4,970,348, Nov. 13 (1990).

(28) P. E. Ellis, Jr., J. E. Lyons and H. K. Myers, Jr., U. S. Patent 4,900,871, Feb. 13 (1990).

(29) P. E. Ellis, Jr., J. E. Lyons and H. K. Myers, Jr., U. S. Patent 4,895,682, Jan. 23 (1990).

(30) P. E. Ellis, Jr., J. E. Lyons and H. K. Myers, Jr., U. S. Patent 4,895,680, Jan. 23 (1990).

(31) J. E. Lyons, P. E. Ellis, Jr., H. K. Myers, Jr., and R. W. Wagner, J. Catal., 141 (1993) 311.

(32) J. E. Lyons and P. E. Ellis, Jr., U.S. Patent 5,120,886, June 9 (1992).

(33) P. E. Ellis, Jr., and J. E. Lyons, "Metal Phthalocyanine Oxidation Catalysts," U.S. patent 5,254,740, issued October 19, 1993.

(34) P. E. Ellis, Jr., and J. E. Lyons, "Nitrated Metalloporphyrins as Catalysts for Alkane Oxidation," U.S. Patent 5,280,115, issued January 20, 1994.

(35) J. E. Lyons and P. E. Ellis, Jr., "Decomposition of Organic Hydroperoxides with Nitrated Porphyrin

Complexes, U.S. Patent 5,345,008, issued September 6, 1994.

(36) P. E. Ellis, Jr. and J. E. Lyons, "Metal Phthalocyanine Catalysts", U.S. Patent 5,354,857, issued October 11, 1994.

(37) P. E. Ellis, Jr. and J. E. Lyons, "Cyano- and Polycyanometalloporphyrins as Catalysts for Alkane Oxidation," U.S. Patent 5,382,662, Issued January 7, 1995.

(38) P. E. Ellis, Jr., J. E. Lyons and S. N. Shaikh, "Novel Iron meso-Nitroporphine Complexes for the Catalytic Reaction of Alkanes with Molecular Oxygen," Catal. Lett., 24, 79 (1994).

(39) H. L. Chen, P. E. Ellis, Jr., T. P. Wijesekera, T. E. Hagan, S. E. Groh, J. E. Lyons and D. P. Ridge, "Correlation Between Gas Phase Electron Affinities, Electrode Potentials and Catalytic Activities of Halogenated Metalloporphyrins", J. Amer. Chem. Soc., 116, 1086 (1994).

(40) J. E. Lyons and P. E. Ellis, Jr., Reactions of Alkanes with Dioxygen: Toward Suprabiotic Systems, Metalloporphyrins in Catalytic Oxidations, R. S. Sheldon, Ed. Marcel Dekker, N.Y., pp 297-324 (1994).

(41) D. E. Winkler and G. W. Hearne, Ind. and Eng. Chem., 33, 655 (1961).

(42) P. D. Taylor and M. T. Mocella, U.S. Patent 4,508,923 (1985).

# Opportunities in Oxidative Natural Gas Conversion
# Alcohols and Ketones Via Direct Air Oxidation of Light Alkanes

Liquid fuels from natural gas

- Methanol-rich oxygenate for:
  - Hydrocarbon fuel precursor
  - Liquid fuel
  - Fuel additive
  - Additive precursor (MTBE)

Chemical oxygenates

- MEK from butane
- Acetone from propane
- Acetaldehyde from ethane
- Formaldehyde from methane

Fuel alcohols from gas components

- Butanols from butane (GTBA)
- IPA from propane
- Methanol
- Ethanol from ethane

# Oxy Synfuels

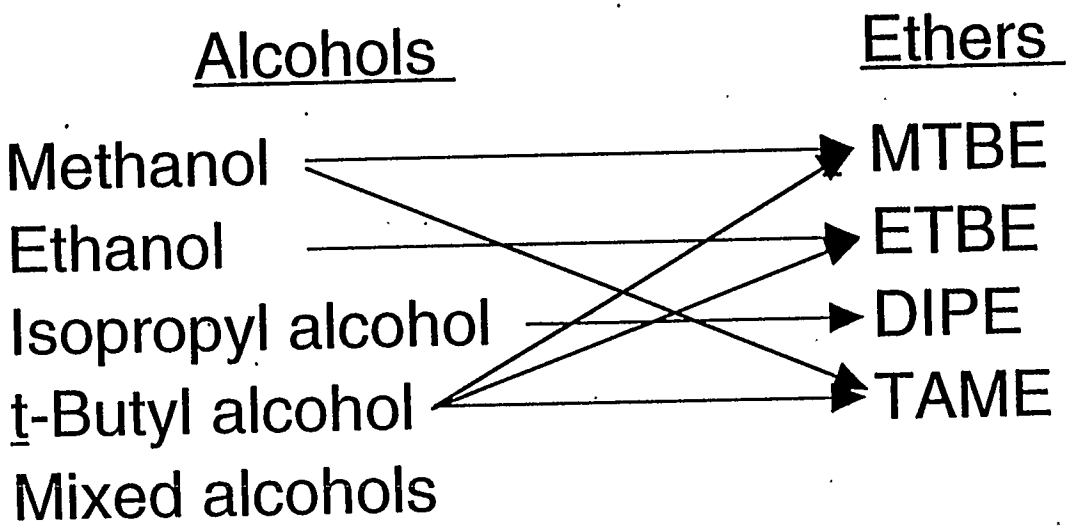


Alcohol-ether blends

# Properties of Ethers and Alcohols

| Property | MTBE | ETBE | GTBA | IPA | ETOH | MeOH |
|---|---|---|---|---|---|---|
| Oxygen, wt % | 18.2 | 15.7 | 21.6 | 26.6 | 34 | 49.9 |
| Sp. gravity | 0.74 | 0.74 | 0.791 | 0.789 | 0.79 | 0.796 |
| Boiling point, °F | 131 | 163 | 181 | 180 | 172 | 149 |
| RVP (lbs/in$^2$) | 7.8 | 2.5 | 1.8 | 1.8 | 2.3 | 4.6 |
| Blending RVP | 9 | 5 | 12 | 14 | 23 | 75 |
| RON BV | 110-122 | 117-121 | ~103 | 113-119 | ~122 | 126 |
| MON BV | 98-102 | 100-105 | ~91 | 95-101 | ~96 | 104 |
| (R+M)/2 BV | 103-110 | ~110 | ~97 | 104-110 | ~100 | 115 |

# Hydrocarbon Reactivity Series

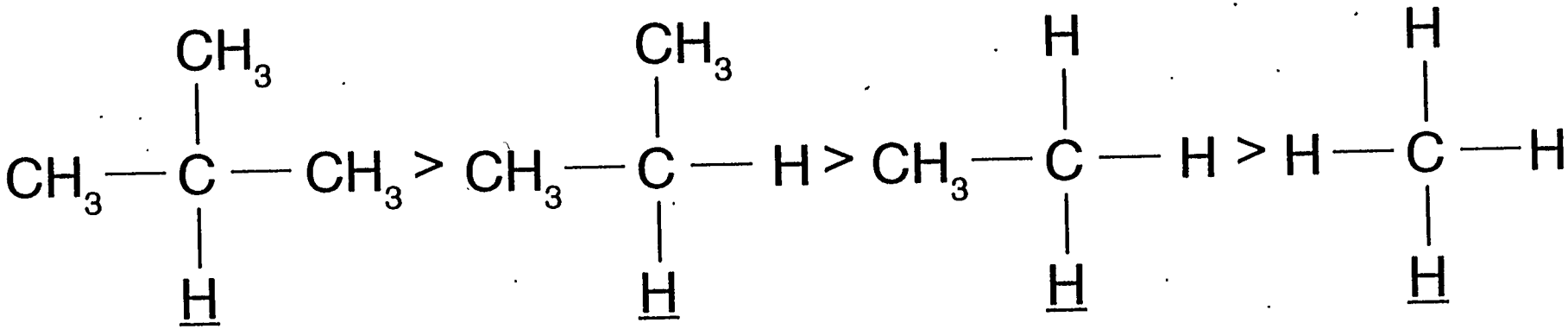


Isobutane (91 Kcal) > Propane (94 Kcal) > Ethane (98 Kcal) > Methane (104 Kcal)

# TBA - Key to Reformulated Gasolines (RFG)

As a gasoline component

- High performance (100 octane)
- Meets Clean Air Act oxygenate requirements
- Good performance characteristics

As an isobutylene precursor

- For alkylate feedstock
- Branched alkanes - good octane
- Environmentally acceptable octane
- Displaces aromatics

As a precursor to MTBE

- Fastest growing chemical (through 1994)
- Largest oxygenate contributor to RFG
- High performance (octane >100)
- Clean burning, environmentally superior

As a precusor to ETBE

- Up-and-coming oxygenate
- All the benefits of MTBE
- Superior vapor pressure properties
- Uses a renewable resource (ethane)

# MTBE - Current Oxygenate of Choice for RFG

- ~30 companies produce MTBE in North America
- These companies operate 44 plants here
- Which produce ~232,000 BPD MTBE
- More plants have been announced
- ARCO is the MTBE volume leader (23% in North America)

# Historical and Current Fuel Applications of Field Butane

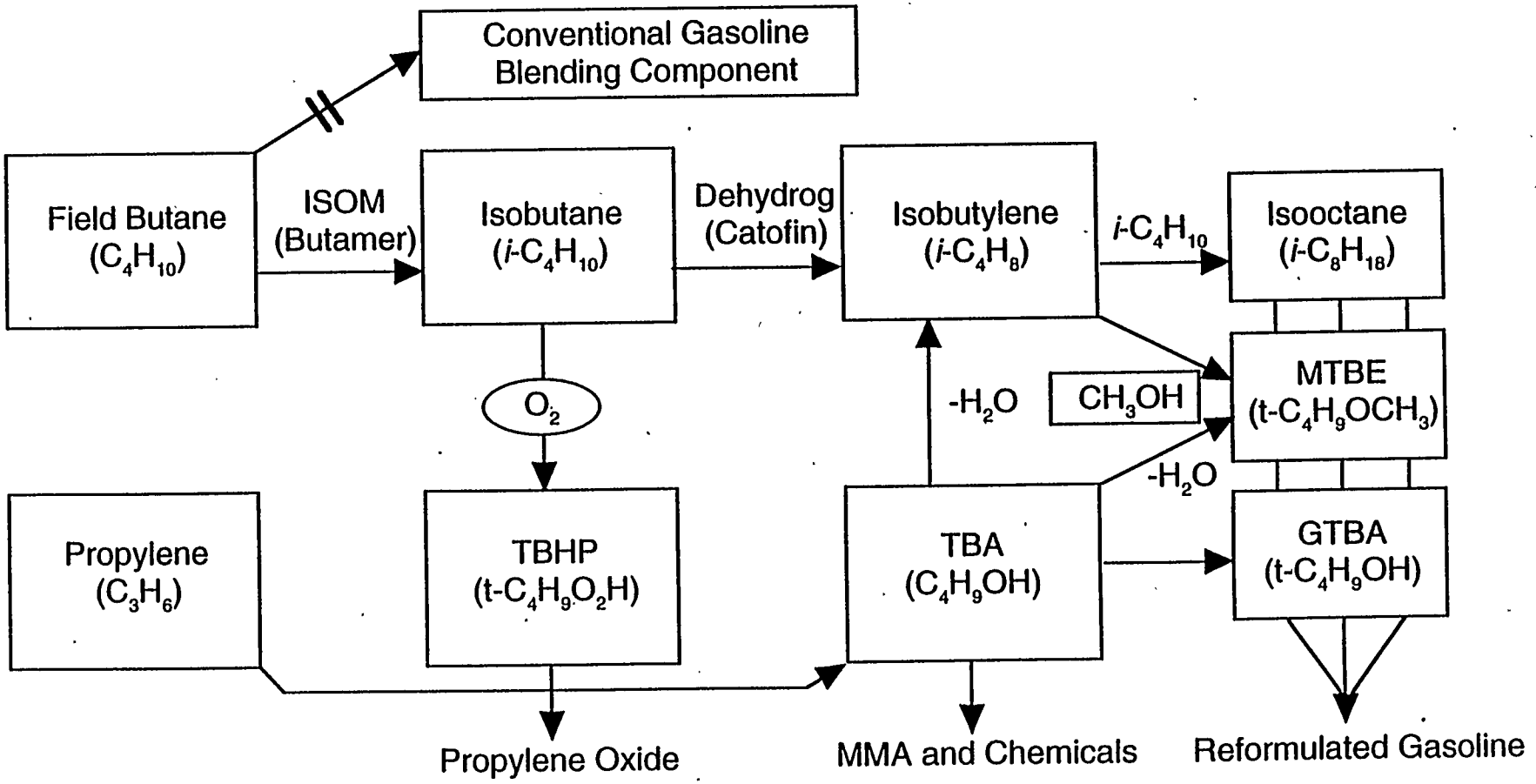


Expensive isobutane dehydrog., limited PO opportunities

# Isobutane Oxidation-Proof-of-Concept Stage

## Process Technology Development Using New Sun Catalysts

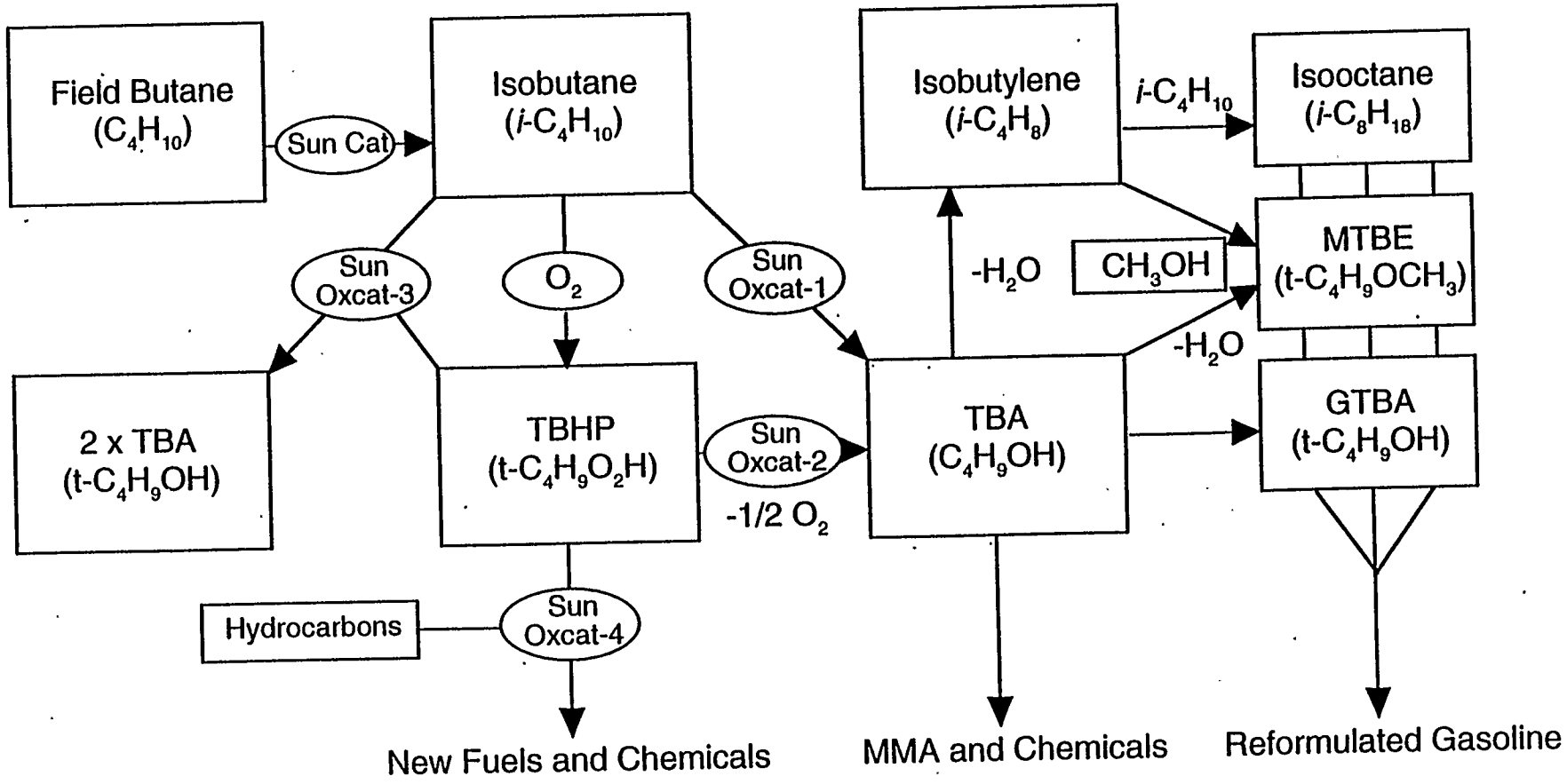


Sun oxcats for product/process flexibility

# Isobutane Oxidation for Reformulated Gasoline

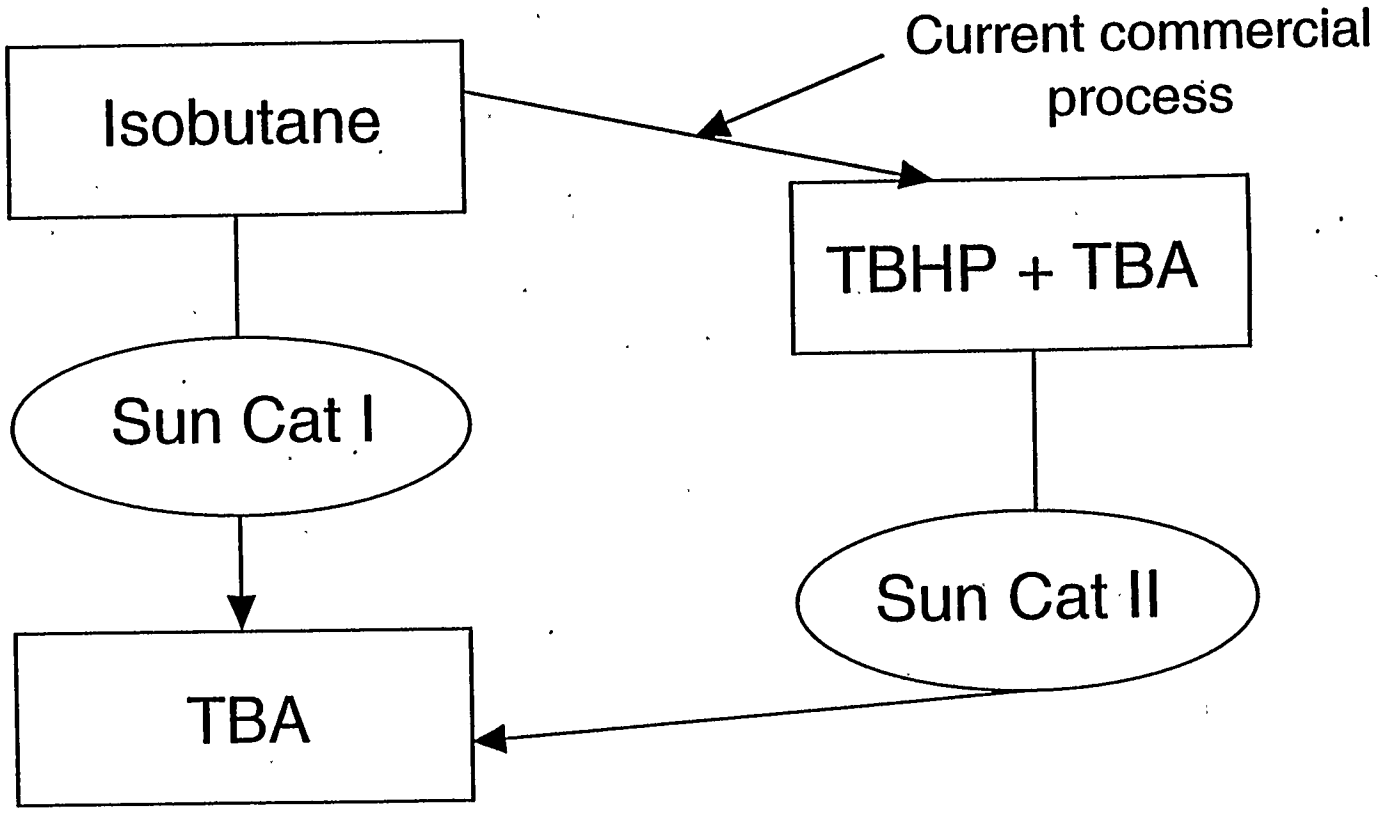

# Cobalt Catalyzed Oxidation of Isobutane

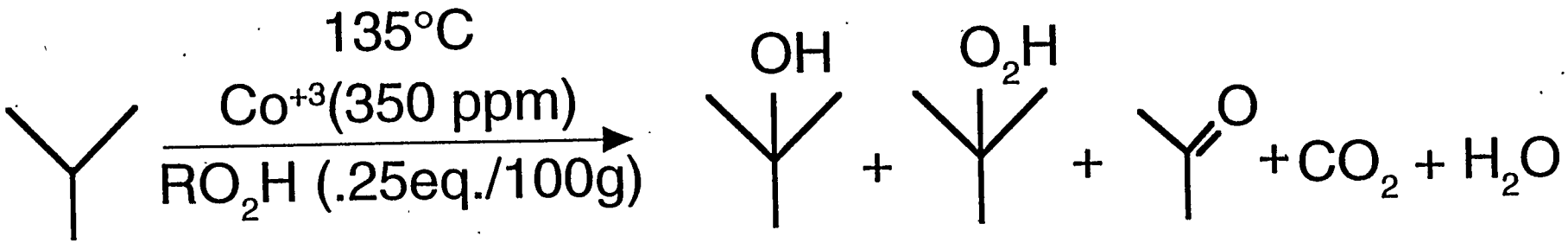


Conv. = 50%  Sel. = 77%  10%  11%

Winkler and Hearns, *Ind. and Eng. Chem.* (1961)

# Biological and Biomimetic Alkane Oxidation

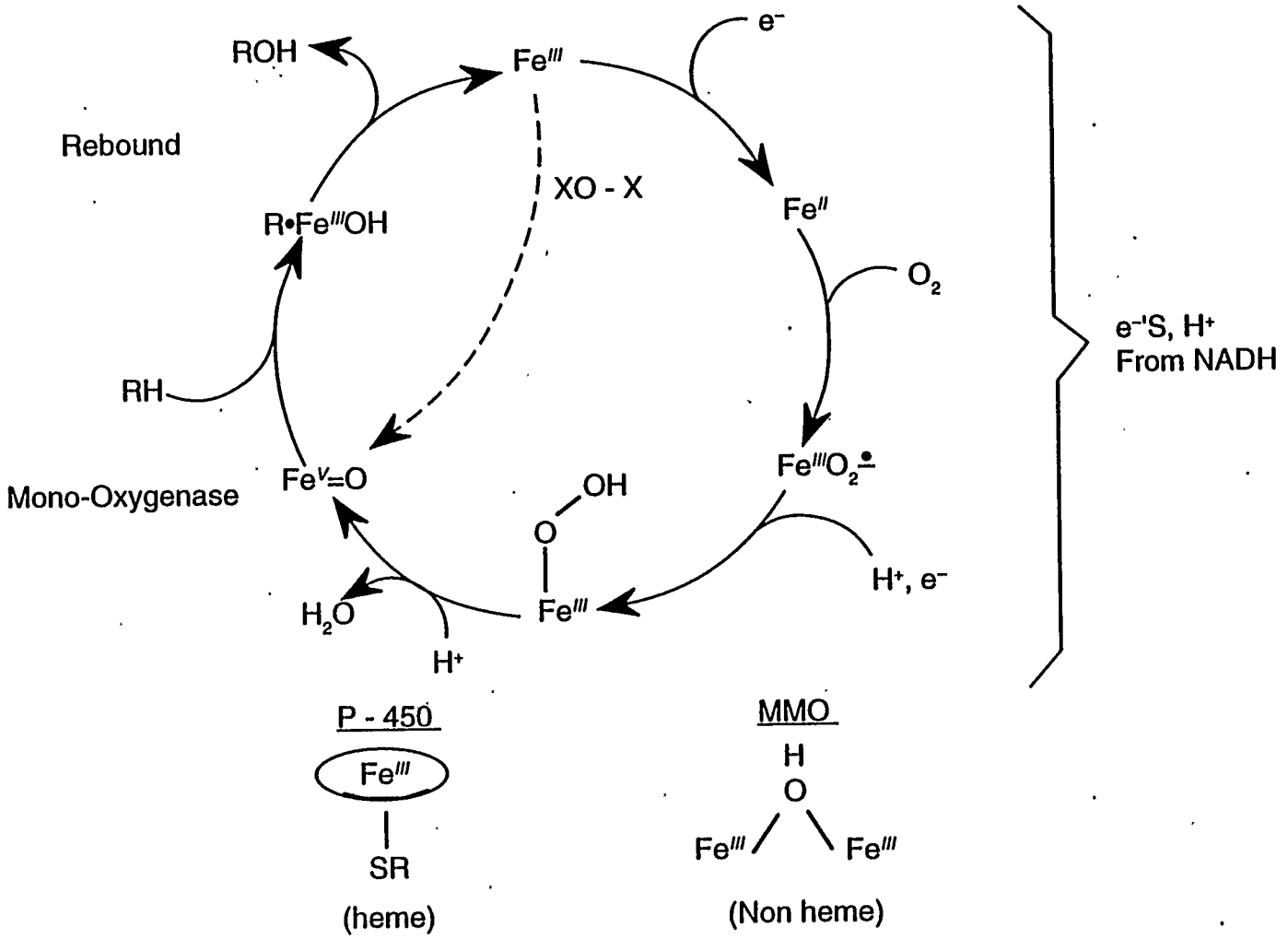

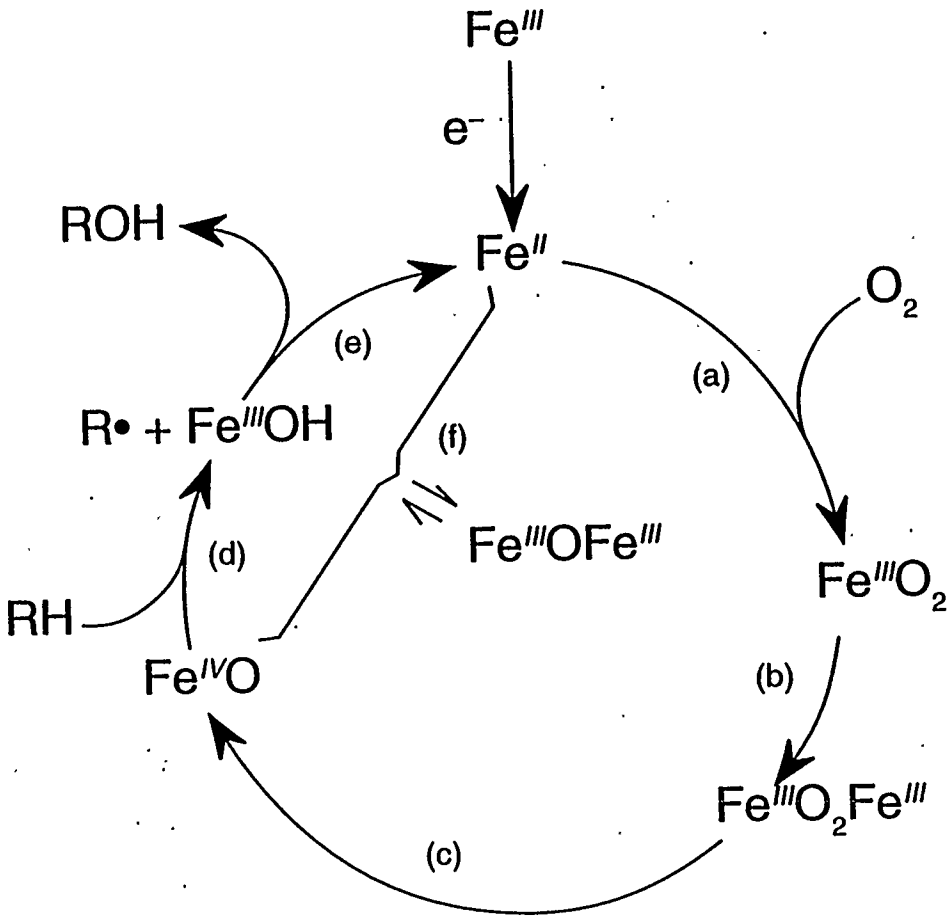


Fe = (Fe) = Porphyrinato Iron

# Substituted Porphyrin Macrocycle

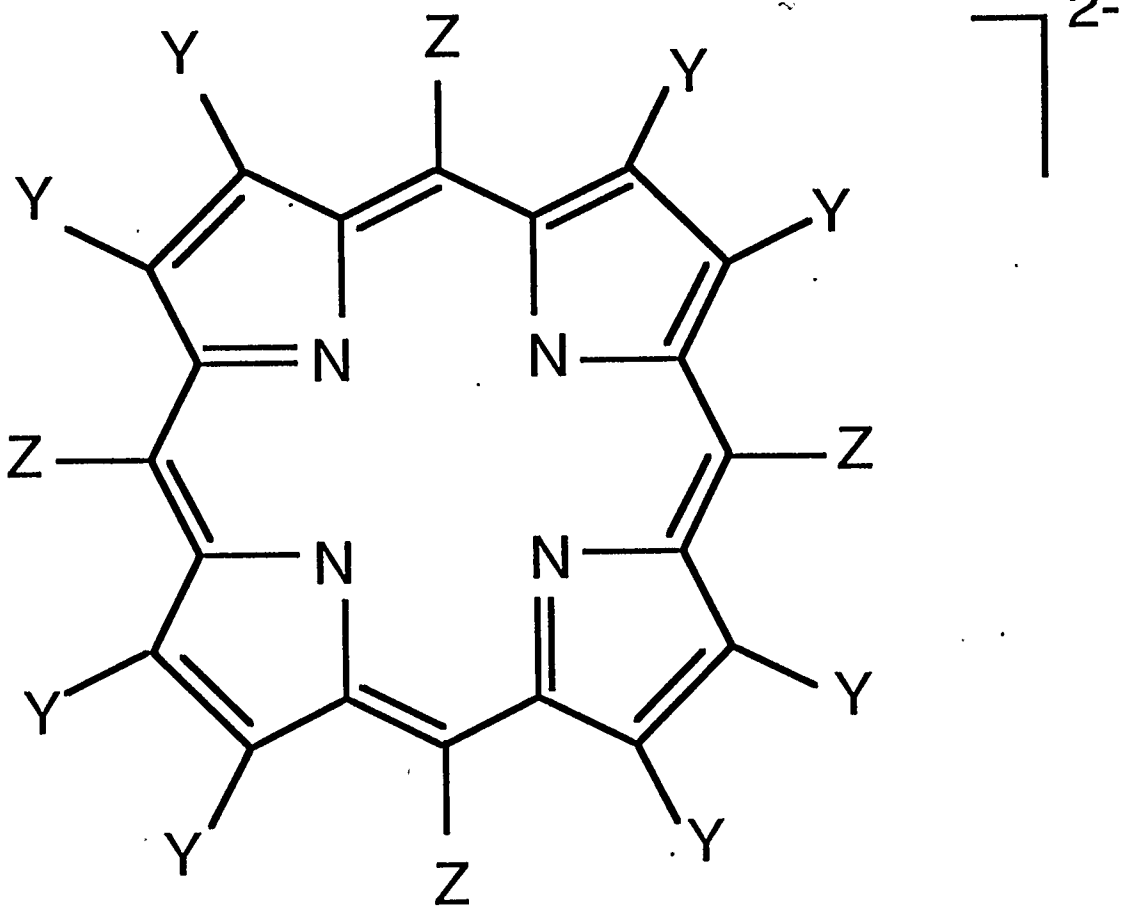

# Isobutane Oxidation for Reformulated Gasoline

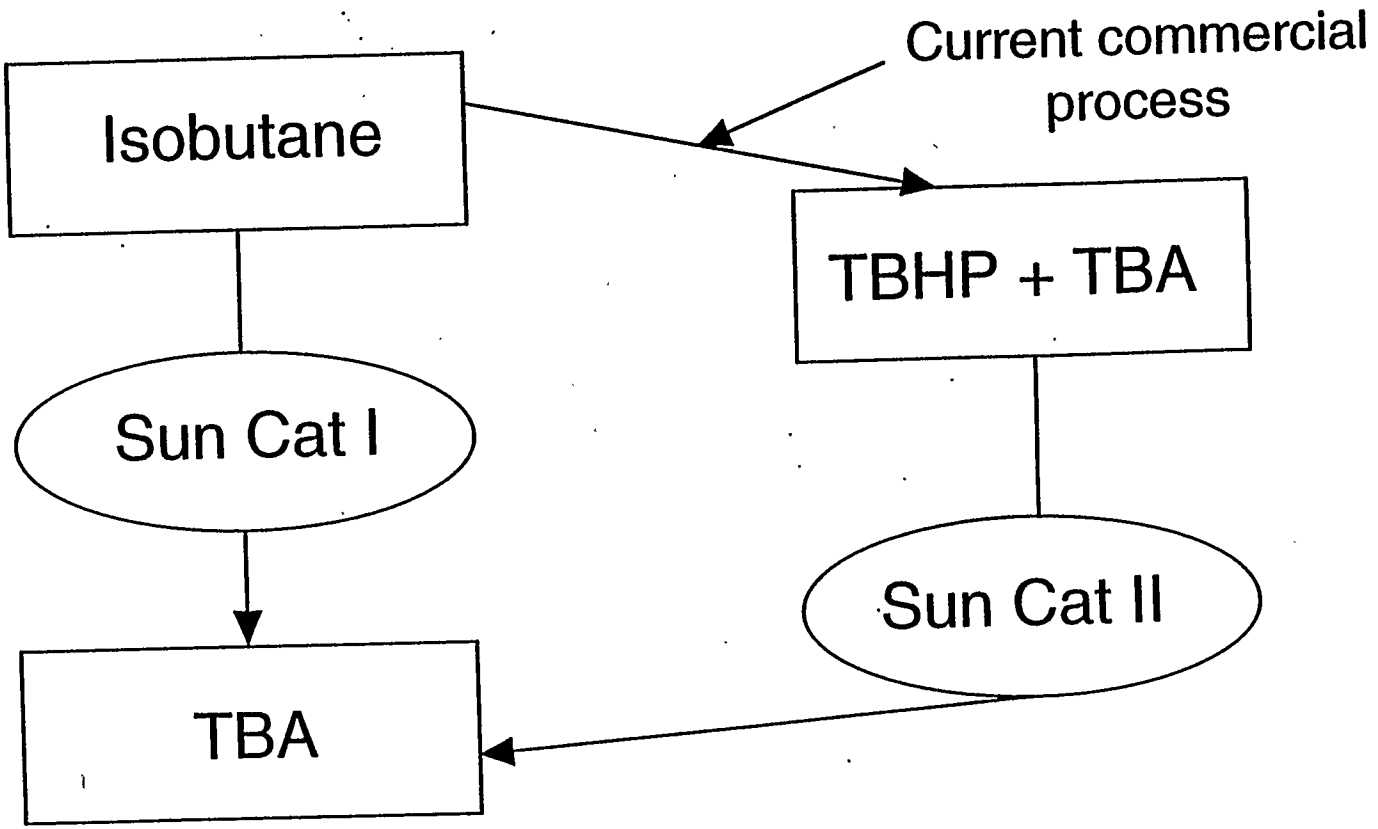

# t-Butyl Alcohol from t-Butyl Hydroperoxide

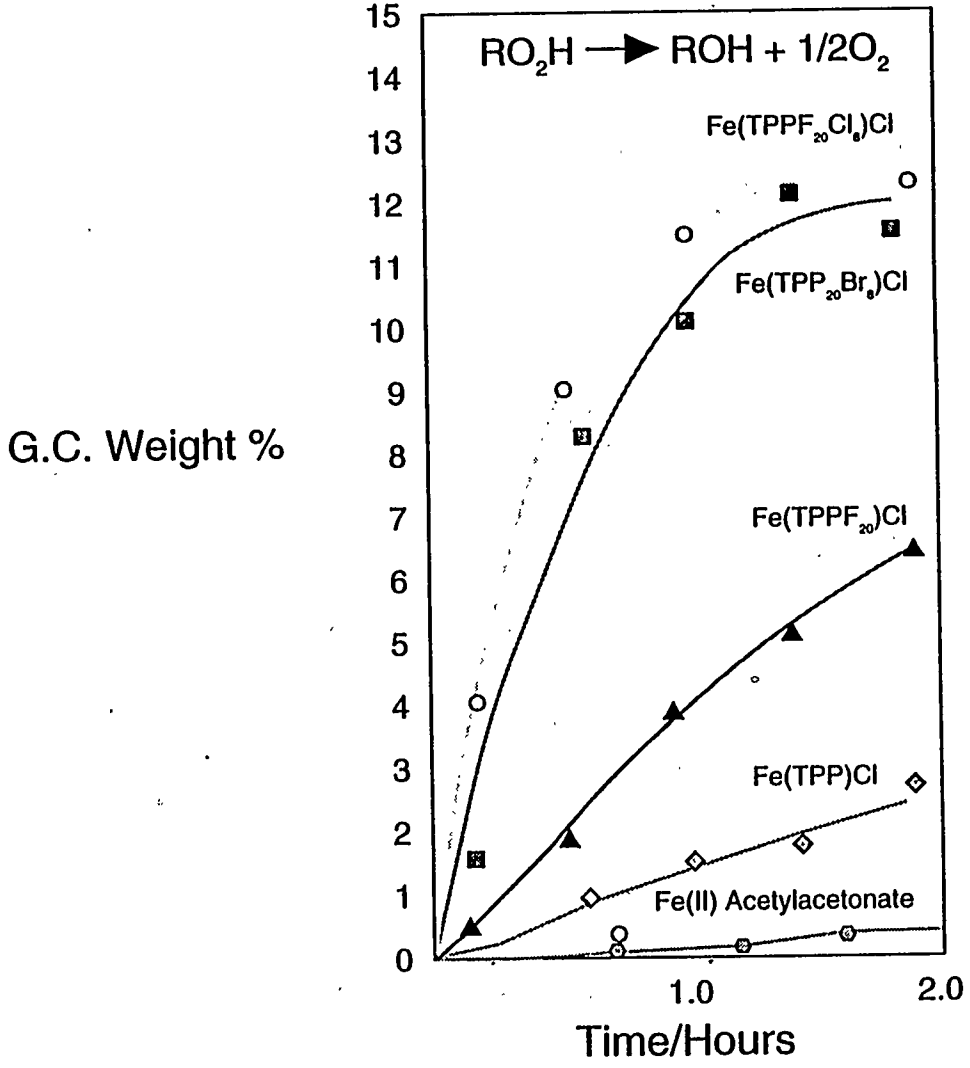

# Conversion of tert-Butyl Hydroperoxide to tert-Butyl Alcohol

| Catalyst | Time Hours | t-$BuO_2H$ Conv., % | Product, Molar Sel., % t-BuOH | $(t\text{-}BuO)_2$ | $(CH_3)_2CO$ |
|---|---|---|---|---|---|
| $Fe(ACAC)_3$ | 2.3 | <5 | 67 | tr | 32 |
| Fe(TPP)Cl | 1.9 | 27 | 82 | 7 | 11 |
| $Fe(TPPF_{20})Cl$ | 3.3 | 72 | 87 | 10 | 3 |
| $Fe(TPPF_{20}\beta\text{-}Br_8)Cl$ | 1.9 | 95 | 90 | 8 | 2 |
| $Fe(TPPF_{20}\beta\text{-}Cl_8)Cl$ | 3.3 | 100 | 90 | 8 | 2 |

[a] The catalyst, $2 \times 10^{-4}$ mmoles, in 2.4 ml p-xylene was rapidly added to a stirred solution of 10 ml t-$BuO_2H$ (90%) in 48 mls benzene. $O_2$ evolved was measured manometrically and liquid samples taken periodically and analyzed by standardized gc

# Relationship Between Catalyst Reduction Potential and Activity

| Catalyst | Fe (III)/(II)[a] $E_{1/2}$ (V) | TBA Yield[b] % at 0.5 HR |
|---|---|---|
| Fe(TPP)Cl | -0.221 | 4.8 |
| $Fe(TPPF_{20})Cl$ | +0.070 | 16.0 |
| $Fe(TPPF_{20}\beta\text{-}Br_8)Cl$ | +0.190 | 51.2 |
| $Fe(TPPF_{20}\beta\text{-}Cl_8)Cl$ | +0.280 | 67.2 |

[a] Cyclic voltammetry in $CH_2Cl_2$, vs. SCE, TBAC - supporting electrolyte, glassy carbon electrode

[b] Room temperature decomposition of TBHP in benzene

# Electron Affinities, Reduction Potentials and Catalytic Activities of Metalloporphyrins



| Species | EA (eV) | $E_{1/2}$ (V) vs. SCE | TO $iC_4$-ox[a] | $TBA^-$ Yield[b] TBHP-dec |
|---|---|---|---|---|
| Fe(TPP)Cl | 2.15 | -.29 | 0 | 4.8 |
| $Fe(TPPF_{20})Cl$ | 3.14 | +.08 | 1160 | 16.0 |
| $Fe(TPPF_{20}\beta Cl_8)Cl$ | 3.35 | +.29 | 1800 | 67.2 |

[a] Moles $O_2$ taken up in 60°C oxidations of isobutane after 6 hours
[b] Yield of TBA from TBHP decomposition in 0.5 hours

# Isobutane Oxidation Schematic of One-Step Process

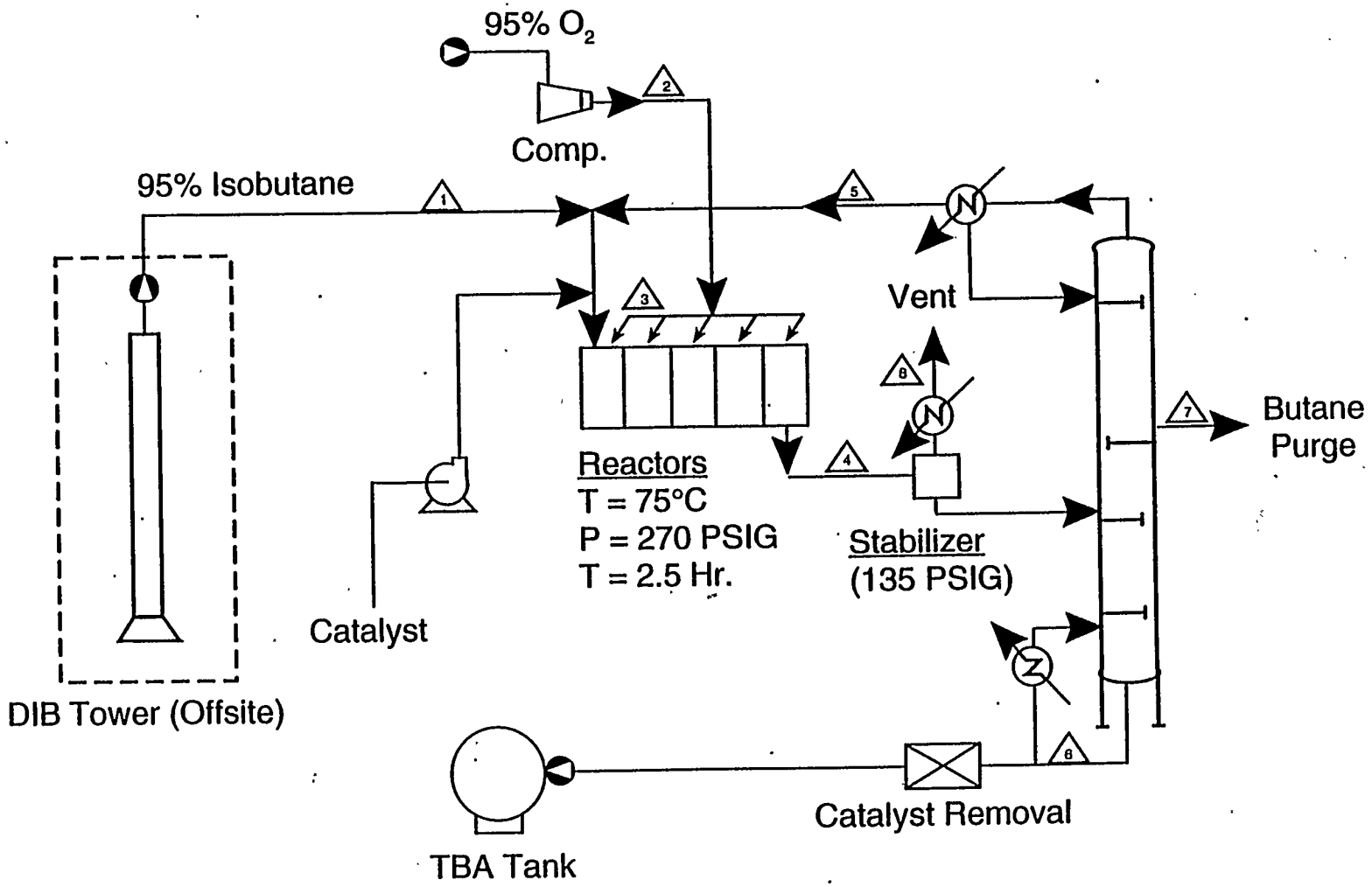

# Experimental Procedures

Reactor

- 500cc autoclave in a barricaded chamber
- $O_2$ addition and T control from outside barricade
- On-line GC product analysis

Procedure

- Catalyst charged before sealing autoclave
- Isobutane (99.7%) charged from 300cc hoke bomb
- Isobutane/cat./cosolvent heated to T in $N_2$
- $O_2$ added to desired P, maintained within 5 psi by total pressure controller

Typical conditions and results

- Catalyst = $Fe(TPPF_{20}\beta\text{-}Cl_8)X$, 200-400 ppm
- Conditions - 80°C, 30-150 psia $O_2$ partial pressure
- Results - 25-50% conversion of $i\text{-}C_4H_{10}$
  - 80-90% selectivity to TBA

# Performance Targets for One-Step Oxidation of Isobutane

## 80°C, 30-50 psia $O_2$, 500-600 psig Total Pressure

| | Grass Roots | Retrofit | Current Best |
|---|---|---|---|
| $IC_4$ Conv., % | 50+ | 30+ | 30+ |
| Reaction time, h | 2.5 | 5 | 5 |
| TBA selectivity, % | 90+ | 85+ | 85+ |
| Cat cost, c/gal MTBE | <3 | <5 | >50 |

# Isobutane Oxidation Schematic of Two-Step Process

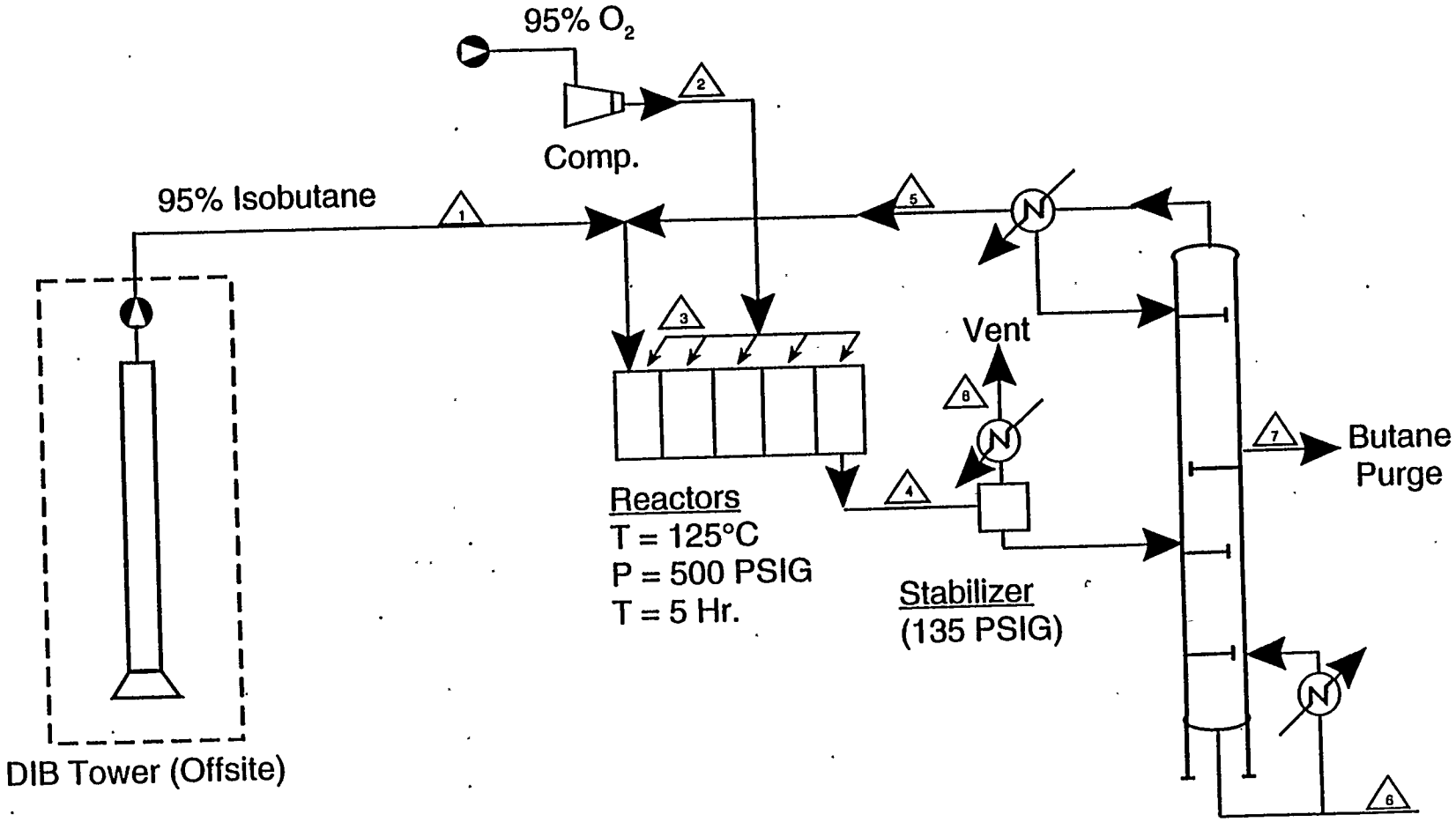

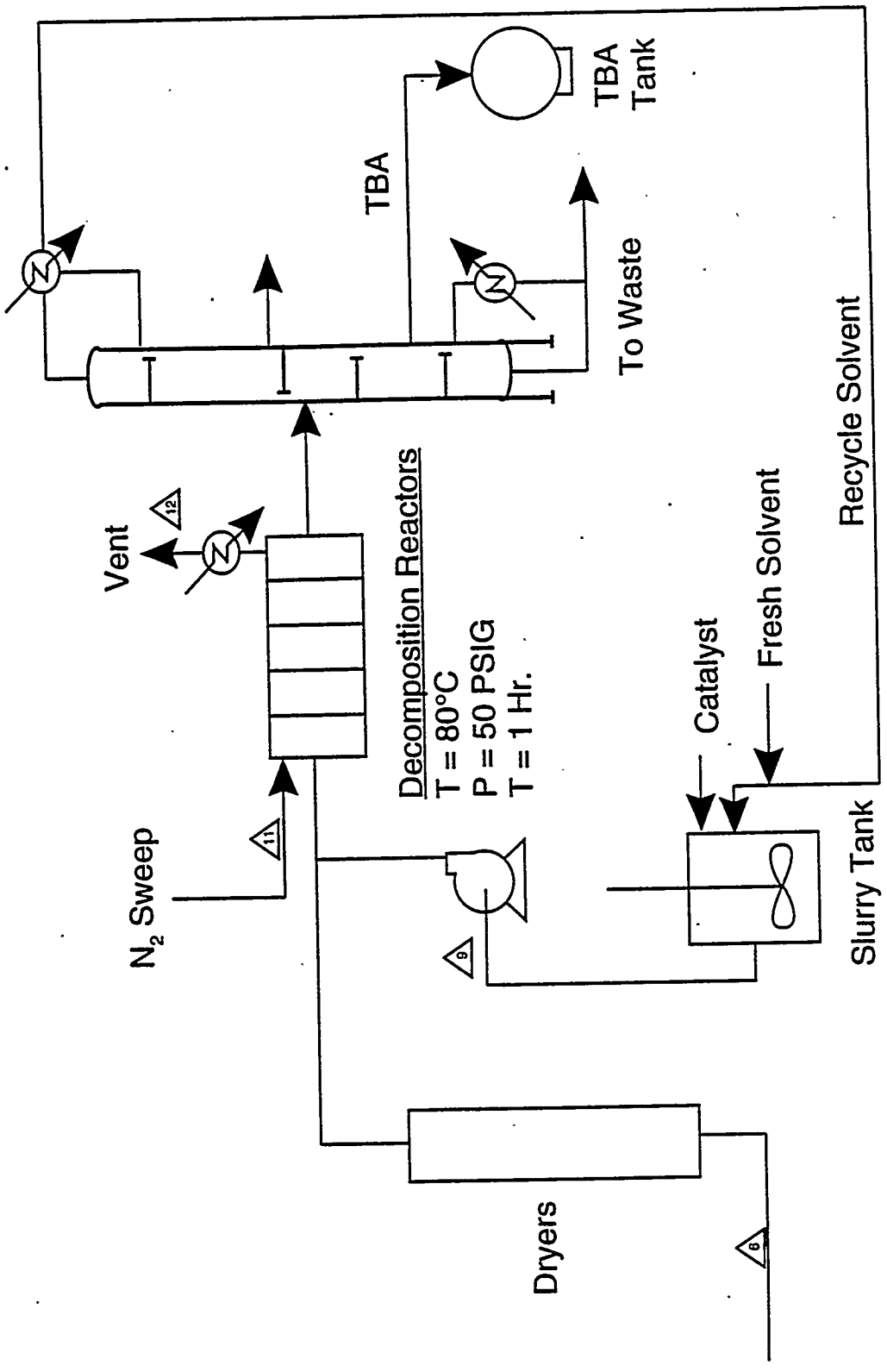
TBA Tank
TBA
To Waste
Recycle Solvent
Vent
Decomposition Reactors
T = 80°C
P = 50 PSIG
T = 1 Hr.
Catalyst
Fresh Solvent
N2 Sweep
Slurry Tank
Dryers

# Isobutane Oxidation Schematic of One-Step Process

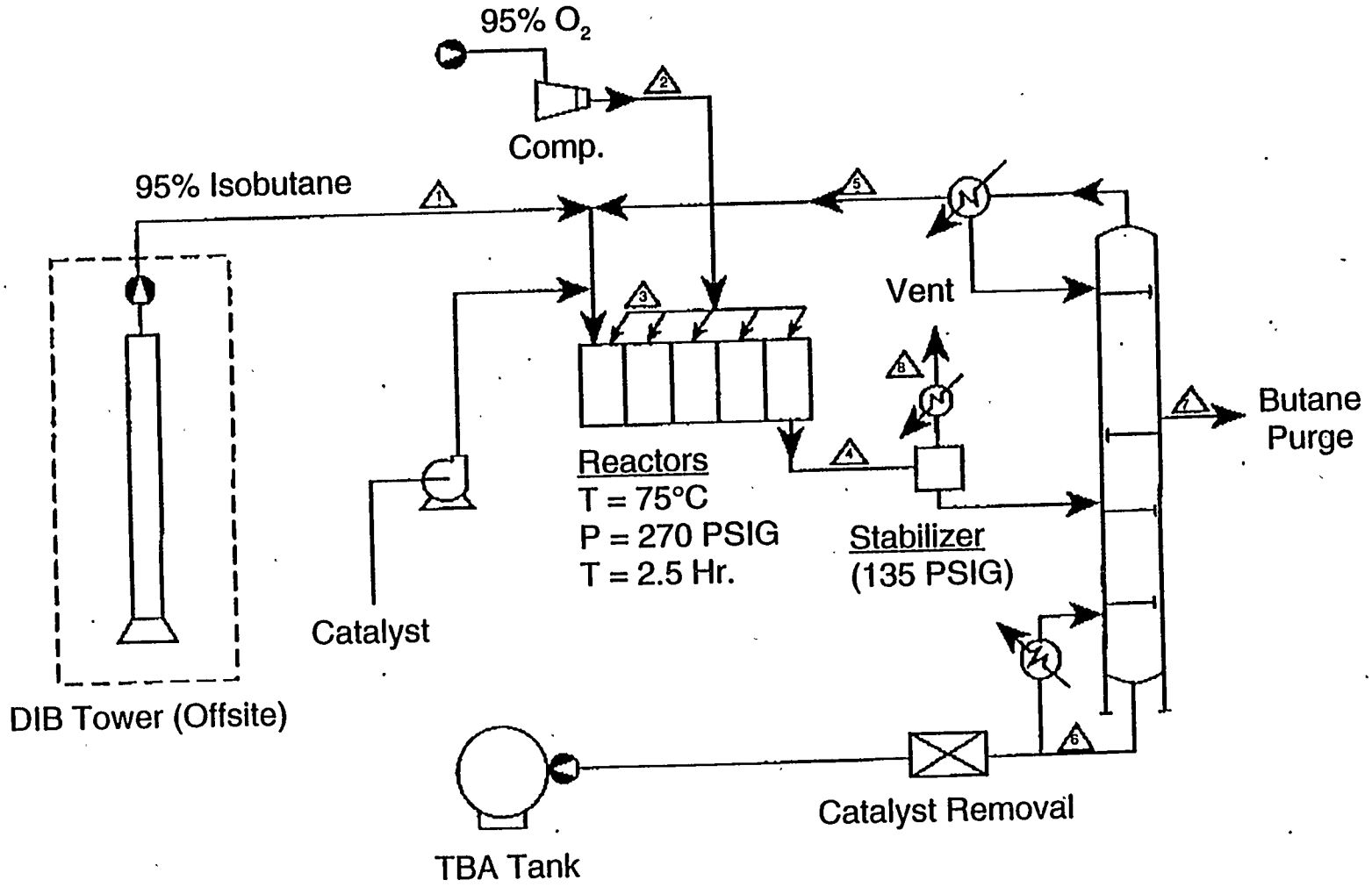

# Decomposition of TBHP

## Experimental Procedures

Reactor

- 50cc autoclave in a barricaded chamber
- T control and flow readings from outside barricade
- Nitrogen purge system avoids build-up of explosive vapors on $O_2$ evolution

Procedure

- TBHP/TBA/co-solvent charged to reactor
- Reactor sealed, pressure tested and heated
- When T has stabilized catalyst solution injected
- Gas flow in and out metered to follow decomposition

Typical conditions and results

- TBHP, 40 wt% in TBA-acetone (51%, 9%) charged
- P = 200 psi with 10 cc/min $N_2$ sweep; 80°C
- Catalyst in TBA added incrementally over time
- Results 87% TBA selectivity at high conversion

# TBHP Decomposition
## Catalyst Cost

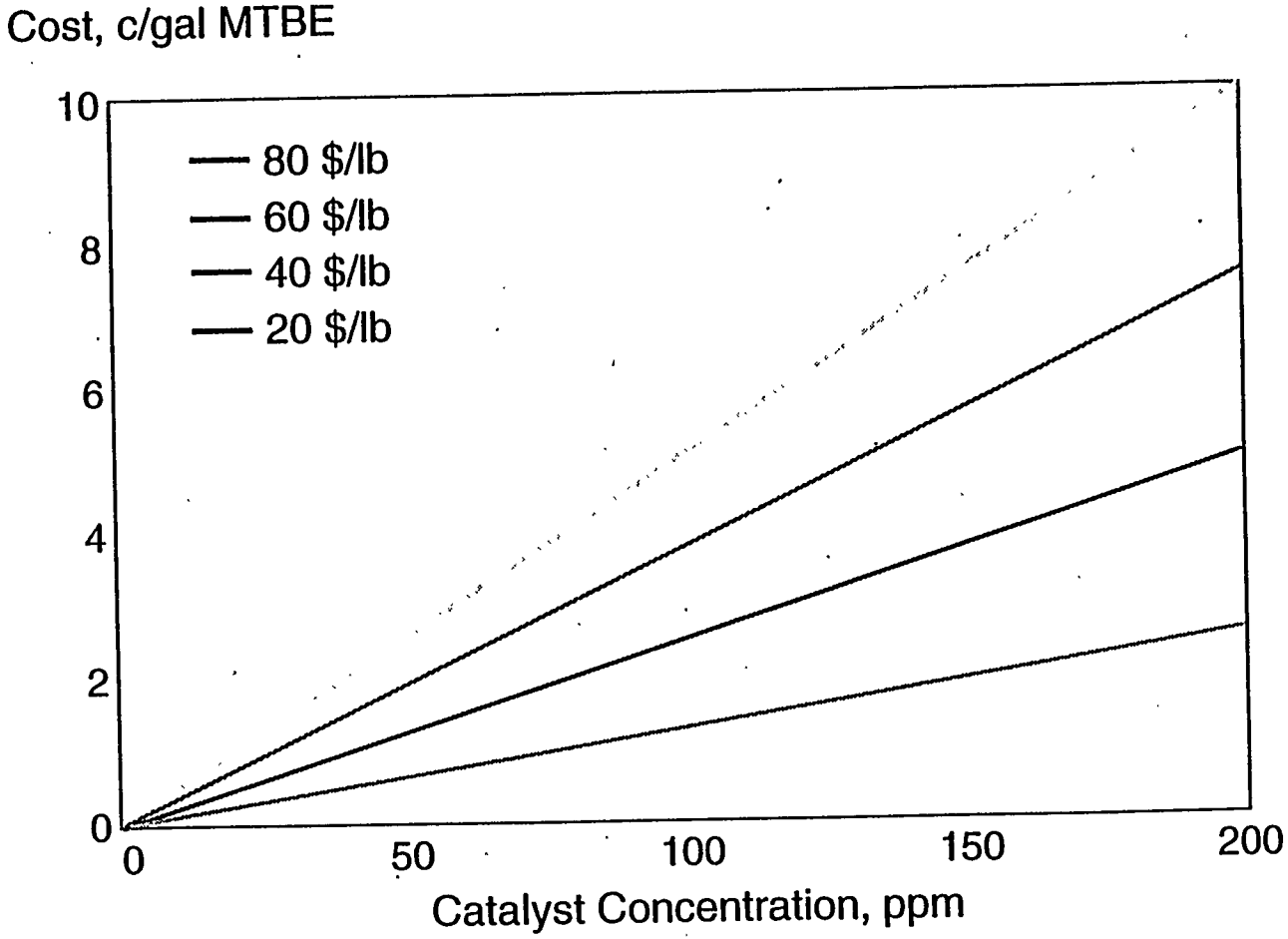

# Isobutane to TBA
## Proof-of-Concept Criteria
## (New Retrofit Process Modes)

**Process Mode 2**

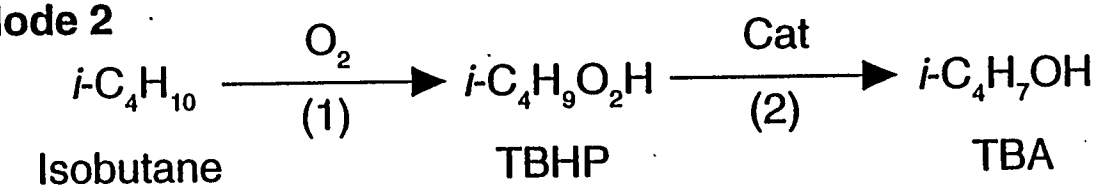


| | | |
|---|---|---|
| Rate: | Proprietary | (Achieved) |
| Catalyst cost: | <$100/lb | (Achieved) |
| TBA selectivity: | ≥85% | (Achieved) |
| (2) Conversion: | 99% | (Achieved) |

**Process Mode 1**

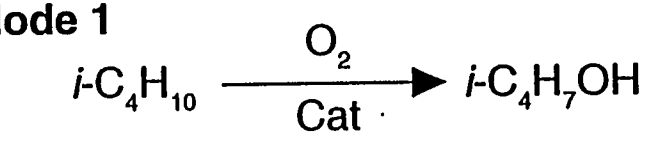


| | | |
|---|---|---|
| Rate: | Proprietary | (Achieved) |
| Catalyst cost: | 5¢/gal. TBA | (Not achieved) |
| TBA selectivity: | ≥85% | (Achieved) |
| Conversion: | 50% | (Achieved) |

# Accomplishments

## Isobutane to TBA - Proof-of-Concept

- Have developed an inexpensive, active catalyst which meets economic criteria for a new two-step process from isobutane to TBA
- Have met three of four key economic criteria for a one-step process from isobutane to TBA
- Have made major advances in catalyst and cost
- Have found a potential joint development partner having a major market position in MTBE from TBA
- Have shelved project pending upturn in fuel oxygenate outlook

# Catalyst Activity vs. Redox Potential

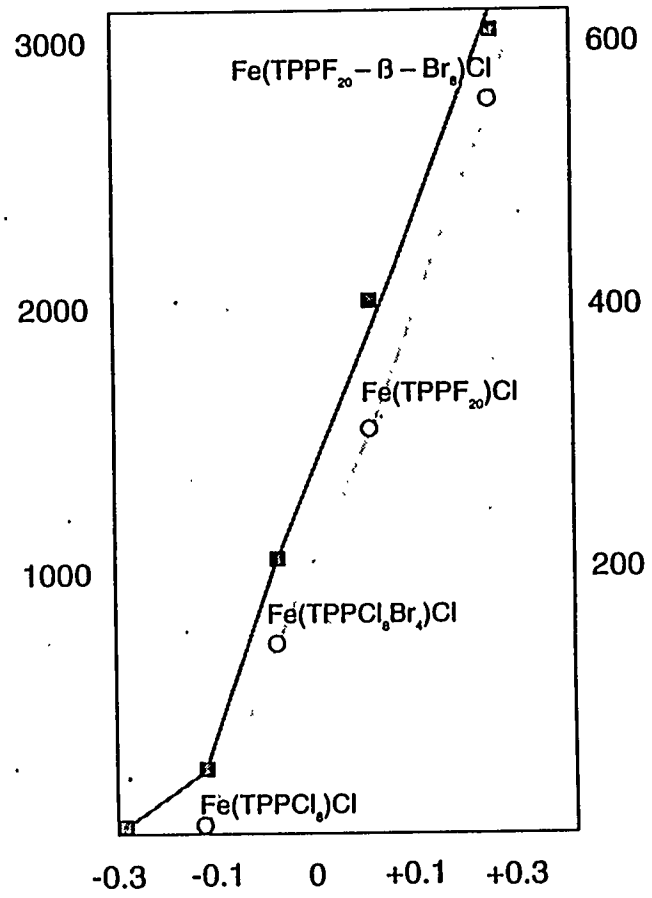


—□— Isobutane Oxidation at 80°C
Moles $O_2$ Consumed/
G • Atom Fe

—○— Propane Oxidation at 125°C
Moles Liquid Product/
G • Atom Fe

# Iron Haloporphyrin - Catalyzed Isobutane Oxidations[a]

| Catalyst | T. °C | T. Hrs | Charge to Reactor $i$-$C_4H_{10}$ | Charge to Reactor $O_2$ | Conversion $i$-$C_4H_{10}$% | Select TBA %[b] | TON[c] |
|---|---|---|---|---|---|---|---|
| $Fe(TPPF_{20}\beta\text{-}Br_8)Cl$ | 80 | 3 | 1870 | 53 | 17 | 87 | 10,660 |
| | 80 | 3 | 1862 | 100 | 28 | 83 | 17,150 |
| | 80 | 3 | 1865 | 47 | 14 | 91 | 8,420 |
| | 25 | 71.5 | 1862 | 53 | 22 | 92 | 13,560 |
| $Fe(TPPF_{20})OH$ | 24 | 143 | 1871 | 53 | 18 | 95 | 12,150 |

[a] Isobutane oxidized by an oxygen - containing gas (75 ATM, diluent = $N_2$), liq. phase (180 ml), 3 hours. $O_2$ added as used

[b] (Moles TBA/molls liquid product) x 100

[c] Models (TBA + acetone) produced/mole catalyst used

## 2B.2 Selective Methane Oxidation Over Promoted Oxide Catalysts

### CONTRACT INFORMATION

| | |
|---|---|
| **Contract Number** | DE-FG21-92MC29228 |
| **Contractor** | Lehigh University<br>Zettlemoyer Center for Surface Studies<br>and Department of Chemistry<br>Bethlehem, PA 18015<br>(215) 758-3577 or 758-3486 |
| **Contractor Project Managers** | Kamil Klier<br>Richard G. Herman |
| **Principal Investigators** | Kamil Klier<br>Richard G. Herman |
| **METC Project Manager** | Rodney D. Malone |
| **Period of Performance** | September 8, 1992 to September 7, 1995 |

### OBJECTIVES

The objective of this research is to selectively oxidize methane to $C_2$ hydrocarbons and to oxygenates, in particular formaldehyde and methanol, in high space time yields under milder reaction conditions than heretofore employed over industrially practical catalysts. In particular, air, carbon dioxide, or oxygen, rather than nitrous oxide, is being used as the oxidizing gas in a continuous flow reactor system and a wide range of reaction conditions, e.g. temperature, pressure, and gas hourly space velocity, is being explored to maximize the space time yields of the desired products. All of the investigated processes are catalytic and aimed at minimizing gas phase oxidation reactions.

### BACKGROUND INFORMATION

Saturated linear hydrocarbons, particularly methane, are major components of natural gas and of the gas produced by certain gasifiers. While methane makes an excellent gaseous fuel, it is desirable to convert it to higher molecular weight products for transportation, storage, and for utilization as chemical feedstocks. The desired reactions are shown below for methane only:

$$CH_4 + 0.5\ O_2 \rightarrow CH_3OH \qquad [1]$$

$$CH_4 + O_2 \rightarrow CH_2O + H_2O \qquad [2]$$

$$2CH_4 + O_2 \rightarrow C_2H_4 + 2H_2O \qquad [3]$$

$$2CH_4 + 0.5\ O_2 \rightarrow C_2H_6 + H_2O. \qquad [4]$$

Another reaction of potential interest is

$$2CH_4 + 2CO_2 \rightarrow C_2H_4 + 2CO + 2H_2O. \quad [5]$$

After Keller and Bhasin described their catalytic research for methane coupling to form $C_2$ hydrocarbons in 1982 (1), many laboratories have been striving to develop efficient methane conversion catalysts and technologies. At present, there is no commercial technology for processes represented by Equations [1]-[5], despite the sizeable patent and open literature on this subject. Various aspects of the state of the art of methane oxidation, including early developments, have been reviewed by Foster in 1985 (2), Gesser et al. in 1985 (3), Pitchai and Klier in 1986 (4), Scurrell in 1987 (5), Lee and Oyama in 1988 (6), Hutchings et al. in 1989 (7), Amenomiya et al. in 1990 (8), Lunsford in 1990, 1991, and 1993 (9-11), Mackie in 1991 (12), Hamid and Moyes in 1991 (13), and Krylov in 1993 (14). Therefore, the literature will not be extensively reviewed here.

## PROJECT DESCRIPTION

While the catalytic oxidative coupling paths [3] and [4] show considerable promise, it is evident from patent examples that the process conditions are still quite severe, in particular that the reaction temperatures of 650-800°C are still too high. Reactions leading to oxygenates (Equations [1] and [2]) are more difficult to conduct selectively, but they have been identified as being very desirable, particularly the oxidation to methanol (15). At the same time, the standard free energy of all the oxidations [1]-[4] is negative over a wide range of temperatures, establishing a thermodynamic driving force for these reactions even at room temperature should an effective catalyst be found. More practical considerations led us to seek a desirable temperature range of 350-650°C. The lower limit is based on experience with the dehydration of most oxide catalysts, which lose water at temperatures ≥350°C. The upper limit of 650°C is in the range of temperatures at which uncontrolled free radical reactions will occur and often will lower the selectivity by driving the oxidation process to CO and $CO_2$. Hence, it is desirable to investigate and develop catalysts that promote partial oxidations of methane to $C_2^+$ hydrocarbons, methanol, or formaldehyde in the temperature range of 350-650°C.

Oxide catalysts were chosen for this research that are surface doped with small amounts of acidic or redox dopants. It was proposed by us that, for example, the very basic $Sr/La_2O_3$ catalyst that is active in the formation of methyl radicals, and therefore of $C_2^+$ products (16,17), can be doped with acidic oxides or other acidic groups to increase further its activity and selectivity to $C_2$ products.

The research being carried out under this U.S. DOE-METC contract is divided into the following three tasks:

| | |
|---|---|
| Task 1. | Maximizing Selective Methane Oxidation to $C_2^+$ Products Over Promoted $Sr/La_2O_3$ Catalysts. |
| Task 2. | Selective Methane Oxidation to Oxygenates. |
| Task 3. | Catalyst Characterization and Optimization. |

Task 1 deals with the preparation, testing, and optimization of acidic promoted lanthana-based catalysts for the synthesis of $C_2^+$ hydrocarbons. Task 2 aims at the formation and optimization of promoted catalysts for the synthesis of oxygenates, i.e. formaldehyde and methanol. Task 3 involves characterization of the most promising catalysts so that optimization can be achieved under Tasks 1 and 2.

## RESULTS

### PART 1. Oxidative Coupling of Methane Over Sulfated-Doped $SrO/La_2O_3$ Catalysts

The basic 1 wt% $SrO/La_2O_3$ catalyst, with a surface area of 6.5 $m^2/g$ has been shown to be a very active methane coupling catalyst (16,17). AMOCO Corp. has prepared a large batch of this catalyst for further investigation and has provided portions of this catalyst to us for catalytic testing. We demonstrated the reproducibility of this catalyst for the conversion of methane from a $CH_4$/air = 1/1 reactant mixture at 0.1 MPa (1 atm) and with gas hourly space velocity (GHSV) = 70,000 ℓ/kg catal/hr, wherein both the molar conversion of $CH_4$ and the %yield of $C_2$ products increased as the temperature was increased in the range of 500 to 675°C (18-20).

### Experimental

In this program of research, the $SrO/La_2O_3$ catalyst was modified by surface doping with sulfate as described elsewhere (18-20). These $SO_4^{2-}/SrO/La_2O_3$ catalysts were produced by the incipient wetness impregnation technique. The appropriate amount of $(NH_4)_2SO_4$ was dissolved in deionized water, the measured quantity of $SrO/La_2O_3$ was added, and the slurry was continuously stirred with a magnetic stirrer until dryness was achieved. This was followed by drying the solid overnight at 120°C and calcination in air at 600°C for 6 hr. Prior to catalytic testing, the samples were activated *in situ* under air (or $O_2$) flow at 500°C for 1 hr unless stated otherwise. The gases used in this study were zero grade purity and were used without further purification

Catalytic testing was carried out in a fixed-bed continuous-flow 9 mm OD (7 mm ID) quartz reactor using 0.1000 g of catalyst. The reactor narrowed to 5 mm ID below the catalyst bed to speed the removal of reaction products from the hot reactor zone. The testing system had two independently controlled inlet gas lines, and a reactant mixtures of $CH_4$/air = 1.0/1.0 or 1.5/1.0 were generally utilized at ambient pressure. The principal products analyzed by on-line sampling of the exit gas using gas chromatography were $CO_2$, $C_2$ ($C_2H_6$ + $C_2H_4$), $C_3$ ($C_3H_8$ + $C_3H_6$), CO and $H_2O$.

### Results

It was shown that approximately 1 wt% $SO_4^{2-}$ doping produced the maximum increases in both the methane conversion level and the selectivity (C mol% basis) to $C_2$ products (18-20). It was also shown that the catalyst was stable in $CH_4$/air = 1/1 at 550°C for over 24 hr. At this temperature, the $CH_4$ conversion was ≈20 mol% (limited by the depletion of oxygen) and the selectivity was ≈50 C mol% to $C_2$ hydrocarbons and ≈50 C mol% to $CO_x$ (18).

Further testing has been carried out and comparisons among the catalysts have been made. This has involved testing a large number of $La_2O_3$-based catalysts, both promoted, i.e. $SrO/La_2O_3$ and $SO_4^{2-}/SrO/La_2O_3$, and unpromoted $La_2O_3$. Each catalyst was tested at 500°C, and then the reaction temperature was sequentially increased to 700°C and then decreased stepwise back to 500°C. To generalize with respect to the effect of the dopants, (i) promoting the $La_2O_3$ catalyst with SrO approximately doubled the conversion of methane and the selectivity to $C_2$ hydrocarbons, and (ii) promoting the $SrO/La_2O_3$ catalyst with $SO_4^{2-}$ approximately doubled the activity and $C_2$ selectivity again.

Figure 1 summarizes the experimental data and clearly shows that the selectivity

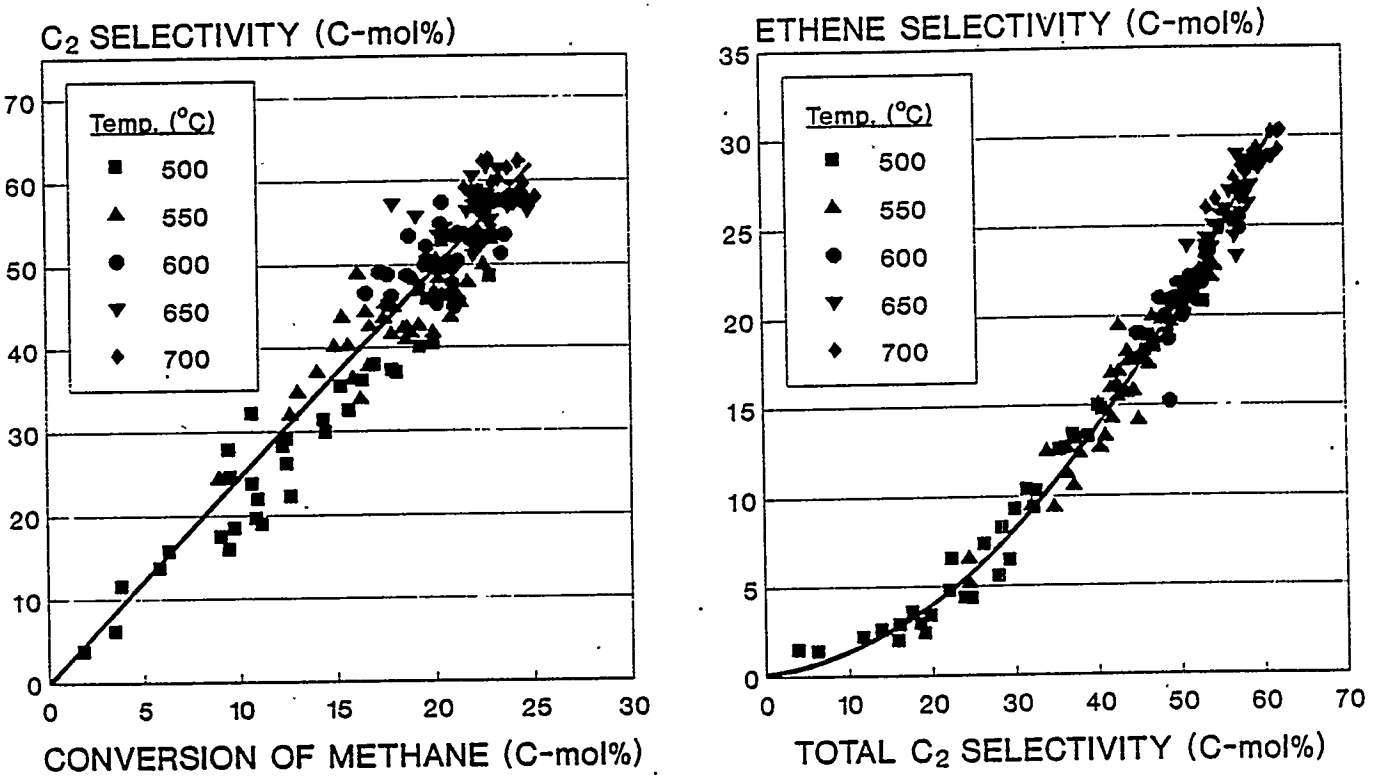


**FIGURE 1.** Correlations of the [A] $C_2$ Hydrocarbon Selectivity with Conversion of Methane and [B] Ethene Selectivity with the Total $C_2$ Hydrocarbon (Ethene + Ethane) Selectivity, where the Testing was carried out with a $CH_4$/air = 1/1 Reactant Mixture at 0.1 MPa and with GHSV = 70,000 ℓ/kg catal/hr. The Data Points Represent Steady State Experiments with $La_2O_3$, 1 wt% $SrO/La_2O_3$, and $SO_4^{2-}/SrO/La_2O_3$ Catalysts, where Sulfate Doping Levels of 1-4 wt% were Utilized. The Experiments were generally carried out by Stepwise Increasing the Reaction Temperature from 500°C to 700°C and then Stepwise Decreasing the Temperature back to 500°C.

toward formation of $C_2$ hydrocarbons is directly related to the level of conversion of the methane reactant, which is controlled by the reaction temperature and quantity of oxygen available. With respect to the synthesis of ethene relative to ethane, Figure 1 also shows that as the selectivity toward the $C_2$ hydrocarbons increased, the proportion of ethene formed increased significantly. For example, as the methane conversion approached 25%, ≈60 C mol% of the products were $C_2$ hydrocarbons, which exhibited a ethene/ethane molar ratio of 1/1.

It was recently stated (21) that successful catalysts for the synthesis of $C_2$ hydrocarbons by the oxidative coupling of methane would meet the following criteria:

1. Have high catalytic activity,
2. Exhibit high selectivity to $C_2$ hydrocarbons,
3. Operate at a reaction temperature between 400 and 600°C, and
4. Have long-term stability under reaction conditions.

The 1 wt% $SO_4^{2-}/SrO/La_2O_3$ catalyst reported here meets these criteria.

**PART 2. Methane Oxidation to Formaldehyde and Methanol Over Supported Oxide Catalysts.**

Since many supported metal oxide catalysts being studied for selective oxidation of methane utilize silica as a support (4,8,22-31), including the $Pd/SiO_2$ catalyst investigated during the previous project (29), the reactivities and selectivities of two common silica supports (fumed Cabosil and Grace 636 silica gel) were determined. These results have been presented previously (18,32). It was found that the ability of the silicas to activate methane below 700°C was low. However, above 700°C, appreciable conversion of methane and oxygen was observed, and the principal oxidation products produced depended on the reaction temperature. For example, lower reaction temperatures favored selectivities toward $CH_2O$ and CO, while higher temperatures, e.g. 780°C enhanced the formation of the $C_2$ hydrocarbons.

Part of the current research is directed to the direct synthesis of formaldehyde at lower reaction temperatures, e.g. 500-650°C, and this research is summarized here.

**Experimental**

The fumed silica (Cabosil EH-5) was obtained from Aldrich with a surface area of 380 $m^2/g$. $TiO_2$ was obtained from Degussa (designated as P-25) and had a surface area of 55 $m^2/g$. $SnO_2$ was also employed as a support and was made from tin(II) acetate from Aldrich by hydrolysis; after calcination at 450°C, its surface area was 20 $m^2/g$.

The doped catalysts were prepared by the incipient wetness impregnation technique. The $TiO_2/SiO_2$ catalysts were prepared *via* a toluene solvent of titanium(IV) isopropoxide ($Ti[OCH(CH_3)_2]_4$) under a $N_2$ atmosphere, while the $V_2O_5$-containing catalysts were prepared using a methanol solution of vanadium(VI) triisopropoxide oxide ($VO[i\text{-}OC_3H_7]_3$) in a $N_2$ environment. $SnO_2/SiO_2$ samples were prepared from an aqueous solution of colloidal $SnO_2$ under ambient conditions. An aqueous solution of ammonium heptamolybdate ($(NH_4)_6Mo_7O_{24}\cdot 4H_2O$ from Matheson, Coleman, and Bell) was used for prepared the $MoO_3$-containing catalysts. After impregnation, each catalyst was dried at room temperature, heated at 120°C overnight, and then calcined at 500°C for 4 hr in flowing air. The metal oxide loading levels on the oxide supports are calculated on the basis of %weight.

Catalytic testing was carried out in the temperature range of 400-630°C in a fixed-bed continuous-flow 9 mm OD (7 mm ID) quartz reactor, and usually 25-200 mg of catalyst was used for each test. A reaction mixture of $CH_4$/air = 1.5/1.0 was used at ambient pressure, and usually a total flow rate (GHSV) of 70,000 ℓ/kg catal/hr was used, but a series of flow rates were employed with some of the catalysts.

The principal products analyzed by on-line sampling of the exit gas using gas chromatography were $CO_2$, $C_2$ ($C_2H_6$ + $C_2H_4$), $C_3$ ($C_3H_8$ + $C_3H_6$), CO and $H_2O$. Condensable water-soluble products, i.e. formaldehyde in particular, were collected in two water-filled scrubbers in series, the first was kept at room temperature and the second at 0°C. Methanol was analyzed by combined GC and GC/MS methods. Formaldehyde was quantitatively determined by the modified Romijn's iodometric titration method (33). The carbon mass balance was always better than 90% and usually better than 95%.

## Results

The conventional steady-state catalytic partial oxidation of methane using air as the oxygen source was carried out with each catalyst at ambient pressure, and the observed conversions and product selectivities for a set of reaction conditions are summarized in Table 1. The high reactant space velocity of 70,000 ℓ/kg catal/hr was used to remove the synthesized products, in particular the formaldehyde, quickly from the heated reaction zone so that secondary oxidizing reactions would be inhibited. Under the reaction conditions employed here, principally the use of reaction temperatures below 700°C, it was shown that the effects on the methane conversion by the reactor and the silica support (by using the empty reactor and the pure Cabosil support) were negligible. For the $SiO_2$ and $MoO_3/SiO_2$ testing, accurate analyses of the products, other than formaldehyde, were very difficult because of the low methane conversion levels.

Testing of the three materials used as catalyst supports demonstrated that the fumed $SiO_2$ exhibit low methane conversion activity. However, the only detectable product was formaldehyde, which resulted in the observed productivity of 24.3 g $CH_2O$/kg catal/hr. The titania was somewhat active for methane conversion, while the $SnO_2$ was very active. However, the latter two catalysts did not produce much formaldehyde, as shown in Table 1. Indeed, the $TiO_2$ catalyst produced predominantly CO, while the $SnO_2$ catalyst formed mainly $CO_2$.

Considering the silica-supported $MoO_3$, $V_2O_5$, $TiO_2$, and $SnO_2$ catalysts, it is clear from Table 1 that the 1 wt% $V_2O_5/SiO_2$ was by far the most active. In addition, an appreciable selectivity toward formaldehyde was obtained with this catalyst, which resulted in a very high formaldehyde productivity of 685 g $CH_2O$/kg catal/hr. At the same time, low selectivities toward $CO_2$ and $C_2$ hydrocarbons (HC) were observed. Adding 3 wt% $MoO_3$ to the 1 wt% $V_2O_5/SiO_2$ catalyst did not significantly alter the catalytic properties of the catalyst, as shown in Table 1, indicating that the $MoO_3$ did not cover the $V_2O_5$ nor influence its catalytic functioning. However, adding 3 wt% $TiO_2$ to the 1 wt% $V_2O_5/SiO_2$ catalyst greatly decreased the catalytic activity of the $V_2O_5/SiO_2$ catalyst but didn't alter the product selectivity.

Finally, Table 1 shows that supporting 1 wt% $V_2O_5$ on titania did not result in an active catalyst for methane conversion to formaldehyde. Supporting the $V_2O_5$ on $SnO_2$ did result in an active methane conversion catalyst (note the lower temperature of 530°C), but the predominant product was $CO_2$, as was observed for all $SnO_2$-containing catalysts tested under these reaction conditions.

<u>$V_2O_5/SiO_2$ Catalysts</u>. Selected data for $V_2O_5/SiO_2$ catalysts having three different doping levels of $V_2O_5$ are given in Table 2. Under the given reaction conditions, the silica support was quite inactive. The 3 wt% $V_2O_5/SiO_2$ catalyst was appreciably more active that the 1 wt% $V_2O_5/SiO_2$ catalyst, as indicated by the lower reaction temperature of 580°C used with the former catalyst. Table 2 shows that decreasing the contact time (doubling the GHSV in two steps) of the reactant mixture over the 3.0 wt% $V_2O_5/SiO_2$ catalyst at 580°C lower the methane conversion level but increased the space time yield of formaldehyde. Finally, increasing the dopant level to 5 wt% and increasing the reaction temperature to 630°C increased the methane conversion and increased the productivity of formaldehyde to 1.44 kg $CH_2O$/kg catal/hr. This increase was more of reflection of the higher reaction temperature than of the higher doping level because under comparable reaction conditions, it was shown that the 5 wt% $V_2O_5/SiO_2$ catalyst

TABLE 1. Methane Oxidation by Air From a $CH_4$/Air = 1.5/1.0 Reactant Mixture at 630°C (except as noted) and 0.1 MPa with GHSV = 70,000 ℓ/kg catal/hr Over $SiO_2$, $TiO_2$, and $SnO_2$ Supports and Supported Catalysts. In Addition to Methane Conversion, the Space Time Yield (STY) of Formaldehyde is Given, as well as the Selectivities (S) of the Products.

| Catalyst | $CH_4$ Conv. (mol%) | $CH_2O$ STY (g/kg/hr) | S $CH_2O$ | S $C_2$ HC | S CO | S $CO_2$ |
|---|---|---|---|---|---|---|
| $SiO_2$ = (F) | 0.05 | 24.3 | 100 | -- | -- | -- |
| $TiO_2$ | 1.55 | 17.6 | 2.3 | -- | 94.0 | 3.6 |
| $SnO_2$ (530°C) | 8.10 | 2.3 | 0.1 | -- | 8.9 | 90.4 |
| 2% $MoO_3$/(F) | 0.08 | 37.9 | 100 | -- | -- | -- |
| 1% $V_2O_5$/(F) | 9.52 | 685 | 15.7 | 1.7 | 76.4 | 6.3 |
| 3% $TiO_2$/(F) | 0.31 | 27.6 | 17.8 | -- | 71.1 | 11.1 |
| 3% $SnO_2$/(F) | 1.60 | 8.8 | 1.1 | 13.7 | 8.7 | 76.3 |
| 1% $V_2O_5$/ 3% $MoO_3$/(F) | 8.47 | 675 | 16.6 | 2.0 | 73.5 | 7.9 |
| 1% $V_2O_5$/ 3% $TiO_2$/(F) | 1.07 | 101 | 18.6 | -- | 76.6 | 4.8 |
| 1% $V_2O_5/TiO_2$ | 0.82 | 14.0 | 3.3 | 1.2 | 73.0 | 22.5 |
| 1% $V_2O_5/SnO_2$ (530°C) | 7.60 | -- | -- | -- | 13.4 | 83.6 |

exhibited lower activity than did the 3 wt% $V_2O_5$-doped catalyst.

The $V_2O_5/SiO_2$ catalysts were studied further to probe the activity of these catalysts as a function of vanadia doping level. This study was conducted so that the methane conversion level could be express in terms of turnover number (TON) per active site under differential conditions at constant temperature and pressure. Thus, the level of $CH_4$ conversion was maintained at a low and rather constant level for all of the catalysts tested by controlling the flow rates (GHSV) of the reactants.

The results are shown in Table 3 for $V_2O_5/SiO_2$ catalysts containing from 0.25 to 5.00 wt% $V_2O_5$. It is seen that a rather constant TON was obtained with these catalysts. This indicates that methane activation and conversion is a unimolecular reaction that requires only one active site.

**TABLE 2.** Methane Oxidation by Air From a $CH_4$/Air = 1.5/1.0 Reactant Mixture Over Different $V_2O_5/SiO_2$ Catalysts at 0.1 MPa. In Addition to Methane Conversion, the Space Time Yield (STY) of Formaldehyde is Given.

| Catalyst | GHSV (ℓ/kg/hr) | Temp. (°C) | $CH_4$ Conv.# (mol%) | $CH_2O$ STY* (g/kg/hr) |
|---|---|---|---|---|
| $SiO_2$ = (F) | 70,000 | 630 | 0.05 | 24.3 |
| 1% $V_2O_5$/(F) | 70,000 | 630 | 9.52 | 685 |
| 3% $V_2O_5$/(F) | 70,000 | 580 | 10.04 | 614 |
| 3% $V_2O_5$/(F) | 140,000 | 580 | 6.86 | 1,022 |
| 3% $V_2O_5$/(F) | 280,000 | 580 | 2.67 | 1,220 |
| 5% $V_2O_5$/(F) | 280,000 | 630 | 5.60 | 1,440 |

#Methane conversion is limited by the availability of oxygen.
*The C-mol% selectivities did not vary appreciably as the space time yields varied over the $V_2O_5/SiO_2$ catalysts, i.e. 13.5-16.6% $CH_2O$ and 76.4-81.3% CO, with the remainder predominantly $CO_2$.

**TABLE 3.** Methane Conversion Turnover Numbers (TON) for Methane Oxidation by Air ($CH_4$/Air = 1.5/1.0) Over $V_2O_5/SiO_2$ Catalysts at 580°C and 0.1 MPa.

| $V_2O_5$ Loading (wt%) | 0.25 | 1.00 | 2.00 | 3.00 | 5.00 |
|---|---|---|---|---|---|
| GHSV (ℓ/kg/hr) | 16,200 | 70,000 | 140,000 | 350,000 | 280,000 |
| $CH_4$ Conv.# (mol%) | 1.7 | 1.0 | 1.1 | 0.8 | 1.1 |
| TON ($10^{-2}s^{-1}$) | 6.8 | 4.5 | 5.0 | 5.9 | 3.8 |

#Methane conversion was maintained at a relatively constant moderate value by variation of the reactant flow rate in order to compare the experimental TON as a function of promoter loading.

Effect of Steam in the Reactant Mixture. Based on the proposal by us (4,32) and others (22,34) that it is the methoxy intermediate that gives rise to formaldehyde, it was thought that hydrolysis of this intermediate should result in the formation of methanol. Therefore, experiments were carried out in which water was injected into the reactant gas stream just above the perheater section of the reactor. The preheater section of the reactor was filled with Pyrex beads, and in this section the water was vaporized into steam and mixed with the $CH_4$/air reactants as they were heated to the reaction temperature before reaching the catalyst.

Since the 1 wt% $V_2O_5/SiO_2$ catalyst was an active catalyst and produced a high space time yield of formaldehyde, it was utilized in this study. The first experiments involved injecting a small steady state quantity of steam into the reactant mixture and determining the effect of temperature on the productivity of the selectively formed oxygenates. The results are summarized in Figure 2, where it is shown that an appreciable space time yield of methanol was formed at temperatures higher than 600°C, e.g. ≈60 g $CH_3OH$/kg catal/hr at 625°C. At the same time, high productivity of formaldehyde was also observed. Therefore, the presence of steam over the catalyst did enhance the formation of methanol.

## Conclusions

Among the dispersed metal oxide catalysts studied for the selective oxidation of methane, the most active catalyst was clearly $V_2O_5/SiO_2$. These high surface area silica-based catalysts impregnated with 1-5 wt% $V_2O_5$ were also found to exhibit low selectivities toward $CO_2$. Although CO was the major product, appreciable selectivities toward formaldehyde were also observed. Indeed, with the $V_2O_5/SiO_2$ catalysts, very high space time yields of formaldehyde of >1 kg $CH_2O$/kg catal/hr) could be obtained even though the conventional single pass %yields were <2%. These results were obtained at relatively high GHSV (70,000-280,000 ℓ/kg catal/hr) but moderate temperatures (530-630°C). Utilizing steam in the $CH_4$/air reactant mixture led to the formation of methanol over the $V_2O_5/SiO_2$ catalyst in the same GHSV and temperature ranges.

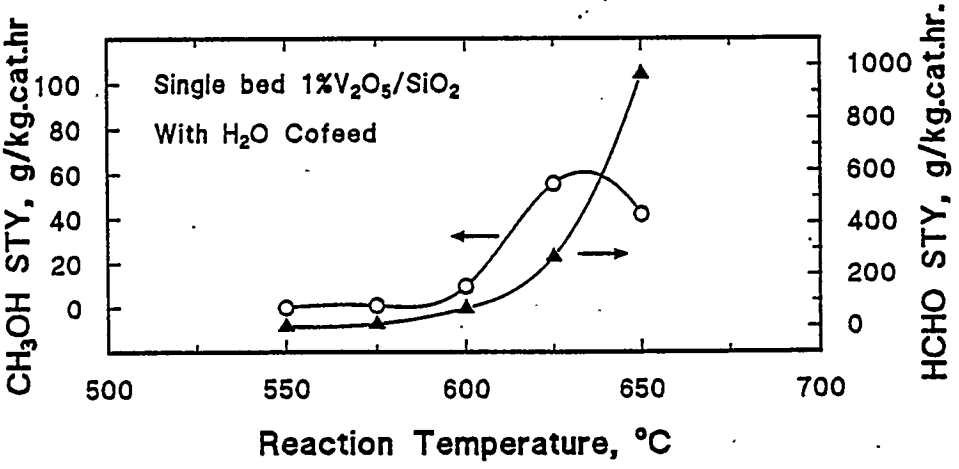


**FIGURE 2.** Space Time Yields of Methanol and Formaldehyde Over 0.1 g of 1 wt% $V_2O_5/SiO_2$ Catalyst at 0.1 MPa. The Reactant Mixture Consisted of $CH_4$/Air/Steam = 140/96/20 with GHSV = 153,600 ℓ/kg catal/hr.

PART 3. Formation of Methanol and Formaldehyde From Methane Over Double Bed Catalysts

Since we have developed (i) a very active catalyst for the synthesis of $C_2$ hydrocarbons from methane, which arise from methyl radicals generated by the catalyst [See PART 1], (ii) a very active catalyst for the synthesis of formaldehyde from methane [see PART 2], and (iii) a process of using steam in the reactant $CH_4$/air mixture that led to the formation of a significant quantity of methanol [see PART 2], a reaction system combining these three technological advances was devised and tested for increasing the formation of methanol as a direct product formed *via* selective oxidation of methane.

This reactor system utilizes a double catalyst bed and is based on the concepts of

(i) the first catalyst bed of $SO_4^{2-}/SrO/La_2O_3$ generates methyl radicals,

(ii) the second catalyst bed traps the methyl radicals to form surface-held methoxy species, and

(iii) the steam in the reactant mixture hydrolyzes the methoxy intermediates to form methanol.

This reaction system is shown schematically in Figure 3.

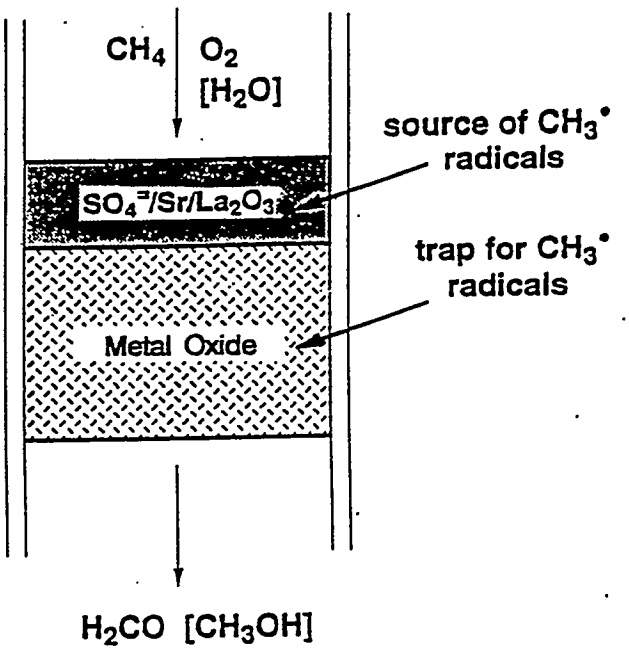


FIGURE 3. A Schematic Representation of the Double Bed Catalyst System Used to Convert Methane to Methanol.

While the first catalyst always consisted of the methyl radical generating $SO_4^{2-}/SrO/La_2O_3$ catalyst, a wide variety of unsupported and supported catalysts was tested as the second bed catalyst. Initial testing was carried out using equal quantities of the two catalysts (0.1 g of each) in each test. The total gas flow rate of GHSV = 72,000 ℓ/kg catal/hr is relative to the total quantity (mass) of the two catalysts present in the reactor. The methanol space time yields of some of these oxides are indicated in Figure 4, where the Mo, V, Cr, and Re oxides were prepared as silica-supported catalysts. As shown here, the most active catalyst and the catalyst that produced the most methanol under these reaction conditions was the 1 wt% $V_2O_5/SiO_2$ catalyst. Therefore, we continued our studies with this catalyst.

Using the 1 wt% $V_2O_5/SiO_2$ catalyst as the second bed catalyst and the $SO_4^{2-}/SrO/La_2O_3$ catalyst as the first bed catalyst, catalytic testing was carried out in the absence of steam in the reactant gas mixture. The resultant catalytic data are shown in Table 4 as a function of the reaction temperature employed. In all cases, high conversion levels of methane were obtained, which was limited by

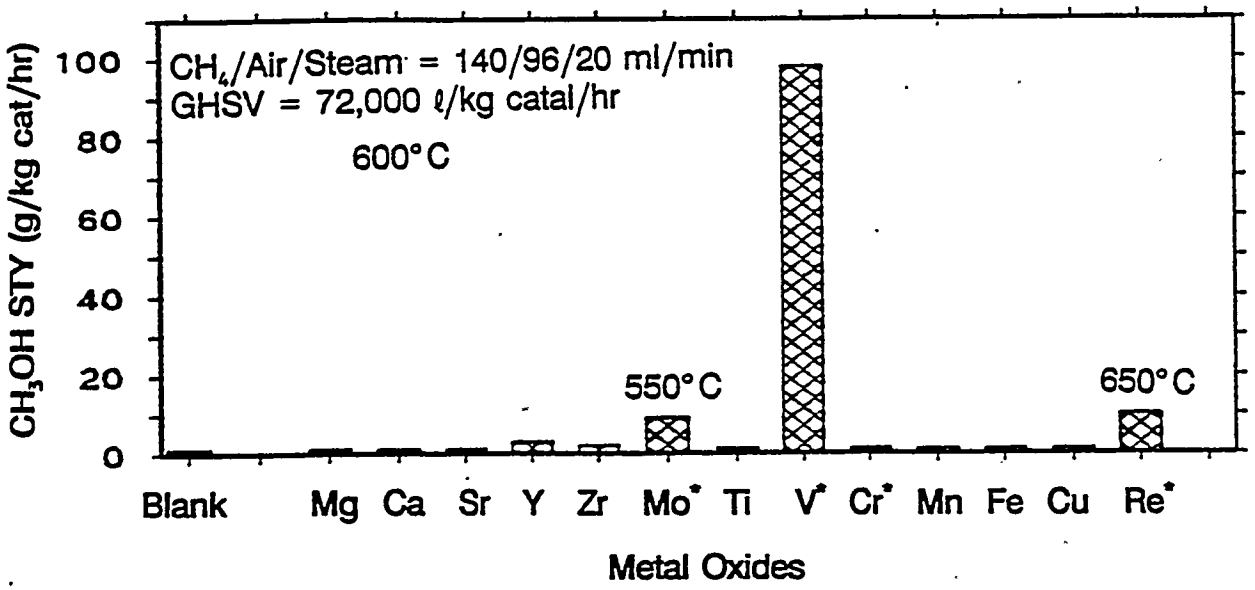


**FIGURE 4.** Methanol Space Time Yields (STY) Obtained From a $CH_4$/Air/Steam Reactant Mixture Over Double Bed Catalysts. The First Catalyst Bed Consisted of 0.1 g $SO_4^{2-}/SrO/La_2O_3$ and the Second Bed Consisted of 0.1 g of the Metal Oxide Catalysts. *Represents Silica-Supported Catalysts.

the availability of oxygen, but distinct differences in selectivities were observed as the temperature was increased from 550°C to 650°C. It is evident that as the reaction temperature was increased, the productivities of all products increased except for $CO_2$. In contrast to the single bed testing of the $V_2O_5/SiO_2$ catalyst where no $C_2$ hydrocarbons were generally observed in the product mixture, the double bed catalyst system produced significantly quantities of $C_2$ hydrocarbons. This is a reflection of the first bed catalyst consisting of $SO_4^{2-}/SrO/La_2O_3$, which generated methyl radicals that were coupled in the gas phase to form the $C_2$ hydrocarbons.

As the reaction temperature was increased stepwise, the methane conversion level gradually increased to a rather constant level of ≈15%, as shown in Table 4. At the same time, the oxygen conversion level followed the same increasing pattern, i.e. increasing from ≈67% to ≈88 mol% as the reaction temperature was increased.

Using fresh portions of the two catalysts, testing was carried out under the same reaction contitions but with the presence of steam in the reactant gas mixture. As indicated in Table 5, the space time yields of both methanol and formaldehyde were significant even at a reaction temperature of 550°C, a temperature at which the single bed $V_2O_5/SiO_2$ catalyst was inactive, as shown Figure 2. Indeed, the productivity of methanol from the double bed reactor reached a maximum of over 100 g/kg catal/hr at 600°C, and the productivity of formaldehyde reached over 1000 g/kg catal/hr at 625 and 650°C. From a comparison of Tables 4 and 5, it can be seen that injection of water into the reactant gas stream apparently retarded the conversion of methane to products to a small degree at the lower temperatures. However, the inhibition was not evident at

**TABLE 4.** The methane conversion and space time yields (STY) of products formed over the double catalyst bed in the absence of steam, where the first bed contained the $SO_4^{2-}/SrO/La_2O_3$ catalyst and the second bed consisted of 1 wt% $V_2O_5/SiO_2$. The bed of each catalyst was 0.10 g and the reactant mixture was steam-free $CH_4$/air ≈ 1.5/1 with GHSV = 141,000 ℓ/kg catal/hr relative to each catalyst and 70,500 ℓ/kg catal/hr for the double catalyst bed.

| Temp. (°C) | Conv. (mol%) | STY (g/kg.hr) | | | | |
|---|---|---|---|---|---|---|
| | | $C_2$ HC | HCHO | $CH_3OH$ | CO | $CO_2$ |
| 550 | 13.8 | 1575 | 167 | 16.8 | 2980 | 11275 |
| 575 | 14.5 | 1946 | 247 | 21.4 | 3586 | 10100 |
| 600 | 15.2 | 2720 | 434 | 38.9 | 3951 | 8165 |
| 625 | 15.5 | 3025 | 746 | 39.5 | 4232 | 6895 |
| 650 | 15.1 | 3577 | 940 | 48.0 | 4234 | 4491 |

**TABLE 5.** The conversion of methane and the space time yields (STY) of products formed over double bed catalysts in the presence of steam. The first bed contained the 1 wt% $SO_4^{2-}/SrO/La_2O_3$ catalyst and the second bed consisted 1 wt% $V_2O_5/SiO_2$. In each case, the bed of each catalyst was 0.10 g and the reactant stream was $CH_4$/air/steam ≈ 1.5/1.0/0.2, with GHSV = 153,000 ℓ/kg catal/hr relative to each catalyst bed and 76,500 ℓ/kg catal/hr for the double catalyst bed.

| Temp. (°C) | Conv. (mol%) | STY (g/kg.hr) | | | | |
|---|---|---|---|---|---|---|
| | | $C_2$ HC | HCHO | $CH_3OH$ | CO | $CO_2$ |
| 550 | 11.1 | 1438 | 210 | 31.4 | 2574 | 8136 |
| 575 | 11.9 | 1782 | 576 | 70.2 | 3228 | 6661 |
| 600 | 12.8 | 2690 | 739 | 104.5 | 3537 | 4687 |
| 625 | 15.3 | 3303 | 1082 | 86.4 | 3815 | 5842 |
| 650 | 14.8 | 3614 | 1248 | 89.1 | 3876 | 3967 |

625°C. Although not given, the conversions of the oxygen reactant corresponding to the data in Table 5 increased from ≈67% to ≈88 mol% as the temperature was increased from 500 to 650°C.

Comparison of the data in Tables 4 and 5 also demonstrates that much higher productivities of the HCHO and $CH_3OH$ oxygenates were obtained in the presence of steam in the reactant gas mixture (Table 5). Therefore, the presence of steam is necessary in order to achieve high productivities of methanol. This is demonstrated graphically in Figures 5A and 5B, where the space time yields of methanol and formaldehyde are shown for the testing in the absence of steam and in the presence of steam, respectively, in the $CH_4$/air ≈ 1.5/1.0 reactant gas mixture.

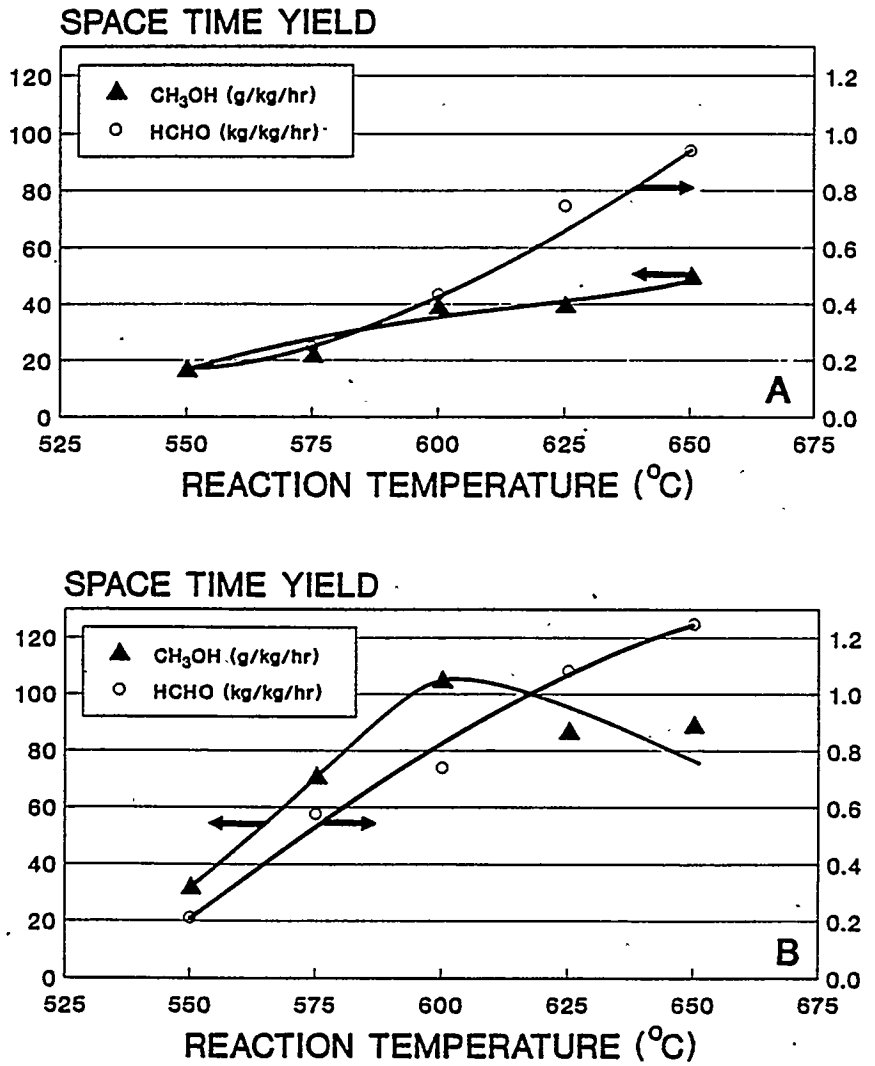


**FIGURE 5.** The Space Time Yields of Methanol and Formaldehyde Over the Double Bed $SO_4^{2-}/SrO/La_2O_3||V_2O_5/SiO_2$ Catalyst System with a $CH_4$/Air Reactant Mixture Flowing at a Rate of 140/96 ml/min, Respectively, that [A] Contained No Steam or [B] Contained Steam Flowing at a Rate of 20 ml/min. See Tables 4 and 5 for Additional Details.

Directions for Optimization. There are several directions in which this reaction system can be optimized. These include optimization of the amount of steam in the reactant gas mixture, the relative sizes of the two catalyst beds, reconfiguration of the reactor so that the primary products are removed from the hot reactor zone (which can be balanced with the gas hourly space velocity), pressure at which the reaction is carried out, and surface areas of the two catalysts.

With the double bed catalyst system, it has been found that the relative sizes of the two catalyst beds are important. With 1 wt% $Re_2O_7/SiO_2$ as the second bed, it has been found that the highest space time yield of methanol was obtained when the first $SO_4^{2-}/SrO/La_2O_3$ catalyst bed was half the weight of the second oxide catalyst bed. These studies are being continued.

Utilizing a $V_2O_5/SiO_2$ catalyst in a single bed, an example of the optimization procedure is examining the effect of increased partial pressure of steam. It has been determined that the amount of steam in the reactant gas mixture is an important variable that affects the conversion of methane, as well as the selectivities of the products. A demonstration of this is shown in Tables 6A and 6B. As the quantity of steam in the reactant mixture was increased to very large proportions, the methane conversion decreased. However, at the same time the selectivities toward CO and $CO_2$ decreased while those toward $CH_3OH$ and $CH_2O$ increased significantly. This was reflected in the higher space time yields obtained for methanol and formaldehyde. Indeed, the space time yields of methanol obtained when the reactant gas mixture consisted of approximately $CH_4$/air/steam ≈ 1.5/1/1 and 1.5/1/1.5 are perhaps the highest ever obtained for a catalytic process under steady state conditions.

Further optimization studies with both single bed and with double bed catalyst reaction systems are being carried out so that the product selectivity is shifted further toward methanol and/or formaldehyde and that the space time yields of these oxygenates are increased to even higher levels.

## OVERALL SUMMARY CONCLUSIONS

Principal accomplishments have been achieved in all three areas of selective catalytic oxidation of methane that have been pursued in this research project. These accomplishments are centered on the development of catalyst systems that produce high space time yields of $C_2$ hydrocarbon products, formaldehyde, and methanol from methane/air mixtures at moderate temperatures and at ambient pressure. The accomplishments can be summarized as the following:

- the $SO_4^{2-}/SrO/La_2O_3$ catalyst developed here has been further optimized to produce 2 kg of $C_2$ hydrocarbons/kg catalyst/hr at 550°C,
- $V_2O_5/SiO_2$ catalysts have been prepared that produce up to 1.5 kg formaldehyde/kg catalyst/hr at 630°C with low $CO_2$ selectivities, and
- a novel dual bed catalyst system has been designed and tested that produces over 100 g methanol/kg catalyst/hr at 600°C.

Further optimization, especially of the methanol synthesis catalyst system, needs to be carried out with these stable oxide catalysts.

**TABLE 6A.** The Methane Conversions Observed Over a 2 wt% $V_2O_5/SiO_2$ (0.1 g) at 0.1 MPa Pressure From a Reactant Mixture Consisting of $CH_4$/Air/Steam = 140/95/variable ml/min.

| Catalyst Test | Steam (ml/min) | GHSV (ℓ/kg/hr) | Temp (°C) | %$CH_4$ Conv. |
|---|---|---|---|---|
| c | 40 | 165,000 | 600 | 11.1 |
| h | 80 | 189,000 | 600 | 6.30 |
| i | 80 | 189,000 | 625 | 8.90 |
| k | 160 | 237,000 | 625 | 4.43 |

**TABLE 6B.** The Methane Conversions, Space Time Yields (STY) of Methanol and Formaldehyde, and the Product Selectivities Observed Over a 2 wt% $V_2O_5/SiO_2$ (0.1 g) at 0.1 MPa Pressure From $CH_4$/Air/Steam = 140/95/variable ml/min.

| Test | Steam | STY (g/kg cat/hr) | | Selectivities (C-mol%) | | | |
|---|---|---|---|---|---|---|---|
| No. | (ml/min) | $CH_3OH$ | HCHO | $CH_3OH$ | HCHO | CO | $CO_2$ |
| c | 40 | 72.0 | 795.2 | 0.7 | 8.0 | 81.9 | 9.4 |
| h | 80 | 181.4 | 795.1 | 2.9 | 23.8 | 76.4 | 6.9 |
| i | 80 | 211.4 | 1241.9 | 2.5 | 15.4 | 74.9 | 7.2 |
| k | 160 | 276.4 | 1281.6 | 6.1 | 30.3 | 54.9 | 8.7 |

## FUTURE WORK

Our research will proceed according to our Year 3 work plan, as described in the **PROJECT DESCRIPTION.** We have finished work under Task 1 with the acid promoted $SrO/La_2O_3$ catalyst that we have shown to be a very active and selective catalyst for the oxidative coupling of methane to ethane and ethene under moderate reaction conditions.

Under Task 2, the objective is to direct methane conversion to the selective formation of oxygenates, especially methanol and formaldehyde. This has involved studying new catalysts and determining the influence of reaction conditions, such as reactant flow rate and gas phase additives such as steam, on enhancing the selectivity toward oxygenates. Catalysts that exhibit high productivities of formaldehyde and of methanol have been

developed. During the remainder of this project, our efforts will be directed toward further improvement in the selectivity of methanol formation directly from methane. Research under Task 3, which involves catalyst characterization and optimization of these very promising catalysts, is being continued in order to obtain the best industrially practical catalysts for the synthesis of oxygenates from methane.

## ACKNOWLEDGEMENTS

This research was partially supported by the AMOCO Corp. under the AMOCO University Natural Gas Conversion Program, and we appreciate receiving the $SrO/La_2O_3$ catalyst from the AMOCO Corp. Most of this experimental research was carried out by Dr. Chunlei Shi, Dr. Qun Sun, Dr. János Sárkány, and Dr. Chuan-Bao Wang.

Further details of this research are provided in quarterly progress reports DOE/MC/29228-5 (January 1994) through -10 (March 1995).

## REFERENCES

1. G. E. Keller and M. M. Bhasin, J. Catal., 73, 9 (1982).
2. N. R. Foster, Appl. Catal., 19, 1 (1985).
3. H. D. Gesser, N. R. Hunter, and C. B. Prakash, Chem. Rev., 85(4), 235 (1985).
4. R. Pitchai and K. Klier, Catal. Rev.-Sci. Eng., 28, 13 (1986).
5. M. S. Scurrell, Appl. Catal., 32, 1 (1987).
6. J. S. Lee and S. T. Oyama, Catal. Rev.-Sci. Eng., 30, 249 (1988).
7. G. J. Hutchings, M. S. Scurrell, and J. R. Woodhouse, Chem. Soc. Rev., 18, 251 (1989).
8. Y. Amenomiya, V. I. Birss, M. Goledzinowski, J. Galuska, and A. R. Sanger, Catal Rev.-Sci. Eng., 32, 163 (1990).
9. J. H. Lunsford, Catal. Today, 6, 235 (1990).
10. J. H. Lunsford, in "*Natural Gas Conversion*" (Studies in Surface Science and Catalysis, Vol. 61), ed. by A. Holmen, K.-J. Jens and S. Kolboe), Elsevier, New York, 3 (1991).
11. J. H. Lunsford, in "*New Frontiers in Catalysis*" ed. by L. Guczi, Elsevier, New York, 103 (1993).
12. J. C. Mackie, Catal. Rev.-Sci. Eng., 33, 169 (1991).
13. H. B. A. Hamid and R. B. Moyes, Catal. Today, 10, 267 (1991).
14. O. V. Krylov, Catal. Today, 18, 209 (1993).
15. F. M. Dautzenberg, in Preprints, Symp. on Methane Activation, Conversion, and Utilization, PACIFICHEM '89, Intern. Chem. Congr. of Pacific Basin Societies, Honolulu, HI, Paper No. 170, pp 163-165 (1989).
16. J. M. DeBoy and R. F. Hicks, Ind. Eng. Chem. Res., 27, 1577 (1988).
17. J. M. DeBoy and R. F. Hicks, J. Catal., 113, 517 (1988).

18. K. Klier and R. G. Herman, "Selective Methane Oxidation Over Promoted Oxide Catalysts," in "*Proceedings of the Fuels Technology Contractors' Review Meeting* (November 1993)," ed. by R. D. Malone, DOE/METC-94/1002 (NTIS/ DE94004065), pp 121-137 (1994).

19. J. Sárkány, Q. Sun, R. G. Herman, and K. Klier, Preprint, Div. Pet. Chem., ACS, 39(2), 226 (1994).

20. J. Sárkány, Q. Sun, R. G. Herman, and K. Klier, "Oxidative Coupling of Methane Over Sulfated $Sr/La_2O_3$ Catalysts," in "*Methane and Alkane Conversion Chemistry*," ed. by M. M. Bhasin and D. N. Slocum, Plenum Press, New York (1995); in press.

21. M. M. Bhasin and K. D. Campbell, Preprint, Div. Pet. Chem., ACS, 39(2), 266 (1994).

22. H.-F. Liu, R.-S. Liu, K. Y. Liew, R. E. Johnson, and J. H. Lunsford, J. Amer. Chem. Soc., 106, 4117 (1984).

23. K. J. Zhen, M. M. Khan, C. H. Mak, K. B. Lewis, and G. A. Somorjai, J. Catal., 94, 501 (1985).

24. S. Kasztelan and J. B. Moffat, J. Chem. Soc., Chem. Commun., 1663 (1987).

25. A. M. Gaffney, C. A. Jones, J. J. Leonard, J. A. Sofranko, and H. P. Withers, in "*Catalysis 1987*," ed. by J. W. Ward, Elsevier, Amsterdam, 523 (1988).

26. N. D. Spencer, J. Catal., 109, 187 (1988).

27. N. D. Spencer and C. J. Pereira, J. Catal., 116, 399 (1989).

28. S. Ahmed and J. B. Moffat, J. Catal., 118, 281 (1989).

29. K. Klier and R. G. Herman, "Methane Oxidation Over Dual Redox Catalysts," in "Proceedings of the Natural Gas Research and Development Contractors' Review Meeting (May 1992)," ed. by R. D. Malone, H. D. Shoemaker, and C. W. Byrer, DOE/METC-92/6125 (DE92001278), pp 251-265 (1992).

30. Q. Sun, J. I. Di Cosimo, R. G. Herman, K. Klier, and M. M. Bhasin, Catal. Letters, 15, 371 (1992).

31. Q. Sun, J.-M. Jehng, H. Hu, R. G. Herman, I. E. Wachs, and K. Klier, "Partial Oxidation of Methane by Molecular Oxygen Over Supported $V_2O_5$ Catalysts: A Catalytic and *in situ* Raman Spectroscopy Study," in "*Methane and Alkane Conversion Chemistry*," ed. by M. M. Bhasin and D. N. Slocum, Plenum Press, New York (1995); in press.

32. Q. Sun, R. G. Herman, and K. Klier, Catal. Letters, 16, 251 (1992).

33. J. F. Walker, "*Formaldehyde*," Reinhold, New York, 489 1964).

34. Y. Tong and J. H. Lunsford, J. Amer. Chem. Soc., 113, 4741 (1991).

# SELECTIVE METHANE OXIDATION OVER PROMOTED OXIDE CATALYSTS

Kamil Klier and Richard G. Herman

with

Chunlei Shi, Qun Sun, Chuan-Bao Wang
and Janos Sarkany

Zettlemoyer Center for Surface Studies
and Department of Chemistry
LEHIGH UNIVERSITY
Bethlehem, PA 18015

Supported by U.S. DOE-METC and AMOCO Corp.

# SELECTIVE METHANE OXIDATION OVER PROMOTED OXIDE CATALYSTS

RESEARCH TASKS:

- Maximizing Selective Methane Oxidation to $C_2$ Products Over Promoted $La_2O_3$ Catalysts
- Selective Methane Oxidation to Oxygenates
- Catalyst Characterization and Optimization

U.S. DOE-METC DE-FG21-92MC29228

# LU Goals for Partial Oxidation of Methane

- Low temperature catalytic conversion to methanol, formaldehyde, $C_2$ HC, $CO/H_2$
- Catalysts: surface-modified oxides
- Process Parameters: include temperature, effects of $CO_2$/steam, pressure, dual bed
- Surface Chemistry: understanding and control of surface dopants, morphology, surface carbon, states and fate of hydrogen and oxygen species, competitive kinetics, poisoning, and stability

# METHANE OXIDATION REACTOR SYSTEM

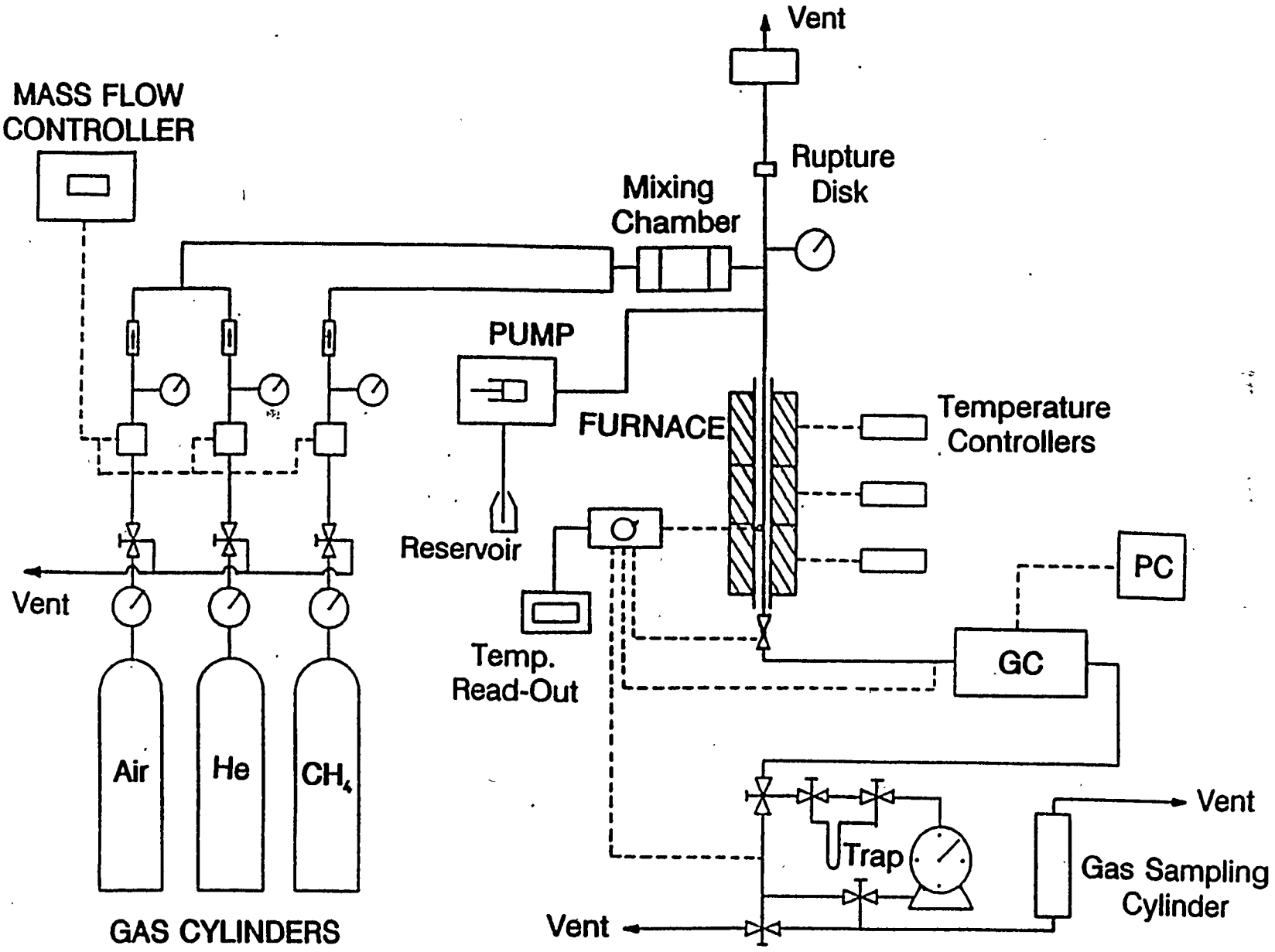

# High Activity Sulfate-Promoted $SrO/La_2O_3$ Catalysts for Selective Oxidation of Methane to $C_2$ Hydrocarbons

# CATALYTIC TEST STUDIES
## (Synthesis of $C_2$ Hydrocarbons)

- Temperature range of 500-700°C was used for testing most of the lanthana-based catalysts at ambient pressure (0.1 MPa).

- $CH_4$/Air = 1-1.5, typically GHSV = 70,000 l/kg catal/hr over 0.1-0.2 g of catalyst in a quartz tubular reactor (6-9 mm OD).

- $CO_2$, CO, $C_2H_6$, $C_2H_4$, $H_2O$ analyzed by GC; $CH_3OH$ by GC & GC/MS; $CH_2O$ by I titration.

# $C_2$ SELECTIVITY *vs* CONVERSION OF METHANE
## $CH_4$/AIR = 1/1 AT 0.1 MPa AND GHSV = 70,000 l/kg catal/hr. [$La_2O_3$, Filled; $SrO/La_2O_3$, Open]

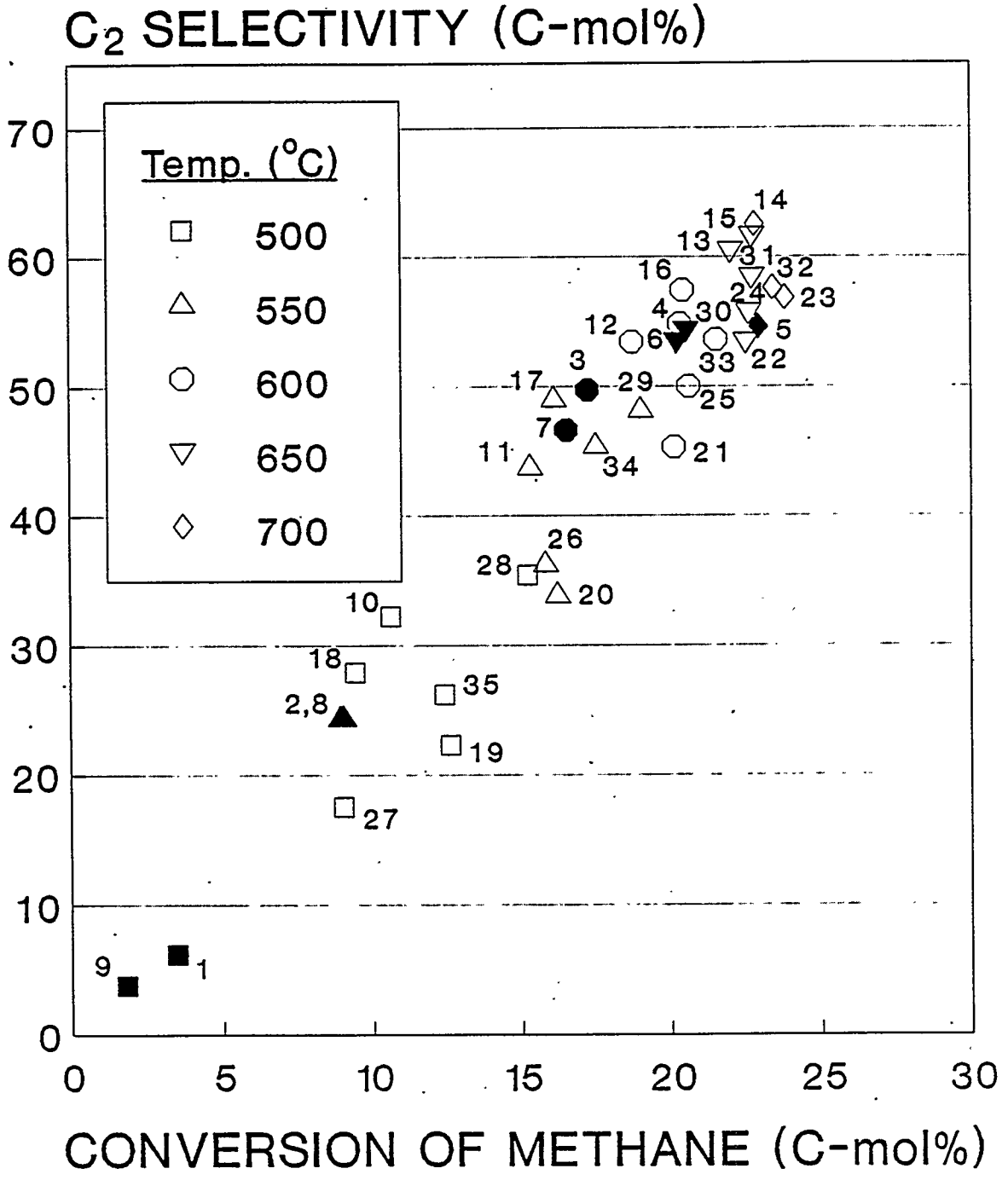

# $C_2$ SELECTIVITY *vs* CONVERSION OF METHANE OVER $SO_4^{2-}/SrO/La_2O_3$ CATALYSTS.

$CH_4$/AIR = 1/1, 0.1 MPa, 70,000 l/kg catal/hr

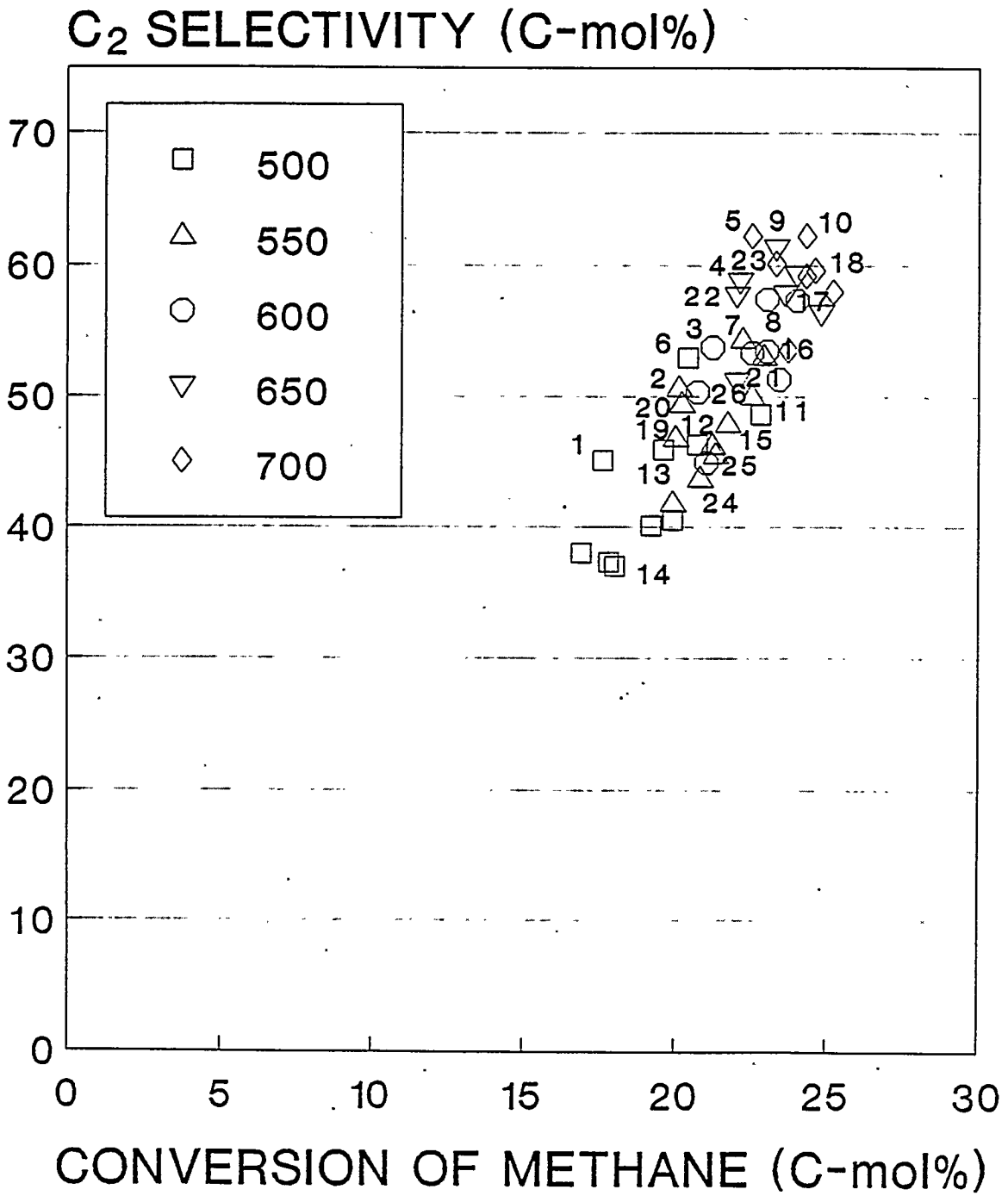

# Selectivity to $C_2^=$ and $C_2$ is a Function of Conversion Only

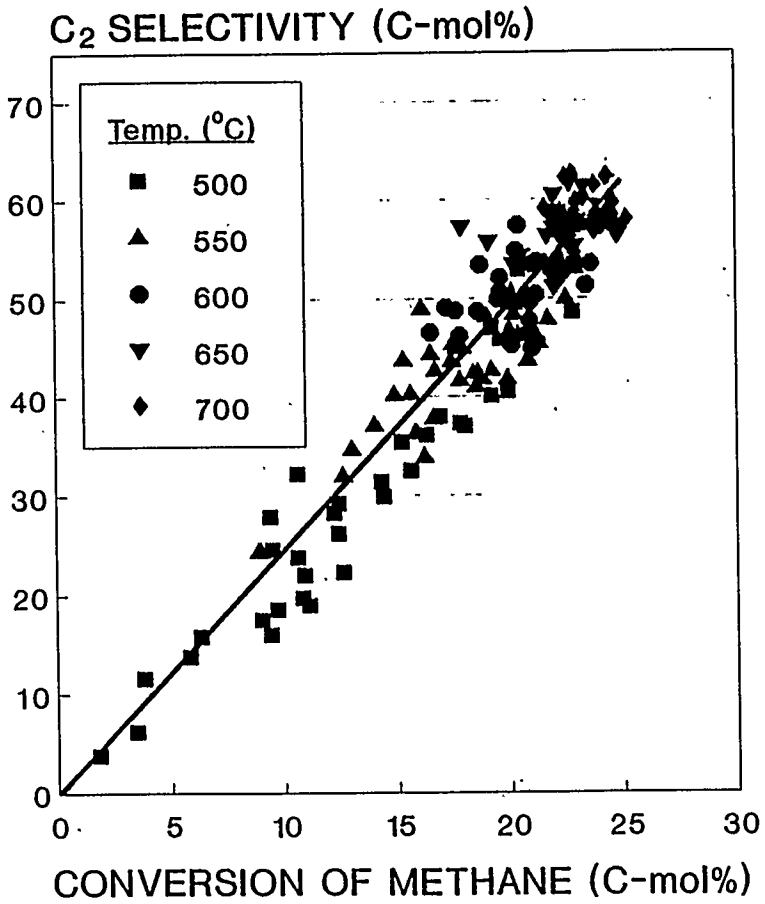


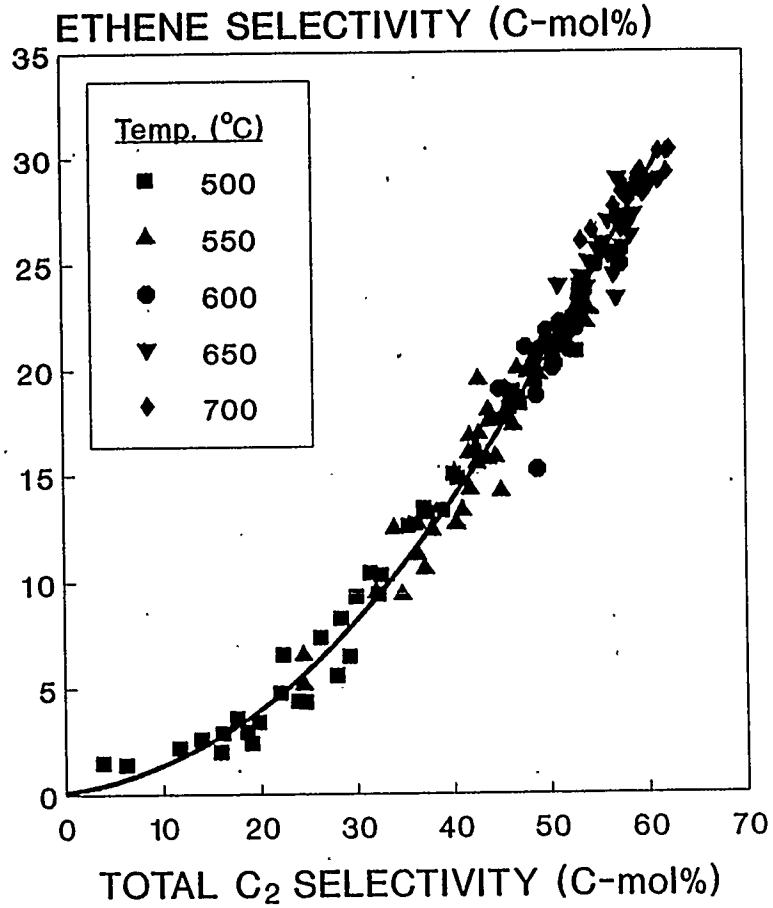

# ACTIVITY

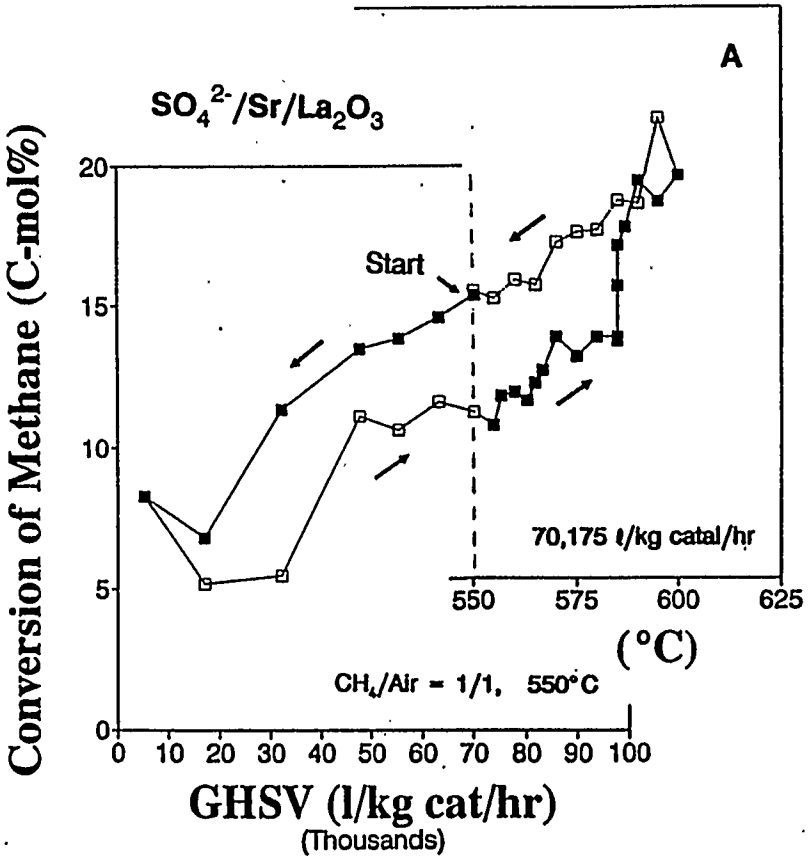


# $C_2$ SELECTIVITY

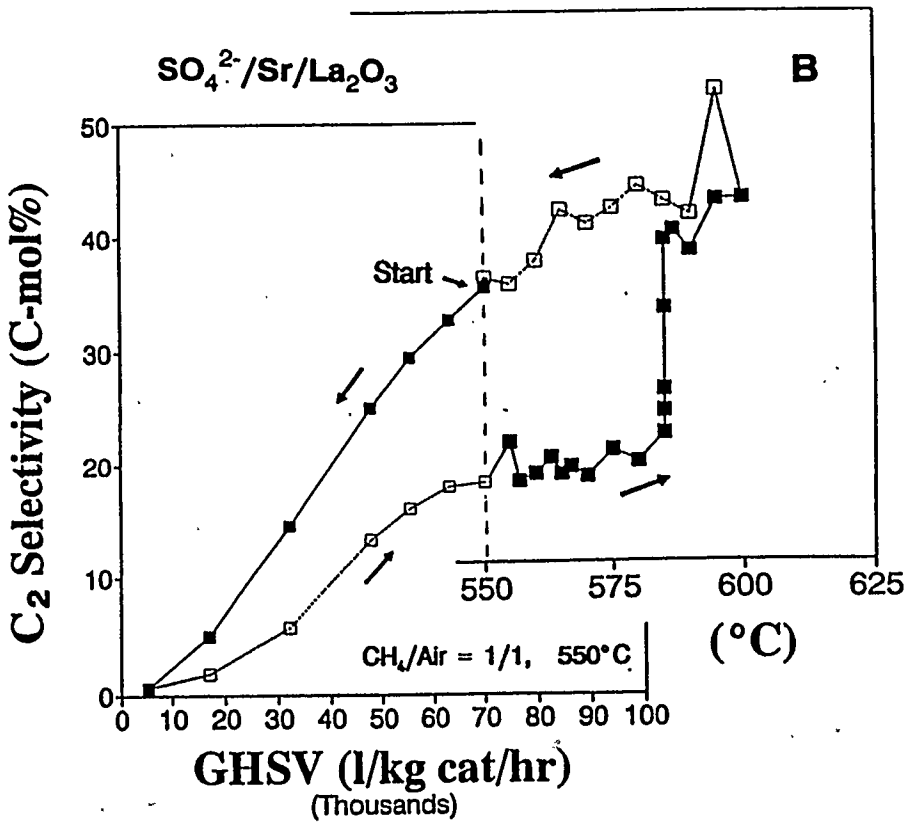

# SUCCESSFUL CATALYSTS FOR OXIDATIVE COUPLING OF METHANE*

- High Catalytic Activity
- High Selectivity to $C_2$ Hydrocarbons
- Operation at 400-600°C
- Long-term Catalyst Stability

*Bhasin, M. M. and Campbell, K. D., *Preprints, Div. Pet. Chem., ACS*, 39(2), 266 (1994).

# Single Bed and Double Bed Catalysts for Selective Oxidation of Methane to Formaldehyde and to Methanol

# CATALYTIC TEST STUDIES
## (Synthesis of Oxygenates)

- Temperature ranges of 500-650°C for oxides and 200-450°C for supported metals (2-4 hr at each temperature) and ambient pressure.

- $CH_4$/Air = 1-1.5, GHSV = 70,000-153,000 l/kg catal/hr over 0.1-0.2 g of catalyst in a quartz tubular reactor (6-9 mm OD).

- $CO_2$, CO, $C_2H_6$, $C_2H_4$, $H_2O$ analyzed by GC; $CH_3OH$ by GC & GC/MS; $CH_2O$ by I titration.

## Methane Oxidation by Air ($CH_4$/Air = 1.5/1.0) Over Supported Metal Oxide Catalysts at 630°C and 0.1 MPa with GHSV = 70,000 ℓ/kg/hr. [S = C-mol% Selectivity]

| Catalyst | $CH_4$ Conv. (mol%) | $CH_2O$ STY (g/kg/hr) | S $CH_2O$ | S $C_2$ HC | S CO | S $CO_2$ |
|---|---|---|---|---|---|---|
| $SiO_2$ = (F) | 0.05 | 24.3 | 100 | -- | -- | -- |
| $TiO_2$ | 1.55 | 17.6 | 2.3 | -- | 94.0 | 3.6 |
| $SnO_2$ (530°C) | 8.10 | 2.3 | 12.5 | -- | 82.2 | 5.3 |
| 2% $MoO_3$/(F) | 0.08 | 37.9 | 100 | -- | -- | -- |
| 1% $V_2O_5$/(F) | 9.52 | 685 | 15.7 | 1.7 | 76.4 | 6.3 |
| 3% $TiO_2$/(F) | 0.31 | 27.6 | 17.8 | -- | 71.1 | 11.1 |
| 3% $SnO_2$/(F) | 1.60 | 8.8 | 1.1 | 13.7 | 8.7 | 76.3 |
| 1% $V_2O_5$/ 3% $MoO_3$/(F) | 8.47 | 675 | 16.6 | 2.0 | 73.5 | 7.9 |
| 1% $V_2O_5$/ 3% $TiO_2$/(F) | 1.07 | 101 | 18.6 | -- | 76.6 | 4.8 |
| 1% $V_2O_5/TiO_2$ | 0.82 | 14.0 | 3.3 | 1.2 | 73.0 | 22.5 |
| 1% $V_2O_5/SnO_2$ (530°C) | 7.60 | -- | -- | -- | 13.4 | 83.6 |

# Methane Oxidation by Air ($CH_4$/Air = 1.5/1.0) Over $V_2O_5/SiO_2$ Catalysts at 0.1 MPa.

| Catalyst | GHSV (ℓ/kg/hr) | Temp. (°C) | $CH_4$ Conv.# (mol%) | $CH_2O$ STY* (g/kg/hr) |
|---|---|---|---|---|
| $SiO_2$ = (F) | 70,000 | 630 | 0.05 | 24.3 |
| 1% $V_2O_5$/(F) | 70,000 | 630 | 9.52 | 685 |
| 3% $V_2O_5$/(F) | 70,000 | 580 | 10.04 | 614 |
| 3% $V_2O_5$/(F) | 140,000 | 580 | 6.86 | 1,022 |
| 3% $V_2O_5$/(F) | 280,000 | 580 | 2.67 | 1,220 |
| 5% $V_2O_5$/(F) | 280,000 | 630 | 5.60 | 1,440 |

#Methane conversion is limited by the availability of oxygen.

*The C-mol% selectivities did not vary appreciably as the space time yields varied over the $V_2O_5/SiO_2$ catalysts; 13.5-16.6% $CH_2O$ and 76.4-81.3% CO.

# Methane Conversion Turnover Numbers (TON) for Methane Oxidation by Air ($CH_4$/Air = 1.5/1.0) Over $V_2O_5/SiO_2$ Catalysts at 580°C and 0.1 MPa.

| $V_2O_5$ Loading (wt%) | 0.25 | 1.00 | 2.00 | 3.00 | 5.00 |
|---|---|---|---|---|---|
| GHSV (ℓ/kg/hr) | 16,200 | 70,000 | 140,000 | 350,000 | 280,000 |
| $CH_4$ Conv.# (mol%) | 1.7 | 1.0 | 1.1 | 0.8 | 1.1 |
| TON ($10^{-2}s^{-1}$) | 6.8 | 4.5 | 5.0 | 5.9 | 3.8 |

#Methane conversion was maintained at a relatively constant moderate value in order to compare the experimental TON as a function of promoter loading.

**Unimolecular reaction requiring a single vanadia active site.**

# Space Time Yields of Formaldehyde and Methanol Over 1 wt% $V_2O_5/SiO_2$ Catalyst (0.1 g) From $CH_4$/Air/Steam = 140/96/20 ml/min (GHSV = 72,000 ℓ/kg catal/hr)

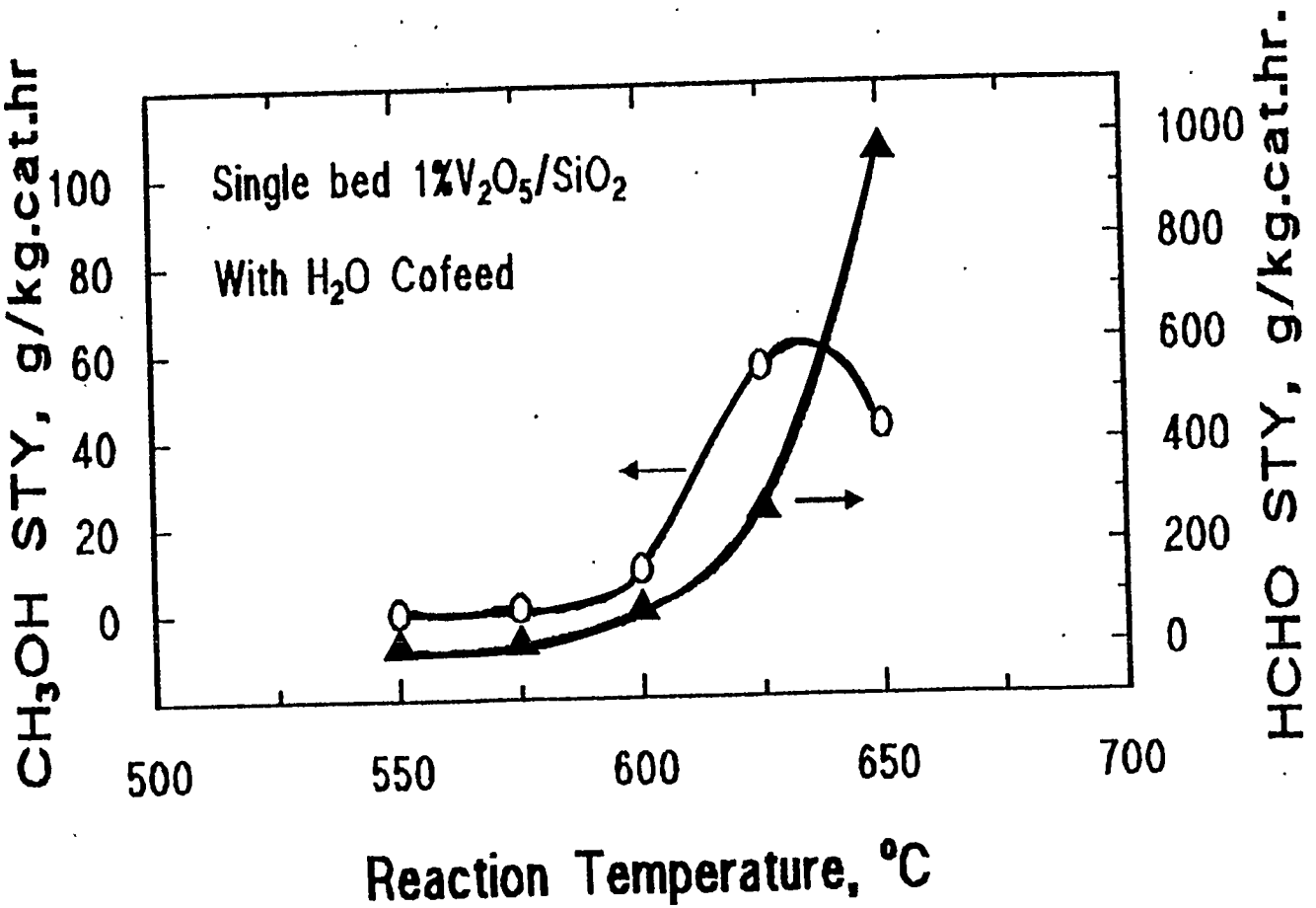

# Double bed experiment for methanol

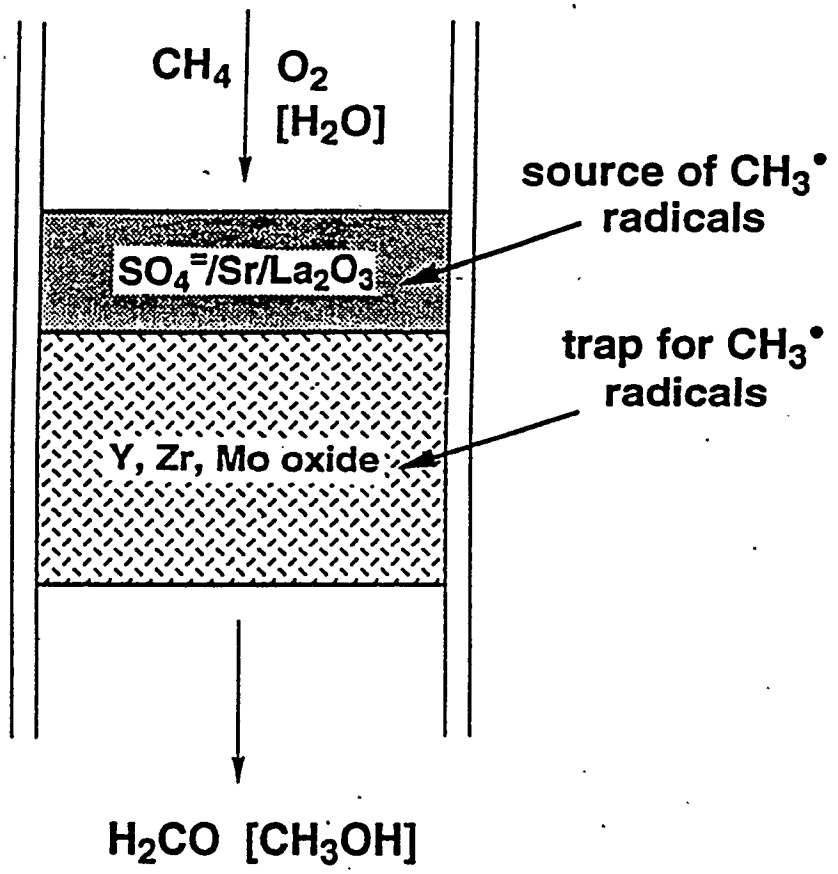


Chemistry: $CH_4 \xrightarrow[S/Sr/La]{} CH_3^{\bullet} \xrightarrow[O^{2-}]{} CH_3O^-$

$H_2O$

$CH_3OH$ $H_2CO$

**Space Time Yields of Methanol Over Double Bed Catalysts. The First Catalyst Bed Consisted of 0.1 g $SO_4^{2-}/SrO/La_2O_3$ and the Second Consisted of 0.1 g Metal Oxide Catalysts. * represents silica-supported catalysts.**

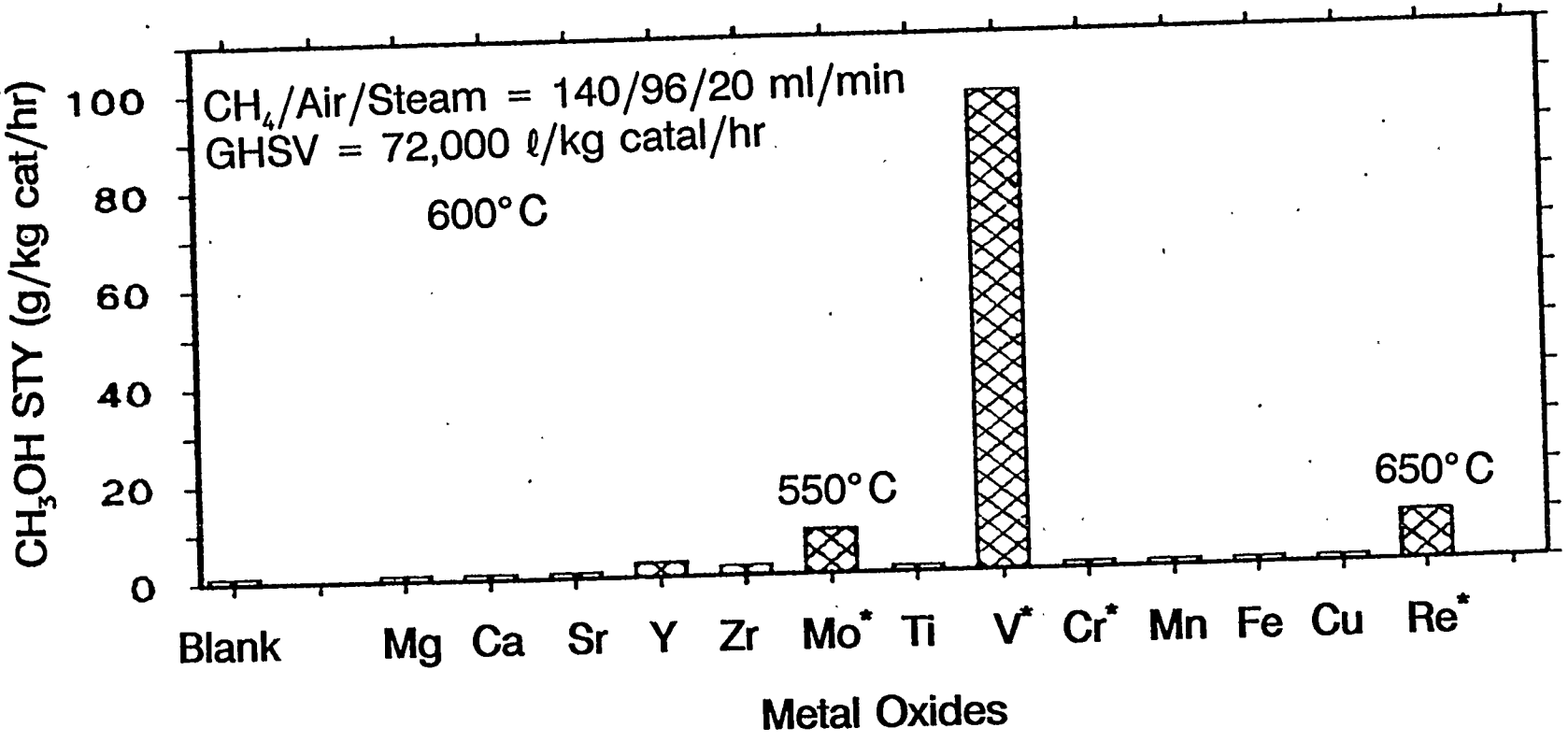

# Space Time Yields of $CH_3OH$ and HCHO Over $SO_4^{2-}/SrO/La_2O_3||V_2O_5/SiO_2$

## $CH_4$/Air = 140/96 ml/min

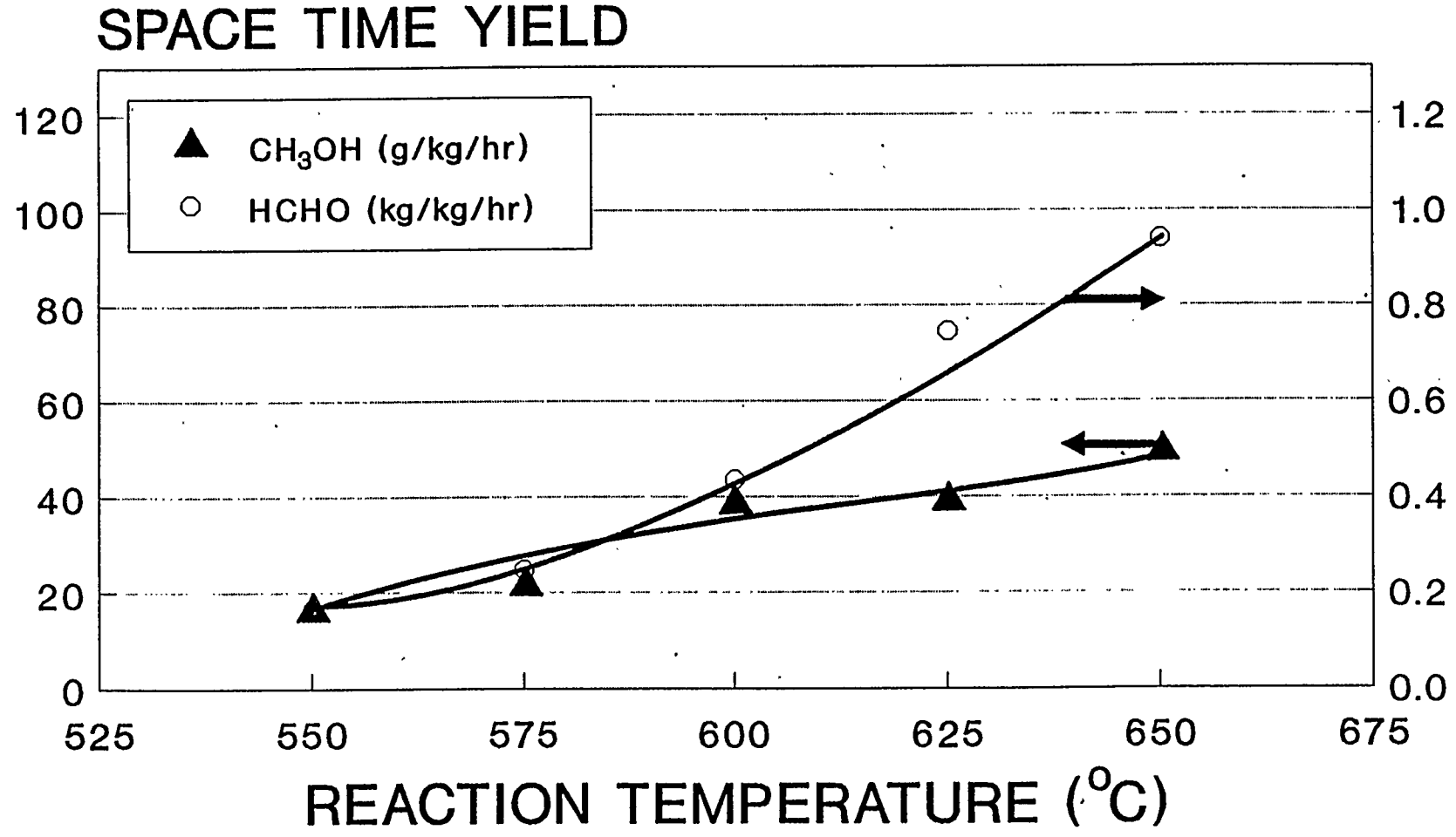

# Space Time Yields of $CH_3OH$ and HCHO Over $SO_4^{2-}/SrO/La_2O_3||V_2O_5/SiO_2$

## $CH_4$/Air/Steam = 140/96/20 ml/min

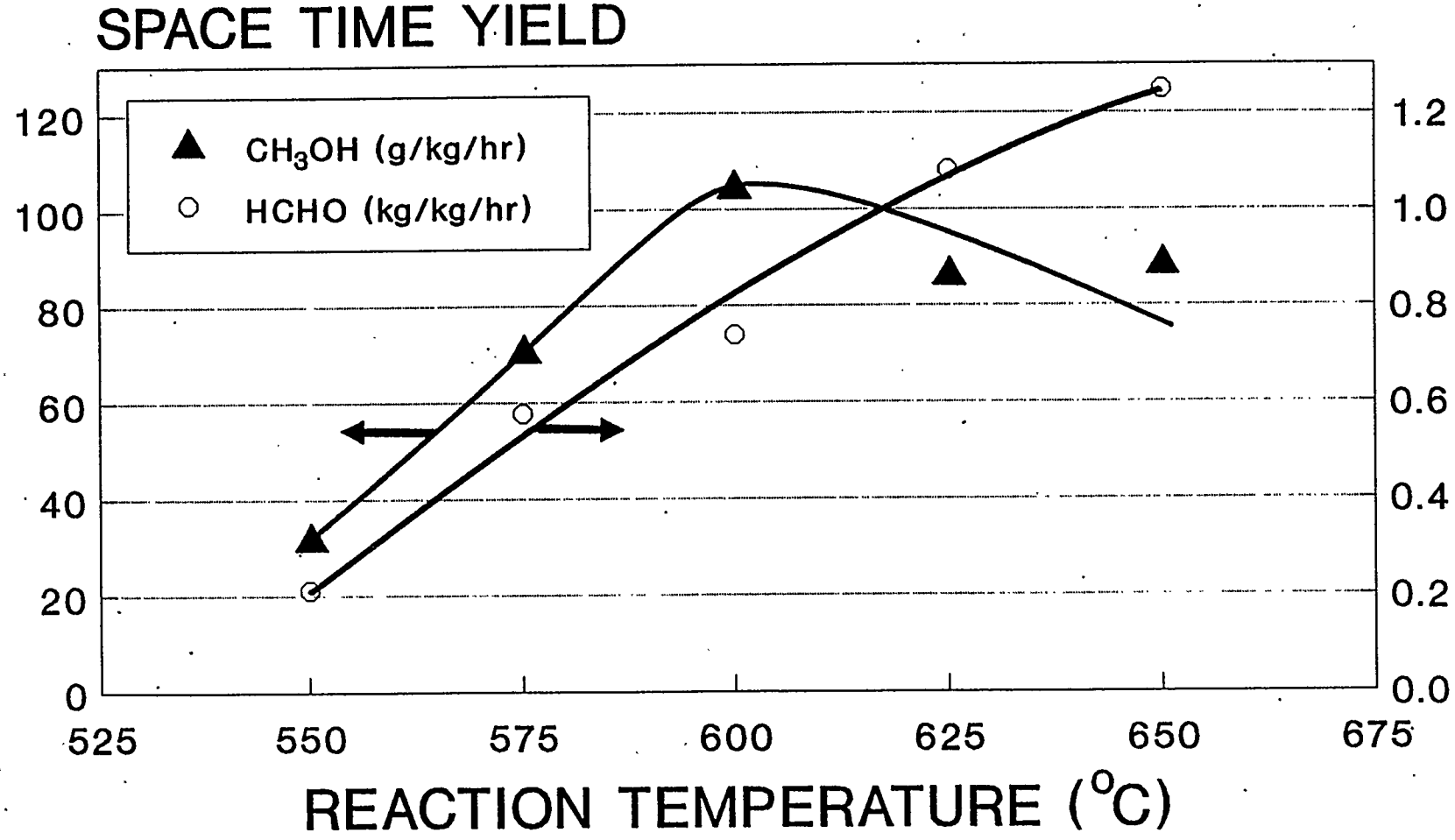

## Methane Conversions and Product Space Time Yields Over Double Bed[a] and Mixed Bed[b] 1 wt% $SO_4^{2-}$ /SrO/$La_2O_3$ (0.1 g) and 1 wt% $V_2O_5/SiO_2$ (0.1 g) Catalysts From $CH_4$/air/steam = 140/95/40 ml/min.

| Temp. (°C) | $CH_4$ Conv. (mol%) | Space Time Yields, g/kg cat/hr (Selectivities, mol%) | | | | |
|---|---|---|---|---|---|---|
| | | $C_2$ HC | HCHO | $CH_3OH$ | CO | $CO_2$ |
| 575[a] | 10.6 | 1782 (33.7) | 524 (4.8) | 78 (0.7) | 3195 (31.3) | 4729 (29.5) |
| 600[a] | 11.4 | 2497 (43.9) | 635 (5.4) | 96 (0.8) | 3214 (29.3) | 3552 (20.6) |
| 625[a] | 13.1 | 2988 (45.8) | 844 (6.3) | 105 (0.7) | 3325 (26.4) | 4140 (20.9) |
| 575[b] | 10.3 | 1812 (35.3) | 7 (0.1) | 23.5 (0.2) | 3354 (33.8) | 4770 (30.6) |
| 600[b] | 10.7 | 2568 (48.1) | 5 (0.1) | 38.4 (0.3) | 3012 (29.2) | 3598 (22.2) |
| 625[b] | 12.4 | 3074 (49.7) | 11 (0.1) | 48.5 (0.4) | 3120 (26.1) | 4442 (23.7) |

[a] Double bed: $SO_4^{2-}$/Sr/$La_2O_3$ was loaded on top of the $V_2O_5/SiO_2$ catalyst.
[b] Mixed bed: well-mixed $SO_4^{2-}$/Sr/$La_2O_3$ and $V_2O_5/SiO_2$ as a uniform bed.

# DIRECTIONS FOR OPTIMIZATION

**Methane Conversions, Product Space Time Yields, and Selectivities Over a 2 wt% $V_2O_5/SiO_2$ Catalyst (0.1 g) at 0.1 MPa Pressure From $CH_4$/Air/Steam = 140/95/variable ml/min.**

| Steam | Temp | $\%CH_4$ | STY (g/kg cat/hr) | | Selectivities (C-mol%) | | | |
|---|---|---|---|---|---|---|---|---|
| (ml/min) | (°C) | Conv. | $CH_3OH$ | HCHO | $CH_3OH$ | HCHO | CO | $CO_2$ |
| 40 | 600 | 11.1 | 72.0 | 795.2 | 0.7 | 8.0 | 81.9 | 9.4 |
| 80 | 600 | 6.30 | 181.4 | 795.1 | 2.9 | 23.8 | 76.4 | 6.9 |
| 80 | 625 | 8.90 | 211.4 | 1241.9 | 2.5 | 15.4 | 74.9 | 7.2 |
| 160 | 625 | 4.43 | 276.4 | 1281.6 | 6.1 | 30.3 | 54.9 | 8.7 |

# SUCCESSFUL CATALYSTS FOR OXYGENATE AND $C_2$ HC SYNTHESIS FROM METHANE

- <u>Summary of 1994 Accomplishments</u>:

- Further optimization of $SO_4^{2-}/SrO/La_2O_3$ to produce 2 kg of $C_2$ HC/kg catal/hr (550°C).

- Preparation of $V_2O_5/SiO_2$ catalysts that produce up to 1.5 kg HCHO/kg catal/hr, with low $CO_2$ selectivities, at 630°C.

- Development of a novel dual bed catalyst system that produces >100 g $CH_3OH$/kg catal/hr at 600°C.

## 2B.4 Conversion Economics for Alaska North Slope Natural Gas

### CONTRACT INFORMATION

| | |
|---|---|
| **Contract Number** | DE-AC07-94ID13223 |
| **Contractor** | Lockheed Idaho Technologies Company<br>P.O. Box 1625<br>Idaho Falls, ID 83415-2213<br>(208) 526-0165<br>(208) 526-0603 |
| **Contractor Project Manager** | Charles P. Thomas |
| **Principal Investigators** | Charles P. Thomas<br>Eric P. Robertson |
| **METC Project Manager** | Rodney D. Malone |
| **Period of Performance** | January 01, 1995 to December 31, 1995 |

**Schedule and Milestones**

**FY95/96 Program Schedule**

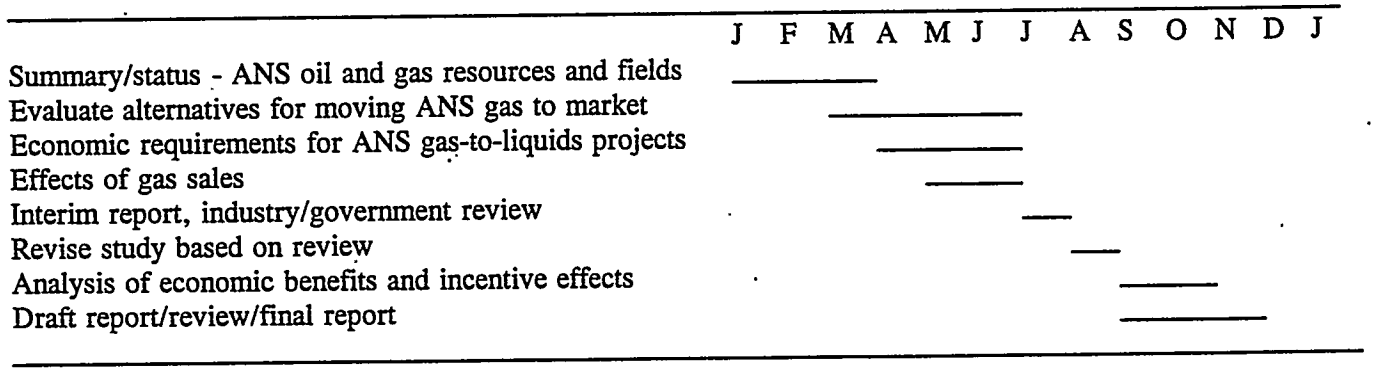


### OBJECTIVES

The purpose of this project is to perform an economic and technical feasibility study of the alternatives for bringing Alaska North Slope (ANS) natural gas resources to market. The economic requirements for gas-to-liquids conversion processes to be viable on the North Slope and the effects such processes would have on the development and utilization of the natural gas resources will be determined and compared to scenarios involving natural gas pipelines, LNG plants, or both. The objectives of the study are as follows:

(a) Review and summarize the ANS oil and gas resources and the status of currently producing fields and known undeveloped fields.

(b) Evaluate alternatives for moving ANS natural gas to market; i.e.. gas pipeline/liquified natural gas (LNG) plant scenarios, and gas-to-liquids conversion technologies that result in hydrocarbon liquids for transport in the Trans-Alaska Pipeline System (TAPS).

(c) Determine the economic requirements for gas-to-liquids conversion processes to be viable on the North Slope.

(d) Evaluate the effects of major gas sales on current and future ANS oil and gas development and production, and on the life of TAPS.

(e) Estimate the effects of major ANS gas sales on industry, state of Alaska, and federal income.

(f) Evaluate the impact alternative taxation and production enhancement incentives could have on development of gas sales capabilities.

## BACKGROUND INFORMATION

The natural gas resources in the developed and known undeveloped fields on the Alaskan North Slope total over 30 trillion cubic feet (Tcf).[1] Undiscovered gas resources on the ANS are estimated to be between 69 and 89 Tcf.[2] **Figure 1** is a map showing the location of the producing and nonproducing units and illustrates the significance of the infrastructure that has developed because of the Prudhoe Bay field. Most, if not all, of the smaller fields would not have been developed without facility cost-sharing made possible by this existing infrastructure, including TAPS. **Table 1** gives the remaining oil reserves and gas resources on the North Slope from the Alaska Department of Natural Resources, Division of Oil and Gas.

Currently, North Slope gas is not marketed off the North Slope except for natural gas liquids (NGLs), which are blended with crude oil for transport in TAPS. Historically and currently, the only market for North Slope gas is as a fuel for oil production facilities and related oil field activities. North Slope gas that is produced is injected back into the reservoirs and will be available for sale when a gas market is developed that will support construction of a gas pipeline system, or technology is developed that can economically convert the natural gas to hydrocarbon liquids that can be transported in TAPS.

**Table 1. Estimated Remaining Reserves[a]**

| | Oil[b] | Gas[c] |
|---|---|---|
| **North Slope Developed** | | |
| East Barrow | - | 6 |
| Endicott | 226 | 894 |
| Kuparuk River | 1,318 | 682 |
| Kuparuk Other | 173 | - |
| Lisburne | 81 | 277 |
| Milne Point | 188 | 13 |
| Niakuk/Alapah | 61 | 33 |
| Point McIntyre | 405 | 300 |
| Prudhoe Bay | 3,432 | 26,000 |
| Prudhoe Bay Other | 7 | 7 |
| South Barrow | - | 4. |
| Walakpa | - | 28 |
| **Undeveloped** | | |
| North Star/Seal Island | 180 | - |
| Pt. Thomson/Flaxman Island | 200 | 3,000 |
| **Total** | 6,271 | 31,244 |

a. From the Alaska Department of Natural Resources (Ref. 1)
b. Millions of barrels
c. Billions of cubic feet

North Slope fields had produced 10.3 billion barrels of oil by the end of 1994, 84% from Prudhoe Bay, 11% from Kuparuk, and 4% from the combined other pools (Reference 1). The ANS historical and projected production for currently producing fields is shown in **Figure 2**. ANS production has accounted for almost 25% of the nations domestically produced oil since production was initiated from the Prudhoe Bay field in 1977. The projected production in **Figure 2** is a composite of individual forecasts developed based on publicly available information obtained from North Slope producers, the Alaska Department of Natural Resources (Oil and Gas Conservation Commission and Division of Oil and Gas), and previous studies performed for the U.S. Department of Energy by the Idaho National Engineering Laboratory (INEL).[3,4] The arrows in **Figure 2** illustrate the potential impact a shutdown of TAPS, resulting from reaching a minimum throughput rate, would have on

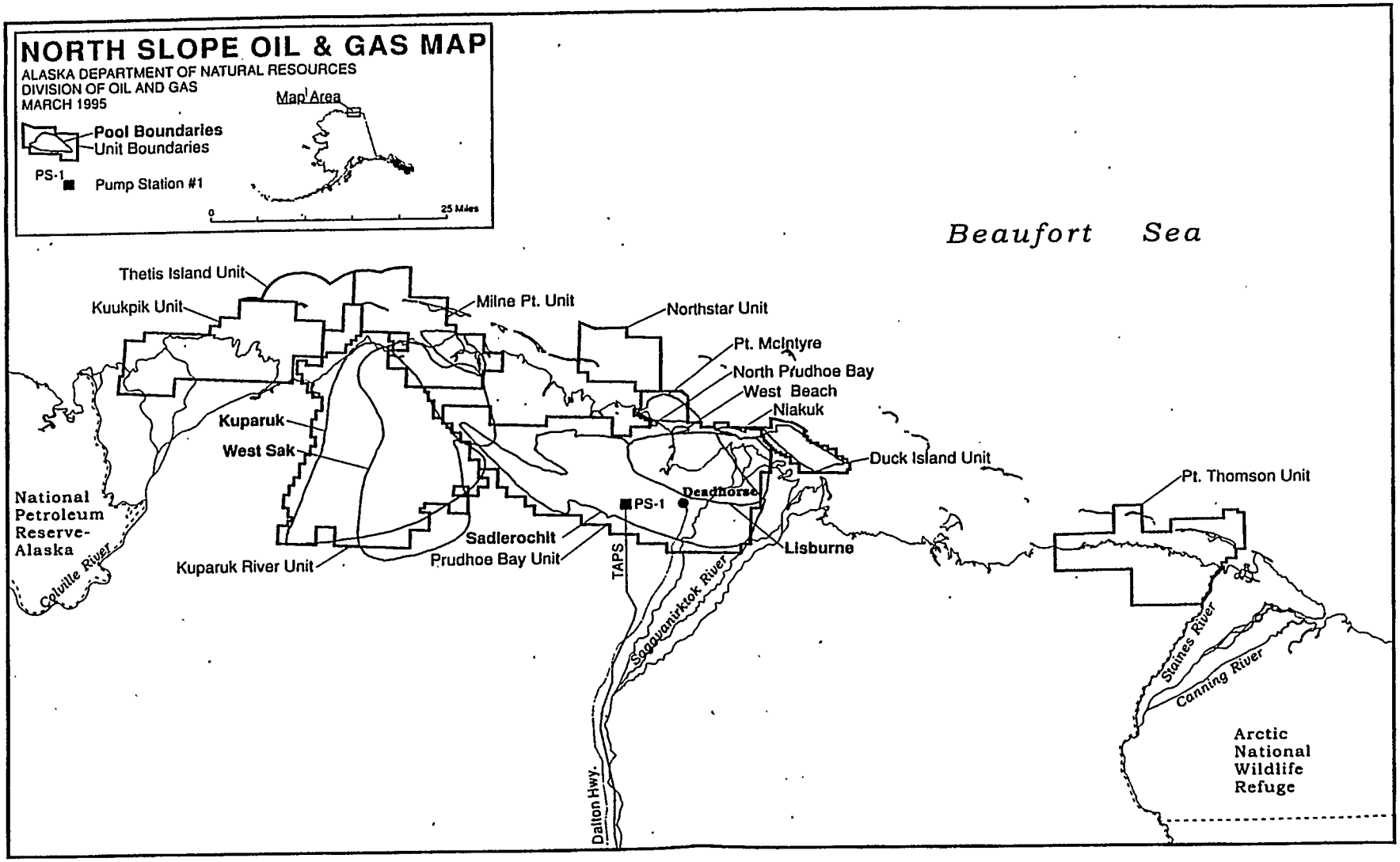


**Figure 1. North Slope Alaska Oil and Gas Map**

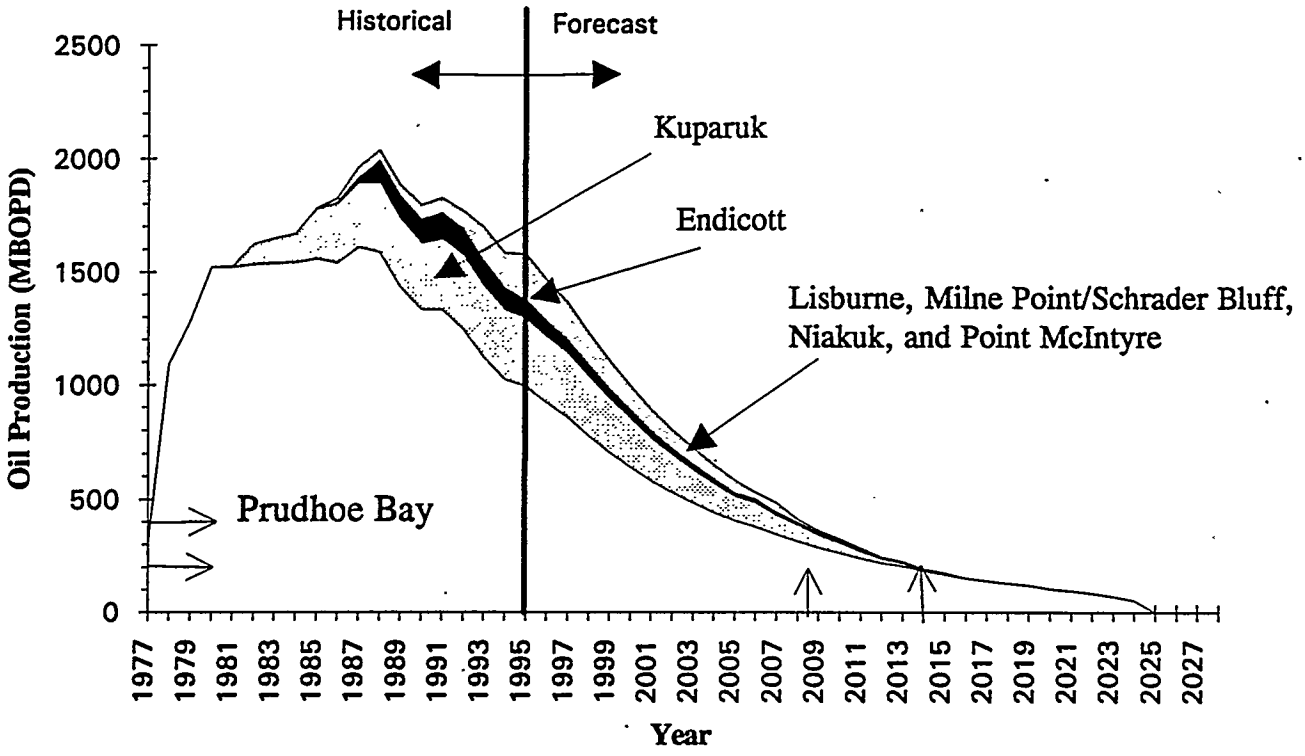


**Figure 2. Historical and projected production for Alaska North Slope**

the production of oil reserves from the North Slope. The actual lower limit for sustained operation has not been determined but would result from technical and economic considerations. A reasonable lower limit has been estimated to range from 400 to 200 thousand barrels per day (MBPD), which corresponds to a time range of 2009 to 2014 unless significant additional production becomes available. A shutdown at 2009 would result in a loss of reserves of about 1 billion barrels (BBO) and a shutdown in 2014 would result in a loss of about 400 million barrels (MMBO).

Since the discovery of the Prudhoe Bay field in 1968, numerous plans and ideas have been proposed for developing markets and a transportation system for North Slope gas. Prudhoe Bay contained 46 Tcf of gas and 23 billion barrels of oil at discovery. The most talked about proposal is the Trans-Alaska Gas System (TAGS), a $14 billion system consisting of a gas-conditioning plant on the North Slope; a 800-mile, 42-inch pipeline; an LNG plant/marine terminal at Valdez; and a LNG tanker fleet. LNG will be transported to Japan and other Pacific Rim countries. Yukon Pacific Corporation (YPC) has secured or satisfied all necessary legal approvals, requirements, and permits for construction of TAGS and export of ANS natural gas to Asia.[5] Construction of the project depends on obtaining long-term sales and purchase contracts with the North Slope owners of the gas supply and the LNG buyers in Asia. YPC believes the large scale of the project, 14 million metric tons of LNG annually, creates economies of scale that will allow this gas to be competitive with LNG projects closer to the Asian markets (Reference 5).

Another project that has been considered is the Alaskan Natural Gas Transportation System (ANGTS), which would involve a 4,783-mile pipeline through

Alaska and Canada to markets in the Lower 48 states. It appears unlikely that this project will be pursued any time in the near future.

Although large LNG markets exist in Pacific Rim countries (a) potential competition from overseas projects (e.g., Qatar, Natuna, and Sakhalin), (b) the large investments required for the TAGS pipeline, and (c) technical and economic factors relating to the best timing for initiation of major gas sales from the Prudhoe Bay Unit (PBU) have kept TAGS from being developed to date.

Except for the gas used for fuel for oil production, the gas that has been produced from the PBU has been reinjected into the reservoir to maintaining reservoir pressure, recycled into the gas cap to strip liquids, and used in a water-alternating-gas enhanced oil recovery project. Major gas sales from the Prudhoe Bay field will have an influence on the oil recovery from the field and could result in a reduction in the total oil recovery achieved depending on the timing and rate of gas sales. The reduction in oil recovery could vary from about 900 MMBO for major gas sales starting as early as 2000, to 400 MMBO for a 2005 start, to no effect for 2015 start.[6] The PBU owners are currently studying the issues and options involved with major gas sales and reviewing the options for reducing the influence on oil recovery.

The other known major gas field on the ANS is the Point Thomson field (see **Figure 1**). The Point Thomson Unit (PTU) covers a gas condensate field about 50 miles east of TAPS Pump Station No. 1. The PTU is listed in the most recent estimates by the Alaska Department of Natural Resources, Division of Oil and Gas (Reference 1) as containing 200 MMB of condensate and 3 Tcf of gas (earlier estimates were 300 MMB condensate and 5 Tcf gas). The PTU currently covers about 83,800 acres and is a deep overpressured reservoir that is located mostly offshore (see **Figure 1** and Reference 4). Development of the Point Thomson field is hindered by the lack of existing infrastructure and facilities that benefit fields in the vicinity of the Prudhoe Bay field. A Point Thomson development must support the construction of field delivery lines to the Prudhoe Bay field area that will encounter five major river crossings and cross the Arctic Coastal plain. The impact of these conditions will not be determined until environmental assessments are conducted.

In addition to the benefits in terms of profits for the industry, and taxes and royalties for the state of Alaska and the federal government from the sale of the gas on the ANS, the future of North Slope oil production beyond the 2009 to 2014 time frame depends on maintaining the viability of TAPS to support future development of known and undiscovered fields. The continued viability of the existing ANS oil and gas production infrastructure and operation of TAPS through discovery and development of new and known undeveloped oil fields will have a very important impact on the U.S. domestic oil supply. Economically viable processes to convert gas to hydrocarbon liquids that can be transported in TAPS could also have a significant impact on the future of the ANS.

Additionally, the ANS has an estimated 40 billion barrels of heavy oil and bitumen in the shallow formations of the West Sak and Ugnu fields (**Figure 1**).[7] The exploitation of these resources depends on maintaining the viability of TAPS until these resources can be economically developed. In addition to the impact of gas-to-liquids processes on the future of the ANS, economic processes for upgrading of heavy oils and tars in remote locations could also have a significant impact.

## PROJECT DESCRIPTION

The economic model developed for the previous North Slope studies performed by the INEL will be updated as needed and used to evaluate the economics of the alternatives for ANS gas sales and the effects of the alternatives on future development and production. The model has been described in detail in References 3 and 4.

The project approach will include the following steps:

(a) The current status of oil and gas resource development will be evaluated. Production, investment, and operating cost forecasts will be developed

for the producing and undeveloped fields that have significance for this study; e.g., the Point Thomson gas condensate field.

(b) Economic evaluations for each field will provide a baseline for current oil reserves using several oil price scenarios and allow a determination of the impact of gas sales scenarios on future oil production.

(c) The Prudhoe Bay field will be evaluated first. Prudhoe Bay without major gas sales, will provide the basis for evaluation of the effects of major gas sales through development of TAGS, or a similar project. A range of producer's gas price net-back values will be used to evaluate the project. The gas net back will be based on Pacific Rim LNG prices tied to the price of crude oil on the world market. Sensitivities of the economics of continued operations and new developments to the net back values for the gas sales will be determined.

(d) Requirements for capital costs, operating costs, and process efficiency for gas-to-liquids conversion processes to be economically viable for Prudhoe Bay, Point Thomson, and other gas resources will be determined for specific field development scenarios. The relative influence of capital costs for power and conversion plants, conversion efficiencies, operating costs, and product value will be determined using estimated costs for existing and emerging gas-to-liquids processes.

(f) The results of the gas-to-liquids conversion requirements will be compared to gas pipeline/LNG sales scenarios.

(g) The feasibility evaluation of gas conversion processes will include the overall impact such processes could have on North Slope production from extended life of the developed fields and development of additional fields.

(h) The impact that alternative taxation and production enhancement incentives could have on economic feasibility will be evaluated. For example, the severance tax calculation for gas could be based on total gas delivered to the conversion plant or an alternative method based on the produced liquid.

## RESULTS

*The results presented in this paper are preliminary; the data gathering phase of the project was initiated on March 6, 1995. The production forecasts and the economic evaluations are subject to change and should not be quoted or used without consultation with the authors.*

The production forecasts, investment forecasts, and operating costs have been updated for Prudhoe Bay, Kuparuk River, Endicott (Duck Island Unit), Lisburne, Milne Point (includes Schrader Bluff), Niakuk, and Point McIntyre. The historical and projected production from these fields is shown in **Figure 2.**

The economic model and the methodology used for the evaluations has been previously described in References 3 and 4. A discount rate of 10%, an inflation rate of 2.2%, and the World Oil Price cases shown in **Figure 3** have been used for the preliminary analyses presented in this paper. The discount rate that industry would use as a hurdle rate to make investment decisions could be much higher than the 10% we have used in this analysis. The inflation rate and the World Oil Price cases are taken from the Energy Information Administration's (EIA) *Annual Energy Outlook 1995*.[8] The World Oil Price cases consist of the reference case and low and high price cases to reflect the uncertainty in world oil markets. The curves in **Figure 3** are in 1995 dollars.

Preliminary results have been obtained for major gas sales from the Prudhoe Bay field for a gas pipeline/LNG plant project, such as TAGS, where the producers receive a gas price at the wellhead based on a gas net-back fraction, and gas-to-liquids conversion plants with assumed input parameters for capital and operating costs and efficiencies.

An evaluation of the economic viability of the TAGS system is not within the scope of this project. It is assumed for the purposes of this work that, if the project is built, it will be able to pay the producers for the gas at the rates assumed. Sensitivities to the producers' gas net-back fraction will be included in the analyses. This case is compared to a hypothetical gas-

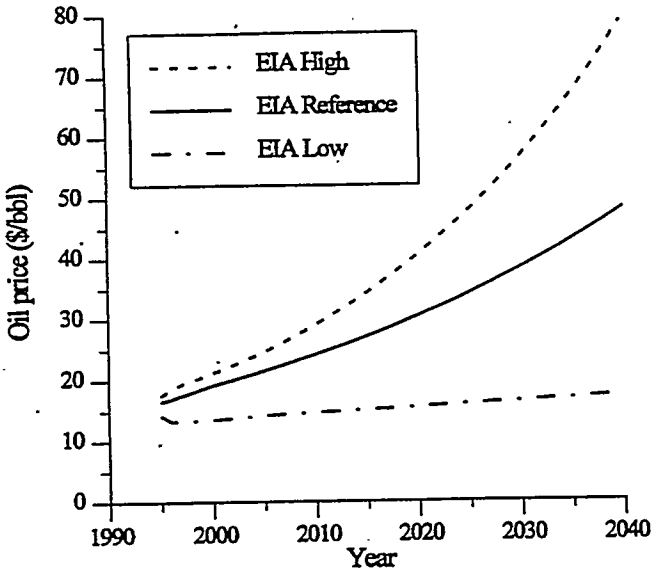


**Figure 3. World Crude Oil Prices (1995 dollars)[8]**

to-liquids conversion plant located in the Prudhoe Bay field and operated by the PBU Owners. Present Worth using a 10% discount rate ($PW_{10}$) is used to compare projects, (present worth is the cumulative after tax cash flow discounted to current year dollars; i.e., 1/1/95 for this study).

**Prudhoe Bay - No Major Gas Sales**

The base case for the Prudhoe Bay field uses the production forecast shown in **Figure 2**, the EIA Reference crude oil price case (**Figure 3**), a TAPS tariff schedule developed for the projected production from the ANS, transportation costs from Valdez to Lower 48 ports (California or Gulf Coast), a quality differential for North Slope crude of -$1.00 (applied to account for the estimated lower value of ANS crude relative to the world oil price), estimated future investments and operating costs, state taxes and royalties, and federal taxes. The wellhead oil price is obtained by subtracting the TAPS tariff, transportation costs, and quality differential from the world oil price. The EIA Reference oil price case with these input parameters results in total economic production from the Prudhoe Bay field of 12.75 BBO or 55.5% of the Original Oil in Place (OOIP). With these input parameters, the field would become uneconomic in 2022. The $PW_{10}$ is $6.5 billion for this case. The present worth at the 10% discount rate ($PW_{10}$) is $11.3 billion for the state of Alaska (severance tax, conservation tax, conservation surtax, ad valorem, income tax, and royalty) and $2.4 billion for the federal government. Early shutdown of TAPS resulting from total ANS production reaching a shutdown limit would reduce this recovery by as much a 400 to 800 MMBO from Prudhoe Bay alone.

**Prudhoe Bay - Major Gas Sales**

The natural gas available from the Prudhoe Bay field is estimated as follows (starting with the original gas in place (OGIP) in the gas cap and oil rim):

| | | |
|---|---|---|
| Gas Cap = 30 Tcf (OGIP) x 0.80 | = | 24.0 Tcf |
| Oil Rim = 16 Tcf (OGIP) x 0.60 | = | 9.6 Tcf |
| **Total Recoverable Gas** | = | 33.6 Tcf |
| Less $CO_2$ @ 12% = 33.6 Tcf x 0.88 | = | 29.6 Tcf |
| Less Fuel: | | |
| Fuel used through 1994 | = | 1.9 Tcf |
| Estimated Future use | = | 5.4 Tcf |
| **Total Fuel Use** | = | 7.3 Tcf |
| Estimated Net After Fuel | = | 22.3 Tcf |
| Less Estimated Liquids Shrinkage | = | 1.5 Tcf |
| **Net For Delivery to Pipeline** | = | **20.8 Tcf** |

Three scenarios have been evaluated to illustrate the relative impact and potential of major gas sales, (a) a pipeline/LNG plant scenario, and (b) two gas-to-liquids projects producing pipeline compatible hydrocarbon liquids.

**Gas Pipeline/LNG Plant.** The economic impact of a gas pipeline/LNG system for major gas sales from the Prudhoe Bay field has been evaluated through the use of a producers gas net-back fraction based on estimated LNG prices in the Asian market (e.g., Japan, Taiwan, S. Korea).

The producer's gas net-back price at the wellhead is the LNG price times a producer's gas net-back fraction; e.g., 15%.

$$\text{LNG Price} = \frac{\text{World Oil Price} \times \text{LNG Parity}}{\text{BTU Conversion}}$$

where,

World Oil Price = Ref. Oil Price (**Figure 3**)

LNG Parity = 1.1

$$\text{BTU Conversion} = \frac{\text{Million (MM) BTU/BBL Oil}}{\text{MM BTU/Mcf gas}}$$

$$= \frac{6.25 \text{ MM BTU/BBL oil}}{1.059 \text{ MM BTU/Mcf gas}}$$

BTU Conversion = 5.9 Mcf/BBL.

The resulting producer's gas net-back price is $0.47/Mcf in 1995 for a gas net-back fraction of 15% for the EIA Reference oil price of $15.67/BBL (1995 dollars). Gas sales are ramped up over a 5-year period to a maximum of 2.4 Bcf/day (i.e., 0.5, 1.0, 1.5, 2.0, 2.4 Bcf/day). The gas available for delivery as LNG to the Asian market, after transportation fuel and losses, is 2.0 Bcf/day, or 14 million metric tons per year for 20 years.

The effect on total oil recovery resulting from less gas being available for pressure maintenance, recycling, and miscible injectant for enhanced oil recovery caused by major gas sales starting in 2005 is estimated to be 400 million barrels of oil. The production forecasts with this reduction in oil reserves and major gas sales are shown in **Figure 4**. The resulting $PW_{10}$ for this case at a 15% gas net back is $8.1 billion. The $PW_{10}$ for the state is $11.5 billion and $3.3 billion for the federal government.

**Gas-To-Liquids Conversion.** For the gas-to-liquids cases, nominal values and costs have been assumed without reference to a particular technology for illustrative purposes. These assumptions will be verified for specific processes in the future work on this project and are presented here as an example of the potential and impact of such processes for application at Prudhoe Bay.

Two cases, a 300,000 barrel per day (BPD) plant and a 200,000 BPD plant, with start up in 2005, and a ramp up of 5 years, have been considered. The lost oil reserves are assumed to be 400 MMBO, the same as for the gas pipeline/LNG plant case. A capital cost of $40,000 per barrel per day (BPD) of hydrocarbon liquid produced is used for both cases. On the North Slope, a power plant and a conversion plant would have to be constructed and both are included in the $40,000/BPD value used for the calculations. One-third of the input gas is used for power plant fuel, and the gas to hydrocarbon liquid conversion efficiency is assumed to be 75%. The value of the product is expected to be of higher value than North Slope crude and is given a $5 per barrel premium; e.g., gasoline or aviation fuel grade. The TAPS tariff varies with the throughput rate; i.e., increased flow reduces the tariff rates. Therefore, a different tariff schedule is required for each case. Severance taxes have been calculated on the gross gas produced rather than on the product sold and valued based on the product sale value.

For the 300,000 BPD plant, the production forecast is shown in **Figure 5**. The plant cost at $40,000/BPD is $12 billion. A gas production rate of 3.6 Bcf/day, removal of 12% $CO_2$, use of 1.2 Bcf/day for fuel, a conversion efficiency of 75%, and a BTU conversion of 5.3 Mcf/BBL results in 300,000 BPD of hydrocarbon liquids. The $PW_{10}$ for this case is $8.2 billion. The $PW_{10}$ for the state of Alaska is $13.8 billion and $3.8 billion for the federal government. The resulting benefit to continued operation of TAPS, assuming a 200 MBOPD lower limit, is 8 years, 2022 versus 2014, and would result in production of almost 2 billion barrels of additional petroleum liquids from the gas conversion. Impact on total ANS production will be determined later in the project.

For the 200,000 BPD gas-to-liquids case (see **Figure 5**), the plant cost at $40,000/BPD is $8 billion. The required gas rate is 2.4 Bcf/day for this case with the same fuel requirements and conversion efficiency. The $PW_{10}$ for this case is $8.7 billion. The $PW_{10}$ for the state of Alaska is $13.2 billion and $3.9 billion for the federal government. The project is extended until

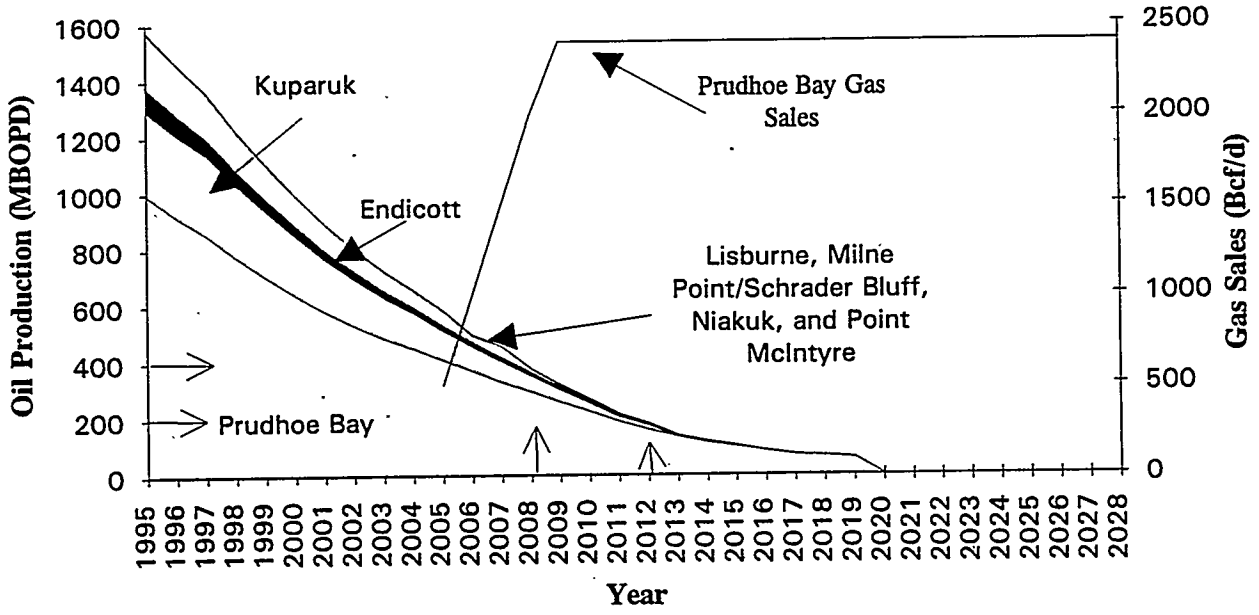


**Figure 4. Prudhoe Bay field production forecast w/major gas sales**

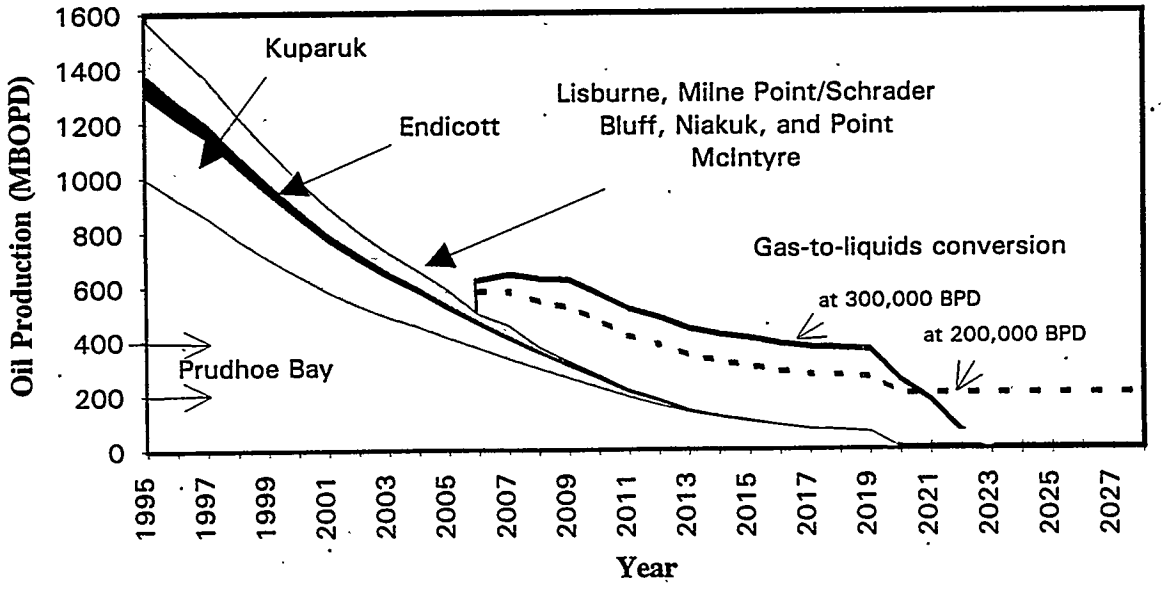


**Figure 5. Prudhoe Bay field w/gas-to-liquid conversion**

2028 using the lower limit for TAPS of 200 MBOPD for an additional 14 years of production compared to the base case. The total oil and hydrocarbon liquid increase is the same as above considering only the Prudhoe Bay field.

## Summary

For the Prudhoe Bay field, this preliminary analysis provides an indication that major gas sales using a gas pipeline/LNG plant scenario, such as TAGS, or a gas-to-liquids process with the cost parameters assumed, are essentially equivalent and would be viable and profitable to industry and beneficial to the state of Alaska and the federal government. The cases are compared in **Table 2** ($1995 dollars, billions) for the Reference oil price case. The reserves would be 12.7 BBO for the base case without major gas sales, 12.3 BBO and 20 Tcf gas for the major gas sales case, and 14.3 BBO for the gas-to-liquids conversion cases.

**Table 2. Preliminary Economics for Natural Gas Sales and Conversion for the Prudhoe Bay Field**

| Project | Life | $PW_{10}$ | State | Federal |
|---|---|---|---|---|
| No Major Gas Sales | 2022 | $6.5 | $11.3 | $2.4 |
| Major Gas Sales | 2028 | $8.1 | $11.5 | $3.3 |
| 300 MBPD | 2022 | $8.2 | $13.8 | $3.8 |
| 200 MBPD | 2028 | $8.7 | $13.2 | $3.9 |

Use of different parameters such will significantly alter these results; e.g., the low oil price case would result in the base case for Prudhoe Bay field becoming uneconomic in 2002 with the operating costs and investments as currently estimated.

## FUTURE WORK

Work was initiated for this project on March 6, 1995 and all the results presented are preliminary and will be reviewed for errors in the input data and assumptions before reaching conclusions about any of the projects.

Future work will include checking the data used, obtaining confirmation of values for the costs and conversion efficiencies associated with specific gas-to-liquids conversion technologies (to the extent such information is known and available); extending the analysis to other fields on the North Slope, particularly the Point Thomson gas field; and reviewing the impact of the alternatives on the future of North Slope development and production.

Sensitivity analysis will be used to determine the effect of the variables such as low and high oil price forecasts, gas net-back fraction, capital costs for power plant and conversion plant construction, gas required to operate the power plant for different gas-to-liquids technologies, timing of project start up, taxation rates and methodologies, value of hydrocarbon product and effect of product type on operation of TAPS.

## REFERENCES

1. State of Alaska, Department of Natural Resources, Division of Oil and Gas. March 1995. "Historical and Projected Oil and Gas Consumption." 3601 C Street, Suite 1380, Anchorage, AK 99503-5948.

2. Mast, R.F., G.L. Dolton, R.A. Crovelli, R.H. Root, E.D. Attanasi, P.E. Martin, L.W. Cooke, G.B. Carpenter, W.C. Pecora, and M.B. Rose. 1989. "Estimates of Undiscovered Conventional Oil and Gas Resources in the United States - A Part of the Nation's Energy Endowment." U.S. Department of Interior, U.S. Government Printing Office, 1989-242-338:80069.

3. Thomas, C.P., T.C. Doughty, D.D. Faulder, W.E. Harrison, J.S. Irving, H.C. Jamison, G.J. White. 1991. "Alaska Oil and Gas: Energy Wealth or Vanishing Opportunity?," U.S. DOE, DOE/ID/01570-H1.

4. Thomas, C.P., R.B. Allaire, T.C. Doughty, D.D. Faulder, J.S. Irving, H.C. Jamison, G.J. White. 1993.

"Alaska North Slope National Energy Strategy Initiative: An Analysis of Five Undeveloped Fields." U.S. DOE, DOE/ID/01570-T164. NTIS/DE93000142. Springfield, VA.: National Technical Information Service.

5. Yukon Pacific Corporation, personal communication. March 1995.

6. ARCO Alaska, Inc., personal communication. March 1995.

7. Mahmood, S.M., D.K. Olsen, and C.P. Thomas. 1995. "Heavy Oil Production from Alaska." In proceedings of the *Sixth UNITAR International Conference on Heavy Crude and Tar Sands*. February 12-17, 1995. Houston, Texas.

8. Energy Information Administration. January 1995. *Annual Energy Outlook 1995*. DOE/EIA-0383 (95).

## 2B.5 Economics of Natural Gas Upgrading


**Contract Number** DE-AC21-90MC27346



**Contractor** K&M Engineering and Consulting Corp.
2001 L Street, N.W., Suite 500
Washington, D.C. 20036
Tel: 202/728-0390
Fax: 202/872-9174



**Other Funding Sources**



**Contractor Project Manager** A. John Rezaiyan

**Principal Investigators** John H. Hackworth
Robert W. Koch

**METC Project Manager** Hsue-Peng Loh



**Period of Performance** May 6, 1994 to April 15, 1995



### ABSTRACT

**Economics of Natural Gas Upgrading**

Natural gas could be an important alternative energy source in meeting some of the market demand presently met by liquid products from crude oil. This study was initiated to analyze three energy markets to determine if greater use could be made of natural gas or natural gas derived products and if those products could be provided on an economically competitive basis. The three markets targeted for possible increases in gas use were motor fuels, power generation, and the chemical feedstocks market.

The economics of processes to convert natural gas to transportation fuels, chemical products, and power were analyzed. The economic analysis was accomplished by drawing on a variety of detailed economic studies, updating them and bringing the results to a common basis. The processes analyzed included production of methanol, MTBE, higher alcohols, gasoline, CNG, and LNG for the transportation market. Production and use of methanol and ammonia in the chemical feedstock market and use of natural gas for power generation were also assessed. Use of both high and low quality gas as a process feed stream was evaluated. The analysis also explored the impact of various gas price growth rates and process facility locations, including remote gas areas. In assessing the transportation fuels market the analysis examined production and use of both conventional and new alternative motor fuels.


### OBJECTIVES

During the past decade, a gas supply surplus has existed in the United States. Future gas supply prospects have also brightened because the estimates of the potential size of

undiscovered gas reserves has increased. At the same time, U.S. oil reserves and production have steadily declined and oil imports have steadily increased.

Reducing the growth in the volume of crude oil imports was an important objective of the Energy Policy Act of 1992. Natural gas could be an important alternative energy source in meeting some of the market demand presently met by liquid products from crude oil. This study was initiated to analyze three energy markets to determine if greater use could be made of natural gas or natural gas derived products and if those products could be provided on an economically competitive basis. In particular, the following three markets were targeted for possible increases in gas use:

- Transportation fuels
- Power generation
- Chemical feedstock

Gas-derived products that could potentially compete in these three markets were identified and the economics of the processes for producing those products were evaluated. The processes considered covered the range from commercial processes to those in early stages of process development. The analysis also evaluated the use of both high quality natural gas and lower quality gases containing $CO_2$ and $N_2$ levels above normal pipeline quality standards.

**Analysis of Gas Derived Products in Transportation Fuels Markets**

Three types of products can be produced from natural gas for use in the transportation fuels market (Exhibit 1). Natural gas is currently used in the production of MTBE, ether which is used in gasoline production both because of its high octane properties and to meet the CAA oxygen content standard required in about 1/3 of the U.S. market. There are other ethers and alcohols that could also potentially be produced from natural gas and compete in the oxygenated gasoline market. While oxygenates command a price premium compared with other gasoline components, the volumes required are limited by octane need and oxygen content requirement as specified by environmental regulations.

Natural gas can also be used to produce synthetic gasoline and diesel. In this instance the issue is the price competitiveness of gas derived gasoline and diesel vs crude oil derived products.

The final avenue of access is production of alternative transportation fuels -- primarily methanol and CNG. Even if the alternative transportation fuels can be produced at a competitive price to gasoline and diesel fuel, they face major hurdles in gaining entry and acceptance in that market. The hurdles that a new fuel faces in establishing a position in the transportation fuels market are summarized in Exhibit 2.

Ideally for most efficient operation, an alternative-fueled vehicle would be an original equipment vehicle/engine system optimized to use the specific fuel. Sometimes in the transition period when the use of the fuel is being established, existing gasoline or diesel vehicles can be converted to use an alternative fuel such as methanol or CNG. Vehicles can also be designed to use either of two fuels (bi-fueled) or a combination (flexible-fueled). These types of vehicles are designed to help the user cope with the problem of finding fuel while the distribution network and number of refueling locations for the alternative fuel is growing.

Exhibit 1
Assessing Increased Use of Gas in the
Transportation Fuels Market

| TYPE OF FUEL | GAS DERIVED PRODUCTS | MARKET PENETRATION | MARKET SIZE |
|---|---|---|---|
| GASOLINE BLEND COMPONENTS | MTBE OTHER ETHERS ALCOHOLS | EASY | LIMITED BY NEED FOR OXYGENATES |
| GASOLINE AND DIESEL | SYNTHESIZED GASOLINE & DIESEL | EASY IF PRICE IS COMPETITIVE | LARGE |
| ALTERNATIVE TRANSPORTATION FUELS | METHANOL CNG | DIFFICULT | LARGE BUT HARD TO PENETRATE |

Exhibit 2
Market Penetration Hurdles for Alternative
Transportation Fuels

- Building a Customer Base of Vehicles Which Can Use the Fuel
- Developing Infrastructure of Delivery and Refueling Facilities
- Gaining Consumer Acceptance of Fuel/Vehicle Systems
  - Cost: Vehicle cost, fuel cost, maintenance and repair cost
  - Convenience: Fuel availability, refueling time, refueling frequency
  - Performance: Start reliability, no stalling, power
  - Safety Perception: As safe or safer than current vehicles

Finally, a new fuel must gain consumer acceptance, which depends on how the consumer assesses the economics, convenience, performance, safety and other factors in choosing to purchase an alternative - fuel vehicle versus a conventional fuel vehicle.

As shown in Exhibit 3, the process routes from natural gas to transportation fuels involve commercial processes such as methanol and MTBE and some processes in the research phase such as production of gasoline or diesel by direct conversion processes such as oxidative coupling or oxyhydrochlorination.

**Economic Evaluation of Gas to Transportation Fuel Conversion Processes**

Data was taken from a variety of previous economic studies to develop the evaluation of the natural gas to transportation fuel economics presented in this study. Only Fischer-Tropsch and oxidative coupling economic data were available from a common source. Since each source of data used somewhat different factors for determining total capital and total operating and maintenance costs, it was decided to accept certain basic data from the economic sources and calculate the rest of the economics using a consistent methodology. All cost were escalated to December 1993 using Nelson-Farrar Indexes reported in the "Oil and Gas Journal".

The current and future prices of natural gas and crude oil in the US are obviously important variables in assessing the economic competitiveness of transportation fuels derived from these two feedstocks. While US gas suppliers have been exceeding needs for the past decade and US crude production has been declining annually, most forecasts of future US energy prices predict a higher growth rate for gas prices compared to crude prices (Exhibit 4). Forecasters see US crude prices as being set in the international crude market, where surplus production capability has existed since the early 1980's. Gas prices in the US are determined in the regional North American market and are based on assessments of the economics of continuing to add future reserves. The assumption of a higher future gas price growth rate makes it more difficult for a process using a gas feed to be economically attractive versus a process using a crude feed. In their most recent energy price forecast, GRI lowered their projection of future gas prices. The GRI forecast was used as a sensitivity case in this analysis.

A summary of the economic analysis of conversion of natural gas to transportation fuels is shown in Exhibit 5. Conversion of natural gas to methanol and MTBE are commercial processes, a number of facilities have been built and are producing and selling a product into the market place at a competitive price. The cost of producing MTBE from natural gas and n-butane was evaluated and estimated to be 86 cents per gallon. Analysis of the gasoline market indicates that MTBE can command a price premium of 30-40 cents per gallon over refinery gasoline gate prices. Thus, MTBE is clearly commercially viable at current gasoline prices and should continue to be competitive in the future.

The economic analysis indicates that methanol can be produced from lower 48 U.S. gas at 44 cents per gallon (cpg). Viewing methanol as an alternative transportation fuel, the 44 cpg must be translated to equivalent gasoline basis, accounting for energy density and efficiency differences. On a gasoline-equivalent basis, methanol would be 74 cpg at the plant gate versus 68 cpg for gasoline. This is not a large differential but development of distribution and refueling infrastructure and

Exhibit 3
Natural Gas Conversion Processes

| |
|---|
| Conversion Processes to Transportation Fuels<br>- Syngas<br>- Methanol<br>- Direct conversion<br>- Compression |
| Commercial Scale Plants Operating<br>- MTBE (via Methanol)<br>- Methanol (via Syngas) |
| Developing Processes<br>- Fischer-Tropsch |
| Research Processes<br>- Oxidative Coupling<br>- Higher Alcohols |

Exhibit 4
Forecasts of U.S. Oil and Natural Gas Prices
(Prices in 1994$)

| | PRICE IN | | | GROWTH RATE |
|---|---|---|---|---|
| FORECAST | 1993 | 2000 | 2010 | 93-2010 |
| 1994 DOE OUTLOOK | | | | |
| GAS ($/MCF) | 1.79 | 2.48 | 3.56 | 4.1% |
| OIL ($/BBL) | 18.65 | 21.25 | 28.88 | 2.6% |
| 1995 DOE OUTLOOK | | | | |
| GAS ($/MCF) | 2.02 | 2.29 | 3.37 | 3.1% |
| OIL ($/BBL) | 16.12 | 19.13 | 24.12 | 2.4% |
| 1995 GRI FORECAST | | | | |
| GAS ($/MCF) | 2.06 | 2.53 | 2.71 | 1.6% |
| OIL ($/BBL) | 16.42 | 18.58 | 20.54 | 1.3% |

**Exhibit 5**
**Comparative Economics of Gas**
**To Transportation Fuel Processes**

| Process | Liquid Phase Methanol | UOP - MTBE | IFP Higher Alcohol | Fischer-Tropsch | Oxidative Coupling | Delivered CNG |
|---|---|---|---|---|---|---|
| Product | Methanol | MTBE | C1-C6 Alcohol | Gasoline or Diesel | Gasoline | CNG |
| Costs (cpg) | | | | | | |
| Feed | 24 | 51 | 36 | 52 | 52 | 28 |
| Other Operating | 7 | 17 | 22 | 28 | 43 | 11 |
| Capital | 12 | 14 | 43 | 58 | 67 | 6 |
| Total | 44 | 86 | 120 | 137 | 169 | 48 |
| Equiv. Gasoline (cpg) | 74 | NA | NA | 137 | 169 | 48 |
| Competing Fuels | Gasoline | Octane Blend Comp'nts | Gasoline Blend Comp'nts | Gasoline | Gasoline | Deliv'd Gasoline |
| Competing Fuel Price (cpg) | 68 | 98 | 68-98 | 68 | 68 | 84 |

gaining consumer acceptance are major obstacles on the path to commercial success for methanol.

The demonstrated processes are processes which have been built at commercial scale and for which cost and technical feasibility have been demonstrated. Conversion of natural gas to liquids using Fischer-Tropsch is placed in this category. There are no operating Fischer-Tropsch gas-to-liquid plants, but there are commercial Fischer-Tropsch units for converting syngas from coal gasification and there are commercial units for generating syngas from natural gas. The estimated cost of producing liquid fuels from natural gas using a Fischer-Tropsch process is 1.37$/gallon. This is double the current production cost of gasoline. If gas prices rise faster than crude, the gap between cost of producing Fischer-Tropsch liquids and gasoline would only widen. The economic hope for a Fischer-Tropsch process using natural gas may lie with utilizing remote gas resources.

The processes that are in a research and development phase include a process to produce higher alcohols from natural gas and oxidative coupling, a direct methane to gasoline process. Using conversion and selectivity assumptions for oxidative coupling previously used in a Bechtel analysis, the cost of producing a gasoline product would be $1.69/gallon. This cost is far above current gasoline prices. Moreover, review of a variety of oxidative coupling research results indicates that the conversion and selectivity used in the economic analysis is beyond those which have practically been achieved.

Several processes have and continue to be studied to convert natural gas to $C_1$-$C_6$ alcohols. In this study, economics were developed for the IFP process and the estimated cost of the product was $1.20/gallon. While the higher alcohols merit a market price premium over gasoline, the IFP alcohol product consists of 50-70% methanol and 16-23% ethanol in the product. Because of such poor selectivity to higher alcohols the process does not look economically attractive. In this process, as in the case of oxidative coupling, the question is, is there sufficient reason to believe that a major process improvement is achievable that can justify further R&D expenditures.

**Economics and Use of Gas in Chemical Feestock and Power Generation Markets**

The use of natural gas in chemical feedstock and in power generation applications is established. This study has analyzed the market for chemical products to assess demand growth and the potential for increased gas usage. Likewise, the issue of increased natural gas use in the power sector was addressed. In each of these applications, use of low quality natural gas (LQNG) was compared with use of high quality natural gas.

The principal uses of natural gas in the chemical feedstock market are in the production of ammonia, methanol and hydrogen (Exhibit 6). The most promising growth area for increased gas usage is in methanol production. U.S. methanol consumption in 1991 was 1.68 billion gallons and in 1995 it is expected to reach 2.75 billion gallons. This growth is primarily attributable to the increased use of methanol to produce MTBE for use in making oxygenated and reformulated gasoline. The high rate of methanol demand growth will diminish after 1995. Use of methanol as a direct transportation fuel is an uncertain factor in assessing longer term demand growth prospects.

**Exhibit 6**
**Use of Natural Gas as a Chemical Feedstock**

| % of Total Natural Gas Consumed as Feedstock | Material Produced | Product Use | US Market Growth |
|---|---|---|---|
| 60 | Ammonia | Fertilizer | Very Low |
| 22 | Hydrogen & Other | Oil Refining | Moderate |
| 18 | Methanol | Transportation Fuels & Chemicals | High |

Ammonia production currently accounts for 60% of the natural gas use as a chemical feedstock. U.S. demand for ammonia, however, has been stagnant and there has been a continuing threat of competition from imports from low gas price regions around the world. There appears to be little chance of ammonia production capacity growth in the U.S. and hence little opportunity for increased natural gas use.

The process economics are summarized in Exhibit 7. As can be seen, using high quality gas, methanol can be produced at a price well below the current market price, but the market is currently very tight. More importantly, future prices are expected to support an acceptable return on investment. On the other hand, ammonia prices, which are currently high, still do not cover the return to capital. Market growth and U.S. facility economics provide a consistently bleak outlook for increasing natural gas use for ammonia production.

Use of gas is increasing as a fuel for power generation due to favorable economics.

**Economics of LQNG**

In all of these cases, use of low quality natural gas (LQNG) as a feed was compared with the use of high quality gas. The low quality gas considered contained 13% $N_2$. A high nitrogen gas was analyzed because it is upgrading a low quality natural gas to a high quality gas. In the methanol case, assuming that the methanol product would sell at the same price when using the LQNG feed as when using high quality gas, the value of the LQNG as a feed would be 2.26$/MMBTU compared to 2.43 $/MMBTU for the high quality gas. For the ammonia case, the value is 2.24 $/MMBTU compared to the 2.43 $/MMBTU, and in the combined-cycle case, the LQNG is valued at 2.32 $/MMBTU. That is a range of 11-24 ¢/MMBTU lower value for the LQNG compared to high quality natural gas. Those values compare very favorably to the cost of upgrading the LQNG via nitrogen rejection which would place a value of only 1.71 $/MMBTU on the LQNG. These results make direct use of LQNG appear to be the path to pursue. There is, however, an important element of the economics not considered -- the transportation of LQNG to the production facility, or transport of the product to the customer.

## Exhibit 7
## Economic Comparison of Natural Gas in Chemical and Power Processes

| Process | Liquid Phase Methanol (LPMEOH) | | Ammonia | | Combined Cycle | | Cryogenic Nitrogen Production |
|---|---|---|---|---|---|---|---|
| Product | Methanol | | Ammonia | | Electric Power | | High Quality Natural Gas |
| Type of Natural Gas Feed | High Quality | Low Quality | High Quality | Low Quality | High Quality | Low Quality | Low Quality |
| Costs ($/per unit product) | | | | | | | |
| Name of Unit | Gallon | Gallon | Short Ton | Short Ton | kWh | kWh | $10^6$ Btu |
| Feed | 0.24 | 0.24 | 50 | 46 | 0.019 | 0.018 | 1.58 |
| Other Operating | 0.07 | 0.07 | 80 | 83 | 0.005 | 0.006 | 0.31 |
| Capital | 0.12 | 0.12 | 57 | 59 | 0.011 | 0.012 | 0.24 |
| TOTAL | 0.44 | 0.44 | 240 | 240 | 0.037 | 0.037 | 2.43 |
| Value of Natural Gas Feed, $/$10^6$ Btu | 2.43 | 2.26[1] | 2.43 | 2.24[1] | 2.43 | 2.32[1] | 1.71[1] |
| Market Price Range of Product, 10/93-10/94, $/Unit | 0.46 to 1.40 | | 104 to 232 | | 0.046 to 0.052 | | 2.43 |

[1]Assumes that product will have the same equivalent price as if produced from high quality natural gas.

In the case of power, it is expensive to transport power, if it can not be marketed locally. In the case of ammonia, there is no need for new production facilities. For methanol, the product is needed on the Gulf Coast and little high $N_2$ gas production is located in that region.

Thus, while the economics for LQNG look favorable, there are limited opportunities because of market and production facilities locations.

**Improving Process Economics and Market Potential**

The economic analysis serves two purposes. First, it provides, as we have seen, the relative cost of providing products using competing process options. Secondly, it establishes sensitivity of the production costs to changes in the cost of feed, reductions in capital cost, or improvements in conversion rates or selectivity.

Some of the sensitivity analysis cases for Fischer-Tropsch (FT) are displayed in Exhibit 8. The exhibit shows that use of a slurry reactor reduces product cost 2$/Bbl. The GRI price growth vs the DOE price forecast would reduce the initial product cost by 4.60 $/Bbl. Large differences are achieved if the technology is employed in a remote gas area where facility construction cost are comparable to the US. With gas prices at 50 ¢/MMBTU product could be produced at 36 $/Bbl and, if plant size were scaled up 4 times, then price could be reduced to 25 $/Bbl.

The indirect conversion processes, such as FT and methanol production are high capital cost processes compared to crude oil conversion processes and as shown in Exhibit 9, the syngas generation step represents 70% of the facility cost. Thus, if improvement could be found in this step, the impact would be significant. While syngas production is viewed as an established process, there are still opportunities for new approaches such as membrane reactor systems.

In the case of the direct conversion processes, poor conversion and selectivity have been the barrier to achieving competitive process schemes. For these processes, marginal improvement will not suffice, new concepts with the potential to break through the yield barriers are needed if these processes are to achieve eventual success.

**Summary**

Achieving greater use of natural gas as an alternative transportation fuel is an uncertain prospect. The US government has set a target of displacing 30 percent of the crude derived fuels for light duty vehicle with non-crude-derived by 2010. CNG has very attractive economics as we have seen but the potential growth on new motor vehicles to 30% faces both political uncertainties in terms of long term commitment to this case and also the obstacles of developing a delivery system infrastructure, refueling technology, refueling outlets, and final consumer acceptance.

Those who deal with the "dismal science" of economics are often viewed as negative people, more focused on the pitfalls, than on the promises. Clearly, the objective of this effort was to provide insights into the more promising vs the less promising in allocating our R&D dollar and efforts. I do hope that we have achieved some degree of success in meeting that objective.

**Exhibit 8**
**Fischer-Tropsch Process Economics Sensitivity Analysis**

| CASE | SYNGAS PROCESS | TYPE FT REACTOR | PLANT LOCATION | CAPACITY MB/D | GAS PRICE: $/MMBTU | | UNIT COST OF PRODUCT: $/BARREL | | | |
|---|---|---|---|---|---|---|---|---|---|---|
| | | | | | INITIAL | GWTH RATE | FEED | O&M | CAP CHRG | PLT GATE |
| 1 | PARTIAL OXIDATION | ARGE FIXED-BED | GULF COAST | 14,500 | 2.43 | 3.1 | 21.68 | 11.91 | 24.53 | 59.61 |
| 2 | PARTIAL OXIDATION | FT SLURRY | GULF COAST | 14,500 | 2.43 | 3.1 | 20.92 | 11.88 | 22.56 | 56.84 |
| 3 | PARTIAL OXIDATION | FT SLURRY | GULF COAST | 14,500 | 2.43 | 1.6 | 20.92 | 11.88 | 22.56 | 54.04 |
| 4 | PARTIAL OXIDATION | FOUR RX SLURRY | GULF COAST | 58,000 | 2.43 | 3.1 | 20.92 | 7.47 | 15.05 | 45.67 |
| 5 | PARTIAL OXIDATION | FT SLURRY | ASIA | 14,500 | 0.50 | 0 | 4.30 | 11.88 | 22.07 | 35.95 |
| 6 | PARTIAL OXIDATION | FT SLURRY | ASIA | 14,500 | 0.00 | 0 | 0.00 | 11.88 | 21.94 | 31.81 |
| 7 | PARTIAL OXIDATION | FT SLURRY | ASIA | 58,000 | 0.50 | 0 | 4.30 | 11.88 | 14.86 | 25.03 |

Exhibit 9

LPMEOH Process

**PROCESS STEPS**

- Production of synthesis gas
- Methanol synthesis in a three stage reactor (1600 psia, 482°F)
- Thermal efficiency approximately 64%

**ECONOMICS**

| | $/Bbl Methanol | |
|---|---|---|
| Natural Gas Feed | 10.08 | |
| Maintenance | 2.74 | |
| Capital Charge | 4.91 | |
| Total | 18.65 | 44 cpg |

**STATUS**

- Commercial process - mature

**POTENTIAL FOR IMPROVEMENT**

- Syngas step is 70% of capital cost
- Significant cost reduction unlikely
- Production cost tied to gas prices

# ECONOMIC EVALUATION AND MARKET ANALYSIS FOR NATURAL GAS UTILIZATION

- Assess Market Potential For Gas-Derived Products
  - Transportation Fuels
  - Chemical Feedstocks
  - Utility Fuels
- Evaluate Process Economics
- Compare Use of Low and High Quality Natural Gas

## ASSESSING INCREASED USE OF GAS IN THE TRANSPORTATION FUELS MARKET

| TYPE OF FUEL | GAS DERIVED PRODUCTS | MARKET PENETRATION | MARKET SIZE |
|---|---|---|---|
| GASOLINE BLEND COMPONENTS | MTBE OTHER ETHERS ALCOHOLS | EASY | LIMITED BY NEED FOR OXYGENATES |
| GASOLINE AND DIESEL | SYNTHESIZED GASOLINE & DIESEL | EASY IF PRICE IS COMPETITIVE | LARGE |
| ALTERNATIVE TRANSPORTION FUELS | METHANOL CNG | DIFFICULT | LARGE BUT GROWTH RATE LIMITING |

# MARKET HURDLES FOR ALTERNATIVE TRANSPORTATION FUELS

- Building a Customer Base of Vehicles Which Can Use the Fuel
- Developing Infrastructure of Delivery and Refueling Facilities
- Gaining Consumer Acceptance of Fuel/Vehicle Systems
  - Cost: Vehicle cost, fuel cost, maintenance and repair cost
  - Convenience: Fuel availability, refueling time, refueling frequency
  - Performance: Start reliablity, no stalling, power
  - Safety Perception: As safe or safer than current vehicles

# GAS CONVERSION PROCESSES

## Routes to Transportation Fuels

- Via syngas
- Via methanol
- Direct conversion
- Compression

## Commercial Scale Plants Operating

- MTBE
- Methanol

## Developing Processes

- Gas via Syn Gas
- Fischer-Tropsch

## Research Processes

- Oxidative Coupling

- Higher Alcohols

## ECONOMIC EVALUATION - ANALYSIS METHODOLOGY

- Data taken from a variety of economic studies.
  Different methods were used to determine
  Capital and Operating & Maintenance Costs.

- Basic determinants of costs were taken from source data.
  e.g., operators per shift

- Other economic data were calculated using factors.
  e.g., startup cost = 20% of Annual Op Cost

- All costs were escalated to 12/93 based on Nelson-Farrar.
  No adjustment was made for differences in capacities.

## FORECASTS OF U.S. OIL AND NATURAL GAS PRICES
## (PRICES IN 1994$)

| FORECAST | PRICE IN 1993 | PRICE IN 2000 | PRICE IN 2010 | GROWTH RATE 93-2010 |
|---|---|---|---|---|
| **1994 DOE OUTLOOK** | | | | |
| GAS($/MCF) | 1.79 | 2.48 | 3.56 | 4.1% |
| OIL($/BBL) | 18.65 | 21.25 | 28.88 | 2.6% |
| **1995 DOE OUTLOOK** | | | | |
| GAS($/MCF) | 2.02 | 2.29 | 3.37 | 3.1% |
| OIL($/BBL) | 16.12 | 19.13 | 24.12 | 2.4% |
| **1995 GRI FORECAST** | | | | |
| GAS($/MCF) | 2.06 | 2.53 | 2.71 | 1.6% |
| OIL($/BBL) | 16.42 | 18.58 | 20.54 | 1.3% |

## COMPARATIVE ECONOMICS OF GAS TO TRANSPORTATION FUEL PROCESSES

| PROCESS | LIQUID PHASE METHANOL | UOP-MTBE | IFP HIGHER ALCOHOL | FISCHER-TROPSCH | OXIDATIVE COUPLING | DELIVERED CNG |
|---|---|---|---|---|---|---|
| PRODUCT | METHANOL | MTBE | C1-C6 ALCOHOL | GASOLINE OR DIESE | GASOLINE | CNG |
| COSTS(cpg) | | | | | | |
| FEED | 25 | 51 | 36 | 52 | 52 | 30-47 |
| OTHER OPR | 7 | 17 | 22 | 28 | 43 | 30 |
| CAPITAL | 12 | 18 | 66 | 57 | 74 | |
| TOTAL | 44 | 86 | 120 | 137 | 169 | 60-77 |
| EQUIV GASO GALLON COST | 74 | NA | NA | 137 | 169 | 60-77 |
| COMPETING FUELS | GASOLINE | OCTANE BLEND COMP'NTS | GASOLINE BLEND COMP'NTS | GASOLINE | GASOLINE | DELIV'D GASOLINE |
| COMPETING FUEL PRICE | 68 | 98 | 68-98 | 68 | 68 | 84 |

# USE OF NATURAL GAS AS A CHEMICAL FEEDSTOCK

| % of Total Natural Gas consumed as Feedstock | Material Produced | Product Use | US Market Growth |
|---|---|---|---|
| 60 | Ammonia | Fertilizer | Very Low |
| 22 | Hydrogen & Other | Oil Refining | Moderate |
| 18 | Methanol | Transportation Fuels & Chem's | High |

## ECONOMIC COMPARISON OF NATURAL GAS TO CHEMICALS AND POWER PROCESSES

| Process | Liquid Phase Methanol (LPMEOH Oil) | | Ammonia | | Combined Cycle | | Cryogenic Nitrogen Production |
|---|---|---|---|---|---|---|---|
| Product | Methanol | | Ammonia | | Power | | High Quality Natural Gas |
| Type of Natural Gas Feed | High Quality | Low Quality | High Quality | Low Quality | High Quality | Low Quality | Low Quality |
| Costs (dollars per unit product) | | | | | | | |
| Name of Unit | Gallon | Gallon | Short Ton | Short Ton | kWh | kWh | $10^6$ Btu |
| Feed | 0.24 | 0.24 | 50 | 46 | 0.019 | 0.018 | 1.58 |
| Other Operating | 0.07 | 0.07 | 80 | 83 | 0.005 | 0.006 | 0.31 |
| Capital | 0.13 | 0.13 | 110 | 111 | 0.013 | 0.013 | 0.54 |
| TOTAL | 0.44 | 0.44 | 240 | 240 | 0.037 | 0.037 | 2.43 |
| Price of Natural Gas Feed, $/$10^6$ Btu | 2.43 | 2.26 | 2.43 | 2.24 | 2.43 | 2.32 | 1.55 |
| Market Price Range of Product, 10/93 - 10/94, $/Unit | 0.46 to 1.40 | | 104 to 232 | | 0.046 to 0.052 | | |

# FISCHER-TROPSCH PROCESS ECONOMICS SENSITIVITY ANALYSIS

| CASE | SYN GAS PROCESS | TYPE FT REACTOR | PLANT LOCATION | CAPACITY MB/D | GAS PRICE:$/MMBTU INITIAL | GWTH RATE | UNIT COST OF PRODUCT: $/BARREL FEED | O&M | CAP CG | PLT GATE |
|---|---|---|---|---|---|---|---|---|---|---|
| 1 | PARTIAL OXIDATION | ARGE FIXED-BED | GULF COAST | 14,500 | 2.43 | 3.1 | 21.68 | 11.91 | 24.53 | 59.61 |
| 2 | PARTIAL OXIDATION | FT SLURRY | GULF COAST | 14,500 | 2.43 | 3.1 | 20.92 | 11.88 | 22.56 | 56.84 |
| 3 | PARTIAL OXIDATION | FT SLURRY | GULF COAST | 14,500 | 2.43 | 1.6 | 20.92 | 11.88 | 22.56 | 54.04 |
| 4 | PARTIAL OXIDATION | FOUR RX SLURRY | GULF COAST | 58,000 | 2.43 | 3.1 | 20.92 | 7.47 | 15.05 | 45.67 |
| 5 | PARTIAL OXIDATION | FT SLURRY | ASIA | 14,500 | 0.50 | 0 | 4.30 | 11.88 | 22.07 | 35.95 |
| 6 | PARTIAL OXIDATION | FT SLURRY | ASIA | 14,500 | 0.00 | 0 | 0.00 | 11.88 | 21.94 | 31.81 |
| 7 | PARTIAL OXIDATION | FT SLURRY | ASIA | 58,000 | 0.50 | 0 | 4.30 | 11.88 | 14.86 | 25.03 |

# LPMEOH PROCESS

## PROCESS STEPS

- Production of synthesis gas
- Methanol synthesis in a three stage reactor. Operates at 1600 psia and 482 exit temperature.
- Thermal efficiency approximately 64%

## ECONOMICS

| | $/Bbl Methanol | |
|---|---|---|
| Natural Gas Feed | 10.35 | |
| Op & Maintenance | 2.74 | |
| Capital Charge | 5.56 | |
| Total | 18.65 | 44 cpg |

## STATUS

- Commercial process - mature
- LPMEOH is an alternative competitive process

## POTENTIAL FOR IMPROVEMENT

- Slight improvement possible, could be optimized
- Syngas step is 70% of capital cost
- Significant cost reduction unlikely
- Production cost tied to gas prices

# 2B.6 An Overview of PETC's Gas-to-Liquids Technology R&D Program

Gary J. Stiegel and Arun C. Bose
Pittsburgh Energy Technology Center

and

Rameshwar D. Srivastava
Burns and Roe Services Corporation
Pittsburgh Energy Technology Center

## ABSTRACT

The overall goal of the Gas-to Liquids Program at the U.S. Department of Energy's Pittsburgh Energy Technology Center (PETC) is to develop technologies for the production of hydrocarbon fuels and premium chemicals from light alkane gases. PETC's current Gas-to-Liquids Program comprises the development of four primary advanced conversion technologies, namely, partial oxidation, oxidative coupling, oxyhydrochlorination, and novel conversion processes.

Based on the current state of development, it can be concluded that, in the near future, one or more of these technologies will reach proof-of-concept demonstration. Oxyhydrochlorination is the most advanced direct conversion technology, and the synthesis of lower cost methyl chloride from natural gas would impact several commercial technologies that utilize methyl chloride as an intermediate to high value products.

Technology development for the partial oxidation of methane to synthesis gas using ceramic membranes could result in significant savings in synthesis gas generation costs by eliminating the air separation plant and replacing the conventional synthesis gas generation loop. A mixed conducting membrane has been developed, and sustained proof-of-principle tests have shown commercially relevant methane conversions and CO selectivities. A multi-channel reactor development and demonstration program has been proposed.


*U.S. Government Printing Office 1995 609-544